

WestminsterResearch

<http://www.westminster.ac.uk/westminsterresearch>

**Production of Polyhydroxyalkanoates and their application for
coronary stent development**

Lukasiewicz, B.

This is an electronic version of a PhD thesis awarded by the University of Westminster.
© Miss Barbara Lukasiewicz, 2017.

The WestminsterResearch online digital archive at the University of Westminster aims to make the research output of the University available to a wider audience. Copyright and Moral Rights remain with the authors and/or copyright owners.

Whilst further distribution of specific materials from within this archive is forbidden, you may freely distribute the URL of WestminsterResearch: (<http://westminsterresearch.wmin.ac.uk/>).

In case of abuse or copyright appearing without permission e-mail repository@westminster.ac.uk

**Production of Polyhydroxyalkanoates and
their application for coronary stent
development**

Barbara Lukaszewicz

**A thesis submitted to the University of Westminster in candidature
for the award of the degree of Doctor of Philosophy**

August 2017

AUTHOR'S DECLARATION

I declare that the present work was carried out in accordance with the Guidelines and Regulations of the University of Westminster. The work is original except where indicated by special reference in the text.

The submission as a whole or part is not substantially the same as any that I previously or am currently making, whether in published or unpublished form, for a degree, diploma or similar qualification at any university or similar institution.

Until the outcome of the current application to the University of Westminster is known, the work will not be submitted for any such qualification at another university or similar institution.

Any views expressed in this work are those of the author and in no way represent those of the University of Westminster.

Signed: Barbara Lukasiewicz

Date: August 2017

ACKNOWLEDGEMENTS

First of all, I would like to express my thankfulness to my supervisor Prof. Ipsita Roy for giving me an opportunity to do this project in her lab. That was an incredible experience, during which I have learnt a lot. I would like to thank her especially for her support and encouragement, which motivated me to work hard in order to achieve my goals.

Secondly, I would like to thank to the ReBioStent Project FP7 consortium for financial support and all our collaborators for their support.

I would like to thank Dr Pooja Basnett for her guidance, constant motivation and support throughout my research adventure.

Thank you Dr Rinat Nigmatullin for valuable advises, guidance and introducing me to the polymers world.

I also would like to thank Dr Stipo Jurcevic for his help and support during haemocompatibility studies and his valuable inputs into this project.

I would like to thank the technical staff from University of Westminster: Thakor, Harry, Luisa, Poulet, Vanita, Jonathan, Glen, Kim, Dinesh, Joe. Special thanks to Neville for his constant support during the experiments involving fermentation.

I am very thankful to the technical staff from UCL: Dr. George Gergiou, Dr. Graham Palmer for their assistance with various techniques as well as Dr Nicola Mordan for her help with different imaging techniques.

I would like to thank all members of the lab, both past and present for your friendship, and time spent together. Thank you, Pooja, Rinat, Moyin, Hima, Elena, Sheila, Isabel, Alex, Christy, Lorena, Prachi, Bijal, Sujata, Manu, Silvia, Peter for all your support during my journey.

I am very grateful to my friends: Malgosia and Darek for their help during writing up period.

I would like to thank my family: my parents and my sisters for their love and encouragement. Thank you for believing in me.

Finally, I would like to dedicate this thesis to my beloved husband, Grzegorz, who was throughout with me during my project. Thank you for taking care of me and being very patient especially in the most difficult time. And thank you for being my inspiration. This work will not be possible without his financial generosity.

ABSTRACT

Development of coronary artery stents have revolutionised the treatment of coronary artery disease. However, the currently available stents have several limitations and side effects, which still need to be addressed. Within this group of biomaterials Polyhydroxyalkanoates (PHAs), which are biopolyesters produced by bacteria, have a great potential in coronary stent development. They are biodegradable, non-toxic and biocompatible. PHAs have a broad range of properties, which can be tailored based on the requirements of the application by an appropriate bacterial strain, carbon source or fermentation conditions.

The main aim of this study was the production of PHAs and their application as a platform material for coronary stent. Poly(3-hydroxybutyrate), P(3HB), short chain length PHA (scl-PHA), was obtained from *B. subtilis* OK2 using glucose as the sole carbon source. *P. mendocina* was selected for the economical production of medium chain length PHA (mcl-PHAs) using waste frying oil as the carbon source. Produced mcl-PHA copolymer was hydrolysed in order to obtain lower molecular weight PHA (oligo-PHA), which was used as the plasticising agent for P(3HB) in order to alter material properties of the scl-PHA polymer. Novel P(3HB)/oligo-PHA blends, using different ratios of P(3HB) and oligo-PHA, which were 100:0 (P(3HB)), 95:5 (P(3HB): oligo-PHA), 90:10 (P(3HB): oligo-PHA) and 80:20 (P(3HB): oligo-PHA) have been developed. Addition of oligo-PHA to P(3HB) resulted not only in the enhancement of mechanical properties of the material, but also improved surface topography and increased the biocompatibility of the scaffolds in comparison to neat P(3HB).

The P(3HB)/oligo-PHA 90/10 blend was selected for the fabrication of radiopaque composites using addition of 1%, 3% and 5% wt barium sulphate. BaSO₄ is well-known contrast agent, commonly used in biomedical applications. The composites were fully characterised with respect to material properties, surface topography and biocompatibility. Preliminary studies, performed by MicroCT confirmed the radiopacity of the composite material. The composites exhibited an increased surface roughness, lower contact angle values and higher protein adsorption in comparison to the neat blend without barium sulphate. The observed cell viability was significantly better in comparison to standard Tissue Culture Plastic (TCP).

The P(3HB)/oligo-PHA 90:10 blend was selected as a base material for tube manufacturing by the dip moulding technique. Mechanical properties of the blend tubes were similar to those obtained for flat films, except for tensile strength, which was slightly higher in tubes. An incubation of tubes in DMEM media at 37°C for 7 weeks resulted in the decrease values of tensile strength, Young's Modulus values and elongation at break in comparison to the tubes stored at room temperature without any media. Additionally, *In vitro* degradation study was carried out on the tubes. After 6 months of incubation in PBS, The P(3HB)/oligo-PHA 90/10 tubes underwent a 30% weight loss. pH of the media has dropped insignificantly, due to release of slightly acidic degradation products. Scanning Electron Microscope (SEM) images confirmed an enlarged porosity in the tube wall with an increased time of incubation.

Furthermore, an investigation of the P(3HB)/oligo-PHA 90/10 tubes coated with PCL-PEG550 with incorporated drugs: rapamycin or tacrolimus was carried out for the development of a drug eluting biodegradable stent. The percentage viability of the HMEC-1 cells was significantly higher on the tubes with tacrolimus compared to the tubes with rapamycin. Controlled release of both drugs was observed within 90 days, which is an encouraging result for the development of biodegradable drug eluting stents. There was a clear cytotoxic effect of rapamycin on the HMEC-1 cells, whereas, presence of tacrolimus did not exhibit similar effect on cell attachment and viability.

Haemocompatibility studies were performed in order to investigate the reaction of blood cells after direct contact with PHAs polymer samples. Obtained results confirmed the non-haemolytic effect of PHAs on erythrocytes and low risk of thrombogenicity. Although all tested materials demonstrated slightly elevated levels of monocytes and neutrophil activation in comparison to fresh whole blood, obtained values were much lower in comparison to poly(L-lactic acid) (PL38), a well-established medical polymer currently used for coronary stent application.

In conclusion, the results obtained in this work confirmed that PHAs have an excellent potential as suitable platform matrices for coronary stent application.

TABLE OF CONTENTS

Chapter 1 Introduction	1
1.1. Coronary artery disease	2
1.2. Coronary stents	3
1.2.1. Bare metallic stents	4
1.2.2. Drug-eluting stents (DES)	6
1.2.3. Biodegradable stents.....	7
1.2.3.1. Absorb Bioresorbable Vascular Scaffold (BVS)	10
1.3. Drugs used in drug eluting stents.....	11
1.3.1. Rapamycin and its analogues	12
1.3.2. Paclitaxel	14
1.3.3. Tacrolimus	15
1.3.4. Dexamethasone.....	16
1.3.5. Antibodies	17
1.4. Biopolymers used as a drug carriers in the prevention of restenosis	18
1.5. Limitations of currently available stents	20
1.5.1. In-stent restenosis	21
1.5.2. Late stent thrombosis.....	24
1.6. Ideal stent requirements.....	26
1.7. Biomaterials used for coronary stent application	27
1.8. Polyhydroxyalkanoates	28
1.8.1. Types of PHAs and their properties	29
1.8.2. Biocompatibility of PHAs	32
1.8.3. Blood-biomaterial interactions.....	33
1.8.4. Biodegradability of PHAs	35
1.8.5. Biosynthesis of Poly(3-hydroxyalkanoates).....	36
1.8.5.1. Synthesis of short chain length polyhydroxyalkanoates	38
1.8.5.2. Synthesis of medium chain length polyhydroxyalkanoates	40
1.8.6. Microbial production of PHAs	41
1.8.6.1. Gram-positive bacteria	41
1.8.6.2. Gram-negative bacteria.....	42
1.8.6.3. Archea	43
1.8.6.4. Mixed microbial cultures (MMC).....	44
1.8.7. Polyhydroxyalkanoate recovery	45
1.8.8. Economical production of Poly(3-hydroxyalkanoates).....	47
1.8.8.1. Cheap carbon sources suitable for PHA production.....	48
1.8.8.2. Genetically engineered strains	49
1.8.8.3. Optimisation of polymer recovery – downstream processes.....	51
1.8.8.4. Efficient fermentation strategies.....	52
1.8.9. Synthesis of PHA blends and composites	52
1.8.10. Applications of PHAs	55
1.8.10.1. Biomedical applications.....	55

TABLE OF CONTENTS

Aims and objectives	62
Chapter 2 Materials and Methods	65
2.1. Materials	66
2.1.1. Bacterial strains	66
2.1.2. Cell line and cell culture materials	66
2.1.3. Chemicals and kits	66
2.2. Media composition.....	67
2.3. Bioreactors	69
2.4. Experimental methods	72
2.4.1. P(3HB) production by <i>Bacillus subtilis</i> OK2 and <i>Bacillus cereus</i> SPV using a range of carbon sources at shaken flask level.....	72
2.4.2. P(3HB) production by <i>Cupriavidus necator</i> using a range of carbon sources at shaken flask level	72
2.4.3. Production of P(3HB) by <i>Bacillus subtilis</i> OK2 in bioreactor.....	73
2.4.4. Production of mcl-PHAs by <i>Pseudomonas mendocina</i> CH50 using a range of carbon sources at shaken flask level	74
2.4.5. Production of mcl-PHAs in bioreactors	74
2.5. Extraction of Poly(3-hydroxyalkanoates) from biomass.....	75
2.5.1. Solvent dispersion method.....	75
2.5.2. Soxhlet extraction	75
2.6. Structural characterization of scl-PHA.....	76
2.6.1. Attenuated Total Reflectance Fourier Transform Infrared Spectroscopy	76
2.6.2. Gas Chromatography-Mass Spectrometry (GC-MS).....	76
2.6.3. Nuclear magnetic resonance (NMR)	77
2.6.4. Thermal analysis - Differential Scanning Calorimetry (DSC).....	77
2.6.5. Molecular weight analysis – Gel Permeation Chromatography	78
2.7. Temporal profiling of the PHA production during fermentation	78
2.7.2. pH measurements	79
2.7.3. Analytical methods.....	79
2.8. Production of oligo-PHA and material characterisation.....	80
2.8.1. Acidic hydrolysis of P(3HHx-3HO-3HD-3HDD).....	80
2.8.2. P(3HHx-3HO-3HD-3HDD) hydrolysis kinetics	81
2.9. Blend film fabrication	81
2.10. P(3HB)/oligo-PHA composite film fabrication with barium sulphate.....	81
2.11. Tubes manufacturing by using dip moulding technique	82
2.11.1. Preparation of the tubes with incorporated drug.....	83
2.11.2. Preparation of composite tubes with barium sulphate	83
2.11.3. Characterization of PHA blends, composites and tubes.....	84
2.11.3.1. Ageing experiments.....	84
2.11.3.2. Tensile test	84
2.11.3.3. Differential scanning calorimetry (DSC)	84

TABLE OF CONTENTS

2.11.3.4. Static contact angle analysis.....	84
2.11.3.5. Scanning electron microscopy (SEM)	85
2.11.3.6. X-ray microtomography (MicroCT).....	85
2.11.3.7. Surface roughness analysis.....	85
2.11.3.8. X-ray diffraction (XRD).....	85
2.11.3.9. Protein adsorption study.....	86
2.12. <i>In vitro</i> release studies of rapamycin using UV-Vis spectrometry.....	86
2.13. <i>In vitro</i> release studies of tacrolimus using High Performance Liquid Chromatography (HPLC).....	86
2.14. <i>In vitro</i> cell culture studies	87
2.14.1. Cell growth and maintenance	87
2.14.2. Sample preparation and cell seeding	87
2.14.3. MTT assay	88
2.14.4. SEM imaging of HMEC-1 cells.....	88
2.14.5. Live/ dead measurements.....	88
2.14.6. Indirect cytotoxicity studies	89
2.15. Haemocompatibility studies.....	89
2.15.1. Haemolysis studies	89
2.15.2. Whole blood clotting.....	90
2.15.3. Monocyte and neutrophil activation studies	91
2.15.3.1. Sample preparation.....	91
2.15.3.2. Whole blood staining with activation antibodies.....	91
2.15.3.3. Flow cytometry analysis	92
2.16. <i>In vitro</i> degradation studies of the tubes	92
2.16.1. Thermal and mechanical properties.....	92
2.16.2. Surface morphology	93
2.16.3. Water uptake, weight loss and pH measurements	93
2.17 Statistical analysis.....	93
Chapter 3 Production and characterisation of scl-PHAs.....	94
3. Introduction.....	95
3.1. Screening experiments.....	96
3.2. Production of P(3HB) using <i>Bacillus subtilis</i> OK2 and glucose as the sole carbon source.....	97
3.3. P(3HB) characterization.....	99
3.3.1. Attenuated Total Reflectance Fourier Transform Infrared Spectroscopy	99
3.3.2. Gas Chromatography Mass Spectrometry (GC-MS)	100
3.3.3. Nuclear Magnetic Resonance (NMR)	102
3.3.4. Molecular weight analysis of P(3HB) produced by <i>Bacillus subtilis</i> OK2	103
3.3.5. Thermal analysis – Differential Scanning Calorimetry (DSC)	104
3.3.6. Mechanical characterisation of the P(3HB) solvent cast films	105

TABLE OF CONTENTS

3.3.7. Thermal analysis of the neat P(3HB) neat films after 7 weeks of storage at room temperature	106
3.3.8. Mechanical characterisation of the neat P(3HB) films after 7 weeks of storage at room temperature	107
3.4. Discussion	109
Chapter 4 Production and characterisation of mcl-PHAs	113
4. Introduction.....	114
4.1. Screening experiments.....	115
4.2. Characterisation of the waste frying oil used to produce mcl-PHAs	117
4.2.1. Attenuated Total Reflectance Fourier Transform Infrared Spectroscopy ..	117
4.2.2. Gas Chromatography Mass Spectrometry (GC-MS)	118
4.2.3. Nuclear Magnetic Resonance (NMR)	120
4.3. Production of P(3HHx-3HO-3HD-3HDD) using <i>Pseudomonas mendocina</i> CH50 and waste frying oil as a sole carbon source.....	123
4.4. Mcl-PHA characterisation.....	124
4.4.1. Attenuated Total Reflectance Fourier Transform Infrared Spectroscopy ..	124
4.4.2. Gas Chromatography Mass Spectrometry (GC-MS)	125
4.4.3. Thermal analysis – Differential Scanning Calorimetry (DSC)	128
4.4.4. Molecular weight analysis – Gel Permeation Chromatography (GPC)	129
4.5. Discussion	130
Chapter 5 Development of Poly(3-hydroxybutyrate)/oligo -PHA blends	136
5. Introduction	137
5.1. Development of oligo-P(3HHx-3HO-3HD-3HDD).....	140
5.1.1. Oligo-PHA characterisation	140
5.1.1.1. Attenuated Total Reflectance Fourier Transform Infrared Spectroscopy (ATR/FT-IR)	141
5.1.1.2. Thermal analysis – Differential Scanning Calorimetry (DSC)	141
5.1.1.3. Molecular weight analysis – Gel Permeation Chromatography (GPC) ..	142
5.2. Development of P(3HB)/oligo-PHA blends.....	143
5.2.1. Blend characterisation.....	144
5.2.1.1. Thermal analysis of the blend films after 7 weeks of storage at room temperature - ageing experiments	144
5.2.1.2. Mechanical characterisation of the blend films after 7 weeks of storage at room temperature - ageing experiments.....	146
5.3. Surface topography studies.....	149
5.3.1. Scanning Electron Microscopy of the P(3HB)/oligo-PHA blends	149
5.3.3. Water contact angle measurements	151
5.3.4. Protein adsorption analysis	152
5.4. <i>In vitro</i> biocompatibility studies.....	153
5.4.1 Cell viability studies	154

TABLE OF CONTENTS

5.4.2. Scanning Electron Microscopy	155
5.4.3 Confocal microscopy of HMEC-1 cells on the P(3HB) and its blends.....	156
5.5. Haemocompatibility studies.....	158
5.5.1. Haemolysis study.....	158
5.5.2. Whole blood clotting.....	159
5.5.3. White cell activation.....	160
5.5.3.1. Whole blood staining	161
5.5.3.2. Blood activation with LPS	162
5.5.3.3. Monocyte and neutrophil activity after incubation with neat P(3HB) and P(3HB)/oligo-PHA blends.....	164
5.6. Discussion.....	165
Chapter 6 Development of Poly(3-hydroxybutyrate)/oligo-PHAs composites	172
6. Introduction	173
6.1. Development of Poly(3-hydroxybutyrate)/oligo-PHAs composites	175
6.2. P(3HB)/oligo-PHA composite characterisation	175
6.2.1. Attenuated Total Reflectance Fourier Transform Infrared Spectroscopy ..	175
6.2.2. Thermal properties of the composites of P(3HB)/oligo-PHA blends with barium sulphate after 7 weeks of storage at room temperature	177
6.2.3. Mechanical properties of the composites of P(3HB)/oligo-PHA blend in ratio 90/10 with barium sulphate after 7 weeks of storage at room temperature.....	179
6.3. Surface analysis	181
6.3.1. Scanning Electron Microscopy (SEM)	181
6.3.2. Surface roughness analysis.....	182
6.3.3. Contact angle measurement	183
6.3.4. Protein adsorption on the surface of the composites containing BaSO ₄ ...	185
6.3.5. XRD analysis.....	186
6.4. <i>In vitro</i> biocompatibility studies.....	187
6.4.1. MTT assay	187
6.4.2. SEM.....	188
6.4.3. Indirect cytotoxicity.....	189
6.4.4. MicroCT scan of the composite samples.....	191
6.5. <i>In vitro</i> haemocompatibility studies.....	192
6.5.1. Haemolysis study.....	192
6.5.2. Whole blood clotting.....	193
6.5.3. Monocytes and neutrophils activity after incubation with P(3HB)/oligo-PHAs composites	194
6.6. Discussion	195
Chapter 7 Poly(3-hydroxybutyrate)/oligo-PHAs tubes manufacturing.....	199
7. Introduction	200
7.1. P(3HB)/oligo-PHA tube manufacturing by dip moulding technique	201

TABLE OF CONTENTS

7.2. Tube characterization.....	202
7.2.1. Tube dimensions	202
7.2.2. Tubes characterisation after 7 weeks of storage at room temperature and incubation in DMEM media at 37° C	202
7.2.2.1. Thermal properties of P(3HB)/oligo-PHA tubes stored for 7 weeks at room temperature	203
7.2.2.2. Mechanical properties of P(3HB)/oligo-PHA tubes stored for 7 weeks at room temperature	204
7.2.2.3. Mechanical properties of the P(3HB)/oligo-PHA tubes after incubation in DMEM media at 37° C for 7 weeks.....	205
7.2.3. Scanning Electron Microscopy of the P(3HB)/oligo-PHA tubes.....	208
7.3. <i>In vitro</i> degradation studies	209
7.3.1. Attenuated Total Reflectance Fourier Transform Infrared Spectroscopy ..	209
7.3.2. Thermal properties – Differential Scanning Calorimetry.....	210
7.3.3. pH measurements during degradation studies of neat PHA tubes.....	211
7.3.4. Weight loss (%) of the neat tubes during degradation studies	212
7.3.5. Water uptake (%) of the neat tubes during degradation studies.....	213
7.3.6. Surface studies of the degraded tubes.....	214
7.4. Manufacturing of the P(3HB)/oligo-PHA 90/10 tubes coated with monolayer of PCL-PEG550	216
7.4.1. Thermal analysis of PCL-PEG550	216
7.4.2. P(3HB)/oligo-PHA 90/10 tubes coated with PCL-PEG550 manufacturing ..	217
7.4.3. Characterisation of P(3HB)/oligo-PHA tubes coated with monolayer of PCL-PEG550.....	217
7.4.3.1. Attenuated Total Reflectance Fourier Transform Infrared Spectroscopy (ATR/FT-IR)	217
7.4.3.2. Thermal properties of the PCL-PEG550 coated PHA tube.....	218
7.4.3.3. Mechanical properties of the PCL-PEG550 coated PHA tube.....	220
7.4.3.4. SEM.....	222
7.5. Manufacturing of P(3HB)/oligo-PHA composite tubes with addition of 5 wt% barium sulphate and their characterization.....	223
7.5.1. Thermal properties.....	224
7.5.2. Mechanical properties.....	225
7.5.3. SEM.....	226
7.5.4. MiroCT.....	227
7.6. <i>In vitro</i> biocompatibility studies of the range of manufactured PHA tubes.....	228
7.6.1. Protein adsorption.....	228
7.6.2. MTT assay	229
7.6.3. Indirect cytotoxicity study	231
7.6.4. SEM.....	232
7.7. <i>In vitro</i> haemocompatibility studies.....	234

TABLE OF CONTENTS

7.7.1. Haemolysis study.....	234
7.7.2. Whole blood clotting.....	235
7.7.3. Monocytes and neutrophils activation.....	236
7.8. Discussion.....	238
Chapter 8 Development of P(3HB)/oligo-PHA tubes with incorporated drug	245
8. Introduction	246
8.1. Drugs characterisation	247
8.1.1. Attenuated Total Reflectance Fourier Transform Infrared Spectroscopy).....	251
8.1.2. Differential Scanning Calorimetry	249
8.2. P(3HB)/oligo-PHA tubes coated with PCL-PEG550 and incorporated drug manufacturing.....	251
8.3. P(3HB)/oligo-PHA tubes coated with PCL-PEG550 and incorporated drug characterisation	252
8.3.1. Attenuated Total Reflectance Fourier Transform Infrared Spectroscopy ..	252
8.3.2. Scanning Electron Microscopy	254
8.3.3. Drug release studies.....	255
8.4. <i>In vitro</i> biocompatibility studies.....	257
8.4.1. Protein adsorption.....	257
8.4.2. Cell viability study.....	259
8.4.3. Scanning Electron Microscopy	260
8.4.4. Indirect cytotoxicity study.....	261
8.5. Haemocompatibility studies.....	262
8.5.1. Haemolysis study.....	262
8.5.2. Whole blood clotting study	263
8.5.3. Monocytes and neutrophil activation	265
8.6. <i>In vitro</i> degradation study	266
8.6.1. Attenuated Total Reflectance Fourier Transform Infrared Spectroscopy ..	266
8.6.2. Thermal properties – Differential Scanning Calorimetry	268
8.6.3. Mechanical properties of the P(3HB)/oligo-PHA tubes coated with PCL-PEG550 with incorporated drugs	270
8.6.4. pH measurements during degradation studies of neat PHA tubes.....	271
8.6.5. Weight loss (%) of the neat tubes during degradation studies	272
8.6.6. Water uptake (%) of the neat tubes during degradation studies.....	273
8.6.7. Surface studies of the degraded tubes.....	274
8.7. Discussion.....	276
Chapter 9 Conclusions and future work	282
9.1. Conclusions.....	283
9.2. Future work	290
References	293

LIST OF FIGURES

Figure 1: Stent implantation in the narrowed artery.....	5
Figure 2: Chemical structure of rapamycin	12
Figure 3: Chemical structure of paclitaxel.....	14
Figure 4: Chemical structure of tacrolimus	15
Figure 5: Chemical structure of dexamethasone	17
Figure 6: Schematic of the arterial wall.	22
Figure 7: Schematic of the restenosis cascade lesion development.....	24
Figure 8: Mechanism of the development of the late in-stent thrombosis in the drug eluting stents in correlation to time after stent deployment	25
Figure 9: Polyhydroxyalkanoates granules inside bacterial cells.	28
Figure 10: The general structure of Polyhydroxyalkanoates.....	29
Figure 11: Biosynthesis pathways of short chain length (scl-PHA) and medium chain length (mcl-PHA) polyhydroxyalkanoates	39
Figure 12: The 5 L stirred tank bioreactor used in this study.....	70
Figure 13: 15L stirred tank bioreactor used in this study.....	71
Figure 14: 20 L stirred stainless steel tank bioreactor used in this study.	71
Figure 15: Schematic representation for the steps involved in the scl-PHAs production in using <i>Bacillus subtilis</i> OK2 and or <i>Bacillus cereus</i> SPV.....	72
Figure 16: Schematic representation for of the steps involved in the PHAs production using <i>Cupriavidus necator</i> or <i>Pseudomonas mendocina</i> CH50.	73
Figure 17: Soxhlet apparatus set up for polymer extraction.	76
Figure 18: PTL-MMB02 Millimeter Grade Desktop Programmable Dip Coater and internal chamber with prepared tubes on the mandrels.....	82
Figure 19: Temporal profile of PHA production by <i>Bacillus subtilis</i> OK2 using Kannan and Rehacek media with 35g/L of glucose as the sole carbon source.	98
Figure 20: ATR-FTIR spectrum of the polymer produced by <i>Bacillus subtilis</i> OK2 with 35g/L glucose as a carbon source.....	99
Figure 21: (A) Gas chromatogram of the polymer extracted from <i>Bacillus subtilis</i> OK2 biomass and (B) mass spectrum of a peak with Rt=4.1 min identified using NIST library as methyl ester of 3-hydroxybutyric acid.....	100
Figure 22: Gas chromatogram of reference standards of methyl esters of 3-hydroxyalkanoates.	101
Figure 23: (A) ¹ H NMR and (B) ¹³ C NMR spectra of P(3HB) confirming the polymer to be P(3HB) homopolymer.....	102
Figure 24: Molecular weight distribution and cumulative molecular weight of neat P(3HB) polymer produced using <i>Bacillus subtilis</i> OK2.....	103
Figure 25: DSC thermograms: first heating cycle and second heating cycle of P(3HB) obtained from <i>Bacillus subtilis</i> OK2 using 35g/L glucose as the sole carbon source. ..	104
Figure 26: Summary of the DSC thermograms of P(3HB) neat films during 1 week, 3 weeks, 5 weeks and 7 weeks of storage (first heating cycle).....	107

LIST OF FIGURES

Figure 27: The evolution of (A) an ultimate tensile strength, (B) elongation at break and (C) Young's modulus during 7 weeks of storage of neat P(3HB).....	109
Figure 28: ATR-FTIR spectrum of the waste frying oil used as a carbon source for mcl-PHAs production indicating the important peaks of the spectrum.....	117
Figure 29: Gas chromatogram of the composition of the waste frying oil used for mcl-PHA production as a carbon source.	118
Figure 30: Mass spectra of peaks obtained by gas chromatography of waste frying oil sample.....	119
Figure 31: (A) ^1H NMR and (B) ^{13}C NMR spectra of waste frying oil used for mcl-PHA production as the carbon source.	121
Figure 32: Temporal profile of PHA production by <i>Pseudomonas mendocina</i> CH50 using MSM medium with 20g/L of waste frying oil as a sole carbon source.....	123
Figure 33: ATR-FTIR spectrum of the polymer produced from <i>Pseudomonas mendocina</i> CH50 with 20g/L waste frying oil as a carbon source	124
Figure 34: Gas chromatogram of the polymer extracted from biomass of <i>P. mendocina</i> CH50. Methyl benzoate was used as an internal standard.	125
Figure 35: Mass spectra of peaks obtained from GC-MS of polymer obtained from <i>P. mendocina</i> and waste frying oil.	126
Figure 36: The thermal properties of the P(3HHx-3HO-3HD-3HDD) copolymer obtained from <i>P. mendocina</i> using waste frying oil as the carbon source.....	128
Figure 37: Molecular weight distribution and cumulative molecular weight of neat P(3HHx-3HO-3HD-3HDD) obtained from <i>Pseudomonas mendocina</i> CH50 using waste frying oil as the carbon source.	129
Figure 38: ATR-FTIR spectrum of the oligo-PHA after 20 hours of hydrolysis.....	141
Figure 39: Summary of thermal properties of the oligo-PHA after of hydrolysis.	142
Figure 40: Solvent cast films of: (A) P(3HB) neat film, (B) P(3HB)/oligo-PHA blend film in ratio 95/5, (C) P(3HB)/oligo-PHA blend film in ratio 90/10, (D) P(3HB)/oligo-PHA blend film in ratio 80/20	144
Figure 41: DSC thermograms of first cycle of P(3HB), oligo-PHA and P(3HB)/oligo-PHA blends (ratios: 95/5, 90/10, 80/20) aged for 7 weeks at room temperature.....	146
Figure 42: The evolution of ultimate tensile strength (A), Young's modulus (B) and elongation at break (C), during aging of neat P(3HB) and its blends with oligo-PHA...	148
Figure 43: SEM images of the neat P(3HB) film and P(3HB)/oligo-PHA blend films. ...	150
Figure 44: Surface roughness of neat P(3HB) and its blends with oligo-PHA	151
Figure 45: Static water contact angle measurements for the neat P(3HB) film and its blends with oligo-PHA (n=3; error bars= \pm SD).	152
Figure 46: Protein adsorption on the films of neat P(3HB) and its blends with oligo-PHA (n=3; error bars= \pm SD).....	153
Figure 47: Cell proliferation study of the HMEC-1 cells on the P(3HB) film and P(3HB)/oligo-PHA blend film samples at day 1, 3 and 7 (n=3; error bars= \pm SD).....	154

LIST OF FIGURES

Figure 48: SEM images of the surfaces of (A) neat P(3HB) and (B-D) P(3HB)/oligo-PHA blends in ratios: 95/5 (B), 90/10 (C), 80/20 (D) respectively after culturing HMEC-1 cells for 7 days.....	156
Figure 49: Representative confocal micrographs of live HMEC-1 cells (green) and dead HMEC-1 cells (red) on different PHA materials at day 7.	157
Figure 50: Haemolysis rates of the P(3HB) and P(3HB)/oligo-PHA blends in percent after 1h of incubation at 37°C (n=3).	158
Figure 51: Whole blood clotting after 30 minutes and 90 minutes of incubation on the neat P(3HB), P(3HB)/oligo-PHA blends and PL38 medical grade.	159
Figure 52: Flow cytometry histograms of stained fresh whole blood without any material with addition of markers (B, C) and without markers (A).	162
Figure 53: Flow cytometry histograms of stained fresh whole blood activated with LPS with two different sets of markers (A, B).	163
Figure 54: Composites of P(3HB)/oligo-PHA in ratio 90/10 with (A) 1 wt%, (B) 3 wt%, (C) 5 wt% of barium sulphate.	175
Figure 55: ATR-FTIR spectrum of the P(3HB)/oligo-PHA composites with BaSO ₄	176
Figure 56: DSC thermograms of P(3HB)/oligo-PHA blend in the ratio 90/10 and composite films with a BaSO ₄ aged for 7 weeks at room temperature.	178
Figure 57: Changes in the ultimate tensile strength (A), Young's modulus (B) and elongation at break (C), during aging of neat P(3HB)/oligo-PHA blend and its composites with BaSO ₄	180
Figure 58: SEM micrographs of surface of (A) P(3HB)/oligo-PHA blend without addition of barium sulphate, P(3HB)/oligo-PHA composite with addition of (B) 1wt%, (C) 3wt% and (D) 5wt% of barium sulphate.	182
Figure 59: Surface roughness of P(3HB)/oligo-PHA blend (90/10) and composites with BaSO ₄ (n=3; error bars=±SD).	183
Figure 60: Static water contact angle measurements of the P(3HB)/oligo-PHA in ratio 90/10 films (n=3) with different concentrations of barium sulphate	184
Figure 61: Protein adsorption to the composites measured by BCA assay.....	185
Figure 62: XRD patterns of P(3HB)/oligo-PHA 90/10 blend and composites with 1%, 3% and 5 wt% BaSO ₄	186
Figure 63: Cell proliferation study of the HMEC-1 cells on the P(3HB)/oligo-PHA composite film samples on day 1, day 3 and day 7 (n=3; error bars=±SD).	187
Figure 64: SEM images of the surfaces of P(3HB)/oligo-PHA blend 90/10 (A) and P(3HB)/oligo-PHA 90/10 composites with 1 wt% BaSO ₄ (B), 3 wt% BaSO ₄ (C) and 5 wt% BaSO ₄ (D) after culturing HMEC-1 cells for 7 days.	189
Figure 65: Indirect cytotoxicity study of the HMEC-1 cells on the P(3HB)/oligo-PHA composites film samples at day 1 and day 3 (n=3; error bars=±SD).	190
Figure 66: MicroCT micrographs demonstrated x-ray absorption by barium sulphate, presented in the concentrations: 0 wt%, 1 wt%, 3 wt% and 5 wt% in the PHAs based composites in comparison with a neat P(3HB)/oligo-PHA blend in ratio 90/10.	191

LIST OF FIGURES

Figure 67: Haemolysis rates of the P(3HB)/oligo-PHA blend and composites with barium sulphate after 1h of incubation at 37°C (n=3).....	192
Figure 68: Whole blood clotting after 30 minutes and 90 minutes of incubation on the neat P(3HB)/oligo-PHA blend 90/10, composites with 1 wt%, 3 wt% and 5 wt% barium sulphate and PL38 (n=3; error bars=±SD).	193
Figure 69: Production of PHA tubes (needle 2.54mm diameter, 78mm length) A-B prepared by using dip coating technique.....	201
Figure 70: Tubes stored for 7 weeks at room temperature, dry (Figure A) and in DMEM media incubated at 37°C (Figure B).....	202
Figure 71: DSC thermograms of P(3HB)/oligo-PHA tubes aged for 7 weeks at room temperature.	204
Figure 72: The changes of ultimate tensile strength (a), Young's modulus (b) and elongation at break (c), during aging of neat P(3HB)/oligo-PHA tubes stored at room temperature and incubated in DMEM media at 37°C for 7 weeks.	207
Figure 73: SEM images of the P(3HB)/oligo-PHA tubes.	208
Figure 74: ATR-FTIR spectrum of the P(3HB)/oligo-PHA tubes during 6 months of degradation study.	209
Figure 75: DSC thermograms of P(3HB)/oligo-PHA tubes during 6 months of degradation study (first heating cycle).	211
Figure 76: pH changes of PBS after incubation with P(3HB)/oligo-PHA tubes for 6 months (n=3).	212
Figure 77: Weight loss (%WL) by the P(3HB)/oligo-PHA tubes for a period of 6 months (n=3).	213
Figure 78: Water absorption (%WU) by the P(3HB)/oligo-PHA tubes for a period of 6 months (n=3).....	214
Figure 79: SEM micrographs of the P(3HB)/oligo-PHA tubes after 6 months of degradation study.	215
Figure 80: DSC thermogram of PCL-PEG550 neat polymer.....	216
Figure 81: ATR/FTIR spectra of neat P(3HB)/oligo-PHA 90/10 tube and P(3HB)/oligo-PHA 90/10 tube coated with monolayer of PCL-PEG550.....	218
Figure 82: DSC thermograms of P(3HB)/oligo-PHA tubes coated with PCL-PEG550 after 1 and 7 weeks of storage (first heating cycle).....	219
Figure 83: The comparison of (A) the ultimate tensile strength, (B) Young's modulus and (C) elongation at break (C) during aging of neat P(3HB)/oligo-PHA tubes and tubes with monolayer of PCL-PEG550 stored at different conditions for 7 weeks.	223
Figure 84: SEM micrographs of P(3HB)/oligo-PHA tube coated with a monolayer of PCL-PEG550.....	228
Figure 85: DSC thermograms of the P(3HB)/oligo-PHA composite tubes with 5 wt% barium sulphate after 1 week and 7 weeks of storage.	225
Figure 86: SEM micrographs of the P(3HB)/oligo-PHA composite tubes with 5 wt% barium sulphate.	227

LIST OF FIGURES

Figure 87: MicroCT micrographs demonstrated x-ray absorption by barium sulphate, presented in the P(3HB)/oligo-PHA composite tubes, containing 5 wt% BaSO ₄	228
Figure 88: Protein adsorption to the neat P(3HB)/oligo-PHA, coated with PCL-PEG550 and composite tubes measured by BCA assay (n=3; error bars=±SD).	229
Figure 89: Cell proliferation study of HMEC-1 cells on the P(3HB)/oligo-PHA neat tubes, coated with monolayer of PCL-PEG550 and composite tubes with 5 wt% barium sulphate tube samples on day 1, day 3 and 7 (n=3; error bars=±SD)..	230
Figure 90: Indirect cytotoxicity study of the HMEC-1 cells on the P(3HB)/oligo-PHA neat tubes, coated with monolayer of PCL-PEG550 and composite tubes with 5 wt% barium sulphate tube samples on day 1 and day 3 (n=3; error bars=±SD).....	231
Figure 91: M images of the surfaces of P(3HB)/oligo-PHA neat tubes (A), PCL-PEG550 coated tubes (B) and composite tubes (C) after culturing HMEC-1 cells for 7 days.....	233
Figure 92: Haemolysis rates of the P(3HB)/oligo-PHA neat tubes, tubes coated with PCL-PEG550 and composite tube with barium sulphate.....	234
Figure 93: Whole blood clotting after 30 minutes and 90 minutes of incubation on the neat P(3HB)/oligo-PHA tubes, coated with PCL-PEG550 and composite tubes with 5 wt% barium sulphate. sulphate and PL38 (n=3; error bars=±SD).	235
Figure 94: ATR/FTIR spectrum of rapamycin powder indicating characteristic peaks typical to chemical bonds observed in rapamycin.	248
Figure 95: ATR/FTIR spectrum of Tacrolimus indicating characteristic peaks typical to chemical bonds observed in tacrolimus.	249
Figure 96: DSC thermograms of rapamycin registered during first heating cycle.....	250
Figure 97: DSC thermograms of tacrolimus registered during first heating cycle.	250
Figure 98: ATR/FTIR spectra of neat P(3HB)/oligo-PHA tube with monolayer of PCL-PEG550 in comparison to P(3HB)/oligo-PHA tube with incorporated rapamycin within PCL-PEG550 coating indicating major peaks characteristic for PHA, PCL-PEG550 and rapamycin and tacrolimus.....	256
Figure 99: SEM micrographs of P(3HB)/oligo-PHA tube coated with monolayer of PCL-PEG550 with incorporated rapamycin.	254
Figure 100: SEM micrographs of P(3HB)/oligo-PHA tube coated with monolayer of PCL-PEG550 with incorporated tacrolimus.....	258
Figure 101: <i>In vitro</i> release profile of rapamycin from P(3HB)/oligo-PHA 90/10 blend tube coated with a monolayer of PCL-PEG550, for a period of 90 days.	256
Figure 102: Cumulative release of tacrolimus within 90 days of study (n=3).	257
Figure 103: Protein adsorption to the P(3HB)/oligo-PHA 90/10 blend tubes with incorporated drugs: rapamycin or tacrolimus in PCL-PEG550 polymeric matrix (n=3; error bars=±SD).	258
Figure 104: Cell proliferation study of the HMEC-1 cells on the P(3HB)/oligo-PHA tubes coated with monolayer of PCL-PEG550 with incorporated rapamycin or tacrolimus samples on day 1, 3 and 7 (n=3; error bars=±SD).	259

LIST OF FIGURES

Figure 105: SEM micrographs of the HMEC-1 cells attached to the surfaces of P(3HB)/oligo-PHA tubes containing rapamycin (A), and tacrolimus (B) after 7 days of culturing.	260
Figure 106: Indirect cytotoxicity study of the HMEC-1 cells on the P(3HB)/oligo-PHA tubes coated with monolayer of PCL-PEG550 with incorporated rapamycin or tacrolimus samples on day 1, 3 (n=3; error bars=±SD).	261
Figure 107: Haemolysis rates of the P(3HB)/oligo-PHA tubes coated with PCL-PEG550 with incorporated rapamycin or tacrolimus after 1h of incubation at 37°C (n=3).	263
Figure 108: Summary of whole blood clotting results after 30 minute and 90 minutes of incubation on the P(3HB)/oligo-PHA tubes coated with PCL-PEG550 with rapamycin or tacrolimus. Tissue culture plastic was used as the control (n=3; error bars=±SD).	264
Figure 109: ATR-FTIR spectrum of the P(3HB)/oligo-PHA tubes with rapamycin (A) and tacrolimus (B) after 3 months incubation in PBS.	267
Figure 110: DSC thermograms of P(3HB)/oligo-PHA tubes with incorporated rapamycin (A) and tacrolimus (B) during 3 months of degradation study.	269
Figure 111: pH changes of PBS after incubation of P(3HB)/oligo-PHA tubes with incorporated rapamycin or tacrolimus for 3 months (n=3).	271
Figure 112: Weight loss (%WL) of the P(3HB)/oligo-PHA tubes with incorporated rapamycin or tacrolimus for a period of 3 months (n=3).	272
Figure 113: Water absorption (%WU) by the P(3HB)/oligo-PHA tubes with incorporated rapamycin or tacrolimus for a period of 3 months (n=3).	273
Figure 114: SEM micrographs of the P(3HB)/oligo-PHA tubes with rapamycin after 3 months of degradation study.	274
Figure 115: SEM micrographs of the P(3HB)/oligo-PHA tubes with tacrolimus after 3 months of degradation study.	275

LIST OF TABLES

Table 1: Summary of material properties typical for mcl-PHA and scl-PHA.	31
Table 2: Experimental set-up for staining with different types of antibodies.	91
Table 3: Summary of the results obtained during screening experiments performed for the production of novel scl-PHA production.....	96
Table 4: Summary of molecular weight analysis of the P(3HB) obtained from <i>Bacillus subtilis</i> OK2 and glucose as the carbon source	104
Table 5: Summary of the thermal properties of the fresh P(3HB) polymer obtained using <i>B. subtilis</i> OK2.....	105
Table 6: Summary of the mechanical properties of neat P(3HB) solvent cast films without storage (n=3).	106
Table 7: Summary of the thermal properties of the P(3HB) films during 7 weeks of storage at room temperature.	106
Table 8: Summary of the mechanical properties of the P(3HB) solvent cast films during 7 weeks of storage at room temperature (n=3).....	108
Table 9: Summary of the screening experiments used for the production of mcl-PHAs by <i>Pseudomonas mendocina</i> CH50 using various carbon sources.....	116
Table 10: Fatty acids composition (mol %) of waste frying oil used for mcl-PHA production.....	120
Table 11: The summary of the chemical shifts observed in ¹ H NMR of the fatty acids presented in the waste frying oil.....	122
Table 12: The summary of the chemical shifts observed in ¹³ C NMR spectrum of the fatty acids presented in the waste frying oil.....	122
Table 13: Monomer composition mcl-PHA synthesised by <i>P. mendocina</i> with waste frying oil as a carbon source.....	127
Table 14: Summary of the thermal properties of the P(3HHx-3HO-3HD-3HDD) copolymer obtained from <i>P. mendocina</i> using waste frying oil as the carbon source.....	128
Table 15: Summary of molecular weight analysis of the P(3HHx-3HO-3HD-3HDD) obtained from <i>Pseudomonas mendocina</i> CH50 using waste frying oil as the carbon source.....	129
Table 16: Summary of hydrolysis kinetics of P(3HHx-3HO-3HD-3HDD) copolymer.....	140
Table 17: Thermal properties of the oligo-PHA after 20 hours of hydrolysis.....	142
Table 18: Summary of molecular weight analysis of the P(3HHx-3HO-3HD-3HDD) obtained from <i>Pseudomonas mendocina</i> CH50 and waste frying oil as the carbon source after 2 hours of hydrolysis.....	143
Table 19: Summary of the thermal analysis of P(3HB)/hydrolysed P(3HHx-3HO-3HD-3HDD) blends during 7 weeks of storage.	145
Table 20: Summary of the mechanical properties of P(3HB)/oligo-PHA blends during 7 weeks of storage (n=3).....	147
Table 21: Summary of median fluorescence intensity (MFI) obtained after incubation of fresh whole blood incubated with neat P(3HB), P(3HB)/oligo-PHA blends in ratios: 95/5,	

LIST OF TABLES

90/10, 80/20 PHAs and PL38 and stained with specific markers in order to evaluate monocyte and neutrophil activity.	161
Table 22: Summary of median fluorescence intensity (MFI) obtained after incubation of fresh whole blood activated with LPS and stained with specific markers in order to evaluate monocyte and neutrophil activity.	163
Table 23: Summary of median fluorescence intensity (MFI) obtained after incubation of fresh whole blood incubated with neat P(3HB), P(3HB)/oligo-PHA blends in ratios: 95/5, 90/10, 80/20 PHAs and PL38; and stained with specific markers in order to evaluate monocyte and neutrophil activity.	164
Table 24: Summary of the thermal properties of the P(3HB)/oligo-PHA composites with 1,3 and 5 wt% barium sulphate during 7 weeks of storage.	177
Table 25: Summary of the mechanical properties of the P(3HB)/oligo-PHA composites with 1,3 and 5 wt% barium sulphate during 7 weeks of storage at room temperature (n=3).	179
Table 26: Summary of median fluorescence intensity (MFI) obtained after incubation of fresh whole blood incubated with P(3HB)/oligo-PHA blend 90/10, P(3HB)/oligo-PHA composites with 1% wt, 3% wt and 5% wt barium sulphate and PL38; stained with specific markers in order to evaluate monocyte and neutrophil activity.	194
Table 27: Summary of the thermal properties of the P(3HB)/oligo-PHA tubes during 7 weeks of storage.	203
Table 28: Summary of the mechanical properties of the P(3HB)/oligo-PHA tubes during 7 weeks of storage at room temperature.	205
Table 29: Summary of the mechanical properties of the P(3HB)/oligo-PHA tubes during 7 weeks of storage in DMEM media at 37° C for 7 weeks.	206
Table 30: Summary of the thermal properties of the P(3HB)/oligo-PHA tubes during 6 months of degradation study.	210
Table 31: Summary of the thermal properties of the P(3HB)/oligo-PHA tubes coated with PCL-PEG550 after 1 and 7 weeks of storage.	219
Table 32: Summary of the mechanical properties of the P(3HB)/oligo-PHA tubes coated with PCL-PEG550 after 1 and 7 weeks of storage (n=3).	220
Table 33: Summary of the thermal properties of the P(3HB)/oligo-PHA composite tubes with 5 wt% barium sulphate after 1 and 7 weeks of storage.	224
Table 34: Summary of the mechanical properties of the P(3HB)/oligo-PHA composite tubes with 5 wt% barium sulphate after 1 and 7 weeks of storage (n=3).	225
Table 35: Summary of median fluorescence intensity (MFI) obtained after incubation of fresh whole blood with P(3HB)/oligo-PHA 90/10 neat tube, P(3HB)/oligo-PHA 90/10 tube coated with PCL-PEG550, P(3HB)/oligo-PHA composite tube with 5% wt barium sulphate and PL38; and stained with specific markers in order to evaluate monocyte and neutrophil activity.	237
Table 36: Dimensions of tubes produced using P(3HB)/oligo-PHA blend coated with PCL-PEG550 with incorporated drug.	251

LIST OF TABLES

Table 37: Summary of median fluorescence intensity (MFI) obtained after incubation of fresh whole blood with P(3HB)/oligo-PHA 90/10 tube coated with PCL-PEG550, P(3HB)/oligo-PHA tube coated with PCL-PEG550 with incorporated rapamycin or tacrolimus and PL38 stained with specific markers in order to evaluate monocyte and neutrophil activity.	265
Table 38: Summary of the thermal properties of the P(3HB)/oligo-PHA tubes containing rapamycin or tacrolimus after 3 months of degradation study.	268
Table 39: Summary of the mechanical properties of the P(3HB)/oligo-PHA tubes with rapamycin or tacrolimus during month 1, 2 and 3 of the degradation study.	270

LIST OF ABBREVIATIONS

PCI: Percutaneous Coronary Intervention
CABG: Coronary Artery Bypass Grafting
BMS: Bare metallic stent
DES: Drug eluting stent
FBR: Foreign body reaction
TE: Tissue Engineering
FDA: United States Food and Drug Administration
SMC: Smooth Muscle Cells
NPs: Nanoparticles
PHA: Polyhydroxyalkanoates
PDLLA: Poly(-D,L-lactic acid)
L-PLCL: Poly(L-lactide-co-caprolactone)
PGA: Poly(glycolic acid)
PLA: Poly(lactic acid)
PLLA: Poly(L-lactic) acid
TCP: Tissue Culture Plastic
PCL: Poly(ϵ -caprolactone)
Scl-PHA: Short chain length polyhydroxyalkanoate
Mcl-PHA: Medium chain length polyhydroxyalkanoate
P(3HB): Poly(3-hydroxybutyrate)
P(3HB-co-3HV): Poly(3-hydroxybutyrate-co-3-hydroxyvalerate)
P(4HB): Poly(4-hydroxybutyrate)
P(3HB-co-4HB): Poly(3-hydroxybutyrate-co-4-hydroxybutyrate)
P(3HB-co-3HHx): Poly(3-hydroxybutyrate-co-3-hydroxyhexanoate)
P(3HO-co-3HHx): Poly(3-hydroxyoctanoate-co-3-hydroxyhexanoate)
P(3HB-co-3HO): Poly(3-hydroxybutyrate-co-3-hydroxyoctanoate)
P(3HO-co-3HD): Poly(3-hydroxyoctanoate-co-3-hydroxydecanoate)
P(3HO-co-3HD-co-3HDD): Poly(3-hydroxyoctanoate-co-3-hydroxydecanoate-co-3-hydroxydodecanoate)
P(3HV): Poly(3-hydroxyvalerate)
P(3HHx-co-3HO-co-3HD-co-3HDD): Poly(3-hydroxyhexanoate-co-3-hydroxyoctanoate-co-3-hydroxydecanoate-co-3-hydroxydodecanoate)
Scl-mcl-PHA: Short chain length-medium chain length polyhydroxyalkanoate
PEG: Polyethylene glycol
PVA: Poly(vinyl alcohol)
CoA: Coenzyme A
MSM: Mineral Salt Medium
OD: Optical Density
DOT: Dissolved Oxygen Tension
GC: Gas Chromatography
GC-MS: Gas Chromatography- Mass Spectrometry
SEM: Scanning electron microscopy
HPLC: High Performance Liquid Chromatography
XRD: X-ray diffraction
FTIR: Fourier Transform Infrared Spectroscopy

LIST OF ABBREVIATIONS

NMR: Nuclear magnetic resonance
DSC: Differential scanning calorimetry
LPS: Lipopolysaccharides
PBS: Phosphate buffer saline
DMEM: Dulbecco's modified Eagle's medium
FBS: Foetal Bovine Serum
MTT: (3-(4,5-Dimethylthiazol-2-yl)-2,5 diphenyltetrazolium bromide
SD: Standard deviation
wt%: Weight percent
 M_n : Average molecular weight
 M_w : Weight average molecular weight
%WU: Water absorption
% WL: Weight loss
C/N: Carbon to nitrogen ratio
 R_t : Retention time
mL: Millilitre
ppm: Parts per million
rpm: Revolutions per minute
mM: Milimolar
 T_g : Glass transition temperature
 T_m : Melting temperature
 T_c : Crystallisation temperature
PDI: Polydispersity index
TS: Tensile strength
 ΔH_f : Enthalpy of fusion
 X_c : Degree of crystallinity
Dcw: Dry cell weight
 R_q : Root mean square
PLGA: Poly(lactic-co-glycolic acid)
BVS: Bioresorbable vascular stent
mTOR: Mechanistic target of rapamycin
PCL-PEG550: Poly(caprolactone-ethylene glycol)– 550
PVP: Poly(vinylpyrrolidone)
MRI: Magnetic Resonance Imaging
PDS: Polydioxanone
SDS: Sodium dodecyl sulphate
HMEC-1: Human microvascular endothelial cells
HaCaT: Immortalized human keratinocytes
MicroCT: Micro computed tomography
EGCG: Epigallocatechin-3-O-gallate

Chapter 1

Introduction

1.1. Coronary artery disease

Coronary artery disease (CAD) is the most important contributor to the mortality and economic burden associated with cardiovascular disease (CVD). CVD is leading cause of death worldwide. In United Kingdom, the mortality due to cardiovascular disease has been placed right after cancer. In 2015 in UK over 158,000 deaths were caused by cardiovascular disease, which is equivalent to 27.4% of all deaths in men and 25.2% in women (BHF statistics, 2017). Only in European Union, cardiovascular disease costs 210 billion euros per year (European Cardiovascular Disease Statistics, 2017). CAD is caused by the deposition of plaque in the coronary artery which results in reduced blood flow and nutrient supply to the heart (Hirase and Node, 2012). This might lead to heart attack, clot formation or stroke. The main risk factors include: high blood pressure, smoking, diabetes, obesity, hypercholesterolemia and sedentary lifestyle (Hamrefors, 2017; Yusuf *et al.*, 2004).

The first successful surgical treatment of coronary artery disease was performed using coronary artery bypass grafting (CABG) in 1960s. This procedure included grafting of a small fragment of an artery taken, usually from another part of the body around the blocked artery to restore blood supply to the heart (Choi *et al.*, 2009). In 1977, the first balloon angioplasty was performed by Grüntzig (Grüntzig *et al.*, 1979). The technique involved placement of a deflated balloon in the narrowed vessel followed by inflation, which resulted in the compression of the plaque towards the vessel walls, hence opening up the artery. In 1987, the first coronary artery stent was implanted by Sigwart and co-workers (Sigwart *et al.*, 1987). The coronary artery stent was designed to provide mechanical support to the vessel wall, which facilitated the opening of the artery and prevented any further narrowing (Nazneen *et al.*, 2012).

Currently CAD treatments require percutaneous coronary intervention (PCI), which involves balloon angioplasty and stent implantation (Iqbal *et al.*, 2013). Only in United Kingdom, 97,376 PCIs were performed in 2015, which is 60% an increase in comparison to 2001. At present, over 80% of cardiovascular interventions in UK involve stent deployment, out of which 85.7% use drug eluting stents (DES) (Ludman *et al.*, NAPCI report, 2015; Sun *et al.*, 2014).

1.2. Coronary stents

Coronary stents are medical devices, which are delivered to the artery in the collapsed form and inflated inside narrowed blood vessel. This results in compressing plaque against the artery wall and restore the normal blood flow (Grabow *et al.*, 2010). It is very important to understand that coronary stent does not act as a tissue engineering scaffold (TES). The main function of stent is to widen and support the narrowed artery, whereas, the main role of tissue engineering scaffold is to repair, replace or regenerate damaged or injured tissues or organs. Tissue engineering scaffold approach requires combination of three main elements, such as biomaterial 3D scaffold, seeded with cells with or without addition of bioactive agents, such as growth factors, in order to simulate body environment, allow cell attachment and new tissue development (O'Brien, 2011; Chan and Leong, 2008). Coronary stents require only suitable material, which will mechanically support blood vessel during natural healing of the artery injured during angioplasty and stent deployment (Waksman, 2006). However, high biocompatibility, non-toxicity, thromboresistance, suitable mechanical properties, are expected from materials considered for stent application as well as TE scaffolds. Additionally, stents can be used as local drug delivery vehicles in order to release drugs and reduce the risk of restenosis, a side effect, associated with stent deployment (Regar *et al.*, 2001), which will be described in details in section 1.5.

Stents are meshed tubular 3D structures, made from metals or polymers. Over 100 types of stents are available in the market, mainly for vascular lesions (Stoeckel *et al.*, 2002). Coronary stent dimensions are designed to have length between 8mm to 38mm and diameter from 2mm to 4mm (Borovetz *et al.*, 2004). Materials for stent manufacturing can be formed into wires, sheets or tubes. The techniques used for stent production are: laser cutting, electrode discharge machining, waterjet-cutting, photochemical etching from tubing, braiding and knitting (Kathuria, 2006; Stoeckel *et al.*, 2002). Coronary stents are known to reduce some major side effects of balloon angioplasty, such as re-narrowing of the artery caused either by reforming of the blockage or new tissue formation (Takayama *et al.*, 2011). Currently available stents can be divided into three main groups: bare metal stents (BMS), drug-eluting stents (DES) and bioresorbable vascular stents (BVS) (Iqbal *et al.*, 2013).

1.2.1. Bare metallic stents

The stents that were initially developed had very high metallic density, resulting in a high incidence of stent thrombosis; accompanied by failure in deployment and embolization (Serruys *et al.*, 1991). Although, stents reduced the risk of restenosis compared to plain balloon angioplasty, there was still a significant risk of in-stent restenosis, which could be associated with high morbidity and mortality. Application of bare metallic stents after balloon angioplasty has eliminated vessel elastic recoil and negative remodelling, which resulted in a significant reduction of restenosis from 30-50% to 20% (Lowe *et al.*, 2002). Stents are delivered to the vessel on a catheter through a guide wire and expanded restoring normal blood flow to the heart (Figure 1). Considering the type of deployment stents can be divided into: balloon-expandable or self-expandable. Depending on the type of expansion, stents require different material properties. For example, self-expanding stents need to have low elastic modulus and high yield stress, due to the specific manufacturing diameters, which should be larger than the diameter of the target structure. Balloon expandable stents must be able to maintain expanded shape and used materials require low yield stress. Therefore, for a balloon expandable stent, 316L stainless steel is the most common choice due to its excellent mechanical properties. However, due to its limited biocompatibility and ferromagnetic properties, other non-corrosive materials have been considered, such as platinum-iridium alloy, tantalum, cobalt-chromium alloy, and titanium (Zahora *et al.*, 2007). For self-expanding stents Nitinol, a nickel-titanium alloy has been widely used because of material shape memory and high elasticity, which allows stent self-expansion during deployment (Barras and Myers, 2000). The drawback of this material is the high risk of immunogenic response due to Ni ions release from the alloy (Shabalovskaya, 1996).

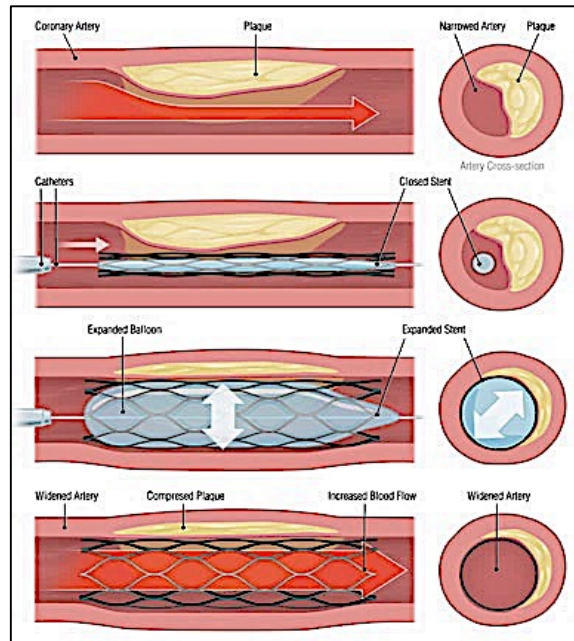


Figure 1: Stent implantation in the narrowed artery. (Source: National Heart, Blood and Lung Institute <https://www.nhlbi.nih.gov/health/health-topics/topics/stents>).

The coronary artery stent is considered as a foreign body; hence there is an inflammatory response triggered by the immune system (Jamshidi *et al.*, 2008). The inflammatory response is a response of the body environment to the injury and implanted material or prosthesis. Usually it involves series of events, including blood-material interaction, acute inflammation, chronic inflammation, foreign body reaction and fibrous capsule development (Anderson *et al.*, 2001). Immediately after contact of biomaterial with tissues and blood, proteins adsorb on the surface of the material and mediate thrombus and provisional matrix formation. This matrix consists mainly fibrin and products released by activated platelets, inflammatory cells and endothelial cells. Acute inflammation occurs within minutes to days after injury. Usually it involves blood proteins infiltration and leukocytes migration from the blood vessel to the site of the injury, followed by neutrophils and monocytes activation. Acute inflammation is dominated by presence of neutrophils, which normally destroy microorganisms and degrades foreign body. However, due to the difference in size between an implant and neutrophils cell, “frustrated phagocytosis” event may occur. This process involves production of free oxygen radicals and lysozyme proteases by leukocytes with an intention to degrade the biomaterial. Neutrophils have very short life span, therefore they are replaced by monocytes, macrophages and lymphocytes, which are

determinants of chronic inflammation, followed by foreign body reaction (FBR) (Anderson *et al.*, 2008). FBR consists an accumulation of macrophages and foreign body giant cells, which may remain for the lifetime of the implant. The last phase of the body response to biomaterials is fibrosis or fibrous encapsulation, which decreases the efficiency of an implant and may leads to its failure (Bryers *et al.*, 2012). Therefore, novel materials are being explored for the production of stents with improved properties, such as higher biocompatibility, greater mechanical strength and tailorable biodegradability (Williams and Martin, 2005).

1.2.2. Drug-eluting stents (DES)

Drug-eluting stents (DES) were developed to reduce or totally eliminate the side effects associated with the application of metallic stents, especially restenosis (Gogas *et al.*, 2012). Drug eluting stents reduced the restenosis rate from 40% to 5%. DES are metallic stents coated with a polymer layer containing drugs, capable of releasing one or more bioactive substance into the blood stream and surrounding tissue. Development of the DES significantly diminished the use of bypass surgery as a treatment of restenosis, which is one of the long-term side effects after stent deployment (Moses *et al.*, 2003). A wide range of different materials and drugs have been tested.

The drug eluting stents have several advantages. The active agents may be delivered directly to a target site in a suitable therapeutic dose, preventing the risk of restenosis and reducing the toxic effects of the systemic delivery of the same drug at higher concentration (Acharya and Park, 2006). The use of DES has been widened from coronary interventions to bifurcation lesions, complex lesions, inlet main trunk and multivessel disease. However, late stent thrombosis has become an issue associated with this type of devices (McFadden *et al.*, 2004).

DES reduced the restenosis rate to up to 10% by the inhibiting effect of drugs on proliferation of vascular smooth muscle cells. Although the restenosis rate was reduced, presence of drugs usually impeded the normal healing process by inhibiting proliferation of endothelial cells. This may lead to a high risk of late thrombosis and require dual antiplatelet therapy (Morice *et al.*, 2002). Moreover, the polymer in the coating layer can cause inflammatory response and hypersensitivity reactions (i.e. dyspnea, rash,

hives, fever), which can lead to myocardial infarction and sudden death (Nebeker *et al.*, 2006; Iakovou and Colombo, 2005).

Development of coronary artery stents was a huge achievement in the invasive cardiology. However, both, bare metallic stents as well as drug eluting stents still have their limitations. Both types of stents provided support to the arterial wall. However, in the long-term perspective, presence of a metallic scaffold in the artery resulted in the development of side effects, such as in stent restenosis and late thrombosis (described in the section 1.5.). Therefore, there was need for a novel solution, which can overcome the limitations of the previous generations of the coronary stents. This is how the concept of biodegradable stents appeared.

1.2.3. Biodegradable stents

The main role of the stent is to provide a mechanical support to the arterial walls until the vessel heals, which is between 6 to 12 months. After this, a permanent implant is not needed. Therefore, the concept of biodegradable stents was introduced that perform their function and then slowly disappear within 18 months. The main advantages of biodegradable stents are: shorter dual-antiplatelet therapy, which reduces the risk of bleeding, no need for surgical removal, absence of a foreign body in the long run reducing the potential inflammatory response and enhances the natural healing process of the artery wall (Waksman, 2006). Arterial wall is very sensitive towards mechanical injury. Only touching with catheter is sufficient to damage the endothelial layer, which results in cell detachment and death of endothelial cells. This causes immediate healing response by platelets adhesion and thrombus formation in order to cover and protect injured place. Healing process is supported by smooth muscle cells proliferation leading to the reconstruction of the arterial wall (Van Erven *et al.*, 1991). Although biodegradable stents were introduced around 20 years ago, most of them have failed during preclinical evaluation (Sun *et al.*, 2014). The polymeric biodegradable stents, which disappear slowly after implantation, are hence promising novel stent technologies that can be loaded with various types of drugs or multiple agents (Peng *et al.*, 1996; Mani *et al.*, 2007). A fully biodegradable coronary stent should meet certain criteria. The stent material as well as its degradation products must be biocompatible. The structural integrity of the stent must be maintained for at least 6

months and full degradation should occur within 18 months. The degradation of the scaffold must not result in the release of large pieces of degraded material into the lumen. The stent must be introduced into the vessel by balloon or self-expansion. The stent must not move after deployment and be equipped with radiopaque markers for safe monitoring (Venkatraman *et al.*, 2008). Hence, many different biomaterials can act as potential platforms for biodegradable coronary artery stents. To date polymers as well as biodegradable metals have been considered. Many different polymers have been investigated, such as poly(L-lactic acid) (PLLA), poly(D,L-lactic acid) (PDLLA) and poly(lactic-co-glycolic acid) (PLGA). However, there have been some concerns related to their immunogenic response and unsuitable mechanical properties (Van der Giessen *et al.*, 1996). Polymers are pliable to deformation. They might require special storage conditions, like for example very low temperatures in order to avoid aging of the material (Waksman and Pakala, 2010). Polymers are not radiopaque in nature, which requires an addition of contrast agents or radiopaque markers. All these properties make the use of polymers as a base material for coronary stent a very challenging application (Agrawal *et al.*, 1992). Many studies have been performed towards overcoming these limitations.

Apart from polymers, some metals, such as magnesium and iron are also being considered for biodegradable coronary stents. Biodegradable metals have exceeded the mechanical properties of the polymers and can be more comparable to stainless steel (SS316L) used as a standard material for coronary stent application (Balcon *et al.*, 1997). The good biocompatibility of magnesium makes it a potential target material for this application. However, it is very unstable in body fluids, which accelerates the degradation. Moreover, the degradation profile of neat magnesium is not suitable for coronary stents. It undergoes rapid degradation, which results in the loss of mechanical stability of the scaffold before the end of the arterial remodelling process. Therefore, alloys of magnesium with other metals, such as aluminium or yttrium with rare earth elements have been developed (Waksman *et al.*, 2009). The results of the clinical trials demonstrated clinical safety of magnesium stents. Struts were not present after 4 months. However, radial strength was lost much earlier and was insufficient to prevent the negative remodelling associated with Percutaneous Coronary Intervention (PCI)

(Erbel *et al.*, 2002). High level of restenosis (around 50%) was observed after 4 months due to the lack of incorporation of any antiproliferative drug. After 1 year, the targeted revascularisation level was only at 45%. This required further improvements, such as increased degradation time and incorporation of drugs. One of the options was to apply a coating with biopolymeric layer, which would decrease the degradation rate of the magnesium alloys as well as can be a matrix for bioactive agents, which can prevent the development of restenosis. Such a stent, AMS-3 Mg alloy, produced by Biotronik, was coated with PLGA containing paclitaxel. Animal studies demonstrated presence of the stent after 4 months. Further improvement was obtained by addition of rare earth elements or other metals, such as calcium, zirconium and lithium. Bioabsorbable stents, containing magnesium and zinc (Zn), calcium (Ca), yttrium (Y) and manganese (Mn) demonstrated improved corrosion resistance in simulated body fluid, promising degradation profile and high biological response in animal models (Hänzi *et al.*, 2010).

Iron is another possible metal considered for stent application, due to its good mechanical properties and high biocompatibility. The first iron-based stent demonstrated promising results (Peuster *et al.*, 2001). The stents were able to provide mechanical support during the remodelling process and beyond. High biocompatibility was maintained. The degradation or corrosion products were non-toxic and did not trigger any inflammatory response. However, the major problem were ferromagnetic properties, which interfere with magnetic resonance imaging during stent deployment (Ramadugu *et al.*, 2016) and very slow degradation rate in the body, which weakened the potential of pure iron to become the perfect material for biodegradable coronary stent development (Peuster *et al.*, 2006). Therefore, iron alloys have been developed to speed up the degradation rate and improve the properties of the material. For example, addition of 20-35% of Mn within the alloy resulted in similar mechanical properties to stainless steel (Hermawan *et al.*, 2008). The *in vitro* degradation rate was 2 times higher, but still insufficient to meet the requirement for an ideal material, i.e. material for coronary stent should be stable for the first 6 months and completely degrade within 18-24 months. There is a lack of results from *in vivo* study on this alloy, which could confirm long-term safety and performance under physiological conditions (Hermawan *et al.*, 2010). Another approach to improve the degradation rate of the iron was

modification of the iron structure using an electroforming process. Obtained material demonstrated more minor microstructure, which resulted in more efficient degradation of the material (Moravej *et al.*, 2010a; Moravej *et al.*, 2010b). Although, concept of biodegradable stent could be an ideal solution for treatment of coronary artery disease, the ideal biomaterial has not been found yet.

1.2.3.1. Absorb Bioresorbable Vascular Scaffold (BVS)

Absorb is the first commercially available fully biodegradable polymeric coronary artery stent, which has been approved by the U.S. Food and Drug Administration (FDA) in 2016. It is made from poly-L-lactic acid (PLA) coated with a layer of poly-D,L-lactic acid (PDLLA). Complete degradation of this scaffold occurs within three years (Okamura *et al.*, 2010). The clinical trial data demonstrated normal functionality of the treated vessels after complete stent disappearance. It contains $100\mu\text{g}/\text{cm}^2$ of everolimus to prevent restenosis. The coating properties allow 80% drug release within 30 days after implantation. The strut thickness is $150\mu\text{m}$ (Ormiston *et al.*, 2008). Polymers are not radiopaque; therefore, platinum markers have been incorporated within the scaffold of the Absorb stent, which allows imaging and monitoring under X-ray (Gogas *et al.*, 2012). After preliminary data, the design of the stent was changed to zigzag segments connected with bridges, to achieve uniform strut distribution and enhanced radial strength and support to the vessel wall (Serruys *et al.*, 2012). PLLA degrades by hydrolysis to the corresponding oligomers, metabolised by the Krebs cycle. Lactic acid is converted to pyruvate and transformed by decarboxylation and oxidation to acetyl-CoA, which can enter Krebs cycle and be eliminated from the body. During first three months of drug release after the stent implantation, revascularisation takes place. Within this time frame, the antiproliferative drug is completely released and radial strength is maintained. Revascularisation is followed by the restoration phase, when hydrolysis of PLLA occurs and entire stent structure becomes unstable. Radial strength decreased steadily and within 6 months neointima covered almost 100% of the struts. After 6 months a resorption phase occurred, where the remaining part of the scaffold was absorbed slowly (Oberhauser *et al.*, 2009). The most significant weight loss was observed between 12 and 15 months (Prabhu and Hossainy, 2006). After stent degradation, the platinum markers remained integrated in the arterial wall and marked

the original site of implantation. Currently, Abbott biodegradable stent, known under the name Absorb GT1 BVS is available in 100 countries. Initial outcomes from clinical trials are similar to the Abbott Xience metallic drug eluting stent. Possible side effects can be related to the device, such as an allergic reaction to the stent material, the drug everolimus, platinum marker or procedure related problems, such as internal bleeding, irritation or infection at the catheter site. Absorb cannot be used for patients with known allergy to PLA or platinum or those that are not able to take aspirin with other antiplatelet agents for an extended period of time. There is still lack of information about clinical performance of the device and its long-term outcomes. This along with device delivery issue and high cost has confined the application of Absorb in the European market (Lu *et al.*, 2016). Absorb BVS revision 1.1 is the second version of the Absorb GT1 BVS, FDA approved. The major improvements in this device were related to the scaffold design. The in-phase zigzag segments linked by bridges replaced the out-of-phase zigzag segments present in the design of the Absorb GT1 BVS. This resulted in the prolonged radial support to the vessel walls. Although second generation of the bioresorbable stent demonstrated improvement in the functionality in the body, it has still some limitations. The most important drawback is related to the rapid ageing of the material, which requires storage at -20°C and the shelf life of the device is only 3 months. Also, expansion of the stent beyond 0.5 mm results in strut fractures. In addition, it cannot be implanted to treat hard-calcified lesions. PLLA degrades to highly acidic products, which can trigger inflammatory response and has poor surface characteristics preventing complete endothelialisation. Surgeons require special training before they are able to carry out the stent deployment procedure. Additionally, Absorb stent is much more expensive in comparison to commonly used bare metallic stents (Gogas *et al.*, 2014).

1.3. Drugs used in drug eluting stents

Drug eluting stents were designed to prevent restenosis, the most common complication after balloon angioplasty. Considering the mechanism of the development of restenosis, a few classes of drugs were proposed. Those included: immunosuppressive, anti-inflammatory, antithrombogenic and anti-proliferative drugs.

Additionally, some research groups are focused on the addition of antibodies, such as anti-CD34 or antiplatelet GPIIb/IIIa as bioactive compounds (Deconinck *et al.*, 2008).

1.3.1. Rapamycin and its analogues

Rapamycin, also known as sirolimus belongs to the group of natural macrolides, which demonstrates immunosuppressive properties (Figure 2). It was isolated in 1975 from *Streptomyces hygroscopicus*. Rapamycin obtained FDA approval in 1999 for application to prevent renal transplant rejection. Few other analogues of rapamycin have been developed, such as everolimus, biolimus-A9 and temrapamycin (Costa and Simon, 2005).

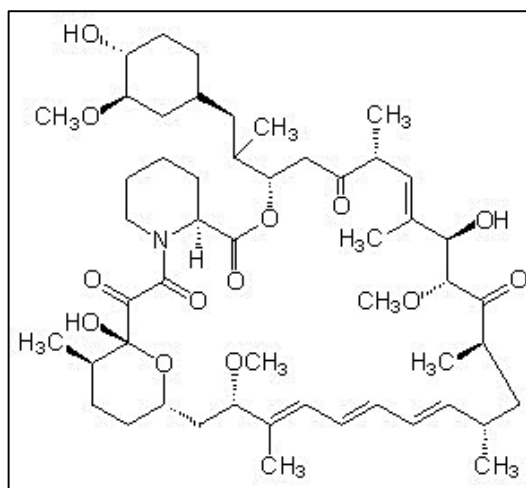


Figure 2: Chemical structure of rapamycin (Pan *et al.*, 2009).

Rapamycin has a form of pro-drug, which can bind to specific proteins, such as 12kDa FK506 binding protein (known as FKBP-12), present in the cytoplasmic matrix (Li *et al.*, 2014). Rapamycin is a hydrophobic drug with low solubility in aqueous solutions. It has lipophilic properties and hence can pass through cell membranes.

Rapamycin inhibits DNA synthesis, by binding to the receptor cytosolic FK-506 binding protein-12 (FKBP12). This is 12kDa in size, which catalyses peptidyl-prolyl cis-trans isomerization. FKBP12 protein is upregulated in neointimal smooth muscle cells (Sabatini *et al.*, 1994). A complex of FKBP12 and rapamycin attaches to the mechanistic target of rapamycin (mTOR) and inhibits its activation. mTOR is a serine-threonine kinase, a protein that regulates cell growth and proliferation, protein synthesis and transcription in the cell cycle. Binding of rapamycin to mTOR is controlled by a raptor, which is a regulatory protein associated with TOR (Schmelzle and Hall, 2000). The actual

mechanism of the inhibiting effect of rapamycin on mTOR at the molecular level is not yet fully understood. The mTOR participates in the transition between, G1 and S phase, connected with DNA replication. It has been observed that rapamycin arrests the cell cycle towards the G1 phase (Braun-Dullaues *et al.*, 1999).

During *in vitro* study, it was found that rapamycin at a concentration 1 ng/mL, inhibited DNA synthesis and cell growth (Marx *et al.*, 1995). In porcine animal model rapamycin stopped restenosis in coronary arteries after angioplasty. Hence, application of Rapamycin resulted in a meaningful reduction in coronary stenosis (Gallo *et al.*, 1999). Metallic stents coated with the nonerodable polymeric matrix with incorporated rapamycin were investigated *in vivo*. It was found that a high dose of rapamycin reduced neointimal formation by 45% in comparison to the control after 28 days (Klugherz *et al.*, 2000). Another study was performed on the porcine model with stainless steel stents coated with a polymeric layer containing rapamycin. The results obtained demonstrated 30% reduction of late in-stent restenosis in comparison to the uncoated stent (Carter *et al.*, 2006). It was reported that long-term systemic treatment with rapamycin after kidney transplantation may give serious adverse effects, such as hypercholesterolemia and hypertriglyceridemia (Morrisett *et al.*, 2002; Brattstrom *et al.*, 1998). Different animals react differently after systemic treatment with rapamycin (Collier *et al.*, 1990). However, none of the side effects listed above were observed after stent implantation (Oberhoff *et al.*, 2002).

Zotarolimus and everolimus are analogues of rapamycin. They demonstrated similar therapeutic activity like rapamycin. Rapamycin analogues were developed in order to improve the hydrophilic properties of the drug, which allows oral and intravenous drug administration. They bind to cytosolic FK-506 binding protein-12 and inhibit the proliferation of smooth muscle cells and T-cells (Kar *et al.*, 2003). Three different zotarolimus eluting stents were studied during clinical trials: Prefer stent, Endeavour stent and zotarolimus-eluting stent, named ZoMaxx™. They were compared with Cypher™ stent loaded with rapamycin. The results were satisfactory (Serruys *et al.*, 2006). No significant differences were observed in comparison to the Cypher™ stent (Kandzari and Leon, 2006). Also, several everolimus stents were studied. The bioactive agent was incorporated within Polylactic acid, PLA and added as an outside monolayer on the metallic stent. The results suggested that the stents containing everolimus were

more efficient in the prevention of restenosis than bare metallic stents (Grube *et al.*, 2004). Overall, rapamycin as well as its analogues efficiently reduced the risk of development of in-stent restenosis (Silber, 2005).

1.3.2. Paclitaxel

Paclitaxel, also known as Taxol was isolated in 1971 from the yew tree, *Taxus brivifolia* (Wani *et al.*, 1971). It belongs to the group of diterpenoids, containing a complex taxane ring in the centre. The side chain bonded to the taxane ring at carbon number 13 and is essential for its antitumor activity (Figure 3). Modification of the side chain (Figure 3) has resulted in the development of the paclitaxel analogue, named docetaxel. The modifications include presence of the hydroxyl group on carbon number 10 and tert-butyl carbamate ester on the side chain in comparison to the acetate group and benzamide present in the paclitaxel (Żwawiak and Zaprutko, 2014).

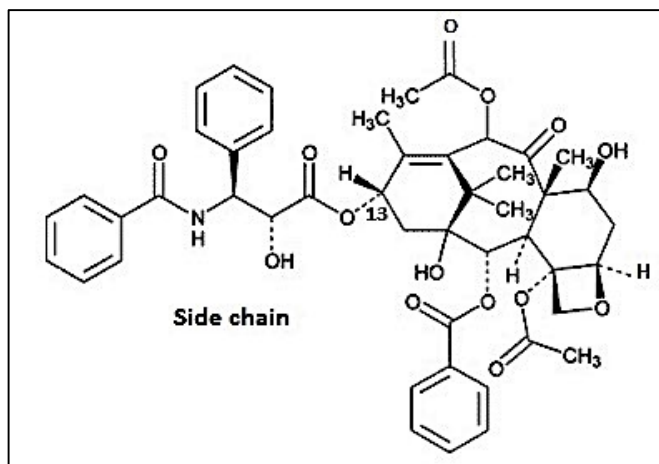


Figure 3: Chemical structure of paclitaxel (Ringel and Horwitz, 1991).

Currently, paclitaxel can be obtained by a semi synthetic process using 10-desacetylbaccatin, which is a precursor found in yew leaves (Nicolaou *et al.*, 1994). One of the drawbacks of this drug is its limited solubility. Therefore, it has to be delivered using a mixture of ethanol and polyethoxylated castor, in ratio 1:1, which may cause reactions of hypersensitivity. Paclitaxel as well as its analogues act as mitotic inhibitors. These drugs are mainly used in the treatment of ovarian, breast, lung, head, bladder, neck and eosophageal cancer (Seidman, 1998). Paclitaxel is one of the cytoskeletal drugs, which specifically binds to the β -tubulin subunit in the microtubules. This results in accelerated accumulation of the microtubules and its derivatives in the mitotic phase

of the cell cycle. This can either trigger cell apoptosis or a return to the G phase without cell division (Rowinsky and Donehower, 1995). Paclitaxel is thus able to disrupt cellular proliferation and migration. Additionally, it has immunomodulatory properties, due to its capacity to induce IL-12 production, which supports immune dysfunctions caused by the tumour (Farb, 2001). Animal models have demonstrated that paclitaxel at a concentration 200 μg per stent reduced neointimal and endothelial cell proliferation up to 180 days. However, the arteries showed incomplete healing (Drachman *et al.*, 2000). Another clinical trial, investigated polymer-free stainless steel stents, containing 2-3 $\mu\text{g}/\text{mm}^2$ of paclitaxel, adhered to the stent surface and demonstrated ordinary antirestenosis effect (Gershlick *et al.*, 2004).

1.3.3. Tacrolimus

Tacrolimus (FK506) (Figure 4) belongs to the group of macrolide lactones, which was isolated from the bacterial strain *Streptomyces tsukubaensis* (Tanaka and Marusawa, 1987). It was applied as an immunosuppressive agent after solid organ transplantation, for example heart, pancreas, lung, liver, kidney (Plosker and Foster, 2000). Tacrolimus belongs to the group of calcineurin inhibitors and can be used in the treatment of autoimmune diseases, such as autoimmune chronic active hepatitis, inflammatory bowel disease, nephrotic syndrome, Crohn's disease, autoimmune inner ear disease (Sadaba *et al.*, 2004; Shapiro *et al.*, 1999; Singer, 1998; Van Thiel *et al.*, 1995).

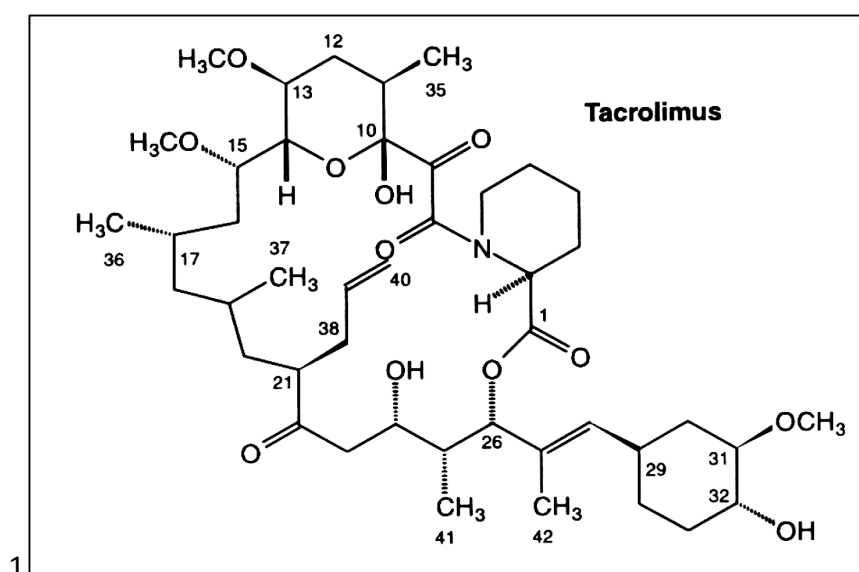


Figure 4: Chemical structure of tacrolimus (Tanaka *et al.*, 1987).

The half-life of tacrolimus inside the human body is from 8.7 to 11.3 hours (Venkataramanan *et al.*, 1995). Tacrolimus can cause several adverse effects, including: neurotoxicity, nephrotoxicity, gastrointestinal toxicity, hyperkalaemia, hypertension, and myocardial hypertrophy (Morales *et al.*, 2001; Nakata *et al.*, 2000). The mechanism of action of tacrolimus is similar to zotarolimus and everolimus, which include inhibition of calcineurin, calcium and calmodulin-dependent phosphatase activity by binding to calcium, calmodulin, and calcineurin through the immunophilin FK506 protein 12. Immunophilins are involved in the protein folding process. Formation of drug-immunophilin complex results in arrested transfer of activated T-cells transcription factor. This encourages the proliferation of helper T-cells, mediated by interleukin-2, which is connected to the immune response associated with allograft rejection (Spencer *et al.*, 1997). Tacrolimus can be metabolised either by the liver or intestinal microsomes (Lampen *et al.*, 1995). The solubility of tacrolimus is within the range 4-12 µg/mL. However, it is highly soluble in organic solvents, such as ethanol, methanol and chloroform (Tamura *et al.*, 2003). Bioavailability of tacrolimus may vary from 5% to 93% (Wallemacq *et al.*, 1998). Around 95% of tacrolimus is eliminated from the body by the biliary route (Moller *et al.*, 1999). Tacrolimus has also been used in drug eluting stents. Recently, a stent named Janus, which has tacrolimus within the carbofilm, a polymer-free monolayer, was demonstrated to be safe for use by patients (Garcia-Tejada *et al.*, 2007).

1.3.4. Dexamethasone

Dexamethasone (Figure 5) belongs to the group of corticosteroid medication, used in the treatment of various inflammatory diseases. It is a very strong anti-inflammatory and immunosuppressive drug, able to inhibit proliferation of fibroblasts, smooth muscle cells and macrophages (Zhou *et al.*, 2005). Therefore, it was considered as a bioactive agent for application in drug-eluting stents.

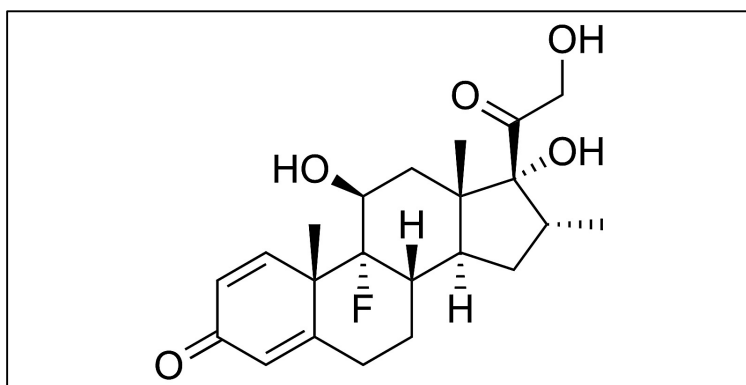


Figure 5: Chemical structure of dexamethasone (Elks and Ganellin, 2014).

Several studies have been performed to investigate possible application of this drug. Han and co-workers studied BiodivYsio Matrix LO stent with a high concentration of dexamethasone. The results were very encouraging. These stents reduced the amount of major cardiac events and in-stent restenosis after 6 months in comparison to the control stents (Han *et al.*, 2006). Another research group investigated stents named Dexamet during clinical trials. It was observed that stents coated with dexamethasone resulted in substantially less lumen loss compared to BMS (Konig *et al.*, 2007). Although, the initial results obtained in animal models were very promising, the data from clinical trials have been contentious (Hämäläinen *et al.*, 2013). Therefore, an idea of incorporating both drugs, such as rapamycin and dexamethasone has appeared (van der Hoeven *et al.*, 2008). However, further studies are required to achieve a final conclusion.

1.3.5. Antibodies

Antibodies have been considered as bioactive agents for coronary stents. The main role of antibodies is this device was to stimulate cell growth in the vessel wall. Faster endothelialisation will result in the faster integration of stents in the arterial wall, which will reduce the risk of thrombosis. Application of stents with antibodies should also reduce the time required for the antithrombogenic drug therapy. Guowei Fu and co-workers developed an efficient method for direct attachment of anti-CD34 antibodies into a nanoporous stainless steel stent. The developed device demonstrated enhanced endothelialisation in both: *in vitro* as well as *in vivo* studies (Guowei Fu *et al.*, 2016). In another study, Aggarwal and co-workers studied antiplatelet GPIIb/IIIa antibody eluting cellulose coated stainless steel stent in an animal model. This study demonstrated, that incorporation of antibodies significantly reduced platelet accumulation in the stent

neighbourhood. However, the effects were temporary and were determined by the presence of antibodies. After complete release of all antibodies, the stent lost its antithrombogenic effect. Therefore, other solutions need to be considered, such as incorporation of antithrombogenic agents, such as heparin, hirudin and glycoprotein IIb/IIIb (Aggarwal *et al.*, 1996).

1.4. Biopolymers used as a drug carriers in the prevention of restenosis

Polymers are used as drug carriers for drug delivery applications. Homopolymers, copolymers, blends of polymers and composites have been investigated. Most of the work has been carried out using biodegradable materials (Ranade and Hollinger, 1996). The main goal for any drug eluting device is to deliver bioactive agent at the right time, to the appropriate location in sufficient concentration over designed period of time (Raval *et al.*, 2010). Controlled drug release is expected from drug eluting stents in order to prevent restenosis without any toxic effect (Wise, 2000). Controlled drug release can be achieved by few mechanisms, such as: diffusion, degradation by surface or bulk-erosion or an active efflux. The main drug release mechanism in DES is based on diffusion, either directly from polymeric matrix or from reservoir systems, where drug is encapsulated inside polymeric structure and release by diffusion through polymeric membrane (Kamath *et al.*, 2006). Polylactic acid, polyglycolic acid and their copolymers have been used in different drug delivery devices due to their high biocompatibility and appropriate degradation profiles for this application. Drug release depends on several factors, such as nature of the drug, polymer degradation rate, water permeability and interactions between drug and polymer surface (Lao *et al.*, 2008). Several biomaterials and different drugs were studied in order to reduce or inhibit the development of restenosis. PLGA was the most commonly used material. Release of the drugs occurred by controlled biological degradation or diffusion (Schliecke and Schmidt, 2003). Wang and co-workers studied multilayer stents where each layer was made using different materials, in order to allow controlled release of rapamycin. PLLA was used as the platform material, as the core of the stent. Whereas PLGA was the matrix for drug incorporation. Cho and co-workers studied poly(lactide-co-caprolactone) films with incorporated epigallocatechin-3-O-gallate (EGCG), which was discovered in green tea.

This substance has antithrombotic, anti-inflammatory and antiproliferative properties. It was found, that EGCG release took place via diffusion. This resulted in the inhibition of smooth muscle cells (SMC) migration, suppression of platelet activation and adhesion (Cho *et al.*, 2008). In another study, rapamycin-eluting stainless steel stent was coated with two layers containing three polymeric biomaterials, such as: PLLA, PLGA and poly(vinylpyrrolidone) (PVP) with incorporated drug. Half amount of the drug was released by day 7, and complete release occurred within 48 days (Dani *et al.*, 2008). Sousa and co-workers (2003) reported significant reduction in-stent restenosis in DES in comparison to bare metallic stents by introduction of rapamycin or paclitaxel within polymeric coating (Sousa *et al.*, 2003).

The fabrication of drug eluting stents can be a challenge. The currently used methods, such as dip coating and spray coating are more suitable for hydrophobic drugs than water-soluble drugs or deoxyribonucleic acid. It was found, that stents coated with oligonucleotides in water soluble polymer demonstrated limited delivery efficiency, which had negative impact on the therapeutic effect of the device. Therefore, nanoparticle-eluting stents were produced by cationic electrodeposition coating technology to overcome this limitation (Nakano *et al.*, 2009). PLGA in general has been a preferred material used in drug delivery related to prevention of restenosis. Additionally, targeting molecules can be attached to the surface of the polymer, which can be recognised by vectors allowing travel to the target tissue. Chorny and co-workers developed magnetic nanoparticles made from PLA with incorporated paclitaxel. The results were up to 10 times more successful than the non-magnetic system in smooth muscle cells (Chorny *et al.*, 2010). Another researcher, Luderer and co-workers, 2011 synthesised PLA nanoparticles loaded with rapamycin for controlled drug delivery. However, produced nanoparticles inhibited viability and proliferation of endothelial as well as smooth muscle cells (Luderer *et al.*, 2011).

1.5. Limitations of currently available stents

Currently, three types of stents, such as bare metallic stents, drug eluting stents and biodegradable stents have been used to treat coronary artery disease. However, each type of these devices has some limitations. For example, application of bare metallic stents results still with high rate of restenosis. Moreover, BMS remain in the body permanently and can lead to complications, mainly, inflammation and in-stent restenosis (Serruys *et al.*, 199). Hypersensitivity reaction to nickel and molybdenum was reported in 10% of patients after BMS implantation (Koster *et al.*, 2000). Drug eluting stents were developed to resolve some issues related to BMS, like for example restenosis. However, deployment of DES resulted in appearance of another side effect, named as late thrombosis, which will be described in section 1.5.2. Moreover, deployment of DES lead to delayed endothelialisation, caused by release of anti-proliferative agents. Endothelial cells are able to covered bare metallic stents within 6-7 months, whereas DES achieve 50% endothelialisation after 3 years (Joner *et al.*, 2006). Drug eluting stents are usually made from metals, hence remain in the body permanently and can lead to similar side effects as BMS (Sun *et al.*, 2013). Also hypersensitivity reaction towards polymeric coatings have been reported in patients after DES deployment (Jeewandara *et al.*, 2014). Biodegradable stents were developed in order to overcome the limitations of previously described stents. However, the results are still not satisfactory. Although, magnesium and iron have been considered as biodegradable metals for stents, due to their high biocompatibility, they represent degradation profile, unsuitable for this application. Magnesium degrades too fast, hence cannot support the vessel wall for required period of time (Erbel *et al.*, 2007). Degradation rate of an iron stent is very slow; hence it acts similarly to the commonly use bare metallic stents (Peuster *et al.*, 2006). Biodegradable polymers on the other hand, have weaker mechanical properties in comparison to metals. Therefore, stent thickness has to be much greater than metallic stents and cannot be used in small blood vessels. Moreover, recoil after expansion have been observed. Polymers cannot be visible under X-Ray, which is additional limitation of this materials (Ramadugu *et al.*, 2016). Limitations associated with biodegradable PLLA polymeric stent have been described previously in section 1.2.3.1.

The major function of stent is to support vessel wall and prevent elastic recoil of the coronary artery. The reaction between the stent and the vessel wall has been extensively studied in animal models (Ashby *et al.*, 2002). It was found that porcine coronary arteries reacted similarly to injury as the human vessels. Balloon angioplasty alone as well as the stent deployment causes serious mechanical injury to the vessel wall. This leads to thick neointima formation within 20-24 days. The thickness is related to the deepness of the injury (Schwartz, 1992).

Stent implantation is usually accompanied by side effects such as thrombosis and in-stent restenosis. The risk of stent thrombosis is the highest in the first month after stent implantation and in 70% cases leads to myocardial infarction or sudden death. Unlike thrombosis, in-stent restenosis usually occurs between 6-12 months of stent implantation (Wilson and Cruden, 2013). In-stent restenosis is defined as the narrowing or lumen loss of over 50% following stent deployment. In-stent restenosis is primarily induced by neointimal proliferation; however, there are a number of known factors, which may affect the appearance of in-stent restenosis, such as diabetes mellitus, lesion length, number of stents, stent design and the lumen diameter (Hoffman and Mintz, 2000). Around 20% of patients with BMS require a second intervention within the first 12 months after stent deployment because of the reduction of the lumen size caused by the development of in stent-restenosis (Fischman *et al.*, 1994).

1.5.1. In-stent restenosis

As mentioned above, balloon angioplasty, followed by stent implantation causes injury to the vessel wall. An artery is a multilayer structure, which contains three major layers (Figure 6). Tunica externa, named also adventitia is the most external layer of the artery wall, which connects the vessel to the surrounding tissues. This layer contains highly dense connective tissue with elastin and collagenous fibres. Tunica media is placed under the adventitia; it is the thickest layer, built mainly from smooth muscle cells. This layer plays a very important role, which is to support the vessel wall and regulation of blood flow and pressure. Tunica intima, called interna is the inner most layer, containing simple squamous epithelium surrounded by connective tissue with elastic fibres (Birkenhauer *et al.*, 2004).

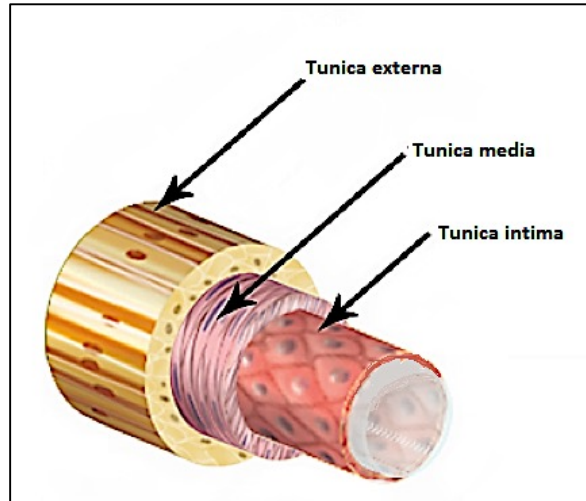


Figure 6: Schematic of the arterial wall. (Source: SEER Training Modules, *Module Name*. U. S. National Institutes of Health, National Cancer Institute. Day of access: 02/02/2017; <https://training.seer.cancer.gov/>).

The changes within the arterial environment that occur right after stent deployment, might lead to in-stent restenosis. Restenosis is developed as an effect of a healing process of the arterial wall caused by mechanical injury during balloon angioplasty and stent implantation. It involves two main processes, neointimal hyperplasia and vessel remodelling (Forrester *et al.*, 1991). The mechanism of in-stent restenosis at the molecular level, occurring after stent deployment, was proposed by Welt and Rogers (2005). Figure 7 demonstrates various phases, which happens after stent implantation until the formation of a restenosis lesion. At the beginning, stent deployment results in the denudation of the most internal layer, named endothelium. In addition, the compression of the plaque can cause delamination within inner layers of the arterial wall, such as tunica media or even externa. The whole artery is stretched. Fibrins along with platelets are embedded directly at the wounded site. The platelets get activated and express P-selectin, an adhesive molecule, which recruits the leucocytes. The leucocytes bind closely across adhesive molecules by direct attachment to platelet receptors or through cross-linking with fibrinogen. In the next stage, the leucocytes migrate through the layer of platelets and fibrin as well as tissues. This is mediated by chemokines, such as interleukin 6 (IL-6), interleukin 8 (IL-8) or monocyte chemoattractant protein (MCP)-1, released by smooth muscle cells (SMCs), present in the arterial wall and resident macrophages. The next step is referred to as the “cellular

proliferation phase". Prolonged release of growth factors by platelets; leukocytes and SMCs stimulate migration of smooth muscle cells into the neointima. The newly-created neointima contains SMC, extracellular matrix and macrophages enrolled within a few weeks. Cell proliferation, observed in this phase, plays a crucial role in further restenosis development. After several weeks, the last phase of remodelling occurs. The main change observed during this period is a higher production of extracellular matrix, composed of various types of collagens and proteoglycans, which are the key elements of the fully formed restenosis plaque (Welt and Rogers, 2002).

Rapamycin, an immunosuppressive drug has been proven to inhibit all phases of the restenosis cascade. It has been reported to inhibit synthesis of collagen and proteins participating in an extracellular matrix formation. Moreover, it inhibits smooth muscle cells migration. Rapamycin is effective within the wide range of 18-1200 μg per 18mm stent length in animal models. The current dose applied on the stent is 140 $\mu\text{g}/\text{cm}^2$ (Costa and Simon, 2005).

However, to date there is only one successful method of treatment for restenosis, called vascular brachytherapy. This method is based on local delivery of either beta or gamma radiation, delivered by specially designed catheter to prevent neointima tissue growth. Brachytherapy has been approved by US FDA as a technique safe to be use for the treatment of the in-stent restenosis. The drawback of this method is that the target vessel revascularization rate is only 20% (Waksman, 2000). There is therefore a real need for an efficient therapy for the prevention of in-stent restenosis.

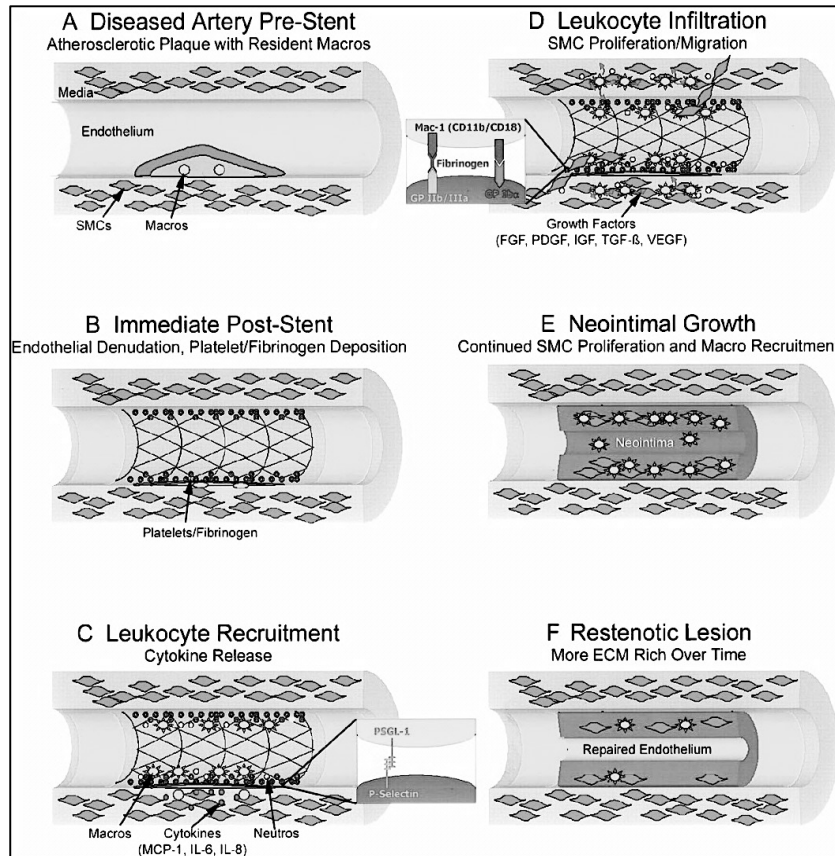


Figure 7: Schematic of the restenosis cascade lesion development. A- vessel structure before intervention, B – changes in the artery environment immediately after stent implantation, C, D- leukocyte recruitment and infiltration associated with constant release of cytokines, E – neointimal thickening and smooth muscle cells proliferation, F – restenosis lesion formed (Taken from: Welt and Rogers, 2002).

1.5.2. Late stent thrombosis

Depending on the time after the stenting procedure thrombosis can be divided into two types: early thrombosis, which occurs within the first 30 days after the procedure, which usually is related to the procedural factors, such as incomplete stent expansion, plaque detachment from residual lesion, internal fractures. The second type, called late thrombosis appears between 1 to 12 months after stent deployment. This type is related to the delayed healing process of the arterial wall (Figure 8) (Joner *et al.*, 2006) and usually results in myocardial infarction or death (Camenzind *et al.*, 2007). Sometimes, thrombosis in drug eluting stents occurs after a year. This is very late thrombosis, which is related to abnormal response of the vessel wall to the implant, which can be caused by a hypersensitive reaction. The new phenomenon, called “neoatherosclerosis”,

which is neointima with atherosclerotic occurrence, seems to have a crucial role in the development of very late thrombosis (Komiya *et al.*, 2015).

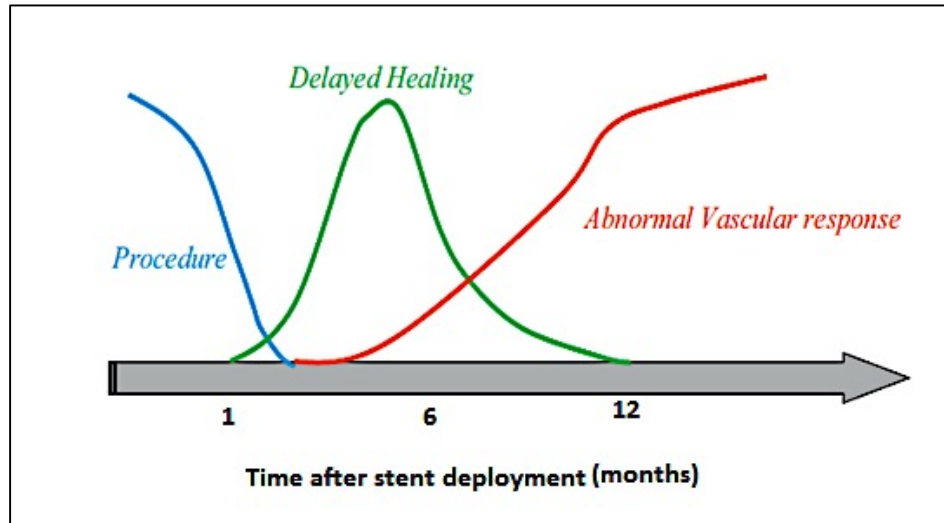


Figure 8: Mechanism of the development of the late thrombosis in the drug eluting stents in correlation to time after stent deployment (Nakazawa, 2011).

The molecular basis of the mechanism of late in-stent thrombosis is still unknown (Fischman *et al.*, 1994; Serruys *et al.*, 1994). There is a hypothesis, that several factors, such as an insufficient expansion of the stent, fracture of the polymer stent, inflammation triggered by metal or polymer and delayed healing might induce platelet aggregation and fibrin deposition in the drug eluting stent, delayed arterial healing caused by incomplete reendothelialization and persistence of fibrin was observed in the patients who died due to late thrombosis, (Morice *et al.*, 2002). Some procedure related factors, such as: smaller final lumen dimensions, caused by stent underexpansion or malapposition, stent length, persistent slow coronary blood flow, placement of multiple stents, positive remodelling play a significant role in late-thrombosis development (Kereiakes *et al.*, 2000). There are also patient-related factors, like advanced age, diabetes, renal failure and stenting in acute myocardial infarction, correlated with an increased risk of stent thrombosis (Park *et al.*, 2006; Ong *et al.*, 2005). The thickness of polymer struts as well as the type of the polymeric material also play an important role (Nakazawa *et al.*, 2011). Moreover, drugs used in DES, which slow down endothelialisation may have a contribution in the development of prothrombogenic conditions (Stähli *et al.*, 2006). Currently, FDA recommends dual antiplatelet therapy

with aspirin and clopidogrel for more than 12 months to prevent DES related thrombosis (Takayama *et al.*, 2011).

1.6. Ideal stent requirements

Requirements for the ideal stent have been clearly formulated (Regar *et al.*, 2001; Sangiorgi *et al.*, 2007; Mani *et al.*, 2007). The perfect stent should be:

- a) biodegradable in nature, to provide scaffolding and allow proper healing; after that to slowly degrade to non-toxic products
- b) flexible, trackable to be able to pass through winding vessels
- c) radio-opaque with good MRI compatibility, to allow monitoring in assessing the *in vivo* location of the stent during deployment and follow-up period
- d) thromboresistant, the material should be compatible with blood and not attract platelets to adhere and accumulate
- e) able to release drugs, stents should act as drug carrier vehicle and provide local drug delivery in a controlled manner
- f) have proper mechanical properties, such as high tensile strength to provide strong mechanical support to the vessel wall; sufficient flexibility in order to be crimped on the balloon catheter supported by a guide wire; the stent should undergo sufficient expansion and conform to the vessel wall
- g) suitable surface characteristics, such as surface chemistry and topography to allow endothelialisation and in case of metallic stents additionally an ability to prevent corrosion induced by formation of oxide films
- h) excellent haemo- and biocompatibility, the material must not cause side effects in the body
- i) relatively inexpensive to manufacture—the stent material should be available to purchase by general patients

1.7. Biomaterials used for coronary stent application

Biomaterials are of great interest for coronary stents due to their high biocompatibility and biodegradability. Poly(L-lactic) acid, poly(D-lactic) acid, polycaprolactone and poly(glycolic) acid have been commonly used for the fabrication of bioresorbable coronary stents (Eberhart *et al.*, 2003). PLLA and PGA have high tensile strength values; therefore, can be used for different types of designs. The complete degradation of PLLA requires 24 months, whereas for PGA it requires from 6 to 12 months. PLLA has been used for several medical applications, especially for devices, which require great strength and toughness from the material, such as orthopaedic and cardiovascular devices or sutures. Moreover, PLLA can be processed by various techniques, such as electrospinning, moulding, extrusion as well as solvent casting (Zilberman and Eberhart, 2006). PCL is a semicrystalline polymer with lower tensile strength and Young's modulus values in comparison to PLLA and PGA. PCL, exhibits much higher flexibility in comparison to PLLA. It has much lower glass transition temperature (-60°C) and melting temperature around 60°C . Polydioxanone (PDS) has also been investigated for coronary stent development, due to its excellent biocompatibility. It has lower strength and glass transition temperature similar to PCL (Pachence and Kohn, 2000). The first bioresorbable stent was developed by Tamai and co-workers. It was called Igaki/Tamai and was made using PLLA, was balloon expandable with a zigzag coil design. The strut thickness was 0.17mm and had self-expanding capacity. However, the initial expansion required high temperature (70°C). Further expansion required the application of a pressure gradient. The most important innovation proposed by Tamai was the unique "zigzag" stent design (Tamai *et al.*, 1999; 2000). Initial results on Igaki/Tamai stents demonstrated reduction of stenosis in a porcine model. Stents showed long-term biocompatibility with minimal immunogenic response after 16 weeks. There were no stent thrombosis events. The restenosis rate after 6 months of clinical trials was 10.5% (Tsuji *et al.*, 2001). The success of a bioresorbable stent is dependent on a combination of several factors, such as excellent biocompatibility, controlled degradation rate, mechanical properties, the manufacturing ability and also a proper design (Zilberman and Eberhart, 2006).

Within the group of biomaterials with great potential in coronary stent development are polyhydroxyalkanoates (PHAs) which are biopolyesters produced by bacteria under nutrient limiting conditions, which will be described in details in the following section.

1.8. Polyhydroxyalkanoates

Polyhydroxyalkanoates (PHAs) are a group of biodegradable biopolymers produced by various microorganisms as an intracellular reserve of carbon and energy (Lu *et al.*, 2009; Kumbhakar *et al.*, 2012; Matias and Rodrigues, 2011). Due to their specific physical and chemical properties, they can be used as a substitute of traditional plastics. PHAs are biodegradable and biocompatible; hence they can be used for a range of medical applications including the production of biodegradable coronary artery stents such as those described in the section 1.3. (Basnett and Roy, 2010; Chen, 2009).

Polyhydroxyalkanoates accumulate in the form of inclusion bodies, 0.2-0.5 microns in diameter, within the cytoplasm (Figure 9). They are produced under conditions of nutrient limitation with one of the growth components, such as nitrogen, sulphur, oxygen, magnesium or phosphorus in limiting concentration, with excess of carbon (Anderson and Dawes, 1990; Khanna and Srivastava, 2005; Chen *et al.*, 2001; Thakor *et al.*, 2006). Various organic compounds such as: carbohydrates, lipids, fatty acids, alkanes, alkenes, organic acids, aromatic compounds, and many others can be used as a carbon source for PHA production (Sudesh *et al.*, 2000).

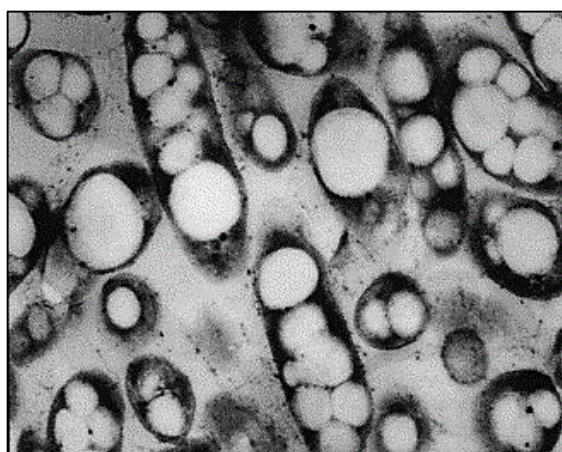


Figure 9: Polyhydroxyalkanoates granules inside bacterial cells. (Source: Chen *et al.*, 2001).

Polyhydroxyalkanoates are esters of 3,-4,-5,-6-hydroxyalkanoic acid. The chemical structure of PHAs is presented in Figure 10. Each monomer unit includes a side chain

group (R), which is usually a saturated alkyl group. Rarely, unsaturated or branched alkyl groups can also be found (Lu *et al.*, 2009).

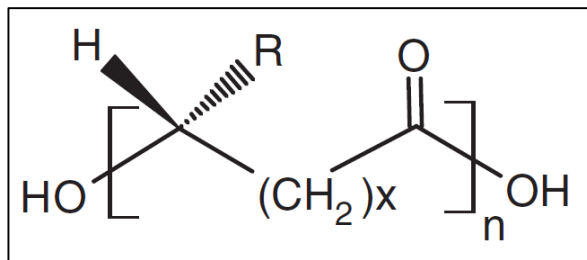


Figure 10: The general structure of Polyhydroxyalkanoates. (x = number of methylene groups in the backbone; n = 1000–10 000; R = alkyl groups, C_1 – C_{13}) (Nigmatullin *et al.*, 2015).

Each PHA molecule contains from 600 to 35,000 (*R*)-hydroxy fatty acid monomer units (Khanna and Srivastava, 2005).

1.8.1. Types of PHAs and their properties

Polyhydroxyalkanoates have some properties similar to traditional plastics, for example: thermoplasticity, hydrophobicity, high molecular weight (Thakor *et al.*, 2006). Physical properties of PHAs are dependent primarily on the number of carbon atoms in the monomer unit. Homopolymers, random copolymers and block copolymers of PHAs can be produced depending on the bacterial species and growth conditions. Over 150 different PHA monomers have been reported so far (Loo and Sudesh, 2007; Gao *et al.*, 2011). Monomers can include aromatic or aliphatic side chains or can be chemically modified in order to improve the functionality and applicability of the polymer (Lu *et al.*, 2009). PHAs are divided into two main groups: short-chain length (scl), where the monomer contains 3 to 5 carbon atoms, and medium- chain length (mcl), where the number of carbon atoms in the monomer is between 6 and 14 (Madison and Huisman, 1999). Scl-PHAs are normally brittle, crystalline, stiff and have high melting temperature. Scl-PHAs can demonstrate different thermal behaviour, due to the various states of the polymer including amorphous, semi-crystalline and crystalline states. Scl-PHAs exhibit double or multiple melting peaks depending on the structure and morphology of the crystals (Ding *et al.*, 2011). However, P(4HB), a scl-PHA is highly elastomeric with high tensile strength, which makes this material very attractive for biomedical applications,

such as sutures. Very often P(4HB) is produced as a copolymer along with P(3HB) after addition of specific precursors, such as 1,4-butanediol or γ -butyrolactone into the feedstock. Mcl-PHAs are biopolymers, which are elastomeric in nature with low melting point, low glass transition temperature. Usually they do not undergo cold-crystallisation. Mcl-PHAs represent a group of soft materials with low tensile strength and very low values of Young's Modulus in comparison to scl-PHAs. Their elastomeric nature increases with the length of the side chain (Khanna and Srivastava, 2005; Williams *et al.*, 1999; Loo and Sudesh, 2007). Their properties make them an attractive group of biomaterials for example for soft tissue engineering (Abe *et al.*, 2012).

Scl-mcl-PHAs are copolymers of short chain length PHAs and medium chain length PHAs and exhibit intermediate properties in comparison to scl or mcl polymers on their own (Matsusaki *et al.* 2000). For example, they exhibit high tensile strength but are also flexible at the same time. Both the thermal and mechanical properties are dominated by the type of monomer present as the major component. For example, P(3HB-co-3HHx) copolymer containing 17mol % 3HHx unit had twice the value of elongation at break as compared to the copolymer with only 10 mol % 3HHx. Melting temperature for these copolymers was in the range 120-127°C. Presence of 3HHx unit did not affect the tensile strength of the material as well as its glass transition temperature (Sudesh *et al.*, 2000; Lauzier *et al.*, 1992).

Blending of scl and mcl-PHAs also allows the production of novel material with intermediate properties, suitable for various applications (Doi *et al.*, 1995). PHA based blends will be described in the section 1.8.9.

Polyhydroxyalkanoates represent group of biopolymers with broad range of properties. PHAs represent several advantages, such as natural origin material, production by using renewable materials, high biocompatibility and non-toxicity. The summary of typical material properties of scl-PHA and mcl-PHA is presented in Table 1.

P(3HB), which belongs to scl-PHA group represents completely different properties than mcl-PHA. Hence, the material selection needs to be based on the final material properties required for chosen application.

Table 1. Summary of material properties typical for mcl-PHA and scl-PHA (Rai *et al.*, 2011; Ojumu *et al.*, 2004; Sudesh *et al.*, 2000).

Material property	Mcl-PHA	Scl-PHA (P3HB)
Thermal properties: <ul style="list-style-type: none"> • Glass transition temperature (T_g) ($^{\circ}\text{C}$) • Melting temperature (T_m) ($^{\circ}\text{C}$) 	-36 to -48	0-15
Mechanical properties <ul style="list-style-type: none"> • Tensile strength (MPa) • Young's Modulus (MPa) • Elongation at break (%) 	1-9	20-40
Crystallinity degree (%)	10-15	1000-3500
	280-1000	4-10
	30-38	60-80
Biocompatibility	Highly biocompatible with several cell lines	Highly biocompatible with several cell lines
Biodegradability	Biodegradable	Biodegradable
Toxicity of polymer and degradation products	Non-toxic	Non-toxic
Processability	Suitable for several techniques without using elevated temperatures, such as solvent casting, dip moulding, freeze-drying, 3D printing, electrospinning	Suitable for several techniques, such as solvent casting, dip moulding, extrusion, electrospinning, freeze-drying, electrospinning, injection moulding

Although, PHAs demonstrate superior properties in comparison to other polymers, PHAs have also few limitations. One of the biggest concerns is related to high production cost and limited availability. Therefore, PHAs cannot compete with cheap synthetic polymers available in large amounts. Another drawback is related to processability. Mcl-PHAs have low temperature of melting, therefore cannot be used for techniques required high temperatures. P(3HB) has much higher T_m value than mcl-PHA, but it demonstrated

susceptibility to thermal degradation in temperature above melting point. Additionally, PHAs are considered as materials exhibiting insufficient mechanical properties: scl-PHA are stronger but brittle, whereas mcl-PHA are very elastomeric but weak (Li *et al.*, 2016). This project will try to address some of the limitations mentioned above, such as economical production of mcl-PHAs, material processability and enhancement of material properties.

1.8.2. Biocompatibility of PHAs

High biocompatibility is required for any material, which meant to be used for medical applications. This would apply to biomaterials, implants, medical devices and prosthesis. The levels of biocompatibility differ between different materials and depend on several factors, such as shape, porosity, functional groups, mechanical properties and surface charge. Human blood contains between 3 to 10mg per 100mL of 3-hydroxybutyric acid (3HB), as a compound associated with ketone body formation (Pawan and Semple, 1983). P(3HB) is found in transmembrane channels in eukaryotic and prokaryotic cell membranes (Reusch, 2000). Therefore, it is expected that implants or sutures made from PHAs containing P(3HB) should not trigger an immune response in the body (Brigham and Sinskey, 2012). Moreover, *in vitro* cell study has confirmed high biocompatibility of P(3HB) towards a range of different cell lines (Misra *et al.*, 2006; Shishatskaya *et al.*, 2004). Sevastianov and co-workers measured the haemocompatibility of PHAs and demonstrated that both P(3HB) and P(3HB-co-3HV) were compatible with blood and do not trigger any immune response (Sevastianov *et al.*, 2003). P(3HB) have been studied intensively for hard tissue engineering and has demonstrated good biocompatibility with several cell lines, such as fibroblasts, chondroblasts or osteoblasts (Köse *et al.*, 2003). Biocompatibility of P(3HB) films has also been confirmed *in vivo*. The tissue reaction to the implanted material did not differ from an inert glass plate (Muhammadi *et al.*, 2015). The high biocompatibility can be explained by the presence of P(3HB) oligomers and HB in animal tissues under normal conditions in comparison to the chemically synthesised polymers, such as polylactides or polyglycolides (Jirage *et al.*, 2013).

Mcl-PHA is another very interesting group of biopolymers. They are usually soft and highly elastomeric. Therefore, they have gained interest as a potential candidate for soft tissue engineering. Bagdadi *et al.*, observed high compatibility of neat P(3HO) cardiac patches with neonatal ventricular rat myocytes (Bagdadi *et al.*, 2017). Blending of scl and mcl-PHA was carried out to obtain materials with intermediate properties. For example, mcl/scl-PHA blends, P(3HO)/P(3HB), have demonstrated good support of growth and proliferation of human microvascular endothelial cells (HMEC-1) (Basnett *et al.*, 2013) as well as NG108-15 neuronal cells (Lizarraga *et al.*, 2015). In another study, Qu and co-workers have reported the development of P(3HB-co-3HHx) scaffold coated with fibronectin and additional surface functionalization by plasma treatment. These modifications led to increased attachment and proliferation of human umbilical vein endothelial cells (HUVECs) as well as smooth muscle cells isolated from the rabbit aorta (RaSMCs) (Qu *et al.*, 2005). The P(3HB-co-3HHx) copolymer promoted differentiation of mesenchymal stem cells into chondroblasts, which can be applied for cartilage regeneration (Yan *et al.*, 2011). Naveen *et al.*, 2015 have observed good biocompatibility of mcl-PHAs with mesenchymal stromal cells (Naveen *et al.*, 2015).

Due to their high biocompatibility, PHAs have become significant candidates as a group of biomaterials for various biomedical applications including their usage for implants, prosthesis, scaffolds and other medical devices in tissue engineering.

1.8.3. Blood-biomaterial interactions

High compatibility of the implant with blood is required especially for the scaffolds or devices used for vascular repair, grafts, stents and heart valves, where contact with blood is constant. Interactions between blood and the material are very complicated and contain many stages connected with each other (Tsai *et al.*, 1999). Healthy endothelium has anticoagulant properties. However, most of the materials, such as polymers or metals, their oxides and alloys, used for medical devices, can activate the body inflammatory response (Ratner, 2007). Immediately after implantation, protein adsorption occurs on the surface, followed by platelet adhesion. If proteins are denatured, coagulation factors are activated, which switches the coagulation cascade and causes an inflammatory response. Appearance of these three elements within a few

minutes after contact with a foreign material lead to thrombus formation and fibrinolysis. Longer contact may result in complete closure of the vessel, or calcification as well as changes in the mechanical properties of the material. Fibrinogen, blood clotting enzymes and blood proteins are crucial for the development of material related to clotting (Forbes and Courtney, 1994). Several studies have been performed towards better recognition of the blood-material interaction mechanisms at a molecular level. Many different types of polymers and other materials have been investigated. Special attention was paid to the materials, which demonstrated low protein adsorption. It was found, that PEG, zwitterionic groups and polycarboxybetaine methacrylate were able to prevent fibrinogen adsorption (Zhang *et al.*, 2006). Blood-material interaction can trigger inflammatory response, which may lead to the implant rejection. Initial contact between the biomaterial and blood results in plasma protein adsorption as well as activation of the plasma cascade systems. The amount of protein attached to the surface differs between the materials (Courtney *et al.*, 1994).

Surface characteristics, such as chemical composition, presence of functional groups, incorporation of particles, crystallinity, roughness, porosity, released products as well as degradation products can affect the interactions between the material and the blood cells (Bacakova *et al.*, 2011). Surface roughness significantly affects platelets adhesion. Higher roughness attracts platelets more than smooth surfaces (Braune *et al.*, 2010). The wettability of the material is also very important. However, the optimum value of the contact angle, required for cell attachment is still controversial. It is commonly known that cells prefer to attach to the weakly hydrophilic surfaces (contact angle around 60°), whereas highly hydrophilic or hydrophobic surfaces have been used to inhibit cell adhesion. Highly hydrophilic surfaces prevent adsorption of proteins. On the other hand, proteins adsorbed to the strongly hydrophobic materials are in inactive form, which inhibit cell adhesion (Bacakova *et al.*, 2011). It is also well known fact, that several cell lines attach and proliferate on the surfaces of PHAs, which are mainly hydrophobic in nature (Chen, 2009). These observations bring to the general conclusion that material-cells interaction is a very complex phenomenon, which depends on several factors and some mechanisms have not yet been discovered.

Restrained hydrophilic and positively charged materials encourage cell attachment due to the adhesion of specific molecules, such as vitronectin and fibronectin, which make

specific sites accessible for the cell adhesion receptors. Surface charge also plays a very important role. The internal wall of the artery is negatively charged, as well as the platelets, hence they repel from the wall. Cells tend to attach to the positively charged surfaces better than to negatively charged surfaces. This can additionally lead to an activation of the complement system and increase the inflammatory response (Franke and Jung, 2012). Therefore, many research groups have focused on the modifications of the surfaces of the materials. There are three different approaches, such as surface passivation, which is a coating with a thin layer of protective material, incorporation of biomolecules, such as mimicking the environment of the vascular wall. Surface passivation requires surface modifications in order to lower or completely eliminate the interactions between the material and proteins. This can be obtained for example by modifications with zwitterionic polymers (Yang *et al.*, 2009). Those are also known as polybetaines, which contain the same number of cationic and anionic groups within the repeating unit and have the overall zero charge (Laschewsky, 2014). The ideal protein resistant material should be hydrophilic, electrically neutral, incorporate hydrogen bond acceptors but be deprived of hydrogen bonds donors (Ostuni *et al.*, 2001).

1.8.4. Biodegradability of PHAs

PHA degradation is defined by a number of factors including weight loss, reduction of molecular weight, degree of crystallinity and change of mechanical properties (Mergaert *et al.*, 1993). PHA degradation are influenced by the properties of the polymer, surface area, type and activity of enzymes, pH, temperature, moisture, salinity, oxygen levels, shape and size of the sample (Boyandin *et al.*, 2013; Hiraishi and Khan, 2003). It has been demonstrated that the copolymer P(3HB-co-4HB) can degrade quicker than the homopolymer P(3HB) (Doi *et al.*, 1990). On the other hand, Boyandin and co-workers demonstrated faster P(3HB) degradation than P(3HB-co-3HV) copolymer. It was found that degradation rate of films was almost two times faster than pellets (Boyandin *et al.*, 2013). P(3HB-co-3HV) is not affected by moisture and does not degrade under normal conditions of storage (Mergaert *et al.*, 1993). The P(3HB) homopolymer was found to degrade within 6 months in the animal models (Kostopoulos and Karring 1994; Luklinska and Bonfield, 1997). Whereas in another experiment, copolymers of P(3HB-co-3HV) and

P(3HB-co-3HHx) degraded completely within 3 months, when implanted subcutaneously (Philip *et al.*, 2007). Degradation rate of PHAs can be accelerated by an addition of other materials, which degrades faster, like for example PLA or gelatine. Li *et al.*, investigated the influence of the addition of maleic anhydride into P(3HB-co-3HHx) copolymer grafts. After 21 weeks, the graft material underwent over 21% weight loss in comparison to the neat copolymer (7.3%) (Li *et al.*, 2008). UV treatment has beneficial impact on the degradation of PHAs. For example, P(3HB-co-3HHx) films made from UV treated polymer powders demonstrated accelerated degradation after 15 weeks. Moreover, UV radiated material enhanced the cell attachment and proliferation of L929 fibroblast cell line (Shangguan *et al.*, 2006). Miller and Williams, investigated gastrointestinal patches, based on P(3HB). After 1 year in the buffer solution, the molecular weight of P(3HB) have decreased by half. Incubation of P(3HB) with enzyme, such as pancreatin resulted in three times accelerated degradation rate in comparison to hydrolytic degradation (Miller and Williams, 1987). In another study, P(3HB) blended with atactic PHB was studied for bowel defect in the rat model. After twenty-six weeks only small residues of patch were present in one animal. The defect was completely healed. The results demonstrated complete degradability of the PHA biomaterial in the time sufficient for such application (Freier *et al.*, 2002). P(3HO) scaffolds, implanted subcutaneously, was relatively slow. After 40 weeks, the molecular weight of implanted P(3HO) was two time lower than the not implanted control (Williams *et al.*, 1999).

1.8.5. Biosynthesis of Poly(3-hydroxyalkanoates)

Polyhydroxyalkanoates play a very important role in bacterial metabolism. PHA granules usually play the role of energy storage during unfavourable conditions, such as nutrient limitation. When the ambient environmental conditions return to those preferred for bacterial culture development, PHA inclusions can be used to support growth. It was discovered, that bacteria, which harbour PHAs have increased tolerance against some agents, such as heat tolerance, osmotic shock or UV irradiation (Kadouri *et al.*, 2005). PHAs can be produced according to various metabolic pathways. The summary of all discovered metabolic pathways up to date is presented in Figure 11. From a total

number of 13 pathways, scl-PHA can be produced by 10 different metabolic pathways (A-J on the figure) and mcl-PHA by 4 (Chen 2010; Lu *et al.*, 2009, Madison and Huisman 1999).

PHA biosynthesis can be carried out by different metabolic pathways in the wild-type as well as genetically modified strains (Figure 11). They are synthesised by several enzymatic reactions from acetyl-CoA, in the presence of substrate specific PHA synthases located in the cytosol of PHA accumulating bacteria (Du and Yu, 2002). Most of the bacteria are able to synthesize scl-PHAs, such as P(3HB) or mcl-PHAs, containing medium chain length 3-hydroxy fatty acids (Koller *et al.*, 2010). The PHA metabolic pathways include several biochemical reactions, such as the Krebs cycle, glycolysis, Calvin Cycle, serine pathway, β -oxidation, *de novo* fatty acid synthesis and amino acid catabolism (Shilalipi and Nirupama, 2012; Steinbüchel *et al.*, 1992). The type of reaction selected for the biosynthesis of PHAs depends mainly on the type of carbon source, availability of nutrients and the bacterial strain used. Metabolism of some bacterial strains, such as *Cupriavidus necator* or *Pseudomonas* sp. is very sensitive towards nutrient balance in the surrounding environment. For example, nutrient-rich conditions inhibit PHA synthesis, due to the production of excess coenzyme A during the Krebs cycle. This results in the blockage of 3-ketothiolase PhaA and the utilization of all acetyl-coA for cell growth (Ratledge and Kristiansen, 2001). Whereas under nutrient limiting conditions in the presence of excess carbon, the concentration of coenzyme A allows acetyl-CoA to be directed to PHA biosynthesis pathways for PHA accumulation (Jung and Lee, 2000). Figure 11 demonstrates various routes of scl-PHA production (labelled from A to J) and mcl-PHA production (routes J-M). It is well known that (*R*)-hydroxyacyl-CoA ([*R*]-3-HA-CoA) is the most common precursor for PHA production. However, the metabolism of cyclohexanol to 6-hydroxyhexanoyl-CoA and 4,5-alkanolactone to 4,5-hydroxyacyl-CoA (4,5-HA-CoA) shown in metabolic routes L and M, have been recently proposed as the alternative precursors, which can lead to PHA biosynthesis (Chen, 2010; Lu *et al.*, 2009). Nevertheless, the possible pathways, L and M require further investigation. Discovery of larger number of metabolic pathways will help bioprocessing engineers to achieve optimal utilisation of the carbon source and enhance polymer production.

1.8.5.1. Synthesis of short chain length polyhydroxyalkanoates

P(3HB) is the most studied polymer from the PHA family. Production of P(3HB) involves three enzymatic reactions involving the enzymes: thiolase, reductase and polymerase. The first reaction involves the condensation of two acetyl coenzyme A (acetyl-CoA) molecules into acetoacetyl-CoA by β -ketoacyl-CoA thiolase (encoded by *phbA*). This is followed by the reduction of acetoacetyl-CoA to (*R*)-3-hydroxybutyryl-CoA by an NADPH-dependent acetoacetyl-CoA dehydrogenase (encoded by *phbB*) occurs. Finally, P(3HB) precursors, (*R*)-3-hydroxybutyryl-CoA monomers are polymerised to poly(3-hydroxybutyrate) by P(3HB) polymerase (encoded by *phbC*). This metabolic pathway is typically found in *Ralstonia eutropha* and *Zooglea ramifera* (Rehm, 2006). Other microorganisms are also able to produce P(3HB) by using completely different metabolic pathways. For example, *Aeromonas caviae* uses an enoyl-CoA hydratase for the formation of the (*R*)-3-hydroxy monomer from crotonyl-CoA or hexenoyl-CoA. It can synthesise copolymer, which contains 3HB and 3HHx units, when olive oil or fatty acids with even number of carbon atoms were used as the sole carbon source. Interestingly, growth on fatty acids mainly resulted in the production of the 3HV unit with slight amount of 3HB (Doi *et al.*, 1995). The metabolic pathway for P(3HB-co-3HHx) copolymer production in *Aeromonas caviae* is similar to the pathway proposed for P(3HB) production from *Rhodospirillum rubrum* by Moskowitz and Merrick. The proposed pathway included two hydratases, each specific to the R and S enantiomer. *R. rubrum* is able to produce P(3HB-co-3HV) from short and medium chain acids, (Moskowitz and Merrick, 1969). This pathway was described 30 years ago. However, Madison and Huisman drew attention to this pathway as a way to obtain scl-mcl-PHA copolymers (Madison and Huisman, 1999). *Methylobacterium rhodesenium* is another example of bacteria, which uses two hydratases for P(3HB) synthesis. In addition, NADH dependent and NADH-independent acetoacetyl-CoA reductases have been characterised. For this strain, the carbon source is crucial for the timing of P(3HB) production. For example, growth on methanol, resulted in the shift of P(3HB) formation until stationary phase, whereas presence of fructose triggered P(3HB) formation during exponential phase (Mothes *et al.*, 2007). Some bacteria, such as *Rhodococcus ruber* and *Nocardia corallina* were able to accumulate PHAs, including 3HV unit when grown on the feed, containing sugars, without addition of typical HV precursors, like valerate or propionate (Valentin and Dennis, 1996). They usually used the methylmalonyl-

1.8.5.2. Synthesis of medium chain length polyhydroxyalkanoates

Mcl-PHAs were discovered by de Smet and co-workers in 1983 (de Smet, *et al.*, 1983). Intense studies discovered that *Pseudomonas* from the rRNA homology group I were able to produce PHAs with the chemical structure directly related to the length of the fatty acid or alkane used as the carbon source (Lageveen *et al.*, 1988). When the carbon source contained between 6 to 12 carbon atoms, PHAs produced had the same main chain length as the carbon source, or were shorter by 2, 4 or 6 carbon atoms in comparison to original compounds (Huisman *et al.*, 1989). Mixtures of two or more different carbon sources reflected on the composition of the copolymers. For example, *P. oleovorans*, when grown on a mixture of octane and 1-octene was able to produce copolymer with the ratio between monomer with double bonds (poly(3-hydroxyoctene) and monomer containing only saturated carbon chains (poly(3-hydroxyoctanoate) varied from 0% up to 50% according to the amount of 1-octene in the feed mixture. Mcl-PHA biosynthesis pathway follows the fatty acid oxidation (Figure 11). Fatty acids are shortened by two atoms of carbon, which are released in the form of acetyl-CoA. The product of the reaction is oxidised from acyl-CoA to 3-ketoacyl-CoA. The precursor of mcl-PHAs, named (*R*)-3-hydroxyacyl-CoA have to be synthesised. Finally, the polymerase synthesises mcl-PHAs. The PHA synthase enzymes have specificity from C₆ to C₁₄ with preference for C₈, C₉ and C₁₀ monomers (Lageveen *et al.*, 1988). Subsequent research suggested that the activity of PHA synthases may affect the molecular weight of the final polymer. In addition, further *in vitro* and *in vivo* analysis implied that the ratio between substrate and enzyme was a major factor, which affected the molecular weight of the final polymer (Kraak *et al.*, 1997).

Pseudomonas species are able to produce mcl-PHAs from carbohydrates. When *Pseudomonas fluorescens* was grown on sugars, the mcl-PHA obtained, contained mainly C₈ and C₁₀ long chains (Huijberts *et al.*, 1992). PHA production from glucose is connected with the fatty acid biosynthesis pathway and utilises (*R*)-3-hydroxyacyl-ACP. When using sugars, additionally this internal product has to be converted to (*R*)-3-hydroxyacyl-CoA. It was found, that *phaG* was responsible for this transformation (Rehm *et al.*, 1998). Few *Pseudomonas* sp. are able to produce scl-mcl copolymers from

unrelated carbon sources, such as carbohydrates or 1,3-butanediol (Steinbüchel and Wiese, 1992). This type of scl-mcl-PHA production is an exception. Usually physical restrictions can limit formation of blended granules, containing both types of PHAs. Even recombinant *Pseudomonas putida*, which contains in addition to *phaC*, a copy of the *R. eutropha phaC* were shown to accumulate separate granules of P(3HB) and mcl-PHA (Preusting *et al.*, 1993).

1.8.6. Microbial production of PHAs

Polyhydroxyalkanoates are produced by over 70 genera of bacteria and *Archea* (Poli *et al.*, 2011; Lu *et al.*, 2009). The specific microbial groups are described in the sections below.

1.8.6.1. Gram-positive bacteria

Gram-positive bacteria have been found to be able to produce PHAs. P(3HB) was discovered for the first time in *Bacillus megaterium* by Lemoigne (Lemoigne, 1926). Within this group of bacteria, several genera, such as: *Bacillus*, *Caryophanon*, *Clostridium*, *Corynebacterium*, *Micrococcus*, *Microlunatus*, *Microcystis*, *Nocardia*, *Rhodococcus*, *Staphylococcus*, *Streptomyces* have been known to be PHAs producers (Lu *et al.*, 2009). Gram-positive bacteria produce mainly scl-PHAs. The polymer yield can be up to 50% dry cell weight (Valappil *et al.*, 2007). Some of the strains are able to produce mcl and scl-mcl-PHA copolymers under specific conditions. For example, *Bacillus megaterium* was found to produce P(3HB) from glycerol and succinic acid in mineral medium with addition of nitrogen. The same strain produced scl-mcl-PHAs in the same media without nitrogen. In addition, the same strain was able to accumulate mcl-PHAs, when grown on octanoic acid in the absence of nitrogen (Shahid *et al.*, 2013). Gram-positive bacteria have lower polymer accumulation in comparison to Gram-negative bacteria. Nevertheless, the main advantage of using Gram-positive bacteria is the lack of lipopolysaccharides (LPS) within the cell wall, which can trigger an immunological response (Ray *et al.*, 2013). It is worth mentioning, that some of the Gram-positive species, mainly *Corynebacterium*, *Nocardia*, *Rhodococcus*, were found to produce lipoglycans, whereas others, such as: *Bacillus*, *Clostridium*, and *Staphylococcus* produce lipoteichoic acids, which have immunogenic properties similar to LPS (Sutcliffe, 1995).

Since then many research groups investigated biocompatibility of PHAs produced by gram positive bacteria. Obtained results confirmed high biocompatibility of these polymers to various cell lines *in vitro* as well as *in vivo* (Francis *et al.*, 2016; Bian *et al.*, 2012; Misra *et al.*, 2010; Valappil *et al.*, 2007).

1.8.6.2. Gram-negative bacteria

A lot of different Gram-negative bacteria are capable of production PHA. For efficient production of scl-PHAs, mainly *Cupriavidus*, *Azohydromonas* (previously classified as *Alcaligenes*) and *Burkholderia* species have been used. For example, *Azohydromonas lata* produced up to 88% dry cell weight of P(3HB) from various carbohydrates, such as: glucose, fructose and sucrose (Wang and Lee, 1997). On the other hand, *Burkholderia* sp. USM could synthesize up to 69 % of dry biomass of P(3HB) from fatty acids (Chee *et al.*, 2010). *Cupriavidus necator* seems to be the most universal strain, which can produce P(3HB) with high yield of up to 88.9% dry cell weight (dcw) from various types of carbon sources, such as CO₂, sugars, *n*-alkanoic acids and vegetable oils (Chakraborty *et al.*, 2009; Gomez *et al.*, 1996). Methylotrophs, are another group of bacteria, able to produce scl-PHAs from alcohols. For example, *Methylobacterium extorquens* utilises methanol to produce P(3HB) (46% dcw), whereas *Paracoccus denitrificans* produced up to 24% dcw of P(3HV) from *n*-pentanol (Mokhtari-Hosseini *et al.*, 2009; Yamane *et al.*, 1996). Methanol is a cheaper carbon source than sugar, therefore selection of methylotrophs can be an option towards reduction of the PHA production cost. However, optimisation studies are required to improve productivity and PHA accumulation rate within the biomass (Khanna and Srivastava, 2005).

Gram-negative bacteria are among the main producers of mcl-PHAs. Various *Pseudomonas* sp. are able to produce a range of mcl-PHA homopolymers as well as copolymers. The average level of polymer yield is around 30% dcw. However, some of the strains, such as *P. putida* mt-2, could produce up to 77 % dcw mcl-PHA from octanoic acid (Shahid *et al.*, 2013). Some *Pseudomonas* species, such as *P. marginalis*, *P. mendocina*, *P. putida* GPo1 and *P. oleovorans* synthesized scl-mcl-PHA copolymers, using a range of *n*-alkanoates and 1,3-butanediol as carbon sources (Lee *et al.*, 1995). The number of strains of *Pseudomonas putida* are able to convert very toxic pollutants containing aromatic compounds to mcl-PHAs (Nikodinovic *et al.*, 2008). Interestingly, *P.*

putida CA-3, *P. aeruginosa* PAO1, *P. frederiksbergensis* GO23, *P. putida* GO16 and *P. putida* GO19 could utilize crude pyrolysis products from a range of plastics for mcl-PHA production (Guzik *et al.*, 2014). PHA accumulation has been observed in Gram-negative bacteria from extreme environments, such as high salinity or high temperatures. For example, the thermophilic *Thermus thermophilus* HB8 utilised whey and produced 35% dcw scl-mcl-PHA copolymer at 70°C (Pantazaki *et al.*, 2009). The halophilic *Halomonas boliviensis* LC1 accumulated 56% dcw of P(3HB) from starch hydrolysate using 0.77M NaCl (Quillaguamán *et al.*, 2004). Application of extremophiles has several advantages such as lower sterility demand and there is no need for pre-treatment of waste effluents. Although, the Gram-negative bacteria represent a wide range of possibilities, the main concern is due to presence of LPS in the outer cell membrane, which may trigger an immunological response and exclude them from biomedical applications (Ray *et al.*, 2013). Endotoxins can be eliminated by repeated solvent extractions with oxidizing agents, like sodium hypochlorite. However, this will further increase the cost of PHA production (Wampfler *et al.*, 2010).

1.8.6.3. Archea

Archea are considered as extremophiles, which can survive in hot springs, salt lakes and oceans (Oren *et al.*, 2008). In *Archea*, only one group of species was found to be able to accumulate PHAs. Those are halophilic species, which require extremely high concentrations of sodium chloride, optimally 5% to grow (Danson and Hough, 1997). The main PHA producers from the *Archeabacteria* belong to the genera: *Haloferax*, *Halalkalicoccus*, *Haloarcula*, *Halobacterium*, *Halobiforma*, *Halococcus*, *Halopiger*, *Haloquadratum*, *Halorhabdus*, *Halorubrum*, *Halostagnicola*, *Haloterrigena*, *Natrialba*, *Natrinema*, *Natronobacterium*, *Natronococcus*, *Natronomonas*, and *Natronorubrum* (Han *et al.*, 2010). They can convert many carbon sources, such as: glucose, fatty acids and complex sources, like starch, biodiesel waste or vinasse (Hermann-Krauss *et al.*, 2013). The main polymers obtained belong to the scl-PHA family. Haloarcheal strains are able to produce homopolymers: P(3HB) and P(3HV) or copolymers containing 3HV and 3HB monomer units. Most of the strains accumulate PHA at a low content, up to 22% dcw. However, *Haloferax mediterranei* was reported as the best PHA producer, which is able to accumulate between 50 to 70% dcw (Bhattacharyya *et al.*, 2012). P(3HB)

production required phosphorus limiting conditions (Lillo and Rodriguez-Valera, 1990). Application of extremely halophilic strains is associated with several challenges including the fact that high salt concentration results in increased cost of the chemicals for media preparation as well results in the corrosion of stainless steel fermenters (Quillaguamán *et al.*, 2010). On the one hand, the risk of contamination is very low, therefore, the costs related to sterilisation can be excluded. Another very interesting aspect is related to polymer recovery. The huge advantage of usage of haloarcheal strain is the ability of the cells to lyse in distilled water and release PHA granules, which can be separated by centrifugation (Chen *et al.*, 2010). This will have a meaningful impact on the reduction of extraction costs as well as make the recovery process simple, solvent free and more ecologically friendly (Poli *et al.*, 2011).

1.8.6.4. Mixed microbial cultures (MMC)

One of the approaches to lower the production cost of PHAs is an application of defined or undefined co-cultures, which contains two or more microorganisms. “Defined” means selected deliberately, according to the targeted outcomes. Presence of an additional strain may lead to the utilisation of more complicated carbon sources, including a mixture of different chemical compounds, which can be toxic or has an inhibiting effect on a single microbial culture. Co-cultures have been successfully applied for PHA production. For example, Nikodinovic and co-workers reported bioconversion of pyrolysis oil into PHAs by three different strains of *Pseudomonas putida*. This carbon source contained mainly a mixture of aromatic compounds, such as: ethylbenzene, toluene, xylene and styrene. Each of the strains was able to utilise only one of the chemical compounds listed above. Overall, higher biomass was obtained and polymer yield was similar to one obtained from the best monoculture. A single bacterial strain used with such complex carbon sources may lead to inhibition of growth of the strain which is not able to utilise a particular carbon source (Nikodinovic *et al.*, 2008). Another approach was used by Ganduri and co-workers, who used co-cultures for P(3HB) production. In this system, one organism was used to convert the carbon source to a product, which was then used by the second strain to produce PHAs. For example, *Lactobacillus delbrueckii* and *Lactobacillus lactis* were used to convert sugars to lactate, which was easily used by *Cupriavidus necator* for P(3HB) production (Ganduri *et al.*,

2005). There was also a trial to moderate biogas, obtained from anaerobic digesters to aerobic PHA production. Preliminary results looked promising, however, this concept still needs further validation (Ha *et al.*, 2012). There are a lot of challenges associated with mixed cultures. One of the challenges is connected to ensure right fermentation parameters, which will result in efficient conversion of the carbon source into PHAs. Sometimes two different types of bacteria require opposite conditions of oxygen supply. Therefore, selection of the right bioreactor design is crucial. Another challenge applies to harvesting and separation of PHA-producers from non-PHA-containing biomass. Extraction of the polymer from both fractions would increase the cost of polymer recovery. Two-stage fermentation systems would be ideal; however, this will further increase production costs (Tan *et al.*, 2014).

Several wild-type bacteria have been previously investigated for the biosynthesis of scl-mcl-PHAs including *Rhodospirillum rubrum*, *Rhodocyclus gelatinosus* and *Rhodococcus* sp. Due to the poor yield of polymers using wild type bacteria, some recombinant strains, such as *Cupriavidus necator*, *Aeromonas hydrophila*, *Pseudomonas putida* or *Escherichia coli* have been used for PHA production (Bhubalan *et al.*, 2010).

1.8.7. Polyhydroxyalkanoate recovery

PHAs accumulate as insoluble granules inside bacterial cells. Polymer can be recovered from the biomass by a process called extraction. The polymer recovery process contains a few steps, which are: polymer extraction, purification, concentration and precipitation. Depending on the method used, the order might change.

The extraction methods, commonly used can be divided into four main groups, such as: solvent extraction, chemical digestion, enzymatic-based digestion or combination methods. Among all of them, solvent extraction is the most commonly used to obtain polymer with high purity. Few solvents, such as: chloroform, 1,2-dichloroethane, propylene carbonate and methylene chloride were studied (Muhammadi *et al.*, 2015). It is worth to mention, that in contrast to mcl-PHAs, scl-PHAs are not soluble in acetone. This solvent can be used to separate the two types of polymers (Yao *et al.*, 1999). Usually, solvent extraction of PHAs occurs due to increased permeability of the membrane by the solvent along with simultaneous dissolution of the polymeric granules

(Kunasundari and Sudesh, 2011). During the extraction step the biomass is treated with solvents for a specified period of time. Cell walls become disrupted, which allows the solvent to penetrate inside the bacterial cells and dissolve polymer granules. During the purification step, debris are separated from the polymer solution either by centrifugation or filtration. The polymer solution is then concentrated by evaporation and precipitated in the ice-cold ethanol, methanol or a mixture of both to obtain the pure polymer.

However, it was observed that solvent extraction in mcl-PHAs resulted in a significant reduction of molecular weight (Ramsay *et al.*, 1994). A novel method for scl-PHA extraction was established by Koller and co-workers, who used the “anti-solvent” acetone under increased temperature and pressure in a closed system, resulting in the recovery of scl-PHAs with similar purity to other established methods. Volatile liquids, such as an acetone along with alcohols and other low molecular ketones were found to be called “scl-PHA anti-solvents” and used at temperature above boiling point and pressure of 7bar. Acetone as a solvent, presented many advantages such as recyclability, affordable price, low impact on molecular weight, suitability for extraction. Special equipment, containing two closed vessels with filtration unit was designed. The main advantage of this method is short time (20 minutes), possibility of solvent recycling and high purity of the product (Koller *et al.*, 2013). In the chemical digestion method sodium hypochlorite was used to dissolve biomass. PHA granules are separated from debris by centrifugation. This method is simple; however, it is well known that polymers recovered by chemical digestion have lower molecular weight in comparison to other extraction methods due to polymer degradation (Berger *et al.*, 1989). To overcome this limitation, sodium hypochlorite can be mixed with chloroform, which can protect the polymer from degradation by sodium hypochlorite (Hahn *et al.*, 1994). Enzymatic digestion requires more gentle conditions than the other two methods. A cocktail of enzymes, containing proteases, nucleases and lysozymes along with detergents, like for example SDS, have been used to eliminate all non-PHA parts of the biomass. PHAs are concentrated through crossflow filtration (Koning *et al.*, 1996). Yang and co-workers reported application of another type of detergent, called linear alkylbenzene sulfonic acid as an alternative to SDS. This resulted in significant reduction (80%) of the amount of required detergent in comparison to SDS. However, the drawback of this method was the amount of polymer

accumulated inside the cells. This method was efficient in the biomass containing larger amounts of PHAs (Yang *et al.*, 2011). The main disadvantage of the chemical methods is a large amount of surfactant-containing wastewater. Moreover, the molecular weight loss in enzymatic digestion is negligible. This method offers a number of advantages, such as lower health risk, easy and more environmentally friendly. However, high price of enzymes, make this process less attractive (Kapritchkoff *et al.*, 2006).

Supercritical CO₂ mixture with other solvents can be applied to recover highly pure PHAs from biomass. This method has been used in industry for extraction of fragrances and caffeine or removal of residual solvents from pharmaceutical products. In combination with other solvents, like for example: ethyl acetate, hexane, THF, methylene chloride and acetylene dichloride, supercritical CO₂ can be used to extract PHAs with a high yield and purity, which might be useful in the reduction of impurities caused by the endotoxin from genetically modified *E. coli* (Williams *et al.*, 1999).

Recently, novel biological methods for P(3HB) recovery have been developed. Biological methods are based on the consumption of dried bacterial biomass by insects or animals. PHA granules were excreted by animals and purified. These methods eliminate usage of hazardous solvents. However, this type of polymer recovery at the industrial scale still has to be confirmed (Kunasundari *et al.*, 2017; Murugan *et al.*, 2016).

1.8.8. Economical production of Poly(3-hydroxyalkanoates)

The main problem associated with large scale production of PHAs is their high cost (Castilho *et al.*, 2009). The carbon source is known as the main contributor in the high price of polyhydroxyalkanoates. The cost of PHA production has been estimated by Lee (1996) as 3–4 US\$/kg, which is 5-10 times more expensive than traditional plastics (Lee, 1996). Production cost of 1kg of polypropylene costs less than a dollar (Suriyamongkol *et al.*, 2007). Over 50% of the total cost of PHA production is the carbon source, used in large quantities during the fermentation process. Various strategies have been explored in order to lower the price and make the whole process more efficient. This includes: using cheap carbon sources, design of genetically engineered strains, enhancement of downstream and upstream processes (Kosseva and Rusbandi, 2018; Singh *et al.*, 2015; Luckachan and Pillai, 2012; Chen, 2009).

1.8.8.1. Cheap carbon sources suitable for PHA production

Cheap carbon sources can be divided into few groups. One of them are molasses, such as sugarcane, sugarbeet and soy molasses. Sugarcane molasses have been used for PHA production. For example, Akaraonye *et al.*, reported successful production of P(3HB) by *Bacillus cereus* SPV and sugarcane molasses. The obtained polymer yield was over 61% dcw in the shaken flasks (Akaraonye *et al.*, 2012). In another report, *Bacillus megaterium* was able to produce P(3HB) from molasses in shaken flasks with a polymer yield of 46.2% dcw (Gouda *et al.*, 2001). Additionally, some recombinant strains, like for example *A. vinelandii* UWD mutant and *E. coli* were able to accumulate PHAs when sugar molasses were used as the carbon source (Liu *et al.*, 1998; Chen *et al.*, 1997). However, the problem associated with general applicability of molasses is related to the downstream decolourisation process. This creates extra cost which diminishes the positive impact on the PHA cost reduction (Chanprateep, 2010). The second group include whey and its hydrolysates, like for example: hydrolysed soy and malt, hydrolysed whey and whey (Koller *et al.*, 2005). Starches are commonly available and are cheap carbon sources. However, most of the bacterial strains were not able to grow on raw starch. It requires further processing, which increases the price of the carbon source. Haas *et al.*, reported high productivity of P(3HB) from saccharified potato starch using *Ralstonia eutropha* (Haas *et al.*, 2008). In another study, Kim and Chang studied various modes of fermentation using *Azotobacter chroococcum* and starch. They obtained the highest yield 74% dcw P(3HB) yield from the shaken flask culture. Oxygen limitation was required to obtain high polymer accumulation (Kim and Chang, 1998). Another group of raw materials to be considered are lignocellulosic raw materials, like: wood, xylose, hemicellulosic hydrolysates, wheat bran (Tamer *et al.*, 1997). Another group of sources of carbon include fats, waste cooking oils and vegetable oils (Solaiman *et al.*, 2006). Several research groups have focused their work on the PHA production from vegetable oils. Especially, *Pseudomonas* species are able to utilise oils and fatty acids for mcl-PHA production. In another study, wild and recombinant *C. necator* were successfully used for efficient PHA production from soybean oil with the final polymer yield above 70% dcw (Kahar *et al.*, 2004). Hassan *et al.*, reported production of PHAs from palm oil by *Rhodobacter sphaeroides* with 67% dcw polymer content (Hassan *et al.*, 1996). Glycerol

from the production of biodiesel is another potential cheap carbon source for PHA production (Baei *et al.*, 2009). Cavalheiro and co-workers reported P(3HB) production from waste glycerol using *C. necator*. The polymer productivity achieved was 1.1g/L and the final yield obtained was 50% dcw (Cavalheiro *et al.*, 2009). In another study, Mozumber *et al.*, reported efficient PHA production and obtained 63% dcw PHA yield by using a three-stage fermentation (Mozumber *et al.*, 2014). An industrial and domestic wastewater were used for economical production of PHAs (Shamala *et al.*, 2012). Few reports demonstrated successful utilisation of wastewater for PHA production. For example, Martinez *et al.*, worked on the production of PHAs from *C. necator* and treated olive mill wastewater and obtained a yield of 55% dcw with 11% of HV monomer (Martinez *et al.*, 2015). Khardenavis *et al.*, obtained 67% dcw PHA accumulation from a mixed culture fed with wastewater derived from rice grain distillery (Khardenavis *et al.*, 2007). Another group of potential carbon sources are agricultural waste, such as: harvestable parts of plants, plant extracts, flower and fruit extracts (Aditi *et al.*, 2015). Koller and co-workers included vinegar waste, food waste, plastic waste and landfill gas as a potential carbon source for PHA production (Koller *et al.*, 2010). However, the lignocellulosic materials require additional treatment, which result in the hydrolysis and sugar monomer formation. Cesario *et al.*, reported 72% dcw PHA accumulation by using *Burkholderia sacchari* DSM17165 from wheat straw hydrolysate (Cesario *et al.*, 2014). Although various carbon sources have been investigated in order to reduce the cost of PHA production, the golden standard for an ideal cheap carbon source has not yet been discovered. Most of the cheap carbon sources require additional processing, which involves expensive enzymes and raises the price of the substrate. In addition to this, further purification of the polymer might be required to avoid presence of any potential contaminants originating from the carbon source, which further increases the production cost (Nor Aslan, *et al.*, 2016).

1.8.8.2. Genetically engineered strains

The cost of PHA using the natural producer, wild type strain *A. eutrophus* was calculated to be within the range 15–30.00\$ per kg (Zinn *et al.*, 2001) which is 18 times more expensive than polypropylene. However, the use of recombinant *E. coli* as a producer of PHA, can lower price to 4.00\$ per kg, which is similar to PLA or other polyesters. The

price of PHAs should not exceed 5.00\$ per kg in order to be economically viable (Lee, 1996).

Development of novel genetically engineered strains is one of the strategies to increase polymer accumulation within the biomass and reduction of total PHA production costs. Engineered *Halomonas*, which overexpress a cell division inhibitor protein MinCD, are able to obtain higher P(3HB) yield and facilitate downstream processing, which reduces the production cost (Tan *et al.*, 2014). Liu and co-workers suggested engineering strains towards higher tolerance of wider range of carbon sources (Liu *et al.* 2014). Using of recombinant *E. coli* gives higher level productivity and high cell density fermentation (Bhatia *et al.*, 2015). Deletion of genes of *E. coli*, such as deletion of *mtgA* and *mreB* improve the production of PHAs thanks to increasing the volumetric capacity of the bacterial cell (Kadoya *et al.*, 2015). Zhang *et al.*, reported construction of an *E. coli* strain, able to produce PHA and succinate by overexpressing the *phaC1* gene from *P. aeruginosa*. This resulted in the production of an mcl-PHA copolymer, containing 3HO and 3HD units, when glycerol, glucose and fatty acids were used as a feedstock (Zhang *et al.*, 2010). Povolito *et al.*, cloned the *E. coli lac* genes along with the PHA depolymerase gene and introduced it into *C. necator*. This resulted in a recombinant strain which was able to grow on waste material with lactose and produced PHAs in higher yield than wild type *C. necator* (Povolito *et al.*, 2010).

PHA synthase, PhaC, is the key enzyme used for the polymerisation of PHAs. Many *phaC* genes have been cloned and resulted in an enhancement of PHA production (Lane and Benton 2015). The modified strain *Rhodospirillum rubrum*, which overexpressed *phaC* genes achieved higher productivity in comparison to the control wild type strain (Jin and Nikolau 2014). Moreover, the *phaC1* gene can be engineered into yeasts, like *Yarrowia lipolytica*, which can result in obtaining precursors for PHAs production. Yeasts are not able to produce PHAs naturally due to the lack of expression of internal PHA synthase. However, they can produce PHA precursors (3-hydroxy-acyl-CoA) as a result of β -oxidation of fatty acids, which can be used as substrates for mcl-PHAs production (Gao *et al.* 2015). Application of highly active synthases can increase polymerisation activity and hence the amount of polymer accumulated inside the bacterial cell within the same period of time. For example, highly active PhaC from *Chromobacterium* sp. USM2 has 8 times more polymerisation activity than the synthase from *C. necator* (Bhubalan *et al.*,

2010). Engineering by changing metabolic pathways is an efficient way to improve PHA productivity. Several metabolic pathways for PHA production have been discovered and described previously in the section 1.9.5. Zhang and co-workers reported combined engineering of serine-deamination pathway and the Entner-Doudoroff (ED) pathway and expressed these in *E. coli*. However, this resulted in excessive accumulation of pyruvate. Therefore, further improvement was made by overexpressing the pyruvate-dehydrogenase complex in order to overcome this limitation. As a result, they obtained enhanced P(3HB) production in *E. coli* from different carbon sources, such as glucose, xylose and glycerol. A large number of research groups have dedicated attention to design bacteria that are able to produce PHAs by both the pathways mentioned above (Zhang *et al.*, 2013). Apart from enhancement of polymer production, manipulation in metabolic pathways can result in obtaining novel types of PHAs with additional desirable properties (Escapa *et al.*, 2011).

1.8.8.3. Optimisation of polymer recovery – downstream processes

PHA granules are hydrophobic, soluble in a range of organic solvents. The traditional approach towards polymer recovery from biomass requires large amounts of toxic solvents, such as chloroform, methylene chloride or acetone, which raise the total cost of the final product (Naranjo *et al.*, 2013). Dimethyl carbonate, named “green solvent”, can be used as a substitute to traditional solvents and effective for the PHA extraction from mixed culture (Samori *et al.*, 2015). Ideally, extracellular secretion of PHAs, which will eliminate the need for separation and purification, can reduce costs significantly. Rahman and co-workers used recombinant *E. coli* to exhibit favourable P(3HB) secretion, hence contribute to the reduction of downstream costs. They developed a system to secrete P(3HB) by using phasins, low molecular weight structural proteins, which bind to the surface of P(3HB) granules. In general, Gram-negative bacteria are able to export compounds by six secretory pathways (Desvaux, *et al.*, 2009). However recombinant proteins can be targeted to type I or II secretory pathways. Type I secretory pathway can translocate proteins up to 900kDa from cytoplasm to extracellular medium in Gram-negative bacteria without protein-periplasm interplay (Mergulhão *et al.*, 2005). Translocation of PHB granules is possible after reduction of the granule size.

Overexpression of phasins, which bind into PHB result in efficient decrease in the size of the PHB granules. Rahman and co-workers demonstrated successful indirect secretion of PHB and phasin PhaP1 from *E. coli* by using signal peptide HlyA via type I secretory pathway. Development of a secretion mechanism will simplify the polymer recovery system by elimination of cell disruption steps involved in the extraction process (Rahman *et al.*, 2013).

1.8.8.4. Efficient fermentation strategies – improvement in upstream processes

Production of PHAs can be improved by improving the fermentation process. PHA biosynthesis involves several variables, such as type of carbon source, temperature, pH, precursor supply, air supply, harvesting time and stirrer speed. Therefore, optimisation of fermentation kinetics has an impact on PHA production. For example, Chen and co-workers, optimised fermentation by mixing cultures, feeding strategies and applied constant pH control over the time of fermentation (Chen *et al.*, 2015). Lack of oxygen in the environment resulted in improved PHA production (Davis *et al.*, 2015). Fermentation strategy plays a very important role in the PHA production. For example, continuous fermentation offers better results in terms of the obtained biomass and polymer productivity as compared to batch cultivation (Amulya *et al.*, 2015; Marang *et al.*, 2014). Koller and Braunegg, 2015 studied a multistage system, containing series of connected continuous bioreactors in order to obtain novel materials with higher polymer productivity. This system will allow production of novel copolymers, containing blocks or larger number of different monomer units to meet the market demands for the material with specific properties (Koller and Braunegg, 2015).

1.8.9. Synthesis of PHA blends and composites

Physical blending with particles or other polymers in the most common approach in order to overcome or improve some of the properties of the materials, such as brittleness in case of scl-PHAs. For example, inorganic particles have a positive impact on toughness and processability of scl-PHAs by decrease in spherulite size and enhancement in nucleation density (Ding *et al.*, 2011). Many different particles were introduced to PHAs, such as of tungsten disulphide inorganic nanotubes, boron nitride,

talc, hydroxyapatite, bioglasses, carbon nanotubes and zinc stearate (Naffakh *et al.*, 2014; Wang *et al.*, 2010; Shan *et al.*, 2011). Organic particles might be introduced to PHAs, such as nano-cellulose, chitosan and bacterial cellulose nanocrystals (Martinez-Sanz *et al.*, 2014). Moreover, addition of nanoparticles, like for example titanium dioxide (TiO₂) or clay, can improve thermal stability of scl-PHAs (Wu *et al.*, 2008; Mook Choi *et al.*, 2003). Addition of reinforcing agents have a positive impact on mechanical properties. For example, P(3HB-co-3HV) and graphene nanocomposites presented significantly higher storage modulus as compared to neat P(3HB-co-3HV) (Sridhar *et al.*, 2013). Another example described addition of hydroxyapatite and silane-modified hydroxyapatite to PHBV and sample preparation by melt extrusion. As a result, the toughness as well as strength and stiffness of the material was improved (Oner and Idotlhan, 2016). Cellulose nanowhiskers were found to be very efficient reinforcing agents for PHBV. They promoted chain orientation and significantly improved tensile strength, Young's modulus value and storage modulus (Patricio *et al.*, 2013).

Blending scl-PHAs with other polymers has a practical and economic impact. This method is simple, quick and cost efficient. Interactions between component polymers within the blends create its miscibility. Usually blends of the polymers can have three different states of miscibility, which are either miscible, immiscible or partially miscible (Yu *et al.*, 2006). Good miscibility may result in uniform polymer blends with novel material properties (Tanadchangsang and Yu, 2013). Added polymers can be either biodegradable (e.g. PHAs, polycaprolactone (PCL), poly(lactic acid) (PLA), poly(butylene succinate) (PBS), poly(propylene glycol), lignin and plant fibers) or non-degradable (e.g. polystyrene, polymethyl methacrylate, polyurethanes) (Jian *et al.*, 2010; Ma *et al.*, 2014; Nagarajan *et al.*, 2013). Many research groups have focused their study on P(3HB)/PLLA blends. For example, Furukawa and co-workers studied P(3HB)/PLLA and P(3HB-co-3HHx)/PLLA blends. They found that both blends were immiscible. However, blends containing P(3HB-co-3HHx) copolymer with PLLA were more compatible. Analysis of the cold crystallisation temperature proposed mixed semicrystalline structure of both developed PHAs/PLLA blend materials described above. PHA copolymers when present within the PLLA matrix in low concentration did not crystallise (Furukawa *et al.*, 2007). Interestingly, blends of P(3HB) with PDLLA prepared at room temperature were immiscible. But the same blends produced at high temperature demonstrated some

level of miscibility. Addition of PDLLA significantly affected the behaviour of P(3HB). A significant decrease of melting temperature and crystallinity of P(3HB) were observed. A slight improvement in the mechanical properties in elongation at break was achieved in comparison to neat P(3HB) (Zhang *et al.*, 1996). Park and co-workers studied the influence of the molecular weight of P(3HB) and monoaxial drawing at glass transition temperatures of the dominant compound in the blend with PLLA on the properties of the materials. Commercially available bacterial origin P(3HB) as well as ultra-high molecular weight P(3HB) obtained from recombinant *E. coli* were used with PLLA. Both systems were immiscible. In the system with commercial P(3HB) dominated blends improvement in the mechanical properties was observed. PLLA played a reinforcing role in this blend, which allowed good interaction between both polymers, which resulted in an increase in the mechanical properties, such as tensile strength and Young's Modulus. Blends based on ultra-high molecular weight P(3HB), the mechanical properties were significantly improved due to the orientation of PLLA chains achieved during the cold drawing as a result of interphase tangling of very long polymeric chains (Park *et al.*, 2004). P(3HB) was also mixed with other PHAs to enhance the properties. Addition of P(3HO) resulted in obtaining an immiscible system and phase separation, which has a negative impact on the mechanical properties of the blend (Dufresne and Vincendon, 2000). In another example, P(3HB) was mixed with P(3HB-co-3HV) copolymer, containing various amounts of the 3HV unit. It was found that increased amount of the 3HV unit resulted in a higher degree of phase separation and weaker miscibility between both components. To obtain co-crystallisation between two or more compounds, certain criteria need to be met including, miscibility at the melt stage, similar crystalline structure and crystallisation rates. In all blends, there is a competition between phase separation and cocrystallisation. Good miscibility prevents phase separation, which allows to meet requirements for cocrystallisation (Saito *et al.*, 2001).

There was also work on the blending of starch and P(3HB) in order to fabricate miscible blends. The blend was compatible, which was confirmed by DSC analysis, i.e. only one glass transition temperature was detected. The optimal amount of starch required to maintain the mechanical property was found to be 30 wt%. Results demonstrated enhanced properties of the blend in comparison to neat P(3HB) as well as a cost reduction, since starch is one of the cheapest biopolymers (Godbole *et al.*, 2003).

The main problem associated with blending is miscibility between the components. Therefore, a lot of different types of compatibilizers, like oxidized polyethylene wax (OPW) have been used to overcome this limitation (Rosa *et al.*, 2007). Another type of material, such as wood flour, tannic acids and plant polyphenols were used to improve mechanical properties of scl-PHAs (Jandas *et al.*, 2013; Gregorova *et al.*, 2009). For example, lignin powder was added to P(3HB) as a nucleating agent. Addition of lignin resulted in reduction of the half-time for crystallisation, but did not change structure of crystals and crystallinity degree. The results obtained confirmed the application of lignin as a proper nucleating agent for the crystallisation of P(3HB) (Weihua *et al.*, 2004).

1.8.10. Applications of PHAs

Due to its characteristics, biodegradable PHAs can be used in a variety of applications including medicine, pharmacy, implants, packaging, chemical industry, food industry, industrial microbiology, cosmetology, agriculture and photography (Ray and Kalia, 2017; Chen, 2010; Ojumu and Solomon, 2004; Thakor *et al.*, 2006). In this thesis, we will focus on the biomedical applications of PHA.

1.8.10.1. Biomedical applications

One of the greatest potential of PHAs is related to the area of medicine, which includes wound management, nerve regeneration, drug delivery system, stents, repair of soft tissue and hard tissue and heart tissue engineering (Misra *et al.*, 2010).

Tissue engineering

The main aim of tissue engineering is to provide products, which can restore, maintain and improve function of injured, diseased or replaced organs, tissues or cells (Langer and Vacanti, 1993). The main approach is to use either biomaterial scaffolds, promoting cell attachment and proliferation; infusion of isolated cells or the combination of both, which is implantation of polymeric scaffolds seeded with special type of cells, depending

on the application (Bettinger, 2009). Tissue engineering scaffolds are designed to provide a support structure for the engineered tissue. Rejection of the implant can be minimized by using autologous cells, and or by administering immunosuppressive drugs (Bell *et al.*, 1981). The properties of the materials for scaffolds in tissue engineering have been already specified by Knight and Evans, 2004. They have to meet certain requirements, such as non-toxicity and high biocompatibility and should be non-carcinogenic. Apart from this they have to be able to be sterilised, deployed by the surgeon, have appropriate mechanical properties and topography which will allow cell attachment and proliferation as well as be able to incorporate drugs and other bioactive molecules, such as growth factors, peptides and antibodies (Ravichandran *et al.*, 2012; Knight *et al.*, 2004).

PHAs have been intensively investigated for biomedical applications. The properties of PHAs can be tailored by adding different types of blocks, various treatments can be performed on the surface to allow the attachment of bioactive agents. Apart from that, scaffolds can be fabricated by a broad range of techniques, which allows the production of the appropriate design suitable for the specific application (Williams *et al.*, 1999). PHAs, its blends and composites have been used for the production of sutures, tacks, staples, screws, bone plates, surgical meshes, repair patches and orthopaedic pins (Dai *et al.*, 2009). Also, several medical devices, such as: stents, nerve conduits, artificial cartilage, wound dressing, artificial skin and drug delivery carriers have been developed using PHAs (Bian *et al.*, 2009; Wang *et al.*, 2008). Rai *et al.*, 2011, reported development of scaffolds based on P(3HO) homopolymer for soft tissue engineering. Material supported attachment and proliferation of human adult low calcium temperature keratinocytes (HaCaT). This study demonstrated suitability of mcl-PHA scaffolds for wound healing applications (Rai *et al.*, 2011). PHA based blends were also considered for various biomedical applications. For example, Basnett *et al.*, 2013 reported development of P(3HO)/P(3HB) blends for biomedical applications. Addition of P(3HB) resulted in the significant improvement of mechanical properties, such as tensile strength and Young's Modulus and the protein adsorption to the surface in comparison to neat P(3HO). Material was considered as highly biocompatible and suitable for various types of medical applications (Basnett *et al.*, 2013). In another study, Lizarraga-Valderrama *et al.*, 2015, demonstrated development of P(3HB)/P(3HO) blends for

peripheral nerve regeneration. Blends with 75 wt% of P(3HB) resulted in significantly higher compatibility to NG108-15 neuronal cells, especially in the context of neurite extension. Therefore, this composition was recommended as potential candidate for nerve conduit in peripheral nerve repair (Lizarraga-Valderrama *et al.*, 2015). Many different types of PHA based composites have been developed for bone tissue engineering. Changing mechanical and topographical properties by addition of other materials have allowed them to be used in a variety of applications. Misra *et al.*, 2010, demonstrated suitability of P(3HB)/BioglassTM composites containing carbon nanotubes as a functional scaffold material for bone tissue engineering (Misra *et al.*, 2010a). In another study Misra *et al.*, reported the development of 3D highly porous P(3HB)/bioglass composite foams for bone tissue engineering. This novel material demonstrated antimicrobial properties against *Staphylococcus aureus* due to the presence of bioglass. Addition of carbon nanotubes induced electrical conductivity. Obtained 3D scaffold allowed vascularisation in the animal model (Misra *et al.*, 2010b). Recently, Akaraonye *et al.*, 2016 reported results on two types of P(3HB) magnetic nanocomposites, containing either magnetic nanoparticles or ferrofluid as smart materials for bone regeneration. Presence of magnetic particles or ferrofluid resulted in enhanced Young's Modulus values and crystallinity. Moreover, scaffolds demonstrated higher biocompatibility to MG-63 cells in comparison to neat P(3HB) and tissue culture plastic. Hence confirm suitability for bone tissue repair (Akaraonye *et al.*, 2016a). In another study, Akaraonye *et al.*, used P(3HB) with microfibrillated bacterial cellulose for articular cartilage regeneration, especially in load bearing joints. The developed 3D scaffolds had high porosity and surface area. The scaffolds demonstrated similar topography to the extracellular matrix and exhibited high biocompatibility towards chondrogenic ATDC5 cells (Akaraonye *et al.*, 2016b). Cheng *et al.*, demonstrated that P(3HB) promoted proliferation of L929 cells by preventing apoptotic and necrotic cell death. This can be useful in the applications, that require regeneration of the large amounts of cells. In another study, they confirmed that P(3HB-co-3HHx) copolymer microparticles also promoted L929 cell proliferation (Cheng *et al.*, 2006).

Cardiovascular tissue engineering

Cardiovascular tissue engineering includes blood vessels regeneration, valves development, heart patch development and coronary stent development. Biomaterials used routinely in cardiovascular tissue engineering include: polymers, such as polylactic acid, polyglycolic acid and hydrogels, like collagen, fibrin and hyaluronic acid (Truskey, 2016). PHAs have also been considered for these applications. For example, Poly(3-hydroxybutyrate) has been studied for cardiovascular applications. Although it belongs to scl-PHA, containing strong and stiff materials, it demonstrated promising results for application in cardiac regeneration or vascular repair. One of the first reports about potential application of P(3HB) as a patch for pericardium regeneration was published in 1992 by Malm and co-workers. After 24 months, the polymer was still present in the sheep model P(3HB) was not found to enhance platelet aggregation (Malm *et al.*, 1992). Two years later the same group studied P(3HB) transannular patches in animal models. Although many macrophages were present, P(3HB) did not accelerate platelet aggregation. Moreover, the regenerated vessel demonstrated similar functionality to the native pulmonary artery (Malm *et al.*, 1994). The P(3HB-co-3HV) copolymer was used along with polylactic acid and polyglycerol sebacate to form fibre sheets as a pericardial patch for myocardium repair. These electrospun fibres were also successfully used to fabricate porous tubing for pericardium repair (Kenar *et al.*, 2010). Badgadi *et al.*, reported various types of cardiac patches based on the neat P(3HO). It was observed, that incorporation of fibres or porosity enhanced cell attachment and proliferation. Therefore, P(3HO) based constructs can be considered as a strong candidate for cardiac tissue regeneration (Bagdadi *et al.*, 2017). In another experiment, P(3HO) was made in to 3D porous scaffolds and seeded with endothelial cells for replacement of the tricuspid heart valve. The seeded cells formed a confluent layer on the scaffold. (Sodian *et al.*, 2000a). Another polymer, Poly(4-hydroxybutyrate), which exhibits exceptional elastomeric properties in comparison to other members of the scl-PHA group was also used in cardiovascular tissue engineering. However, it has demonstrated rapid degradation *in vivo*, which limited its applicability in this area (Chen and Wu, 2005). However, P(4HB) was also used as a replacement of the pulmonary valve in an animal model. After 24 weeks, there was no stenosis or thrombosis observed. The results

obtained confirmed the suitability of this material for pulmonary valve repair (Stock *et al.*, 2000). In another study Sodian *et al.*, studied P(4HB) as a bulk material for heart valve fabrication. However, P(4HB) did not meet the requirements during *in vivo* study. The material had prolonged degradation rate, and was stable in the body environment, which led to incomplete replacement and could potentially cause side effects (Sodian *et al.*, 2000b). P(3HB-co-4HB) copolymer was used for the development of artificial blood vessels. The amount of elastin found in the animal model was 160% higher than the P(3HB-co-3HHx) studied previously for this application (Cheng *et al.*, 2008). Coronary stents are demanding medical devices, which require specific material properties. One of the very important factors to consider is the excessive vascular smooth muscle cell proliferation, which might be induced by injury to the vessel wall or insufficient re-endothelialisation. Application of suitable biopolymers can solve these problems. Ideal stent requirements were listed in the section 1.7. The stent should be stable inside the body, made from the non-immunogenic and non-toxic materials. The material should demonstrate high biocompatibility towards endothelial cells to reduce immunogenic response and the development of restenosis. Most of the tested biomaterials tested for coronary stent development demonstrated tissue incompatibility (Regar *et al.*, 2001). PHAs can be considered for this application. Various types of PHAs have been investigated for this application. For example, Basnett *et al.*, 2013 reported P(3HO)/P(3HB) blends for biomedical application, especially coronary artery stents. Blends demonstrated improved mechanical properties and enhanced biocompatibility in comparison to neat P(3HO) (Basnett *et al.*, 2013). Another example is the ReBioStent (2013-2016) Project, an European Union's Seventh Framework Programme (FP7). One of the main approaches of this project was to investigate the use of PHAs for the development of Reinforced Bioresorbable Therapeutic Drug Eluting Stents.

Drug delivery

Polyhydroxyalkanoates are considered as very attractive group of materials for drug delivery. This is due to their proven biocompatibility and material properties, such as degradation kinetics and non-toxicity. Moreover, PHAs as natural biopolymers are produced according to natural metabolic pathways without any additional chemical

catalysts, which usually are toxic and can contaminate the final polymer after chemical synthesis. Apart from that, PHAs demonstrate higher stereochemical purity as compared to synthetic materials, which can be produced as a mixture of both configurations and require additional separation after synthesis (Pouton and Akhtar, 1996). PHAs were considered as drug delivery vehicles for the first time in 1980s, when neat P(3HB) and P(3HB-co-3HV) copolymer were investigated as a vehicle for oral drug administration (Korsatko *et al.*, 1983; Gould *et al.*, 1987). Since then research in this area has progressed substantially. P(3HB) and PLA microspheres have been compared in order to release the anticancer agent, lomustine by Bissery *et al.*, 1985. It was found, that the amount of drug released from P(3HB) was higher, possibly due to greater porosity (Bissery *et al.*, 1985). Various polymers from the PHA family have been studied for controlled drug delivery, due to their diverse properties. PHAs degrade much slower than polylactides, therefore they can be successfully used for prolonged drug delivery (Gogolewski *et al.*, 1993). Also, material properties of the scl-PHAs allow formulation of microspheres and nanoparticles with encapsulated drugs. Various types of PHAs have been explored as a polymer matrix for different drug delivery devices. For example: *In vitro* release study of P(3HB-co-3HV) rods containing antibiotics, such as gentamycin or sulperazone demonstrated presence of drugs in the body within 2 weeks. P(3HB-co-3HV) copolymer, containing 20% 3HV within the monomer unit demonstrated controlled release of antibiotics for up to 60 days (Gurselt *et al.*, 2002). In another similar study, Rossi and co-workers obtained similar results. Higher amount of 3HV within the scl-PHA copolymer resulted in sustainable drug release for a longer period of time and the amount of released drugs were higher than in neat P(3HB). Moreover, the drug delivery systems were haemocompatible and did not induce any negative effect on the blood cells (Rossi *et al.*, 2004). Francis *et al.*, reported production of P(3HB) based microspheres and multifunctional scaffolds, microsphere/composite scaffolds with encapsulated gentamycin for bone tissue regeneration. Controlled slow release of the drug was achieved in the composite scaffold, whereas burst release of the same drug was observed from neat P(3HB) microspheres (Francis *et al.*, 2011; Francis *et al.*, 2010). Zinn *et al.*, 2001, demonstrated a rapid release of rifampicin and tetracycline encapsulated in neat P(3HB) microspheres. These results indicated the influence of the degree of crystallinity on the release kinetics. The PHAs with lower crystallinity were

more suitable for cumulative release profiles (Zinn *et al.*, 2001). P(3HHx-co-3HO), mcl-PHAs copolymer, was mixed with a polyamidoamine dendrimer to create drug delivery system for tamulosin, a drug used for treatment of benign prostate hyperplasia. This construct was found to enhance the release of the drug *in vivo* (Wang *et al.*, 2003). Also, P(3HB) microspheres, containing the anti-cancer drug, rubomycin, inhibited the proliferation of carcinoma cells in the mice model (Shishatskaya *et al.*, 2008). PHA granule binding proteins, called PhaP were used in the receptor-mediated targeted drug delivery system, containing PHA nanoparticles with hydrophobic drugs, PhaP and ligands linked to it. PhaP-PHA nanoparticles complex were transported to targeted cells, which were hepatocellular carcinoma cells. The ligand-PhaP-PHA drug delivery system demonstrated effectiveness *in vitro* as well as *in vivo* in the animal models (Yao *et al.*, 2008).

Hence, Polyhydroxyalkanoates are a group of biomaterials with very high potential towards biomedical applications. Their unique properties, such as high biocompatibility, biodegradability, non-toxicity and tuneable mechanical and thermal properties make them especially attractive for medical devices, such as coronary stents. Moreover, some PHA-based products have received the FDA clearance. For example, Tephaflex absorbable sutures, which is first PHAs-based medical device, made from P(4HB) gained FDA clearance in 2007. That was a mile stone in the use of PHAs in biomedical areas. In 2009 Aesculap AG received CE Mark for MonoMax monofilament absorbable sutures in Europe, made from Tephaflex fibers (Chen, 2009).

Aims and objectives

The main aim of this project was to obtain novel biomaterials, based on PHAs, using *Pseudomonas mendocina* CH50 and *Bacillus subtilis* OK2, suitable for medical device development with focus on coronary artery stents.

Specific objectives of this project were:

1. Production of the novel PHAs by using different bacterial strains and a range of various carbon sources and their characterisation.

Screening experiments were performed in order to obtain novel PHAs. The polymers produced were chemically characterised using Fourier Transform Infrared Spectroscopy (FTIR) and chemically identified using Gas Chromatography Mass Spectrometry (GC-MS). Selected materials were characterised further by Nuclear Magnetic Resonance (NMR) analysis. Thermal properties of the selected materials were studied using Differential Scanning Calorimetry (DSC) and mechanical properties were tested using tensile testing.

2. Development of novel, biocompatible and biodegradable P(3HB)/oligo-PHA blends.

Three different compositions of the blends of P(3HB)/oligo-PHA were studied with respect to their mechanical properties using tensile testing and thermal properties using DSC. In addition, the microstructural properties were investigated using Scanning Electron Microscopy (SEM), surface roughness analysis, protein adsorption and contact angle measurement. Thermal and mechanical properties were also studied during 7 weeks of storage at the room temperature in order to investigate the effect of ageing on the properties of the blends. Biocompatibility of these P(3HB)/oligo-PHA blends were tested using human dermal microvascular endothelial cells (HMEC-1). Haemocompatibility studies were also carried out to investigate the reaction of the blood cells after direct contact with the material.

3. Development of novel, biocompatible and biodegradable multifunctional 2D biodegradable P(3HB)/oligo-PHA composites with barium sulphate as a radiopaque agent.

A selected blend film composition P(3HB/oligo-PHA) 90/10 was mixed with different amounts of barium sulphate in order to obtain radiopaque composites. Materials were characterised with respect to their mechanical properties using tensile test, thermal properties using DSC and microstructural properties using SEM, MicroCT, protein adsorption and contact angle measurements. They were also characterised for their bioactivity using HMEC-1 cells to assess their suitability in the development of biodegradable stents. Direct and indirect cytotoxicity studies were performed. Haemocompatibility studies were carried out to investigate the reaction of the blood cells after direct contact with the material.

4. Manufacturing of the P(3HB)/oligo-PHA tubes by dip moulding technique.

P(3HB)/oligo-PHA 90/10 blend were selected for tube manufacturing by the dip moulding technique as a potential candidate for coronary stent application. Tubes were characterised with respect to the mechanical and thermal properties within 7 weeks of storage at room temperature in order to investigate the effect of ageing on the properties of the material. Tubes were also incubated in DMEM media at 37°C in order to mimic *in vivo* conditions and observe influence of the body environment on the material properties. In addition, microstructural studies were performed using SEM, microCT and protein adsorption studies. HMEC-1 were grown on the tubes to assess their biocompatibility to the developed biomaterial. Direct and indirect cytotoxicity studies were performed. Haemocompatibility studies were carried out to investigate the reaction of the blood cells after direct contact with the material. Degradation studies were also carried out to confirm suitability of the selected materials for coronary stent application.

5. Incorporation of the drugs, such as rapamycin or tacrolimus in the P(3HB)/oligo-PHA tubes coated with PCL-PEG550 as a platform material for development of drug eluting biodegradable stent.

P(3HB)/oligo-PHA 90/10 blend tubes were coated with PCL-PEG550 with incorporated rapamycin or tacrolimus ($1-1.5\mu\text{g}/\text{mm}^2$) and were characterised for their mechanical properties using tensile testing, thermal properties using DSC and surface properties

using SEM and microCT. Biocompatibility of these blend tubes containing drugs were investigated using HMEC-1 to investigate the effect of drug loading. Direct and indirect cytotoxicity studies were performed. Haemocompatibility studies were carried out to investigate the reaction of the blood cells after direct contact with the material. Degradation studies were also carried out to confirm suitability of the selected materials for coronary stent application. Drug release studies were carried out using High Performance Liquid Chromatography (HPLC) or UV-VIS for tacrolimus and rapamycin respectively.

Chapter 2

Materials and Methods

2.1. Materials

2.1.1. Bacterial strains

Various types of PHAs were produced by *Cupriavidus necator* (NCIMB 10442), *Pseudomonas mendocina* CH50 (NCIMB 10541), obtained from the National Collection of the Industrial and Marine Bacteria (NCIMB), *Bacillus cereus* SPV, obtained from the University of Westminster culture collection and *Bacillus subtilis* OK2, obtained from Prof. Fujio Kawamura, Department of Life Sciences, Rikkyo University. Strains cultures were stored on agar plates in the fridge at +4°C or as glycerol stock in the freezer at -80°C.

2.1.2. Cell line and cell culture materials

Human dermal microvascular endothelial cells (HMEC-1) were obtained from the University of Westminster's cell line collection.

2.1.3. Chemicals and kits

All the chemicals were purchased from Sigma-Aldrich (Dorset, UK) and VWR (Leicestershire, UK). Distilled water was used for all experiments. Cell culture media and other reagents were purchased from Sigma-Aldrich, Thermo Fisher Scientific (Dartford, UK) and Lonza (Basel, Switzerland). Live/Dead viability/Cytotoxicity Kit was purchased from Thermo Fisher Scientific (Dartford, UK) and PromoCell (Heidelberg, Germany). Protein estimation was done using the BCA estimation kit purchased from Sigma-Aldrich. Biodiesel waste was obtained from Dr. Godfrey Kyazze's lab at the University of Westminster (London, UK). Waste frying oil was obtained from Lion King Café (London, UK). FITC Mouse Anti-Human CD66b, PE Mouse Anti-Human CD11b, PE Mouse Anti-Human CD86, PerCP Anti-Human CD45 antibodies were purchased from BD Biosciences (San Jose, US). Haemocompatibility study was carried out by Dr. Jurcevic's lab at University of Westminster. Rapamycin was purchased from LC Laboratories (Woburn, USA). Tacrolimus was purchased from VWR (Leicestershire, UK). Suspension of BaSO₄ nanoparticles and isopropyl alcohol was provided by Lucideon Limited (Staffordshire,

UK). PCL-PEG550 block copolymer was synthesised by Vornia Biomaterials Ltd. (Dublin, Ireland).

2.2. Media composition

Various types of media compositions were used during this study as listed in the section below.

Nutrient Broth No 2 composition (Sigma Aldrich, UK)

Chemical compound	Amount (g/L)
Meat peptone	4.3
Casein peptone	4.3
Sodium chloride	6.4

Mineral Salt Medium (MSM) composition – second stage (Rai *et al.*, 2011):

Medium constituent	Concentration (g/L)
Ammonium sulphate	0.45
Sodium hydrogen phosphate	3.42
Potassium dihydrogen phosphate	2.38
Magnesium sulphate	0.40
Trace elements solution	1.0 mL

MSM media composition – production media (Tian *et al.*, 2000):

Medium constituent	Concentration (g/L)
Ammonium sulphate	0.50
Sodium hydrogen phosphate	3.80
Potassium dihydrogen phosphate	2.65
Magnesium sulphate	0.40
Trace elements solution	1.0 mL

CHAPTER 2

Composition of Trace elements solution (TES) (Rai *et al.*, 2011):

Constituent	Concentration (g/L)
CoCl ₂	0.22
CaCl ₂	7.80
FeCl ₃	9.70
NiCl ₃	0.12
CrCl ₃ ·6H ₂ O	0.11
CuSO ₄ ·5H ₂ O	0.16

List of carbon sources used for PHAs production with MSM media:

Carbon source	Concentration (g/L)	Bacterial strain
Glycerol	20	<i>Pseudomonas mendocina</i> CH50
Waste frying oil	20	<i>Pseudomonas mendocina</i> CH50
Sugarcane molasses	20	<i>Pseudomonas mendocina</i> CH50
Rapeseed oil	20	<i>Pseudomonas mendocina</i> CH50
Grapeseed oil	20	<i>Pseudomonas mendocina</i> CH50
Sunolive oil	20	<i>Pseudomonas mendocina</i> CH50
Sucrose, biodiesel waste	10; 20	<i>Pseudomonas mendocina</i> CH50
Lauric acid, 1,4-butanediol	10; 10	<i>Pseudomonas mendocina</i> CH50
Sucrose, γ-butyrolactone	20; 10	<i>Pseudomonas mendocina</i> CH50
Biodiesel waste	50	<i>Pseudomonas mendocina</i> CH50
Rapeseed oil, sucrose	10; 10	<i>Pseudomonas mendocina</i> CH50
Glucose, heptanoic acid	5; 0.3	<i>Pseudomonas mendocina</i> CH50
Sucrose, valeric acid	20; 1.0	<i>Pseudomonas mendocina</i> CH50
Sodium octanoate, hexanoic acid	2.5; 2.3	<i>Cupriavidus necator</i>
Rapeseed oil, fructose	10; 10	<i>Cupriavidus necator</i>
γ-butyrolactone	10	<i>Cupriavidus necator</i>
Sodium octanoate, γ-butyrolactone	3.34; 10	<i>Cupriavidus necator</i>

Modified Kannan and Rehacek (K-R) medium composition – production media

(Kannan and Rehacek, 1970):

Medium constituent	Concentration (g/L)
Ammonium sulphate	5.0
Potassium chloride	3.0
Yeast extract	2.5
Glucose	35.0

List of carbon sources used for PHA production with K-R media:

Carbon source	Concentration (g/L)	Bacterial strain
Fructose	20	<i>Bacillus cereus</i> SPV
Glucose	35	<i>Bacillus subtilis</i> OK2

2.3. Bioreactors

5 L Bioreactor

The 5 L bioreactor used in this study was a stirred tank with 2 Rushton turbine impellers and buffers. The vessel was a 320 series Fermac (Electrolab Biotech Ltd, Tewkesbury, UK) and total volume was 5 L (Figure 12). The working volume used in this study was 3.5L. The vessel temperature was controlled with a wrap-around heating belt. pH was controlled by Hamilton, EasyFerm Plus K8 120mm pH sensor. Dissolved oxygen tension (DOT) was controlled by Hamilton, OxyFerm K8 FDA 120mm dO sensor. The bioreactor sterilization was carried out in an autoclave at 121°C for 30 minutes.



Figure 12: The 5 L stirred tank bioreactor used in this study (Fermac 320, Electrolab Biotech Ltd).

15 L Bioreactor

15L bioreactor (Aplikon Biotechnology) was a stirred tank with 2 Rushton turbine and marine impellers with an outside diameter of 45mm, 60 mm 75 mm or 85 mm (Figure 13). The vessel was a single wall glass autoclavable bioreactor and total volume was 15 L. The working volume used in this study was 10L and the aspect ratio working volume was 1.5. The vessel temperature was controlled by Pt-100 sensor in thermo well in top plate and with a wrap-around heating jacket via bioreactor wall. The pH was controlled by 12 mm classic pH sensor AppliSens (Sensor Innovation). Dissolved oxygen tension (DOT) was controlled with 12 mm classic polarographic DO₂ sensor (AppliSens 425mm) (Sensor Innovation) electrodes. The optical density was measured online by non-invasive biomass monitor Bug Lab BE 2100. The process was monitored online using BioXpert software. The bioreactor sterilization was carried out in an autoclave at 121°C for 30 minutes.



Figure 13: 15L stirred tank bioreactor used in this study (Applikon Biotechnology).

20 L Stainless Steel Bioreactor

The 20 L bioreactor was a stirred tank with 2 Rushton turbine impellers and buffers. The vessel was a 420 FerMac series and total volume was 20 L (Figure 14). The vessel temperature was controlled with a standard Pt 100 temperature sensor. pH was controlled by Hamilton, EasyFerm Plus K8 325mm pH sensor. Dissolved oxygen tension (DOT) was controlled by stainless steel polarographic dO sensor, Hamilton, OxyFerm K8 FDA 325mm.



Figure 14: 20 L stirred stainless steel tank bioreactor used in this study (Electrolab Biotech Ltd).

2.4. Experimental methods

2.4.1. P(3HB) production by *Bacillus subtilis* OK2 and *Bacillus cereus* SPV using a range of carbon sources at shaken flask level.

The PHAs production using *B. subtilis* OK2 and *B. cereus* SPV strains was carried out using one-stage seed culture preparation (Valappil *et al.*, 2007). Sterile nutrient broth (10% of the final volume) was inoculated with a single colony of the bacterial strain taken from the agar plate and cultured for 16 hrs at 30°C at 150rpm in shaking incubator. The grown culture was then used for inoculating the PHA production media and incubated for 48hrs at 30°C at 150rpm (modified Kannan and Rehacek medium, (section 2.2.) After 48hrs, cells were harvested, centrifuged, washed with distilled water and homogenised for 10 minutes using T25 basic homogeniser (IKA Labortechnik). The obtained biomass was lyophilised. PHAs were extracted from lyophilised cells. Figure 15 shows a schematic representation of the steps involved in the production of PHAs from *Bacillus* sp.

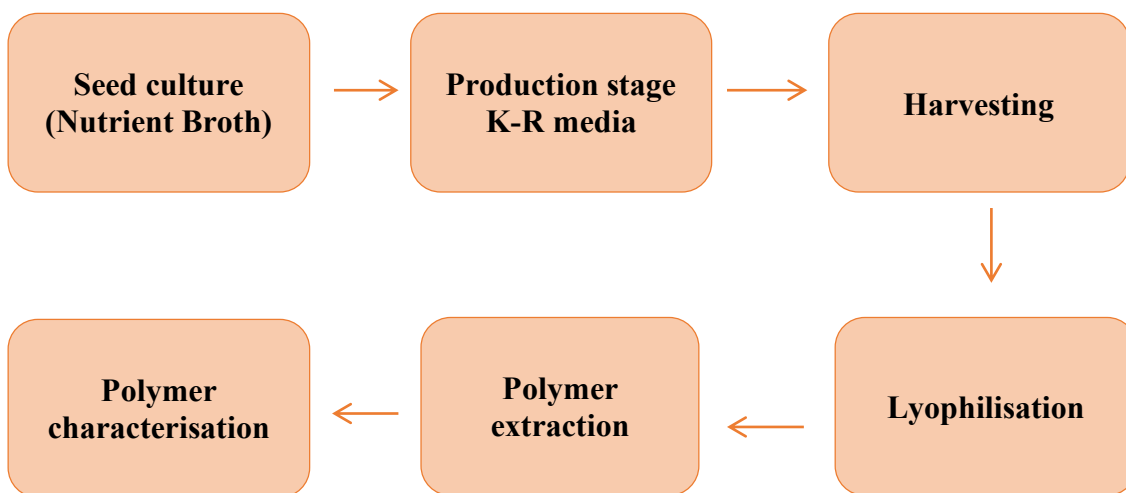


Figure 15: Schematic representation for the steps involved in the scl-PHAs production in using *Bacillus subtilis* OK2 and or *Bacillus cereus* SPV.

2.4.2. P(3HB) production by *Cupriavidus necator* using a range of carbon sources at shaken flask level

The PHA production using *C. necator* was carried out using a two-stage seed culture preparation used previously when culturing *Pseudomonas mendocina* CH50 (Rai *et al.*,

2011; Basnett *et al.*, 2013). Sterile nutrient broth (1% of the final volume of production media) was inoculated with a single colony of the bacterial strain taken from the agar plate. The culture in mid-log phase was then used for inoculating the PHA MSM second stage media (composition in section 2.2.). After 24 hours, second stage culture was used to inoculate production media (MSM, section 2.2.) and incubated for 48hrs at 30°C at 150rpm. After 48hr cells were harvested. The downstream process remained the same as described in the section 2.4.1. Figure 16 shows a schematic representation of the steps followed for PHA production using a two-stage culture and MSM media.

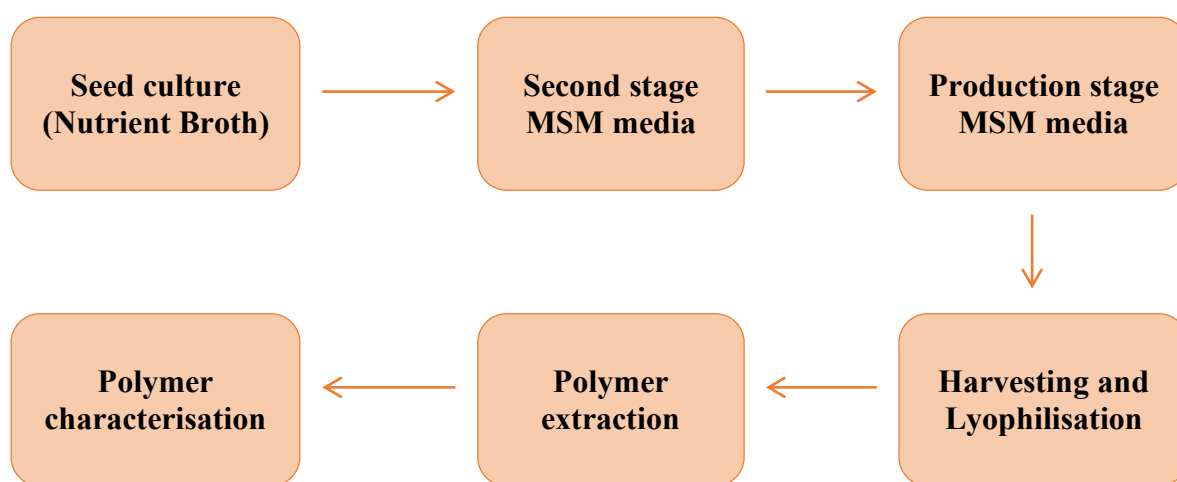


Figure 16: Schematic representation for of the steps involved in the PHAs production using *Cupriavidus necator* or *Pseudomonas mendocina* CH50.

2.4.3. Production of P(3HB) by *Bacillus subtilis* OK2 in bioreactor

The P(3HB) production was carried out in 5L and 20 L bioreactors. Bioreactors were sterilized with distilled water. K-R media salts and glucose were sterilised separately and added to the bioreactor aseptically. Sterile nutrient broth (10% of the final volume of production media) was inoculated with a single colony of *Bacillus subtilis* OK2 taken from the agar plate. The culture in mid-log phase was then used for inoculating the bioreactor. The air flow rate was set at 1vvm. The stirrer speed was set to 200rpm. pH was adjusted to 6.8 at the beginning of the fermentation. Bacteria were grown for 48 hours, at 30°C, 200rpm (Akaraonye *et al.*, 2010). The culture was harvested, centrifuged, washed twice

with water, homogenised and freeze-dried. Polymer was extracted by Soxhlet extraction (described in section 2.5.2.).

2.4.4. Production of mcl-PHAs by *Pseudomonas mendocina* CH50 using a range of carbon sources at shaken flask level

The mcl-PHA production using *P. mendocina* was carried out using a two-stage seed culture preparation as described in the section 2.4.2. Sterile nutrient broth (1% of the final volume of production media) was inoculated with a single colony of *P. mendocina* taken from the agar plate. The culture in mid-log phase was then used for inoculating the PHA MSM second stage media (composition shown in section 2.2.) and grown at 30°C, 200 rpm for 24 hr. Obtained second stage culture was used to inoculate production media (MSM, table in section 2.2.) and grown at 30°C, 140rpm for 48 hours (Rai *et al.*, 2011; Bagdadi *et al.*, 2017). The volume of the seed culture used was 10 % of the final working volume of the production media. After 48hrs cells were harvested and the downstream process remained the same as described in the section 2.4.2.

2.4.5. Production of mcl-PHAs in bioreactors

The mcl-PHA production was carried out in 5L and 20 L bioreactors. Bioreactors were sterilized with distilled water and waste frying oil. MSM salts, magnesium sulphate were sterilised separately and added to the bioreactor aseptically. Trace elements solution was filtered through 0.22µm filters and added to the bioreactor before the inoculation. The bioreactor was inoculated with second stage seed inoculum (10% of the final working volume of the bioreactor). The air flow rate was set at 1vvm. The stirrer speed was set to 200rpm. pH was adjusted to 7.0 at the beginning of the fermentation. Bacteria were grown for 48 hours, at 30°C, 200rpm (Rai *et al.*, 2011c; Basnett *et al.*, 2017). The obtained culture was harvested, centrifuged, washed twice with 10% ethanol, homogenised and freeze-dried. Polymer was extracted by Soxhlet extraction as described in the section 2.5.2.

2.5. Extraction of Poly(3-hydroxyalkanoates) from biomass

2.5.1. Solvent dispersion method

Polymer yield was estimated by extraction of the dried biomass by using chloroform/sodium hypochlorite dispersion method (Hahn *et al.*, 1993). Lyophilised biomass was milled in to the fine powder and placed in the conical flasks. Per every 0.3g of biomass 5mL of 80% sodium hypochlorite solution in distilled water and 22.5mL of chloroform were added into biomass and mixed well. The biomass was incubated for 2 hours at 30°C in the orbital shaker (140rpm). After incubation, the slurry was centrifuged for 20 minutes at 3900rpm. This resulted in phase separation. Three layers were formed. The top two layers, containing sodium hypochlorite and cell debris were discarded. The bottom layer, containing chloroform and dissolved polymer was collected, filtered and concentrated. Polymer was precipitated using ice-cold methanol in the ratio 1:10 under continuous stirring (Rai *et al.*, 2011). Polymer yield was calculated as a percentage of dry cell weight, using the formula:

$$\text{Polymer yield (\% dcw)} = (\text{polymer weight/biomass}) * 100$$

2.5.2. Soxhlet extraction

The PHA extraction was carried out using the two-stage Soxhlet extraction (modified from Soxhlet, 1879). For this, dried biomass was weighed, crushed into the fine powder, placed in the extraction thimble (Whatman 28mmx100mm) obtained from GE Healthcare Life Sciences. The thimble with biomass was placed inside the Soxhlet extractor attached to round bottom flask, which contained methanol and boiling stones (Figure 17). The system was attached to the condenser and refluxing was carried out at 90°C for 16 hours. In the first stage, biomass was depleted from organic substances soluble in methanol. After this the solvent was discarded and replaced with chloroform and refluxing at 80°C for 24 hours in order to isolate PHAs from the biomass. Obtained chloroform solution with dissolved polymer was concentrated in a Büchi Rotavapor (R-215) and polymer was precipitated out in ice-cold methanol and dried at room temperature. The polymer yield was calculated using the formula described in the section 2.5.1.



Figure 17: Soxhlet apparatus set up for polymer extraction.

2.6. Structural characterization of scl-PHA

The structural characterization of the polymer obtained from *B. subtilis* OK2, *B. cereus* SPV and *C. necator* was carried out using FTIR, GC-MS and NMR.

2.6.1. Attenuated Total Reflectance Fourier Transform Infrared Spectroscopy (ATR/FT-IR)

The ATR-FTIR spectra of the polymers were recorded using the Perkin-Elmer Spectrum Two Spectrometer in the range between 4000 to 450 cm^{-1} . The spectral resolution was 4 cm^{-1} and spectra were generated as an average of 4 scans (Shah, 2014).

2.6.2. Gas Chromatography-Mass Spectrometry (GC-MS)

Chemical characterisation of the obtained polymer was carried out by GC-MS analysis conducted on samples of polymers subjected to methanolysis, which results in the formation of volatile esters detectable by GC. 20mg of the polymer sample were dissolved in 2mL of chloroform. 2mL of the 15% of sulphuric acid solution in methanol was added and mixed well. 20 μL of methyl benzoate was used as an internal standard. Methanolysis was carried out for 4 hours. For mcl-PHAs and waste frying oil the

methanolysis was carried out for 16 hours. Next, the incubation tubes with the reaction mixture were cooled down on ice for 2 minutes. 2mL of water was added to the mixture and vigorously mixed. Tubes were left on the stand until two layers separated. The organic layer was collected and dried over 10mg of sodium sulphate and sodium bicarbonate, filtered using Whatman No 1 filter paper and transferred to the vial for further analysis (modified from Lageveen *et al.*, 1988).

GC-MS analysis was carried out using a Varian GS/MS system consisting Chrompack CP-3800 gas chromatograph and Saturn 200 MS/MS block. The chromatograph was equipped with a capillary column (Elite-5MS, Perkin Elmer, UK) 30 m in length 0.25mm internal diameter and 0.25 m film thickness. The sample (1 μ L) in chloroform was injected with helium (1mL/min) as the carrier gas. The injector temperature was 225 $^{\circ}$ C and the column temperature was increased from 40 to 240 $^{\circ}$ C at 18 $^{\circ}$ C/min and held at the final temperature for 10 min for polymer samples and prolonged up to 25 minutes for waste frying oil.

2.6.3. Nuclear magnetic resonance (NMR)

The chemical structure of obtained polymers was determined by 13 C and 1 H NMR spectroscopy. 20mg of polymer were dissolved in 1 mL of the deuterated chloroform (CDCl_3) and transferred into an NMR tube. The chemical shifts were referenced against the residual solvent signals 7.26ppm and 77.0ppm for 1 H and 13 C respectively. NMR spectra were analysed using the MestRec software package. The NMR analysis was carried out at the Department of Chemistry, University College London, UK.

2.6.4. Thermal analysis - Differential Scanning Calorimetry (DSC)

Thermal analysis of polymers was conducted using a DSC 214 Polyma (Netzsch, Germany) equipped with Intracooler IC70 cooling system, which provides measurements from -70 $^{\circ}$ C. Temperature ramps were performed under nitrogen flow of 60 mL per min. The initial temperature was -70 $^{\circ}$ C. The sample was heated from -70 to 170 $^{\circ}$ C (mcl-PHAs) or 200 $^{\circ}$ C (scl-PHAs) at heating rate of 10 $^{\circ}$ C per min, kept in molten state at 200 $^{\circ}$ C for 2 min to eradicate sample thermal history and cooled down to -70 $^{\circ}$ C at a cooling rate of 20 $^{\circ}$ C \cdot min $^{-1}$. The second heating cycle from -70 to 170 $^{\circ}$ C (mcl-PHAs)

or 200°C (scl-PHAs) was conducted at scanning speed of 10°C·min⁻¹. For mcl-PHAs DSC thermograms were analysed using Proteus 7.0 software.

2.6.5. Molecular weight analysis – Gel Permeation Chromatography

The molecular weight of the polymer described by the number average molecular weight, (M_n) and weight average molecular weight, (M_w) was determined by carrying out Gel Permeation Chromatography analysis (GPC). PLgel 5 μ m MIXED-C (300x7.5 mm) column were calibrated using the narrow molecular weight polystyrene standards from 162 Da to 15.000 kDa. The eluent used was chloroform. 2 mg/mL of polymer was introduced into the GPC system at a flow rate of 1 mL/min. The eluted polymer was detected with a refractive index detector. The data were collected and analysed using “Agilent GPC/SEC” software.

2.7. Temporal profiling of the PHA production during fermentation

The progress of the fermentation was monitored by taking samples in 3 hour intervals and analysed them in order to estimate glucose and nitrogen concentration, biomass content, pH, dissolved oxygen tension, optical density and polymer accumulation.

2.7.1 Optical density measurements and biomass estimation

Bacterial growth was monitored by measuring the optical density (OD). The optical density of the bacterial culture was measured at 450nm (*Pseudomonas mendocina* CH50) or 600nm (*Bacillus subtilis* OK2) in the spectrophotometer using media as a blank (Single Beam Spectrophotometer, SB038, Cadex Inc.). Biomass (dry cell weight) was obtained by weighing the dried pellet of the cells obtained after centrifugation of the grown culture at 13,200rpm for 10 minutes (Heraeus Pico 17 Centrifuge, Thermofisher Scientific, MA, US).

2.7.2. pH measurements

Collected samples were centrifuged at 13,200 rpm for 10 minutes. pH of the supernatant was measured using Seven Compact pH meter (Mettler Toledo Ltd., Leicester).

2.7.3. Analytical methods

Reagents

Dinitrosalicylic acid (DNS) reagent (Miller, 1959):

Chemical compound	Amount (g/L)
NaOH	10.0
Sodium sulphite	0.5
Dinitrosalicylic acid	10.0
Phenol	2.0

Phenol-nitroprusside buffer (Rai *et al.*, 2011c):

Chemical compound	Amount (g/L)
$\text{Na}_3\text{PO}_4 \cdot 12\text{H}_2\text{O}$	3.0
$\text{C}_6\text{H}_7\text{NaO}_7$	3.0
$\text{C}_{10}\text{H}_{16}\text{N}_2\text{O}_8$	0.3
EDTA	6.0
$\text{Na}_2 [\text{Fe}(\text{CN})_5\text{NO}] 2\text{H}_2\text{O}$	0.02

Alkaline hypochlorite reagent (Rai *et al.*, 2011c):

Chemical compound	Amount (mL/100mL)
NaOCl	2.5
1M NaOH	40.0

Glucose estimation

Glucose concentration was performed using Dinitrosalicylic acid (DNS) assay (modified from Miller, 1959). 2-hydroxy-3,5-dinitrobenzoic acid (3,5-dinitrosalicylic acid) is reacting with reducing sugars to 3-amino-5-nitrosalicylic acid, which gives brown colour product in the presence of reducing sugar. 1mL of diluted supernatant was incubated with 1mL of the DNS reagent (section 2.7.3.) in the water bath at 90°C for 10 minutes.

330 μ L of 40% sodium potassium tartrate solution was added to the reaction test tubes to prevent colour disappearance. The absorbance was read at 575nm. Distilled water was used as a negative control. Glucose concentration was calculated from the calibration curve.

Nitrogen estimation

Nitrogen in the ammonia form was estimated by using phenol-hypochlorite method (Rai *et al.*, 2011c). 250 μ L of diluted sample was mixed with 100 μ L of nitroprusside reagent (Section 2.7.3.), 150 μ L of alkaline reagent (section 2.7.3.) and incubated in the absence of light for 45 minutes. The absorbance was read at 635nm. Ammonium sulphate was used as a positive control. Distilled water was used as a negative control. Nitrogen concentration was calculated from the calibration curve prepared for ammonium sulphate.

Polymer content estimation

Polymer yield was estimated by extraction of the dried biomass by using chloroform/sodium hypochlorite dispersion method as described in the section 2.5.1.

2.8. Production of oligo-PHA and material characterisation

2.8.1. Acidic hydrolysis of P(3HHx-3HO-3HD-3HDD)

The mcl-PHA produced by *P. mendocina* using waste frying oil as the sole carbon source was subjected to partial depolymerisation by acidic hydrolysis (Tepha patent, 2001, patent). Hydrolysis of PHAs in acetic acid solution provides mild conditions leading to a slow well-controlled depolymerisation of aliphatic polyester chains. For this, 2g of the dry mcl-PHA copolymer was suspended in 200mL of 83% solution of glacial acetic acid in distilled water and boiled at 100-105°C for 20 hours. After the reaction was completed, 50mL of distilled water was added to the solution and the flask was washed twice with 50mL of chloroform. The mixture was transferred into the separating funnel. The organic layer was collected, dried over sodium sulphate, filtered and partially concentrated using the rotary evaporator. To complete evaporation of the volatile

solvent, the product was kept in the oven at 40°C until the constant weight was achieved. The material obtained was characterised by using FTIR, GC-MS, NMR, DSC and GPC.

2.8.2. P(3HHx-3HO-3HD-3HDD) hydrolysis kinetics

P(3HHx-3HO-3HD-3HDD) copolymer was hydrolysed as described in the section 2.8.1. 7mL samples were collected in 3 hour intervals and processed to obtain polymer. The amount of polymer recovery was calculated by using formula:

$$\% \text{ polymer recovery} = (\text{weight of dry oligo-PHA (g)} / 0.077\text{g}) * 100,$$

where 0.077g was the total weight of polymer expected in 7mL of the sample

2.9. Blend film fabrication

The neat and blend films fabrication was carried out by dissolving 0.5 g of polymers: P(3HB) and hydrolysed P(3HHx-3HO-3HD-3HDD) in ratios: 95/5; 90/10 and 80/20 in 10 ml of chloroform and pouring the polymer solution in 60 mm diameter glass petri dishes (Lizarraga-Valderrama *et al.*, 2015). The polymer was dried at room temperature in the incubator Stuart S160 (Bibby Scientific Limited, Staffordshire, UK) until complete solvent evaporation.

2.10. P(3HB)/oligo-PHA composite film fabrication with barium sulphate

The composite film fabrication was carried out in two steps: firstly 0.5 g of polymers: P(3HB) and hydrolysed P(3HHx-3HO-3HD-3HDD) in ratio 90/10 was mixed barium sulphate (BaSO_4), density 4.49g/cm^3 was milled using ZrO_2 milling media and dispersed in isopropanol (9 wt%), particle size: 0.3-3.0 μm (Lucideon, UK) to obtain final concentrations of 1, 3 and 5 wt% BaSO_4 , in chloroform. The composite solution was poured into glass petri dishes and dried at the room temperature in order to allow complete evaporation of isopropyl alcohol. 0.5g of dried composite material was further dissolved in 10mL of chloroform and cast in the 60 mm diameter glass petri dishes. The polymer was dried at room temperature in the incubator Stuart S160 (Bibby Scientific Limited, Staffordshire, UK) until complete solvent evaporation. Isopropyl alcohol has higher boiling temperature (82.6°C) than chloroform (61.2°C), which results in different

evaporation rates of both solvents at room temperature. Hence presence of both solvents may affect uniform composite formation and has negative effect on the material morphology (e.g. increased porosity). Therefore, two-step composite films fabrication was performed in order to avoid this detrimental effect.

2.11. Tubes manufacturing by using dip moulding technique

The blend of P(3HB)/P(3HHx-3HO-3HD-3HDD) in ratio 90/10 was selected for tube manufacturing. Polymer concentration of 4 wt% in chloroform was used for the formation of tubes. Chloroform/1,1,2,2-tetrachloroethane solvent system with composition 70:30 wt/wt% was prepared (method optimised in the lab). Addition of 1,1,2,2-tetrachloroethane enabled to obtain stable solution of P(3HB), oligo-PHA in chloroform at room temperature. Higher boiling point of 1,1,2,2-tetrachloroethane (146.7°C) in comparison to chloroform (61.2°C) allows obtaining an optimal evaporation rate during tube formation and drying.

Tubes were prepared by the dip moulding technique using PTL-MMB02 Millimeter Grade Desktop Programmable Dip Coater (1-200 mm/min) (Figure 18).

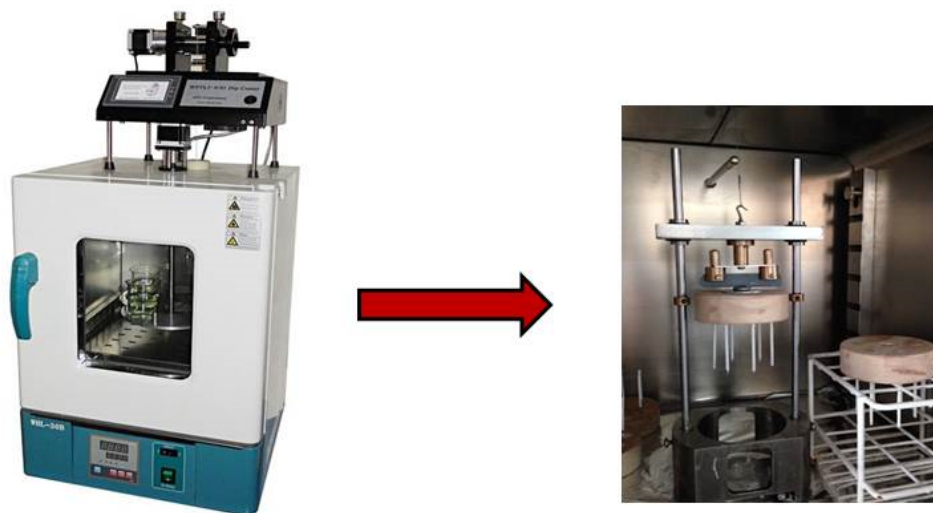


Figure 18: PTL-MMB02 Millimeter Grade Desktop Programmable Dip Coater (right) and furnace with prepared tubes on the mandrels (left).

The tubes were produced using mandrels of 2.3-mm diameter using a homemade tooling which held 6 mandrels. The settings for mandrel movement were 150 and 200 for up and down movement correspondingly. Dwell time of 1 sec was used to keep the

mandrel in the solution while drying time of 30 secs was set to allow partial drying of the coating between the coating cycles. The total number of cycles was 20. Every 5 cycles, the drying time was extended until 3 minutes. Coated mandrels were dried in the furnace at 50°C overnight, removed from the mandrels and stored at room temperature for further testing. Dip moulding conditions were optimised in order to produce tubes with wall thickness around 150 µm in order to compare PHAs with currently existing polymeric stents. Strut thickness of currently available biodegradable polymeric stent “Absorb” is 150 µm. Uniformity of manufactured tubes were confirmed by SEM. Preliminary mechanical tests were conducted to characterise tensile properties of the tubes.

2.11.1. Preparation of the tubes with incorporated drug

The neat tubes prepared were coated with an additional layer of polymer with incorporated drug. For the polymeric coating 12 wt/wt% solution of PCL-PEG 550 in tetrahydrofuran (THF) was prepared. The amount of drug required for coronary stent application is 1-1.5 µg/mm² (Van der Hoeven *et al.*, 2005; Serruys *et al.*, 2002). Hence, the concentration of drug (tacrolimus or rapamycin) in the polymer solution was 1.44 wt %, based on polymer deposition per mm². Dried PHA tubes were coated in the PCL-PEG 550 solution at room temperature using dip coating technique. The dwell time was 1s, drying time 30s for 1 cycle. The coated tube was left for 24 hours to dry. Tubes were measured, removed from the mandrels and characterised.

2.11.2. Preparation of composite tubes with barium sulphate

Composite material was prepared in two stages as described in the section 2.10. For this, 4g of the blend of P(3HB)/oligo-PHA in the ratio 90/10 was dissolved in chloroform with 5 wt% barium sulphate solution in isopropanol (9 wt%). The solution obtained was casted into the glass petri dish and dried completely. For tube manufacturing, 4 wt/wt% solution of the composite material in chloroform and of 1,1,2,2-tetrachloroethane (70:30) was prepared at room temperature and used for tube fabrication as described in the section 2.11.

2.11.3. Characterization of PHA blends, composites and tubes

2.11.3.1. Ageing experiments

Obtained PHA based blends, composites and tubes were stored at ambient temperature for a period of 1, 3, 5 and 7 weeks and analysed with respect to their thermal and mechanical properties.

2.11.3.2. Tensile test

Tensile testing was carried out using a 5942 Testing Systems (Instron) equipped with 500N load cell at room temperature. The test was conducted using films of 5 mm width and length of 3.5-5.0 cm. Before the measurement, thickness and width of the specimen was measured in several places and an average value was used for the calculation of the cross-sectional area. The gauge length of the sample holder was 23 mm. The deformation rate was 5 mm per minute. Young's modulus, ultimate tensile strength and elongation at break were calculated from the stress-strain curve. The average values for 3 specimens were calculated. The data analysis was carried out using the BlueHill 3 software.

2.11.3.3. Differential scanning calorimetry (DSC)

The focus of the DSC analysis was on characterisation of aged samples of known history. Therefore, the data presented were obtained from a single heating run from -70 to 200°C using the method described in the section 2.6.4.

2.11.3.4. Static contact angle analysis

Static contact angle study was performed to measure the hydrophobicity/hydrophilicity of the PHA films. This was carried out using the KSV Cam 200 optical goniometer (Helsinki, Finland). About 200µL of deionized water was dropped onto the surface of the films using a gas tight micro-syringe. Soon after the water droplet made contact with the sample, a total of 10 images were captured with a frame interval of one second. The analysis of the images was performed using the KSV Cam software. Analysis was carried out at Eastman Dental Institute, University College London, UK.

2.11.3.5. Scanning electron microscopy (SEM)

Surface topography of the PHA film was studied using SEM. The film samples were mounted on aluminium stubs (8mm in diameter) and these were gold coated using a EMITECH-K550 gold sputtering device for 2mins. A JOEL 5610LV-SEM was used to record images of the surface topography of both film types. The SEM images were taken with an acceleration voltage of 10 kV at 10 cm working distance. This study was carried out at the Eastman Dental Hospital, University College London.

2.11.3.6. X-ray microtomography (MicroCT)

Tubes and composite films were cut in to pieces between 2-4mm long and about 1mm wide and mounted upright into the MicroCT holder and placed on the MicroCT stage within the SEM. Bruker SEM software was used to operate the stage to obtain the X-Ray images of the sample. Series of X-Ray images was collected as the sample was turned through 180° at 1° intervals. The images were then reconstructed using Bruker software CTan, CTvox and analysed at the Eastman Dental Institute, UCL, UK.

2.11.3.7. Surface roughness analysis

The surface roughness of the films was measured using a Sony Proscan 1000 Laser Profilometer (Tokyo, Japan). The laser used was model 131A, which had a measuring range of 400-600µm, a resolution of 0.02µm and a maximum output of 10mW. Scans of 0.5 mm² were obtained from each sample. Nine random coordinates were selected from each specimen in order to measure the root mean square roughness (R_q).

2.11.3.8. X-ray diffraction (XRD)

X-ray diffraction (XRD) analysis was performed on neat P(3HB) films, blends with oligo-PHA and composites with BaSO₄. Samples were analysed on a Brüker D8 Advance diffractometer in flat plate geometry, using Ni filtered Cu K_α radiation. Data was collected from 10 to 100° with a primary beam slit size of 0.6 mm. A Brüker Lynx Eye silicon strip detector was used and a step size of 0.02° and a count time of 0.1 s per step. Samples were analysed at the Eastman Dental Institute, UCL, UK.

2.11.3.9. Protein adsorption study

Protein adsorption assay was performed using foetal bovine serum, (FBS). 1 cm² polymer samples were incubated in 400µl of FBS at 37°C for 24hrs. After incubation, the samples were rinsed 3 times with phosphate buffer saline, (PBS) and incubated in 1mL of 2% sodium dodecyl sulphate (SDS) in PBS for 24 hrs at room temperature under vigorous shaking. The total amount of proteins adsorbed on the surface of the samples was quantified using the Bicinchoninic Acid Protein Assay Kit (The Thermoscientific, Pierce, Hemel Hempstead, UK). The absorbance of the samples was measured spectrophotometrically at 562nm against a calibration curve, using bovine serum albumin. The samples incubated in PBS were used as a negative control (Misra *et al.*, 2010). The assay was carried out in triplicate.

2.12. *In vitro* release studies of rapamycin using UV-Vis spectrometry

2cm long tubes coated with a polymer layer with incorporated rapamycin were immersed in 2mL of PBS release medium in triplicate and incubated at 37°C for 90 days. A sample volume of 1 ml was collected at predetermined time points and each aliquot were replaced with fresh buffer throughout the entire release study. The drug content in the sample was analysed using Lambda 35 UV-Vis spectrometer (PerkinElmer, Waltham, USA) at 278nm wavelength. Rapamycin standards in methanol were prepared by serial dilutions and analysed using a UV-Vis spectrometer. The concentration of released drug was calculated from the standard curve (Ma *et al.*, 2011).

2.13. *In vitro* release studies of tacrolimus using High Performance Liquid Chromatography (HPLC)

The release studies of the P(3HB)/oligo-PHA tubes with incorporated tacrolimus were carried out as described in the section 2.12. Tacrolimus concentration during release study was measured as described by Patel *et al.*, 2013. A HPLC system containing C18 60RP column (dimensions 250nmx4.6mm, 5µm in particle size) was used to measure the amount of the tacrolimus released to PBS from the incubated tubes. A methanol and water solution (80:20) was used as the mobile phase (pH=6.0 adjusted with 1N HCl) at a

flow rate of 1 ml/min. The column oven temperature was set to 50°C. The UV detection wavelength was 210 nm and 20µl sample was injected (Ultimate 3000 HPLC, Dionex, Thermofisher). Tacrolimus standards were prepared by serial dilutions in acetonitrile. The released tacrolimus concentration was calculated from the standard curve. Obtained data was analysed by using Chromeleon 7.2 chromatography data system software.

2.14. *In vitro* cell culture studies

2.14.1. Cell growth and maintenance

Human microvascular endothelial cells (HMEC-1) were grown in DMEM supplemented with 10 % heat inactivated foetal bovine serum, 1% v/v of penicillin and streptomycin solution (10,000 units of penicillin and 10 mg streptomycin per mL in 0.9% NaCl) and 1% L-glutamine, grown at 37°C with 95% air and 5 % of CO₂ humidified incubator. Media was pre-warmed at 37°C. Cell passages were carried out, when 70% confluence was obtained. For cell passage, cells were rinsed with PBS and detached from the flask using a 2mL of 10x 2.5% trypsin at 37°C for 2 minutes. The reaction was stopped by addition of 8mL of supplemented DMEM media. Cells were centrifuged at 1000rpm for 5 min and the resulting pellet was resuspended in fresh supplemented DMEM. Cells were seeded in sterile 75 cm² tissue culture flasks and cultured at 37°C with 95% air and 5 % of CO₂ humidified incubator.

2.14.2. Sample preparation and cell seeding

P(3HB) neat and blend film constructs were cut in to 13mm diameter circles and sterilized under the UV light for 30 minutes each side. All film samples were soaked in 24well plate in 1mL of supplemented DMEM medium for 16hrs prior to cell seeding. Cell culture studies were performed in triplicates. HMEC-1 cells at 70 % confluence were used for the cell seeding. Cells were counted by using Trypan Blue (1:5) in the haemocytometer. Around 20,000 cells were seeded on the pre-wetted constructs in a 24 well plate. TCP was used as positive control. Wells containing media without cells were used as negative control. Plates were incubated at 37°C with 5 % of CO₂ and media was changed every 2 days. Cell proliferation was assessed at day 1, 3 and 7 of incubation.

2.14.3. MTT assay

The MTT (3-(4,5-Dimethylthiazol-2-yl)-2,5-diphenyltetrazolium bromide) colourimetric assay (modified from Mosmann, 1983) was performed on the constructs containing the cells at 24, 48 and 72 hrs. For this, 500 μ l of a 12mM MTT solution in PBS were added to each well at day 1, 3 and 7 and the plates were incubated for four hours at 37°C with 5% of CO₂. After incubation, the liquid was discarded from each well and 200 μ l of DMSO was added and kept for 15 minutes at 37°C. 200 μ l of the resulting solution were transferred to 96 well plates and the absorbance at 540 nm was measured on a FluoStar Optima plate reader (SMG Labtech). The absorbance of the samples was normalised with respect to the positive control (standard tissue culture plastic). The difference in the surface areas of the tissue culture plate wells and the films were considered for the calculation of the % cell viability on the films.

2.14.4. SEM imaging of HMEC-1 cells

For the SEM imaging, HMEC-1 cells seeded on the PHA films were fixed using 4% paraformaldehyde. These samples were dehydrated by several treatments with different solutions of ethanol (20%, 50%, 70%, 90%, 100%) for 10 minutes, dried by immersion in hexamethylsilizalane for 2-5 minutes and left in a fume cupboard for at least an hour, gold coated and viewed under the SEM as described in the section 2.12.3.5.

2.14.5. Live/ dead measurements

Live/dead viability assay was done using fluorescence dyes, such as: Calcein AM and Ethidium homodimer-1. Calcein-AM is used to determine viable cells, by conversion of non-fluorescent form of Calcein, present in live cells to green fluorescent form by intracellular esterase. Ethidium homodimer-1 emits red fluorescence while bounded into DNA of dead cells. After growing the cells for 1, 3 and 7 days on the polymer scaffolds, the culture medium was removed and cells rinsed with Dulbecco's Phosphate Buffered Saline (DPBS). Then 300 μ L of working solution, which contains 2 μ M Calcein AM and 4 μ M Ethidium homodimer-1 in DPBS were added directly to cells and incubated for 30-45 minutes in the absence of light at room temperature (ThermoFisher Scientific

LIVE/DEAD™ Viability/Cytotoxicity Kit Protocol). Following incubation, about 2mL of the DPBS was added to a 6 well plate. The samples were imaged using 40xW objective under the confocal microscope (Leica TCS SP2).

2.14.6. Indirect cytotoxicity studies

Indirect cytotoxicity study was performed in order to confirm their biocompatibility. Cytotoxicity of different extracts obtained after incubation of PHAs samples with DMEM media for 24 hours was measured by the MTT assay. 10mm discs of P(3HB)/oligo-PHA composites or 10mm tubes were prepared, placed in the polystyrene 24-well plate and sterilised under UV lamps for 30minutes on each site. 500µl of DMEM media was added into each well, containing scaffolds. All samples were prepared in triplicate. Simultaneously, HMEC-1 cells were seeded at 20,000 cells per well in 24-well plates in 500µl of culture medium and were incubated at 37 °C. After 24 h of incubation, the media was removed. The HMEC-1 cell monolayer was washed with DPBS and exposed to 500µl of the extract obtained after incubation with PHA based scaffolds and incubated for 24 and 72 hours. After that cells were washed with DPBS and quantified by MTT assay as described in section 2.14.3.

2.15. Haemocompatibility studies

Haemolysis, whole blood clotting assays and monocytes/neutrophils activation studies were performed to investigate haemocompatibility of the PHAs blends, composites and tubes after direct contact with blood.

2.15.1. Haemolysis studies

Haemolysis study was performed according to the protocol provided by Wang *et al.*, 2013 with some modifications. Lithium heparin whole blood was diluted 4:5 in sterile 0.9% (v/v) sodium chloride solution. For the films, discs of 10 mm diameter were prepared, washed with sterile 0.9% NaCl and placed into the wells of 24 well plate (Sigma-Aldrich, Dorset, UK). For the tubes, the 0.0045g of polymer tubes (an equivalent polymer weight to the 10mm discs) were washed with sterile 0.9% NaCl and placed inside the 24 well plate. All the samples were prepared in triplicates and incubated for

30 min at 37°C with 980µl sodium chloride solution. Standard tissue culture plastic with 980µl sodium chloride was used as negative control. Wells containing 980 µl of distilled water instead of NaCl were used as positive control. To each well 20µl of pre-diluted blood was added, mixed and incubated for 60 min at 37°C and centrifuged at 3000 rpm for 5 min. 200 µl of supernatant were transferred to a 96 well plate and the absorbance was measured at 540 nm. The haemolysis ratio (HR, in %) was calculated by using formula:

$$\text{Haemolysis ratio (\%)} = (A - A_{\text{neg}}) / (A_{\text{pos}} - A_{\text{neg}}) \times 100\%$$

where A is the absorbance of the sample, A_{neg} is the absorbance of the negative control and A_{pos} is the absorbance of the positive control.

2.15.2. Whole blood clotting

The whole blood clotting assay was performed as previously described by Motlagh *et al.*, 2006 and Huang *et al.*, 2005 with some modifications. 800µl 0.1M calcium chloride was added to 4 ml of tri-potassium ethylenediaminetetraacetic acid (K_3 -EDTA) whole blood in order to activate coagulation cascade. 10 mm diameter film samples or 45mg tubes were prepared and placed into the wells of a polystyrene 24 well plate (Sigma-Aldrich, Dorset, UK). For the tubes, the 45mm of polymeric tubes (an equivalent weight of polymer present in the 10mm discs) were placed inside the 24 well plate. 50µl of activated blood was applied directly on the material, placed into each well. For the negative control 100 µl of 0.9% sodium chloride in 1 ml of blood was used as negative control. TCP was used as the control. After 30 and 90 min of incubation at ambient temperature the coagulation was stopped by the addition of 1.5mL distilled water. The erythrocytes not trapped in the thrombus were lysed by addition of distilled water, releasing free haemoglobin. After 5 minutes, 200 µl were transferred to a 96 well plate and the absorbance was measured at 540 nm. All samples were prepared in triplicate. The size of the formed blood clot was calculated as the percentage of blood clotting:

$$\text{Blood clotting (\%)} = (A_{\text{neg}} - A) / (A_{\text{neg}} - A_{\text{pos}}) \times 100\%$$

where A_{neg} is the absorbance of the negative control, A is the absorbance of the sample and A_{pos} is the absorbance of the positive control.

2.15.3. Monocyte and neutrophil activation studies

Monocytes and neutrophils are two types of white blood cells taking essential part of innate immune system. They take part in acute inflammatory response. They can be activated for example by lipopolysaccharide, present in cell wall of Gram negative bacteria. In this study, mcl-PHA was produced by *Pseudomonas mendocina*, which is Gram negative organism. Therefore, activation study on both types of white blood cells will be performed in order to investigate the response of monocytes and neutrophils after direct contact with PHA based materials.

2.15.3.1. Sample preparation

For leukocyte activation analysis, samples which contained 4.5mg of polymer were incubated for 16 hours with 1mL of blood at 37° C. Whole blood and blood activated with LPS (100ng/mL) were used as negative and positive control respectively. Two types of antibodies were used: an activation antibody, which is CD11b-PE and selective antibodies, such as CD86-PE, CD45-PerCP and CD66b-FITC, which allow accurate location of neutrophils and monocytes during flow cytometry analysis.

Table 2: Experimental set-up for staining with different types of antibodies.

No. Experiment	Blood sample	Antibodies
1.	Non-activated whole blood	CD86-PE+CD45-PerCP
2.	Non-activated whole blood	CD11b-PE+CD66b-FITC
3.	LPS activated whole blood	CD86-PE+CD45-PerCP
4.	LPS activated whole blood	CD11b-PE+CD66b-FITC
5.	Whole blood after incubation with PHAs	CD86-PE+CD45-PerCP
6.	Whole blood after incubation with PHAs	CD11b-PE+CD66b-FITC

2.15.3.2. Whole blood staining with activation antibodies

For leukocyte activation analysis, 100µL of whole blood, blood activated by LPS and blood after incubation with PHAs was added to flow cytometry and fluorescence-activated cell sorting (FACS) tubes containing 10µL of monoclonal anti-human

antibodies: CD66B conjugated with fluorescein isothiocyanate (CD66b-FITC), CD86 conjugated with phycoerythrin (CD86-PE), CD11b conjugated with phycoerythrin (CD11b-PE) and CD45 conjugated with peridinin chlorophyll protein (CD45-PerCP). The samples were gently shaken and incubated for 20 min in the absence of light at room temperature. Erythrocytes were then lysed with 2 ml of lysing buffer and incubated for 10 minutes at 37° C. Samples were centrifuged at 1500rpm for 5 minutes, the supernatant was discarded and replaced with 2mL of PBS and centrifuged again at the conditions mentioned above. The supernatant was discarded and replaced by 200µL of flow cytometry fixing buffer (containing 4% formaldehyde) and were analysed by using flow cytometry. Fresh whole blood without antibodies was used as negative control.

2.15.3.3. Flow cytometry analysis

Flow cytometry analyses were carried out in a centralized laboratory using a Cyan ADP flow cytometer (Beckman Coulter, Inc., Brea, USA), equipped with a 488nm laser, 530/40 and 575/25nm band pass filters, and a 750-nm long pass filter. Determination of CD11b expression on neutrophils and monocytes was performed as described in the section 2.16.3.2. Cell-associated fluorescence was measured using the 575/25-nm filter. The mean of the relative fluorescence intensity (MFI) from logarithmically amplified data expressed as linear value was recorded and compared.

2.16. *In vitro* degradation studies of the tubes

In vitro degradation studies of the fabricated tubes were carried out according to the protocol described by Misra *et al.*, 2008. The P(3HB)/oligo-PHA tubes were studied for a period of 6 months. Tubes were weighed and incubated in 5mL of phosphate buffer saline (PBS) at 37°C. All the degradation related studies were carried out in triplicates. Samples were characterized in order to study mechanical, thermal, molecular weight, water uptake and weight loss, pH change, and surface morphology.

2.16.1. Thermal and mechanical properties

Tubes collected from PBS solution after each time point were characterized in order to study changes in thermal and mechanical properties according to protocols described in the section 2.6.4-2.6.5.

2.16.2. Surface morphology

SEM analyses of the surface of the degraded tubes were carried out at the end of the 1st, 2nd, 3rd, 4th, 5th and 6th month study to see changes in the surface morphology of the tubes occurring due to its degradation. The sample preparation and methodology was the same as described in section 2.11.3.5.

2.16.3. Water uptake, weight loss and pH measurements

Degradation kinetics was also determined by measuring the % water uptake (%WU) and % weight loss (% WL). For these, weight of the dried tubes was recorded. Tubes were immersed in PBS and kept under static conditions at 37°C until the desired time point. At the end of each time point the tubes were collected and analysed for water uptake and weight loss behaviour. For measuring the % WU, the immersed samples were removed at given time points, the surface was gently wiped with a tissue paper and the weight was recorded. Similarly, for measuring the weight loss, the samples were removed from the PBS, dried at 37°C overnight and weighed dry. Water uptake and weight loss were calculated using the following equations:

$$\%WU = ((M_1 - M_2) / M_2) * 100$$

$$\%WL = ((M_0 - M_2) / M_0) * 100,$$

where M_0 – initial weight of the tube before incubation, M_1 – weight of the wet tube after incubation, M_2 – weight of the dry tube after incubation.

The pH changes of the media were then measured at the end of each incubation time point.

2.17 Statistical analysis

Obtained results were presented with their mean standard deviation (mean value \pm SD). Data were compared using Student's t-test and ANOVA. The differences were considered significant when p-value was below 0.05 ($p < 0.05$). p-value greater than 0.05 ($p > 0.05$) was interpreted as no significant difference.

Chapter 3

Production and characterisation of short chain length Poly(3-hydroxyalkanoates)

3. Introduction

Polyhydroxyalkanoates have been widely explored as a group of promising biomaterials, for biomedical applications (Rai *et al.*, 2011). They represent a broad range of properties, which depends on the number of carbon atoms within the monomer unit (Laycock *et al.*, 2013). Short chain length Poly(3-hydroxyalkanoates), include PHAs with monomer length between 3 to 5 carbon atoms within the monomer unit (Verlinden *et al.*, 2007). Most of the polymers from this group of PHAs have the material properties, such as: high crystallinity, thermal properties similar to thermoplastics, as well as high stiffness and tensile strength (Pena *et al.*, 2014). However within this group of PHAs, the P(4HB) polymer is an exception. Unlike other scl-PHAs, P(4HB) has low melting temperature, high tensile strength and is highly elastomeric. Scl-PHAs are represented by 3-hydroxypropionate (3HP), which contain 3 carbon atoms within the monomer unit, 3-hydroxybutyrate (3HB) or 4-hydroxybutyrate (4HB) with 4 carbon atoms and 3-hydroxyvalerate (3HV) with 5 carbon atoms. In addition, there are scl-PHA copolymers which include Poly(3-hydroxybutyrate-co-3-hydroxyvalerate), P(3HB-co-3HV), poly(3-hydroxybutyrate-co-4-hydroxybutyrate), P(3HB-co-4HB), which represent intermediate properties between both monomers which are dictated by the main monomer unit within the copolymer (Akaraonye *et al.*, 2010). Scl-PHAs can be produced by different types of bacterial strains including *Bacillus sp.*, *Cupriavidus necator*, Cyanobacteria (*Spirulina platensis*), *Burkholderia sacchari* and *Methylobacterium sp.* (Jau *et al.*, 2005; Mendonca *et al.*, 2013; Yezza *et al.*, 2006). Each bacterial strain has different levels of polymer accumulation within the cell as well as different material properties. Scl-PHAs have been used in several biomedical applications, such as drug delivery, bone tissue engineering, nerve regeneration, sutures and heart valves (Chen and Wang, 2013; Grage *et al.*, 2009; Masaeli *et al.*, 2012). The main application for PHAs in this work was to develop biodegradable coronary artery drug eluting stents. Coronary stents are known to be a very demanding medical device, which require particular material properties, such as strength and stiffness. On the other hand, it also needs a certain amount of elastomeric property in order to be crimpable and deployable within the artery. Currently, only one polymeric stent is available in the market, made using poly(L-lactic acid) PLLA, a stiff polymer (Abbott, USA). Although this product is currently being used

by clinicians, it presents several limitations as mentioned in the section 1.4.1. Polyhydroxyalkanoates can be an alternative solution to PLLA as a platform for coronary artery stents. Hence, the main objective of this study was to produce scl-PHAs using a range of carbon sources and different bacterial strains. The selected materials were subjected to thorough analysis in order to fully characterise the properties of the chosen material.

3.1. Screening experiments

Screening experiments were carried out in order to obtain scl-PHAs using four different bacterial strains, such as: *Pseudomonas mendocina* CH50, *Cupriavidus necator*, *Bacillus cereus* SPV and *Bacillus subtilis* OK2. A range of different carbon sources were studied as described in the section 2.2. A summary of the results obtained is shown in the Table 3.

Table 3: Summary of the results obtained during screening experiments performed for the production of novel scl-PHA production.

Bacterial strain	Carbon source	Polymer yield (% dcw)	GC-MS results
<i>Bacillus cereus</i> SPV	Fructose	7.5	3HB
<i>Bacillus subtilis</i> OK2	Glucose	30.8	3HB
<i>Cupriavidus necator</i>	Sodium octanoate, hexanoic acid	12.2	3HB
	Rapeseed oil, fructose	9.0	3HB
	Butyrolactone	6.7	3HB
	Sodium octanoate, butyrolactone	18.6	3HB
<i>Pseudomonas mendocina</i> CH50	Rapeseed oil, sucrose	22.5	3HB
	Glucose, heptanoic acid	17.2	3HB
	Sucrose, valeric acid	7.0	3HB, 3HV

Depending on the carbon source, mainly the P(3HB) homopolymer was obtained. *Bacillus* species were grown on carbohydrates as the sole carbon source. Both conditions resulted in P(3HB) production. The polymer yield obtained from *B. subtilis* OK2 was much higher (30.8% dcw) than *B. cereus* SPV (7.5% dcw) when grown using fructose as the only carbon source. It is well known that *Bacillus* species are able to metabolise sugars and produce scl-PHAs, mainly homopolymer P(3HB) (Faccin *et al.*, 2013). *Cupriavidus necator* produced P(3HB), when grown on several different carbon sources. The obtained polymer yield was from 6.7% dcw when grown using γ -butyrolactone as the sole carbon source to 18.6% dcw when γ -butyrolactone and sodium octanoate were used as the carbon sources. *C. necator* is a well-known strain used for PHA production. It has been used mainly for P(3HB) production. However, it is also able to produce P(3HB-co-4HB). Engineered strains can be used to produce scl-mcl-PHA copolymers, such as P(3HB-3HHx). P(3HB) was obtained also from *Pseudomonas mendocina* CH50 when mixed carbon sources, such as glucose with heptanoic acid or sucrose with rapeseed oil, were used. The obtained polymer yield was 17.2% dcw and 22.5% dcw respectively. P(3HB-co-3HV), a scl-PHA copolymer was obtained by *Pseudomonas mendocina* CH50 when valeric acid was used along with sucrose as the precursor for 3HV monomer unit within the copolymer. Although, *Pseudomonas* species are well studied as the main sources for mcl-PHAs, in this study, *P. mendocina* was able to produce also short chain length PHAs.

The P(3HB) polymer obtained from *Bacillus subtilis* OK2 was selected for further studies since it had the highest polymer yield. This was characterised with respect to thermal properties, mechanical properties, molecular weight and chemical identification.

3.2. Production of P(3HB) using *Bacillus subtilis* OK2 and glucose as the sole carbon source

P(3HB) production by *Bacillus subtilis* OK2 using glucose was carried out as described in the section 2.4.3. The fermentation was carried out in the 15L bioreactor for 48 hours. The fermentation profile of *Bacillus subtilis* OK2 grown with 35g/L of glucose was studied for 48 hours (Figure 19). Samples were taken at 3 hour intervals. Biomass, Optical

Density (OD_{600nm}), pH, glucose consumption and polymer yield were monitored as described in the section 2.7.

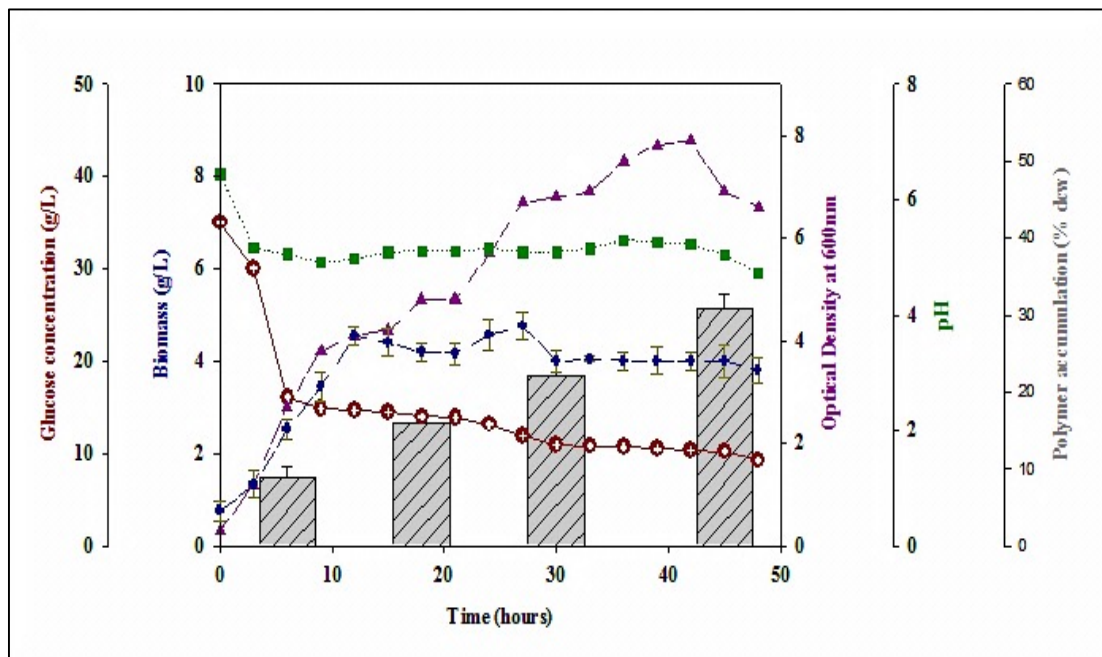


Figure 19: Temporal profile of PHA production by *Bacillus subtilis* OK2 using Kannan and Rehacek media with 35g/L of glucose as the sole carbon source. polymer yield (% dcw), optical density at 600nm, pH, biomass (g/L), glucose concentration (g/L).

During fermentation, the optical density (OD) increased gradually until 42 hours and reached a maximum value of 7.9. After that point, the OD values decreased. Biomass concentration increased along with the optical density of the bacterial culture up to 27 hours. Maximum biomass concentration of 4.7g/L was obtained at 27 hours and then found to decrease. The pH of the production medium was set to 6.8 at the beginning of the process. During fermentation, the pH decreased from 6.8 until 4.7 at 48 hours. Utilisation of the carbon source was investigated as well. The results showed that the glucose concentration decreased from its initial concentration of 35 g/L to 9.3 g/L at the end of the fermentation. Polymer production started at 9 hrs of the fermentation and the maximum polymer yield (% dcw) was obtained at 48 hours was 30.8% dcw.

In this study production of PHA was carried out as a one-step batch cultivation process in 5L bioreactor using this relatively unexplored bacterial strain. The final biomass obtained was 3.8 g/L, and polymer yield was 30.8 % dcw at the end of fermentation at 48 hours.

3.3. P(3HB) characterization

Obtained polymer was chemically characterised using Attenuated Total Reflectance Fourier Transform Infrared Spectroscopy (ATR-FTIR), Gas Chromatography–Mass Spectrometry (GC-MS) and Nuclear Magnetic Resonance (NMR) as described in the sections 2.6.1.-2.6.3. Molecular weight analysis was performed according to the method described in the section 2.6.5.

3.3.1. Attenuated Total Reflectance Fourier Transform Infrared Spectroscopy (ATR/FT-IR)

The adsorption spectrum of the polymer produced *Bacillus subtilis* OK2 is shown in Figure 20.

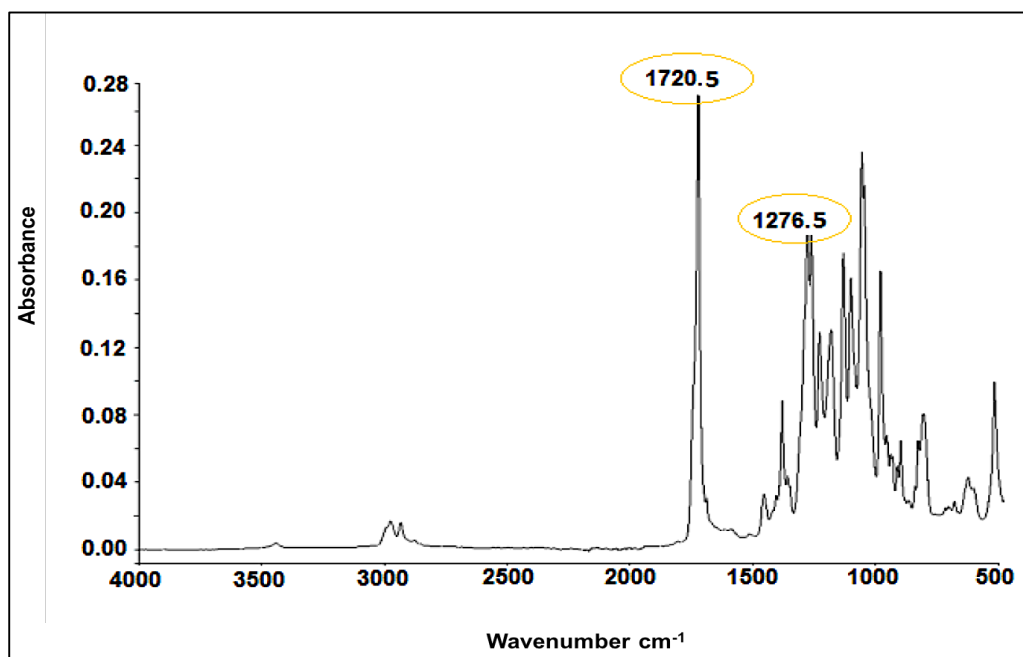


Figure 20: ATR-FTIR spectrum of the polymer produced by *Bacillus subtilis* OK2 with 35g/L glucose as a carbon source with major characteristic peaks at 1720.5 cm⁻¹ for carbonyl group (C=O) and 1276.5cm⁻¹ for –CH group.

FTIR-ATR analysis of the isolated polymer revealed absorption bonds at 1720.5 cm⁻¹ and 1276.5 cm⁻¹ (Figure 20) corresponding to the ester carbonyl group and the -CH group, respectively. These bands are characteristic for scl-PHAs (Sun *et al.*, 2007) and hence this result confirmed the production of a scl-PHA.

3.3.2. Gas Chromatography Mass Spectrometry (GC-MS)

The isolated polymer was subjected to methanolysis prior to GC-MS analysis, as described in the chapter 2.6.2. The result in chromatograms is presented in the Figure 21A.

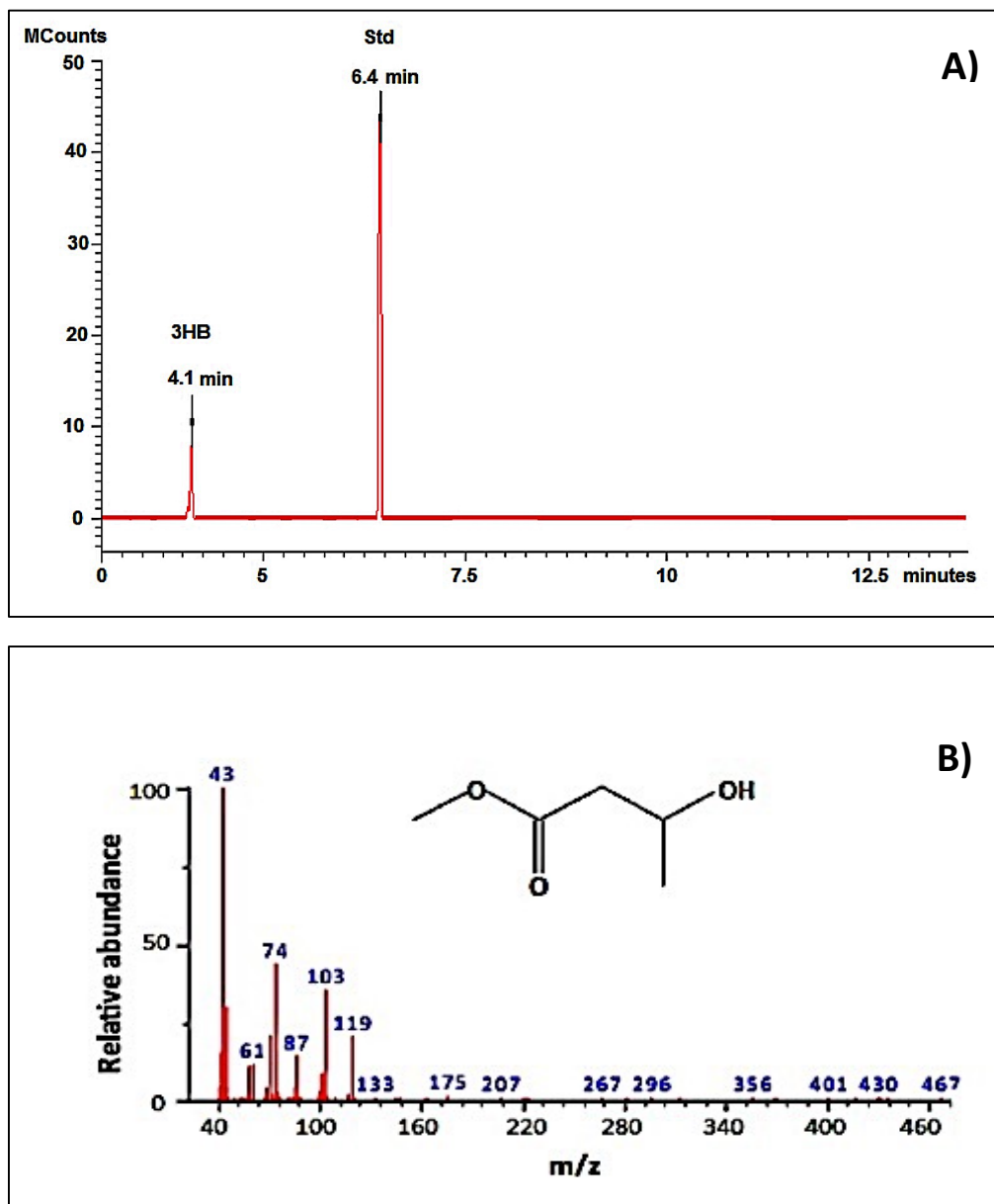


Figure 21: (A) Gas chromatogram of the polymer extracted from *Bacillus subtilis* OK2 biomass and (B) mass spectrum of a peak with $R_t=4.1$ min identified using NIST library as methyl ester of 3-hydroxybutyric acid. Methyl benzoate was used as an internal standard (Std).

The GC chromatogram showed one peak at $R_t=4.1$ min. The system was calibrated using reference standards of various methyl esters of 3-hydroxyalkanoates (Figure 22).

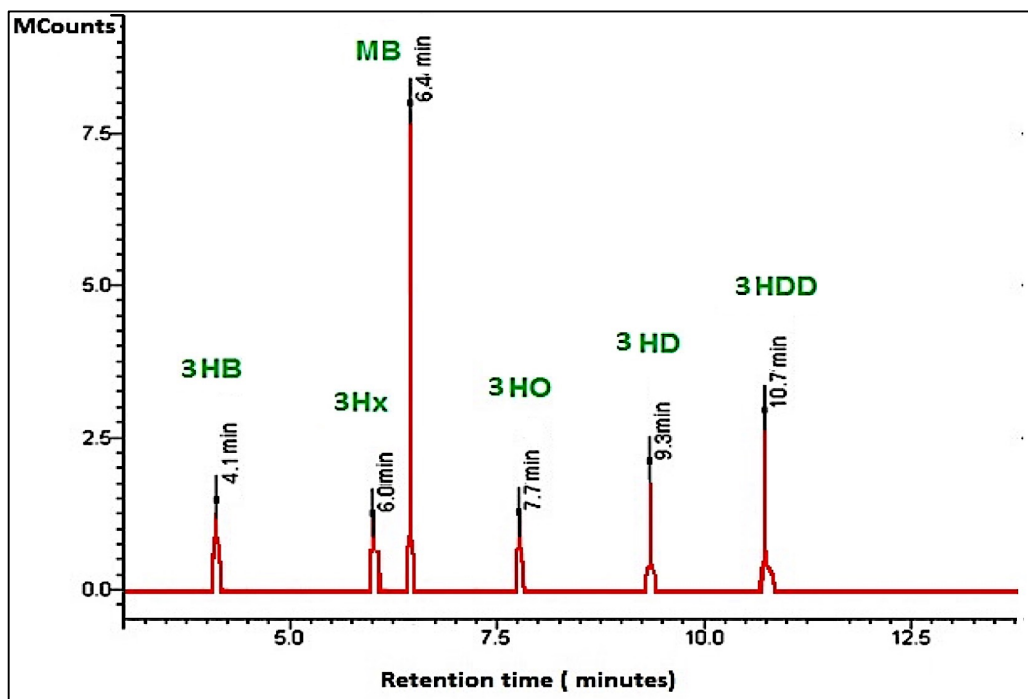


Figure 22: Gas chromatogram of reference standards of methyl esters of 3-hydroxyalkanoates: 3-hydroxybutyrate (3HB), 3-hydroxyhexanoate (3HHx), 3-hydroxyoctanoate (3HO), 3-hydroxydecanoate (3HD), 3-hydroxydodecanoate (3HDD). Methyl benzoate (MB) was used as an internal standard.

According to the standard chromatogram (Figure 22), the peak observed at 4.1 minutes (Figure 21A) corresponded to the methyl esters of 3-hydroxybutyric acid (3HB). Methyl benzoate was used as the internal standard ($R_t=6.4$ min.).

Mass spectra analysis further demonstrated that the peak with $R_t=4.1$ minutes was comparable with the MS spectrum of the methyl ester of 3-hydroxybutyric acid in the MS library obtained from the National Institute of Science and Technology (NIST) (Figure 21B). The $m/z=103$ peak was due to the cleavage between carbon atoms number 3 and 4. The peak at $m/z=74$ was obtained by McLafferty rearrangement of the methyl ester. The ion $m/z=43$ was obtained due to the saturated alkanolic part of the molecule and from the methyl ester moiety (Rijk *et al.*, 2005).

3.3.3. Nuclear Magnetic Resonance (NMR)

^1H and ^{13}C NMR confirmed the chemical structure of the obtained scl-PHA polymer produced by *B. subtilis* OK2 using glucose as the sole carbon sources. The ^1H NMR spectrum (Figure 23A) of the scl-PHA copolymer obtained from *B. subtilis* OK2, grown on glucose showed 3 peaks corresponding to the three different proton environments from P(3HB) (Figure 23A). Signals of the methine protons (-CH) at 5.3 ppm corresponded to the protons bonded to carbon number 3 (-CH- group). The peak present at 1.3 ppm corresponded to the terminal methyl group (-CH₃). The signal at 2.48 ppm corresponded to the methylene protons (-CH₂) bonded to carbon number 2.

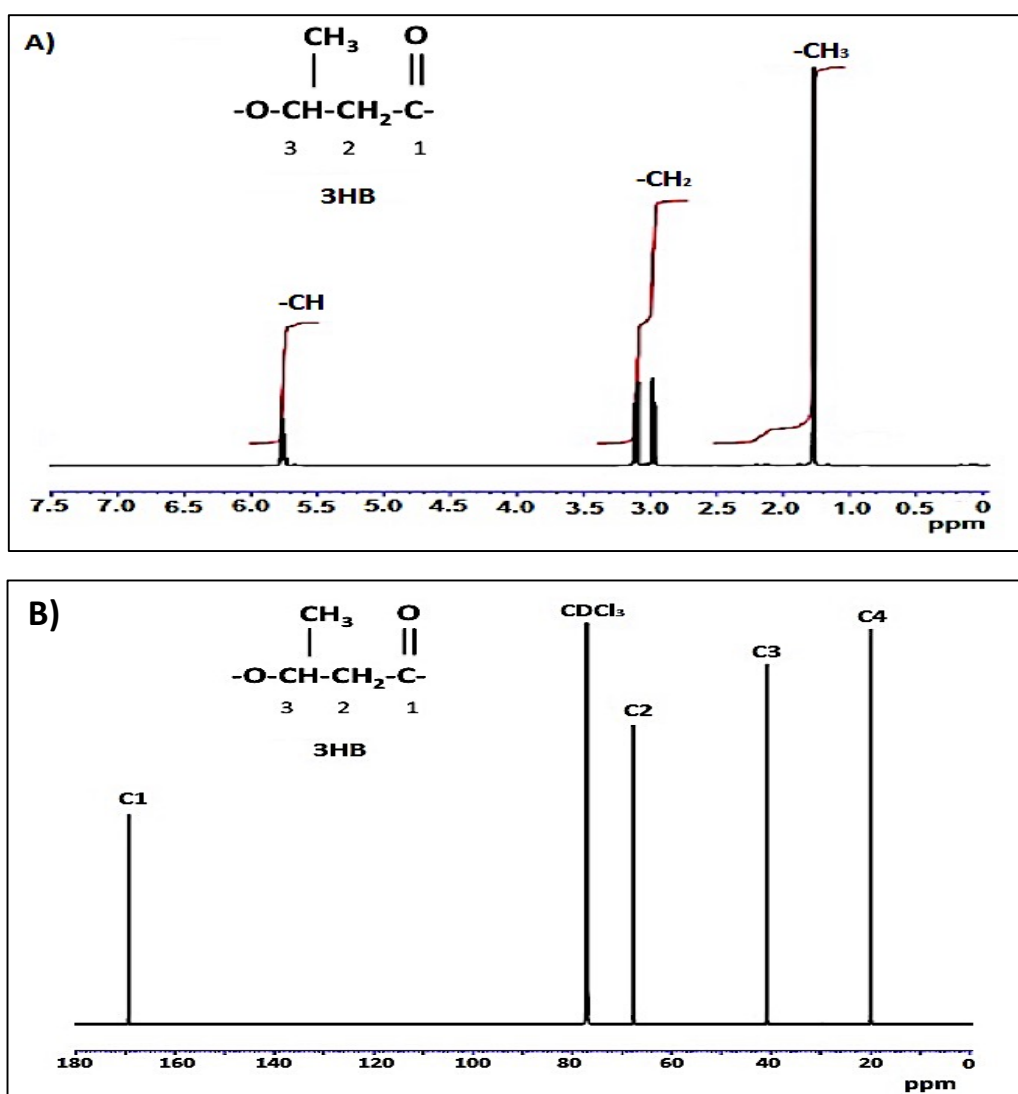


Figure 23: (A) ^1H NMR and (B) ^{13}C NMR spectra of P(3HB) confirming the polymer to be homopolymer P(3HB). The structure of P(3HB) is shown as an insert within the spectra.

The ^{13}C NMR spectrum showed 4 peaks related to the different atoms of carbon (Figure 23B). The peak at the chemical shift of 77.4 ppm corresponded to the carbon of the solvent CDCl_3 . The peaks present at 169.4 ppm, 67.8 ppm, 40.7 and 19.9 corresponded to C1 (C=O group), C3 (-CH- group), C2 (-CH₂- group) and the terminal carbon atom C₄ (-CH₃ group) in the 3-hydroxybutyrate monomer unit.

The chemical shifts of 3HB were similar to those obtained from previous studies (Doi *et al.*, 1986).

The ^1H NMR and ^{13}C NMR analysis confirmed the structure of the scl-PHA as the P(3HB) homopolymer.

3.3.4. Molecular weight analysis of P(3HB) produced by *Bacillus subtilis* OK2

Gel Permeation Chromatography was used to characterize molecular weight of the P(3HB) homopolymer. The results obtained are shown in Table 4 and Figure 24.

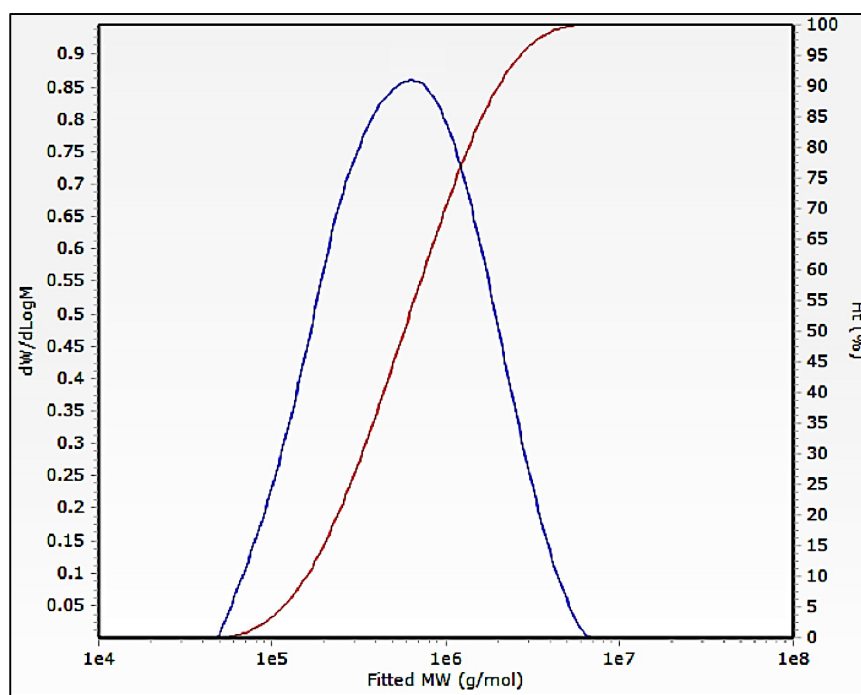


Figure 24: Molecular weight distribution (—) and cumulative molecular weight (—) of neat P(3HB) polymer produced using *Bacillus subtilis* OK2.

Table 4: Summary of molecular weight analysis of the P(3HB) obtained from *Bacillus subtilis* OK2 and glucose as the carbon source; where M_w = weight average molecular weight, M_n = number average molecular weight, PDI= polydispersity index.

Polymer sample	M_w (kDa)	M_n (kDa)	PDI
P(3HB)	582.4	306.7	1.9

As shown in Table 4, GPC analysis demonstrated that the weight average molecular weight (M_w) of the P(3HB) homopolymer was 582.4 kDa and the poly dispersity index was 1.9. These values were similar to those obtained by Reddy *et al.*, 2009, who reported the production of P(3HB) from *Bacillus* sp. 88D with the molecular weight range from 523-627kDa.

3.3.5. Thermal analysis – Differential Scanning Calorimetry (DSC)

DSC studies were carried out to analyse the thermal properties of the freshly produced P(3HB) polymer. Summary of the thermal properties are presented in the Table 5 and in the Figure 25. The glass transition temperature (T_g) of the polymer was -10.7°C . A melting event was observed at 169.5°C .

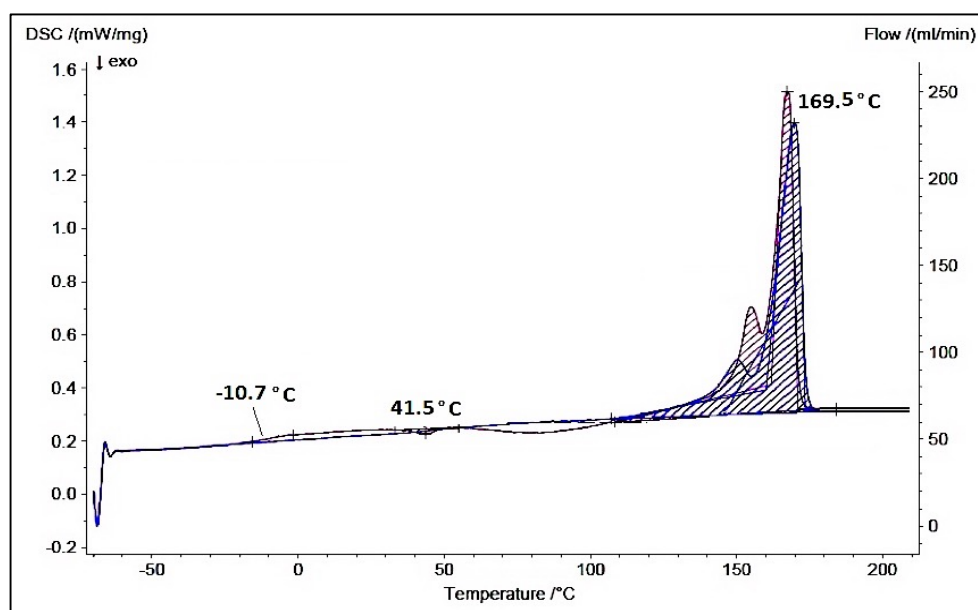


Figure 25: DSC thermograms: first heating cycle (—) and second heating cycle (---) of P(3HB) obtained from *Bacillus subtilis* OK2 using 35g/L glucose as the sole carbon source.

The figure shows the normalised DSC heating curves with peak for glass transition temperature, $T_g = -10.7^\circ\text{C}$ and peak for melting temperature, $T_m = 169.5^\circ\text{C}$.

First heating cycle is used in general, to remove the thermal history of the material. The actual thermal properties of the material appear during second heating cycle. However ageing experiments are an exception. For those studies, the first heating cycle is considered.

Table 5: Summary of the thermal properties of the fresh P(3HB) polymer obtained using *B. subtilis* OK2. Where, T_m = melting temperature, T_g = glass transition temperature, T_c = crystallisation temperature, ΔH_f = enthalpy of fusion.

Polymer sample	T_m ($^\circ\text{C}$)	T_g ($^\circ\text{C}$)	T_c ($^\circ\text{C}$)	ΔH_f (J/G)
P(3HB)	169.5	-10.7	41.5	82.5

The observed T_g and T_m values were similar to that observed for the short chain length PHAs (T_m above 60°C and T_g above -25°C) (Zhang *et al.*, 2009). Wellen and co-workers studied the melting behaviour of P(3HB) and confirmed the presence of a complex peak, which could be spread into three separate peaks with different intensities and melting temperatures (Wellen *et al.*, 2013). The glass transition temperature highly influences the polymer morphology and mechanical properties. Below its T_g , the polymer is in a glassy state and is in a hard and brittle state; while above T_g the polymer is in a rubbery state and is relatively soft (Chanprateep *et al.*, 2010).

3.3.6. Mechanical characterisation of the P(3HB) solvent cast films

P(3HB) neat films were characterised in order to obtain the mechanical properties of the polymer using tensile test as described in the section 2.11.3.2. Three different parameters have been measured, such as: tensile strength, which is a measure of the strength, Young's Modulus, which is a measure of the stiffness and elongation at break, which is a measure of ductility of the material. The summary of the mechanical properties is shown in Table 6.

Table 6: Summary of the mechanical properties of neat P(3HB) solvent cast films without storage; including tensile strength, elongation at break and Young’s modulus (n=3).

Polymer sample	Tensile strength (MPa)	Young’s Modulus (GPa)	Elongation at break (% strain)
P(3HB) film	19.2±2.1	0.8±0.01	22.3±3.4

Fresh P(3HB) films have tensile strength 19.2±2.1MPa, elongation at break 22.3±3.4% and Young’s Modulus 0.8±0.01GPa. The values obtained for tensile strength as well as Young’s Modulus were lower than generally reported in literature. However, the elongation at break is much higher (Pachekoski *et al.*, 2009). In this experiment, material properties were obtained using fresh films within 3 days after complete solvent evaporation. To investigate the influence of the time of storage, known as “material ageing”, on the thermal and mechanical properties of the P(3HB) neat films, DSC and tensile test analysis were performed after 1, 3, 5 and 7 weeks of storage at room temperature, as described in sections 2.11.3.1.-2.11.3.3.

3.3.7. Thermal analysis of the neat P(3HB) neat films after 7 weeks of storage at room temperature

Thermal properties of the solvent cast films were studied for 7 weeks, in order to understand the impact of ageing on the material. The results obtained are summarised in Table 7 and Figure 26.

Table 7: Summary of the thermal properties of the P(3HB) films during 7 weeks of storage at room temperature. Where, T_m = melting temperature, T_g = glass transition temperature, T_c = crystallisation temperature, ΔH_f = enthalpy of fusion.

Time of storage (weeks)	T_g (°C)	T_c (°C)	T_m (°C)	ΔH_f (J/g)
1	-2.8	35.9	172.3	83.22
3	-1.0	40.1	173.0	82.16
5	-1.7	41.6	174.2	84.35
7	0.2	51.5	172.5	85.86

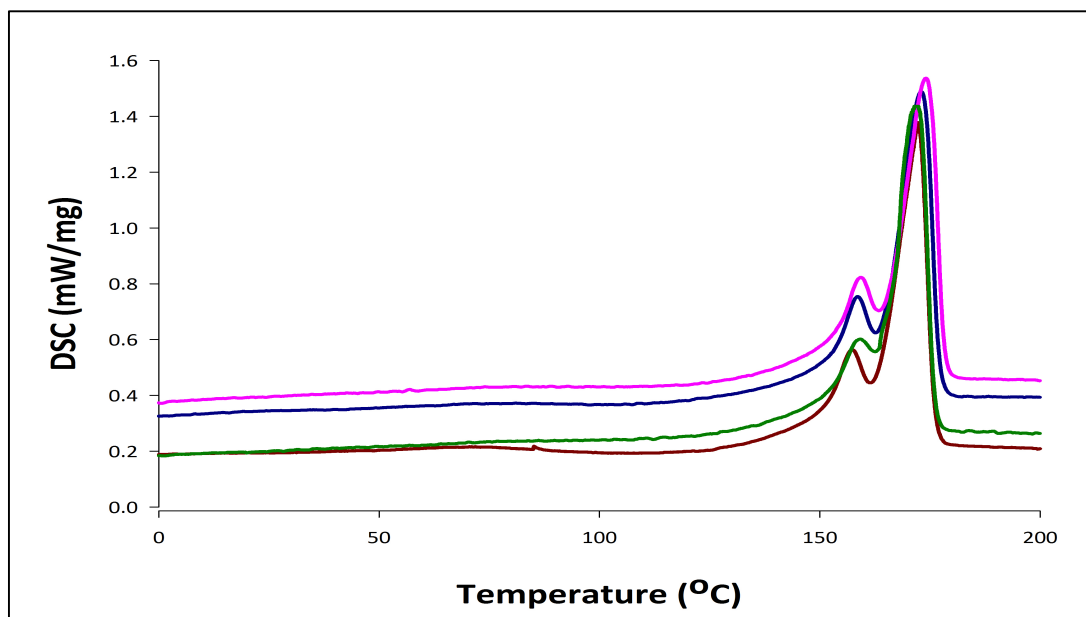


Figure 26: DSC thermograms of P(3HB) neat solvent cast films during 1 week (-), 3 weeks (-), 5 weeks (-) and 7 weeks (-) of storage at room temperature indicating melting peaks (first heating cycle).

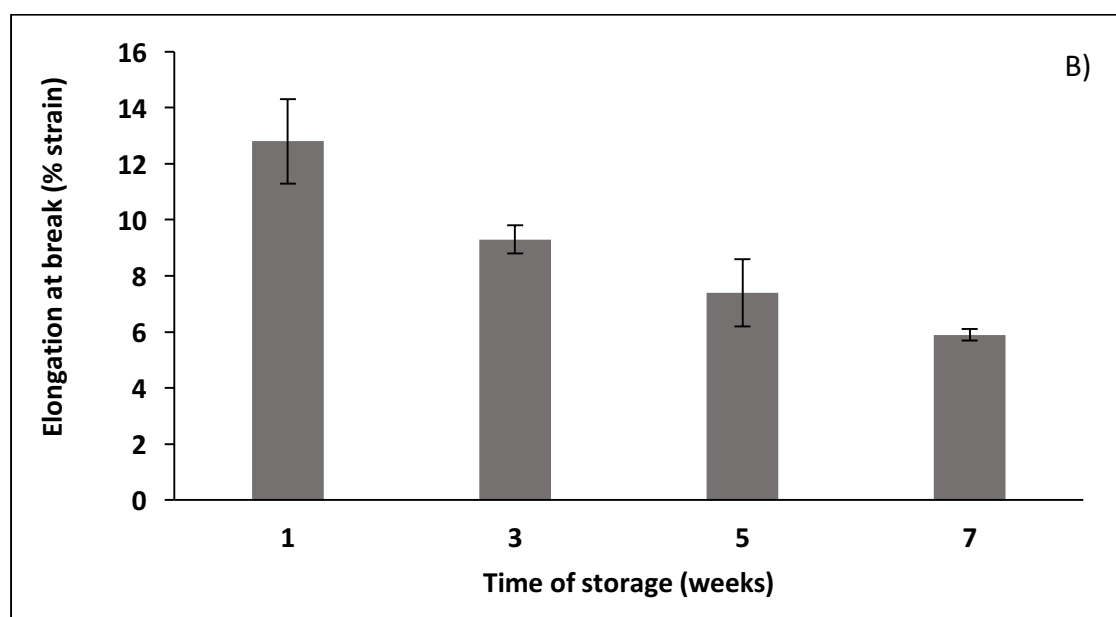
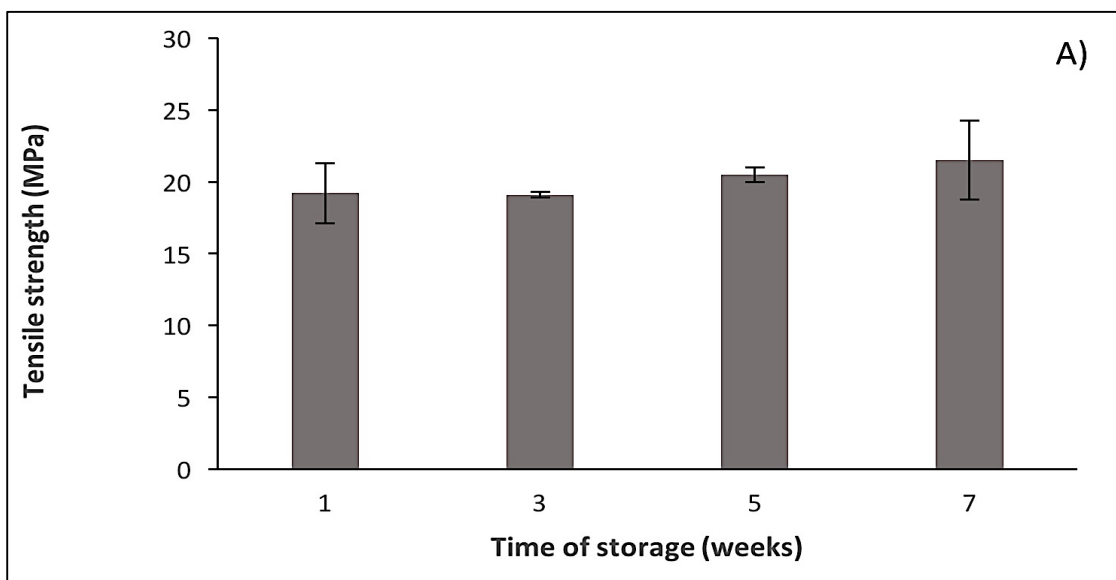
The time of storage has clearly influenced the thermal properties of the material. The glass transition temperature increased from -2.8°C to 0.2°C after 7 weeks of storage. Changes were also observed in the cold crystallisation temperature as in the enthalpy of fusion. T_c values increased from 35.9°C to 51.5°C , ΔH_f values followed the trend of T_c and increased from 83.2 to 85.8 J/g. However, 7 weeks of storage did not result in changes in the melting temperature.

3.3.8. Mechanical characterisation of the neat P(3HB) films after 7 weeks of storage at room temperature

Mechanical properties of the solvent cast films were also carried out for 7 weeks, in order to check the effect of ageing on the material. The results obtained are summarised in Table 8 and Figure 27A-C.

Table 8: Summary of the mechanical properties of the P(3HB) solvent cast films during 7 weeks of storage at room temperature; including tensile strength, elongation at break and Young's Modulus (n=3).

Time of storage (weeks)	Tensile strength (MPa)	Young's Modulus (GPa)	Elongation at break (% strain)
1	19.2±2.1	0.8±0.01	12.8±1.5
3	19.1±0.2	0.9±0.08	9.3±0.5
5	20.5±0.5	1.1±0.06	7.4±1.2
7	21.5±2.7	1.3±0.1	5.9±0.2



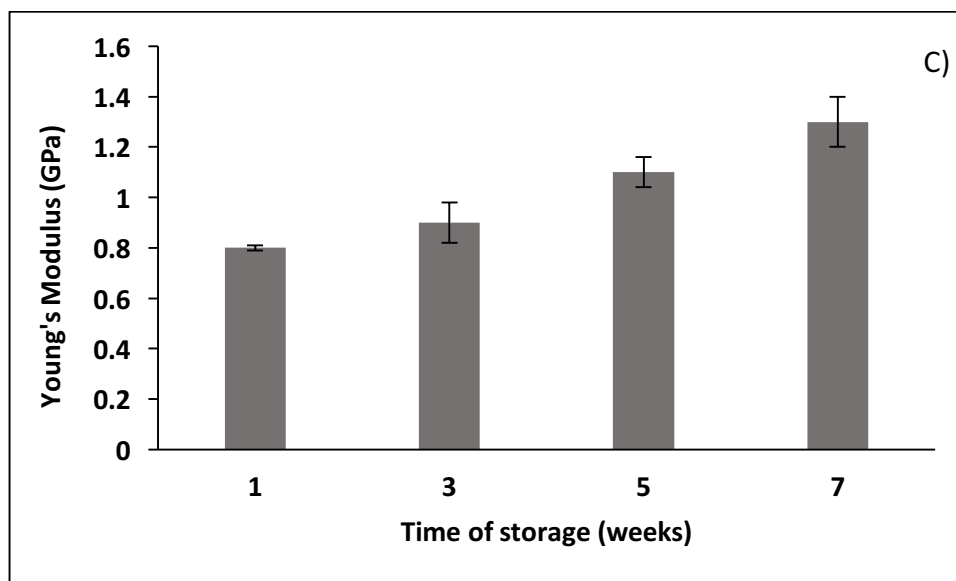


Figure 27: The evolution of (A) an ultimate tensile strength, (B) elongation at break and (C) Young's modulus during 7 weeks of storage at room temperature of neat solvent cast P(3HB) films.

Ageing has influenced the mechanical properties of the P(3HB) films. The tensile strength has slightly increased from 19.2 ± 2.1 MPa at week 1 to 21.5 ± 2.7 MPa after 7 weeks of storage. The Young's Modulus values significantly increased from 0.8 ± 0.01 GPa after week 1 to 1.3 ± 0.1 GPa after week 7. Elongation at break decreased from $12.8 \pm 1.5\%$ after week 1 to $5.9 \pm 0.2\%$ strain after week 7. Hence, ageing of P(3HB) enhanced its strength and stiffness but decreased its elastomeric properties. The material became more brittle with time.

3.4. Discussion

Recent studies demonstrated that various wild-type as well as genetically engineered microorganisms are able to accumulate scl-PHAs. P(3HB) is one of the most explored polyesters within the family of Polyhydroxyalkanoates (Karbasi *et al.*, 2012). The polymer yield, varies depending on the bacterial strain used, carbon source, conditions, fermentation mode and PHA production media (Shahid *et al.*, 2013). For example: *Alcaligenes latus* was able to accumulate more than 75% dcw of P(3HB), when grown on sucrose. *Bacillus sp.*, cultured on sugarcane produces over 90% dcw of P(3HB) (Mozejko-Ciesielska and Kiewisz, 2016). P(3HB) have been produced commercially by several

companies, such as: Biomer (Germany), PHB Industrial S.A. (Brazil) and Jiangsu Nantian Group (China) (Chen, 2009; Bugnicourt *et al.*, 2014).

In this study four different wild-type strains: *Bacillus cereus* SPV, *Bacillus subtilis* OK2, *Cupriavidus necator* and *Pseudomonas mendocina* CH50 were studied with respect to the production of scl-PHAs. All microorganisms studied were able to produce PHAs, mainly P(3HB). *Bacillus* sp. and *Cupriavidus necator* are well known P(3HB) producers. Several metabolic pathways are involved in PHA production as described in the Chapter 1. The main enzyme involved in the biosynthesis of PHAs is the PHA synthase. There are four classes of PHA synthases, class I PHAs synthases, found in *Ralstonia eutropha*, class II, occurring in *Pseudomonas aeruginosa*, class III, present in *Allochromatium vinosum* and class IV in *Bacillus megaterium* (Rehm, 2003). *Pseudomonas* sp. are mainly mcl-PHA producers, whereas *C. necator* is known to mainly produce P(3HB) and copolymers, such as P(3HB-co-3HV) or P(3HB-co-4HB) (Wong *et al.*, 2012, Bhubalan *et al.*, 2010; Timm and Steinbüchel, 1992).

In this study a novel strain, *Bacillus subtilis* OK2 was used for P(3HB) production. Production of P(3HB) by *Bacillus subtilis* OK2 has only been reported by Sukan *et al.*, 2015. The main advantage of using *Bacillus subtilis* over *Bacillus cereus* is that *B. subtilis* is classified as GRAS bacteria (“Generally Recognised as Safe”). Moreover, *B. subtilis* OK2 in contrast to Gram-negative bacteria does not contain lipopolysaccharides, known endotoxins, as structural components of the cell wall. Therefore P(3HB) produced by *B. subtilis* OK2 minimizes the risk of material-mediated immunogenic reactions in humans. Out of all the bacterial strains tested in this work, *Bacillus subtilis* OK2 produced the highest amount of P(3HB) polymer, 30.8% dry cell weight, when glucose was used as the only carbon source. Sukan *et al.*, 2015 have reported production of P(3HB) from *Bacillus subtilis* OK2 at the level of 41% dcw. However, in his study orange peel was used as the carbon source. Akaraonye *et al.*, 2012 observed production of P(3HB) by *B. cereus* SPV with a yield of up to 61% dcw, when grown on sugarcane molasses as the carbon source. *Pseudomonas* sp. are mainly used for mcl-PHA production, however, in this study, P(3HB) as well as P(3HB-co-3HV) have been produced using *P. mendocina*, albeit at a relatively low yield.

The P(3HB) homopolymer produced by *Bacillus subtilis* OK2 was selected for further analysis. FTIR, NMR and GC-MS analysis confirmed that the polymer obtained was

indeed polyester of 3-hydroxybutyric acid. Due to its specific material properties, P(3HB) has been extensively studied for the application mainly in bone tissue regeneration and drug delivery (Luef *et al.*, 2015). For example, nanofibre mats of P(3HB) with incorporated kanamycin were tested against *S. aureus* and over 95% of the drug was successfully released within first 8 hours (Naveen *et al.*, 2010). In another study Shishatskaya *et al.*, reported positive results, obtained after implantation of P(3HB) sutures in the Wistar rat models (breed of albino rat; first rat model organism developed for medical and biological research) (Shishatskaya *et al.*, 2004).

P(3HB) was characterised with respect to the molecular weight of the material, which was detected and found to be 582.4 kDa. The molecular weight of a polymer is one of the most significant properties affecting the processability of the polymer. It has also been shown, that different bacterial strains are able to produce P(3HB) with different molecular weight. Taniguchi *et al.*, 2003, observed production of P(3HB) from *C. necator* with a molecular weight 530 kDa, when grown on sesame oil, whereas Kahar *et al.*, 2004 reported P(3HB) production from *C. necator* with molecular weight 1.2 MDa, when grown on soybean oil. Kusaka *et al.*, 1999, reported synthesis of P(3HB) with ultrahigh molecular weight from 5.0 MDa to 20.0 MDa from recombinant *E. coli*, harbouring genes from *Ralstonia eutropha* H16. Rai *et al.*, 2011 compared various techniques of P(3HO) extraction using different solvents. Soxhlet extraction resulted in the low polymer yield but the highest purity product, which is crucial in biomedical applications. The molecular weight of the polymer obtained from Soxhlet extraction was comparable with the molecular weight of the polymer obtained from solvent extraction using chloroform, but much larger than that obtained using the solvent dispersion method (Rai *et al.*, 2011).

In order to fully understand the mechanical and thermal properties is it necessary to look at the changes in the properties of P(3HB) films after storage time. The thermal properties of fresh P(3HB) films and after 7 weeks of ageing were found to be different especially for glass transition temperature and cold-crystallisation temperature. The two parameters, i.e. the melting event as well as enthalpy of fusion remain stable. From literature, the thermal properties of P(3HB) are: T_g value in the range 2-10°C and T_m between 174 to 178°C (Reddy *et al.*, 2009; Akaraonye *et al.*, 2012; Ashby *et al.*, 2012; Zhang *et al.*, 1996). However, there was no record about the age of the characterised

material. T_g and T_m values obtained in this study were lower than the values found in the literature. The largest changes were observed in the cold-crystallisation temperature, which increased from 36 °C to 51.5 °C. In this study, melting peak for P(3HB) obtained was a double peak. This is with an agreement with literature. Multiple melting peaks of P(3HB) have been reported previously as a consequence either of conditions used during DSC analysis, polymorphism, different size, maturation and stability of crystals or physical ageing of the material (Gunaratne and Shanks, 2005).

It is well known that the P(3HB) polymer becomes increasingly brittle with the time of storage due to secondary crystallization, which occurred during ageing. This has an effect on the tensile strength, elongation at break and Young's Modulus values. This increased brittleness of the material also results in an increase of stiffness and strength of the material. The usual mechanical properties of P(3HB) reported in the literature are: Young's Modulus round 1.1-3.5GPa, tensile strength 19-35MPa and elongation at break 0.4-5.0% (Chanprateep *et al.*, 2010; Sigh *et al.*, 2015; Sudesh *et al.*, 2000). However, the age of the studied material was not mentioned. All three mechanical properties of P(3HB) produced from *B. subtilis* OK2 in this study were within the ranges mentioned in the literature.

The mechanical properties of the P(3HB) produced in this work were found to be unsuitable for use as a platform for coronary stent development. The elongation at break value was found to be too low since the stent need to be crimped and then expanded by ballooning. This can perhaps be achieved by creating blends of P(3HB) with more elastomeric mcl-PHAs. The final material should have a high tensile strength of 30-50 MPa, Young's modulus above 1 GPa and an elongation at break around 10%.

In conclusion, this study has demonstrated the ability of various bacterial strains to produce mainly P(3HB) using a range of the different carbon sources. This work confirmed the capability of a Gram-positive GRAS organism, *Bacillus subtilis* OK2 to produce P(3HB) with high polymer yield. Characterisation of the material verified the thermal and mechanical properties typical to P(3HB). Due to its high brittleness, P(3HB) has to be mixed with more elastomeric PHAs to be more suitable for coronary stent application.

Chapter 4

Production and characterisation of medium chain length Poly(3-hydroxyalkanoates)

4. Introduction

Polyhydroxyalkanoates are an emerging group of biomaterials, which can be an alternative to the traditional, petroleum based plastics. PHAs are produced by a wide variety of bacterial species usually under nutrient limiting conditions with excess of carbon source. Scl-PHAs have been produced and characterised as described in Chapter 3. The second type of PHAs is medium chain length polyhydroxyalkanoates (mcl-PHAs), which contain from 6 to 14 carbon atoms within the monomer unit (Oliveira *et al.*, 2007). This group of PHAs have different material properties in comparison to scl-PHAs. Mcl-PHAs are very elastomeric, have low crystallinity, low melting temperature and glass transition temperature (Rai *et al.*, 2011). The drawback of mcl-PHAs is their low Young's modulus and tensile strength values, therefore, they cannot be used in load bearing applications. Also, their low T_g and T_m values make them suitable only for very specific applications, due to restricted methods of processing. Among mcl-PHAs are commonly represented by 3-hydroxyhexanoate (3HHx), which has 6 carbon atoms within the monomer unit, 3-hydroxyheptanoate (3HHp) with 7 carbon atoms, 3-hydroxyoctanoate (3HO), containing 8 atoms, 3-hydroxydecanoate (3HD), containing 10 carbon atoms and 3-hydroxydodecanoate, with 12 carbon atoms within the monomer unit (Basnett *et al.*, 2017). Within mcl-PHA group, a lot of different types of copolymers have been produced, such as poly(3-hydroxyhexanoate-co-3-hydroxyoctanoate) P(3HHx-3HO), poly(3-hydroxyoctanoate-co-3-hydroxydecanoate) P(3HO-3HD) and poly(3-hydroxyoctanoate-co-3-hydroxydecanoate-co-3 hydroxydodecanoate) P(3HO-3HD-3HDD) (Anderson and Dawes, 1990). Mcl-PHAs can be produced by different types of *Pseudomonas* sp., such as *P. aeruginosa*, *P. putida*, *P. oleovorans*, *P. mendocina*, *P. ragnenesii*, *P. guezenei* and *P. stutzeri* (Simon-Collin, 2009; Simon-Collin, 2012). Mcl-PHA production was also achieved by using *Comamonas testosteronii* or recombinant *E. coli* (Thakor *et al.*, 2006; Wang *et al.*, 2012). Mcl-PHAs have been used in several biomedical applications, such as: soft tissue engineering or biological adhesives (Chen and Wu, 2005; Williams *et al.*, 1999; Pouton and Akhtar, 1996). They can also be used as an additive to scl-PHAs to enhance the elastomeric properties of the scl-PHAs. High production cost is one of the main limiting factors, which reduces the widespread application of mcl-PHAs (Singh *et al.*, 2009). Therefore, various strategies have been

introduced to make the PHA production more economically efficient. These will include: PHA production from mixed cultures (Choi and Lee, 1997), genetically engineered microorganisms, cheap carbon sources (Luckachan and Pillai, 2012) as well as changes in fermentation strategies towards continuous fermentation with high cultures density (Chen, 2009). Many different solutions have been tested to improve the yields, productivity and decrease the production costs of PHAs, to make them commercially available. Over 50% of the total cost is due to the price of carbon source. Various types of cheap carbon sources and waste materials, such as vegetable oils, waste crops, and side products from fuel industry have been explored in order to significantly reduce the total production cost (Anjum *et al.*, 2016; Ciesielski *et al.*, 2015).

The main objective of this study was to produce mcl-PHAs using *Pseudomonas mendocina* CH50 using a range of cheap carbon sources and renewable materials. The selected material was subjected to thorough analysis in order to fully characterise the properties of the chosen material.

4.1. Screening experiments

Screening experiments were carried out to obtain novel mcl-PHAs using *Pseudomonas mendocina* CH50. The range of different carbon sources, including cheap carbon sources, such as waste frying oil, sugarcane molasses, vegetable oils and biodiesel waste have been investigated. A summary of the results is shown in the Table 9. Depending on the type of carbon source, various mcl-PHAs copolymers have been synthesised. The monomer units, which are present in the most of the conditions are 3-hydroxyoctanoate (3HO) and 3-hydroxydecanoate (3HD). The polymer yield (% dcw) is also shown in the Table 9.

Table 9: Summary of the screening experiments used for the production of mcl-PHAs by *Pseudomonas mendocina* CH50 using various carbon sources.

Bacterial strain	Carbon source	Polymer yield (% dcw)	GC-MS results
<i>Pseudomonas mendocina</i> CH50	Glycerol	4.2	3HO, 3HD
	Waste frying oil	38.0	3HHx, 3HO, 3HD, 3HDD
	Sugarcane molasses	14.0	3HO, 3HD
	Rapeseed oil	15.27	3HO, 3HD
	Grapeseed oil	10.42	3HO, 3HD, 3HDD
	Sunolive oil	8.8	3HO, 3HD
	Biodiesel waste	38.9	3HHx, 3HO, 3HD, 3HDD
	Sucrose, biodiesel waste	16.8	3HO, 3HD
	Lauric acid, 1,4-butanediol	5.2	3HO, 3HD, 3HDD
	Sucrose, butyrolactone	4.33	3HO, 3HD

As seen in Table 8, all studied carbon sources resulted in mcl-PHA accumulation. *Pseudomonas* sp. are well-known mcl-PHA producers from different types of carbon sources. The copolymer P(3HO-3HD) was produced using glycerol, sugarcane molasses, rapeseed oil, sunolive oil, and mixture of sucrose with biodiesel waste or γ -butyrolactone. The terpolymer P(3HO-3HD-3HDD) was obtained from grapeseed oil and lauric acid mixed with 1,4-butanediol. A unique mcl-PHA copolymer, containing 4 monomer units: 3HHx, 3HO, 3HD, 3HDD was obtained when *P. mendocina* was grown using waste frying oil and biodiesel waste. Obtained polymer yield was around 38-39.0% dcw.

Due to its high yield and polymer composition, the novel mcl-PHA copolymer obtained from *Pseudomonas mendocina* CH50 with 20g/L of waste frying oil was selected for further studies.

4.2. Characterisation of the waste frying oil used to produce mcl-PHAs

Waste frying oil, used as the carbon source was chemically characterised using Attenuated Total Reflectance Fourier Transform Infrared Spectroscopy (ATR-FTIR), Gas Chromatography–Mass Spectrometry (GC-MS) and Nuclear Magnetic Resonance (NMR) as described in the sections 2.6.1.-2.6.3.

4.2.1. Attenuated Total Reflectance Fourier Transform Infrared Spectroscopy (ATR/FT-IR)

Preliminary characterisation of the waste frying oil was carried out using ATR/FTIR. In the ATR/FT-IR spectrum (Figure 28) two sharp absorption bands at 2923.1 and 2853.6 cm^{-1} were observed and could be assigned to $-\text{CH}_2$ asymmetric vibrations and to $-\text{CH}_3$ asymmetric vibrations respectively. In addition, a small peak at 3009 cm^{-1} , which corresponds to $=\text{C}-\text{H}$ (configuration *cis*) stretching was also observed. The spectra also revealed absorption bands at 1743.6 cm^{-1} corresponding to the ester carbonyl group, a short peak at 1655.0 cm^{-1} corresponding to $-\text{C}=\text{C}-$ (*cis* configuration) stretching, peaks at 1463.8 cm^{-1} and 1377.5 cm^{-1} , corresponding to $-\text{C}-\text{H}$ bending and two peaks at 1236.2 and 1161.1 cm^{-1} corresponding to the $-\text{CO}$ stretching group and $-\text{CH}_2$ bending. There was also observed absorption bands at 722.2 cm^{-1} , which could be assigned to $-(\text{CH}_2)$ bending.

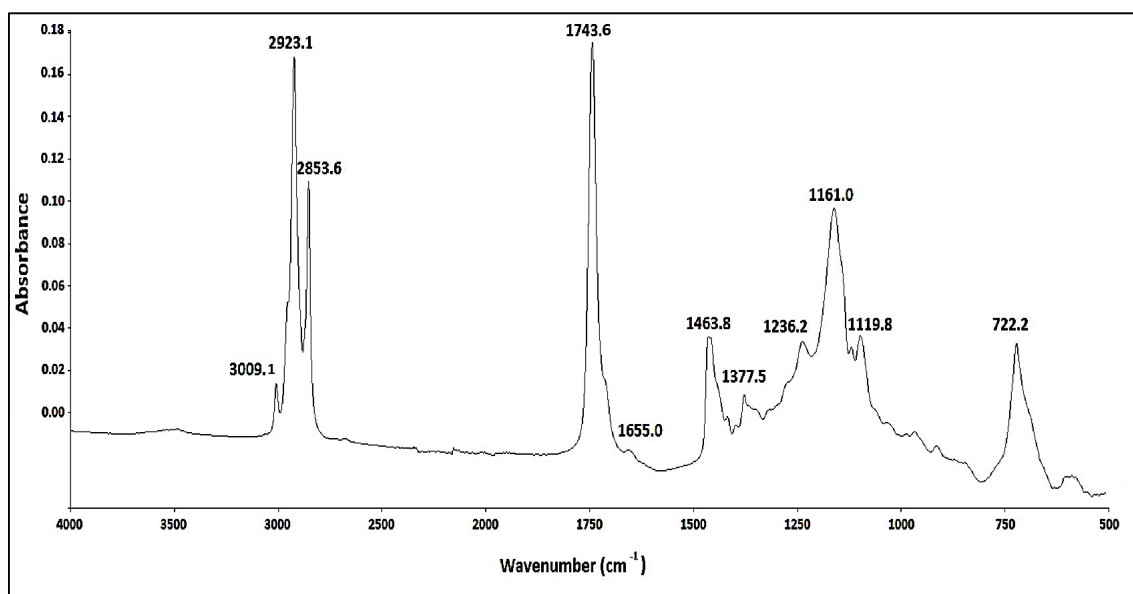


Figure 28: ATR-FTIR spectrum of the waste frying oil used as a carbon source for mcl-PHAs production indicating the important peaks of the spectrum.

This analysis confirmed the presence of characteristic bands of fatty acids. Sbihi *et al.*, 2015 have observed similar adsorption peaks, obtained from the analysis and characterisation of fatty acids present in fat from goat milk (Sbihi *et al.*, 2015). Also, Gomez *et al.*, 2011 have observed similar FTIR spectra obtained from the analysis of vegetable oils (Gomez *et al.*, 2011).

4.2.2. Gas Chromatography Mass Spectrometry (GC-MS)

Chemical composition of obtained PHAs polymer was identified by Gas Chromatography-Mass Spectrometry analysis. The GC chromatogram showed three peaks at $R_t=12.3$ minutes, $R_t=13.4$ minutes and $R_t=13.7$ minutes. Methyl benzoate was used as the internal standard ($R_t=6.5$ minutes) The peaks obtained were analysed using the NIST library (Figure 29).

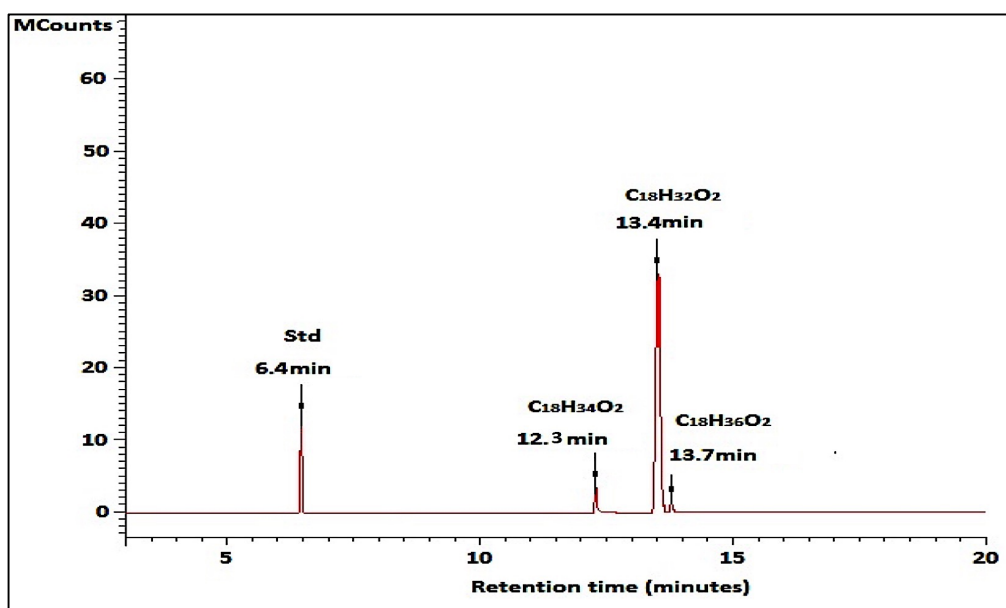


Figure 29: Gas chromatogram of the composition of the waste frying oil used for mcl-PHA production as a carbon source. Methyl benzoate was used as an internal standard (Std).

The mass spectra analysis demonstrated that the peak with $R_t=12.3$ minutes was comparable with the MS spectrum of the methyl ester of 9-octadecenoic acid, known also as oleic acid (Figure 30A). Peak with $R_t=13.4$ minutes was comparable with the MS spectrum of the methyl ester of 9,12-octadecadienoic acid, known as linoleic acid (Figure 30B). Peak with $R_t=13.7$ minutes was comparable with the MS spectrum of

CHAPTER 4

octadecanoic acid also known as stearic acid (Figure 30C). In all mass spectra m/z ion peaks characteristic for fatty acids have been observed. Similar MS spectra for oleic acid as well as linoleic acid are presented in the AOCS Lipids Library (source: <http://lipidlibrary.aocs.org>).

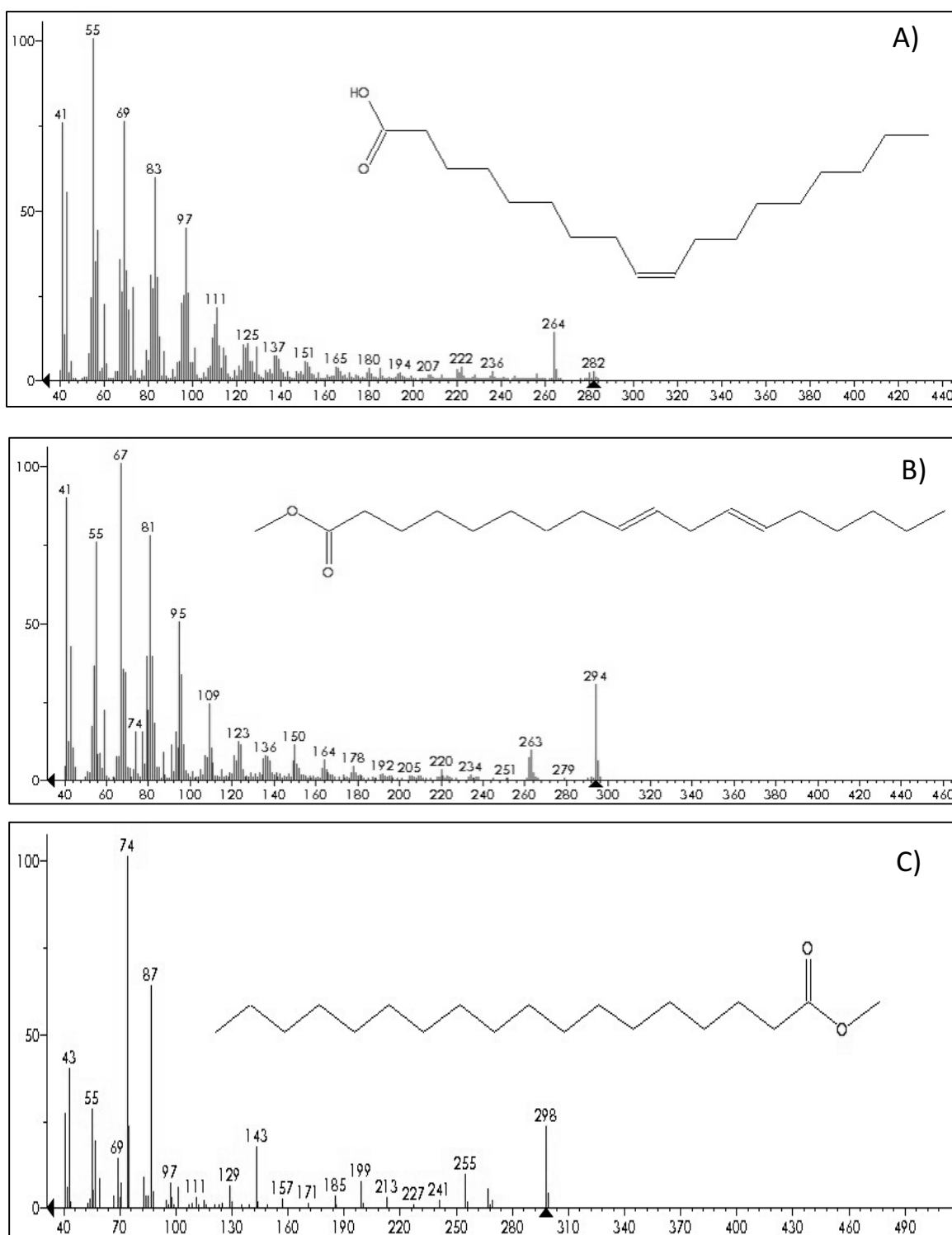


Figure 30: Mass spectra of peaks obtained by gas chromatography of waste frying oil. Retention times (A) 12.3 min, (B) 13.4 min and (C) 13.7min identified using the NIST

library as methyl esters of 9-octadecenoic acid, 9,12-octadecadienoic acid and octadecanoic acid respectively.

Hence, the composition of waste frying oil was confirmed as 9-octadecenoic acid (oleic acid), 9,12-octadecadienoic acid (linoleic acid) and octadecanoic acid (stearic acid). The dominant compound in waste frying oil was linoleic acid 90.5mol%, whereas the amount of oleic acid was only 8.6 mol % and stearic acid 0.9mol% (Table 10).

Table 10: Fatty acids composition (mol %) of waste frying oil used for mcl-PHA production.

Fatty acid	Molar content (mol %)
$C_{18}H_{34}O_2$	8.6
$C_{18}H_{32}O_2$	90.5
$C_{18}H_{36}O_2$	0.9

4.2.3. Nuclear Magnetic Resonance (NMR)

1H and ^{13}C NMR further confirmed the chemical structure of the composition of the waste frying oil. The 1H NMR spectrum (Figure 31A) of the waste frying oil showed 7 peaks corresponding to the different proton environments from the fatty acids (Figure 31A). Individual signals derived from protons bonded to the carbon atoms for octadecanoic acid, 9-octadecenoic acid and 9,12-octadecadienoic acid are listed in Table 11, 12.

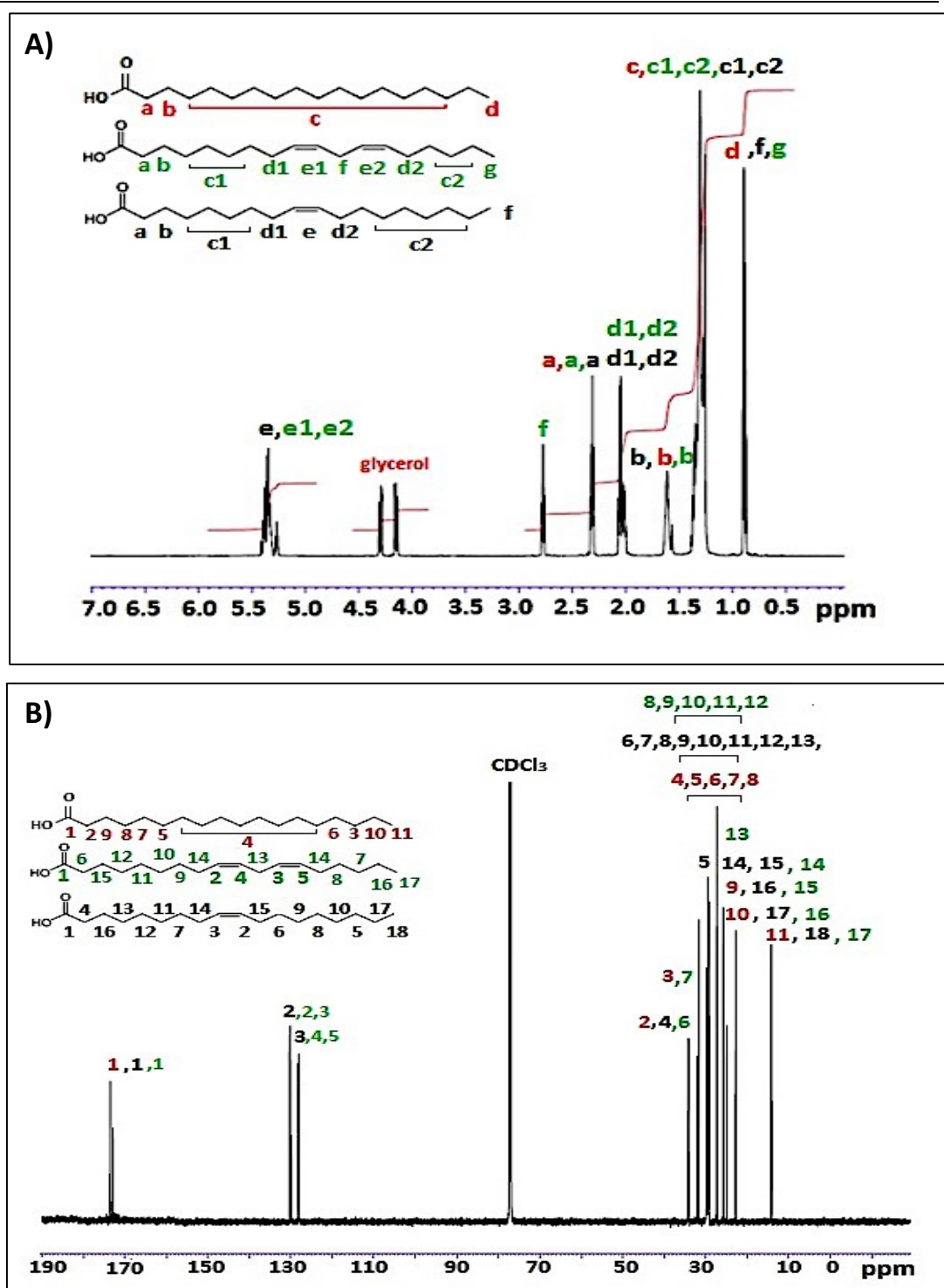


Figure 31: (A) ^1H NMR and (B) ^{13}C NMR spectra of waste frying oil used for mcl-PHA production as the carbon source. Chemical structures of stearic acid $\text{C}_{18}\text{H}_{36}\text{O}_2$ (red), linoleic acid $\text{C}_{18}\text{H}_{32}\text{O}_2$ (green) and oleic acid $\text{C}_{18}\text{H}_{34}\text{O}_2$ (black) are shown as an insert within the spectra.

Table 11: The summary of the chemical shifts observed in ^1H NMR of the fatty acids presented in the waste frying oil.

	δ , ppm	Proton group and bonded carbon atoms in Octadecanoic acid (red colour)	Proton group and bonded carbon atoms in 9-Octadecenoic acid (black colour)	Proton group and bonded carbon atoms in 9,12-Octadecadienoic acid (green colour)
a.	5.3	-	e-CH=CH-	e1, e2 - CH=CH-
b.	2.7	-	-	f-CH ₂ -CH=
c.	2.3	a-CH ₂ -	a-CH ₂ -	a-CH ₂ -
d.	2.0	-	d1, d2-CH ₂ -CH=	d1, d2-CH ₂ -CH=
e.	1.6	b-CH ₂ -	b-CH ₂ -	b-CH ₂ -
f.	1.3	c-(CH ₂) _n -	c1, c2-(CH ₂) _n -	c1, c2-(CH ₂) _n -
g.	0.9	d-CH ₃	f-CH ₃	g-CH ₃

The ^{13}C NMR spectrum showed 11 peaks related to signals from different atoms of carbon (Figure 31B). The peak at the chemical shift 77.4 ppm corresponds to the carbon of the solvent CDCl_3 . The summary of chemical shifts in ^{13}C NMR of octadecanoic acid, 9-octadecenoic acid and 9,12-octadecadienoic acid are listed in Table 12.

Table 12: The summary of the chemical shifts observed in ^{13}C NMR spectrum of the fatty acids presented in the waste frying oil.

	δ , ppm	Octadecanoic acid	9-Octadecenoic acid	9,12-Octadecadienoic acid
1.	180.2	C1	C1	C1
2.	130.2	-	C2	C2-C3
3.	128.1	-	C3	C4-C5
4.	34.1	C2	C4	C6
5.	31.5	C3	C5	C7
6.	29.3	C4-C8	C6-C13	C8-C12
7.	27.2	-	-	C13
8.	25.7	C9	C14-C15	C14
9.	24.7	-	C16	C15
10.	22.6	C10	C17	C16
11.	14.1	C11	C18	C17

Both NMR spectra: ^1H and ^{13}C , confirmed the composition of the waste frying oil obtained by GC-MS analysis. The waste frying oil has 3 main compounds listed below: 9,12-octadecadienoic acid, 9-octadecenoic acid and octadecanoic acid.

4.3. Production of P(3HHx-3HO-3HD-3HDD) using *Pseudomonas mendocina* CH50 and waste frying oil as a sole carbon source

The growth profile of *Pseudomonas mendocina* CH50 grown with 20g/L of waste frying oil as a sole carbon source was studied for 48 hours (Figure 32). Samples were taken in 3 hour intervals. Biomass, optical density (OD_{450nm}) and pH were monitored. Polymer yield and nitrogen concentration were estimated.

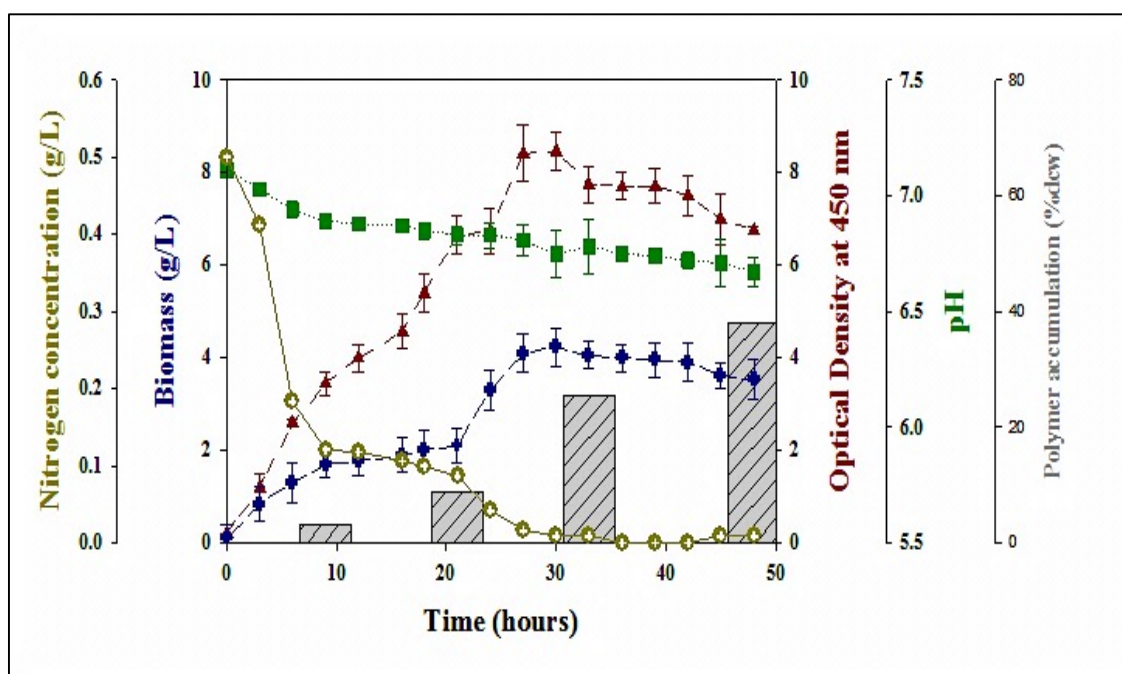


Figure 32: Temporal profile of PHA production by *Pseudomonas mendocina* CH50 using MSM medium with 20g/L of waste frying oil as a sole carbon source. polymer yield (% dcw), Optical Density at 450nm, pH, biomass (g/L), nitrogen concentration (g/L).

It was observed that the Optical Density (OD) increased gradually until 30 hours and reached a maximum value 8.5. After that the OD decreased. Biomass concentration increased along with the optical density of the bacterial culture until 30 hours. A maximum biomass concentration of 4.2g/L was obtained at 30 hrs and then the values decreased. pH of the production medium was set to 7.0. During the fermentation, pH

decreased from 7.0 until 6.67 at 48 hours. Concentration of nitrogen decreased from its initial value of 0.5 g/L to 0.01 g/L within 27 hours of fermentation indicating that a nitrogen-limiting environment was maintained during the fermentation. The polymer yield increased from 3.1% dcw at 9 hours to 38.0% dcw after 48 hours.

4.4. Mcl-PHA characterisation

Obtained polymer was chemically characterised using Attenuated Total Reflectance Fourier Transform Infrared Spectroscopy (ATR-FTIR), Gas Chromatography–Mass Spectrometry (GC-MS) as described in the sections 2.6.1.-2.6.2. Molecular weight analysis was performed according to the method described in the section 2.6.5.

4.4.1. Attenuated Total Reflectance Fourier Transform Infrared Spectroscopy (ATR/FT-IR)

Preliminary characterisation of the polymer was carried out using ATR/FTIR. FTIR spectra revealed presence of an absorption bands at 1736.9 cm^{-1} corresponding to the ester carbonyl group and at 1162.2 cm^{-1} corresponding to the -CO stretching group, characteristic of mcl-PHAs (Randriamahefa *et al.*, 2003) (Figure 33). The bands at 2955.4 cm^{-1} , 2925.9 and 2856.8 cm^{-1} correspond to the aliphatic C-H group of the pendant alkyl group found in mcl-PHAs. This analysis confirmed the presence of bands characteristic for mcl-PHAs suggesting the production of mcl-PHA by *P. mendocina* using waste frying oil as a carbon source.

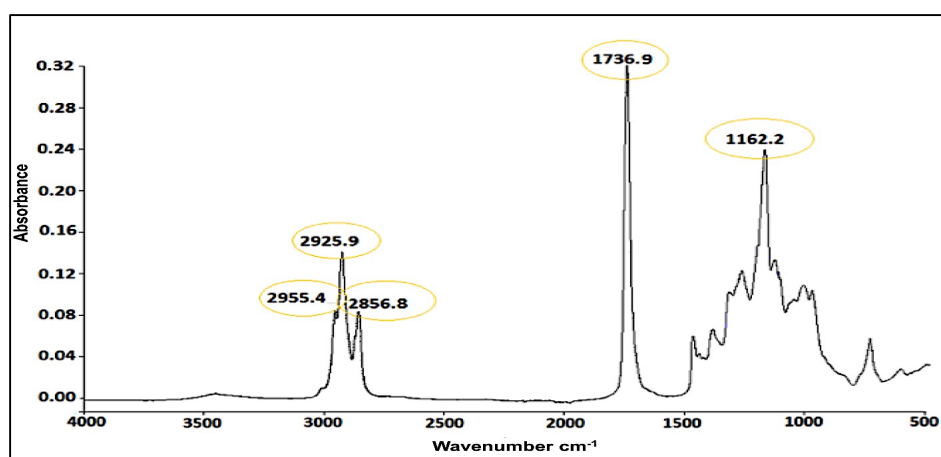


Figure 33: ATR-FTIR spectrum of the polymer produced from *Pseudomonas mendocina* CH50 with 20g/L waste frying oil as a carbon source indicating the important peaks of the spectrum characteristic for mcl-PHAs.

FTIR analysis confirmed the presence of the peaks, characteristic of medium chain length PHAs (Simon-Colin *et al.*, 2008).

4.4.2. Gas Chromatography Mass Spectrometry (GC-MS)

The GC chromatogram showed four peaks at $R_t=5.9$ min, $R_t=7.7$ min, $R_t=9.3$ min, $R_t=10.7$ min (Figure 34). The chromatographic system was calibrated using reference standards of various methyl esters of 3-hydroxyalkanotes as presented in Figure 22. According to the calibration, the peaks observed corresponded to the methyl esters of the 3-hydroxyhexanoic acid (3HHx), 3-hydroxyoctanoic acid (3HO), 3-hydroxydecanoic acid (3HD) and 3-hydroxydodecanoic acid (3HDD), respectively. Methyl benzoate was used as the internal standard ($R_t=6.4$ min) (Figure 34).

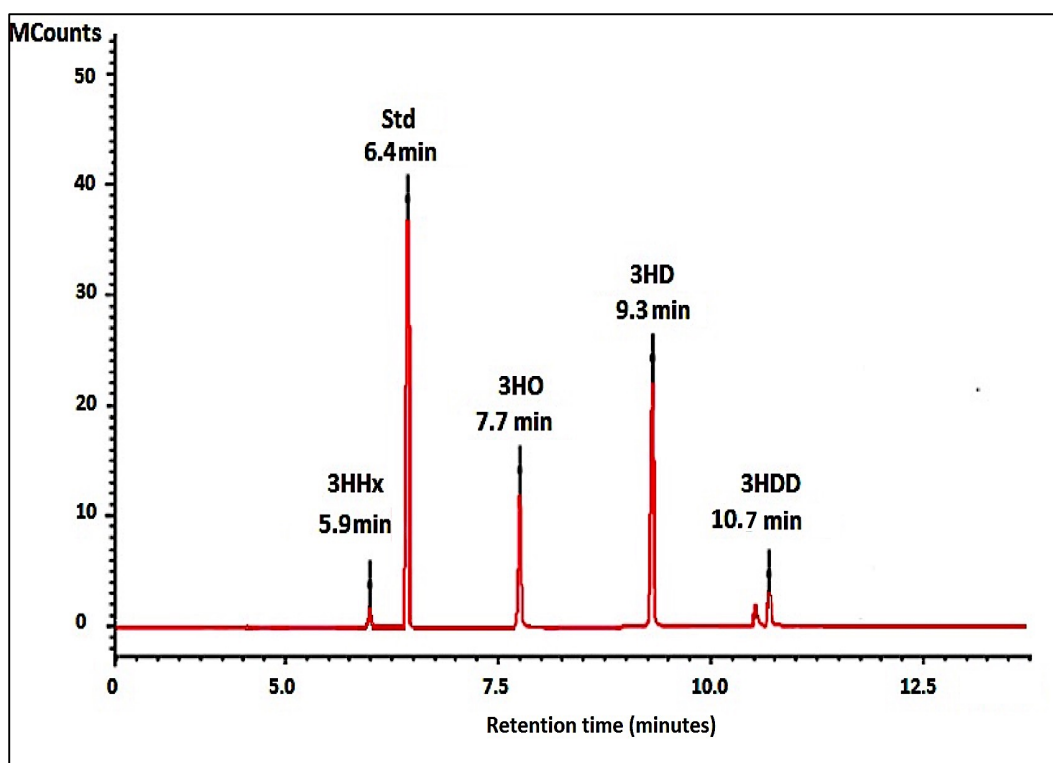


Figure 34: Gas chromatogram of the mcl-PHA polymer produced by *Pseudomonas mendocina* CH50 using waste frying oil as the carbon source. Methyl benzoate was used as an internal standard.

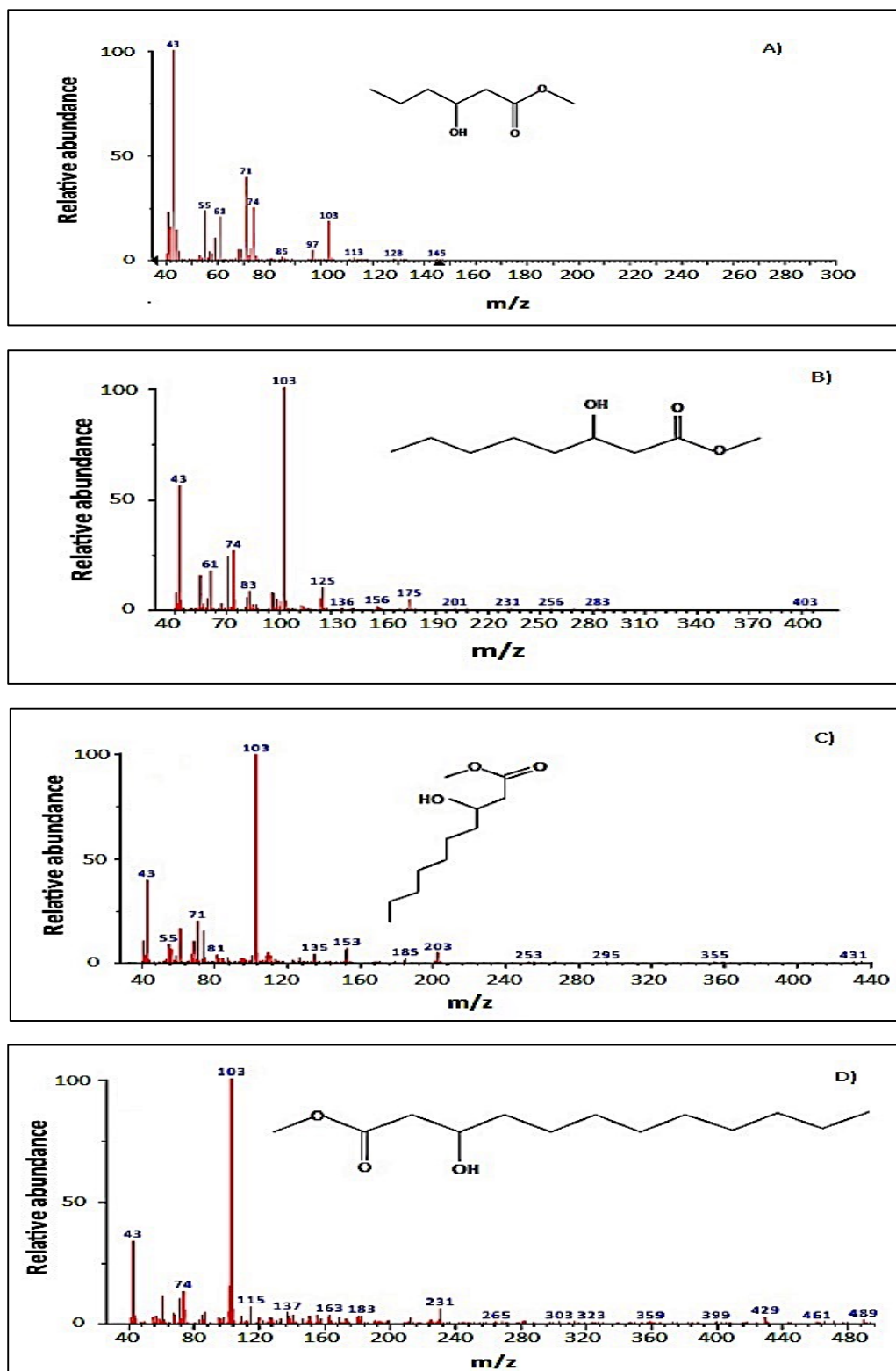


Figure 35: Mass spectra of peaks obtained from GC of polymer produced by *P. mendocina* and waste frying oil. Retention times (A) 6.0 min, (B) 7.7 min, (C) 9.3 min and (D) 10.7 min identified using the NIST library as methyl esters of 3-hydroxyhexanoic acid, 3-hydroxyoctanoic acid, 3-hydroxydecanoic acid, and 3-hydroxydodecanoic acid respectively.

The mass spectra obtained demonstrated that the peak with $R_t=5.9$ minutes was comparable with the MS spectrum of the methyl ester of 3-hydroxyhexanoic acid (Figure 35A). The peak with $R_t=7.7$ minutes was comparable with the MS spectrum of the methyl ester of 3-hydroxyoctanoic acid (Figure 35B). Peaks with $R_t=9.3$ and $R_t=10.6$ minutes are similar with the MS spectra of the methyl ester of 3-hydroxydecanoic acid and 3-hydroxydodecanoic acid respectively (Figure 35C and D). In all mass spectra m/z ion peaks characteristic for PHAs have been observed, such as peak $m/z=103$ (α cleavage between carbon atoms number 3 and 4), peak at $m/z=74$ (McLafferty rearrangement of the methyl ester). The ion $m/z=43$ as described in section 3.3.2.

The composition of the obtained polymer was confirmed as P(3HHx-3HO-3HD-3HDD). The dominant monomer units in these copolymers were 3-hydroxyoctanoate and 3-hydroxydecanoate. Table 13 presents the molecular composition of the mcl-PHA synthesised by *P. mendocina* using waste frying oil. The monomer content was derived from the GC-MS results using the calibration curve obtained using methyl esters of 3-hydroxyalkanoates with different alkanic acids described in the Chapter 3. As can be seen from the Table 13, the shortest (C6) and the longest (C12) monomer units were only slightly more than 10 mol%, with the rest of the polymer consisting of almost equal fractions of 3-hydroxyoctanoate and 3-hydroxydecanoate.

Table 13: Monomer composition mcl-PHA synthesised by *P. mendocina* with waste frying oil as a carbon source.

	Molar content, mol%
3HHx	7.6
3HO	45.4
3HD	41.8
3HDD	5.2

4.4.3. Thermal analysis – Differential Scanning Calorimetry (DSC)

Thermal analysis of the P(3HHx-3HO-3HD-3HDD) mcl-PHA copolymer were performed by DSC as described in section 2.6.2. Summary of the results are presented in Figure 36 and Table 14.

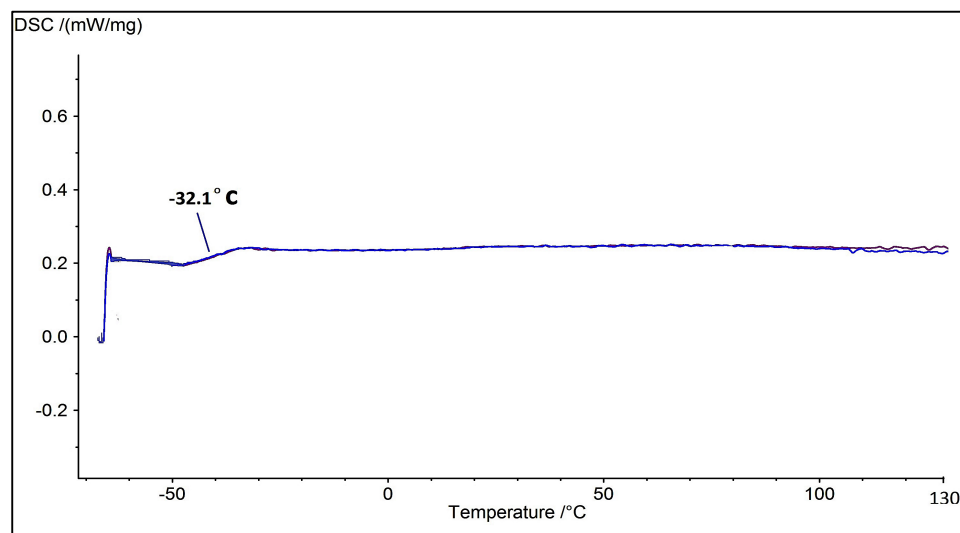


Figure 36: The DSC thermogram of the P(3HHx-3HO-3HD-3HDD) copolymer obtained from *P. mendocina* using waste frying oil as the carbon source. (—) first heating cycle, (—) second heating cycle.

Table 14: Summary of the thermal properties of the P(3HHx-3HO-3HD-3HDD) copolymer obtained from *P. mendocina* using waste frying oil as the carbon source; Where, T_m = melting temperature, T_g = glass transition temperature, T_c = crystallisation temperature.

Polymer sample	T_m (°C)	T_g (°C)	T_c (°C)
P(3HHx-3HO-3HD-3HDD)	-	-32.1	-

The mcl-PHA copolymer, P(3HHx-3HO-3HD-3HDD), obtained from vegetable waste frying oil as a carbon source was found to be rubbery amorphous in nature. Neither a melting event nor a cold-crystallisation temperature were detected. Glass transition temperature of the mcl-PHA copolymer was -32.1°C as seen in Table 14. The polymer was sticky at room temperature.

4.4.4. Molecular weight analysis – Gel Permeation Chromatography (GPC)

Molecular weight analysis was carried out according to the procedure described in the section 2.6.5. The results of the molecular weight analysis of the mcl-PHA copolymer obtained using *P. mendocina* CH50 and waste frying oil are shown in Figure 37 and Table 15.

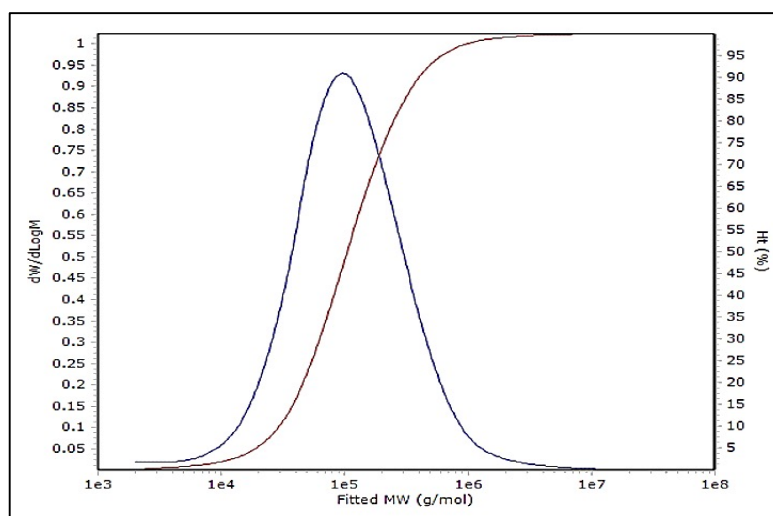


Figure 37: Molecular weight distribution (—) and cumulative molecular weight (—) of neat P(3HHx-3HO-3HD-3HDD) obtained from *Pseudomonas mendocina* CH50 using waste frying oil as the carbon source.

Table 15: Summary of molecular weight analysis of the P(3HHx-3HO-3HD-3HDD) obtained from *Pseudomonas mendocina* CH50 using waste frying oil as the carbon source. M_w = weight average molecular weight, M_n = number average molecular weight, PDI= polydispersity index.

Polymer sample	M_w (kDa)	M_n (kDa)	PDI
P(3HHx-3HO-3HD-3HDD)	210.7	56.6	3.7

The molecular weight (M_w) of the P(3HHx-3HO-3HD-3HDD) obtained in this study was 210.7 kDa, which is higher than that observed in the literature for different types of mcl-PHAs.

4.5. Discussion

It has been known from literature that various types of *Pseudomonas* sp. are able to accumulate mcl-PHAs, mainly copolymers. In this study, *Pseudomonas mendocina* CH50 was investigated in order to produce mcl-PHAs using different carbon sources, including cheap carbon sources and renewable materials. According to the literature *Pseudomonas* sp. readily use fatty acids for PHA production. Production of mcl-PHA copolymers by *Pseudomonas mendocina* CH50 using waste frying oil has not been reported so far. Waste frying oil was selected for the production of the mcl-PHA copolymer, identified as P(3HHx-3HO-3HD-3HDD). Prior to PHA production, the composition of the carbon source was investigated and confirmed by GC-MS and NMR analysis. Analysis of waste frying oil confirmed the composition as: linoleic acid, oleic acid and stearic acid. Linoleic acid and oleic acid are unsaturated fatty acids. Linoleic acid contains two double bonds, including the 9 and 12 carbon atoms within the fatty acid chain. Oleic acid has only one double bond present at carbon 9. Both detected fatty acids have 18 carbon atoms within the carbon chain. Each vegetable oil contains a unique composition of saturated and unsaturated fatty acids. All fatty acids, detected in the waste frying oil were mainly originated from vegetable oils, obtained from corn, cottonseed, soybean, peanuts and sunflower (Demirbas, 2003). However, the ratios of specific components were different from that obtained in this project. This can be explained by the fact that mixed vegetable oil, rather than a pure source of oil was used for frying.

Vegetable oils are most widely studied as a potential carbon source for PHA production with the various bacterial strains, like *Cupriavidus necator* and *Pseudomonas* sp. According to literature, P(3HB) concentration of up to 90% dry cell weight was obtained from *C. necator* using canola oil and fructose in a three-stage fermentation (Lopez-Cuellar *et al.*, 2011). Cruz *et al.*, 2015 reported P(3HB) production from *Cupriavidus necator* DSM 428 using cooking oil with a yield of 63±10.7% dcw. *Cupriavidus necator* was also used for PHA production using emulsified palm oil and yields obtained varied from 37% dcw (Martino *et al.*, 2014) in a batch fermentation up to 79% dcw in a multiple batch bioreactor system (Budde *et al.*, 2011). Waste frying oil has also been investigated by Verlinden and co-workers, 2011, who observed an enhanced P(3HB) production using

waste frying oil (polymer yield 1.2g/L) in comparison to pure vegetable oils (0.62g/L) in shaken flasks. Follonier *et al.*, 2014 reported mcl-PHA production yield of 23.3% dcw, when grape pomace was used together with waste frying oil as the carbon source. Similarly, Hwan *et al.*, 2008 observed mcl-PHA copolymer production with yields of about 23.5% dcw from waste frying oil. Hwan *et al.*, 2008 observed accumulation of 23.5% dcw of mcl-PHAs using *Pseudomonas* sp. DR2 and waste frying oil as the carbon source. Gamal *et al.*, 2013 compared three different fermentation strategies using *Pseudomonas fluorescens* and waste frying oil as the carbon source for PHA production. One-stage fermentation resulted with 33.7% dcw polymer accumulation after 60 hours. Two-stage batch fermentation gave 50.1% dcw polymer yields after 54 hours. High cell density culture with continuous feeding resulted in the highest polymer content of 55.3% of dry cell weight after 54 hours. Waste materials, usually comprise many different compounds in their composition. According to results obtained, *Pseudomonas mendocina* CH50 seems to have preference for complex carbon sources rather than single fatty acids. Silva-Queiroz *et al.*, reported challenges in the production of custom-made mcl-PHA polymers from complex carbon sources, such oils and fatty acids due to complexity of the metabolism of this compound (Silva *et al.*, 2009).

In this work, high polymer yield (38% dcw) was obtained in *Pseudomonas mendocina* CH50 and 20g/L of waste frying oil as the carbon source. The mineral salt medium was used to ensure nitrogen limitation. Nutrient limitation is one of the major factors that stimulate PHA production. In addition, excess of carbon source is required for most of the bacterial strains (Rai *et al.*, 2011). In this study nitrogen limiting conditions were provided from 27 hours of the fermentation, when ammonium sulphate was completely consumed by bacteria. In this study, only batch fermentation was carried out in the bioreactor. It is well known from the literature that a fed-batch feeding strategy can enhance mcl-PHA production to obtain polymer yield of up to 75.5% dcw (Jiang *et al.*, 2013). Also, achieving high cell densities is required for PHA production, because those polymers are accumulated as inclusion bodies inside the cell (Ienczak *et al.*, 2013). For PHA production, high cell density of the culture means 100g/L total concentration of biomass with polymer content of 60-70% dcw (Ryu *et al.*, 1997). Obtaining large amount of biomass and polymer yield will reduce the total cost of PHA production. For future work, as a part of the optimization process to enhance further copolymer production, a

fed batch approach with different feeding strategies or high cell density fermentation needs to be explored.

Polymer obtained by using *Pseudomonas mendocina* CH50 and waste frying oil was confirmed as mcl-PHA and the chemical structure and monomer composition of the polymer showed presence of FTIR peaks characteristic for medium chain length PHA (Simon-Colin *et al.*, 2008). The chemical structure of the obtained polymer was also confirmed by GC-MS. Four different monomer units, including: 3HHx, 3HO, 3HD and 3HDD were identified. Ashby *et al.*, 2004 has reported production of mcl-PHA, which contains 3-hydroxyoctanoic, 3-hydroxydecanoic and 3-hydroxytetradecadienoic acid when *P. corrugata* grown on various concentrations of biodiesel waste. In the literature, different mcl-PHA copolymers were obtained, when waste-frying oil was used as the carbon source. Follonier *et al.*, 2014, reported copolymer, which contains 5 different monomer units: 3-hydroxyhexanoate, 3-hydroxyoctanoate, 3-hydroxydecanoate, 3-hydroxydodecanoate, and 3-hydroxytetradecanoate within the polymer chain. Hwan and co-workers, 2008 produced mcl-PHA copolymer, which contain 5 different monomer units, such as: 3-hydroxyhexanoate, 3-hydroxyoctanoate, 3-hydroxydecanoate, 3-hydroxytetradecanoate and 3-hydroxyhexadecanoate. Mcl-PHAs composition depends on the type of the bacterial strain used for polymer production. Mozejko *et al.*, 2011 used two different strains of *Pseudomonas* sp. and waste rapeseed oil as a carbon source. Obtained polymer for *Pseudomonas* GI01 contains 3 different monomer units: 3-hydroxyoctanoate, 3-hydroxydecanoate and 3-dodecanoate, whereas strain *Pseudomonas* GI06 was able to produce mcl-PHA copolymer, containing 3-hydroxyhexanoate, 3-hydroxyoctanoate, 3-hydroxydecanoate and 3-dodecanoate within the polymer chain. This composition is similar to the mcl-PHA copolymer obtained in this study.

The P(3HHx-3HO-3HD-3HDD) mcl-PHA copolymer was produced using cheap carbon sources, such as waste frying oil, to overcome the main problem associated with large-scale production of PHAs such as high cost. Different approaches towards economical production of PHA were described in details in the section 1.8.8. Using cheap carbon sources is one of the main approaches, which were investigated. Each year, only in Europe, 24 million tons of vegetable oils are consumed. Hence, large amounts of waste frying oil are available (OECD-FAO, 2017). For the few past years production of biodiesel

using waste frying oil or biopolymers gained attention from many research projects. This has two positive effects, such as reduction of the cost production as well as elimination of waste material from the environment. During the process of frying oil is continuously or repeatedly treated at high temperature in the presence of moisture and air. This causes three different types of degradation reactions, such as hydrolysis, oxidation and polymerisation, which create various types of chemical compounds, such as free fatty acids, ketones and aldehydes as well as aromatic triglycerides (Choe and Min, 2007; Gertz, 2000).

To date, there are no published results, which describe mcl-PHA production using waste frying oil and *Pseudomonas mendocina* CH50. In this study production of mcl-PHA was carried out as a two-step batch cultivation process in a 5L bioreactor. The maximum polymer yield obtained was 38.0 % dcw at 48 hours. Nutrient limitation is one of the factors that stimulate PHA production in the presence of excess carbon for most of the bacterial strains (Rai *et al.*, 2011). In this study, nitrogen-limiting conditions were provided from 27 hours of the fermentation, when ammonium sulphate was completely consumed by bacteria. In this study only batch fermentation was carried out in the bioreactor. For the future work, as a part of the optimization process to enhance further copolymer production, a fed batch approach with different feeding strategies or high cell density fermentation (Chen, 2009) should be considered. It is well known from the literature that fed-batch feeding strategy can enhance mcl-PHA production to obtain polymer yields up to 75.5% dcw (Jiang *et al.*, 2013). High cell densities are good for PHA production, because these polymers are accumulated as inclusion bodies inside the cell (Ienczak *et al.*, 2013). For optimal PHA production, high cell density of the culture with 100g/L total concentration of biomass and polymer content of 60-70% dcw (Ryu *et al.*, 1997) is required. Obtaining such high biomass and polymer yield will reduce the total cost of PHA production.

It is well known from literature, that most of the mcl-PHAs have properties similar to rubbers and both: glass transition as well as a melting event have been observed. The typical thermal properties for mcl-PHAs are: melting temperature in a range between 40 °C to 60 °C and glass transition temperature from -50 °C to -25 °C (Rai *et al.*, 2011). The glass transition temperature decreases with an increasing length of side chains or number of unsaturated bonds within the polymer chain (Haba *et al.*, 2007). However,

Mozejko and Ciesielski, 2013, reported synthesis of different mcl-PHAs, which showed glass transition temperature ranging from -14°C to -55°C and melting temperatures around $83\text{-}86^{\circ}\text{C}$, which is much higher than usually observed in mcl-PHAs. The mcl-PHA copolymer obtained in this study was amorphous in nature. Only glass transition temperature was detected at -32°C , which corresponded with the values presented in the literature. Polymer thermal properties depend on the number of carbon atoms within the aliphatic chains of individual monomers. Longer chains and presence of unsaturated groups in the side chains increase the number of amorphous regions within polymer chain, which might cause disturbance in the crystallisation process. This can explain the more adhesive nature of the produced polymer rather than the ability to create films (Muangwong *et al.*, 2016). There are reports that demonstrate mcl-PHA production which are amorphous in nature. Follonier and co-workers, 2015 as well as Muangwong *et al.*, 2016 have obtained amorphous mcl-PHA copolymer using different carbon sources and bacterial strains.

The molecular weight of the obtained copolymer in this study was 210.7 kDa. There are several factors which can influence the molecular weight of the PHAs, such as: concentration of the PHA synthase, PHA depolymerase activity, polymer recovery technique, bacterial strain as well as culture conditions, such as temperature or pH might affect the molecular weight of the final polymer (Tsuge, 2016; Bugnicourt *et al.*, 2014). Different researchers have reported production of mcl-PHAs with a range of molecular weight values from 60 to 330kDa. For example, Martelli and co-workers (2012) produced P(3HO-3HD-3HDD) copolymer, which had a molecular weight 140 kDa. Gumel *et al.* 2012, reported the molecular weight of mcl-PHAs obtained from *Pseudomonas putida* Bet001 using various carbon sources to be between 55-77.7kDa. Mozejko and Ciesielski, 2013 observed production of mcl-PHA copolymers using *Pseudomonas sp.* GI01 with the molecular weight range from 60 to 110kDa. On the other hand, Preusting *et al.*, 1990 have observed production of mcl-PHAs using *P. oleovorans* with the molecular weight of over 300kDa. Hence, the molecular weight of the polymer produced in this project was within the range of values demonstrated by other labs.

In conclusion, this study has demonstrated the ability of the selected strain, *Pseudomonas mendocina* CH50 to produce mcl-PHAs, mainly copolymers, using a range of different carbon sources, including cheap carbon sources and waste materials. PHA

yield of 38.0% dcw was obtained using waste frying oil as the sole carbon source. The obtained mcl-PHA copolymer contained four different monomer units within the repeatable unit in the polymer chain. This study confirmed the possibility of utilization of vegetable waste frying oil as the carbon source by *Pseudomonas mendocina* CH50 for economically efficient PHA production.

Chapter 5

Development of Poly(3-hydroxybutyrate)/oligo -PHA blends

5. Introduction

Polyhydroxyalkanoates (PHAs) are the natural biopolyesters, intensively studied for biomedical applications. PHAs are biocompatible, non-toxic, biodegradable and have been widely studied for wound management, coronary stents, nerve regeneration, bone tissue engineering, drug delivery and soft tissue engineering (Hazer *et al.*, 2012). P(3HB) is well known representative of scl-PHAs family. Mechanical properties of P(3HB), such as stiffness and brittleness make it suitable for hard tissue engineering, such as bone regeneration. Neat P(3HB) and its copolymers have been suggested for many biomedical applications, such as: bone tissue regeneration, drug delivery systems, nerve conduits, sutures, wound management and soft tissue engineering (Williams and Martin, 2005). Various approaches have been taken to improve the properties of the biomaterials. Physical blending is one of the approaches to obtain novel material with different properties, superior to the materials already existing (Chen and Wu, 2005). PHAs have been blended with various types of materials, such as: polyhydroxyalkanoates (Lizarraga-Valdemarra *et al.*, 2015; Nerkar *et al.*, 2014; Basnett *et al.*, 2013; Zhao *et al.*, 2003), rubbers (Bhatt *et al.*, 2008; Calvão *et al.*, 2012), starch (Paruleka and Mohanty, 2007; Godbole *et al.*, 2003), synthetic polymers (Zhao *et al.*, 2012; Furukawa *et al.*, 2005; Cara *et al.*, 2003; Koyama and Doi, 1997).

However, the results obtained are still not satisfactory. The problem with blending between two different types of polymers is poor miscibility of the system, which leads to a phase separation (Chen and Luo, 2009). Addition of low molecular weight compounds, such as hydrolysed polymers, might have an improvement in the blend miscibility by acting as the plasticisers. Poor compatibility in P(3HB) blends with other polymers is well documented including P(3HB) blends with other PHAs. Therefore P(3HB) blends are multiphase polymer systems, the properties and stability of which depend on their processing and morphological structure (Larsson *et al.*, 2016; Jacob *et al.*, 2002; Verhoogt *et al.*, 1994; Scandola *et al.*, 1992).

Plasticizers are small molecules incorporated into polymeric materials in order to enhance their flexibility and processability (Platzer, 1982). Plasticizers are mainly added to hard and brittle polymers in order to decrease glass transition temperature (T_g), elastic modulus and increase elastomeric properties of the blend (Sears and Darby, 1982).

The main role of the plasticizer is to separate neighbouring polymer chains and reduce interaction between them. This will result in a lower T_g and influencing the final material properties. In order to be used as a plasticiser every substance has to meet certain criteria. This include: low volatility, temperature stability, odourless, compatibility with the polymer, efficiency, permanence (Sachin *et al.*, 2016). Selection of the right compound requires compromise, since none of the known plasticisers can meet all the criteria at that time (Edmund, 1965).

Although plasticisers interact with polymer chains, they are not chemically bound to the polymer. Hence, they can leach out with the time and accumulate in the environment (Erythropel *et al.*, 2014; Staples *et al.*, 1997). There has been reports regarding health and safety concerns of the degradation products of various plasticisers (Horn *et al.*, 2004.). Therefore, many research groups have been working extensively in order to develop safer alternatives, which will demonstrate comparable plasticising effect, faster biodegradation, lower toxicity and reduced leaching from the polymeric matrix (Erythropel *et al.*, 2016; Wadey, 2003). Plasticisers can be used with short chain length polyhydroxyalkanoates, like P(3HB) or P(3HBV) to improve their elasticity. Various types of ester-type substances have been tested (Vieira *et al.*, 2011; Mekonnena *et al.*, 2013). Different types of esters of citric acid, known as biocompatible compatibilisers, have been an attractive additive for PHAs (Ghiya *et al.*, 1995; Hull, 1990).

Biomedical applications require from any biomaterials including various additives, plasticisers and fillers high biocompatibility, non-toxicity, degradability, processability and cost effectiveness. Although the issue of environmental impact of plasticisers is currently widely recognised (Oehlmann *et al.*, 2009; Beauchesne *et al.*, 2007; Cadogan, 1991), the current literature is deficient in testing cytotoxicity of implantable plasticised polymer materials.

Additionally, migration of low molecular weight plasticisers from polymeric matrix into surrounding tissues may not only lead to toxicity effects but also drastically alter materials properties before the degradation of the implanted material (Snejdrova and Dittrich, 2012). The smaller the plasticizer molecule, the greater its volatility and, therefore, the rate at which it is lost from the plasticised product (Li *et al.*, 2008). Increase in molecular weight of plasticisers reduce migration speed or fully prevents migration, which led to the development of oligomeric plasticizers. Oligomeric

analogues of a polymer could be an ideal approach since it offers good affinity between the polymer and the plasticiser. Similar chemical structure of plasticiser and polymeric matrix is the oldest known plasticizer-polymer system (Sachin *et al.*, 2016). Oligomeric plasticisers have been studied already. Polyethylene glycol (PEG) and polypropylene glycol have been used as plasticising agents for PLLA (Laia *et al.*, 2004). Oligomers of lactic acid have been successfully used to improve flexibility of synthetic biodegradable PLLA (Burgos *et al.*, 2014) or PLLA/P(3HB) blends (Abdelwahaba *et al.*, 2012). However, oligomers of PHAs have not yet been widely explored as additives for the improvement of P(3HB) flexibility. There were only two reports, where synthetic atactic P(3HB) diols (El-Taweela *et al.*, 2004) and oligomeric P(3HB) (Meszynska *et al.*, 2016) were used as additives to P(3HB). Natural plasticisers are very attractive group of additives (Garcia-Garcia *et al.*, 2017). Hence, plasticisers based on PHAs can be very attractive compounds, due to natural origin, biodegradability and non-toxicity. They can be very attractive alternative for petroleum based plasticisers and allow obtaining fully compostable materials. Oligomeric derivatives of PHAs can be produced by using various techniques, such as: alkaline or acidic hydrolysis, transesterification, thermal degradation or ester reduction (Crétois *et al.*, 2016).

The main aim of this part of the work was to develop more flexible P(3HB) based blends using oligomeric form of mcl-PHA copolymer in order to enable the application of P(3HB) in coronary artery stents. In this study, three different blends of P(3HB)/oligo-PHA in ratios: 95/5, 90/10 and 80/20 have been developed. Materials were fully characterized in order to obtain their thermal and mechanical properties. Evolution of various properties have been studied during material storage for 7 weeks. *In vitro* biocompatibility of the blends was tested with human dermal microvascular endothelial cells HMEC-1 to evaluate the potential of new biodegradable material in applications such as coronary artery stent. Additionally, haemocompatibility studies, including haemolysis and blood clotting studies, as well as white cell activation studies were performed in order to study the blood cell behaviour after direct contact with new material.

5.1. Development of oligo-P(3HHx-3HO-3HD-3HDD)

MCl-PHA copolymer produced by *Pseudomonas mendocina* CH50 using waste frying oils as the carbon source was subjected to an acidic hydrolysis for 20hrs as described in the section 2.8.1. in order to obtain low molecular weight oligomers (oligo-PHA). Samples were collected in 3 hours intervals. Polymer recovery of the hydrolysis reaction is presented in Table 16.

Table 16: Summary of hydrolysis kinetics of P(3HHx-3HO-3HD-3HDD) copolymer.

Time (hours)	Polymer amount (μg)	Polymer obtained (% recovery)
3	156	21.2
6	166	22.6
9	288	39.2
12	346	47.1
15	459	62.5
17	464	63.1
19	560	76.7
20	1450	92.0

The yield of the reaction increased gradually with the time from 21.2% after 3 hours up to 92% at the end of the reaction. The polymer obtained after 20 hours was characterised further by FTIR, DSC and GPC analysis.

5.1.2. Oligo-PHA characterisation

The hydrolysed P(3HHx-3HO-3HD-3HDD) was a waxy material. The material was characterised in order to investigate the influence of the acidic conditions on the chemical and thermal properties as well as molecular weight of the polymer.

5.1.2.1. Attenuated Total Reflectance Fourier Transform Infrared Spectroscopy (ATR/FT-IR)

The final oligomeric product of hydrolysis obtained after 20 hours was characterised by ATR/FT-IR spectroscopy. The absorption peaks corresponded to peaks typical for mcl-PHAs and the P(3HHx-3HO-3HD-3HDD) copolymer (Figure 38) before hydrolysis as described in the section 4.4.1.

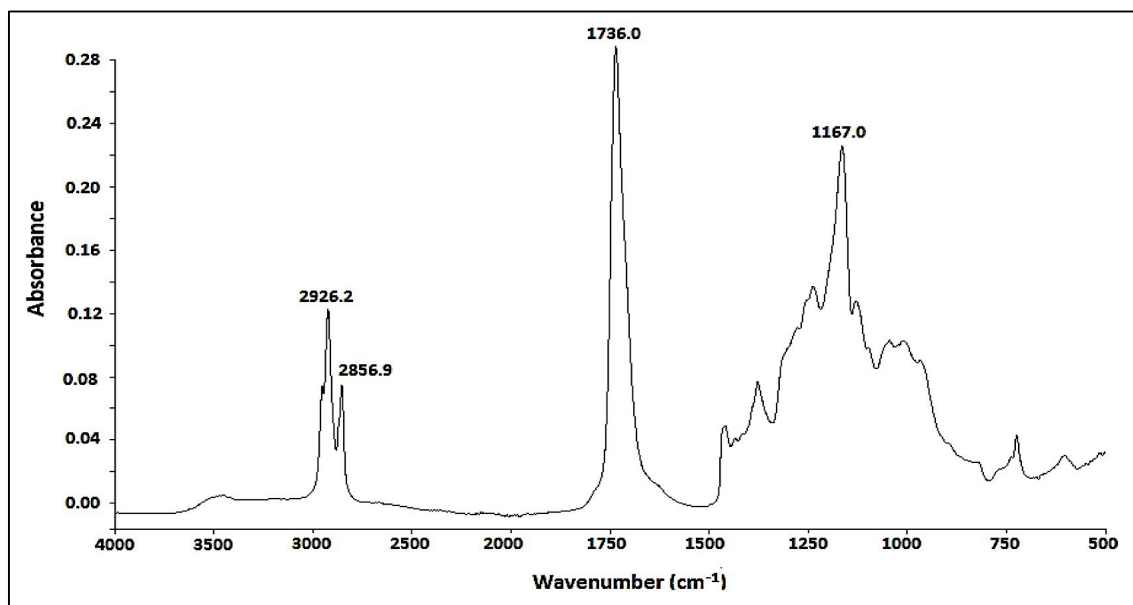


Figure 38: ATR-FTIR spectrum of the oligo-PHA obtained from *Pseudomonas mendocina* CH50 and waste frying oil as the carbon source after 20 hours of hydrolysis indicating peaks characteristic for mcl-PHAs.

Four main adsorption peaks were observed at: 2926cm^{-1} , 2856cm^{-1} , 1726cm^{-1} and 1167.04cm^{-1} , which correspond to C-H group, carbonyl group and -CO stretching respectively (Figure 36). There was no difference in the spectrum between hydrolysed and non-hydrolysed P(3HHx-3HO-3HD-3HDD).

5.1.2.2. Thermal analysis – Differential Scanning Calorimetry (DSC)

The thermal properties of the hydrolysed P(3HHx-3HO-3HD-3HDD) copolymer were analysed by DSC. The thermogram of the hydrolysed polymer is shown in the Figure 39. The summary of the thermal properties of hydrolysed polymer are presented in the Table 17.

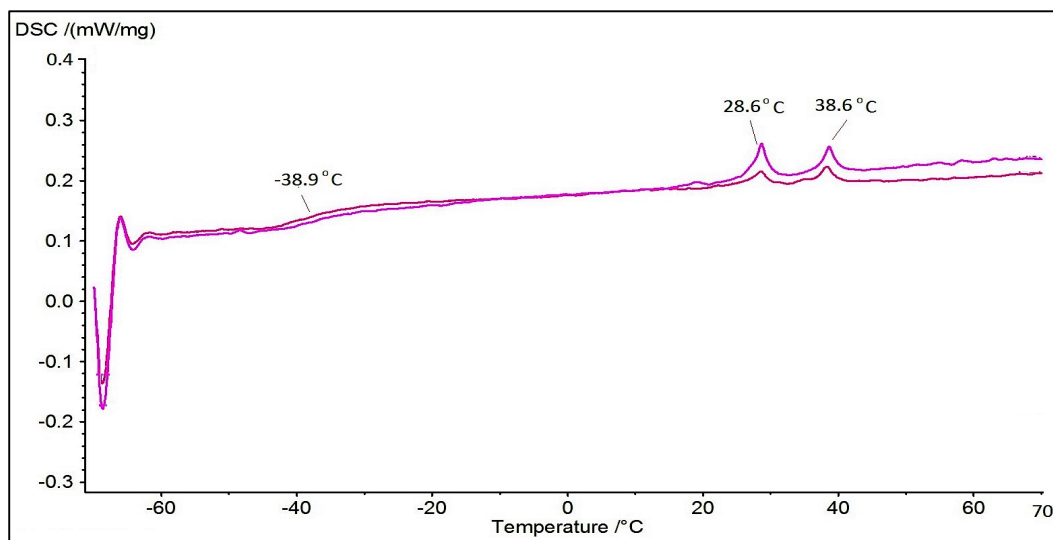


Figure 39: Summary of thermal properties of the oligo-PHA after 20 hours of hydrolysis. (—) first heating cycle, (—) second heating cycle.

Table 17: Thermal properties of the hydrolysed P(3HHx-3HO-3HD-3HDD) after 20 hours of hydrolysis. T_m = melting temperature, T_g = glass transition temperature, T_c = crystallisation temperature.

Polymer sample	T_m	T_g	T_c
Hydrolysed P(3HHx-3HO-3HD-3HDD)	28.6°C 38.6°C	-38.9°C	-

Oligomeric mcl-PHA demonstrated presence of glass transition temperature at -38.9 °C and two different melting events at 28.6°C and 38.6°C. T_c was not detected, which is a typical characteristic of mcl-PHAs.

5.1.2.3. Molecular weight analysis – Gel Permeation Chromatography (GPC)

The summary of the results of the molecular weight analysis of the hydrolysed mcl-PHA copolymer obtained using *P. mendocina* CH50 and waste frying oil are shown in the Table 18.

Table 18: Summary of molecular weight analysis of the P(3HHx-3HO-3HD-3HDD) obtained from *Pseudomonas mendocina* CH50 and waste frying oil as the carbon source after 2 hours of hydrolysis. M_w = weight average molecular weight, M_n = number average molecular weight, PDI= polydispersity index.

Polymer	M_w , kDa	M_n , kDa	PDI
oligo-PHA	10	4.6	2.2

The GPC results obtained (Table 17) clearly confirmed that hydrolysis of the P(3HHx-3HO-3HD-3HDD) copolymer has occurred. The molecular weight of the hydrolysed polymer was reduced significantly and measured as 10kDa. The polydispersity index obtained was 2.2. The molecular weight of the hydrolysed P(3HHx-3HO-3HD-3HDD) copolymer was over 20-fold lower than the original copolymer described previously in the section 4.4.4.

5.2. Development of P(3HB)/oligo-PHA blends

P(3HB) was blended with oligo-PHA in ratios: 95/5, 90/10 and 80/20 (Figure 40) to obtain blends for coronary stent application and fully characterised. In order to evaluate the potential of the oligomeric mcl-PHA derivative as a plasticizer for P(3HB), the influence of oligo-PHA additives on thermal and mechanical properties of P(3HB) were studied using blend films prepared by solvent casting technique. P(3HB) embrittlement during the storage is a well-known complex phenomenon which is mainly attributed to a secondary crystallisation and ageing of the amorphous phase (Barham *et al.*, 1984). Therefore, the changes of thermal and mechanical properties of neat P(3HB) and its blends with oligo-PHAs was monitored for a period of 7 weeks for samples stored at room temperature.

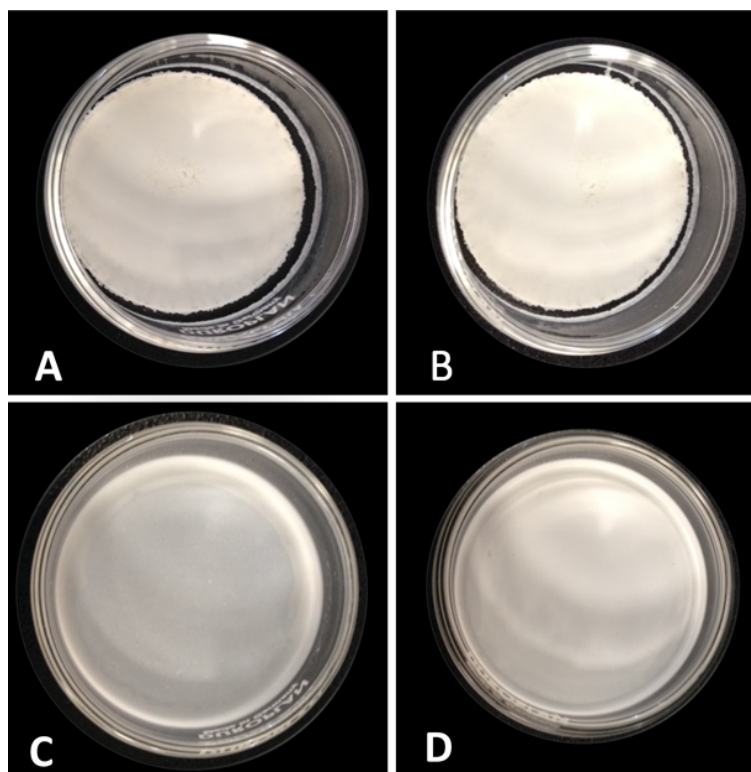


Figure 40: Solvent cast films of: (A) P(3HB) neat film, (B) P(3HB)/oligo-PHA blend film in ratio 95/5, (C) P(3HB)/oligo-PHA blend film in ratio 90/10, (D) P(3HB)/oligo-PHA blend film in ratio 80/20; diameter: 60mm.

5.2.1. Blend characterisation

Blend films were characterised with respect to their thermal, mechanical and topographical properties. Additionally, biocompatibility and haemocompatibility studies were performed in order to confirm non-toxicity and safety of the biomaterials.

5.2.1.1. Thermal analysis of the blend films after 7 weeks of storage at room temperature - ageing experiments

Thermal properties of the solvent cast films were studied for 7 weeks, in order to check the effect of ageing on the material. The results obtained are summarised in Table 19.

Table 19: Summary of the thermal analysis of P(3HB)/hydrolysed P(3HHx-3HO-3HD-3HDD) blends during 7 weeks of storage. T_m = melting temperature, ΔH_{app} = enthalpy of fusion, ΔH_{norm} = enthalpy of fusion normalised to P(3HB), X_c = crystallinity degree.

Week	Sample	T_m , °C	ΔH_{app} , Jg ⁻¹	$\frac{\Delta H_{norm}}{Jg_{P(3HB)}^{-1}}$	X_c , %*
2	P(3HB) neat	174.8	82.5	82.5	56.5
	95/5 blend	174.2	66.9	70.4	48.2
	90/10 blend	167.0	67.5	71.0	48.6
	80/20 blend	171.4	-	-	-
5	P(3HB) neat	175.2	84.4	84.4	57.8
	95/5 blend	170.4	62.6	69.6	47.7
	90/10 blend	173.9	65.1	72.3	49.5
	80/20 blend	167.2	43.1	53.9	36.9
7	P(3HB) neat	176.6	85.9	85.9	58.8
	95/5 blend	171.7	-	-	-
	90/10 blend	174.8	56.5	70.6	48.4
	80/20 blend	173.0	43.3	54.1	37.1

- X_c , the crystallinity degree of P(3HB) was calculated using the formula:

$$X_c = \frac{\Delta H_{norm}}{\Delta H_0} \times 100, H_0 = 146 \text{ J/g.}$$

The enthalpy of fusion of P(3HB) from *B. subtilis* OK2 was found to increase during the storage for 7 weeks (Table 18), confirming the previously reported secondary crystallisation of P(3HB). Total enthalpy of fusion (ΔH_{app}) was lower for all blends as compared with neat P(3HB). Also, addition of the oligo-PHA resulted in a small decrease of melting temperature (T_m), between 2 to 5 °C. No further changes in the enthalpy of fusion and melting temperature were observed after 7 weeks of ageing indicating completion of P(3HB) crystallisation within 7 weeks. Normalised enthalpy (ΔH_{norm}) of fusion indicated slower rate of crystallisation of P(3HB) in blends in comparison to neat P(3HB).

Crystallinity degree of P(3HB) (X_c) in blends 95/5 and 90/10 was calculated as 48%, which is 20% less in comparison to neat P(3HB). Addition of 20% wt of oligo-PHA resulted in

further drop in crystallinity degree up to 37% after 7 weeks of storage at room temperature.

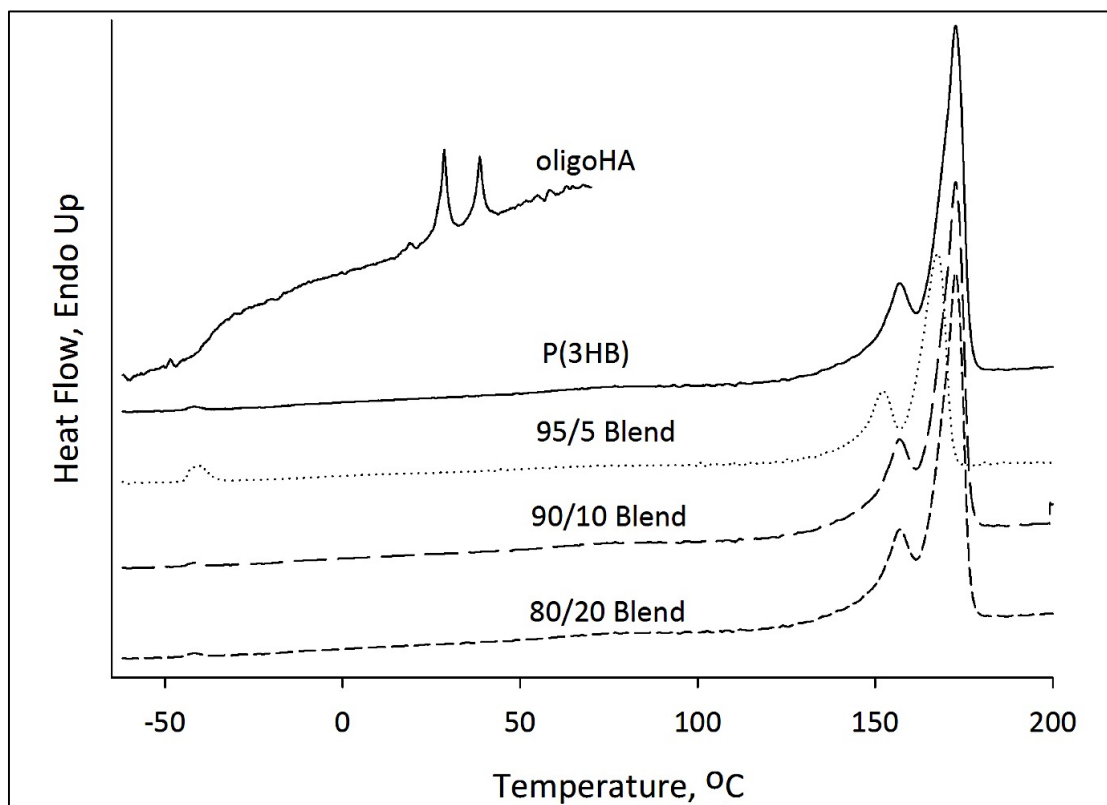


Figure 41: DSC thermograms of first cycle of P(3HB), oligo-PHA and P(3HB)/oligo-PHA blends (ratios: 95/5, 90/10, 80/20) aged for 7 weeks at room temperature.

DSC thermograms (Figure 41) of blends did not show a thermal event in the range characteristic for oligo-PHA melting temperature in the blends containing 20 wt% of oligo-PHA. Hence, the thermal properties indicated that obtained blend materials were miscible and compatible systems.

5.2.1.2. Mechanical characterisation of the blend films after 7 weeks of storage at room temperature - ageing experiments

Mechanical properties of the solvent cast films were measured for 7 weeks, in order to check the effect of storage for 7 weeks at room temperature on the ageing on the material. The results obtained are summarised in Table 20 and Figure 42.

Table 20: Summary of the mechanical properties of P(3HB)/oligo-PHA blends during 7 weeks of storage (n=3).

Time of storage (week)	Blend composition P(3HB)/P(3HHx-3HO-3HD-3HDD)	Tensile test (MPa)	Young's Modulus (MPa)	Elongation at break (% strain)
0	95/5	16.9±0.2	600±100	45.9±1.3
	90/10	15.1±0.5	600±100	47.0±0.4
	80/20	11.4±0.05	300±40	52.8±2.4
2	95/5	11.6±0.1	900±100	36.1±3.5
	90/10	12.4±0.5	900±20	24.2±4.7
	80/20	11.3±0.2	890±5	39.0±4.1
5	95/5	12.8±0.4	1000±100	4.9±3.0
	90/10	8.3±0.6	660±40	11.2±3.4
	80/20	5.3±0.2	420±40	18.6±3.5
7	95/5	12.9±0.8	1040±90	3.8±0.4
	90/10	14.8±0.7	1240±80	6.2±0.8
	80/20	6.4±0.4	480±30	13.3±3.8

Material ageing has influenced the mechanical properties of the P(3HB)/oligo-PHA blend films. For P(3HB)/oligo-PHA blend in ratio 95/5 the tensile strength decreased from 16.9±0.2MPa at week 1 to 12.9±0.8 MPa after 7 weeks of storage; the Young's Modulus values significantly increased from 600±100MPa after week 1 to 1040±90 MPa after week 7 and an elongation at break decreased from 45.9±1.3% after week 1 to 3.8±0.4% strain after week 7. Similar trend was observed for P(3HB)/oligo-PHA blend in ratio 90/10. the tensile strength decreased from 15.1±0.5MPa at week 1 to 14.8±0.7MPa after 7 weeks of storage; the Young's Modulus values significantly increased from 600±100MPa after week 1 to 1240±80MPa after week 7 and an elongation at break decreased from 47.0±0.4% after week 1 to 6.2±0.8% strain after week 7. For P(3HB)/oligo-PHA blend in ratio 80/20 the tensile strength decreased from 11.4±0.05MPa at week 1 to 6.4±0.4MPa after 7 weeks of storage; the Young's Modulus values significantly increased from 300±40MPa after week 1 to 480±30MPa after week 7 and an elongation at break decreased from 52.8±2.4% after week 1 to 13.3±3.8% strain after week 7.

Hence, ageing of P(3HB) enhanced its strength and stiffness but reduced its elastomeric properties. The material became more brittle with time.

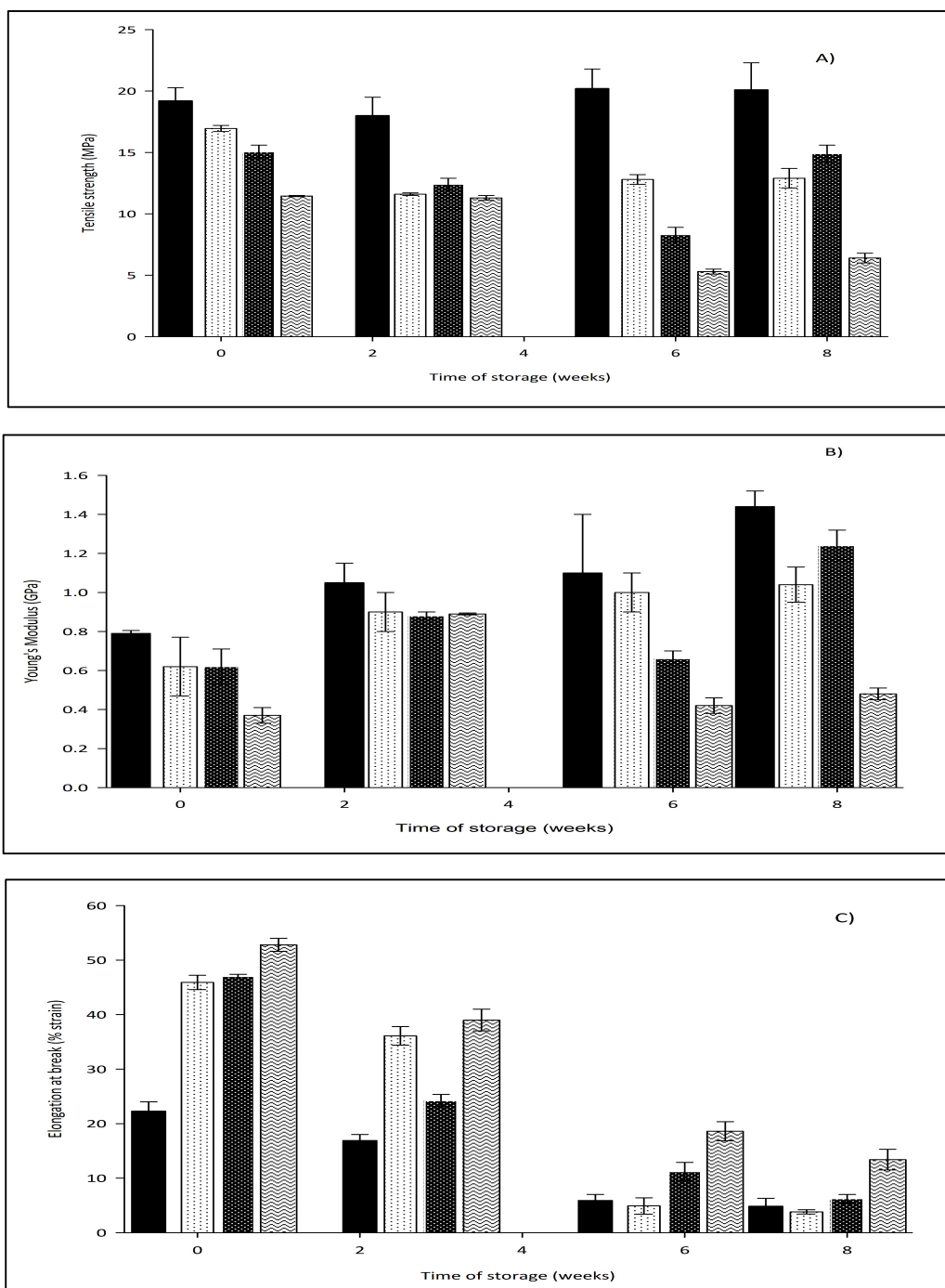


Figure 42: The summary of tensile strength (A), Young's modulus (B) and elongation at break (C), during aging of neat P(3HB) and P(3HB)/oligo-PHA blends after 7 weeks of storage at room temperature. (■) P(3HB), (□) 95/5 blend, (▣) 90/10 blend, (▤) 80/20 blend.

The embrittlement behaviour is a characteristic material property of P(3HB). Addition of oligo-PHA had a great impact on the mechanical properties of P(3HB). Increased

concentration of oligo-PHA in P(3HB)/oligo-PHA blends resulted in obtaining materials with lower tensile strength and Young's Modulus values than neat P(3HB). Only a 5 wt% addition of oligo-PHA decreased the ultimate tensile strength and Young's modulus by 35% and 28%, respectively. Elongation at break demonstrated an opposite trend. Higher values were obtained for the blend composition with the highest concentration (20 wt%) of oligo-PHA. After 7 weeks of storage at room temperature, elongation at break of the 95/5 blend was similar to that of neat P(3HB). However, when the content of oligo-PHA exceeded 10 wt%, improvement in plasticity was observed and elongation at break for the 80/20 blend reached almost 14%.

In summary, an addition of oligo-PHA resulted in obtaining materials with novel properties in comparison to neat P(3HB), which can be suitable for biomedical applications, such as coronary stents.

5.3. Surface topography studies

5.3.1. Scanning Electron Microscopy of the P(3HB)/oligo-PHA blends

SEM was used to examine topography of neat P(3HB) and P(3HB)/oligo-PHA films. As can be seen from SEM images shown in Figure 43, all materials had similar irregular surface topography. Few circular pores were observed on the surface of all tested

materials.

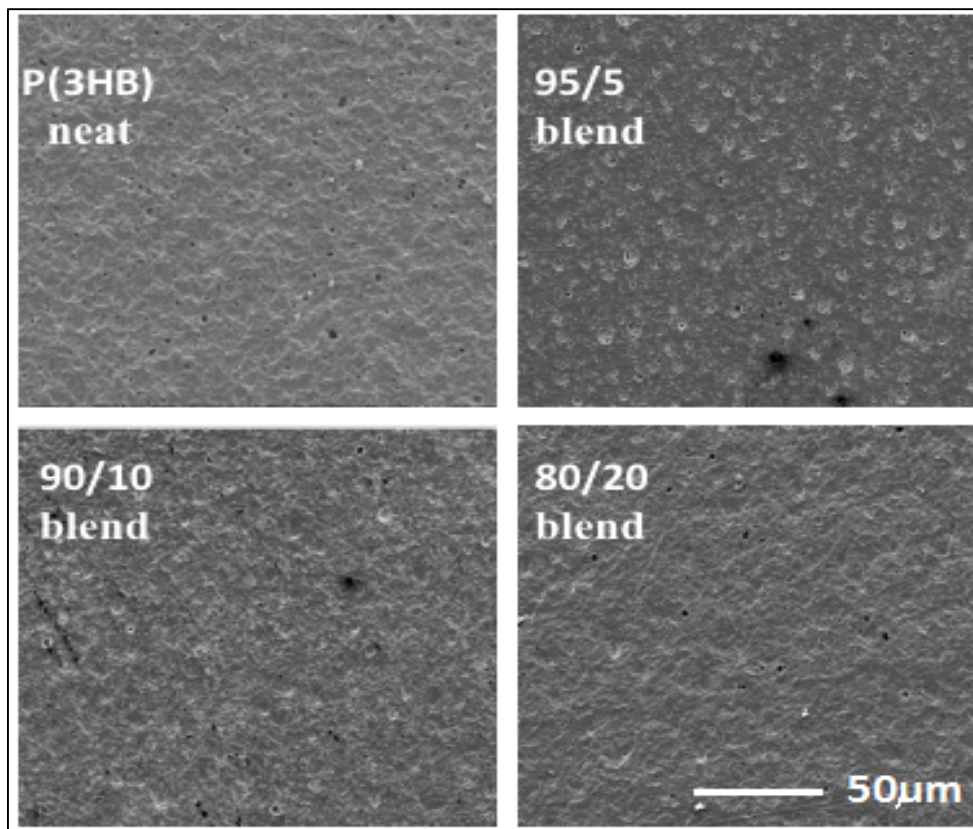


Figure 43: Scanning electron micrographs of the neat P(3HB) film and P(3HB)/oligo-PHA blends.

The surface of both the neat and the blend films appeared to have a rough surface. Surface roughness measurements were carried out to confirm the SEM data.

5.3.2. Surface roughness analysis

Generally, surfaces of all the materials appeared to be rough. Roughness was further characterised quantitatively as the root mean square roughness (R_q) using laser profilometry (Figure 44). The mean square roughness of the P(3HB) neat film was $0.64 \pm 0.04 \mu\text{m}$. With the increase of content of oligo-PHA in the blends the surface roughness rose from $0.8 \pm 0.02 \mu\text{m}$ for 95/5 blend and $1.2 \pm 0.02 \mu\text{m}$ for 80/20 blend. The roughness of the blend films was significantly higher in comparison to neat P(3HB).

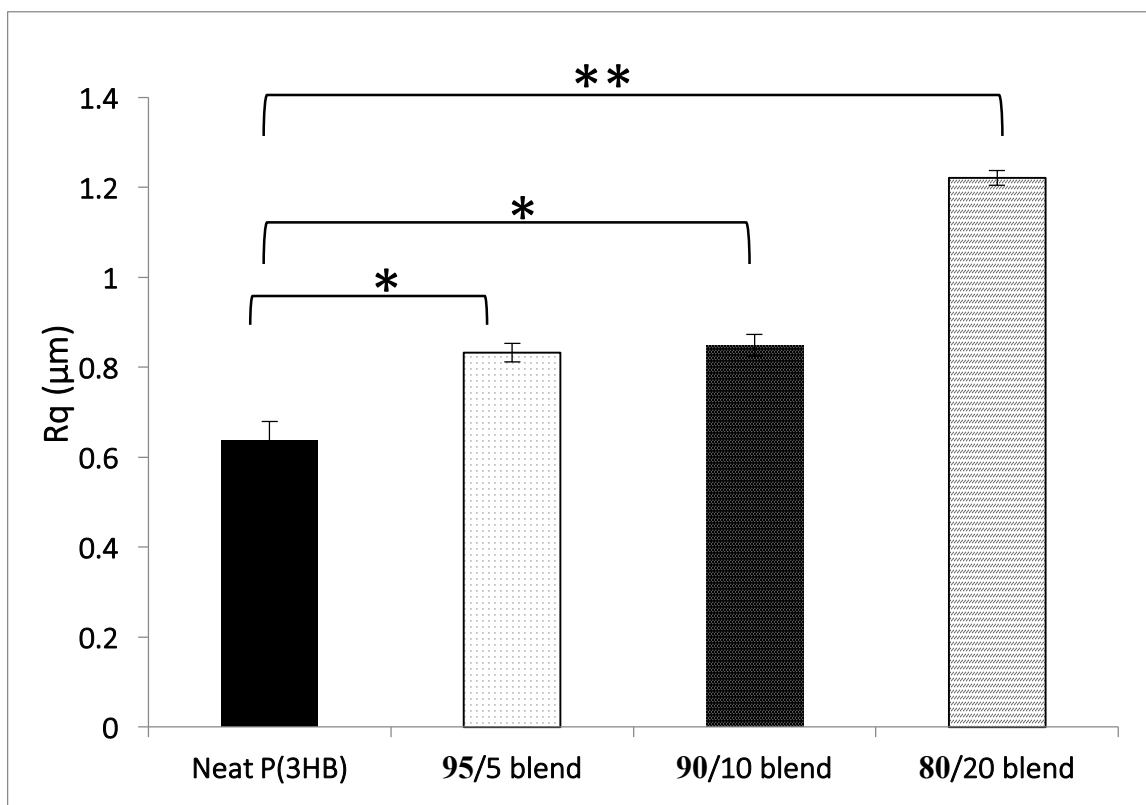


Figure 44: Surface roughness analysis of neat P(3HB) and its blends with oligo-PHA (n=3; error bars=±SD). The data were compared with the neat P(3HB) using ANOVA. * indicates $p < 0.05$ and ** indicates $p < 0.005$.

These results obtained from surface roughness measurements confirmed the SEM findings that surface of the all samples tested were rough. With an increase of concentration of oligo-PHA higher surface roughness was observed. The difference was significant in comparison to the neat P(3HB) film.

5.3.3. Water contact angle measurements

Water contact angle and protein absorption represent physiologically relevant surface properties of materials. P(3HB) is a hydrophobic biopolymer of which films exhibited a water contact angle of $87.5 \pm 7.4^\circ$ (Figure 45). There was a steady increase in values of water contact angles for the blends with the increase in content of oligo-PHA reaching $118 \pm 7^\circ$ for 80/20 blends. All blend films had significantly higher contact angle values in comparison to that of neat P(3HB). The longer hydrophobic aliphatic chains of oligo-PHA

contribute to the increase of hydrophobicity of P(3HB)/oligo-PHA blends. However, increase in surface roughness of the blends might also lead to the higher water contact angle values.

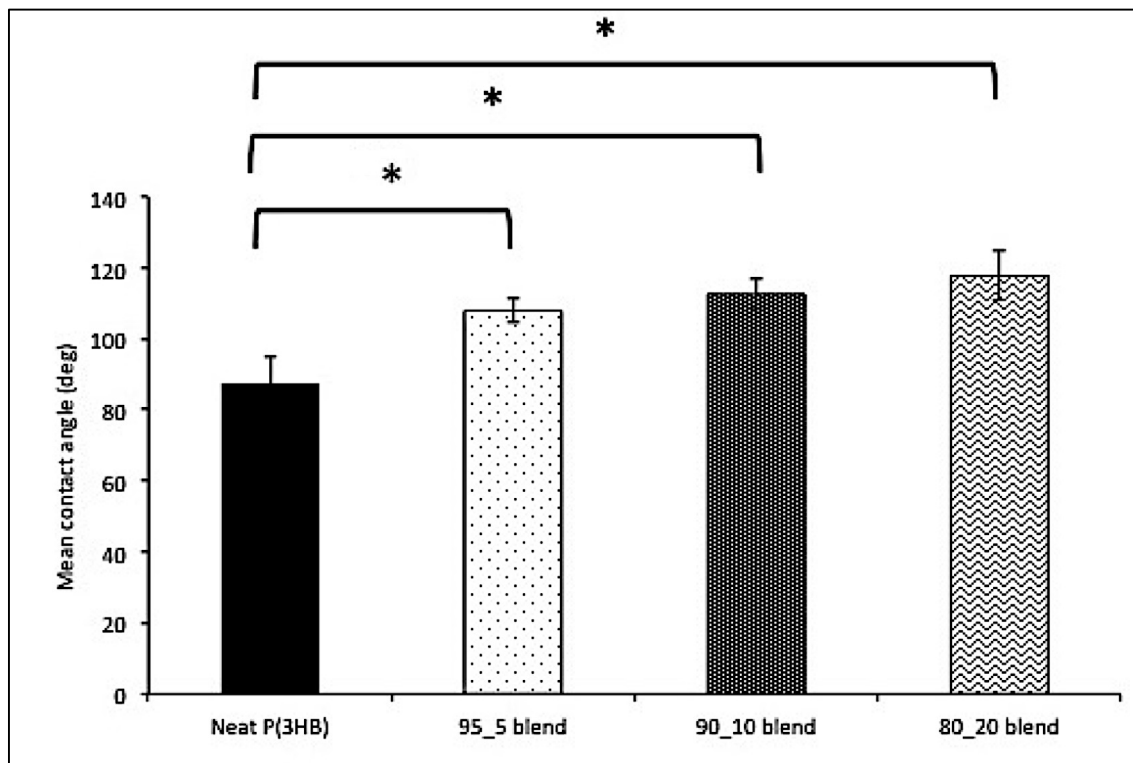


Figure 45: Static water contact angle measurements for the neat P(3HB) film and its blends with oligo-PHA (n=3; error bars=±SD). The data were compared with neat P(3HB) using ANOVA. * indicates p-value < 0.05.

Materials, which have contact angle value higher than 70° are considered as hydrophobic in nature. Bearing in mind this definition, all tested film samples were hydrophobic. And the hydrophobicity increased with the increased concentration of the hydrolysed mcl-PHA copolymer. It has been observed, that cells prefer to attach to the weakly hydrophilic surfaces (contact angle around 60°), whereas highly hydrophilic or hydrophobic surfaces have been used to inhibit cell adhesion (Bacakova *et al.*, 2011).

5.3.4. Protein adsorption analysis

The affinity of the materials towards proteins were evaluated by bicinchoninic acid assay with Foetal Bovine Serum (FBS) as a model protein. It was found that total protein adsorption was 90±3, 105.6±15, 145±35 and 300±35 µg/cm² for the neat P(3HB) film

and 95/5, 90/10 and 80/20 blends respectively. There was no significant difference between P(3HB) and 95/5 blend. There was significant difference between the 90/10 and 80/20 blend in comparison to the neat P(3HB) film (** $p=0.006$ and *** $p=0.0001$ respectively) (Figure 46).

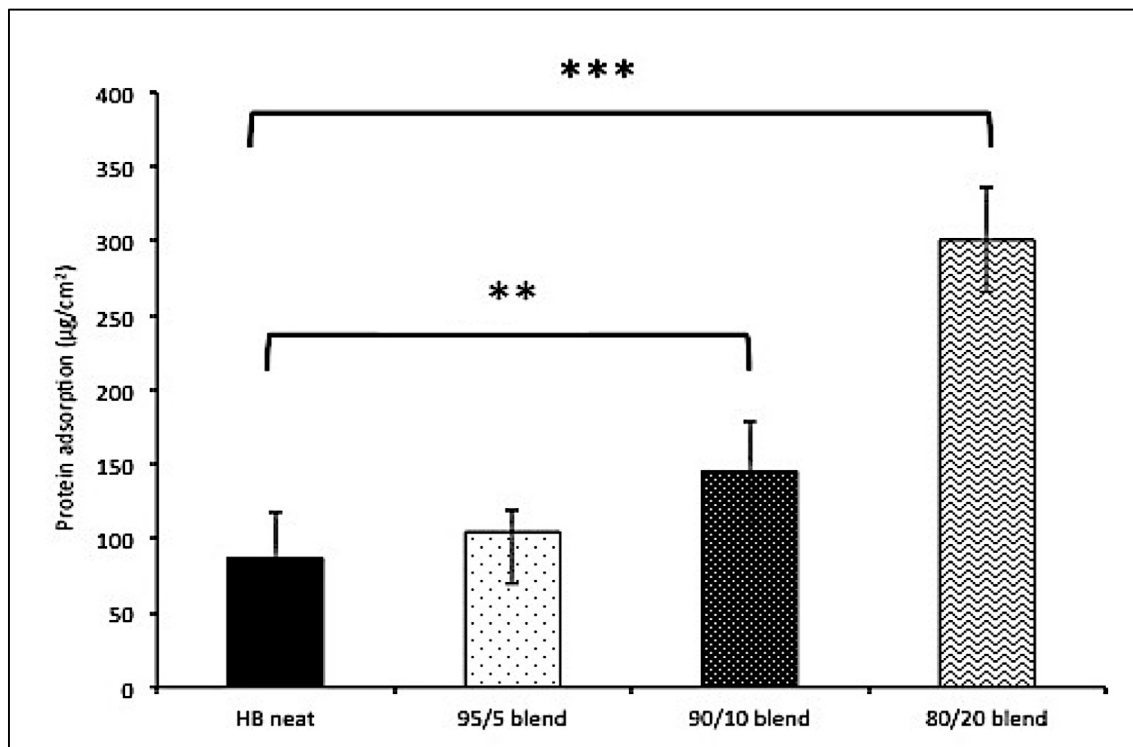


Figure 46: Protein adsorption on the films of neat P(3HB) and P(3HB)/oligo-PHA blends ($n=3$; error bars= \pm SD). The data were compared with neat P(3HB) using ANOVA. ** indicates $p<0.005$ and *** indicates $p<0.0005$.

The amount of protein adsorbed on the film samples increased with the addition of the oligo-PHA and was almost three times higher for the 80/20 blend compared with neat P(3HB).

5.4. *In vitro* biocompatibility studies

The carbon source used for P(3HHx-3HO-3HD-3HDD) production was a waste material. Therefore, it was crucial to evaluate the biocompatibility of the developed materials in order to consider them for any biomedical applications.

5.4.1 Cell viability studies

Preliminary *in vitro* cell culture studies were carried out using a human dermal microvascular cell line. Therefore HMEC-1 was chosen to investigate the possibility of using softer P(3HB)-based materials with improved plasticity as materials for scaffolds in coronary stent applications. The results of biocompatibility studies are presented in Figure 47.

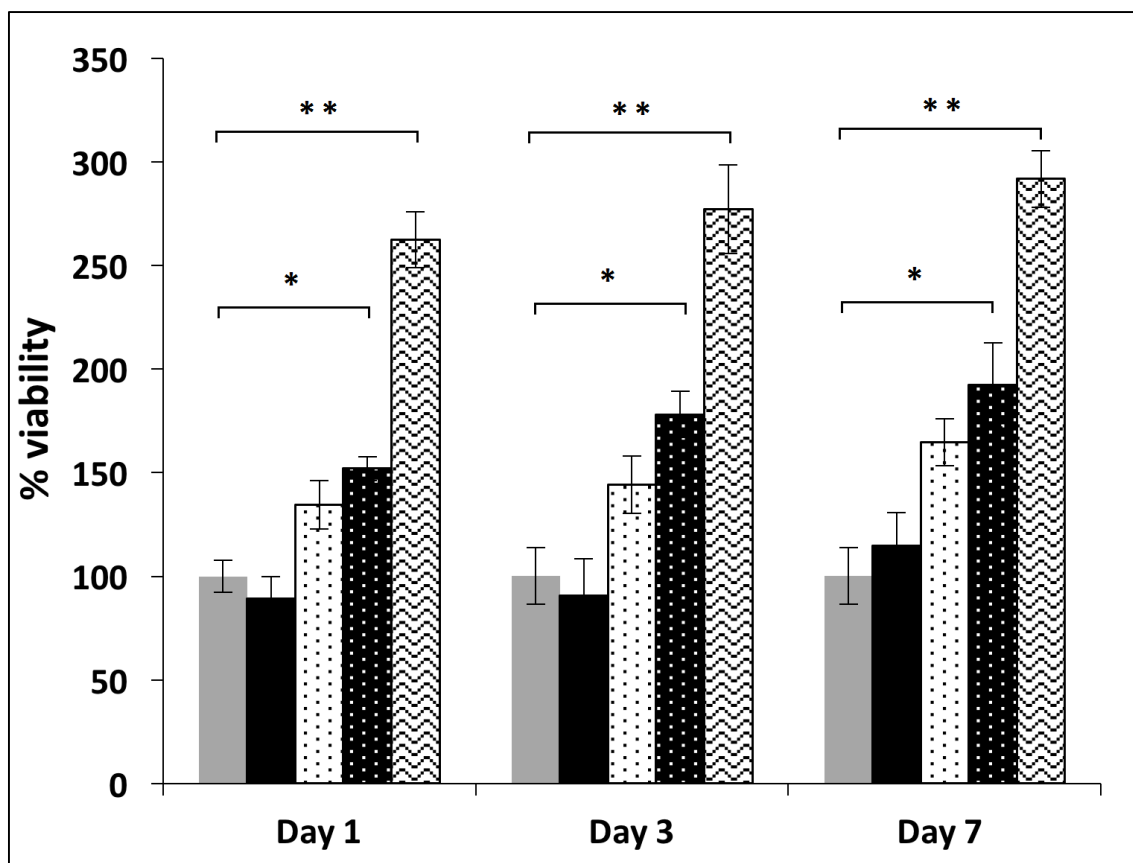


Figure 47: Cell proliferation study of the HMEC-1 cells on the P(3HB) film and P(3HB)/oligo-PHA blend film samples at day 1, 3 and 7 (n=3; error bars=±SD). The data were compared with standard tissue culture plastic (positive control), which was normalised to 100% using ANOVA. * indicates $p < 0.05$ and ** indicates $p < 0.005$. (■) TCP, (■) P(3HB), (◻) 95/5 blend, (◻) 90/10 blend, (◻) 80/20 blend.

Cell proliferation on the P(3HB) film samples was $89.1 \pm 2.2\%$ on day 1, $90.8 \pm 1.2\%$ on day 3 and $114.6 \pm 1.7\%$ on day 7 compared to the TCP. The differences were not statistically significant in comparison to TCP. Growth of HMEC-1 cells on the P(3HB) film was lower at day 1 and 3 in comparison with the TCP. The growth of the HMEC-1 cells on the surface of the 95/5 blend was higher than TCP on day 1, 3 and 7. The differences were

not statistically significant, when compared with standard tissue culture plastic. HMEC-1 cell viability on films of the 90/10 blend was also higher at every time point in relation to TCP: $152 \pm 0.5\%$, $178.2 \pm 2.2\%$ and $192 \pm 1.6\%$ at day 1, 3 and 7 respectively. The differences were statistically significant in comparison to TCP at day 1 (* $p=0.019$), day 3 (* $p=0.021$) and day 7 (** $p=0.0016$). The highest viability of the HMEC-1 cells was achieved on the surface of the 80/20 blend which supported $262.4 \pm 2.7\%$, $277.1 \pm 4.4\%$, $291.7 \pm 2.1\%$ of viable cells compared with TCP on day 1, 3 and 7 respectively. The differences were statistically significant in comparison to TCP on day 1 (** $p=0.0048$), day 3 (** $p=0.0022$) and day 7 (** $p=0.0031$).

Overall, the results obtained demonstrated higher biocompatibility of all samples in comparison to TCP. However, the highest cell adhesion was observed for P(3HB)/oligo-PHA 80/20 blend within the 7-day period. Hence, in conclusion, P(3HB) as well as all blends were biocompatible. Higher adhesion of the HMEC-1 cell line to the 90/10 and 80/20 P(3HB)/oligo-PHA composition in comparison to the TCP indicated the possibility of their application as a platform material in coronary stent application.

5.4.2. Scanning Electron Microscopy

Cell adhesion and proliferation was further characterised using SEM imaging. Micrographs presented in Figure 46 revealed that HMEC-1 cells adhered and proliferated evenly across the surface. Cell density evidently increased with a higher concentration of oligo-PHA within the blend, which is in agreement with the results of the MTT assay. This order of the materials ability to support cell proliferation also matched the order of increasing surface roughness, hydrophobicity and protein absorption. Overall, all PHA-based materials supported HMEC-1 cell attachment and proliferation demonstrating good biocompatibility. Addition of oligo-PHA improved cell proliferation with the highest cell viability achieved for 90/10 and 80/20 blends (Figure 48).

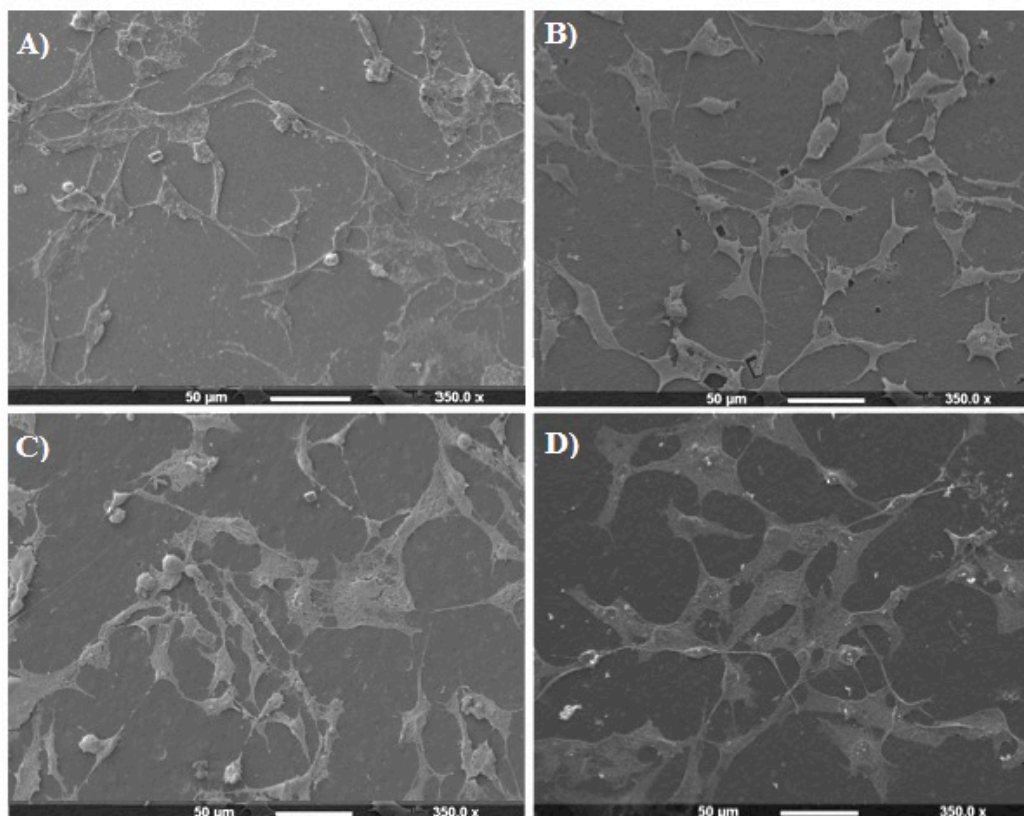


Figure 48: Scanning electron micrographs of the surfaces of (A) neat P(3HB) and P(3HB)/oligo-PHA blends in ratios: 95/5 (B), 90/10 (C), 80/20 (D) after culturing HMEC-1 cells for 7 days.

HMEC-1 cells adhered to the surface of the materials had spindle-shaped morphology, typical to healthy endothelial cells. With respect to the results obtained, neat P(3HB) as well as all blends of P(3HB)/oligo-PHA supported the growth of the HMEC-1 cell line. However, blends with higher amount (over 10 wt%) of oligo-PHA appeared to support better cell attachment and proliferation.

5.4.3 Confocal microscope of HMEC-1 cells on the P(3HB) neat and P(3HB)/oligo-PHA blends

Confocal imaging was performed to support the results obtained in viability studies and SEM. HMEC-1 cells on the P(3HB) neat film as well as P(3HB)/oligo-PHA blends were stained with Calcein AM and Ethidium homodimer-1. The images obtained (Figure 49) demonstrated high cell adhesion and growth on all types of scaffolds on day 7.

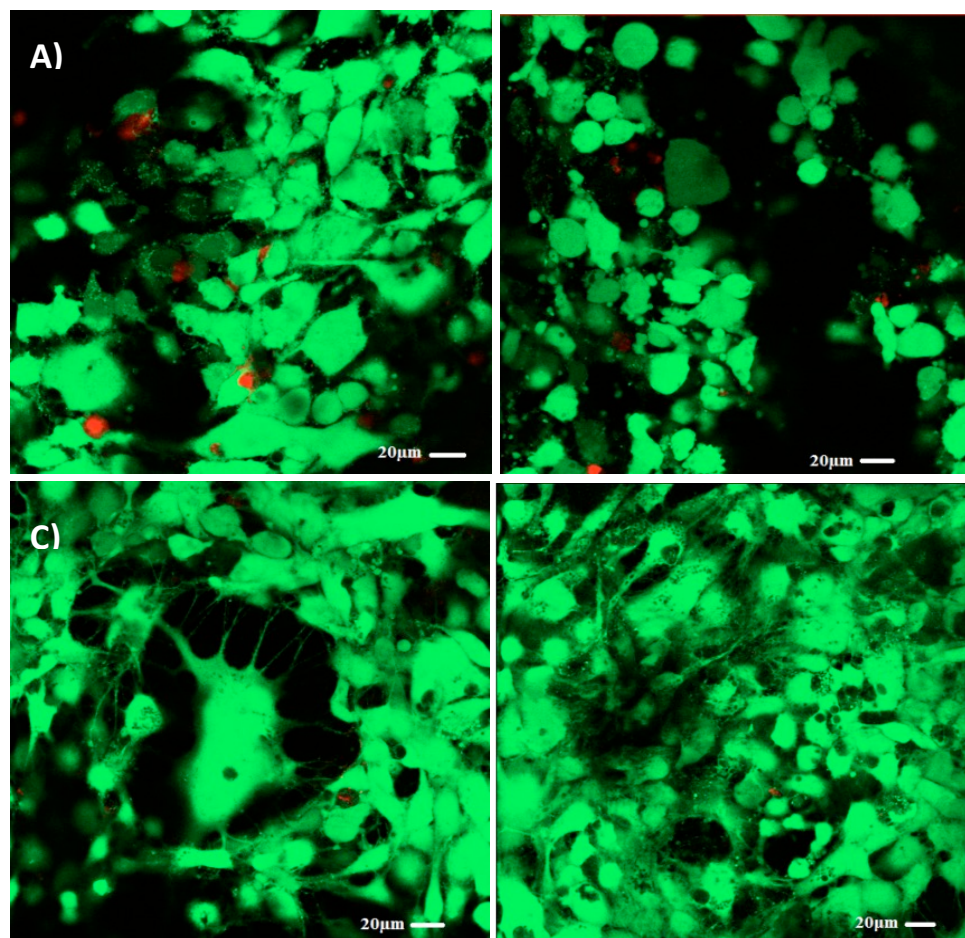


Figure 49: Representative confocal micrographs of live HMEC-1 cells (green) and dead HMEC-1 cells (red) on different PHA materials at day 7. (A) Neat P(3HB) film, (B) P(3HB)/oligo-PHA in ratio 95/5 blend film, (C) P(3HB)/oligo-PHA in ratio 90/10 blend film, (D) P(3HB)/oligo-PHA in ratio 80/20 blend film.

HMEC-1 cells attached and proliferated on the surface of developed biomaterials. Green colour of the cells indicates presence of alive cells. Confocal images further confirmed results obtained by MTT assay and SEM imaging, indicating high biocompatibility of the neat P(3HB) and P(3HB)/oligo-PHA blends to the HMEC-1 cell line.

5.5. Haemocompatibility studies

P(3HB) neat film and P(3HB)/oligo-PHA blends were subjected to haemocompatibility studies, which included haemolysis studies, whole blood clotting as well as monocyte and neutrophils activation.

5.5.1. Haemolysis study

Haemolysis study was performed on P(3HB) neat films as well as P(3HB)/oligo-PHA blends to check if the materials would cause haemolysis, which is lysis of the red blood cells after direct contact with fresh whole blood. Damaged red cells will release free haemoglobin, which can be measured spectrophotometrically. The results obtained are shown in Figure 50. Distilled water was used as positive control. 0.9% NaCl solution was used as a negative control.

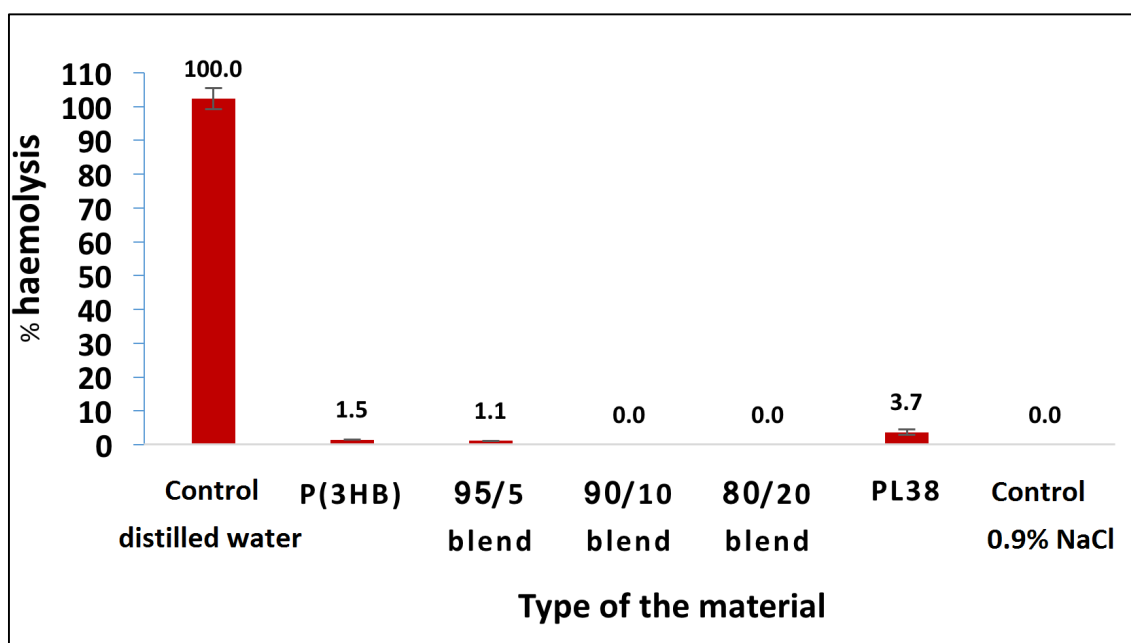


Figure 50: Haemolysis rates of the P(3HB) and P(3HB)/oligo-PHA blends in percent after 1h of incubation at 37°C (n=3). All the film samples were compared with the control, (0.9% NaCl) calculated as 0% haemolysis using ANOVA. No significant difference.

Erythrocytes underwent haemolysis after direct contact with distilled water, whereas 0.9% NaCl solution did not cause lysis of red blood cells. Among the PHAs tested, none of the materials caused haemolysis. The percent of haemolysis observed for neat P(3HB) and 95/5 P(3HB)/oligo-PHA blend was 1.5% and 1.1% respectively. Additionally, PL38

medical grade was tested in order to compare with the haemocompatibility of the PHAs. The percent of haemolysis was 3.7%. For the blends with an addition of oligo-PHA over 10 w%, the percent of haemolysis was 0%. According to the criteria, described by van Oeveren, 2013, a material can be classified as haemolytic, when % haemolysis is higher than 5%. The results obtained demonstrated that PHAs are non-haemolytic (% haemolysis 0-2%) materials, whereas PL38 is slightly haemolytic (% haemolysis 2-5%). According to the ISO 10993-4:2002 standard, the % haemolysis value should be below 5%. All tested materials demonstrated haemolysis at levels below 5%. This result showed that all tested films had low potential to destroy red blood cells.

5.5.2. Whole blood clotting

Whole blood clotting experiment was performed to investigate the potential procoagulant properties and thrombogenicity of the materials. Red blood cells not trapped in the blood clot were lysed by addition of distilled water and released free haemoglobin, which was measured spectrophotometrically. The summary of the results obtained after 30 and 90 minutes are shown in Figure 51.

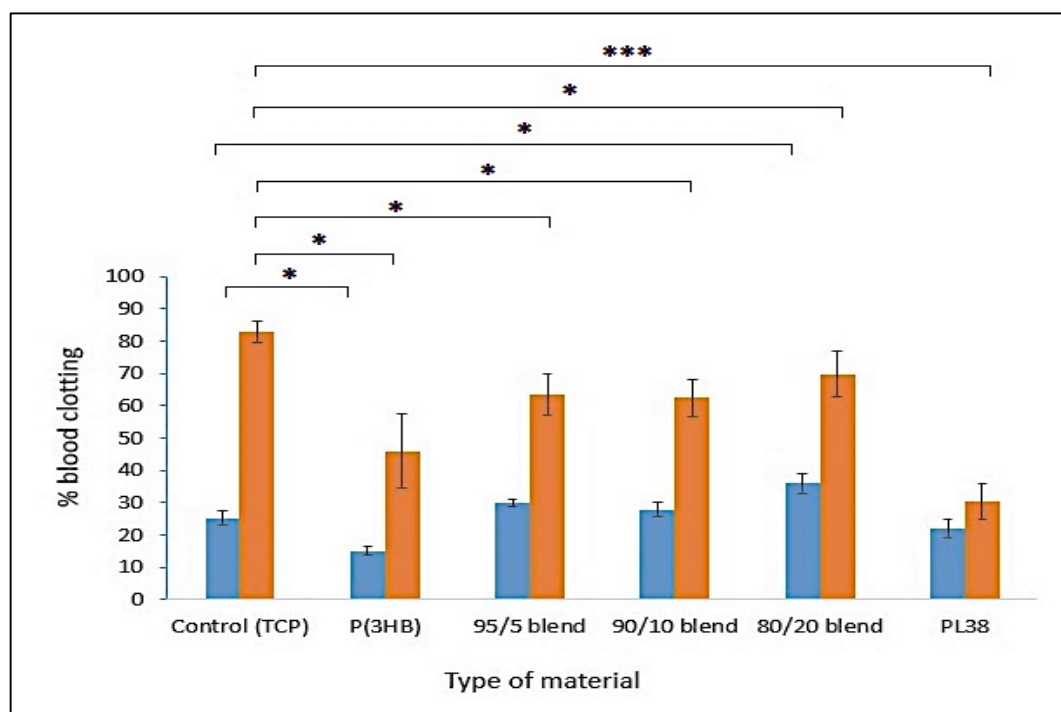


Figure 51: Whole blood clotting after 30 minutes (■) and 90 minutes (■) of incubation on the neat P(3HB), P(3HB)/oligo-PHA blends and PL38 medical grade (n=3; error

bars= \pm SD). The data were compared with standard tissue culture plastic using ANOVA. *indicates $p < 0.05$ and *** indicates $p < 0.0005$.

The results obtained indicate that after 30 minutes of incubation, the P(3HB) neat film demonstrated $15.1 \pm 1.3\%$ blood clotting, which was significantly lower blood clotting rate than the positive control, tissue culture plastic (TCP) with a value of $25.2 \pm 0.2\%$ (* $p = 0.0175$). P(3HB)/oligo-PHA blend in the ratio 80/20 showed significantly higher blood clotting ($36.1 \pm 0.3\%$) rate in comparison to the positive control (* $p = 0.0107$) after 30 minutes. All other materials, after 30 minutes resulted in higher % blood clotting than the positive control. However, the differences were not significant. With the increase of time, the % blood clot increased in all tested materials as well as in the positive control. After 90 minutes the control blood exhibited $82.9 \pm 3.3\%$ blood clotting. The neat P(3HB) film exhibited $45.9 \pm 1.1\%$ blood clotting, P(3HB)-oligo-PHA blends had % blood clotting over 62.4-69.7%. PL38 resulted in a decrease in blood clotting after 90 minutes ($30.2 \pm 0.5\%$) in comparison to TCP. This difference was highly significant (*** $p = 0.0008$) in comparison to the standard tissue culture plastic.

5.5.3. White cell activation

White cell activation was performed on monocytes and neutrophils. Fresh whole blood activated with LPS (10ng/mL) was used as a positive control. Non-activated blood was used as a negative control. PL38, commonly used for medical applications, was used as a biomaterial control. The activation was evaluated by flow cytometry after staining whole blood with specific markers, as described in the section: 2.15.3.2. CD11b is an activation marker for neutrophils and monocytes. CD11b regulates leukocyte adhesion and migration to mediate the inflammatory response. Other markers, such as CD86-PE, CD45-PerCP and CD66b-FITC were used in this study were to select the right fraction of the cells during flow cytometry analysis. Obtained results are expressed as the Median Fluorescence Intensity (MFI).

5.5.3.1. Whole blood staining

Whole blood was incubated at 37°C overnight and stained with the markers listed in Table 1. The results obtained are shown in Table 21 and Figure 52.

Table 21: Summary of median fluorescence intensity (MFI) obtained after incubation of fresh whole blood incubated with neat P(3HB), P(3HB)/oligo-PHA blends in ratios: 95/5, 90/10, 80/20 PHAs and PL38 and stained with specific markers in order to evaluate monocyte and neutrophil activity. Fresh whole blood without any markers were used as a control.

No.	Sample	Markers	Monocyte activity (MFI)	Neutrophil activity (MFI)
1.	Fresh whole blood	-	0	0
2.	Fresh whole blood	CD86-PE	114.9	157.1
		CD45-PerCP	109.4	117.6
3.	Fresh whole blood	CD11b-PE	135.9	140.9
		CD66B-FITC	202.6	162.8

Fresh blood without any antibodies did not demonstrate any activity as expected.

Fresh blood incubated with selective and activation markers demonstrated low level of activity for monocytes as well as for neutrophils.

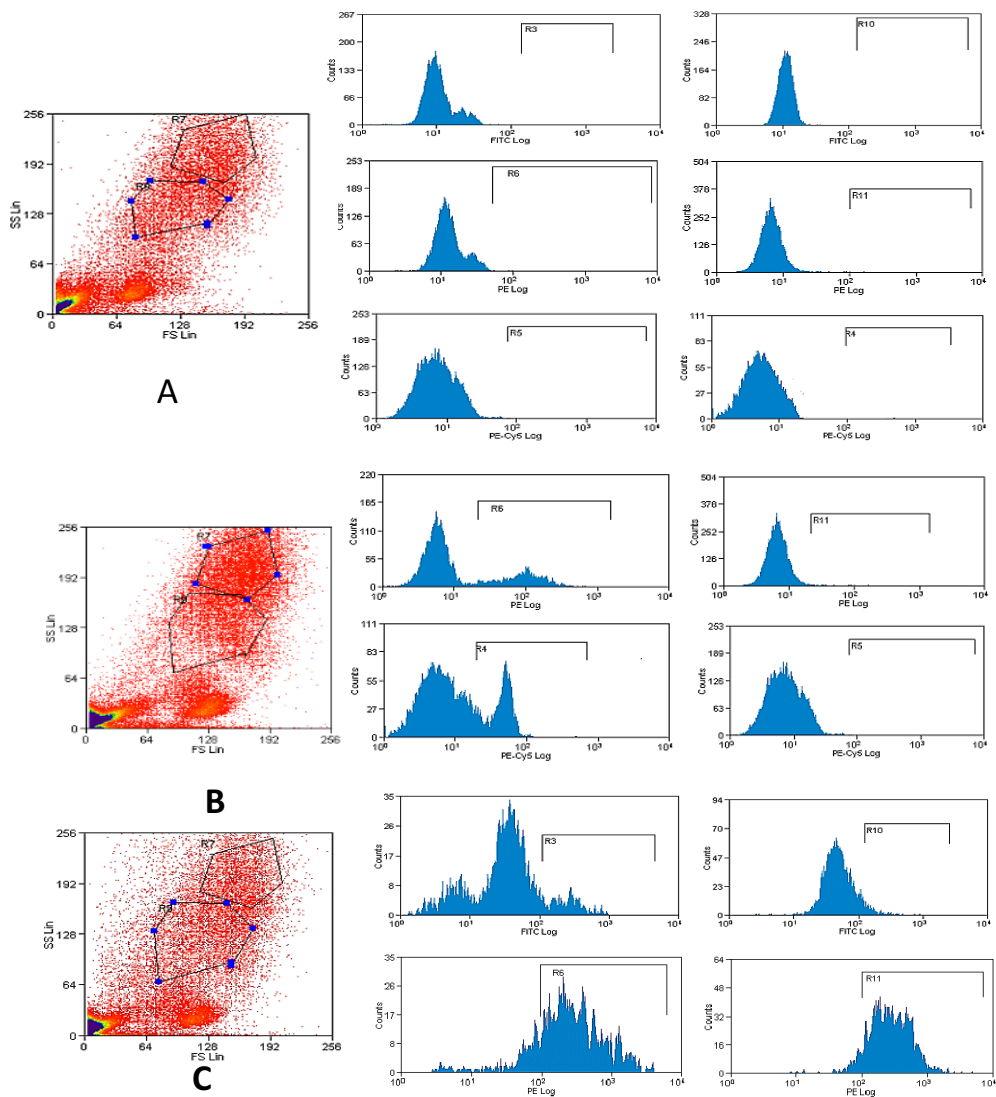


Figure 52: Flow cytometry histograms of stained fresh whole blood without any markers (A) and whole blood with addition of markers (B, C). Results are considered as significant when more than 500 events were recorded.

5.5.3.2. Blood activation with LPS

Whole blood was incubated with LPS (10ng/mL) at 37°C overnight and stained with the markers listed in Table 2. The results obtained were summarised in Table 22 and Figure 53.

Table 22: Summary of median fluorescence intensity (MFI) obtained after incubation of fresh whole blood activated with LPS and stained with specific markers in order to evaluate monocyte and neutrophil activity.

No.	Sample	Markers	Monocytes activity (MFI)	Percentage change (%)	Neutrophils activity (MFI)	Percentage change (%)
1.	Fresh whole blood+LPS	CD86-PE	162.8	41.7	146.2	-
		CD45-PerCP	113.5	3.7	117.8	0.17
2.	Fresh whole blood+LPS	CD11b-PE	715.2	426.3	1104.6	683.9
		CD66B-FITC	175.1	-	225.9	38.7

LPS is present in the cell walls of Gram negative bacteria. It is also known as an endotoxin.

From the results obtained it is evident that LPS triggered an increased activity of monocytes and neutrophils. CD11b-PE is a marker of activation for both: neutrophils and monocytes. It is an adhesion molecule and its expression increases several hours after cell activation. This blood samples were incubated overnight; therefore, higher activity of CD11b-PE was expected. Other markers did not demonstrate higher activity in presence of LPS.

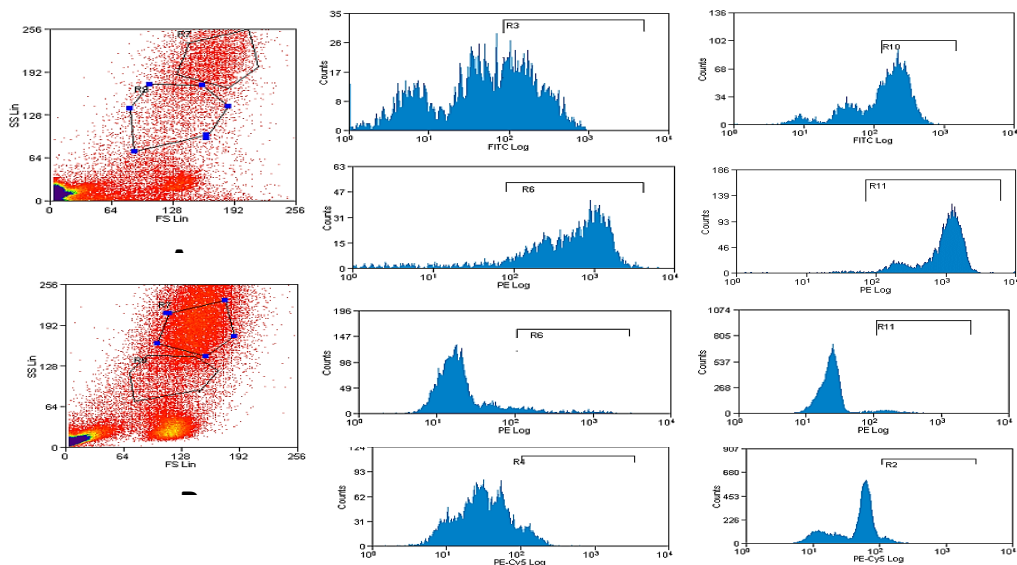


Figure 53: Flow cytometry histograms of stained fresh whole blood activated with LPS with two different sets of markers (A, B).

Fresh whole blood activation with the same concentration of LPS (10ng/mL) tested after 16 hour of incubation at 37°C resulted in much higher values of CD11b-PE for monocytes as well as neutrophils. The percentage change in the MFI value of CD11b-PE marker in the blood activated with LPS was 426.3% and 683.9% higher in comparison to the fresh whole blood. In conclusion, addition of LPS was able to activate both fractions of white blood cells. This aspect needs to be consider during purification of the PHA polymers obtained from Gram negative bacteria, containing LPS within the cell wall. Traces of LPS present within the polymer can lead to accelerated white blood activation and inflammatory response from the body against the polymeric material. Therefore, maximum LPS levels, accepted in the biomaterial have been strictly regulated. For implants which will be in contact with cardiovascular system, the maximum acceptable level of LPS is 20 endotoxin units (20EU) per device (FDA, 1987).

5.5.3.3. Monocyte and neutrophil activity with neat P(3HB) and P(3HB)/oligo-PHA blends

P(3HB), P(3HB)/oligo-PHA blends and PL38 were incubated with whole blood at 37°C overnight and stained with the markers listed in Table 2. Summary of the results obtained are shown in Table 23.

Table 23: Summary of median fluorescence intensity (MFI) obtained after incubation of fresh whole blood incubated with neat P(3HB), P(3HB)/oligo-PHA blends in ratios: 95/5, 90/10, 80/20 PHAs and PL38; and stained with specific markers in order to evaluate monocyte and neutrophil activity.

Sample	Markers	Monocytes Activity (MFI)	Percentage change (%)	Neutrophils Activity (MFI)	Percentage change (%)
P(3HB) neat	CD86-PE	176.5	53.6	117.3	-
	CD45-PerCP	51.3	-	79.1	-
	CD11b-PE	464.2	241.5	955.3	578.0
	CD66B-FITC	-	-	-	-
95/5 blend	CD86-PE	113.5	-	121.9	-
	CD45-PerCP	94.7	-	86.1	-
	CD11b-PE	665.1	389.4	742.32	426.8
	CD66B-FITC	117.6	-	113.5	-

90/10 blend	CD86-PE	217.4	89.2	162.6	3.5
	CD45-PerCP	135.9	0.0	117.8	0.17
	CD11b-PE	517.4	280.7	742.3	426.8
	CD66B-FITC	311.97	53.9	175.1	7.5
80/20 blend	CD86-PE	126.4	10.0	136.9	-
	CD45-PerCP	121.9	11.4	94.7	-
	CD11b-PE	431.4	217.4	556.3	294.8
	CD66B-FITC	-	-	-	-
PL38	CD86-PE	106.6	-	101.6	-
	CD45-PerCP	113.5	3.7	101.8	-
	CD11b-PE	597.7	339.8	1584.1	1024.3
	CD66B-FITC	135.9	-	131.1	-

Results obtained after staining blood samples, exposed to various polymer samples demonstrated different levels of activity of monocytes as well as neutrophils. The neat P(3HB) film triggered higher activity of both fractions. An activation marker: CD11b demonstrated higher activity in all tested comparison to the non-activated blood. For neat P(3HB) film, the percentage change of median fluorescence activity was 241.5% for monocytes and 578% for neutrophils higher than fresh whole blood. P(3HB)/oligo-PHA blends also demonstrated elevated values in comparison to control. Among all tested materials, PL38 demonstrated the highest percentage changes for monocytes (339.8%) and neutrophils (1024.3%) activation in comparison to fresh whole blood. Neutrophils activation levels were 34% higher in comparison to blood activated by LPS.

5.6. Discussion

Embrittlement of P(3HB) is a well-recognised phenomenon which limits applications of P(3HB) including biomedical applications. Therefore, addition of oligo-PHA was studied for the development of novel materials based totally on PHAs.

Oligomerisation of mcl-PHA was achieved by acidic hydrolysis which resulted in an mcl-PHA with molecular weight around 10 kDa. Presence of single melting peak during DSC analysis of P(3HB)/oligo-PHA blends (Figure 41) confirmed good compatibility of the oligo-PHA with the P(3HB). It is worth noting that both thermal and mechanical properties of the P(3HB)/oligo-PHA blends were characterized with respect to material ageing in order to evaluate embrittlement of P(3HB)-based material. The P(3HHx-3HO-

3HD-3HDD) copolymer after hydrolysis presented different thermal properties than the same material before hydrolysis. The glass transition temperature for oligo-PHA copolymer was at -39°C . Two melting events were detected: at 28.6°C and 38.6°C . The observed low value of T_g as typical to mcl-PHAs. Melting events observed in the thermograms were at lower temperatures than mcl-PHAs. Although the addition of oligo-PHA to P(3HB) caused only a small decrease in melting temperature, it led to a significant drop in the crystallinity of P(3HB). Meszynska and co-workers (2015) reported application of oligomeric compounds of P(3HB) as plasticiser into P(3HB-co-4HB) copolymer. However, oligo-PHB worked more like nucleating agent, rather than plasticiser. Oligo-PHB did not have any influence on the glass transition temperature or crystallisation temperature. Melting temperature of the new system and crystallinity degree increased significantly in comparison to neat P(3HB-co-4HB) copolymer. Type of plasticiser can have detrimental effect on the material properties. The same polymer (P(3HB-co-4HB)), mixed with monoglyceride acetate demonstrated totally different thermal properties than P(3HB-co-4HB) mixed with oligo-PHB. Glass transition temperature and crystallisation temperature decreased, while other parameters did not change. Observed changes in glass transition temperature confirmed plasticisation effect of studied additive (Meszynska *et al.*, 2015). Presence of plasticiser results in an increase in free volume and polymer chains mobility between polymer chains, which leads to decrease in glass transition in the materials (D'Amico *et al.*, 2016).

Addition of oligo-PHA have an influence on the mechanical properties of the material. Presence of plasticiser resulted in decrease of Young's Modulus, tensile strength and an increase of an elongation at break. This result is in agreement with literature. Ghiya and co-workers studied addition of butyryltriethyl citrate to P(3HB). Obtained material presented lower value of Young's Modulus and higher elongation at break in comparison to neat P(3HB) (Ghiya *et al.*, 1995). In another study reported by Meszynska and co-workers (2015), an addition of monoglyceride acetate to P(3HB-co-4HB) confirmed results obtained in this study. However, an addition of oligomeric form of P(3HB) to the same copolymer resulted in different mechanical properties of the final material. Material became more stiff and strong, without loss of any elastomeric properties (Meszynska *et al.*, 2015). Experiments performed by Garcia-Garcia and co-workers (2017) also demonstrated plasticising effect of vegetable oil derivatives, such as

maleinized linseed oil and an epoxidized fatty acid ester on P(3HB). Mechanical properties of new material, demonstrated similar trend to these obtained in this study (Garcia-Garcia *et al.*, 2017). It is worth mentioning that various types of plasticisers react differently with PHAs. For example, in another study, Requena and co-workers studied effect of five various plasticisers, such as three different molecular weight polyethylene glycols (PEG200, PEG1000 and PEG4000), lauric and stearic acids on P(3HB-co-3HV) copolymer. As a result, among all tested compounds, only addition of PEG1000 resulted in slight improvement of elastomeric properties in P(3HB-co-3HV) copolymers films (Requena *et al.*, 2016). Another very important aspect was related to the concentration of the plasticiser. Panaitescu and co-workers (2016) reported that properties of the material obtained after addition of plasticiser depends on the amount of the compound added. Higher concentration of plasticisers may result in sudden drop in the properties of the material, which can be a consequence of phase separation and limited compatibility between polymer and an additive (Panaitescu *et al.*, 2016). The mechanical properties of both neat P(3HB) and P(3HB)/oligo-PHA blends gradually changed during the 7-week ageing. Although the addition of oligo-PHA did not eliminate the increase in stiffness of the P(3HB)-based materials attributed to the ageing processes, oligo-PHAs had a clear plasticising effect on the P(3HB) resulting in softer, more elastomeric materials. The plasticising effect of the oligo-PHAs resulted in obtaining P(3HB)-based materials with a wider range of mechanical properties with the potential of their applications as coronary stents.

Addition of the oligo-PHAs also resulted in changes in the surface topography. With an increase of the amount of plasticizer, the surface roughness, static contact angle as well as protein adsorption increased significantly. The exact mechanism of an enhancement in surface roughness by addition of oligomeric mcl-PHA plasticiser to P(3HB) is not fully understood due to shortage of relevant literature. Different approaches have been taken, in order to increase surface roughness of PHAs. These include mainly surface modifications, such as plasma treatment, laser micropatterning, chemical modifications (Slepicka *et al.*, 2017). Surface roughness can be also affected by using different processing techniques. For example, Yu and co-workers, 2009 reported that solvent cast PHA films had higher surface roughness than compression moulded films (Yu *et al.*, 2009). An increase in surface roughness after addition of various compounds, such as

cellulose, organoclay, carbon nanotubes, hydroxyapatite, bioglass into PHAs, have been reported previously (Ma *et al.*, 2017; Basnett *et al.*, 2013; Bittmann *et al.*, 2013; Francis *et al.*, 2010).

An increase of surface roughness results in an enlargement of surface area, which might explain an increased protein adsorption on the surface of the blend films in comparison to neat P(3HB). It is known from literature, that protein adsorption is higher on a rough surface compared to the smooth, flat surface (Chen *et al.*, 2009). Inability of the proteins to attach to the surface of the implant could trigger an inflammatory response and lead to the rejection of the implant (Das *et al.*, 2007). Protein adsorption is correlated with surface roughness and hydrophobicity of the material. The more hydrophilic material, the less amount of protein will adsorb. However, they will remain in active conformation (Baujard-Lamotte *et al.*, 2008). However, it is worth mentioning, that various proteins demonstrate different affinity towards materials. For example, albumin prefer to adsorb on the hydrophobic surfaces in comparison to fibronectin, which prefers more hydrophilic materials (Iuliano *et al.*, 1993). Both proteins: albumin and fibronectin supports each other. For example, adsorbed albumin inhibits conformational changes in fibronectin and allows fibronectin RGD active sites to be more accessible to cells (Anselme *et al.*, 2010). In general, mcl-PHAs have higher contact angle values due to increased hydrophobicity of the material induced by the longer length of monomer chains. Surface roughness is one of the crucial factors which is measured while evaluating any biomaterial for biomedical applications (Das *et al.*, 2007). Numerous studies have revealed that most of the cells prefer to attach on a rough surface as compared to the smooth surface. An uneven or a rough surface provides the cells with several adhesion points that allow them to migrate and proliferate (Hao and Lawrence, 2004). Restrained hydrophilic and positively charged materials encourage cell attachment due to the adhesion of specific molecules, such as vitronectin and fibronectin, which make specific sites accessible for the cell adhesion receptors (Bacakova *et al.*, 2011).

The human dermal microvascular cell line was used for *in vitro* assessment of attachment and proliferation of cells relevant to coronary stent application. Biocompatibility studies confirmed that P(3HB)/oligo-PHA materials were not cytotoxic. HMEC-1 cells evenly colonised the surface of films and exhibited a typical healthy

morphology. All P(3HB)/oligo-PHA materials showed better ability to support cell growth compared with control standard tissue culture plastic. Cell proliferation on the surface of blends improved compared with the neat P(3HB) and increased with the larger content of oligo-PHA. Protein adsorption occurs as a first step before cells attach and spread over the surface (Anselme *et al.*, 2010). The mechanism of cell adhesion to biomaterial has been extensively studied. Immediately, after implantation, biomaterial is covered with proteins from blood and body fluids. Cells are able to sense foreign surfaces by this adsorbed protein layer and respond to it accordingly. Process of cells adhesion can be divided into few phases: at early stage physico-chemical interaction between cells and material occurs by Van der Waals forces and ionic forces. Cells attach to the surface, spread, express cytoskeleton proteins and integrins. In the next stage, clustering of integrin receptors occurs, followed by cytoskeleton reorganisation and cell spreading on the surface of the biomaterial (Trepap *et al.*, 2008). In general, cells prefer to attach to rougher than smoother surfaces. However, the lever of roughness is individual for each cell type (Korovessis *et al.*, 2002). For example, Kunzler and co-workers demonstrated that osteoblasts more favoured rough surfaces, while fibroblast definitely prefer smooth materials (Kunzler *et al.*, 2007). Improved affinity of P(3HB)/oligo-PHA blends towards proteins could contribute to the materials enhanced ability to support cell proliferation. Also by variation of the amount of plasticiser varied the mechanical properties of the blend. There is growing research interest in demonstrating the role of substrate mechanics in the behaviour and function of individual cells, in particular material stiffness (Han *et al.*, 2016). Pelham and Wang (1997), demonstrated that rat kidney epithelial cells and 3T3 fibroblasts responded differently to varied flexibility of the material (Pelham and Wang, 1997). In another study, Lo and co-workers (2000), demonstrated influence of material rigidity on 3T3 fibroblasts cell movement. Cells could sense stiffness of the material and migrated in the direction of more rigid substrate (Lo *et al.*, 2000).

The enhancement of HMEC-1 cell proliferation on slightly softer blends could be a result of the fact that better mimic the physiological biomechanical environment of these cells. Bhattacharyya and co-workers (2010), reported enhanced adhesion and growth rate of human aortic endothelial cells (HAEC) on the surfaces containing increased number of -COOH functional groups on the surface. It was possible to generate favourable

environment for increased endothelial cell adhesion and proliferation by adjusting surface chemistry as well as polymer film thickness (Bhattacharyya *et al.*, 2010).

The compatibility of P(3HB) and P(3HB)/oligo-PHA blends after direct contact with blood were investigated. All materials demonstrated a non-haemolytic effect on the erythrocytes. Addition of low molecular weight mcl-PHA resulted in deceleration of blood clotting after 90 minutes. Haemocompatibility is a crucial factor during material evaluation, especially for biomedical applications. There is only one publication, where the haemocompatibility of P(4HB) was analysed (Liu *et al.*, 2014). The blood-scaffold response is a very complex mechanism of several reactions, quite complicated to perform in one study (Ratner, 2007). Many different experiments need to be carried out to evaluate the biomaterials appropriately. This should include effect on haematology, coagulation, thrombosis as well as the immunological response (Hanson and Ratner, 2004). Neutrophils and monocytes were found to be major factors in the immunological response, especially with cardiovascular devices (Gorbet and Sefton, 2004). Indicators of leucocyte activation, such as upregulation of CD11b has been observed *in vivo*, for example after angioplasty (Takala *et al.*, 1996; Serrano *et al.*, 1997). Therefore, activation of both fractions was studied after contact with PHA films. Although the life of neutrophils is very short (8-20 hrs), activation triggered by LPS can prolong this time to 60hrs (Cassatella, 2009). Monocytes circulate between 36-104hrs in the blood stream and then migrate into tissues and differentiate into macrophages (Anderson, 1993). Bacteria and their metabolites can induce activation of both: neutrophils and monocytes (Gorbet and Sefton, 2004). LPS is released after destruction of the entire cell (Lynn and Golenbock, 1992). It can cause strong immunogenic response in human and animals (Lemke, 1994). FDA approved the acceptable level of endotoxin in medical devices to be 0.5EU/mL or 20EU/device for products, which directly or indirectly contact cardiovascular system (FDA, 1987). Leucocytes can be activated by 0.01 ng/ml of LPS, an equivalent of 0.05 EU/ml (Weingarten *et al.*, 1993).

P(3HB) was produced by Gram-positive bacteria, free from the presence of LPS. Therefore, it was worth investigating further, the reason behind obtaining this result. One of the hypothesis might be an ability of some of the Gram-positive bacteria to produce macroamphiphiles including lipoglycans and lipoteichoic acids (LTA), which have highly immunogenic properties, similar to LPS (Ray *et al.*, 2013). Surprisingly PL38,

certified to be produced under GMP conditions and widely used for biomedical applications also induced very high neutrophil activation (over 1500.MFI), even higher than LPS (1100.0MFI). This may be caused by some chemical impurities in the material, which react with the blood in a similar way like LPS.

In conclusion, addition of oligo-PHA resulted in an improved material properties in comparison to neat P(3HB). This include mechanical properties, surface topography and biological performance. P(3HB)/oligo-PHA blend 90/10 exhibited the most suitable characteristics for coronary artery stent application. Therefore, this composition will be selected for further experiments.

Chapter 6

Development of radiopaque Poly(3-hydroxybutyrate)/oligo- PHAs composites

6. Introduction

Polyhydroxyalkanoates are natural origin biopolyesters, produced by various types of bacteria. They have been widely studied in order to be used in various fields, such as packaging, food industry, photography, medicine, drug delivery, chemical industry and coatings (Ali and Jamil, 2016; Kushwah *et al.*, 2016; Chen, 2012). PHAs represent a broad range of properties, which make them very attractive biomaterials for different applications. They can be mixed with other components to create blends, described in previous chapter. PHAs can be also used to produce materials, named as composites. A composite contains a matrix, usually polymeric in nature and different kind of fillers, such as fibres, inorganic salts, bioglass and ceramics, cellulose, beer spent grains and empty fruit bunches from oil palm. (Chiulan *et al.*, 2016; Cunha *et al.*, 2015; Khan *et al.*, 2014; Pardo-Ibanez *et al.*, 2014; Misra *et al.*, 2006). The main role of fillers is to improve the mechanical properties, such as tensile strength and Young's modulus of the base material by reinforcement or to improve functionality of the material, such as additional value to the compatibility or radiopaque properties, by acting as a contrast agent. Composites can be produced by various techniques, such as a solvent casting, melt extrusion, hot pressing, cross-linking and melt-blending (De Arenaza *et al.*, 2015).

Radiopacity is a property exhibited by some of the materials, which allows them to be visible under X-ray. These materials are able to absorb X-rays and occur white on radiographs (Hunter and Taljanovic, 2003). Chemical elements with high density and high atomic number exhibit higher radiopacity. Hence, those materials have been used as markers for coronary stents made from Fe, Cr, Co, Ni and their alloys (Dobranszky *et al.*, 2014). Several markers have been used in coronary stents in order to improve x-ray absorption and allow surgeons more efficient stent deployment, follow-up monitoring or stent dislocation (Kutryk *et al.*, 2000; Fischell, 2000). Markers can be made from gold, platinum, silver, niobium, tantalum, zirconium, tungsten and hafnium (Fulkerson *et al.*, 2004; Lam *et al.*, 1998) and manufactured using various techniques, such as crimping, extrusion, laser micro-welding or braiding (Paszenda, 2010). They can have different shapes, such as rings or discs, and are usually located on the proximal and distal ends of

the stent struts (Scott *et al.*, 2004). Some of radiopaque markers, like for example tantalum have been studied as powder and be integrated within stent (Nagy *et al.*, 2014). Several studies confirmed significant increase of visibility of the stent containing markers in comparison to neat metallic stents (Nagy, 2014; Wiskirchen *et al.*, 2004; Wiskirchen *et al.*, 2003). Polymeric materials are not radiopaque in nature. Hence, addition of radiopaque agents is required in order to be able to be implanted within the artery. Commercially available, polymeric biodegradable stent, named Absorb (Abott Vascular, US) has four platinum beads incorporated: two at the proximal and two at distal end of the scaffold (Rzeszutko, 2013).

Barium sulphate is one of the radiopacifiers, which are able to absorb X-ray and has been used in biomedical applications. Different salts or oxides of heavy metals can be used, such as bismuth, barium, tantalum or tungsten (Chen *et al.*, 2014). However, at the moment, barium sulphate is a commonly used for biomedical applications (Meagher *et al.*, 2013). Application of BaSO₄ allows surgeons correct implant insertion and monitoring over time (Ricker *et al.*, 2008). Barium sulphate have been used already with various materials such as polylactic acid, polyurethanes, polymethylmethacrylate and polypropylene (Baleani and Viceconti, 2010; Kurtz *et al.*, 2005).

The main aim of this part of the project was to develop radiopaque P(3HB)-based materials using barium sulphate for development of medical devices, such as coronary stents. One of the P(3HB)/oligo-PHAs blend in ratio 90/10 was selected for composites preparation. Three different concentrations of barium sulphate were investigated as an additive to create radiopaque composites. Materials were fully characterized in order to evaluate the thermal and mechanical properties. *In vitro* biocompatibility of the composites was tested with human dermal microvascular endothelial cells (HMEC-1) to evaluate the potential of new biodegradable material in applications such as coronary artery stent. Haemocompatibility studies were carried out in order to study the impact of the composite materials on blood cells. Additionally, microCT measurements were performed to study the potential application of barium sulphate as a contrast agent for coronary stents.

6.1. Development of Poly(3-hydroxybutyrate)/oligo-PHAs radiopaque composites

Three types of P(3HB)/oligo-PHA in ratio 90/10 composites with 1 wt%, 3 wt% and 5 wt% barium sulphate (Figure 54) were prepared as described in section 2.10. and fully characterised. P(3HB) was blended with oligo-PHA in the ratio 90/10 and mixed with BaSO_4 to obtain radiopacity and be suitable for coronary stent application. The thermal and mechanical properties of P(3HB)/radiopaque composites were studied using films prepared by solvent casting during 7 weeks of storage at ambient temperature. The mechanical properties of the composites, such as the tensile strength, Young's Modulus and elongation at break were measured at four time points (week 1, 3, 5, 7).

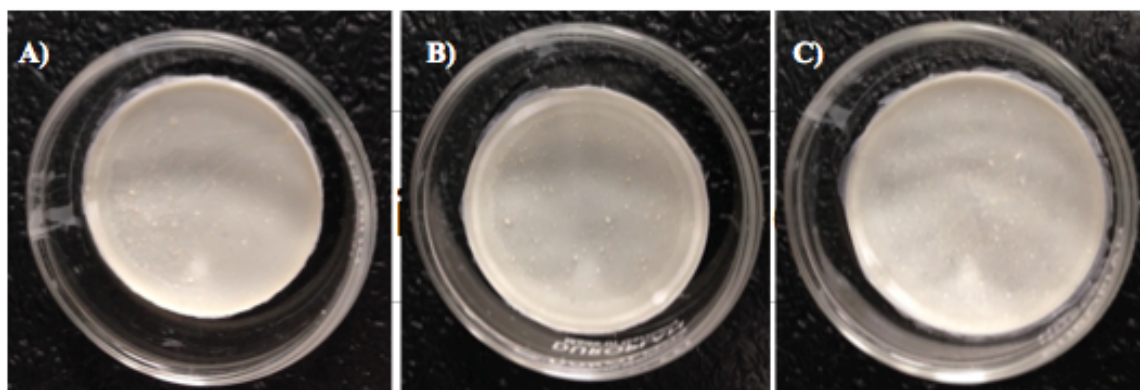


Figure 54: Composite solvent cast films of P(3HB)/oligo-PHA in ratio 90/10 with (A) 1 wt%, (B) 3 wt%, (C) 5 wt% of barium sulphate. Film diameter: 60mm.

6.2. P(3HB)/oligo-PHA composite characterisation

Solvent cast composite films were characterised with respect to their thermal, mechanical and topographical properties. Additionally, biocompatibility and haemocompatibility studies were performed in order to confirm non-toxicity and safety of the biomaterials.

6.2.1. Attenuated Total Reflectance Fourier Transform Infrared Spectroscopy (ATR/FT-IR)

Preliminary characterisation of the P(3HB)/oligo-PHA composites with barium sulphate was carried out using ATR/FTIR. FTIR spectra (Figure 55) revealed absorption bands centred in the region $1131.4\text{--}1043.7\text{ cm}^{-1}$ with a shoulder at 978.5 cm^{-1} , corresponding

to the symmetrical vibration of sulphate group ($-\text{SO}_4^{2-}$). Two absorption peaks at: 625cm^{-1} and 606cm^{-1} , corresponded to the out of plane bending vibration of sulphate (Ramaswamy *et al.*, 2011; Shen *et al.*, 2007).

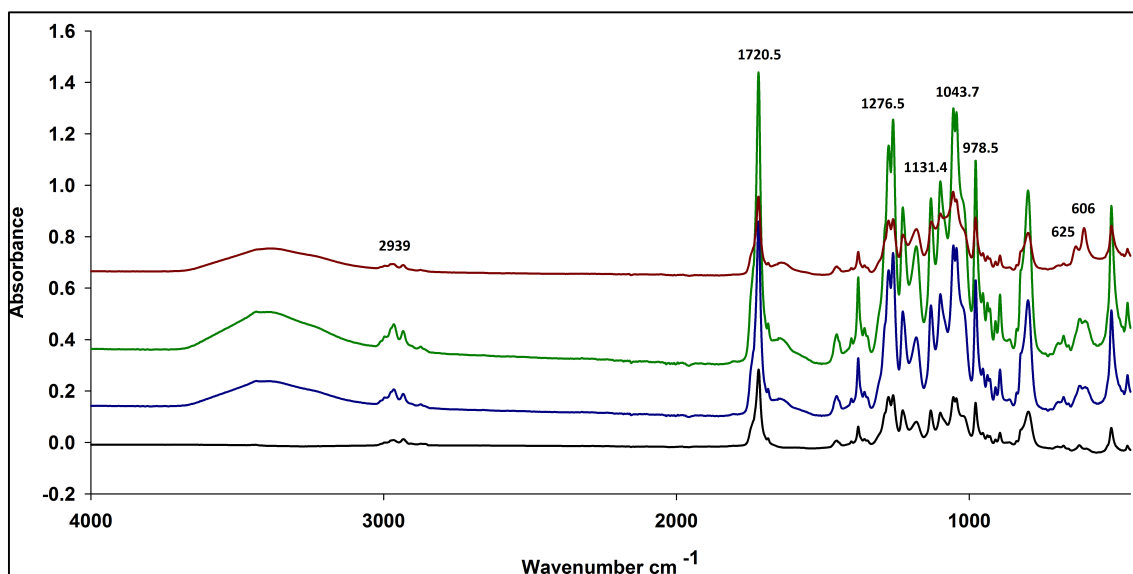


Figure 55: ATR-FTIR spectrum of the P(3HB)/oligo-PHA composites with barium sulphate. (—) P(3HB)/oligo-mcl-PHA 90/10 blend without barium sulphate, (—) composite film containing 1% barium sulphate, (—) composite film containing 3% barium sulphate, (—) composite film containing 5% barium sulphate indicating characteristic peaks for PHAs and SO_4^{2-} .

FTIR-ATR analysis of the composites revealed absorption bands at 1720.5 cm^{-1} and 1276.5 cm^{-1} corresponding to the ester carbonyl group and the $-\text{CH}$ group, respectively. Obtained values are typical to scl-PHAs, as described in the section 3.3.1. The weak absorption bands at 2938cm^{-1} , 2991cm^{-1} and 2939 cm^{-1} could be assigned to the aliphatic C-H group of the pendant alkyl group found in mcl-PHAs. The peak, observed at 1182 cm^{-1} corresponded to the $-\text{CO}$ stretching group, characteristic of mcl-PHAs as described in the section 4.4.1.

FTIR analysis of the PHA based composites with barium sulphate confirmed the presence of chemical bonds, which belongs to scl-PHAs, mcl-PHAs and sulphate anions from BaSO_4 .

6.2.2. Thermal properties of the composites of P(3HB)/oligo-PHA blends with barium sulphate after 7 weeks of storage at room temperature

The thermal properties of the P(3HB)/oligo-PHA composites during 7 weeks of storage were analysed by DSC. The summary of the results obtained is presented in Table 24 and Figure 56.

Table 24: Summary of the thermal properties of the P(3HB)/oligo-PHA composites with 1,3 and 5 wt% barium sulphate during 7 weeks of storage. T_m = melting temperature, T_g = glass transition temperature, T_c = crystallisation temperature, ΔH_f =enthalpy of fusion.

Time of storage (week)	Concentration of Barium sulphate	T_g (°C)	T_m (°C)	ΔH_f (J/g)	T_c (°C)
1	1 wt%	-11.6	171.3±1.1	88.1±8.5	53
	3 wt%	-4.2	168.2±0.3	74.3±1.9	53.8
	5 wt%	-8.4	167.5±1.9	75.5±3.5	45.9
3	1 wt%	-2.9	169.2±1.6	87.3±1.1	52.5
	3 wt%	-4.3	168.8±2.0	81.0±4.2	53.9
	5 wt%	-2.5	170.4±1.5	77.2±4.3	52.9
5	1 wt%	-2.2	169.7±1.9	82.7±2.1	55.3
	3 wt%	-2.1	169.8±1.6	83.9±0.9	58.3
	5 wt%	-2.6	170±1.9	78.9±0.8	56.8
7	1 wt%	-3.2	169.1±1.5	84.2±3.02	53.8
	3 wt%	-3.3	169.1±2.1	85.5±3.5	55.2
	5 wt%	-4.1	168.3±1.6	80.9±2.3	51

Addition of barium sulphate affects the thermal properties of the composites (Table 24 and Figure 56). With the increase of the concentration of barium sulphate, T_m , T_c and ΔH_f values decreased.

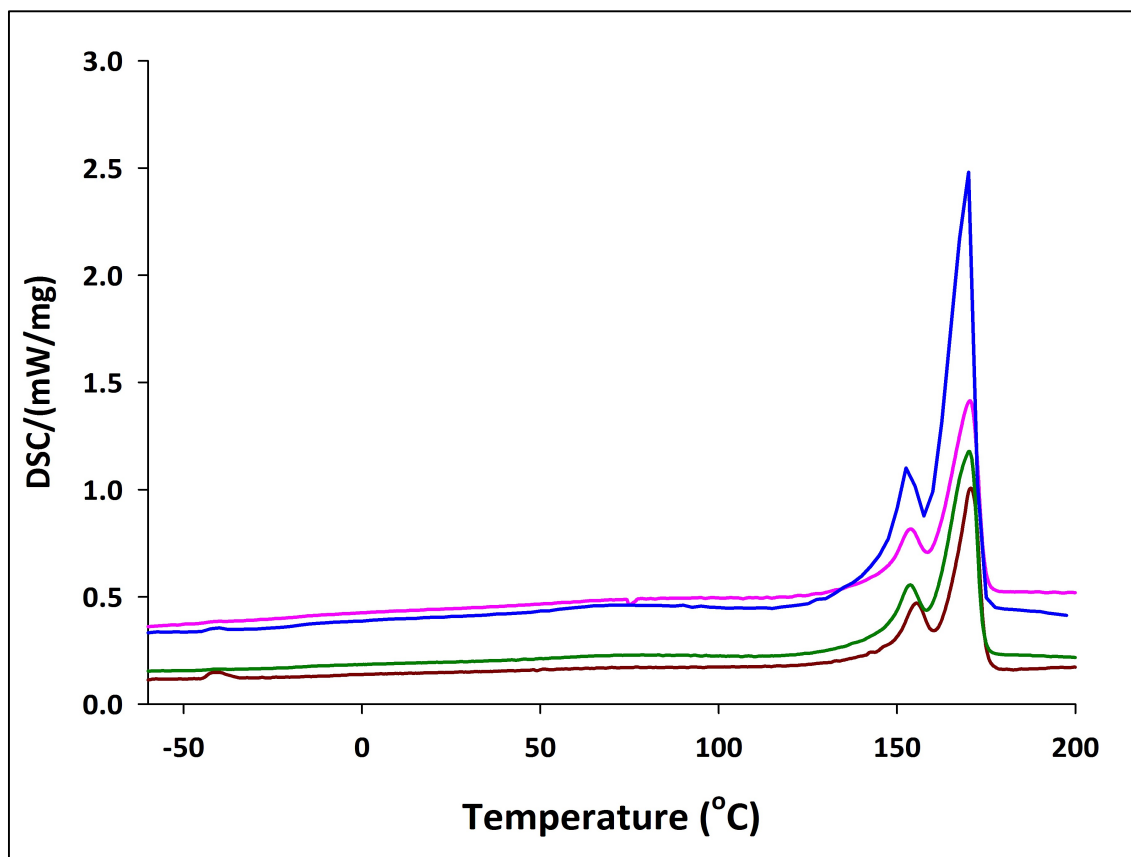


Figure 56: DSC thermograms of P(3HB)/oligo-PHA blend in the ratio 90/10 and composite films with addition of 1%, 3% and 5 wt% of BaSO₄ stored for 7 weeks at room temperature. (—) 0 wt% barium sulphate film, (—) 1 wt% barium sulphate composite film, (—) 3 wt% barium sulphate composite film, (—) 5 wt% barium sulphate composite film indicating melting peaks.

The glass transition temperature for all compositions of P(3HB)/oligo-PHA have changed during 7 weeks of storage. The cold crystallisation temperature remained stable for 1 and 3 wt% and has increased (from 45.9 to 52.9°C) for 5 wt% concentrations of barium sulphate within 3 weeks. After 3 weeks, no changes in T_c values were observed. The T_m value decreased for 1 wt% barium sulphate concentration as compared to the neat blend was observed at similar temperatures for 3 wt% barium sulphate and increased in the sample with 5 wt%. ΔH_f decreased for composite with 1 wt%, remain the same for 3 wt% of barium sulphate and increased for 5 wt% of barium sulphate in comparison to P(3HB)/oligo-PHA without barium sulphate.

6.2.3. Mechanical properties of the composites of P(3HB)/oligo-PHA blend in ratio 90/10 with barium sulphate after 7 weeks of storage at room temperature

Mechanical properties of the solvent cast composite films with addition of 1, 3, 5 wt% barium sulphate were carried out for 7 weeks, in order to check the effect of the addition of the radiopaque agent on the mechanical properties of the material. The results obtained summarised in Table 25 and Figure 57.

Table 25: Summary of the mechanical properties of the P(3HB)/oligo-PHA composites with 1,3 and 5 wt% barium sulphate during 7 weeks of storage at room temperature (n=3).

Time of storage (week)	Concentration of Barium sulphate	Tensile test (MPa)	Young's Modulus (MPa)	Elongation at break (% strain)
1	1 wt%	12.9±1.3	520±60	14.2±0.2
	3 wt%	11.2±0.4	430±120	9.1±0.3
	5 wt%	13.1±1.9	680±140	7.9±1.1
3	1 wt%	18.2±0.9	1310±50	8.4±0.4
	3 wt%	18.1±0.9	1250±30	7.9±1.7
	5 wt%	18.5±3.2	1230±70	4.7±0.1
5	1 wt%	17.1±1.5	1160±140	4.3±0.7
	3 wt%	17.1±0.8	1250±7	4.5±0.1
	5 wt%	16.0±0.6	1070±280	4.3±0.1
7	1 wt%	16.2±2.1	1020±100	4.4±0.8
	3 wt%	14.6±1.3	920±80	4.9±0.6
	5 wt%	14.1±0.3	1110±70	4.3±0.5

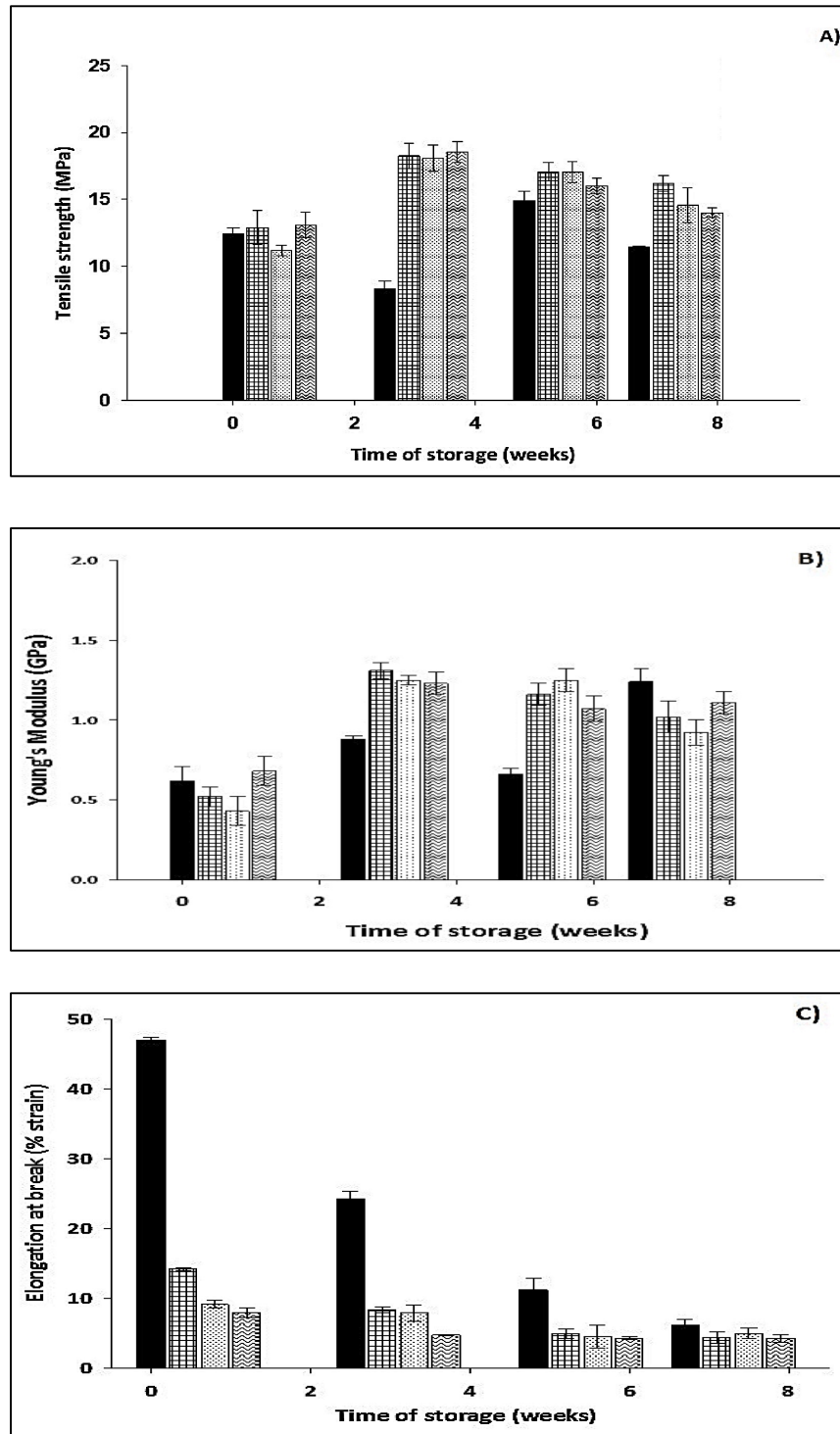


Figure 57: Changes in the ultimate tensile strength (A), Young’s modulus (B) and elongation at break (C), during storage of neat P(3HB)/oligo-PHA blend and its composites with BaSO₄ for 7 weeks at room temperature. (■) 0% barium sulphate film, (▣) 1% barium sulphate composite film, (▤) 3% barium sulphate composite film, (▥) 5% barium sulphate composite film.

After 3 weeks of ageing, the mechanical properties of the P(3HB)/oligo-PHAs composite films with barium sulphate had changed. For the composite with addition of 1 wt% barium sulphate, elongation at break decreased after 7 weeks of storage from $14.2 \pm 0.2\%$ to $4.3 \pm 0.2\%$. Young's modulus increased significantly from 0.5 ± 0.1 MPa to 1250 ± 7 MPa. Tensile strength increased after 7 weeks from 12.9 ± 1.3 MPa to 16.2 ± 2.1 MPa. Addition of barium sulphate in 3 wt% to the P(3HB)/oligo-PHAs blend in the ratio 90/10 resulted in decrease of the elongation at break after 7 weeks of storage from $9.9 \pm 6.1\%$ to $4.9 \pm 1.6\%$. Young's modulus increased from 0.4 ± 0.1 MPa to 0.9 ± 0.1 GPa. The tensile strength increased after 7 weeks from 11.2 ± 0.4 MPa to 14.6 ± 1.3 MPa. For the composition with the addition of 5 wt% barium sulphate, elongation at break decreased after 3 weeks of storage from $7.9 \pm 6.1\%$ to $4.3 \pm 0.5\%$. Young's modulus value increased from 0.7 ± 0.1 MPa to 1.1 ± 0.1 GPa. Tensile strength increased after 7 weeks from 13.1 ± 1.9 MPa to 14.1 ± 0.3 MPa. The results obtained suggest that addition of barium sulphate in all three compositions resulted in an increase of the tensile strength and Young's modulus in comparison to the P(3HB)/oligo-PHAs blend. An increase of the concentration of the barium sulphate within the blend improved the material strength and stiffness. Addition of barium sulphate resulted in a decrease of the elongation at break, hence, the material became more brittle. The minimum amount of barium sulphate required in order to obtain sufficient material radiopacity needs to be confirmed in future work.

6.3. Surface analysis

6.3.1. Scanning Electron Microscopy (SEM)

SEM and laser profilometry were used to examine the topography of polymer films. As can be seen from SEM images presented in Figure 58, P(3HB)/oligo-PHA 90/10 solvent cast film with an addition of BaSO_4 had similar surface topography and demonstrated visible irregularities with various protuberances in comparison to neat P(3HB) film, which appeared to be smoother and even.

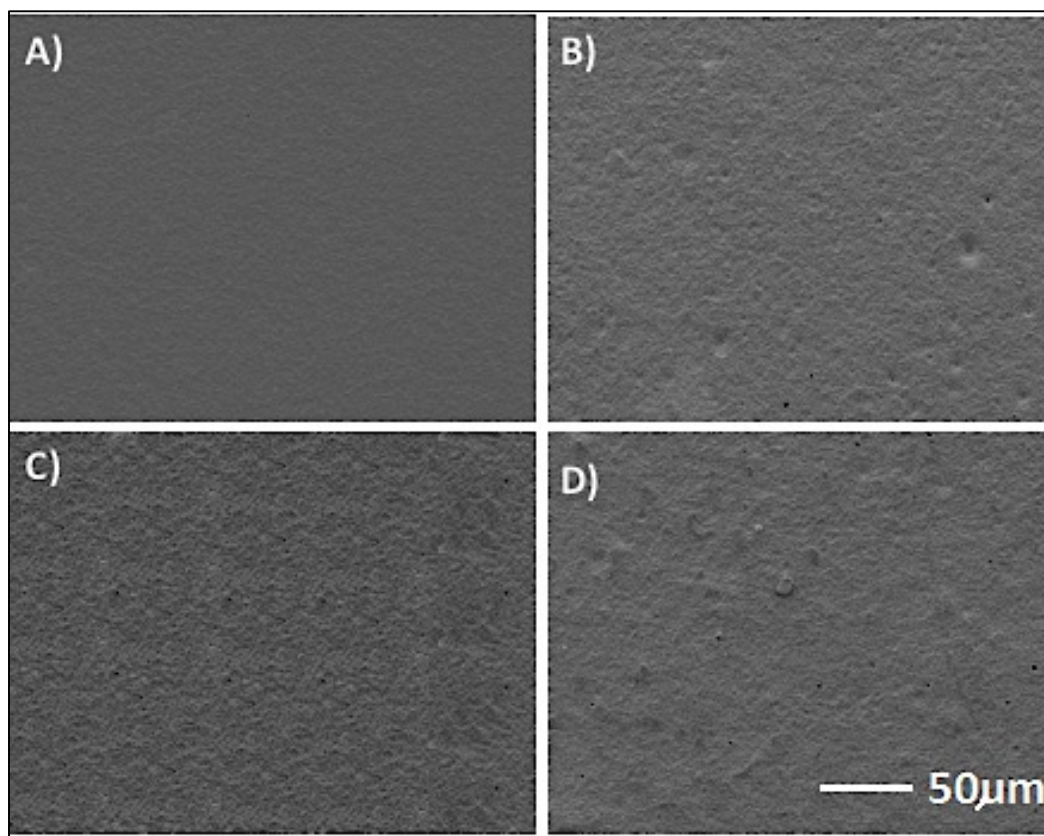


Figure 58: SEM micrographs of the surface of (A) P(3HB)/oligo-PHA blend without addition of barium sulphate, P(3HB)/oligo-PHA composite with addition of (B) 1wt%, (C) 3wt% and (D) 5wt% of barium sulphate.

The surface of composite films appeared to have a rougher surface than P(3HB)/oligo-PHA blend. The surface roughness measurements were carried out to confirm the SEM data.

6.3.2. Surface roughness analysis

Composites roughness was characterised quantitatively as the root mean square roughness (R_q) using laser profilometry (Figure 59). The roughness of the P(3HB)/oligo-PHA in the ratio 90/10 was $0.9 \pm 0.04 \mu\text{m}$. With an increase in the content of BaSO_4 in the composites the surface roughness increased from $1.1 \pm 0.02 \mu\text{m}$ for 1 wt% BaSO_4 to $1.6 \pm 0.06 \mu\text{m}$ for 5 wt% BaSO_4 concentration. Surface roughness value of composite with the highest amount of BaSO_4 (5 wt%) was significantly higher than the neat P(3HB)/oligo-PHA blend.

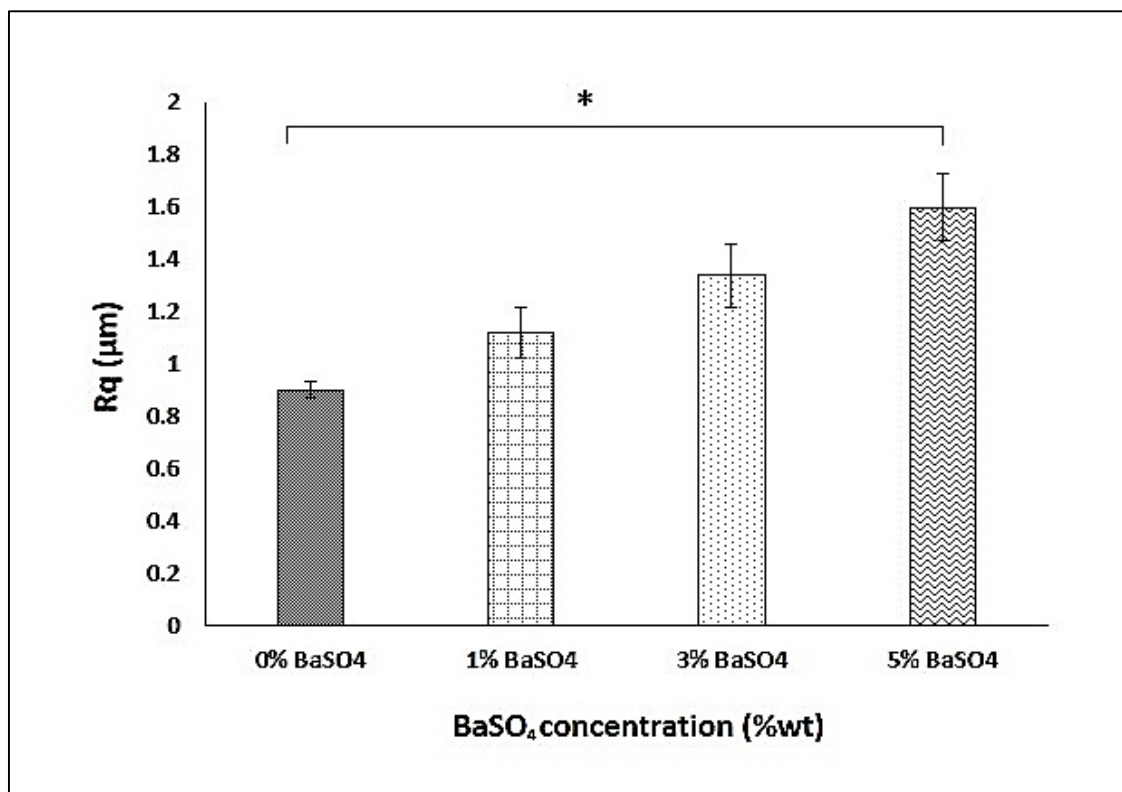


Figure 59: Surface roughness of P(3HB)/oligo-PHA blend (90/10) and composites with BaSO₄ (n=3; error bars=±SD). The data were compared with P(3HB)/oligo-PHA 90/10 blend film without addition of barium sulphate using ANOVA. * indicates $p < 0.05$.

Results obtained from surface roughness measurements confirmed further the SEM findings. The surface of the all composite samples resulted with root mean square (R_q) value greater than 1. SEM images of the surface topography for P(3HB)/oligo-PHAs with an addition of BaSO₄ composites demonstrated rough surfaces. With an increase in surface roughness with the concentration of BaSO₄ the difference was significant for composition with the 5 wt% BaSO₄ in comparison to the neat P(3HB)/oligo-PHA blend film. Higher surface roughness of the P(3HB)/oligo-PHA composites with an increase concentration of barium sulphate might have an impact on biocompatibility of the composite materials.

6.3.3. Contact angle measurement

Static contact angle study was performed to measure the hydrophobicity of the solvent cast P(3HB)/oligo-PHAs composites samples. The results of the water contact angle measurements have been summarised in Figure 60.

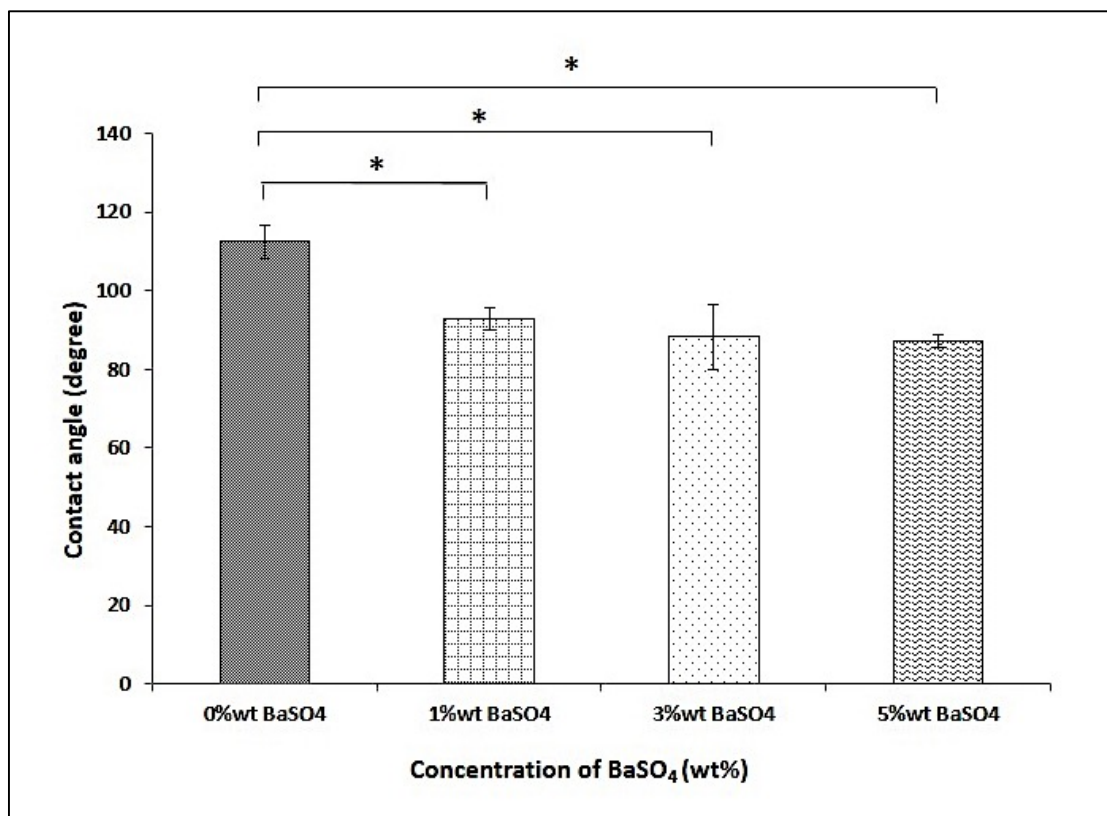


Figure 60: Static water contact angle measurements of the P(3HB)/oligo-PHA in ratio 90/10 films (n=3) with different concentrations of barium sulphate (n=3; error bars=±SD). The data were compared with P(3HB)/oligo-PHA 90/10 blend film without addition of barium sulphate using ANOVA. * indicates $p < 0.05$.

Obtained results demonstrated that the water contact angle was higher than 70 degrees in all tested materials, therefore materials were hydrophobic in nature. Addition of barium sulphate decreased the value of water contact angle, hence the related hydrophobicity. Neat blend of P(3HB)/oligo-PHAs has contact angle value 112.5 ± 4.3 degrees, whereas addition of 5% BaSO₄ reduced static contact angle values to 87.2 ± 1.5 degrees. The results obtained of the water contact angle were significantly lower for the composites in comparison to the P(3HB)/oligo-PHAs blend in ratio 90/10. Although, contact angle values for P(3HB)/oligo-PHA composites demonstrated lower values, materials are still considered as hydrophobic. However, it will be interesting to observe the reaction of endothelial cells to the surface of P(3HB)/oligo-PHA composite materials during biocompatibility study.

6.3.4. Protein adsorption on the surface of the composites containing barium sulphate

The affinity of the materials towards proteins were evaluated by using the bicinchoninic acid assay as described in section 2.11.3.9. It was found that total protein adsorption was 145 ± 3.5 , 156.4 ± 4.6 , 173 ± 14 and 175.4 ± 4.6 $\mu\text{g}/\text{cm}^2$ for the neat P(3HB)/oligo-PHA 90/10 blend film and P(3HB)/oligo-PHA composites with an addition of 1 wt%, 3 wt%, 5 wt% BaSO_4 respectively (Figure 61). There was a significant difference between all tested composites in comparison to the tissue culture plastic (* $p=0.011$, * $p=0.0206$ and ** $p=0.0079$ respectively) (Figure 61).

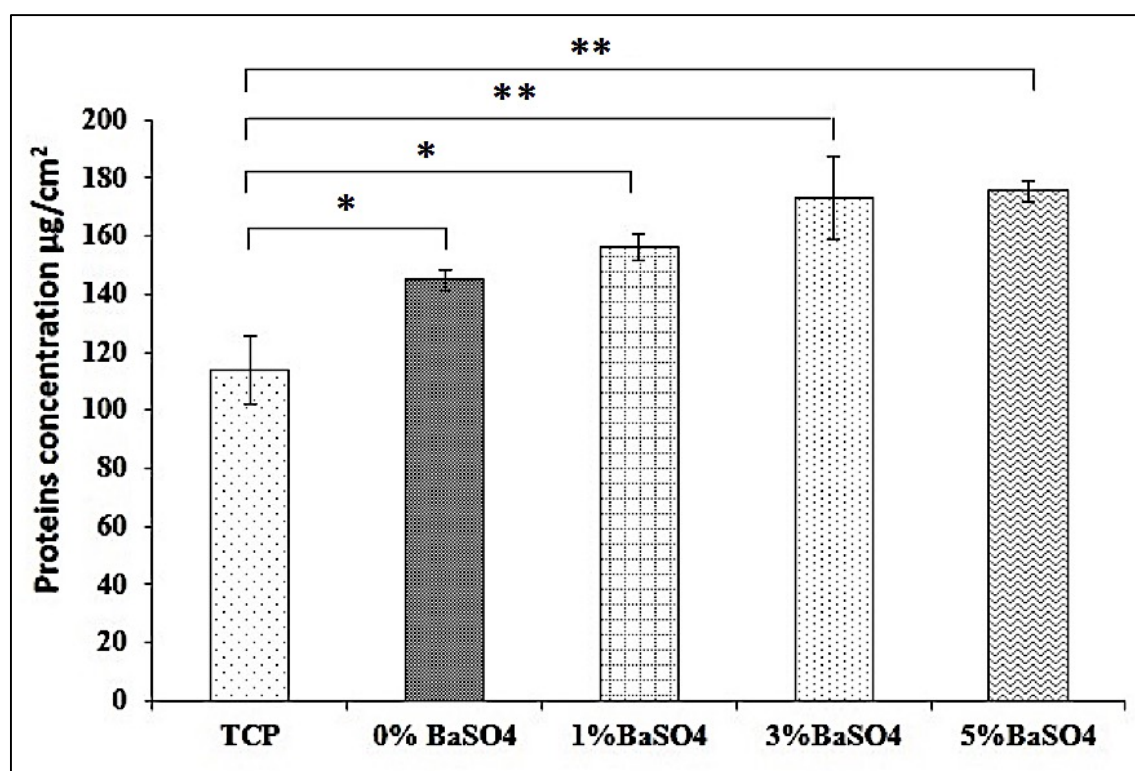


Figure 61: Protein adsorption to the composites measured by BCA assay ($n=3$; error bars= \pm SD). The data were compared with standard tissue culture plastic using ANOVA. * indicates $p < 0.05$ and ** indicates $p < 0.005$.

Composites with barium sulphate were characterized with higher concentration of proteins adsorbed on the surface in comparison with TCP (positive control). The amount of proteins adsorbed on the TCP was 114.7 ± 11.7 $\mu\text{g}/\text{cm}^2$. All the composites exhibited higher protein adsorption than the control and the P(3HB)/oligo-PHA 90/10 blend.

6.3.5. XRD analysis

The effect of addition of barium sulphate on crystallinity of the materials as well as identification of presence of BaSO_4 was studied using X-ray diffraction, described previously in the Chapter 2, section 2.11.3.8. Summary of XRD patterns for P(3HB)/oligo-PHA blend with 0%, 1%, 3% and 5% barium sulphate are shown in the Figure 62.

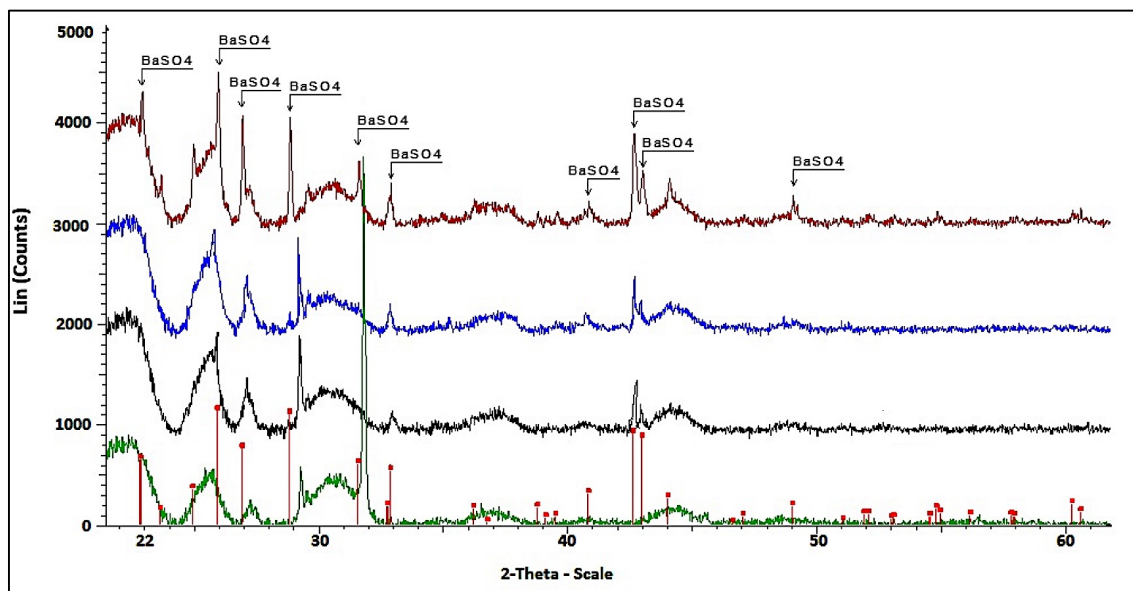


Figure 62: XRD patterns of P(3HB)/oligo-PHA 90/10 blend and composites with 1%, 3% and 5 wt% BaSO_4 . (—) P(3HB)/oligo-mcl-PHA 90/10 blend without barium sulphate, (▲) barium sulphate powder, (—) composite film containing 1% barium sulphate, (—) composite film containing 3% barium sulphate, (—) composite film containing 5% barium sulphate.

In the composite samples, there was an increased in the peak intensity with an increase of the BaSO_4 concentration. The intense peaks, such as 25° , 26° , 28° , 33° , 42.5° and 43° were characteristic of BaSO_4 and present in all concentrations of barium sulphate. The intensity of these peaks increased with increased concentration of BaSO_4 . Some peaks, such as 22.5° , 31.5° , 44° or 49° were much less intense and detected only in the composite sample with 5 wt% of BaSO_4 . None of these peaks were observed in the neat P(3HB)/oligo-PHA in 90/10 blend.

6.4. *In vitro* biocompatibility studies

Biocompatibility of the composite samples were investigated by cell viability studies and SEM imaging of the scaffolds.

6.4.1. MTT assay

MTT assay was used to evaluate cell adhesion and proliferation. Attachment and proliferation of the HMEC-1 cells on the film samples were studied over a period of 1, 3 and 7 days. The standard tissue culture plastic was used as the positive control for these experiments. The results of biocompatibility studies are presented in Figure 63.

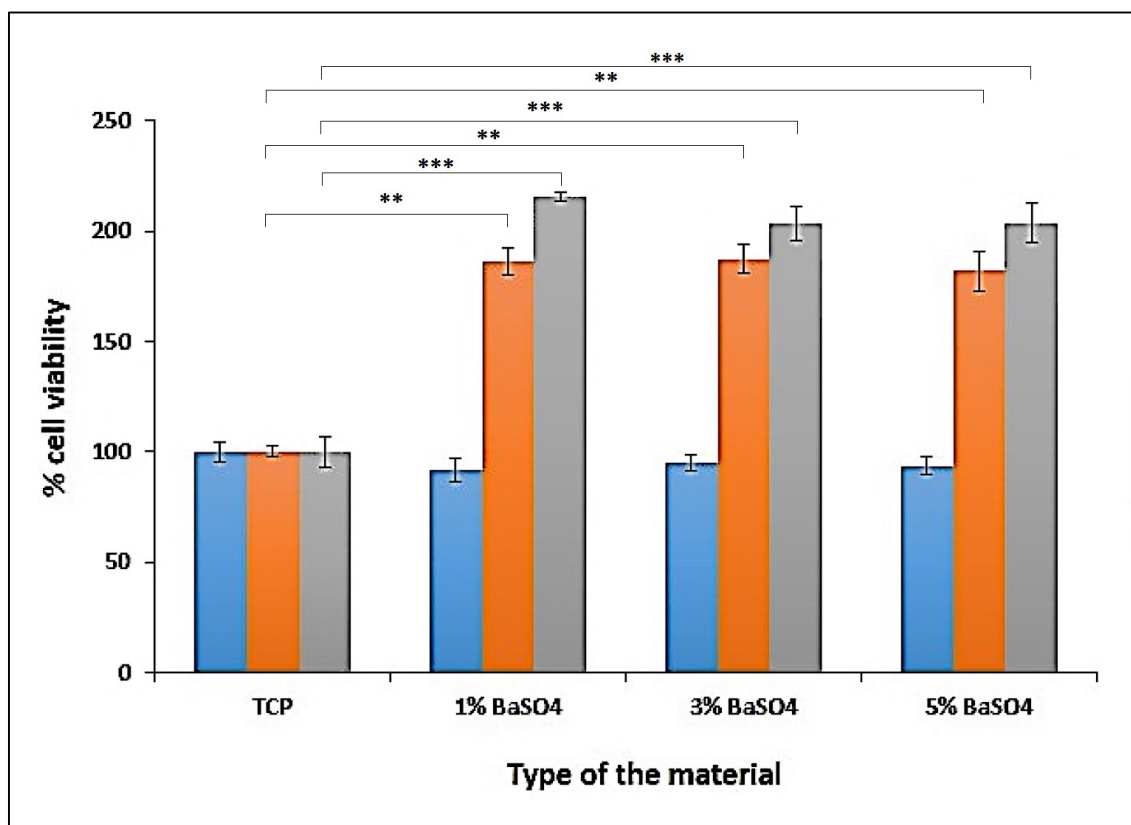


Figure 63: Cell proliferation study of the HMEC-1 cells on the P(3HB)/oligo-PHA composite film samples on day 1 (■), day 3 (■) and day 7 (■) (n=3; error bars=±SD). The results were compared with standard tissue culture plastic, which was normalised to 100% using ANOVA. * indicates $p < 0.05$, ** indicates $p < 0.005$ and *** indicates $p < 0.0005$.

Cell proliferation on the surface of composite films was slightly lower than TCP at day 1, but higher at day 3 and day 7. The observed cell viability on the composite film samples

with 1 wt% barium sulphate was $91.6 \pm 5.4\%$ on day 1, $186.4 \pm 6.0\%$ on day 3 and $215.5 \pm 2.0\%$ on day 7 as compared to that TCP. The differences were statistically significant for results from day 3 and 7 ($***p=0.0005$ and $**p=0.0013$ respectively). The growth of the HMEC-1 cells on the surface of 3 wt% BaSO₄ composite was $95.2 \pm 5.4\%$ on day 1 and $187.4 \pm 6.5\%$ and $203.5 \pm 8.0\%$ at day 3 and 7 respectively. The differences were statistically significant ($**p=0.0088$, $**p=0.0075$) in comparison to TCP on day 3 and 7. Similarly, HMEC-1 cell viability on films with 5 wt% BaSO₄ was lower at day 1 ($93.7 \pm 4.0\%$) and higher on day 3 and 7 in relation to TCP: $182.2 \pm 9.0\%$ and $203.6 \pm 4.5\%$ respectively. The differences were statistically significant in comparison to TCP at day 3 ($*p=0.0182$) and day 7 ($***p=0.0009$).

The results obtained demonstrated higher biocompatibility of all tested composite samples in comparison to TCP. However, the highest cell adhesion was observed for P(3HB)/oligo-PHA composite with 1 wt% BaSO₄ within 7-day period. The results obtained confirmed that all composites were non-cytotoxic.

6.4.2. SEM

Cell adhesion and proliferation was further characterised using SEM imaging. SEM images presented in Figure 64 revealed that HMEC-1 cells adhered and proliferated evenly across the surface. Cell density was comparable between the samples. The increase in cell adhesion and proliferation on the composites also matched the increasing surface roughness and protein absorption. All PHA-based materials supported HMEC-1 cell attachment and proliferation, hence demonstrating good biocompatibility. Addition of barium sulphate improved cell proliferation with the highest cell viability achieved for the composite with 1 wt% BaSO₄.

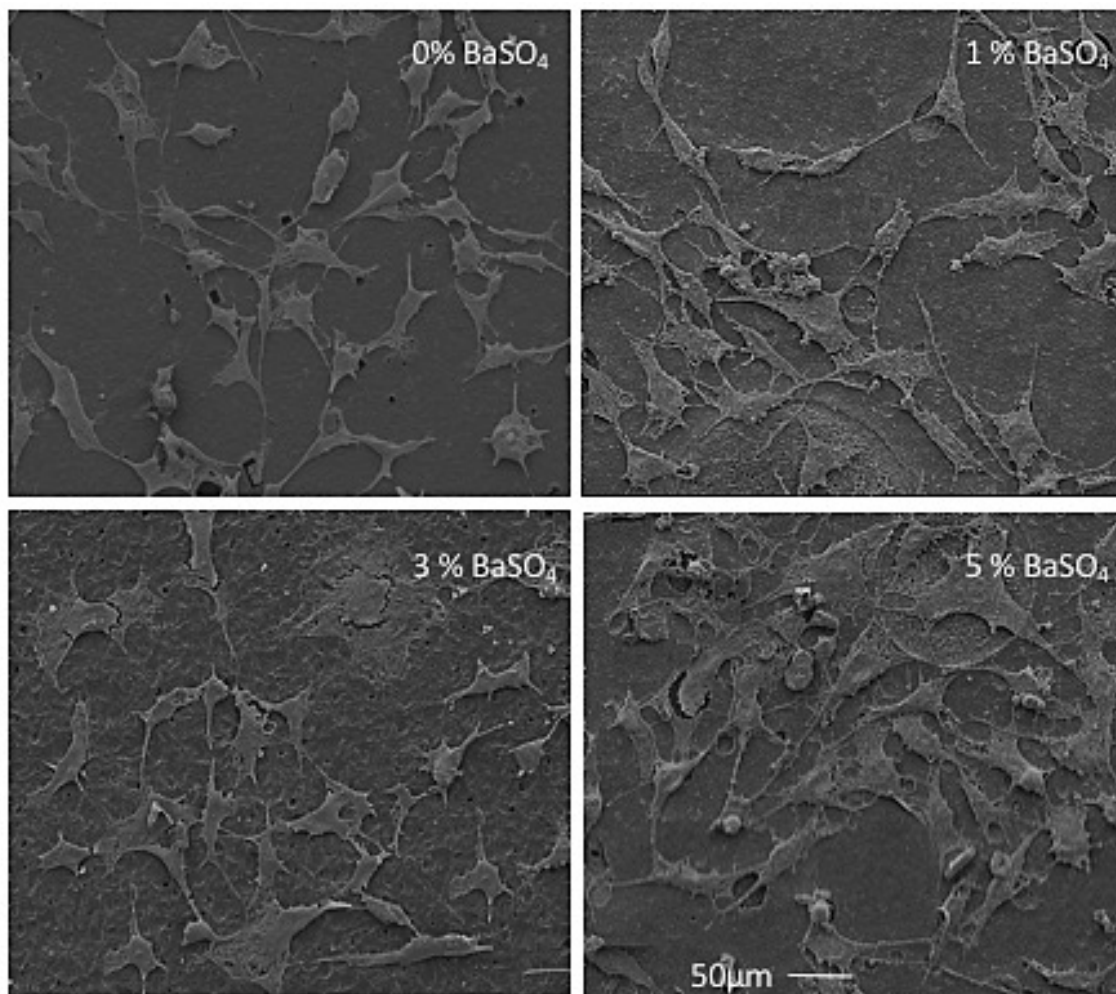


Figure 64: SEM images of the surfaces of P(3HB)/oligo-PHA blend 90/10 (A) and P(3HB)/oligo-PHA 90/10 composites with 1 wt% BaSO₄ (B), 3 wt% BaSO₄ (C) and 5 wt% BaSO₄ (D) after culturing HMEC-1 cells for 7 days.

With respect to the results obtained, composites of barium sulphate with P(3HB)/oligo-PHAs supported the growth of HMEC-1 cell line. Addition of barium sulphate did not inhibit cell attachment or proliferation.

6.4.3. Indirect cytotoxicity

The indirect cytotoxicity test was performed to investigate the influence of any substances released from the P(3HB)/oligo-PHA composite materials on the HMEC-1 cell line. Cells without an extract were used as negative control. 70% methanol instead of media or extract was used as a positive control. Endothelial cells were selected for this

study to mimic the environment present in the human body after stent implantation. This device would be in direct contact with the endothelium, therefore the HMEC-1 cell line, an endothelial cell line was chosen. The summary of the results obtained are shown in Figure 65.

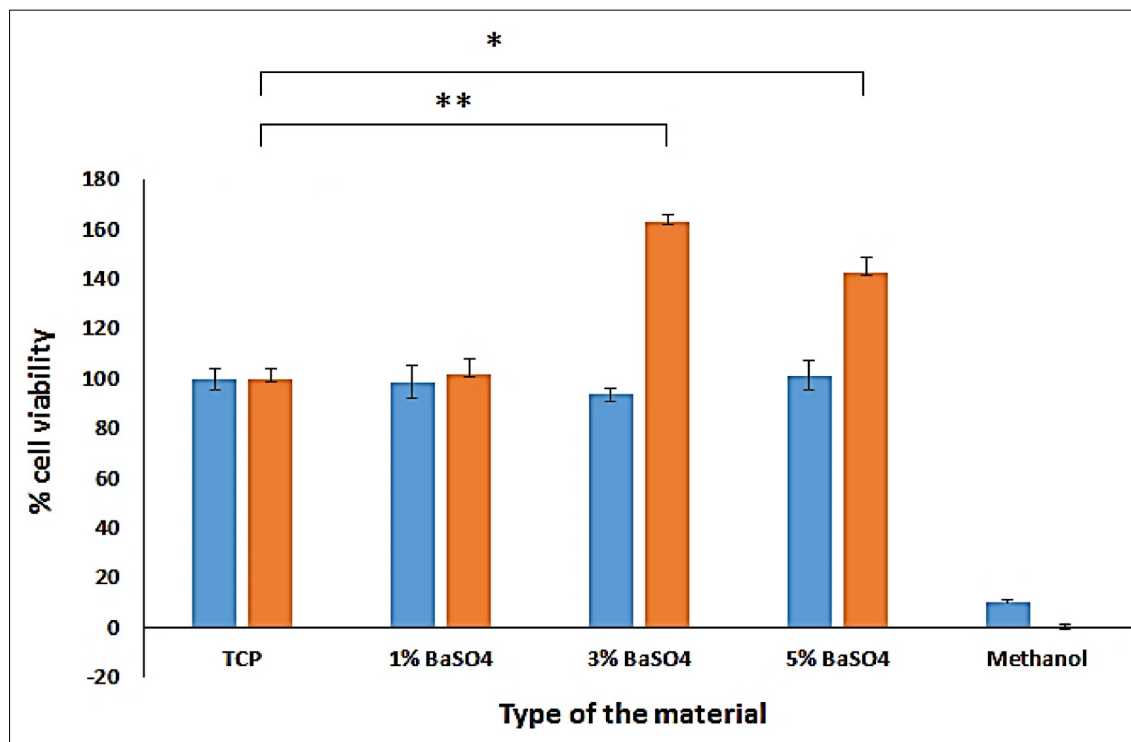


Figure 65: Indirect cytotoxicity study of the HMEC-1 cells on the P(3HB)/oligo-PHA composites film samples at day 1 (■) and day 3 (■) (n=3; error bars=±SD). The data were compared with standard tissue culture plastic, which was normalised to 100% using ANOVA. * indicates $p < 0.05$ and ** indicates $p < 0.005$.

Cell proliferation on the composite film samples with 1% barium sulphate was $98.7 \pm 6.7\%$ on day 1 and $101.4 \pm 8.4\%$ on day 3 compared to the TCP. The differences were not statistically significant. The growth of HMEC-1 cells on the composite film was similar on day 1 and 3 to TCP. The growth of the HMEC-1 cells on the surface of 3 wt% BaSO₄ composite was higher than TCP on day 3 (163 ± 8.9). The difference was statistically significant (** $p = 0.0079$). HMEC-1 cell viability on composite films with 5 wt% BaSO₄ was also higher on day 3 in relation to TCP: $142.6 \pm 4.8\%$. The difference was statistically significant in comparison to TCP on day 3 ($*p = 0.04$). The highest viability of the HMEC-1 cells was achieved after treatment with an extract from composite samples

with 3 wt% barium sulphate in comparison to TCP after 3 days of incubation (Figure 65). The results obtained confirmed an absence of any cytotoxic substances were released from the composite. Moreover, extracts obtained after incubation of composites containing 3 wt% and 5 wt % BaSO₄ supported the cells attachment and proliferation better than tissue culture plate. Therefore, PHA based composites with BaSO₄ can be strongly considered as potential materials for biomedical applications, such as coronary stents.

6.4.4. MicroCT scan of the composite samples

MicroCT scans were performed to investigate a radiopacity of the composites, containing barium sulphate. The images are presented in the Figure 66.

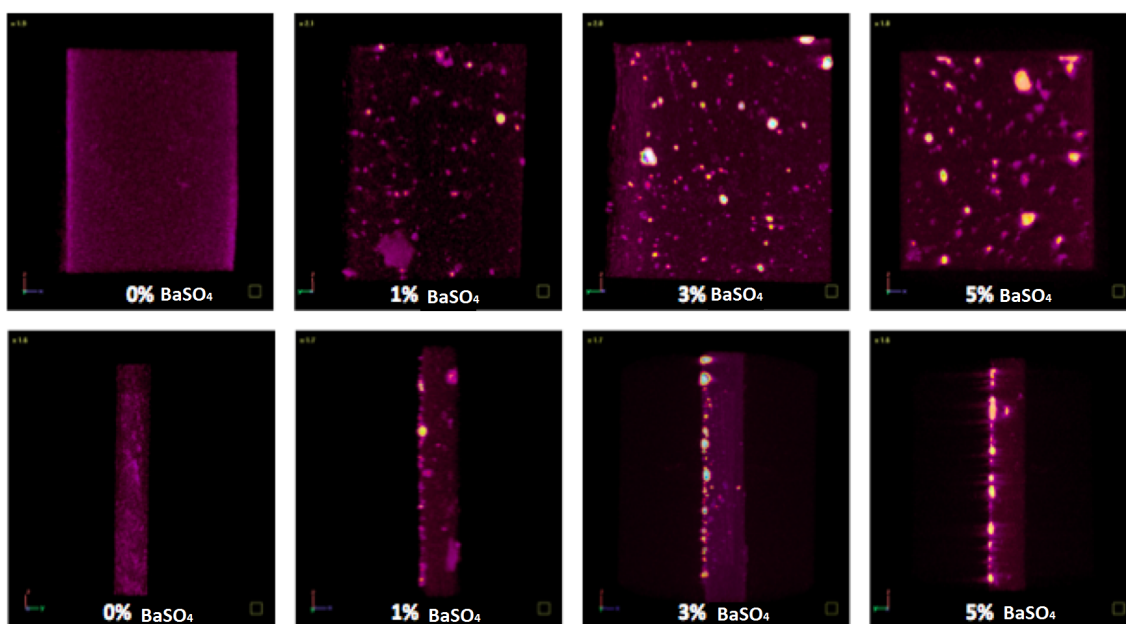


Figure 66: MicroCT micrographs demonstrated x-ray absorption by barium sulphate, presented in the concentrations (from the left to right): 0 wt%, 1 wt%, 3 wt% and 5 wt% in the PHAs based composites in comparison with a neat P(3HB)/oligo-PHA blend in ratio 90/10.

From the micrographs presented in the Figure 66 it is evident that the intensity of the signals is higher with an increased concentration of barium sulphate. The control sample, such as neat P(3HB)/oligo-PHAs 90/10 blend did not exhibited these signals as expected.

The results obtained suggest possibility of application of barium sulphate as a radiopaque agent for coronary stent application.

6.5. *In vitro* haemocompatibility studies

P(3HB) neat film and P(3HB)/oligo-PHA blends were subjected to haemocompatibility studies, which includes haemolysis studies, whole blood clotting as well as monocytes and neutrophils activation.

6.5.1. Haemolysis study

Haemolysis study was performed on P(3HB)/oligo-PHAs composites with barium sulphate to check an effect of the materials on the erythrocytes after direct contact with fresh whole blood. The analysis was performed as described in section 2.15.1. The results obtained are shown at the Figure 67.

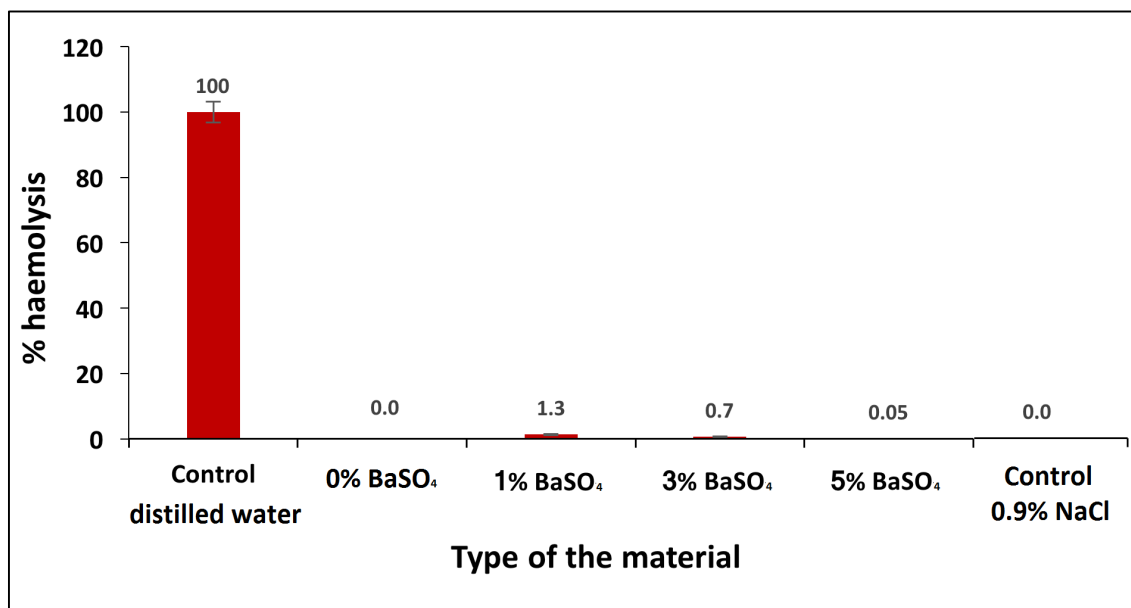


Figure 67: Haemolysis rates of the P(3HB)/oligo-PHA blend and composites with barium sulphate after 1h of incubation at 37°C (n = 3). All the film samples were compared to the control with 0.9% NaCl using ANOVA. No significant difference.

All tested PHA based materials confirmed the non-haemolytic effect on erythrocytes. The percent of haemolysis 1.3%, 0.7% and 0.05% was obtained for composites with 1 wt% BaSO₄, 3 wt% BaSO₄ and 5 wt% BaSO₄ respectively.

6.5.2. Whole blood clotting

Whole blood clotting experiments were performed to investigate the potential thrombogenicity of the materials as described previously in section 2.15.2. The summary of the results obtained after 30 and 90 minutes are demonstrated in Figure 68.

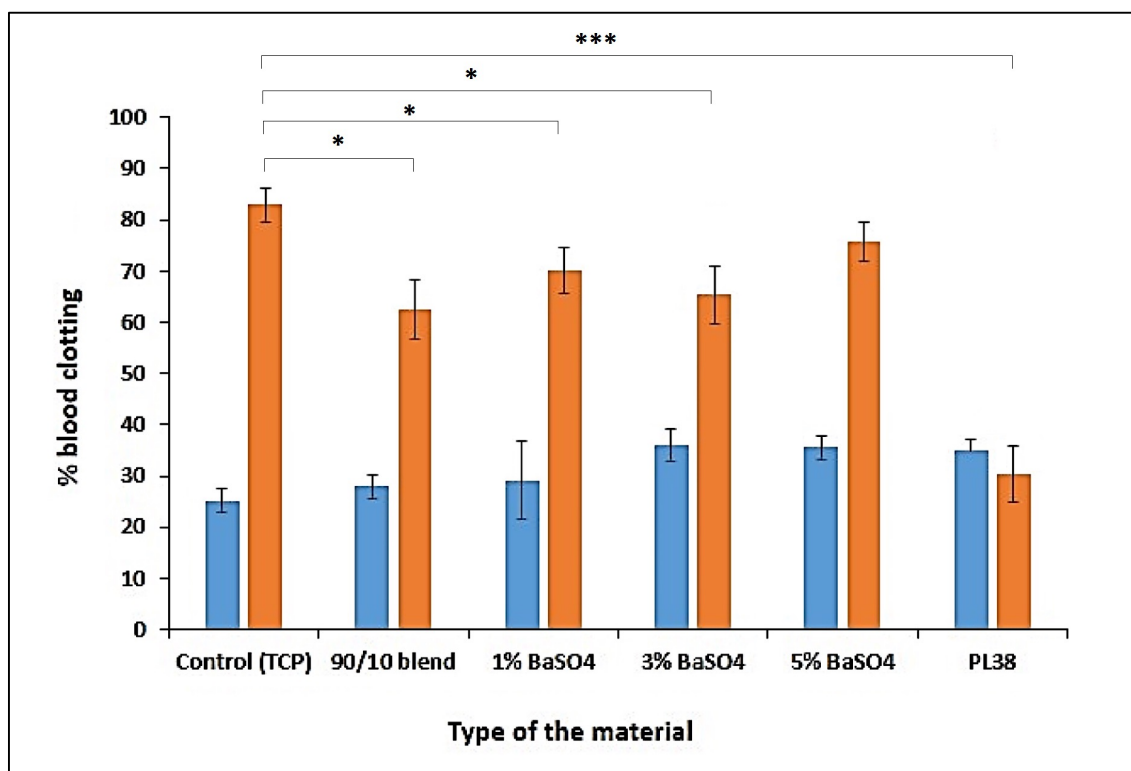


Figure 68: Whole blood clotting after 30 minutes (■) and 90 minutes (■) of incubation on the neat P(3HB)/oligo-PHA blend 90/10, composites with 1 wt%, 3 wt% and 5 wt% barium sulphate and PL38 (n=3; error bars=±SD). The data were compared with standard tissue culture plastic using ANOVA. *indicates $p < 0.05$ and *** indicates $p < 0.0005$.

The results obtained indicated that all tested materials enhanced the activation of the coagulation cascade. After 30 minutes of incubation, composite with 1% barium sulphate demonstrated $29.2 \pm 2.6\%$ blood clotting. Addition of BaSO₄ at level 3 wt% resulted in an increased % blood clotting after 30 minutes to $36.0 \pm 3.1\%$, which was significantly higher blood clotting rate than positive control $25.2 \pm 0.2\%$ (* $p=0.014$). P(3HB)/oligo-PHA composite with 5 wt% barium sulphate showed blood clotting rate $35.5 \pm 2.3\%$ after 30 minutes. With the increase of time, the % blood clot increased in all tested materials as well as in positive control. After 90 minutes the blood control demonstrated $82.9 \pm 3.3\%$ blood clotting. P(3HB)/oligo-PHA composites with 1 wt%, 3

wt% and 5 wt% of barium sulphate resulted with blood clotting rate: 69.9±4.4%, 65.7±5.7% and 75.7±3.7% respectively. The results obtained for composites with 1 wt% and 3 wt% barium sulphate were considered as significantly lower than positive control (*p=0.026 and *p=0.036). There was no difference between TCP and composite sample with 5% BaSO₄. Addition of barium sulphate resulted in higher blood clot rate formation than neat blend. However, the results obtained were lower than positive control. To summarise, composites of P(3HB)/oligo-PHA with barium sulphate did not demonstrate increased risk of thrombogenicity and can be consider as a biomaterial for medical applications, such as coronary stent.

6.5.3. Monocytes and neutrophils activity in the P(3HB)/oligo-PHAs composites

P(3HB)/oligo-PHAs composites with different amounts of barium sulphate were incubated with whole blood at 37°C overnight and stained with the markers listed in the section 2.15.3.1. Summary of the results obtained in the Table 26.

Table 26: Summary of median fluorescence intensity (MFI) obtained after incubation of fresh whole blood incubated with P(3HB)/oligo-PHA blend 90/10, P(3HB)/oligo-PHA composites with 1% wt, 3% wt and 5% wt barium sulphate and PL38; stained with specific markers in order to evaluate monocyte and neutrophil activity.

Sample	Markers	Monocytes Activity (MFI)	Percentage change (%)	Neutrophils Activity (MFI)	Percentage change (%)
P(3HB)/oligo-PHAs 90/10 blend	CD86-PE	217.4	89.2	162.6	3.5
	CD45-PerCP	135.9	24.2	117.8	0.17
	CD11b-PE	576.4	324.1	797.9	466.2
	CD66B-FITC	311.97	53.9	175.1	7.5
P(3HB)/oligo-PHAs 90/10 composite	CD86-PE	151.5	31.8	117.6	-
	CD45-PerCP	86.5	-	88.1	-

with 1 wt% BaSO ₄	CD11b-PE	769.7	466.4	955.2	577.9
	CD66B-FITC	117.6	-	113.5	-
P(3HB)/oligo-PHAs 90/10 composite with 3 wt% BaSO ₄	CD86-PE	135.9	18.3	116.7	-
	CD45-PerCP	82.1	-	86.8	-
	CD11b-PE	991.2	629.3	1187.7	742.9
	CD66B-FITC	105.6	-	175.1	7.5
P(3HB)/oligo-PHAs 90/10 composite with 5 wt% BaSO ₄	CD86-PE	126.4	10.0	136.9	-
	CD45-PerCP	121.9	11.4	94.7	-
	CD11b-PE	991.2	629.3	1027.5	629.2
	CD66B-FITC	121.9	-	157.2	-

Results obtained after staining blood samples, which were exposed to various polymer samples demonstrated different levels of activity of monocytes as well as neutrophils. All tested samples containing BaSO₄ presented elevated activity in the marker CD11b-PE. The percentage change of MFI in the composites increased with larger amounts of barium sulphate. The MFI values were between 466.4-629.3% for monocytes and 577.9-742.9% for neutrophils in comparison to control and almost 2-fold higher in comparison to P(3HB)/oligo-PHA blend without barium sulphate. The results obtained suggest, that addition of barium sulphate cause an increased activation of neutrophils and monocytes with an increase of the concentration of barium sulphate.

6.6. Discussion

Barium sulphate usually occurs as a white powder, used as x-ray positive contrast agent for imaging or diagnostics purposes. BaSO₄ cannot be metabolized or absorbed in the physiological conditions. It is excreted from the body in unchanged form (Widmark, 2007). Barium sulphate has been used as a contrast agent in biomedical applications, such as bone cement (Lewis, 1997), microdamage detection (Wang *et al.*, 2007) or

gastrointestinal radiography (Skucas, 1989). It exhibits high x-ray attenuation and good biocompatibility (Leng *et al.*, 2008).

Barium sulphate has been used as one of the compounds in bone cements or contrast oral tablets. However, it has been reported that presence of BaSO₄ can facilitate macrophage differentiation to osteoclasts, which contribute to bone resorption and loosening of prosthesis and implants (Lewis *et al.*, 2005; Sabokbar *et al.*, 1997).

In this study, an addition of barium sulphate changed the properties of the composite materials. The differences are more evident in the mechanical properties of composites. As expected the most affected factor was the elongation at break. Addition of BaSO₄ resulted in an increase of the brittle nature of the material. Elongation at break in all composites with addition of barium sulphate was significantly lower than without. During storage changes in the tensile strength and Young's Modulus were observed. Both factors increased after 3 weeks of storage and then decreased after that. In the material without addition of filler the Young's Modulus increased after 7 weeks of storage. Composite stiffness and strength were improved significantly after 3 weeks. However, after 7 weeks of storage, the improvement was much less prominent. Minari *et al.*, 2000 reported that addition of BaSO₄ resulted in decrease of the strength on the material. De Arenaza *et al.*, 2015, demonstrated an enhancing effect of addition of barium sulphate on the mechanical properties of materials, such as polylactic acid (De Arenaza *et al.*, 2015). However, an addition of barium sulphate could lead to negative effects to the materials, such as: fatigue crack initiation in methacrylic bone cements (Ricker *et al.*, 2008). Barium sulphate used as a filler is expected to enhance the material properties, such as mechanical properties, optical characteristics and flow behaviour, which allows BaSO₄ application in pigments, printing inks, glasses, polymers and medicine (Van Leuween, 1998). Additionally, BaSO₄ particles can be modified in order to improve reaction with polymer. Wang and co-workers demonstrated enhanced reinforcement effect of BaSO₄ particles on natural rubber when modified by 5 wt% stearic acid. Achieved tensile strength was 14.4MPa and elongation at break 516%, which was 240% and 172% higher in comparison to non-modified BaSO₄ (Wang *et al.*, 2011). In another study, Wang and co-workers demonstrated increased Young's Modulus values with an increase amount of filler. High content of BaSO₄ had negative effect on the yield stress of the composite materials (Wang *et al.*, 2003). Presence of

barium sulphate particle can result with different material properties. Yan and co-workers (2016) reported that composites made from polytetrafluoroethylene (PTFE) granular powder containing barium sulphate (BaSO_4) demonstrated tensile strength 19.4MPa and elongation at break 420% in comparison to 16.4-17.3MPa and 260-370% strain for PTEE non-granular powder (Yan *et al.*, 2016).

An addition of barium sulphate also resulted in changes of the surface topography of the materials. A significant increase of surface roughness was observed. Especially in the composite with 5 wt% of BaSO_4 the value of mean root square was 87% higher than P(3HB)/oligo-PHA blend without addition of barium sulphate. For some medical devices, like for example catheters, an increased roughness of the surfaces can be a negative factor (Baleani and Viceconti, 2011). Addition of 5 wt% of BaSO_4 have decreased the contact angle values around 33% in comparison to neat blend. This can be explained by the hydrophilic nature of the barium sulphate surface, which can be wetted easily, although is insoluble in water (Bala *et al.*, 2006). Also, addition of barium sulphate had an impact on protein adsorption. The amount of proteins attached to the composite materials was significantly higher in comparison to TCP or the neat blend. The amount of absorbed proteins on the surface of composite with 5 wt% BaSO_4 was 47% higher as compared to tissue culture plastic and 19% higher than neat PHA blend.

The amounts of radiopacifier used in different materials varies between 7 wt% to 60 wt%. However, Dios and co-workers observed that an addition of BaSO_4 at concentration 5 wt% to the floating drug delivery system was sufficient to obtain a radiopacity (Dios *et al.*, 2016). All tested composite materials with concentrations of barium sulphate (1-5 wt%) resulted in successful absorbability by X-ray, the intensity of the signal increased with higher amount of barium sulphate.

Addition of barium sulphate also resulted in a significant increase of cell viability of HMEC-1 after day 3 and 7. In the indirect cytotoxicity analysis, the cell viability results were similar to those obtained in cell viability studies. The highest cell viability was obtained in case of 3 wt% concentration of barium sulphate. This experiment confirmed non-toxic effect on the HMEC-1 cells. Moreover, higher amounts of barium sulphate supported growth and proliferation of endothelial cells. High adhesion of the HMEC-1 cell line to all types of tested composites in comparison to the TCP indicated the possibility of application as a platform material in coronary stent. However, considering

the other factors, such as mechanical properties as well as radiopacity, 5 wt% addition of BaSO₄ might be most reasonable choice.

In this study, presence of barium sulphate in the composites did not affect the haemocompatibility of the tested materials. According to ISO 10993-4:2002 standard, all tested films had low potential to destroy red blood cells. All composites did not present any haemolytic properties or enhanced blood clot formation. However, they presented much higher activation of neutrophils and monocytes as shown by the marker CD11b. Similarly, Lazarus *et al.*, 1994 reported an increased secretion of inflammatory mediators due the presence of BaSO₄ particles in the periprosthetic tissue (Lazarus *et al.*, 1994).

The results obtained in this project confirmed the non-toxic effect of barium sulphate on the endothelial cells. The differences in the material properties between different concentrations of barium sulphate were minor. The main aim of this study was to develop radiopaque material, suitable for coronary stent application using barium sulphate as a radiopacifier. Hence, in conclusion, the composite with 5 wt% of BaSO₄ would be the most reasonable choice for stent application because of its strong X-ray absorption and improved surface topography which resulted in enhanced biocompatibility with human endothelial cells.

Chapter 7

Poly(3-hydroxybutyrate)/

oligo-PHAs tubes manufacturing

7. Introduction

Polymeric materials can be processed by using different techniques. Selection of the suitable manufacturing technique depends on the material properties as well as final application. Many techniques have been applied to the synthetic polymers, such as phase separation, gas foaming, freeze drying, solvent casting, particulate leaching, thermal processing, moulding, rapid prototyping or electrospinning (Kim *et al.*, 2012; Chung and King, 2011; Dhandayuthapani *et al.*, 2011).

Polyhydroxyalkanoates represent a group of natural polymers with broad range of material properties. They can be processed by using different techniques, such as electrospinning, solvent casting, spin casting, melt extrusion, to form films, fibres, 3D structures, tubes and foams (Thellen *et al.*, 2012). Solvent casting has been widely used to study initial properties of the materials. Some of the applications required flat scaffolds, therefore this technique can be applied directly. The main benefit of the solvent casting technology is obtaining materials by unique drying of the polymer solution without additional mechanical or thermal treatment (Siemann *et al.*, 2005). Fabrication of 3D structures is much more complicated. There are few factors, which can be considered during material processing, such as solvents, quantities of the material, stability of the solution, processing conditions. Coronary stent applications, require tubular structures. Melt extrusion is a well-known technique, commonly used to produce tubes. However, this method has some limitations, such as requirement of substantial quantities of the material, a large amount of waste material, not very suitable for sticky polymers (LaFontaine *et al.*, 2016).

Dip moulding is a technique, widely used for manufacturing 3D structures or coating already made articles. It required small quantities of material and is a simple piece of equipment. The process is also cheaper than melt extrusion. Important parameters which require an optimisation, include the right choice of the solvents, stability of the solution, correct temperature and time of drying. Processing of the single polymer is much easier than mixture of two different types of the materials, therefore preparation of blends or composites is much more challenging by using this method (Parameswaranpillai *et al.*, 2014).

The main aim of this part of the project is to develop P(3HB)/oligo-PHA based tubes using the dip moulding technique for development of medical devices, such as coronary

artery stents. Based on the results obtained for solvent cast films, one of the P(3HB)/oligo-PHA blends in ratio 90/10 was selected for tube manufacturing. Three different types of tubes were prepared: neat P(3HB)/oligo-PHA neat tube, P(3HB)/oligo-PHA tube coated with PCL-PEG550 and P(3HB)/oligo-PHA composite tube with an addition of 5 wt% barium sulphate. The tubes were fully characterized with respect to their thermal and mechanical properties. *In vitro* biocompatibility of the tubes was tested with human dermal microvascular endothelial cells HMEC-1 to evaluate the potential of new biodegradable material in an application as coronary artery stents. Haemocompatibility studies were carried out in order to study the impact of the tubular structures on blood cells. Additionally, microCT scanning was performed to study radiopacity of the composite tube, containing barium sulphate as a contrast agent.

7.1. P(3HB)/oligo-PHA tube manufacturing by dip moulding technique

The P(3HB)/oligo-PHA blend in ratio 90/10 was selected for tube manufacturing by the dip moulding technique. The P(3HB)/oligo-PHA blend 90/10 was dissolved in a mixture of solvents, such as chloroform and 1,1,2,2-tetrachloroethane in ratio 70:30 wt/wt at room temperature. The polymer solution was clear and stable at room temperature. Metallic moulds (needles) with 2.54mm diameter and 78mm length were coated with polymer solution in order to create tubes (Figure 69). Tubes were made and dried at 50 °C. The process parameters included: 20 cycles, 2s dwelling time and 30s drying time between the cycles. After every 5 cycles, extended drying time up to 3 minutes was used. Coated needles were dried at 50 °C for 24 hours, measured with Vernier caliper and removed from the needles after being cooled down to the room temperature.

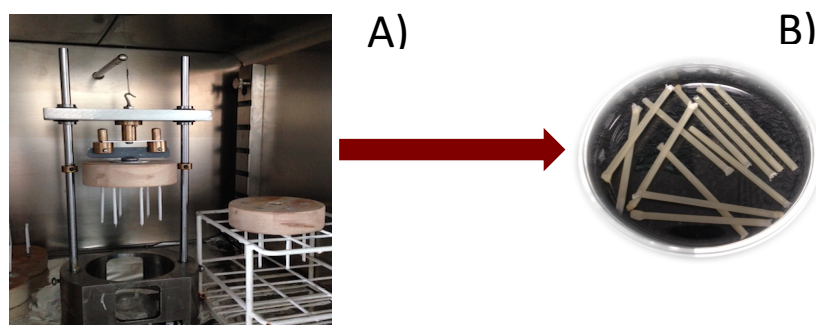


Figure 69: Production of PHA tubes (needle 2.54mm diameter, 78mm length) A-B prepared by using dip coating technique.

7.2. Tube characterization

Obtained tubes were characterised with respect to their thermal and mechanical properties after 7 weeks of storage. Additionally, *In vitro* degradation studies for 6 months were performed.

7.2.1. Tube dimensions

Coated moulds were measured using the Vernier caliper in 3 places and recorded as the outer diameter. The outer diameter of the tubes was measured as 2.7 ± 0.01 mm. Hence, the obtained P(3HB)/oligo-PHA tubes had wall thickness 146 ± 3.2 μ m.

7.2.2. Tubes characterisation after 7 weeks of storage at room temperature and incubation in DMEM media at 37° C

Tubes were stored for 7 weeks at room temperature (Figure 70A) in order to study ageing of the material. Some of the tubes were incubated in the DMEM media at 37°C (Figure 70B) in order to mimic an environment, which is similar to the human body. The influence of the hydrophilic environment and body temperature on the mechanical properties of the material was investigated.

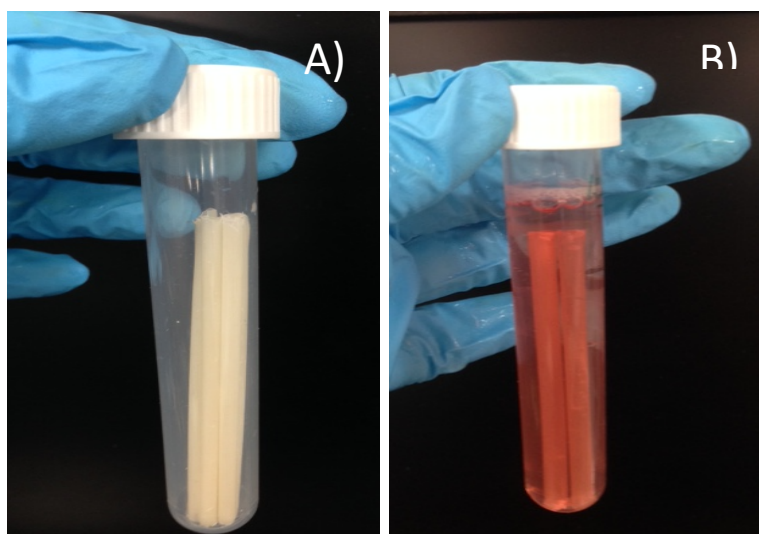


Figure 70: Tubes stored for 7 weeks at room temperature, dry (Figure A) and in DMEM media incubated at 37°C (Figure B).

7.2.2.1. Thermal properties of the tubes stored for 7 weeks at room temperature

Thermal properties of the tubes were studied by using Differential Scanning Calorimetry as described in the section 2.6.4. The results obtained were listed in the Table 27. The thermograms from the first heating cycle of the tubes, studied at week 1, 3, 5 and 7 of storage are shown in the Figure 71.

Table 27: Summary of the thermal properties of the P(3HB)/oligo-PHA tubes during 7 weeks of storage. T_m = melting temperature, T_g = glass transition temperature, T_c = crystallisation temperature, ΔH_f =enthalpy of fusion.

Time of storage (week)	T_g (°C)	T_m (°C)	ΔH_f (J/G)	T_c (°C)
1	1.1	166.00	83.3	58.6
3	2.7	167.6	69.1	56.9
5	3.4	171.4	70.2	54.1
7	2.5	172.6	79.3	60.4

The thermal properties of the tubes had changed during 7 weeks of storage. The glass transition temperature increased from 1.1°C to 2.5°C after 7 weeks. Temperature of melting increased from 166°C to 172.6°C. Similarly, cold-crystallisation temperature increased from 58.6°C to 60.4°C. The value of enthalpy of fusion decreased from 83.3 J/g to 79.3 J/g. However, significant decrease was observed after week 3 and 5. The values of ΔH_f have dropped down about 16% in comparison to week 1.

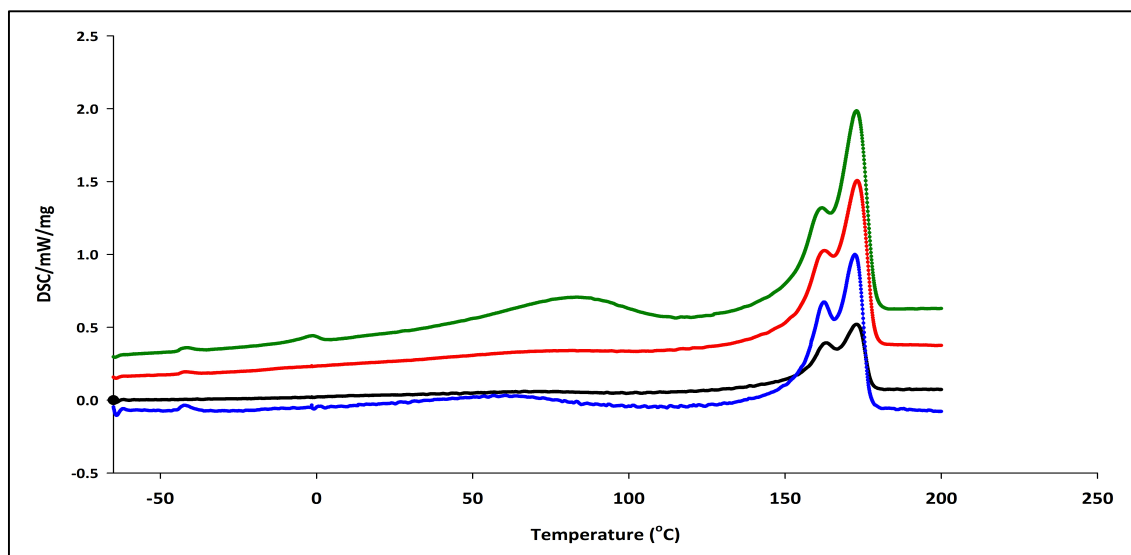


Figure 71: DSC thermograms of P(3HB)/oligo-PHA tubes stored for 7 weeks at room temperature illustrating melting peaks. (■) week 1, (■) week 3, (■) week 5 and (■) week 7.

The DSC thermograms represent the first heating cycle during DSC analysis. This part of the analysis is very important during ageing experiments, which main aim to study changes in thermal properties within a selected period of time. In this cycle only melting events were present in all tested samples. The temperature of melting increased slightly within 7 weeks of storage. All melting peaks obtained were double peaks, characteristic for P(3HB) and described in previous chapters.

7.2.2.2. Mechanical properties of the tubes stored for 7 weeks at room temperature

The analysis of the mechanical properties of the P(3HB)/oligo-PHA tubes stored at room temperature were carried out for 7 weeks, in order to study the material properties during ageing. The results obtained are summarised in Table 28.

Table 28: Summary of the mechanical properties of the P(3HB)/oligo-PHA tubes during 7 weeks of storage at room temperature.

Week	Tensile strength (MPa)	Elongation at break (% strain)	Young's Modulus (MPa)
1	15.7±2.8	14.6±1.9	510±17
3	18.5±1.8	9.9±0.9	1280±170
5	20.5±4.6	8.6±1.3	1230±50
7	21.6±2.6	6.5±1.2	1270±40

As expected after 7 weeks of ageing at room temperature, the mechanical properties of the P(3HB)/oligo-PHA tubes changed. The tensile strength increased from 15.7±2.8 MPa at week 1 to 21.6±2.6 MPa at week 7. Similarly, Young's modulus values increased from 0.5±0.01GPa to 1.27±0.04GPa. The material became stronger and stiffer with the time. Elongation at break decreased from 14.6±1.9% to 6.5±1.2%, which confirmed brittle nature of the material. The material behaviour of the tubes followed the trend observed in the flat P(3HB) based blend films, described in details in the Chapter 5, section 5.2.1.2.

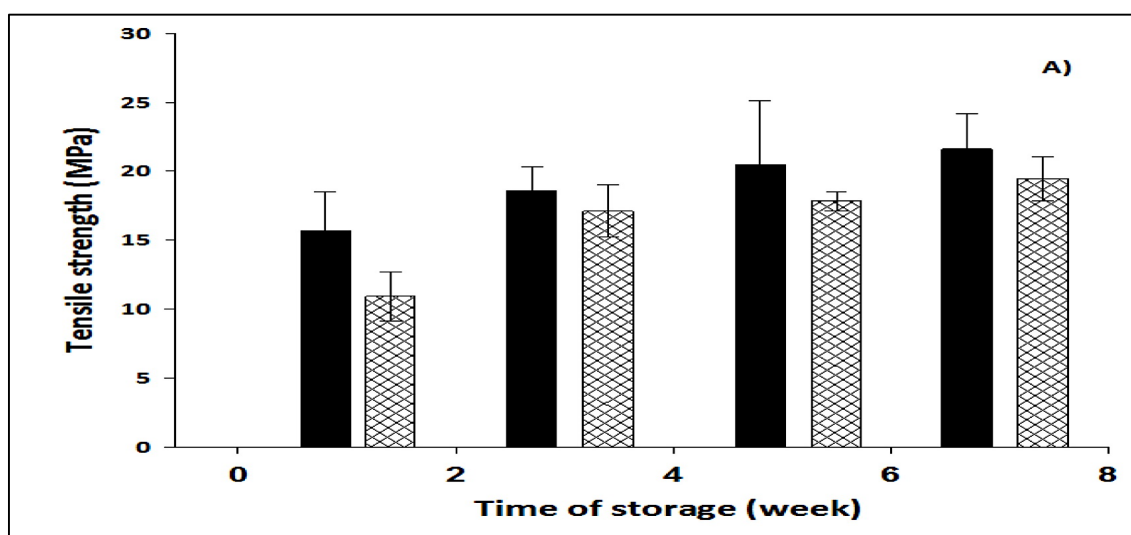
7.2.2.3. Mechanical properties of the tubes after incubation in DMEM media at 37° C for 7 weeks

In order to check the effect of the hydrophilic environment and body temperature on the mechanical properties of the material, the analysis of the mechanical properties of the tubes incubated in DMEM media at 37° C were carried out for 7 weeks. The summary of the mechanical properties of the tubes stored at room temperature and at 37°C for 7 weeks were demonstrated in Table 29 and Figure 72.

Table 29: Summary of the mechanical properties of the P(3HB)/oligo-PHA tubes during 7 weeks of storage in DMEM media at 37° C for 7 weeks.

Week	Tensile strength (MPa)	Elongation at break (% strain)	Young's Modulus (MPa)
1	10.9±3.9	8.4±0.9	360±40
3	17.1±1.9	7.3±1.1	690±90
5	17.8±0.1	6.2±0.1	690±10
7	19.5±1.6	3.9±0.4	740±30

After 7 weeks of incubation in DMEM media at 37°C, the mechanical properties of the P(3HB)/oligo-PHA tubes had changed. The tensile strength increased from 10.9±3.9 MPa at week 1 to 19.5±1.6 MPa at week 7. Similarly, Young's modulus values increased from 0.36±0.04 GPa to 0.74±0.03 GPa. Material became stronger and stiffer with the time. Elongation at break decreased from 8.4±0.9% strain to 3.9±0.4 MPa after week 7, which is 53% lower than value obtained at week 1. The results obtained confirmed the relative brittle nature of the material. Material behaviour of the tubes followed the general trend observed in the flat P(3HB) based blend films, described previously in Chapter 5.



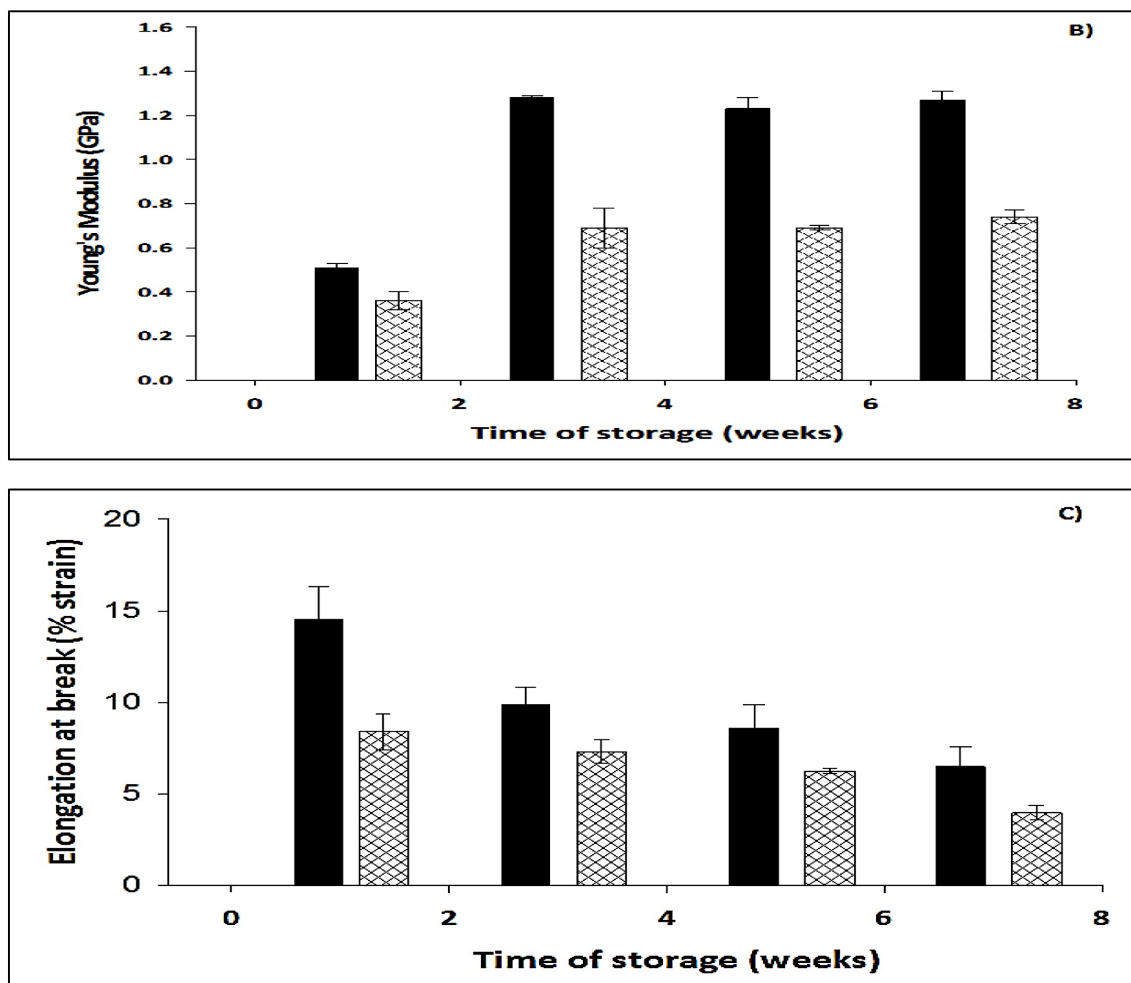


Figure 72: The changes of ultimate tensile strength (A), Young's modulus (B) and elongation at break (C), during aging of neat P(3HB)/oligo-PHA tubes stored at room temperature (■) and incubated in DMEM media at 37°C (⊠) for 7 weeks.

The results obtained clearly suggest that tubes underwent the same embrittlement phenomenon as the flat films. However, it is worth to notice that the storage conditions played crucial role in order to shape the final material properties. From the Figure 72 it is clear that tubes incubated at 37°C demonstrated significant differences in the stiffness and elongation of the material. On the other hand, the differences between values of tensile strength were not that high. Tubes incubated at 37°C exhibited Young's Modulus values 60% lower than tubes stored at room temperature. Elongation at break was 40% lower after 7 weeks of incubation at 37°C in comparison to the tubes stored at room temperature. Overall, tubes stored in the DMEM media and body temperature environment became more brittle as well as less stiff than tubes storage at room temperature. Hence, in future we need to investigate, which of the factors: hydrophilic

environment, presence of different organic compounds such as proteins or higher temperature is a determinant factor to cause changes to the material.

7.2.3. Scanning Electron Microscopy of the P(3HB)/oligo-PHA tubes

Microstructural studies of P(3HB)/oligo-PHA tubes were performed using Scanning Electron Microscopy. The surface of the cross-intersection demonstrated that material is uniform (Figure 73A). Very small irregular pores are present in the wall of the tube as an effect of the increased chloroform evaporation at 50°C during dip moulding process. Surface of the tube was smooth and even. Pores are not visible on the outer surface of the tube (Figure 73C). SEM imaging allowed measuring the wall thickness. Presented tube on the Figure 73D has wall thickness $145.6 \pm 0.5 \mu\text{m}$, which confirmed results obtained, measured by caliper. Wall thickness on the studied tube was quite uniform and homogenous (Figure 73B). Therefore, the chosen processing conditions were appropriate to formulate tubular structures using the dip moulding technique.

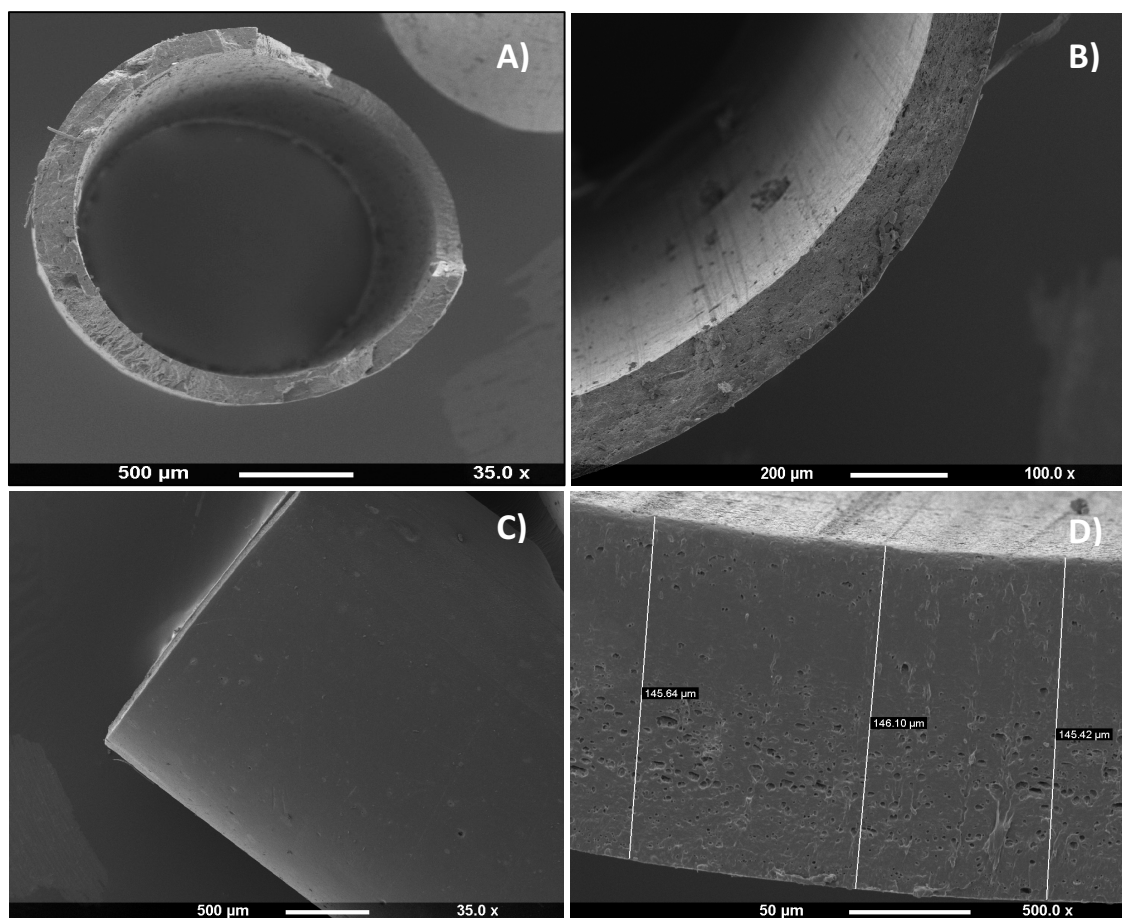


Figure 73: SEM images of the P(3HB)/oligo-PHA tubes: cross section (A), wall topography (B) surface of the tube (C), wall thickness (D),

7.3. *In vitro* degradation studies

In vitro degradation study was carried out for period of 6 months at 37°C in phosphate buffered saline solution (PBS), at pH=7.4 to mimic *In vivo* environment and to investigate the degradation behaviour of the P(3HB)/oligo-PHA neat tubes.

7.3.1. Attenuated Total Reflectance Fourier Transform Infrared Spectroscopy (ATR/FT-IR)

FTIR was carried out on the tubes to investigate the changes in the chemical structure during the incubation time. Figure 74 illustrates the ATR/FTIR spectra obtained for the tubes after month 1, 3 and 6 of degradation studies.

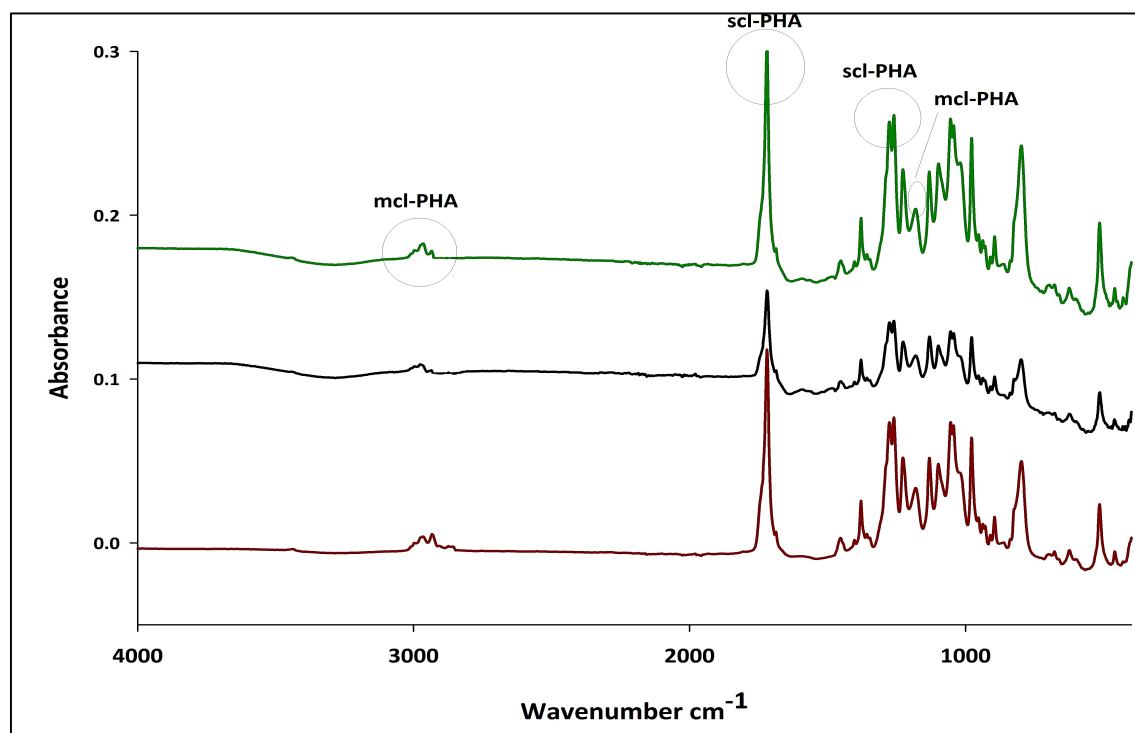


Figure 74: ATR-FTIR spectrum of the P(3HB)/oligo-PHA tubes during 6 months of degradation study. (—) month 1, (—) month 3, (—) month 6.

There were no differences between the spectra obtained after month 1 and 6. All the chemical bonds, which have been detected are typical to P(3HB)/oligo-PHA blends, such as peak at 1720.5 cm^{-1} and 1276.5 cm^{-1} corresponding to the ester carbonyl group and the -CH group, respectively (scl-PHA) and the weak absorption bands at 2938 cm^{-1} , 2991 cm^{-1} and 2939 cm^{-1} assigned to the aliphatic C-H group of the pendant alkyl group

found in mcl-PHAs and the peak, observed at 1182 cm^{-1} corresponded to the -CO stretching group, characteristic of mcl-PHAs. The intensity of the signals obtained for C-H and -CO bonds for mcl-PHA decreased within 6 months time.

7.3.2. Thermal properties – Differential Scanning Calorimetry

DSC analysis was carried out in order to study changes in the thermal properties in the material caused by tubes degradation. A summary of the results obtained has been listed in Table 30. First heating cycle thermograms are illustrated in the Figure 75.

Table 30: Summary of the thermal properties of the P(3HB)/oligo-PHA tubes during 6 months of degradation study. T_m = melting temperature, T_g = glass transition temperature, T_c = crystallisation temperature, ΔH_f =enthalpy of fusion.

	Month 1	Month 2	Month 3	Month 4	Month 5	Month 6
T_g (°C)	-3.1	-4.5	-4.7	1.1	-0.4	-2.7
T_m (°C)	175.5	173.4	174.8	175.6	173.7	172.7
T_c (°C)	53.9	51.5	50.1	59.1	59.3	51.3
ΔH_f (J/g)	72.2	71.6	78.7	72.3	78.6	79.3

During 6 months of degradation study, the thermal properties of the materials changed. Glass transition temperature slightly increased from -3.1°C at month 1 to -2.7°C at month 6. Melting temperature decreased from 175.5°C to 172.7°C after month 1 and 6 respectively. Similarly, the cold-crystallisation temperature decreased. The enthalpy of fusion values had increased from 72.2 J/g to 79.2 J/g . Hence, there was a significant change in the thermal behaviour of the tubes from month 4 to 6.

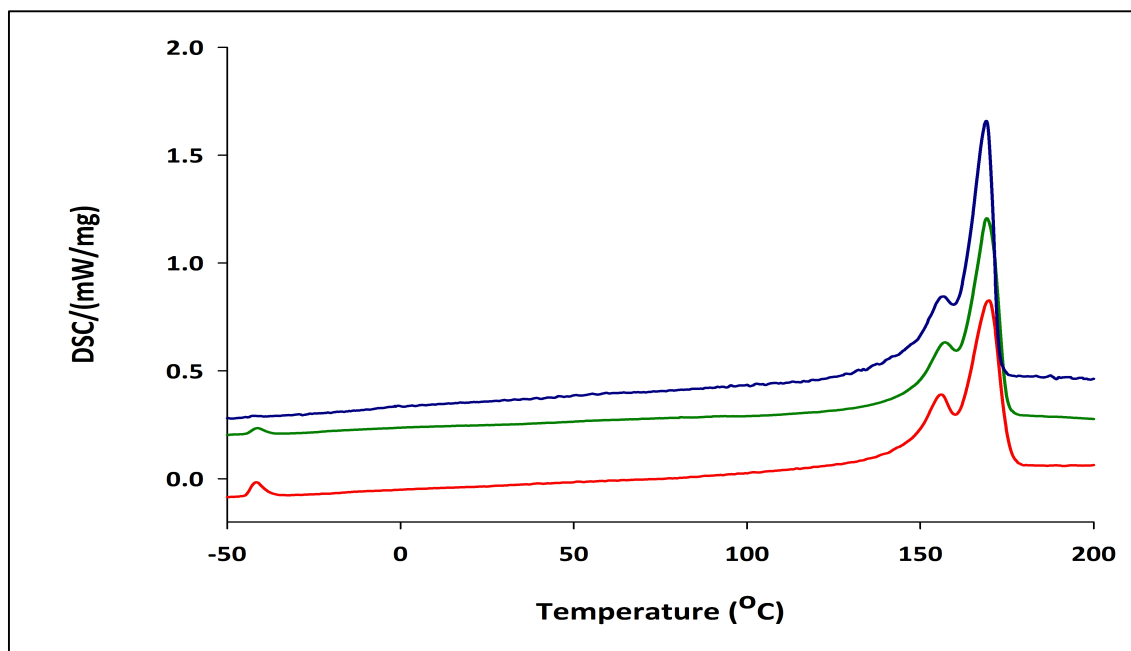


Figure 75: DSC thermograms of P(3HB)/oligo-PHA tubes during 6 months of degradation study (first heating cycle) illustrating melting peaks. The thermal properties of the tubes after 1 month (■), 3 months (■) and 6 months (■).

The DSC thermograms in the Figure 75 presents the first heating cycle of tubes after months 1, 3 and 6 of degradation. During degradation studies and ageing experiments results obtained in the first cycle are very important. DSC analysis of the tubes during degradation study demonstrated presence only melting events during first heating cycle. There was slight decrease in the temperature of melting, observed between tubes after month 1 and 6. Glass transition was not observed in the first cycle at any measured time point.

7.3.3. pH measurements of the PBS during degradation studies of neat PHA tubes

PBS, in which the tubes were incubated were studied in order to monitor any changes in the pH. The results obtained were presented in the Figure 76.

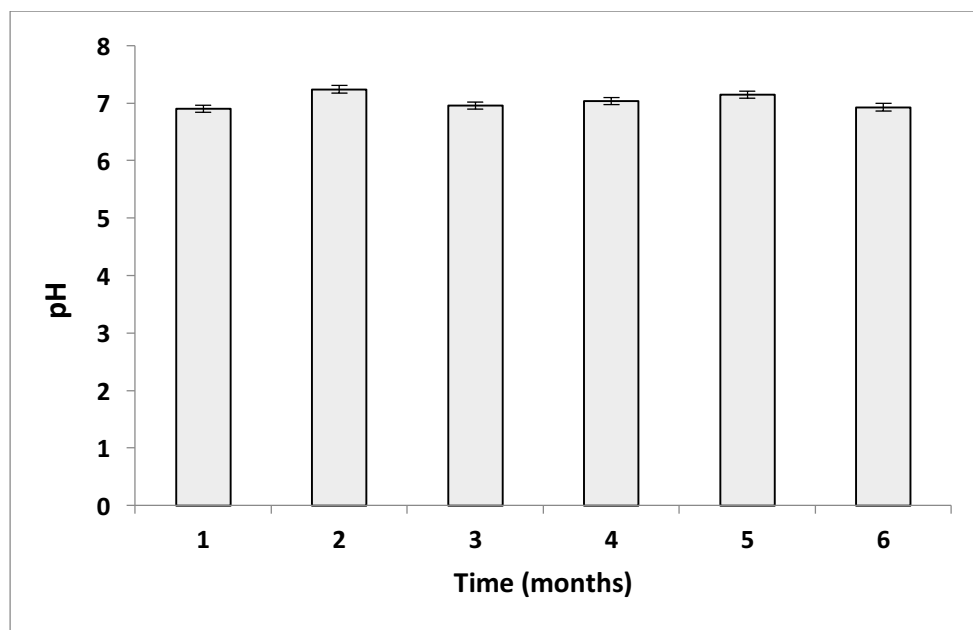


Figure 76: pH changes of PBS after incubation with P(3HB)/oligo-PHA tubes for 6 months ($n=3$; error bars \pm SD), no significant difference in comparison to month 1, ANOVA.

The pH of PBS was 7.4 at the beginning of the study. After 6 months of incubation at 37°C the final pH was 6.9 ± 0.05 . The results obtained in this study suggest release of slightly acidic product during the degradation process, which cause a decrease in pH. However, the pH changes were not significant.

7.3.4. Weight loss (%) of the neat tubes during degradation studies

Percentage of weight loss was measured at month 1, 2, 3, 4, 5 and 6 of degradation study as described previously in the section 2.16.3. The summary of the results has been illustrated in Figure 77.

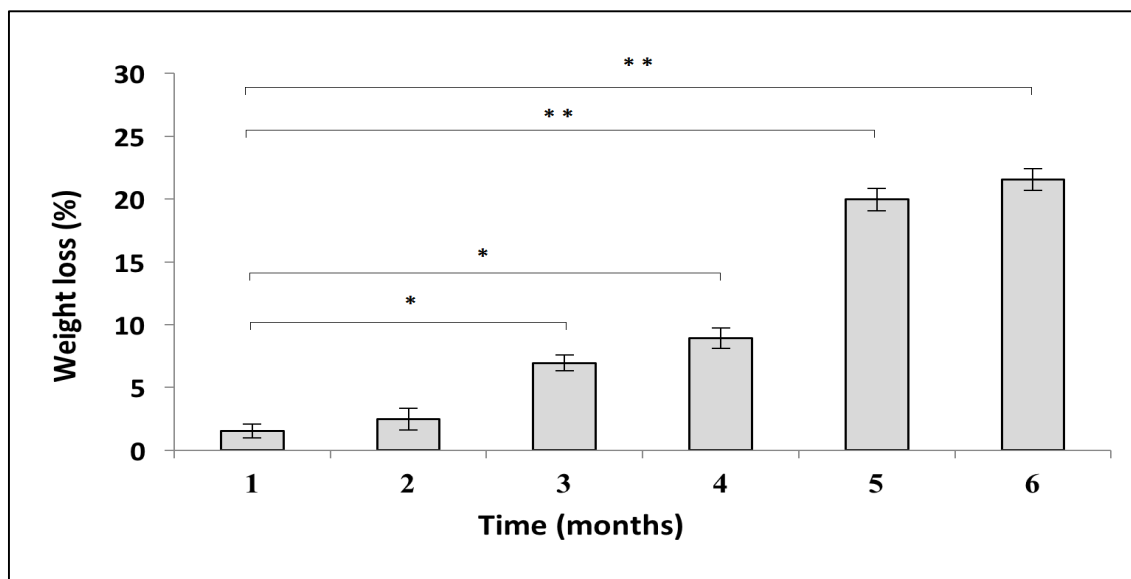


Figure 77: Weight loss (%WL) by the P(3HB)/oligo-PHA tubes during a period of 6 months (n=3). Results were compared to % weight loss after month 1 using ANOVA. * indicates $p < 0.05$, ** indicates $p < 0.005$.

The results obtained suggest a gradual increase in the weight loss, observed in the tubes during degradation study. Initial weight loss at month 1 and 2 was below 3%. The most rapid weight loss was observed after month 4 of degradation study. After 6 months, the obtained weight loss of the tubes was $21.6 \pm 0.8\%$.

7.3.5. Water uptake (%) of the neat tubes during degradation studies

Percentage of water uptake (%WU), which is an amount of water absorbed by the material during incubation was measured at month 1, 2, 3, 4, 5 and 6 of degradation study as described previously in the section 2.16.3. the summary of the results has been illustrated in the Figure 78.

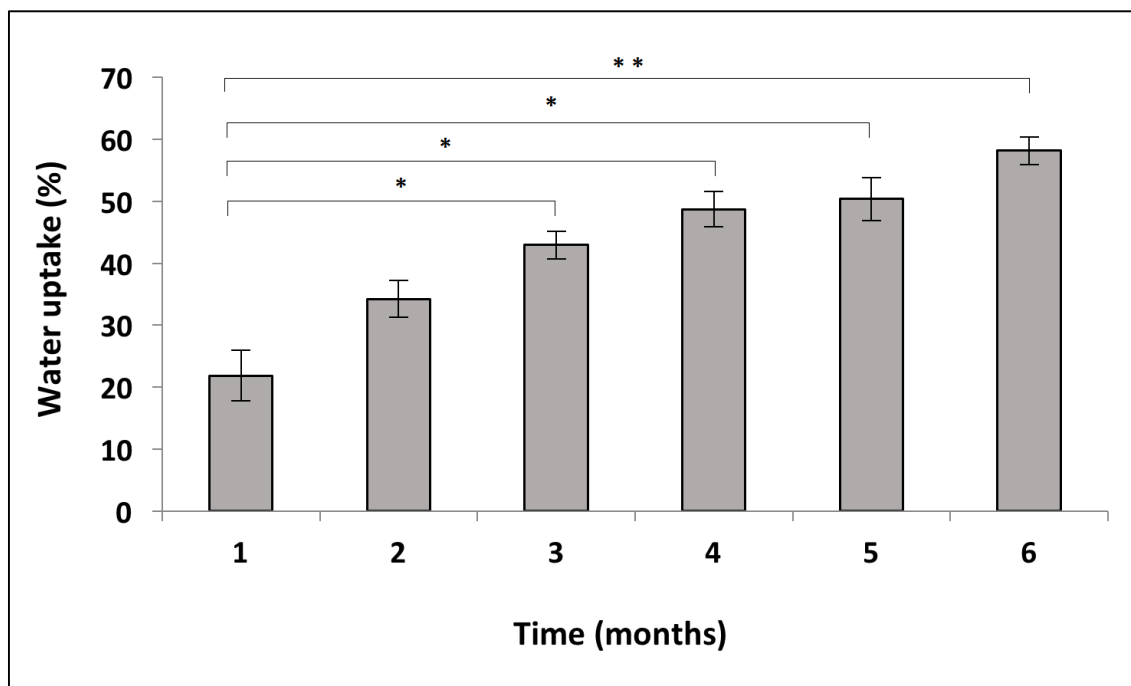


Figure 78: Water absorption (%WU) by the P(3HB)/oligo-PHA tubes for a period of 6 months (n=3). Results were compared to % water uptake after month 1 using ANOVA. * indicates $p < 0.05$, ** indicates $p < 0.005$.

The results obtained illustrated the amount of absorbed water by the tubes during 6 months of degradation study. The water uptake increased steadily from month 1 to 6. The final WU value obtained in this study after month 6 was $58.1 \pm 2.2\%$. The most significant increase was between month 1 and 2 of incubation.

7.3.6. Surface studies of the degraded tubes

After each time point during degradation studies tubes were rinsed with distilled water, dried and imaged using Scanning Electron Microscope as described in section 2.16.2. SEM analyses of the surface, cross section, wall thickness of the tubes was carried out to analyse any structural changes that occur due to degradation. SEM images of the tubes obtained after 6 months of degradation studies are presented in the Figure 79.

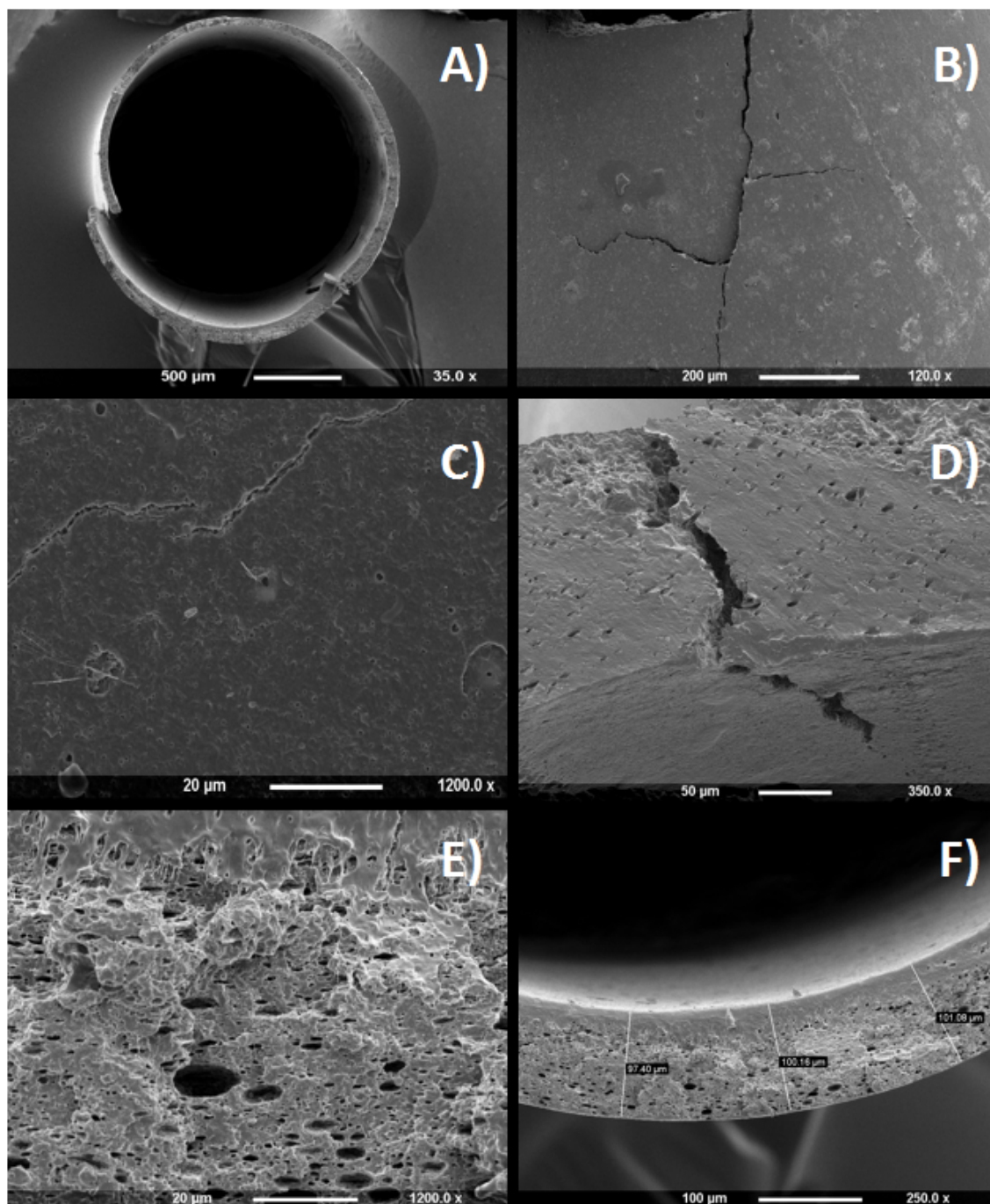


Figure 79: SEM micrographs of the P(3HB)/oligo-PHA tubes after 6 months of degradation study. (A) tube cross section, (B, C, D) outer surface of the tube, (E) wall microstructure, (F) wall thickness.

SEM images confirmed the degradation process on the tubes after 6 months. Degradation proceeded on the surface of the tubes along with decreasing wall thickness, which decreased 30% as compared to that before the incubation (Figure 79F). This affected tube stability (Figure 79A). Tubes became very fragile and brittle. Fractures were observed on the surface of the tubes (Figure B-D). The walls exhibited enhanced

porosity, which was much higher in the outer surface of the tube (Figure 79E), i.e. the increased porosity began from the outer part of the tube and progressed towards the core. Increased porosity allowed higher water penetration through the material wall. The internal surface did not show any changes in topography of the tubes. The results obtained in this study suggest that P(3HB)/oligo-PHA tubes undergo degradation process by surface erosion.

7.4. Manufacturing of the P(3HB)/oligo-PHA 90/10 tubes coated with PCL-PEG550

P(3HB)/oligo-PHA tube were coated with a monolayer of PCL-PEG550 as described in the section 2.11.1. and characterised in order to investigate the influence of the coating on the properties of the tube.

7.4.1. Thermal analysis of PCL-PEG550

PCL-PEG550 is a synthetic block polymer. The DSC thermograms are presented in the Figure 80.

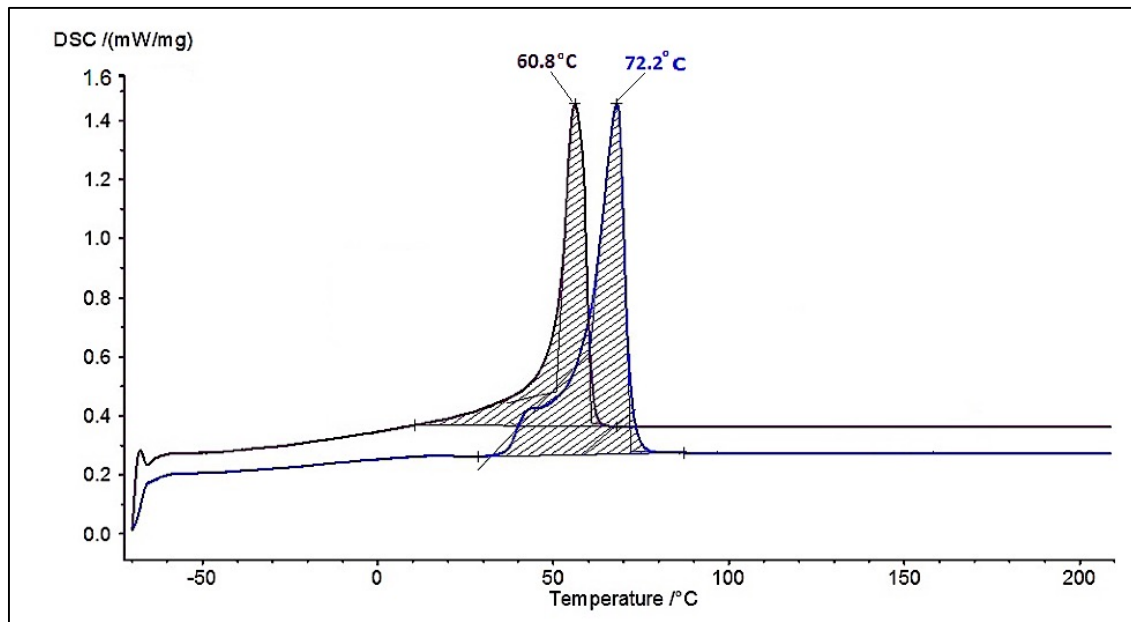


Figure 80: DSC thermogram of PCL-PEG550 neat polymer. (—) first heating cycle, (—) second heating cycle.

For PCL-PEG550 only one melting event was present in both heating cycles. The glass transition temperature as well as cold-crystallisation temperature for PCL-PEG550 were

not detected. The melting temperature of the PCL-PEG550 is 60.8°C, which is higher than mcl-PHAs and lower than scl-PHAs.

7.4.2. P(3HB)/oligo-PHA 90/10 tubes coated with PCL-PEG550 manufacturing

Mandrels with a layer of P(3HB)/oligo-PHA were coated with PCL-PEG550 monolayer and left to dry at room temperature. The resulting tubes were measured with a caliper in 3 places and recorded as the outer diameter. The difference between outer diameter of the mould was calculated as wall thickness. The difference between outer diameter of neat tube and coated tube was used to obtain the thickness of the coating.

Obtained tube had wall thickness $187 \pm 3.1 \mu\text{m}$. the size of the PCL-PEG550 monolayer was calculated as $36 \pm 2.3 \mu\text{m}$.

7.4.3. Characterisation of P(3HB)/oligo-PHA tubes coated with monolayer of PCL-PEG550

P(3HB)/oligo-PHA tubes coated with PCL-PEG550 were chemically characterised by using FTIR. Mechanical and thermal properties were studied during 7 weeks of storage at room temperature. Microstructural analysis was performed using Scanning Electron Microscopy.

7.4.3.1. Attenuated Total Reflectance Fourier Transform Infrared Spectroscopy (ATR/FT-IR)

ATR/FTIR spectrum of coated P(3HB)/oligo-PHA tube was different in comparison to the neat P(3HB)/oligo-PHA tube (Figure 81). Chemical bonds from PCL and PEG were present in addition to PHAs, described previously in Chapter 5. There was an adsorption peak at 2947cm^{-1} and 2872cm^{-1} , which corresponded to the asymmetric stretching $-\text{CH}_2$ and symmetric $-\text{CH}_2$ respectively. These bonds were more intense in the coated tubes, which confirmed the presence of another polymer, such as PCL-PEG550. The carbonyl bond at 1721cm^{-1} is slightly shifted in comparison to the neat tube, due to the presence of additional polymer. Asymmetric C-O-C- stretching bond was present at 1239.8cm^{-1} and symmetric -C-O-stretching at 1166.8cm^{-1} . Additionally, the ether bond was present at

1045 cm^{-1} , and -C-H bending bond at 1366.1 cm^{-1} , typical for the PEG part of the coated layer.

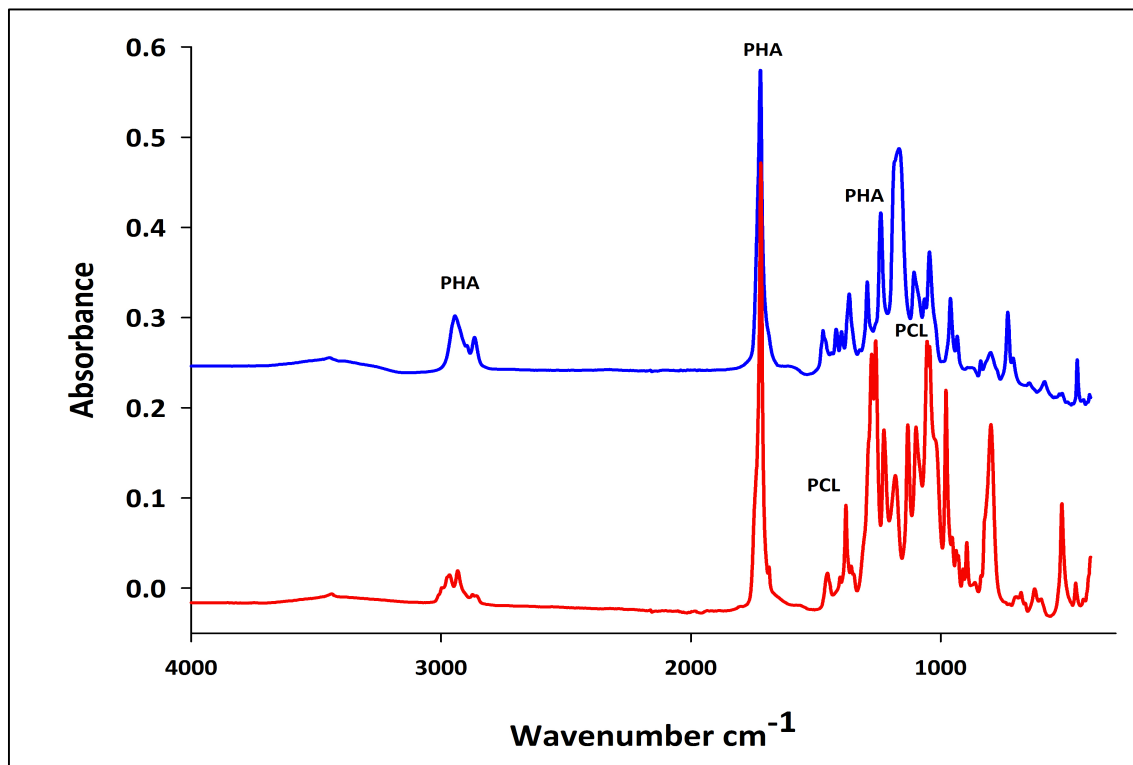


Figure 81: ATR/FTIR spectra of neat P(3HB)/oligo-PHA 90/10 tube (■) and P(3HB)/oligo-PHA 90/10 tube coated with PCL-PEG550 (■).

The obtained ATR/FTIR spectra of the tubes confirmed presence of the PCL-PEG550 unit on the surface of the tube due to the absorbance observed at 1045 cm^{-1} , 1366.1 cm^{-1} .

7.4.3.2. Thermal properties of the PCL-PEG550 coated PHA tube

DSC analysis of the PCL-PEG550 coated PHA tube was carried out in order to study the thermal behaviour of the coated tube after week 1 and 7 of storage at room temperature. The summary of the data is listed in the Table 31. The DSC thermograms from first heating cycle are presented in the Figure 82.

Table 31: Summary of the thermal properties of the P(3HB)/oligo-PHA tubes coated with PCL-PEG550 after 1 and 7 weeks of storage. T_m = melting temperature, T_g = glass transition temperature, T_c = crystallisation temperature, ΔH_f =enthalpy of fusion.

Time of storage (week)	T_g (°C)	T_m (°C)	ΔH_f (J/G)	T_c (°C)
1	1.1	166.0	83.3	58.6
		64.0	2.6	
7	2.7	167.6	69.1	56.9
		61.3	5.5	

DSC analysis also confirmed the presence of PCL-PEG550 compound by exhibiting a small melting event around 60°C, which is melting temperature of PCL-PEG550, described in section 7.4.1. Two melting events suggested that coated tube is a separated system with the bulk polymer being the P(3HB)/oligo-PHA blend and PCL-PEG550 as a coating. There was only one glass transition temperature detected. After 7 weeks of storage the glass transition temperature as well as melting temperature related to P(3HB) increased. Temperature of melting of PCL-PEG550 decreased from 64°C at week 1 to 61.3°C at week 7. On the other hand, the cold-crystallisation temperature as well as enthalpy of fusion presented an opposite trend. The largest change for ΔH_f values, were after week 7, the enthalpy of the PHAs decreased about 17% in comparison to week 1 and enthalpy related to PCL-PEG550 increased twice in comparison to week 1.

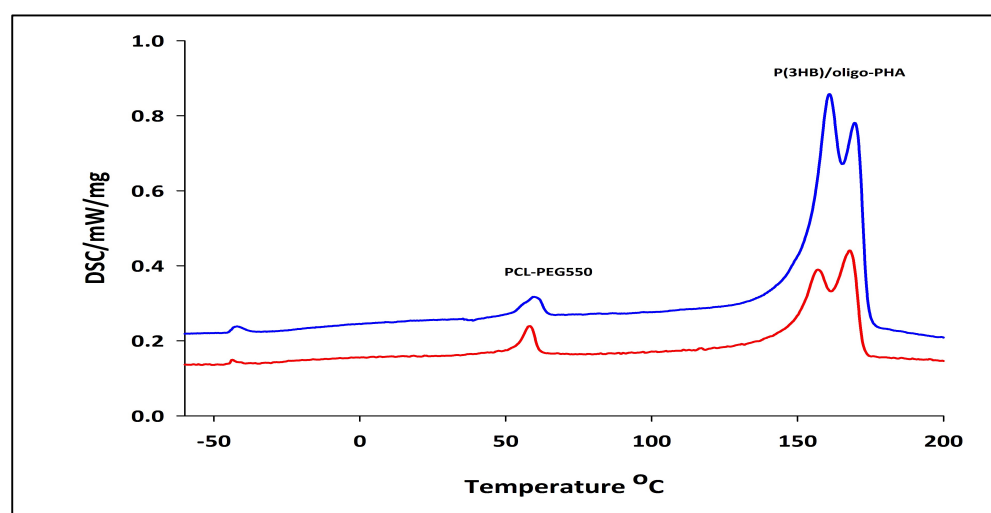


Figure 82: DSC thermograms of P(3HB)/oligo-PHA tubes coated with PCL-PEG550 after 1 (■) and 7 (■) weeks of storage (first heating cycle) indicating melting peaks.

The first heating cycles presented in the Figure 82 showed two different melting events, related to two different compounds in the tested tube: PHA-based core of the tube and PCL-PEG550 coating, which forms a monolayer on the outer surface of the tube.

7.4.3.3. Mechanical properties of the PCL-PEG550 coated PHA tube

The analysis of the mechanical properties of the P(3HB)/oligo-PHA tubes coated with PCL-PEG550 stored at room temperature were carried out for week 1 and 7, in order to check the properties during material ageing. The results obtained are summarised in Figure 83 and Table 32.

Table 32: Summary of the mechanical properties of the P(3HB)/oligo-PHA tubes coated with PCL-PEG550 after 1 and 7 weeks of storage (n=3).

Week	Tensile strength (MPa)	Elongation at break (% strain)	Young's Modulus (GPa)
1	16.7±1.5	9.3±1.3	0.7±0.1
7	29.2±1.0	7.9±0.6	1.4±0.1

After 7 weeks of ageing at room temperature, the mechanical properties of the P(3HB)/oligo-PHA tubes coated with PCL-PEG550 had changed. The tensile strength increased significantly from 16.7±1.5 MPa at week 1 to 29.2±1.0 MPa at week 7. Similarly, Young's modulus values increased from 0.7±0.1 GPa to 1.4±0.1 GPa. Material became stronger and stiffer with the time. The elongation at break decreased slightly from 9.3±1.2% strain to 7.9±0.6%.

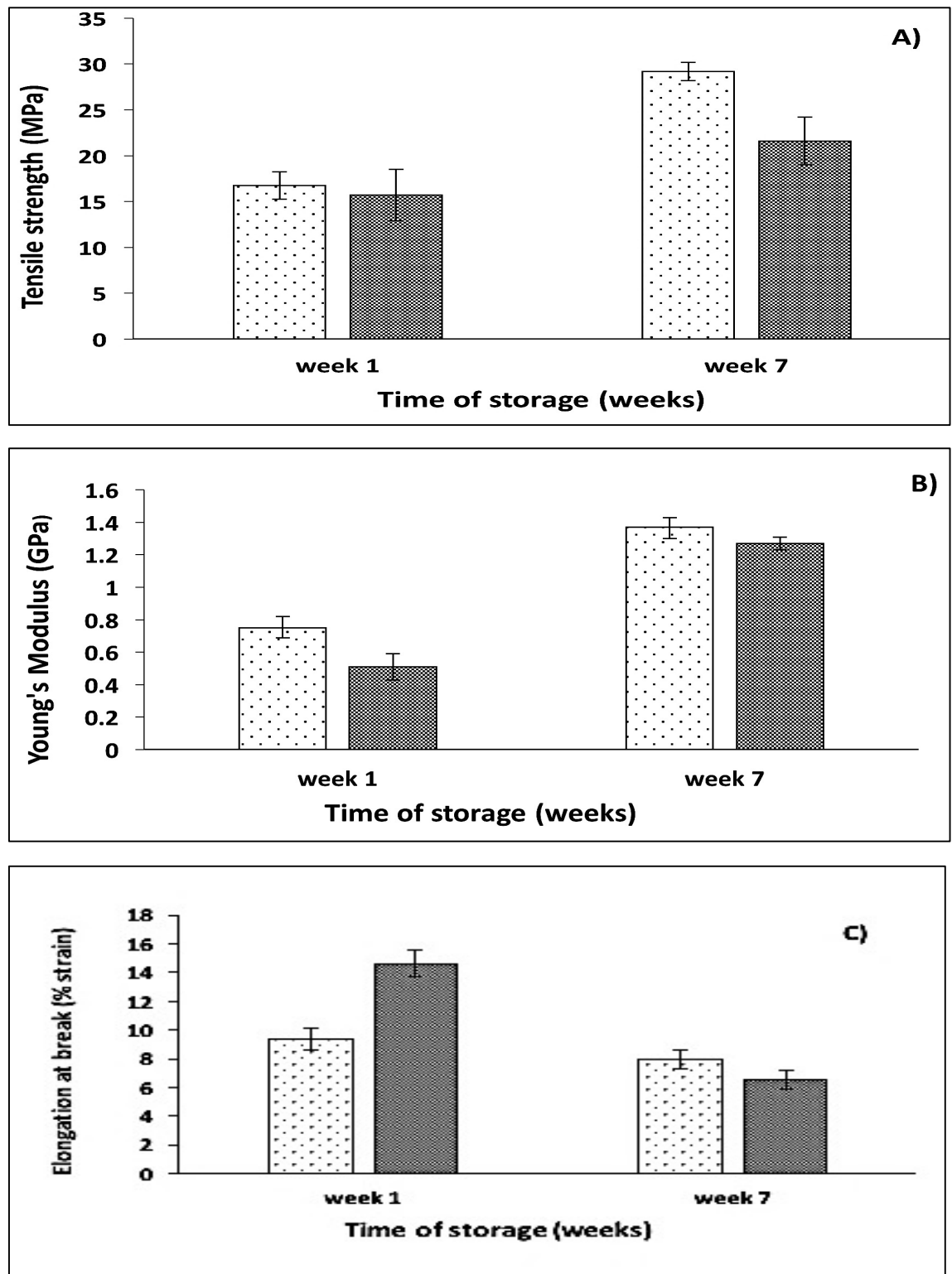


Figure 83: The summary of (A) the ultimate tensile strength, (B) Young's modulus and (C) elongation at break (C) during storage of neat P(3HB)/oligo-PHA neat tubes and tubes with monolayer of PCL-PEG550 for 7 weeks. (□) P(3HB)/oligo-PHA tube with PCL-PEG550 coating, (■) P(3HB)/oligo-PHA neat tube.

The tubes coated with PCL-PEG550 presented slightly different mechanical properties in comparison to neat P(3HB)/oligo-PHA tubes. Initially, tensile strength values were similar. However, after 7 weeks of storage the PCL-PEG550 coated tube had 30% higher tensile strength than neat P(3HB)/oligo-PHA tube. Coated tube had a slightly higher Young's Modulus. At first, the initial elongation at break of the coated tube is 30% lower than the neat tube. However, after 7 weeks of storage PCL-PEG550 coated tube demonstrated stronger, stiffer and more elastomeric properties in comparison to the neat tube.

7.4.3.4. SEM

Microstructural studies of P(3HB)/oligo-PHA tubes coated with PCL-PEG550 were performed using Scanning Electron Microscopy. The surface of the tube cross-intersection (Figure 84A) demonstrated that the obtained tube had uniform structure. Presence of the coating, which covered surface of the tube was confirmed. The thickness of the coating evaluated by SEM was $35.9 \pm 0.2 \mu\text{m}$ (Figure 84B). The surface of the tube is smooth and even as presented on the Figure 84C. Pores are not visible from the outer surface of the tube (Figure 84D) confirming that the tube was well formed. Therefore, the chosen processing conditions were appropriate to formulate tubular structures by using the dip moulding technique coated with a monolayer of PCL-PEG550 by dip coating.

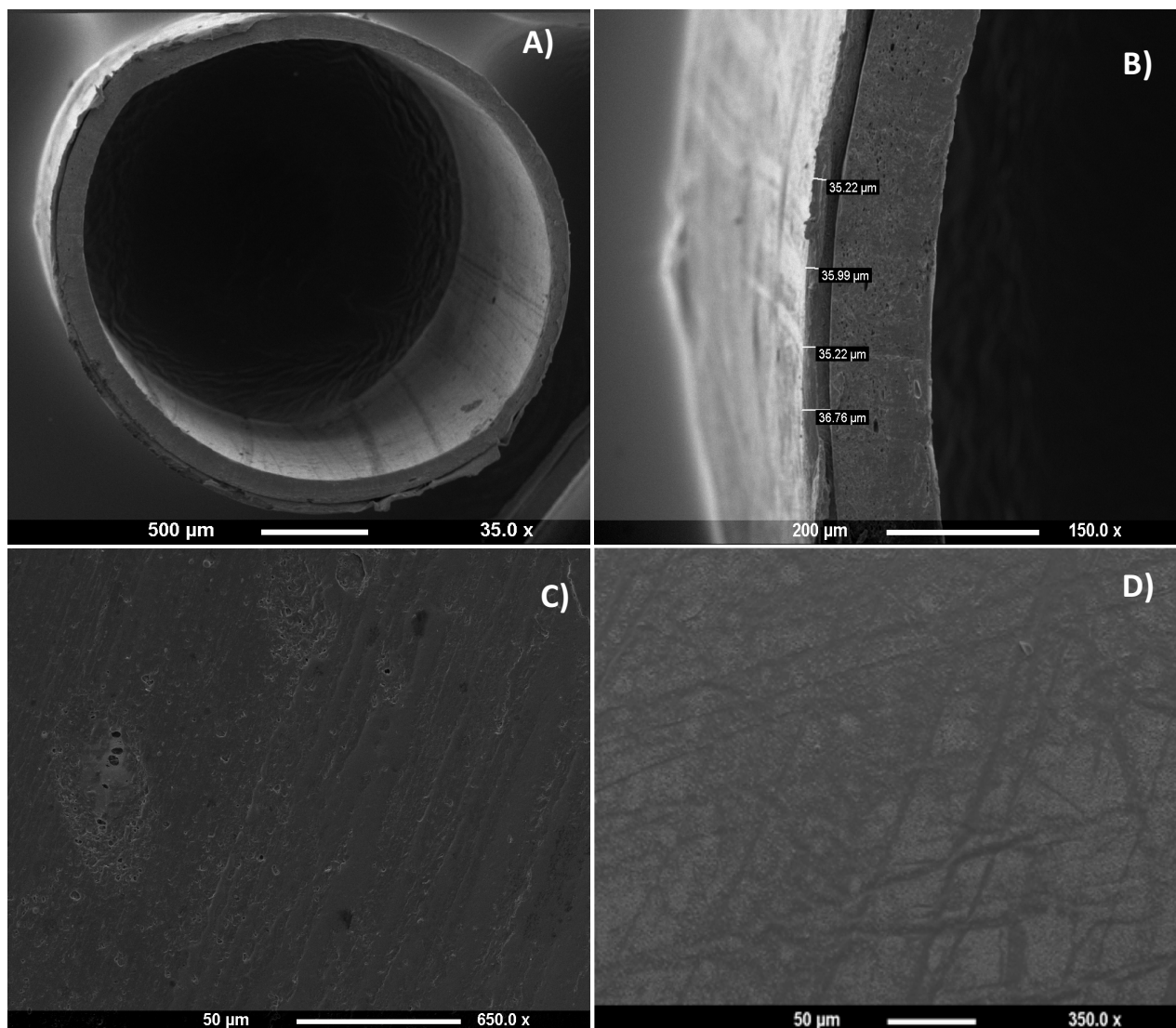


Figure 84: SEM micrographs of P(3HB)/oligo-PHA tube coated with a monolayer of PCL-PEG550: (A) cross-section, (B) tube wall with coating thickness measurement, (C) inner surface of the tube, (D) tube outer surface.

7.5. Manufacturing of P(3HB)/oligo-PHA composite tubes with addition of 5 wt% barium sulphate and their characterization

The composite tube manufacturing was performed as described in the section 2.11.2. The coated mandrels were measured using a caliper at 3 places and recorded as outer diameter. The difference between outer diameter of the size of the mould was calculated as wall thickness. Obtained P(3HB)/oligo-PHA composite tubes containing 5 wt% BaSO₄ had wall thickness 170 ± 2.2 µm.

7.5.1. Thermal properties

DSC analysis of the composite tubes were carried out in order to study the thermal behaviour of the coated tube after week 1 and 7 of storage at room temperature. The summary of the data is listed in the Table 33. The DSC thermograms from first heating cycle after week 1 and 7 are presented in the Figure 85.

Table 33: Summary of the thermal properties of the P(3HB)/oligo-PHA composite tubes with 5 wt% barium sulphate after 1 and 7 weeks of storage. T_m = melting temperature, T_g = glass transition temperature, T_c = crystallisation temperature, ΔH_f =enthalpy of fusion.

Time of storage (week)	T_g (°C)	T_m (°C)	ΔH_f (J/G)	T_c (°C)
1	-1.7	173.8	79.1	53.4
7	-4.7	173.6	71.7	49.9

DSC analysis confirmed changes in the thermal behaviour of the material. After 7 weeks of storage the glass transition temperature has decreased. The temperature of melting remained stable within the period of 7 weeks. The cold-crystallisation temperature as well as the enthalpy of fusion presented similar trend. The largest changes were observed for the ΔH_f values, where after week 7, enthalpy of the composite tube decreased by about 10% in comparison to week 1. The T_c value decreased from 53.4°C to 49.9°C.

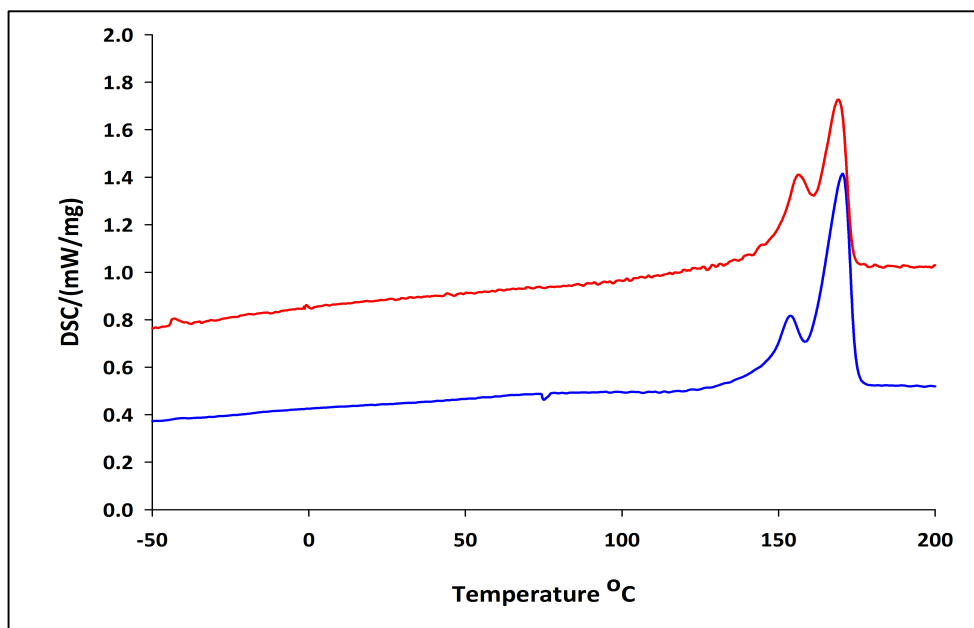


Figure 85: DSC thermograms of the P(3HB)/oligo-PHA composite tubes with 5 wt% barium sulphate after 1 week (■) and 7 weeks (■) of storage illustrating melting peaks.

The first heating cycles are presented in the Figure 85, which showed only melting event, related to the tested composite tubes. The temperature of the melting remained the same after 7 weeks of storage.

7.5.2. Mechanical properties

The analysis of the mechanical properties of the P(3HB)/oligo-PHA composite tubes stored at room temperature were carried out for 7 weeks, in order to check the material properties during material ageing. The results obtained are summarised in Table 34.

Table 34: Summary of the mechanical properties of the P(3HB)/oligo-PHA composite tubes with 5 wt% barium sulphate after 1 and 7 weeks of storage (n=3).

Week	Tensile strength (MPa)	Elongation at break (% strain)	Young's Modulus (GPa)
1	18.9±0.6	7.9±1.2	1.2±0.1
7	20.7±1.4	2.9±0.2	1.4±0.1

After 7 weeks of ageing at room temperature, the mechanical properties of the P(3HB)/oligo-PHA tubes had changed. The tensile strength increased from 18.9 ± 0.56 MPa at week 1 to 20.7 ± 1.4 MPa at week 7. Similarly, the Young's modulus values increased from 1.2 ± 0.1 GPa to 1.4 ± 0.1 GPa. The material became stronger and stiffer with the time. The elongation at break drastically decreased from $7.89 \pm 1.24\%$ strain to 2.9 ± 0.2 MPa, which confirmed the brittleness of the material. Material behaviour of the composite tubes observed during 7 weeks of storage at room temperature, followed the trend observed in the flat P(3HB) based composite films, described in details in Chapter 6.

7.5.3. SEM

Microstructural studies of P(3HB)/oligo-PHA composite tubes with 5% wt BaSO₄ were performed using Scanning Electron Microscopy. The surface of the cross section of the tube demonstrated that tubular structure of the stent was uniform (Figure 86A). Porosity of the material was not visible from the outer surface of the tube as well as within the tube wall (Figure 86B-D). The surface of the tube was even with some irregularities due to the presence of BaSO₄ particles (Figure 86D). The chosen processing conditions were appropriate to formulate tubular composite structures by using the dip moulding technique.

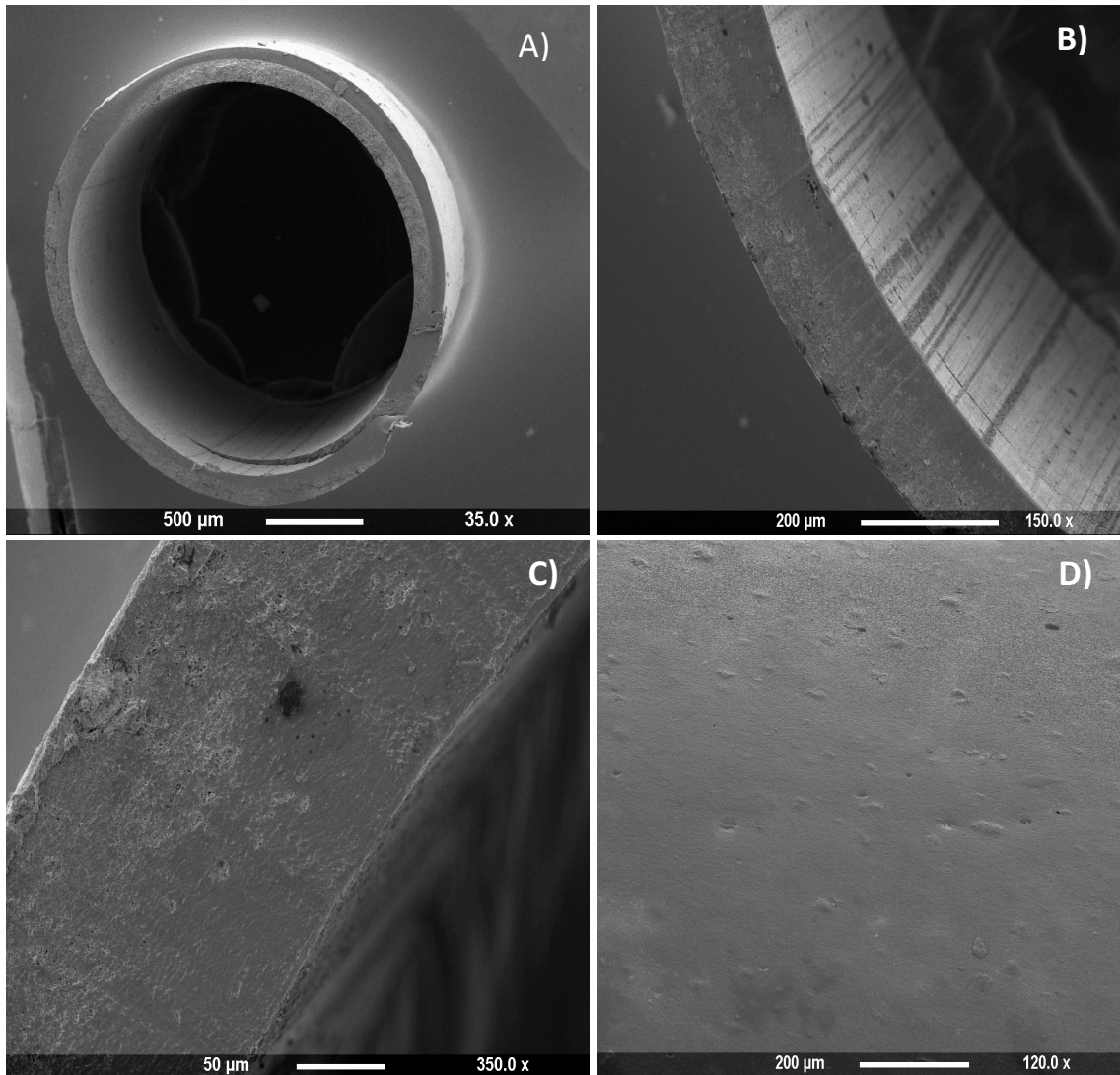


Figure 86: SEM micrographs of the P(3HB)/oligo-PHA composite tubes with 5 wt% barium sulphate: (A) tube cross-section, (B) wall thickness, (C) wall microstructure, (D) tube outer surface.

7.5.4. MicroCT

The composite tube was subjected to a microCT scan to observe barium sulphate particles, which has the characteristic of high X-ray attenuation (Figure 87).

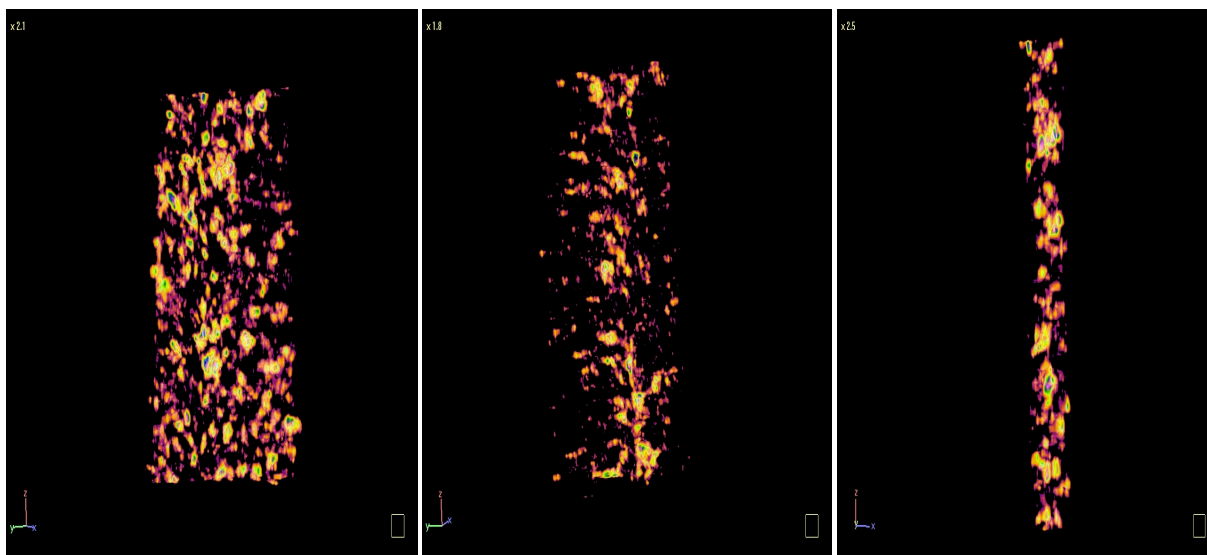


Figure 87: MicroCT micrographs demonstrated x-ray absorption by barium sulphate, presented in the P(3HB)/oligo-PHA composite tubes, containing 5 wt% BaSO₄.

From the micrographs presented in the Figure 87 it is evident that the barium sulphate was distributed uniformly within the polymeric matrix. The results obtained confirmed radiopacity of the composite tubes and possibility of using the composite for the application in the development of coronary stent prototypes.

7.6. *In vitro* biocompatibility studies of the range of manufactured PHA tubes

Neat P(3HB)/oligo-PHA tubes, coated tubes and composite tubes were characterised in order to evaluate their functionality as platform materials for biomedical applications.

7.6.1. Protein adsorption study

Bicinchoninic acid assay was used to evaluate the affinity of the materials towards proteins as described in section 2.11.3.9. It was found that total protein adsorption was 180.2 ± 4.5 , 225.6 ± 5.6 and $170.7 \pm 7.1 \mu\text{g}/\text{cm}^2$ for the neat P(3HB)/oligo-PHA neat tube, PCL-PEG550 coated tube and P(3HB)/oligo-PHA composite tube with 5 wt% barium sulphate respectively. All tested materials demonstrated higher protein adsorption than TCP. However, the results were significant only for tube coated with monolayer of PCL-PEG550 (* $p=0.019$). There was no significant difference between tissue control plastic and neat P(3HB)/oligo-PHA tube or PHA based composite tube with 5% wt BaSO₄ (Figure 88).

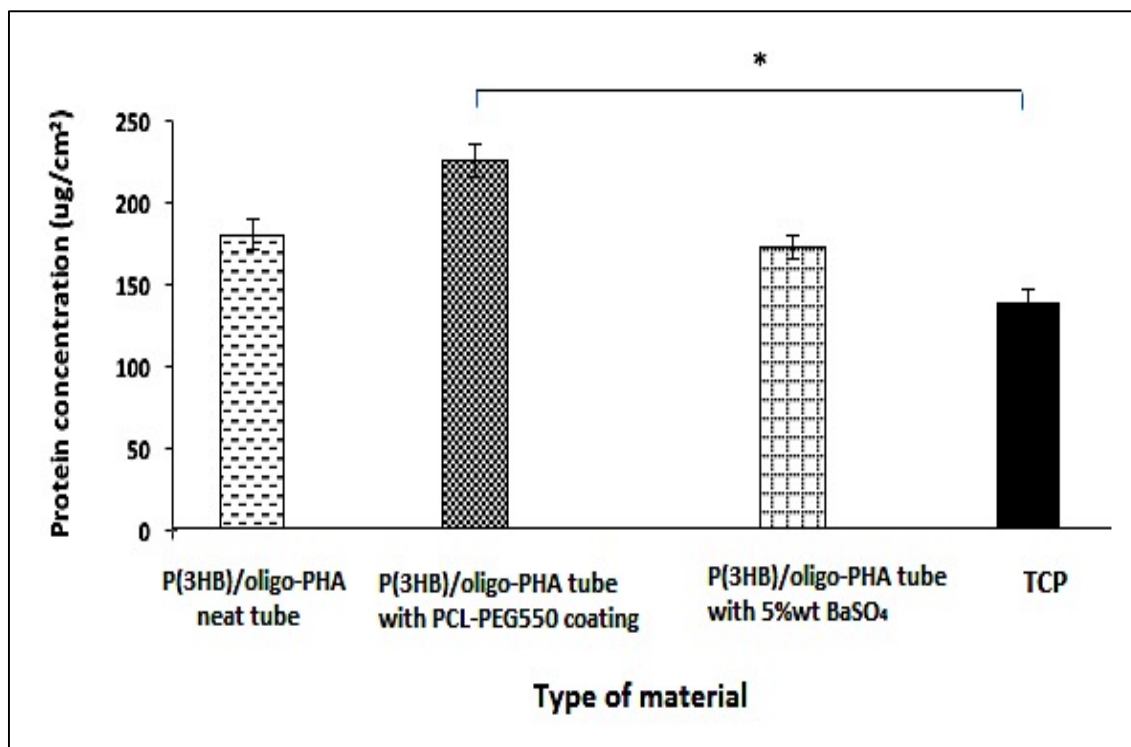


Figure 88: Protein adsorption to the neat P(3HB)/oligo-PHA, coated with PCL-PEG550 and composite tubes measured by BCA assay (n=3; error bars=±SD). The data were compared with standard tissue culture plastic using ANOVA. * indicates $p < 0.05$. P(3HB)/oligo-PHA tubes with coating layer of PCL-PEG550 adsorbed significantly higher concentration of proteins on the surface in comparison with TCP (positive control). The amount of proteins adsorbed to the TCP was $137.5 \pm 7.8 \mu\text{g}/\text{cm}^2$.

7.6.2. MTT assay

The MTT assay was used to evaluate cell adhesion and proliferation. Attachment and proliferation of HMEC-1 cells on the tube samples were studied over a period of 1, 3 and 7 days. The standard tissue culture plastic was used as the positive control for these experiments. The results of biocompatibility studies are presented in Figure 89

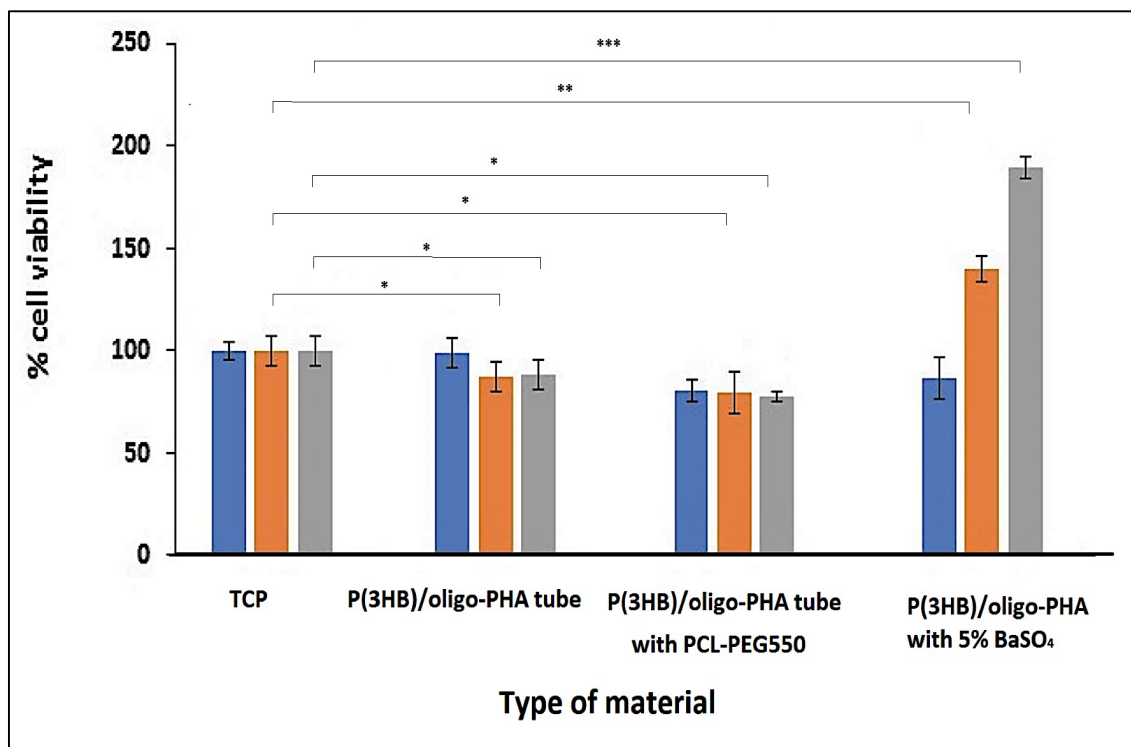


Figure 89: Cell proliferation study of HMEC-1 cells on the P(3HB)/oligo-PHA neat tubes, coated with monolayer of PCL-PEG550 and composite tubes with 5 wt% barium sulphate tube samples on day 1 (■), day 3 (■) and 7 (■) (n=3; error bars=±SD). The data were compared with standard tissue culture plastic using ANOVA. * indicates $p < 0.05$, ** indicates $p < 0.005$ and *** indicates $p < 0.0005$.

Cell proliferation on the surface of neat P(3HB)/oligo-PHA tubes was similar to TCP at day 1, but lower at day 3 and day 7. The observed cell viability on the tube samples was $98.7.6 \pm 7.6\%$ at day 1, $86.7 \pm 6.0\%$ at day 3 and $88.2 \pm 2.0\%$ at day 7 as compared to the TCP. The differences were statistically significant for results from day 3 and 7 (* $p=0.014$ and * $p=0.017$ respectively). The growth of the HMEC-1 cells on the surface of PCL-PEG550 coated tube was $80.0 \pm 5.2\%$ at day 1 and $79.4 \pm 4.5\%$ and $77.5 \pm 2.0\%$ at day 3 and 7 respectively. The differences were statistically significant for day 3 and 7 (* $p=0.013$, * $p=0.011$) in comparison to TCP. On the other hand, HMEC-1 cell viability on the composite tubes with 5 wt% BaSO₄ was slightly lower on day 1 ($87.7 \pm 3.5.0\%$) and higher on day 3 and 7 in relation to TCP: $140.5 \pm 6.5\%$ and $189.9 \pm 4.9\%$ respectively. The differences were statistically significant in comparison to TCP at day 3 (** $p=0.0082$) and day 7 (** $p=0.0001$).

The results obtained demonstrated higher biocompatibility of the P(3HB)/oligo-PHA composite tube with 5 wt% BaSO₄ in comparison to TCP, whereas the neat P(3HB)/oligo-PHA tube and PCL-PEG550 coated tube exhibited lower cell attachment on the surface. The highest cell adhesion was observed for P(3HB)/oligo-PHA composite tube with 5 wt% BaSO₄ within 7 days. The higher adhesion of the HMEC-1 cell line to the composite tube in comparison to the TCP indicated the possibility of application as a platform material in coronary stent application.

7.6.3. Indirect cytotoxicity study

Indirect cytotoxicity test was performed using MTT assay to investigate the influence of any leachable substances released from neat P(3HB)/oligo-PHA tube, P(3HB)/oligo-PHA tube with PCL-PEG550 coating and P(3HB)/oligo-PHA tube with 5% BaSO₄ into DMEM media on the HMEC-1 cell line. Cells without an extract were used as the negative control. 70% methanol instead of media or extract was used as a positive control. Results obtained were summarised in the Figure 90.

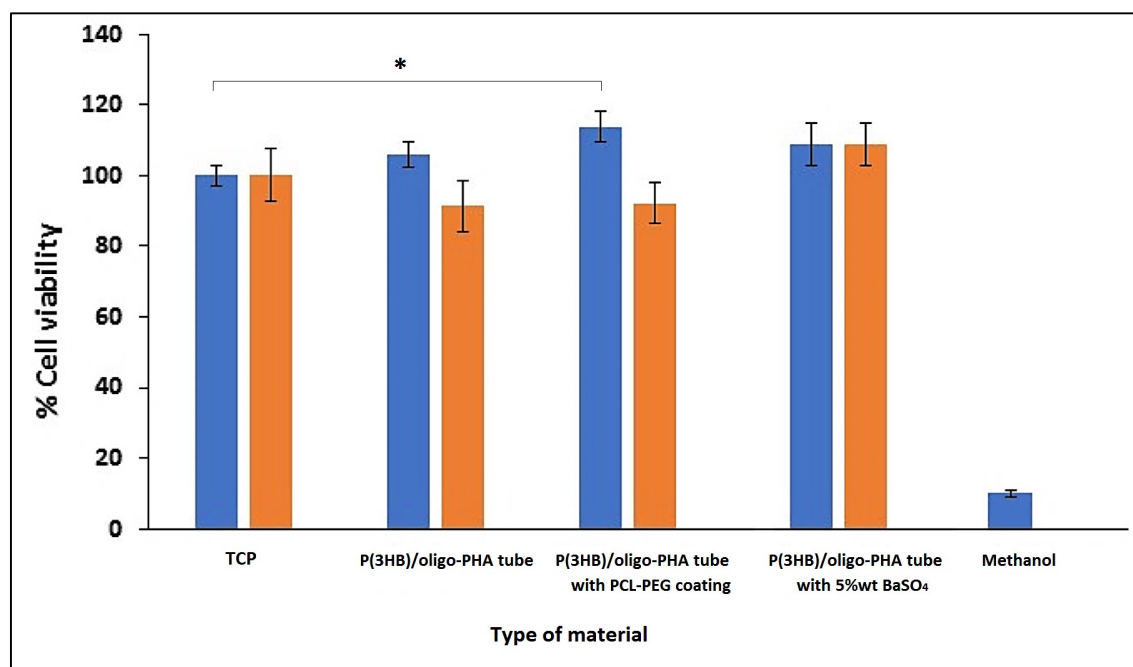


Figure 90: Indirect cytotoxicity study of the HMEC-1 cells on the P(3HB)/oligo-PHA neat tubes, coated with monolayer of PCL-PEG550 and P(3HB)/oligo-PHA composite tubes with 5 wt% barium sulphate tube samples on day 1 (■) and day 3 (■) (n=3; error

bars= \pm SD). The data were compared with standard tissue culture plastic using ANOVA. * indicates $p < 0.05$, ** indicates $p < 0.005$ and *** indicates $p < 0.0005$.

Cell proliferation on the neat P(3HB)/oligo-PHA tube extract was $106.0 \pm 3.5\%$ at day 1 and $91.4 \pm 4.4\%$ at day 3 compared to the TCP. The differences were not statistically significant. The growth of HMEC-1 cells treated with an extract from the neat P(3HB)/oligo-PHA tube was similar on day 1 and 3 to TCP. The growth of the HMEC-1 cells with extract from PCL-PEG550 coated tube was higher than TCP on day 1 (113.9 ± 4.3). The difference was statistically significant (* $p = 0.035$). HMEC-1 cell viability in the extract from P(3HB)/oligo-PHA composite tube with 5 wt% BaSO₄ was also higher on day 1 and 3 in relation to TCP: $108.06 \pm 4.8\%$ and $109.1 \pm 6.0\%$. The difference was not significant in comparison to TCP. The highest viability of the HMEC-1 cells was achieved after treatment with an extract from coated tubes in comparison to TCP after 1 day of incubation. The results obtained confirmed an absence of any cytotoxic substances released from the composite. All tested extracts supported the cells attachment and proliferation similar to the standard tissue culture plastic. Therefore, PHAs based tubes can be considered as potential materials for biomedical applications, such as coronary stent prototype production.

7.6.4. SEM

Cell adhesion and proliferation was further characterised using SEM microscopy. SEM images presented in Figure 91 revealed that HMEC-1 cells adhered and proliferated on the surface of the tubes. Cell density was much higher for composite tube with an addition of 5 wt% of barium sulphate. All PHA-based materials supported HMEC-1 cell attachment and proliferation demonstrating good biocompatibility. Addition of barium sulphate improved cell proliferation with the highest cell viability was achieved for composite tube.

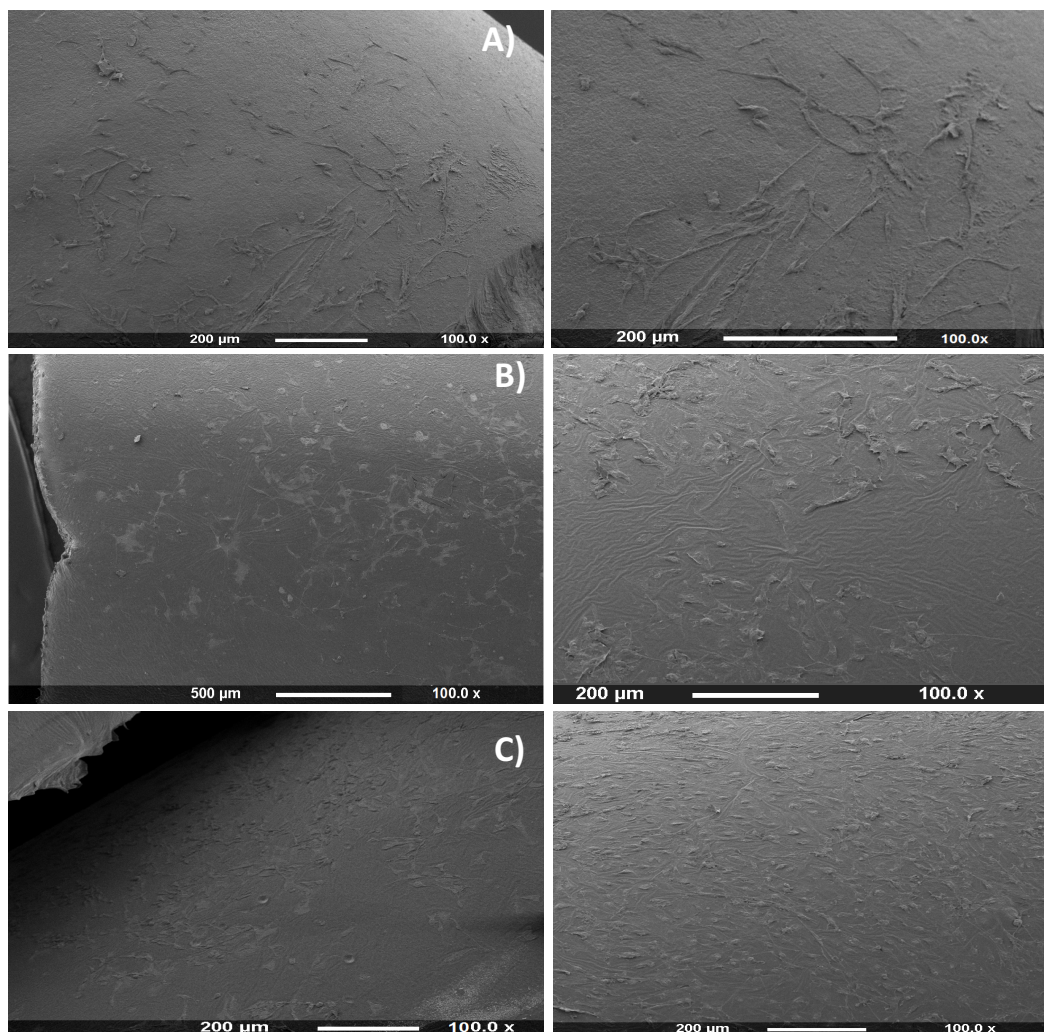


Figure 91: SEM images of the surfaces of P(3HB)/oligo-PHA neat tubes (A), PCL-PEG550 coated tubes (B) and P(3HB)/oligo-PHA composite tubes with 5 wt% BaSO₄ (C) after culturing HMEC-1 cells for 7 days.

With respect to the results obtained, all tested materials based on P(3HB)/oligo-PHAs supported the growth of HMEC-1 cell line. However, the addition of barium sulphate resulted in much higher cell attachment after 7 days of incubation. Presence of PCL-PEG550 in the coating did not have any negative impact on the biocompatibility of the tested materials to the endothelial cell line.

7.7. *In vitro* haemocompatibility studies

P(3HB)/oligo-PHA neat tubes, PCL-PEG550 coated tubes and P(3HB)/oligo-PHA composite tubes with 5 wt% barium sulphate blends were subjected to haemocompatibility studies, which includes haemolysis studies, whole blood clotting as well as monocytes and neutrophils activation.

7.7.1. Haemolysis study

Haemolysis study was performed on PHAs based tubular structures to investigate an effect of the materials on the erythrocytes after direct contact with fresh whole blood. The analysis was performed as described in the section 2.15.1. The results obtained are shown at the Figure 92.

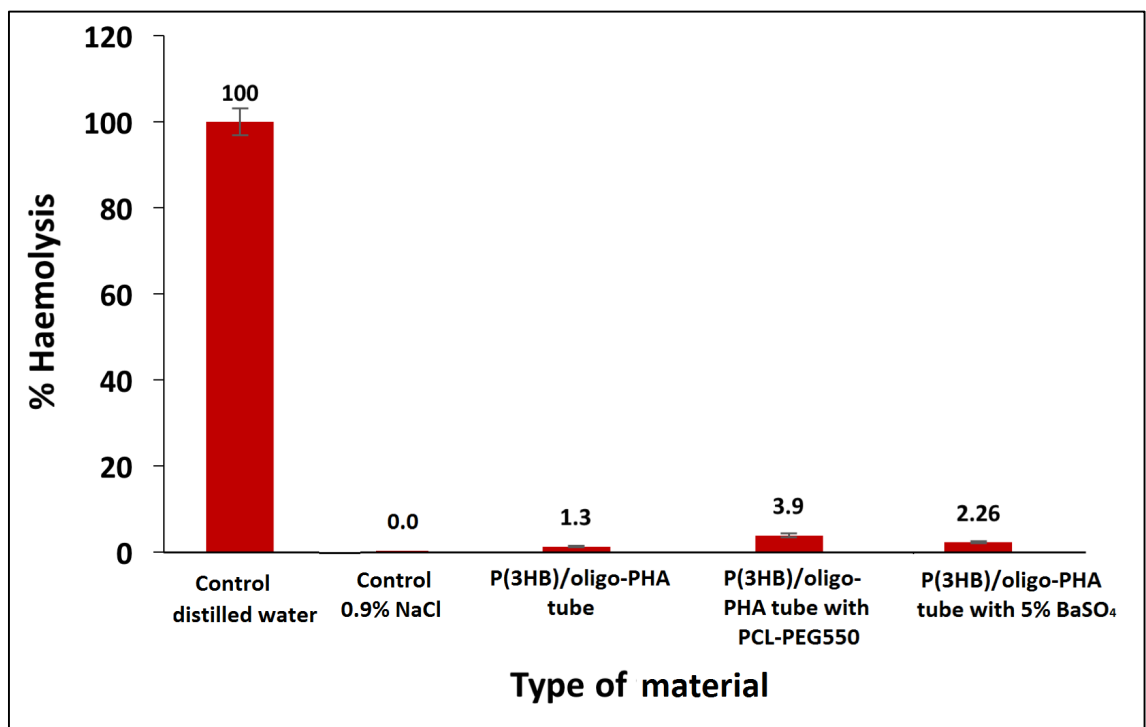


Figure 92: Haemolysis rates of the P(3HB)/oligo-PHA neat tubes, tubes coated with PCL-PEG550 and composite tube with barium sulphate after 1h of incubation at 37°C (n=3). Results were compared to TCP using ANOVA. No significant difference.

All tested types of tubes presented non-haemolytic effect on erythrocytes. A percent haemolysis of 1.3%, 3.9% and 2.3% was obtained for the neat tube, coated tube and composite tube respectively. The results were not significant in comparison to TCP.

According to ISO 10993-4:2002 standard, all tested tubes demonstrated low potential to destroy red blood cells.

7.7.2. Whole blood clotting

Whole blood clotting experiment was performed to investigate the potential thrombogenicity of the different types of tubes as described previously in the section 2.15.2. The summary of the results obtained after 30 and 90 minutes are shown in Figure 93.

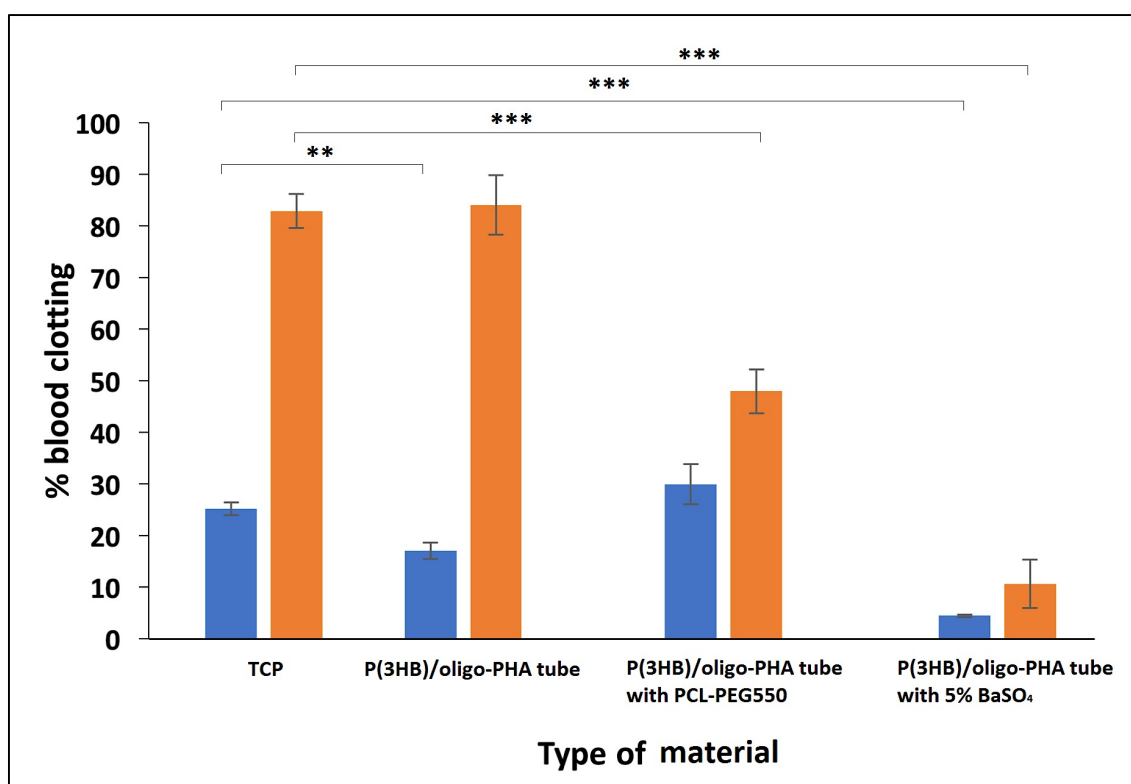


Figure 93: Whole blood clotting after 30 minutes (■) and 90 minutes (■) of incubation on the neat P(3HB)/oligo-PHA tubes, coated with PCL-PEG550 and composite tubes with 5 wt% barium sulphate. sulphate and PL38 (n=3; error bars=±SD). The data were compared with standard tissue culture plastic using ANOVA. **indicates $p < 0.005$ and *** indicates $p < 0.0005$.

The results obtained indicate that P(3HB)/oligo-PHA neat tube and the PCL-PEG550 coated tube enhanced the activation of the coagulation cascade, whereas, the composite tube containing BaSO₄ did not demonstrate similar effect. After 30 minutes

of incubation, neat PHA tube demonstrated $17.0 \pm 1.6\%$ blood clotting. Addition of PCL-PEG550 as a coating resulted in increased % blood clotting after 30 minutes to $29.9 \pm 3.1\%$. P(3HB)/oligo-PHA composite tube with 5 wt% barium sulphate exhibited a blood clotting rate of $4.5 \pm 0.2\%$ after 30 minutes. With the increase of time, the % blood clot increased in all tested materials as well as in the control. After 90 minutes the blood control demonstrated $82.9 \pm 3.3\%$ blood clotting. P(3HB)/oligo-PHA neat tube resulted in slight increase in the blood clotting rate up to $84 \pm 5.7\%$. PCL-PEG coated tube presented decreased blood clotting rate ($47.9 \pm 2.2\%$) in comparison to the control ($82.9 \pm 3.3\%$). The result was significant ($***p=0.0006$). The results obtained for the composite tubes were considered as significantly lower than the positive control ($***p=0.0001$). Addition of barium sulphate resulted in much lower blood clotting than neat P(3HB)/oligo-PHA tube or PCL-PEG550 coated tube. To summarise, all tested materials did not demonstrate increased risk of thrombogenicity and can be considered as a biomaterial for medical applications, such as coronary stent.

7.7.3. Monocytes and neutrophils activation

Three different types of tubes: neat P(3HB)/oligo-PHA, PCL-PEG550 coated tube and P(3HB)/oligo-PHA composite tube with 5% wt BaSO₄ were incubated with whole blood at 37°C overnight and stained with the markers listed in the section 2.15.3.1. Summary of the results obtained was demonstrated in Table 35.

Table 35: Summary of median fluorescence intensity (MFI) obtained after incubation of fresh whole blood with P(3HB)/oligo-PHA 90/10 neat tube, P(3HB)/oligo-PHA 90/10 tube coated with PCL-PEG550, P(3HB)/oligo-PHA composite tube with 5% wt barium sulphate and PL38; and stained with specific markers in order to evaluate monocyte and neutrophil activity.

Sample	Markers	Monocytes Activity (MFI)	Percentage change (%)	Neutrophils Activity (MFI)	Percentage change (%)
P(3HB)/oligo-PHA 90/10 tube	CD86-PE	181.5	57.9	162.6	3.5
	CD45-PerCP	225.4	106.0	121.9	3.6
	CD11b-PE	536.8	294.9	666.1	372.7
	CD66B-FITC	188.2	-	279.9	71.9
P(3HB)/oligo-PHA 90/10 tube coated with PCL-PEG550	CD86-PE	209.7	82.5	175.3	11.6
	CD45-PerCP	135.9	0.0	76.3	-
	CD11b-PE	498.9	267.1	586.8	316.5
	CD66B-FITC	168.8	-	279.8	71.8
P(3HB)/oligo-PHA 90/10 composite tube with 5% BaSO ₄	CD86-PE	140.9	22.6	116.7	-
	CD45-PerCP	94.7	-	86.8	-
	CD11b-PE	857.7	531.1	991.2	603.5
	CD66B-FITC	105.6	-	117.6	-

Results obtained after staining blood samples, which were exposed to various types of tubes demonstrated different levels of activity of monocytes as well as neutrophils. All tested samples presented higher activity of the activation marker CD11b-PE. However, the level of activity was lower than in the samples activated by addition of LPS (Chapter 5, Table 21). Among three types of tubes, P(3HB)/oligo-PHA tube coated with PCL-PEG550 demonstrated the lowest values of CD11b marker: 267.1% for monocytes and 316.5% for neutrophils activity higher than control. The percentage change of MFI for P(3HB)/oligo-PHA tube was 294.9% for monocytes and 372.7% for monocytes and

neutrophils respectively in comparison to control. P(3HB)/oligo-PHA composite tube with 5 wt% BaSO₄ demonstrated percentage change 531.1% for monocytes and 603.5% for neutrophils activation marker CD11b in comparison to control. The results obtained further confirmed, that addition of barium sulphate causes an increased activation of neutrophils and monocytes, which was indicated previously in Chapter 6. It is worth mentioning, that percentage change of MFI of composite tube was lower than flat composite films described previously in the Chapter 6.

7.8. Discussion

In this study three types of tubes were prepared using the dip moulding technique, such as neat P(3HB)/oligo-PHA tube in the ratio 90/10, P(3HB)/oligo-PHA tube coated PCL-PEG550 and composite tube, prepared by addition of 5 wt% barium sulphate to the P(3HB)/oligo-PHA blend. The tubes were characterised in order to obtain thermal and mechanical properties, topography studies as well as biocompatibility. The tubes were subjected to ageing for 7 weeks in order to obtain final material properties.

Storage of fabricated tubes for 7 weeks at room temperature resulted in changes in thermal and mechanical properties of neat P(3HB)/oligo-PHA tubes. After 7 weeks of storage, neat tubes stored at room temperature demonstrated an increase in the glass transition temperature, cold-crystallisation and melting temperature within the time of storage. Tensile strength and Young's Modulus values increased, whereas elongation at break decreased, as expected. Material behaviour during storage time is closely related to material ageing. Changes in the properties of P(3HB) and its copolymers during storage time at room temperature has been already recognised. Elongation at break is the main parameter, which change within the time of storage and is a measurement of material increased brittleness. The main process, which causes P(3HB) ageing during storage at room temperature is called post-crystallisation (Wen *et al.*, 2011; Hong *et al.*, 2011). All three parameters, which determine mechanical properties for the tubes were similar to those obtained for the flat films, except the tensile strength, which was 25% lower for the films in comparison to the tubes. This might be explained by applying completely different conditions during tube preparation, such as presence of an additional solvent (1,1,2,2-tetrachloroethane) and temperature of 50°C during dip

coating and drying time. While solvent cast films were prepared by dissolving PHAs in chloroform only at room temperature. Dip coating allows partial solvents evaporation from each layer after each dipping cycle, whereas in solvent cast technique, solvent evaporation rate is lower and chloroform gradually evaporates from the surface of the polymer solution until thin film remains. It has been reported previously, that processing technique has great impact on the material properties (Renstadt *et al.*, 1998). Interestingly, the changes in the mechanical properties of the tubes incubated in the DMEM media at 37°C for the period of 7 weeks resulted in much lower values for all measured parameters in comparison to the tubes stored dry at room temperature. Tubes in DMEM medium became more brittle and less stiff in comparison to the materials storage at room temperature. Results obtained were in an agreement with literature, that temperature and hydrophilic environment has a crucial impact on the mechanical properties of the material (Lyu and Untereker, 2009). Coronary stents will be placed inside the artery and constantly surrounded by blood in body, hence material properties obtained after incubation of tubes in DMEM media at 37°C can help to predict the material behaviour inside the human body.

Biodegradability of polyhydroxyalkanoates depends not only on their own material properties, such as crystallinity, presence of functional groups, but also on the surface area and the conditions in the surrounding environment, such as pH, temperature, moisture, presence of nutrients or microbial activity (Sudesh *et al.*, 2000; Doi *et al.*, 1989). Highly crystalline materials require longer time to degrade in comparison to semi-crystalline or amorphous materials (Miller *et al.*, 1977). Hydrolysis preferably occurs around the chain ends, which are usually placed in the amorphous part of the polymer (Yavuz *et al.*, 2002). When amorphous regions are degraded, hydrolytic attack progress within crystalline domains, leading to their degradation. Molecules in the amorphous regions are loosely packed and more susceptible towards reacting species or solvents than in crystalline region (Yavuz *et al.*, 2002). Also, molecular weight seems to be a very important factor. It was found, that PHAs with low molecular weight are more susceptible degradation. The thermal properties of the materials have an influence on the degradation rate. Generally, with an increase of melting temperature, the biodegradability of the material decrease (Philip *et al.*, 2007). Anjum and co-workers

reported that PHAs can degrade in aquatic environments within 254 days at temperature below 60°C (Anjum *et al.*, 2016).

In general, polymer degradation takes place mostly through scission of the main chains or the side-chains of the polymer structure. It can be induced by thermal activation, photolysis, oxidation, radiolysis or hydrolysis (Doi and Fukuda, 1994; Benicewicz and Hopper, 1991). The degradation process via hydrolysis can occur with or without the presence of enzymes; it can be catalysed by the presence of acid or base in the environment (Rydz *et al.*, 2015; Ikada and Tsuji, 2000). Different factors can trigger the degradation process, like for example temperature. Therefore, one of the very important aspects to consider are processing conditions and chosen fabrication techniques. For example, melt extrusion and injection moulding require high temperature and shear rate, which might lead to certain level of degradation of the material. Injection moulding causes partial orientation, usually higher in the external layer, than the core of the mould. This can trigger faster degradation of the material in the core of the mould rather than from the outer layer. Also, various additives, such as plasticizers, stabilizers, lubricants, antioxidants, salts might either enhance or decelerate degradation rate of the materials (Azevedo and Reis, 2004; Yoshie *et al.*, 2000). In this study, *In vitro* degradation studies demonstrated high percentage of water adsorption and accelerated weight loss after 3 months of incubation. Minor changes in the pH during the degradation suggested absence of the highly acidic products released during polymer degradation. It is a well-known that the degradation products released from synthetic polymers, such as PLLA are highly acidic, which can trigger an elevated immunogenic response in the body (Mani *et al.*, 2007; Liu *et al.*, 2006). Hydrolytic degradation of PHAs is a slow process, which can take up to several months (Marois *et al.*, 2000; Doi *et al.*, 1990). Addition of polymers or plasticizers can increase the degradation rate of P(3HB). Addition of hydrophilic as well as amorphous materials enlarge water adsorption which speeds up hydrolysis (Freier *et al.*, 2002). The influence of addition of PLA and PEG to PHAs on degradation was studied. PLA and PEG enhanced the degradation rate only in PHBV, without any effect on the degradation of P(3HO) due to incompatibility of the system (Renart *et al.*, 2004). In this study, an addition of oligo-PHA accelerated the degradation rate of the PHA tubes. It was already observed by Zhang and co-workers, that addition of amorphous polymers or plasticizers can lead to

advanced degradation (Zhang *et al.*, 1996). The blend of P(3HB) with the oligomer of P(3HHx-3HO-3HD-3HDD) was a compatible system and plasticising effect occurred. Hence, this could accelerate degradation. It is worth mentioning, that PHA-based tubes, studied in this project degraded by surface erosion, which is a typical property of PHAs. In this study, an increased porosity was observed in the external layer of the tube. This can support the statement mentioned above. Another reason for enhanced porosity might be possible migration of oligo-PHA from the polymeric matrix. Plasticiser migration is one of the most important problems associated with this process (Papakonstantinou and Papaspyrides, 1994). Plasticisers do not bond to the polymeric chains. They penetrate the polymeric matrix, increase free volume, keep near chains in the distance and allow increased movement of polymer chains (Reinecke *et al.*, 2011). In this study, after 3 months of degradation studies, tubes became fragile, brittle and very difficult to handle without damaging the structure.

In the second part of study P(3HB)/oligo-PHA tubes were coated by a monolayer of PCL-PEG550. FTIR analysis have proven the presence of chemical bonds typical to PCL and PEG within the tube. Thermal analysis of the coated tubes demonstrated the presence of the PCL-PEG by the appearance of an additional melting event, observed around 60°C, which is a melting temperature of PCL (Sui *et al.*, 2015). DSC analysis of the coated tubes demonstrated presence two different melting points, which suggest presence of two different types of polymers, which are not miscible with each other. One peak belongs to PCL-PEG550 at 60°C and second peak at 167 °C is characteristic for P(3HB)/oligo-PHA blend (Chapter 5, Figure 41). Storage of the coated tubes resulted in changes in thermal and mechanical properties. The glass transition temperature increased, whereas, cold-crystallisation temperature and enthalpy of fusion, related to PHAs decreased. This behaviour was similar to the neat tube. With respect to the mechanical properties, tensile strength of the material as well as stiffness have improved significantly. Initially, the elongation at break of the coated tube was lower than the neat tube and decreased slightly within 7 weeks. The presence of PCL-PEG550 has a positive impact on the mechanical properties of the tube, such as strength, stiffness and ductility, which makes this material very attractive for coronary stent application. Presence of synthetic coating (PCL-PEG550) reduced the deteriorating effect of material ageing on the elongation at

break of the tubes. Elongation at break decreased only 16% in the PCL-PEG550 coated tubes in comparison to 66% reduction in case of the neat P(3HB)/oligo-PHA tubes.

The third type of tubes was prepared from P(3HB)/oligo-PHA 90/10 blend with an addition of 5 wt% barium sulphate. Within 7 weeks of storage the glass transition temperature, enthalpy of fusion and cold-crystallisation temperature decreased. There was no impact on melting temperature within 7 weeks of storage. Addition of barium sulphate drastically influenced the elongation at break. The composite tube became very brittle after 7 weeks of storage. However, the material became much stronger and stiffer after week 7 in comparison to week 1. Addition of barium sulphate also had an impact on the topography and structure of the tubes. SEM micrographs confirmed complete absence of porosity within the tube wall structure. This can be explained by the fact, that BaSO₄ particles could act as fillers of potential spaces within polymeric matrix. The surface of the tube was rougher due to the presence of the BaSO₄ particles in comparison to the neat P(3HB)/oligo-PHA tube. This is with agreement with data obtained earlier, where the solvent cast film composites with an addition of 5% wt BaSO₄ resulted in significant increase of surface roughness (Chapter 6, Figure 59). Additionally, presence of barium sulphate lead in obtaining intense signals by high x-ray absorption, which confirmed the radiopacity of the tube.

Protein adsorption studies revealed higher protein attachment to all types of studied tubes in comparison to TCP. Protein adsorption is a first step in the integration between implanted material and tissue (Horbett, 2004). However, the differences were significant only for the PCL-PEG550 coated tube in comparison to standard tissue culture plastic. This might be explained by the wettability of the material. PCL-PEG550 has a contact angle of around 61°, whereas PHAs have usually much higher values of contact angle. The biocompatibility study resulted in much higher cell viability obtained for the composite tube in comparison to TCP and other tubes tested. Neat and coated tube had relatively lower cell viability. This can be explained by different surface topography of the tube. Neat tube and coated tube had very smooth and even surface, which might affect cell attachment. Presence of particles, allow obtaining rougher and enlarge surface area, which creates attachment points for cells (Hao and Lawrence, 2004). It will be worth to investigate further an influence of barium ions on the functional behaviour of the endothelial cells. SEM images confirmed results obtained from the

MTT assay. SEM micrographs clearly demonstrated increased cell density on the tubes with an addition of barium sulphate in comparison to neat P(3HB)/oligo-PHA tube and PHA tube coated with PCL-PEG550. Obtained results suggest, that surface roughness was a crucial factor required for high endothelial cell attachment. Considering other factors, important for cell attachment and proliferation, such as protein adsorption or wettability of the material, endothelial cells should drive more towards P(3HB)/oligo-PHA tube coated with PCL-PEG550. Material stiffness is another factor, recently gaining much attention in correlation to cell attachment (Gu *et al.*, 2012). However, in this study there was no difference between Young's Modulus values between composite and PCL-PEG550 coated tube.

Biodegradable polymers always release low molecular weight compounds into the surrounding environment as a result of degradation. Those foreign compounds might enter the cell or interact with the surface, leading to abnormal functionality (Ikada and Tsuji, 2000). Indirect cytotoxicity study confirmed non-toxic effect of an extract released from the materials incubated in the media. Moreover, PCL-PEG550 coated tube demonstrated higher cell viability after day 1 as compared to TCP.

All type of tested tubes did not have any haemolytic effect towards red blood cells. Neat P(3HB)/oligo-PHA tube demonstrated blood clotting rate similar to the control. PCL-PEG550 coated tube and the composite tube resulted in decelerated blood clot formation. This can be explained by the presence of poly (ethylene glycol) unit, which is a well-known anti-coagulant due to presence of an ether oxygen within the monomer units, which hinder proteins adsorption (Meyers and Grinstaff, 2012). Moreover, barium ions seem to block an activation of the coagulation cascade, probably by displacement of Ca ions, which are required to trigger blood clotting process. All tested tubes demonstrated elevated monocytes and neutrophils activity. However, the values were lower than that obtained for the solvent cast flat films. The highest activity was obtained for the composite tube, due to presence of barium sulphate, which is a well-known trigger for white cell activation (Lazarus *et al.*, 1994). The 3D tubular structure of studied PHA constructs did not have any detrimental effect on the blood cells.

The results obtained confirmed high biocompatibility of the P(3HB)/oligo-PHA based tubes to HMEC-1 cells. Therefore, all the tubes tested can be suitable candidates for coronary stent application. The composite P(3HB)/oligo-PHA tube with barium sulphate

presented an additional advantage over the neat P(3HB)/oligo-PHA and PCL-PEG550 coated P(3HB)/oligo-PHA tube, such as presence of radiopacity and higher biocompatibility.

Chapter 8

Development of P(3HB)/oligo- PHA tubes with incorporated drug

8. Introduction

Drug eluting stents (DES) were discovered as a second generation of stent, to overcome the limitations accompanied to bare metallic stents, such as restenosis. The drug was released locally rather than in a systemic manner. DES usually contain three parts: stent, coating and bioactive agent (Ako *et al.*, 2007). Initially, the results obtained from clinical trials were very promising. However, the long-term side effects appeared, such as thrombosis, which can lead to sudden death (Windecker and Meier, 2007). As a polymeric matrix, non-biodegradable, biodegradable and biological polymers have been studied (Puskas *et al.*, 2009). Four classes of drugs, such as: anti-inflammatory, antiproliferative, antithrombogenic and immunosuppressive have been taken into consideration for DES (Grube *et al.*, 2002). Several different drugs have been tested so far. The most common are the immunosuppressive drugs, which belongs to the “limus” family, such as: sirolimus, everolimus, tacrolimus, zotarolimus, biolimus A9, as well as actinomycin D, dexamethasone or paclitaxel (Khan *et al.*, 2012)., described previously in the section 1.5. Many research groups have been focusing on the development of appropriate drug delivery systems, to allow controlled drug delivery of the bioactive agent. Rapamycin, also referred as sirolimus is a macrocyclic antibiotic produced by natural fermentation which exhibits potential immunosuppressive properties. It has the ability to block several phases in the development of the restenosis cascade (van der Hoeven *et al.*, 2005). Tacrolimus is an immunosuppressive agent, which has less inhibitory effect on the cells attachment and migration in comparison to rapamycin, therefore can be considered as promising agent to be use in coronary stents (Matter *et al.*, 2006). Although first DES were based on metals, a lot of attention was put towards bioresorbable materials, such as biodegradable polymers or corrodible metals. None of the materials have met all specific requirements, such as high biocompatibility, appropriate mechanical properties, degradation kinetics and inflammation. There is still high demand for the development of novel materials (Ramcharitar and Serruys, 2008). Polyhydroxyalkanoates are biopolyesters, which were not studied extensively in coronary stents, but have been studied as drug delivery vehicles. They are very promising materials for drug delivery systems due to proven biodegradability, non-toxicity and biocompatibility (Williams and Martin, 2005). Mainly P(3HB) and its copolymers, such as: P(3HB-co-3HV) and P(3HB-co-4HB) were explored for drug delivery

applications. Microspheres, nanoparticles, rods, discs, biodegradable implants, films with different drugs, such as: gentamycin, aspirin, cefoperazone, doxorubicin, tetracycline and ampicillin have been developed (Nigmatullin *et al.*, 2015). P(3HB)/P(3HO) blends were proposed as a matrix for drug carrier in DES (Basnett *et al.*, 2013).

Both drugs, rapamycin and tacrolimus are considered as the bioactive agents for coronary stents. Therefore, the main aim of this part of the project was to develop P(3HB)/oligo-PHA based tubes using the dip moulding technique with incorporated drugs, such as rapamycin or tacrolimus for the development of medical devices, such as coronary stents. Each drug was dissolved in the PCL-PEG550 polymeric matrix and applied on the surface of the tube as a monolayer. The materials were fully characterized. *In vitro* biocompatibility of the tubes was tested with human dermal microvascular endothelial cells (HMEC-1) in order to evaluate the potential of new biodegradable material in applications such as coronary artery stent. Haemocompatibility studies were carried out in order to study the impact of the tubes with incorporated drugs on blood cells. Additionally, drug release studies were carried out in order to investigate the rate of drug elution from the device. *In vitro* degradation study was also performed on the PCL-PEG550 coated P(3HB)/oligo-PHA tubes to investigate the degradation rate of the coated PHA tubes with incorporated drugs.

8.1. Drugs characterisation

Analysis of the chemical nature and thermal properties of rapamycin and tacrolimus powders were carried out using Fourier Transform Infrared Spectroscopy and Differential Scanning Calorimetry respectively.

8.1.1. Attenuated Total Reflectance Fourier Transform Infrared Spectroscopy (ATR/FT-IR)

The ATR/FTIR spectrum of rapamycin (Figure 94) present few chemical bonds, characteristic of rapamycin. There is an adsorption peak at 2947cm^{-1} which corresponds to asymmetric stretching $-\text{CH}_2$. The carbonyl bond is present at the wavenumber 1716.3

cm^{-1} . Additionally, two bonds, typical to imines are present at 1644.6 cm^{-1} (C=N) and 1633.6 cm^{-1} (C-N) respectively.

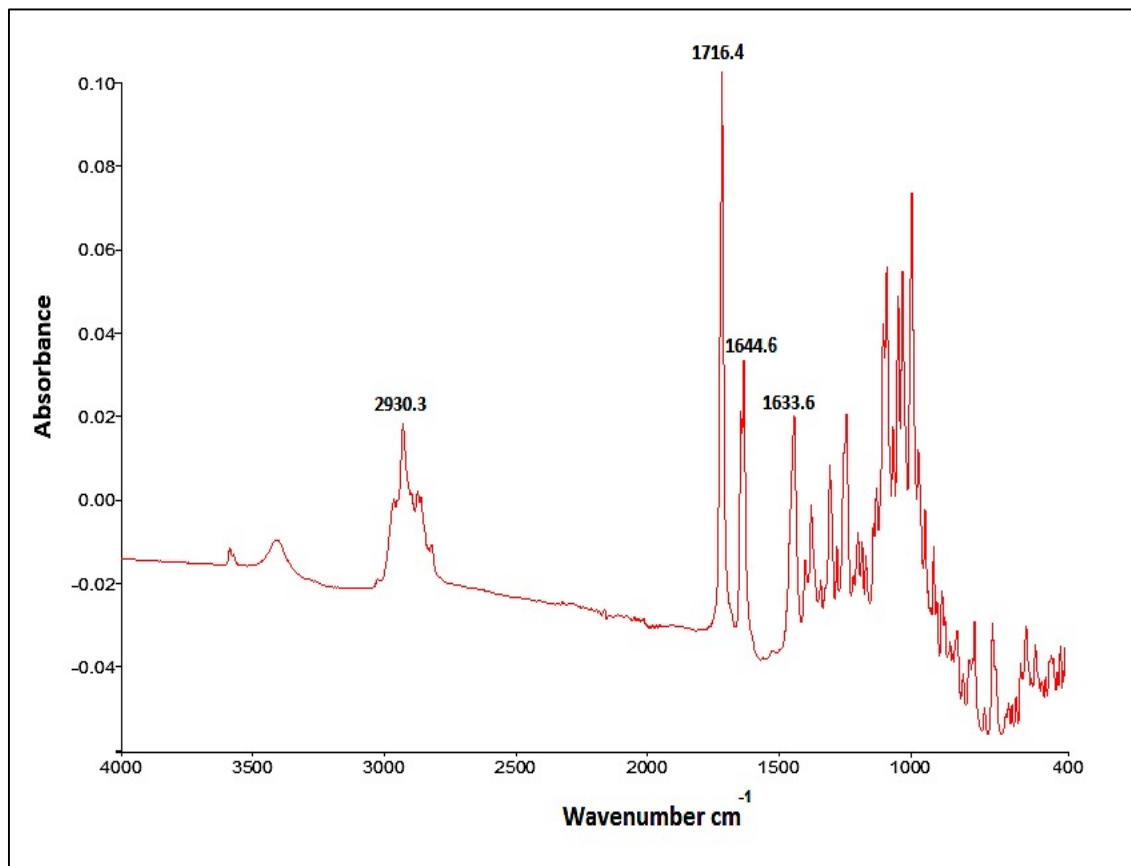


Figure 94: ATR/FTIR spectrum of rapamycin powder indicating characteristic peaks corresponding to chemical bonds observed in rapamycin.

The tacrolimus powder exhibited various peaks related to the functional groups present in the structure of tacrolimus (Figure 95). There was a peak at 3438 cm^{-1} , which corresponded to O-H stretching vibration. Carbonyl group C = O (ester and ketone) stretching vibrations were present at 1739.8 cm^{-1} . An absorption peak at 1692.3 cm^{-1} and 1636.4 cm^{-1} corresponded to the keto-amide group C=O and C=C stretching vibration respectively. Additionally, the C–O (ester) stretching vibration was present at 1191.2 cm^{-1} and the ether group C–O–C (ether) stretching vibration at 1087.2 cm^{-1} .

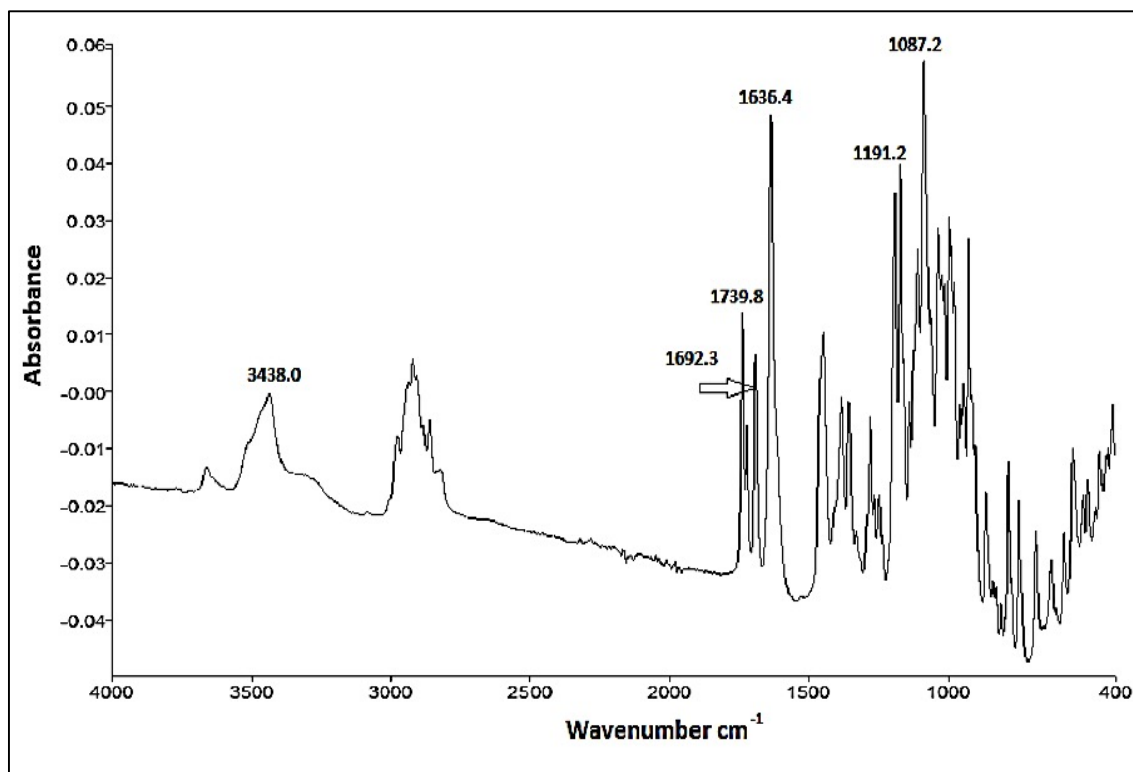


Figure 95: ATR/FTIR spectrum of tacrolimus indicating characteristic peaks corresponding to chemical bonds observed in tacrolimus structure.

Obtained ATR/FTIR spectra of the rapamycin and tacrolimus represent chemical bonds, typical of their chemical structures, corresponded with literature (Patel *et al.*, 2013).

8.1.2. Differential Scanning Calorimetry

DSC analysis of the rapamycin and tacrolimus powder was carried out in order to study thermal properties of the drugs. The thermograms are shown in the Figure 96 and 97 for rapamycin and tacrolimus respectively.

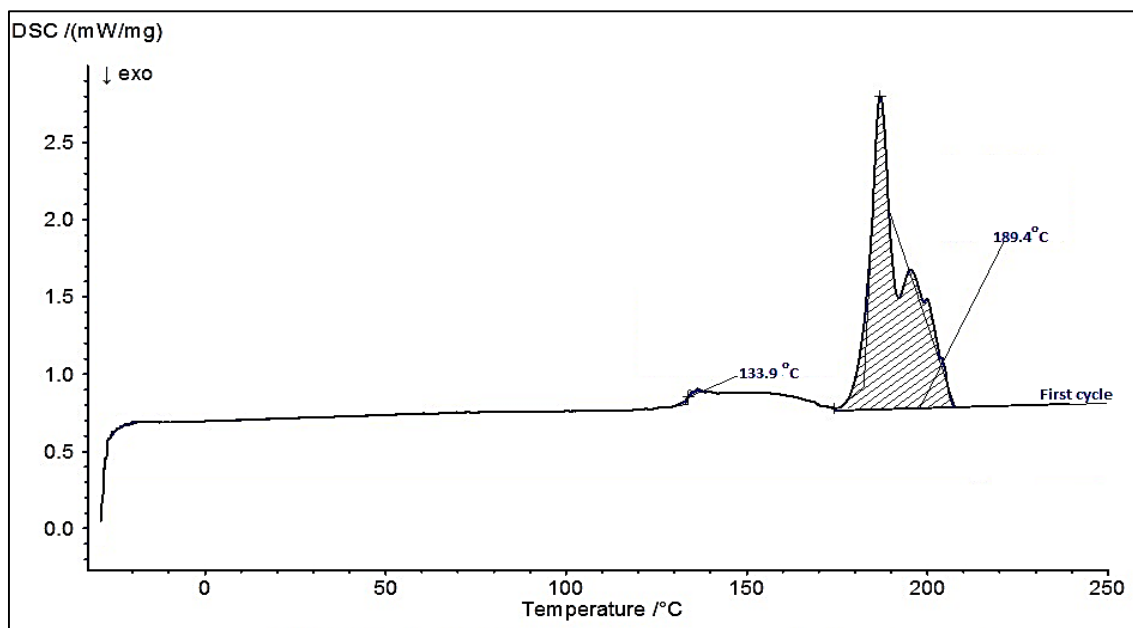


Figure 96: DSC thermograms of rapamycin registered during first heating cycle.

One heating cycle was performed during DSC analysis in order to obtain the thermal properties of the drugs. The thermogram for rapamycin, presented in the Figure 96 demonstrated the presence of melting event at 189.4°C. There was also thermal event, similar to a glass transition temperature at 133.9°C. Obtained melting peak was a multiple peak, which demonstrated polymorphic structure and maturity of crystals of rapamycin.

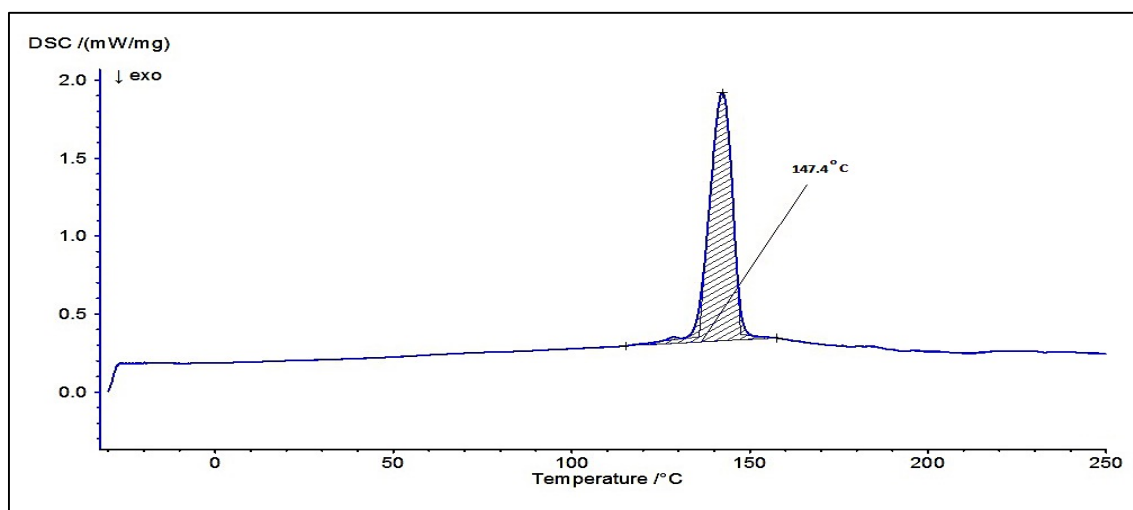


Figure 97: DSC thermograms of tacrolimus registered during first heating cycle.

The DSC thermogram of tacrolimus powder (Figure 97) demonstrated the presence only one melting event at 147.4°C. Glass transition as well as cold-crystallization were not

detected in the first cycle, as expected. The observed value was slightly higher than that reported by Patel and co-workers, i.e. 129.6°C (Patel *et al.*, 2012; Yamashita *et al.*, 2003).

8.2. P(3HB)/oligo-PHA tubes coated with PCL-PEG550 and incorporated drug manufacturing

Mandrels with layers of P(3HB)/oligo-PHA were coated with PCL-PEG330 monolayer with incorporated drugs: rapamycin or tacrolimus at a concentration of 1.2 $\mu\text{g}/\text{cm}^2$ of the material as described in the section 2.11.1. Prepared tubes were measured with a calliper in 3 places and this was recorded as the outer diameter. The difference between the outer diameter of the mould was calculated as wall thickness and expressed in Table 36 with standard deviation. The difference between the outer diameter of neat tube and coated tube was calculated to be the thickness of the coating.

Table 36: Dimensions of tubes produced using P(3HB)/oligo-PHA blend coated with PCL-PEG550 with incorporated drug.

Material	Outer diameter (mm)	Wall thickness (μm)	Coating thickness (μm)
Neat P(3HB)/oligo-PHA 90/10 tube coated with PCL-PEG-550 with incorporated Rapamycin	2.7 \pm 0.004	183.5 \pm 4.3	31.5 \pm 1.7
Neat P(3HB)/oligo-PHA 90/10 tube coated with PCL-PEG-550 with incorporated Tacrolimus	2.7 \pm 0.002	191.6 \pm 1.4	34.2 \pm 2.2

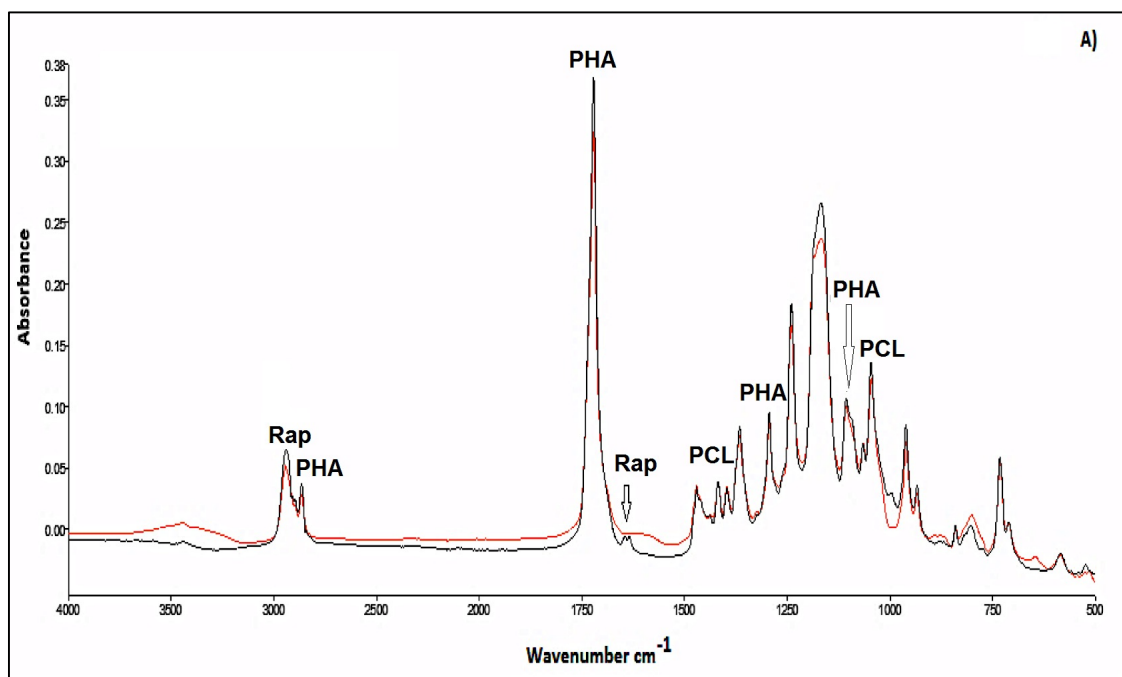
The obtained tube had a wall thickness 183.5 \pm 4.3 μm and coating thickness with rapamycin of 31.5 \pm 1.7 μm . The wall thickness of the tubes with tacrolimus was 191.6 \pm 1.4 μm and monolayer size was 34.2 \pm 2.2 μm .

8.3. P(3HB)/oligo-PHA tubes coated with PCL-PEG550 and incorporated drug characterisation

P(3HB)/oligo-PHA tubes with incorporated drugs were characterised with respect to their thermal, mechanical and topographical properties. Additionally, biocompatibility and haemocompatibility studies were performed in order to confirm non-toxicity and safety of the biomaterials.

8.3.1. Attenuated Total Reflectance Fourier Transform Infrared Spectroscopy (ATR/FT-IR)

FTIR spectroscopy was performed on the P(3HB)/oligo-PHA 90/10 blend tubes coated with PCL-PEG550 and rapamycin or tacrolimus using the method described in section 2.6.1. This was done to confirm presence of the drugs within polymeric matrix placed in the external layer of the tube. The ATR/FTIR spectrum of the PHA blend tube coated with rapamycin or tacrolimus in comparison with neat blend coated tubes is shown in Figure 98A-B.



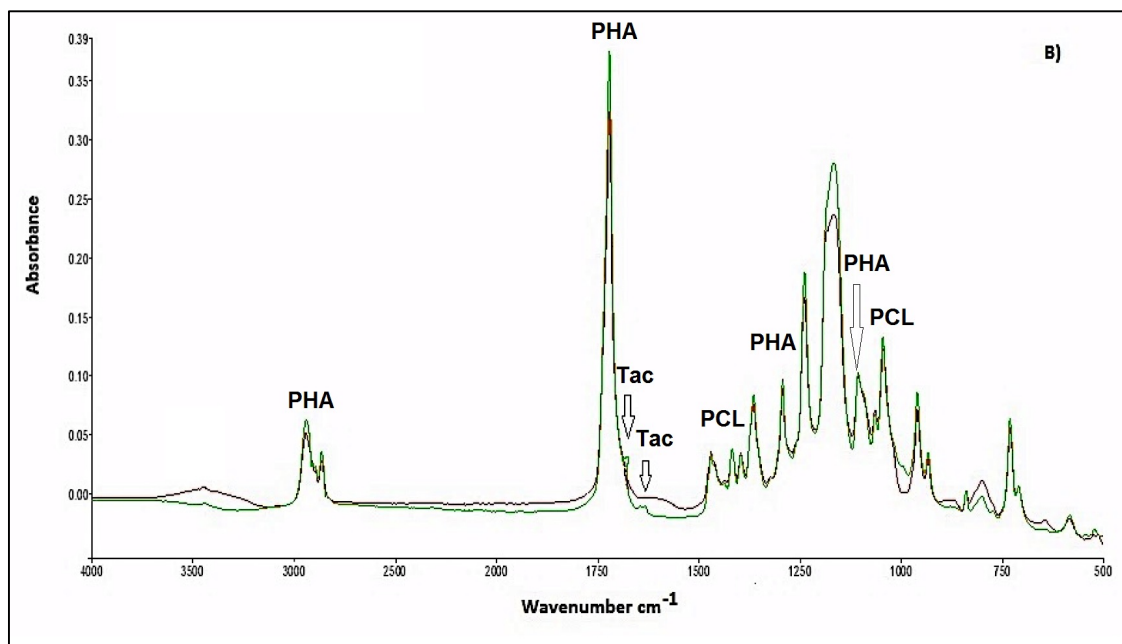


Figure 98: (A) ATR/FTIR spectra of neat P(3HB)/oligo-PHA tube with monolayer of PCL-PEG550 (—) in comparison to P(3HB)/oligo-PHA tube with incorporated rapamycin within PCL-PEG550 coating (—) indicating major peaks characteristic for PHA, PCL-PEG550 and rapamycin. (B) ATR/FTIR spectra of neat P(3HB)/oligo-PHA tube with monolayer of PCL-PEG550 (—) in comparison to P(3HB)/oligo-PHA tube with incorporated tacrolimus within PCL-PEG550 coating (—) Indicating major peaks characteristic for PHA, PCL-PEG550 and tacrolimus.

The spectrum of coated PHA-tube with rapamycin (Figure 98A) demonstrated presence of weak chemical bonds typical of rapamycin, as described in the section 8.1.1. in Figure 94. Those are adsorption peaks at: 2947cm^{-1} , 1644.6 cm^{-1} and 1633.6 cm^{-1} . Rapamycin have been loaded successfully into the polymeric matrix, which was coated on the P(3HB)/oligo-PHA 90/10 blend tube.

The spectrum of coated PHA-tube with tacrolimus (Figure 98B) demonstrated presence of weak chemical bonds typical to tacrolimus, as described in the section 8.1.1. in Figure 95. Those were adsorption peaks at: 3438cm^{-1} , 1739.8 cm^{-1} , 1692.3 cm^{-1} and 1636.4 cm^{-1} . Drug tacrolimus had been successfully loaded into the polymeric matrix, which was coated on the P(3HB)/oligo-PHA 90/10 blend tube.

In conclusion, presence of both drugs was detected in the PHA based tubes coated with PCL-PEG550 with drug.

8.3.2. Scanning Electron Microscopy

SEM images of cross section of the P(3HB)/oligo-PHA tubes with incorporated rapamycin confirmed that the material was uniform (Figure 99A). Presence of the coating, which covered surface of the tube was detected. The thickness of the coating evaluated by SEM was $36.0 \pm 0.6 \mu\text{m}$ (Figure 99D). The surface of the tube is smooth and even; pores are not visible from the outer surface of the tube (Figure 99C). Tube wall thickness was measured as $180.7 \pm 0.5 \mu\text{m}$ (Figure 99B).

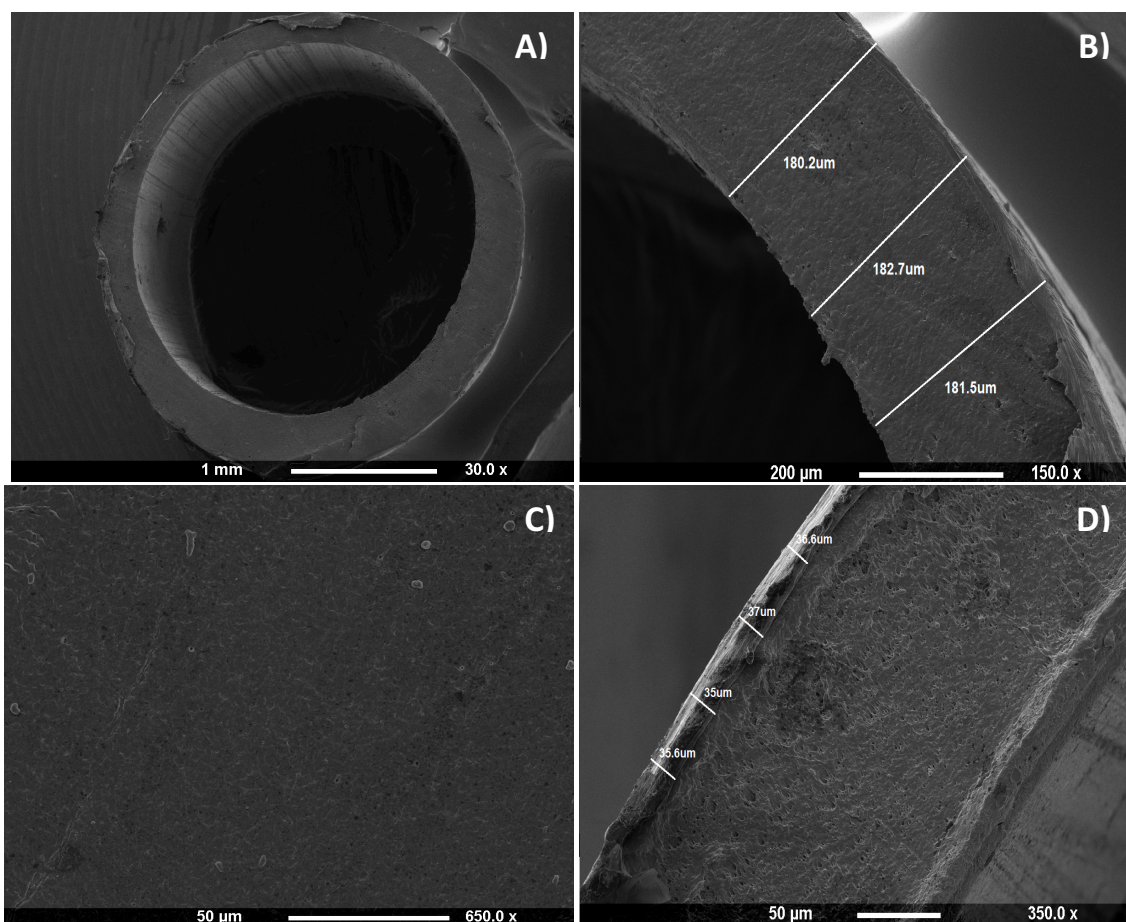


Figure 99: SEM micrographs of P(3HB)/oligo-PHA tube coated with monolayer of PCL-PEG550 with incorporated rapamycin. (A) tube cross-intersection, (B) tube wall structure, (C) tube surface, (D) coating thickness.

SEM images of cross section of the P(3HB)/oligo-PHA tubes with incorporated tacrolimus confirmed that the material was uniform (Figure 100). The thickness of the coating by SEM was $36.1 \pm 0.8 \mu\text{m}$ was also confirmed (Figure 100D). The surface of the tube was smooth and even as shown in the Figure 100C. Pores are not visible from the outer

surface of the tube or throughout the wall thickness. Obtained tube wall thickness was measured as $180.7 \pm 0.5 \mu\text{m}$ (Figure 100B).

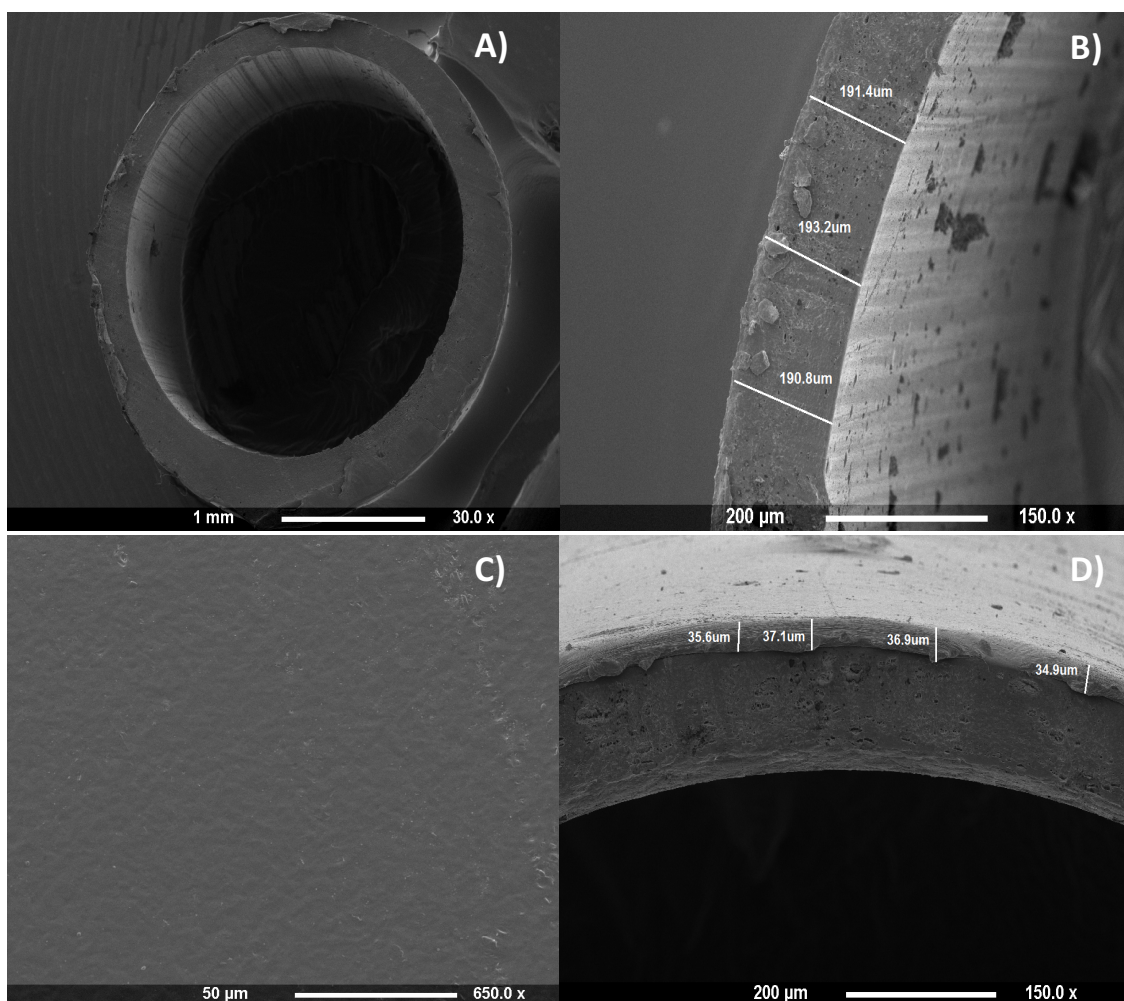


Figure 100: SEM micrographs of P(3HB)/oligo-PHA tube coated with monolayer of PCL-PEG550 with incorporated tacrolimus. (A) tube cross-intersection, (B) tube wall structure, (C) tube surface, (D) coating thickness.

8.3.3. Drug release studies

The release of rapamycin from the P(3HB)/oligo-PHA 90/10 blend tube containing rapamycin incorporated within PCL-PEG550 polymeric matrix was carried out as described in section 2.12. for a period of 90 days. The results obtained during *In vitro* release study were summarised in Figure 101.

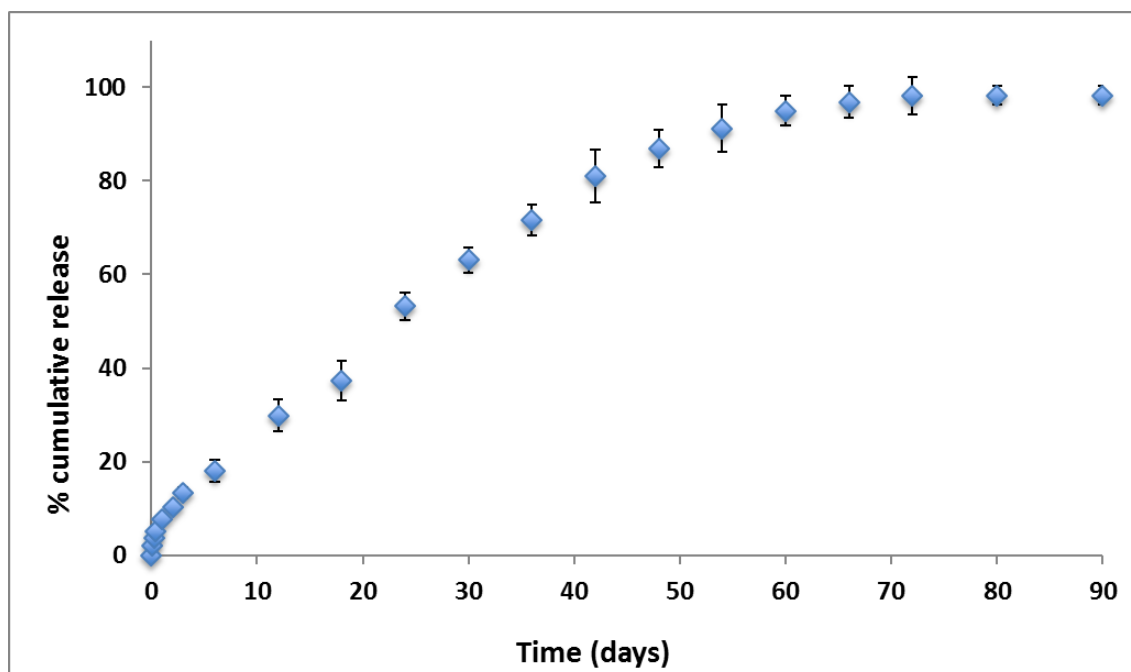


Figure 101: *In vitro* release profile of rapamycin from PCL-PEG550 polymeric coating of P(3HB)/oligo-PHA 90/10 blend tube for a period of 90 days (n=3).

Rapamycin was released slowly at a constant rate throughout the period of release. Burst release was not observed. However, slightly faster release was noticed within first 24 hours. This might be due to the release of drug attached to the surface of the matrix. After 1 day of incubation $7.6 \pm 0.6\%$ of rapamycin was released. Within 12 days almost 30% of the drug was released. During the first 30 days $62.2 \pm 2.5\%$ was released. After 30 days, the rate of release slowed down. After 48 days 86.8% of rapamycin was released. After 72 days, no further release was recorded. In this study, cumulative release of rapamycin of 98.2% occurred within a period of 90 days.

The release of tacrolimus from the P(3HB)/oligo-PHA 90/10 blend tube containing monolayer of PCL-PEG550 with tacrolimus was carried out as described in section 2.13 for a period of 90 days. The results obtained during *In vitro* release study were summarised in Figure 102.

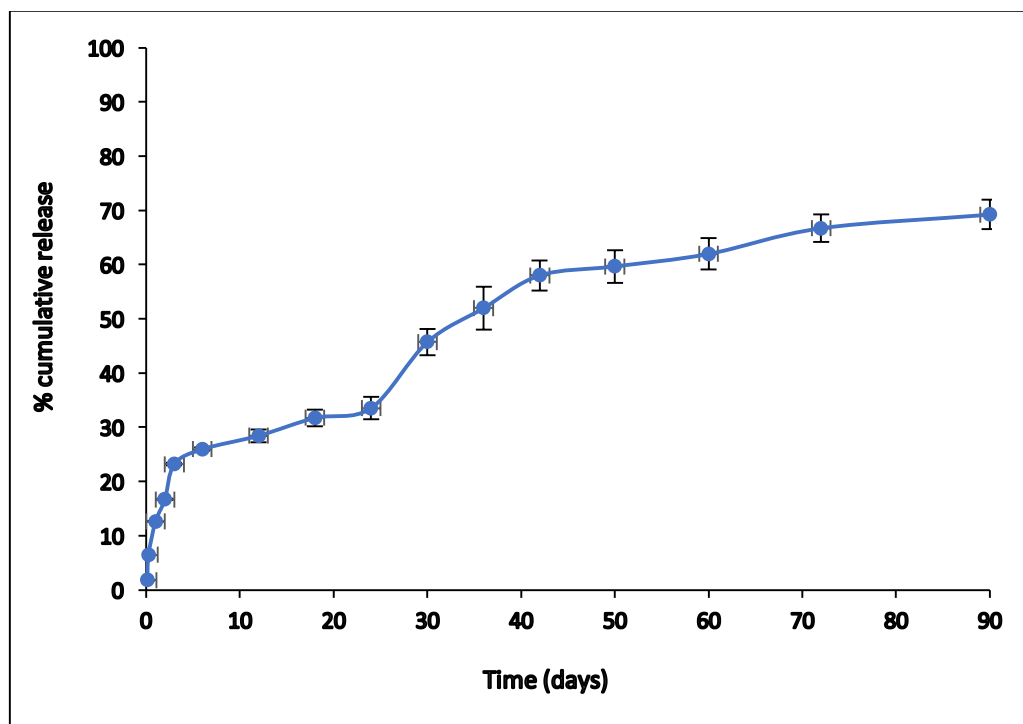


Figure 102: Cumulative release profile of tacrolimus from PCL-PEG550 polymeric coating of P(3HB)/oligo-PHA 90/10 blend tube for a period of 90 days (n=3).

Tacrolimus was released slowly throughout the period of study. Burst release was observed within first 3 days of incubation. This might be due to the release of drug attached to the surface of the matrix. After 1 day of incubation $12.6 \pm 0.4\%$ of tacrolimus was released. Within 18 days around 32% of the drug was released. During the first 30 days $45.7 \pm 2\%$ was released. After 24 days, the rate of release increased. After 48 days 60.0% of tacrolimus was released. In this study, cumulative release of tacrolimus of 69.2% occurred within a period of 90 days.

8.4. *In vitro* biocompatibility studies

Neat P(3HB)/oligo-PHA 90/10 tubes coated with PCL-PEG550 monolayer, containing rapamycin or tacrolimus were characterised in order to evaluate their functionality as a platform materials for biomedical applications.

8.4.1. Protein adsorption

Bicinchoninic acid assay was used to evaluate the potential of the materials towards proteins as described in the section 2.11.3.9. It was found that total protein adsorption was 189.9 ± 7.6 and 150.6 ± 6.9 $\mu\text{g}/\text{cm}^2$ for the P(3HB)/oligo-PHAs blend tube containing tacrolimus or rapamycin in the PCL-PEG550 matrix respectively. Both tested materials demonstrated higher protein adsorption than TCP. However, the results were significant only for tube containing tacrolimus (* $p=0.033$). There was no significant difference between the tissue control plastic and tube with incorporated rapamycin (Figure 103).

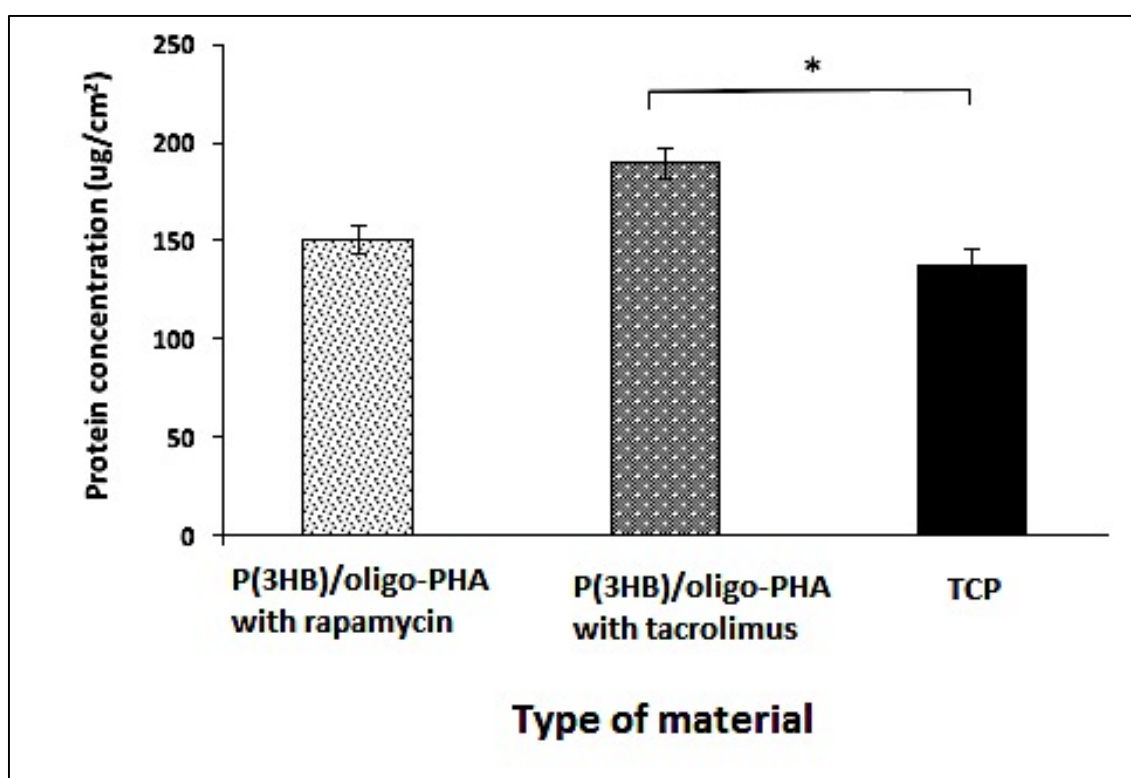


Figure 103: Protein adsorption to the P(3HB)/oligo-PHA 90/10 tubes with PCL-PEG550 coating with incorporated drugs: rapamycin or tacrolimus ($n=3$; error bars= \pm SD). The data were compared with standard tissue culture plastic using ANOVA. * indicates $p < 0.05$.

The tubes with tacrolimus demonstrated higher concentration of proteins adsorbed on the surface in comparison with TCP (positive control). The amount of proteins adsorbed to the TCP was 137.5 ± 7.8 $\mu\text{g}/\text{cm}^2$. The presence of drug did not demonstrate inhibiting effects on the amount of protein adsorbed on the surface of the tubes. Moreover,

incorporated tacrolimus enhanced proteins affinity towards P(3HB)/oligo-PHA tube coated with PCL-PEG550.

8.4.2. Cell viability study

MTT assay was used to evaluate cell adhesion and proliferation. Attachment and proliferation of HMEC-1 cells on the tube samples were studied over a period of 1, 3 and 7 days. The standard tissue culture plastic was used as the positive control for these experiments. The results of biocompatibility studies are presented in Figure 104.

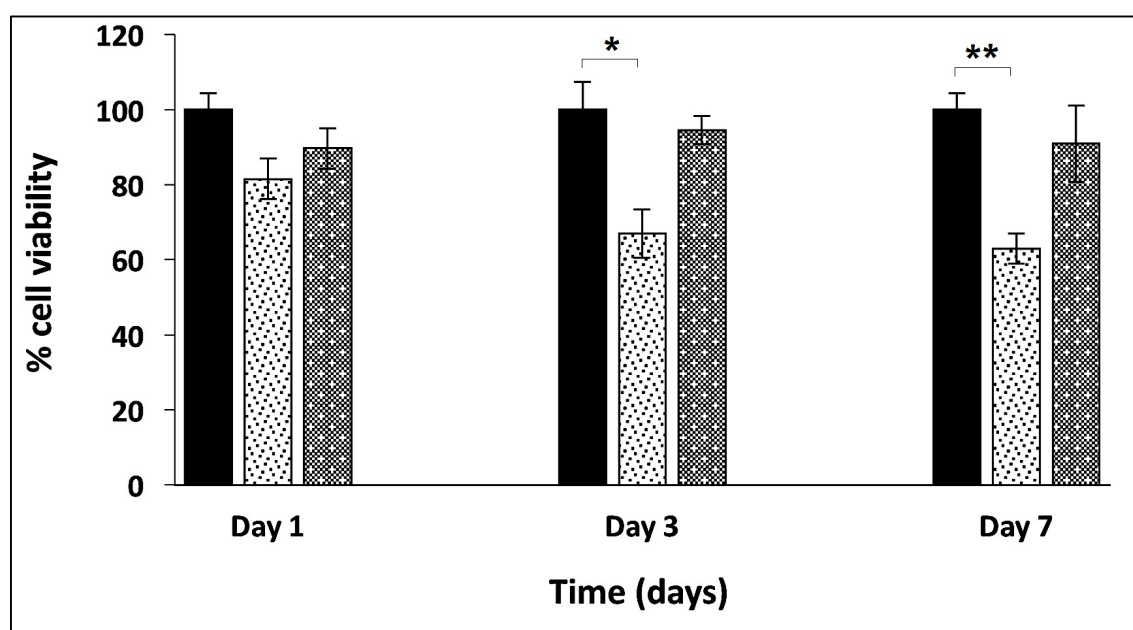


Figure 104: Cell proliferation study of the HMEC-1 cells on the P(3HB)/oligo-PHA tubes coated with monolayer of PCL-PEG550 with incorporated rapamycin or tacrolimus samples on day 1, 3 and 7 (n=3; error bars=±SD). The data were compared with standard tissue culture plastic, which were normalized to 100% using ANOVA. * indicates $p < 0.05$ and ** indicates $p < 0.005$. (■) standard tissue culture plastic, (□) tube with incorporated rapamycin, (▣) tube with incorporated tacrolimus.

Cell proliferation on the surface of P(3HB)/oligo-PHA 90/10 blend tubes with incorporated tacrolimus within PCL-PEG550 matrix was slightly lower in comparison to TCP on day 1, 3 and 7. The cell viability obtained on the tube samples was $89.6 \pm 5.4\%$ on day 1; $94.4 \pm 3.7\%$ on day 3 and $90.9 \pm 2.5\%$ on day 7 as compared to the TCP. The differences were not statistically significant for all the results obtained. The growth of

the HMEC-1 cells on the surface of tube with rapamycin was lower in comparison to the control. The cell viability observed was: $81.5 \pm 2.4\%$ on day 1 and $66.6 \pm 4.9\%$ and $62.9 \pm 4.0\%$ on day 3 and 7 respectively. The differences were statistically significant for day 3 and 7 ($*p=0.022$, $*p=0.012$) in comparison to TCP on day 3 and 7. Presence of rapamycin within the polymeric matrix had a negative impact on the viability of the HMEC-1 cells.

The results obtained demonstrated higher biocompatibility of the tube with incorporated tacrolimus in comparison to rapamycin. Therefore, this drug should be considered for application in coronary stents.

8.4.3. Scanning Electron Microscopy

Cell attachment and morphology was further characterised using SEM imaging. SEM images presented in Figure 105 revealed that HMEC-1 cells adhered to and proliferated on the surface of the tubes. However, much higher cell density for the tube containing tacrolimus in comparison to rapamycin was observed. The cell morphology was similar in both tested materials. HMEC-1 cells exhibited spindle-shape morphology, typical for this cell line. Additionally, cell-to-cell interactions were observed.

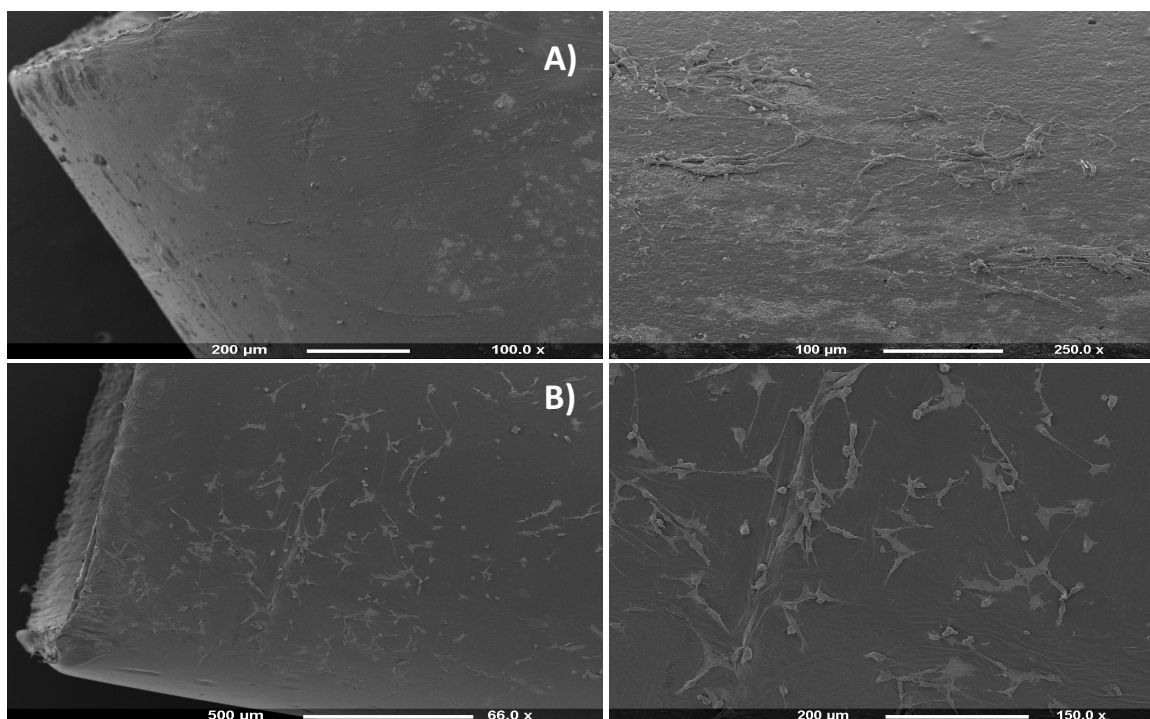


Figure 105: SEM micrographs of the HMEC-1 cells attached to the surfaces of P(3HB)/oligo-PHA tubes containing rapamycin (A), and tacrolimus (B) after 7 days of culturing.

With respect to the results obtained, not all tested materials based on P(3HB)/oligo-PHAs supported the growth of HMEC-1 cell line. Addition of tacrolimus into P(3HB)/oligo-PHA tube demonstrated much higher biocompatibility to the endothelial cell line in comparison to rapamycin, which distinctly inhibited growth of the HMEC-1 cells.

8.4.4. Indirect cytotoxicity study

Indirect cytotoxicity test was performed to investigate the influence of the substances released from the tubes with incorporated drugs, such as rapamycin or tacrolimus on the HMEC-1 cell line. Cells with fresh DMEM medium were used as negative control. 70% methanol instead of media or extract was used as the control.

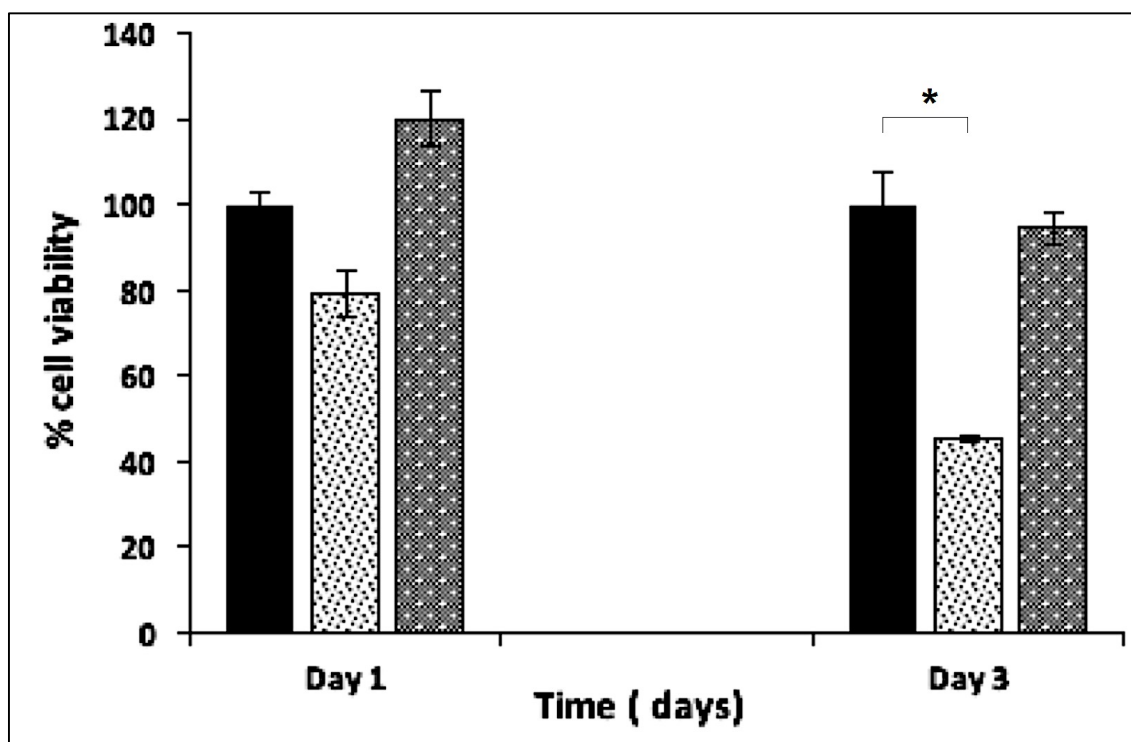


Figure 106: Indirect cytotoxicity study of the HMEC-1 cells on the P(3HB)/oligo-PHA tubes coated with monolayer of PCL-PEG550 with incorporated rapamycin or tacrolimus samples on day 1, 3 (n=3; error bars=±SD). The data were compared with standard tissue culture plastic containing DMEM medium, which were normalised to 100% using ANOVA. * indicates $p < 0.05$. (■) fresh DMEM medium, (▨) extract from the tube containing rapamycin (▩) extract from the tube containing tacrolimus.

Cell proliferation on the P(3HB)/oligo-PHA tube with tacrolimus was $119.9 \pm 4.3\%$ on day 1 and $94.4 \pm 3.8\%$ on day 3 compared to TCP. The differences were not statistically significant. The growth of HMEC-1 cells on the extract from tube containing tacrolimus was similar on day 1 and 3 to TCP. The growth of the HMEC-1 cells with an extract from P(3HB)/oligo-PHA tube with rapamycin was lower than TCP on day 1 (79.2 ± 2.3) and day 3 (45.1 ± 0.5). The difference was statistically significant (** $p=0.0033$) for the result obtained after day 3. The highest viability of the HMEC-1 cells was achieved after treatment with an extract from tube with incorporated tacrolimus in comparison to TCP after 1 day of incubation. The results obtained suggest that no cytotoxic substances were released from the tube containing tacrolimus. This drug did not inhibit the growth of HMEC-1 cells. An opposite effect was observed with rapamycin. This drug definitely interfered with endothelial cells and inhibited their attachment and proliferation. Therefore, PHAs tubes with tacrolimus can be strongly considered as potential materials for biomedical applications, such as coronary stents.

8.5. Haemocompatibility studies

P(3HB)/oligo-PHA tubes with incorporated drugs, such as rapamycin or tacrolimus were subjected to haemocompatibility studies, which includes haemolysis studies, whole blood clotting as well as monocytes and neutrophils activation.

8.5.1. Haemolysis study

Haemolysis study was performed on P(3HB)/oligo-PHA tubes with tacrolimus and rapamycin in order to investigate an effect of the materials on erythrocytes after direct contact with fresh whole blood. The analysis was performed as described in the section 2.15.1. The results obtained are shown at the Figure 107.

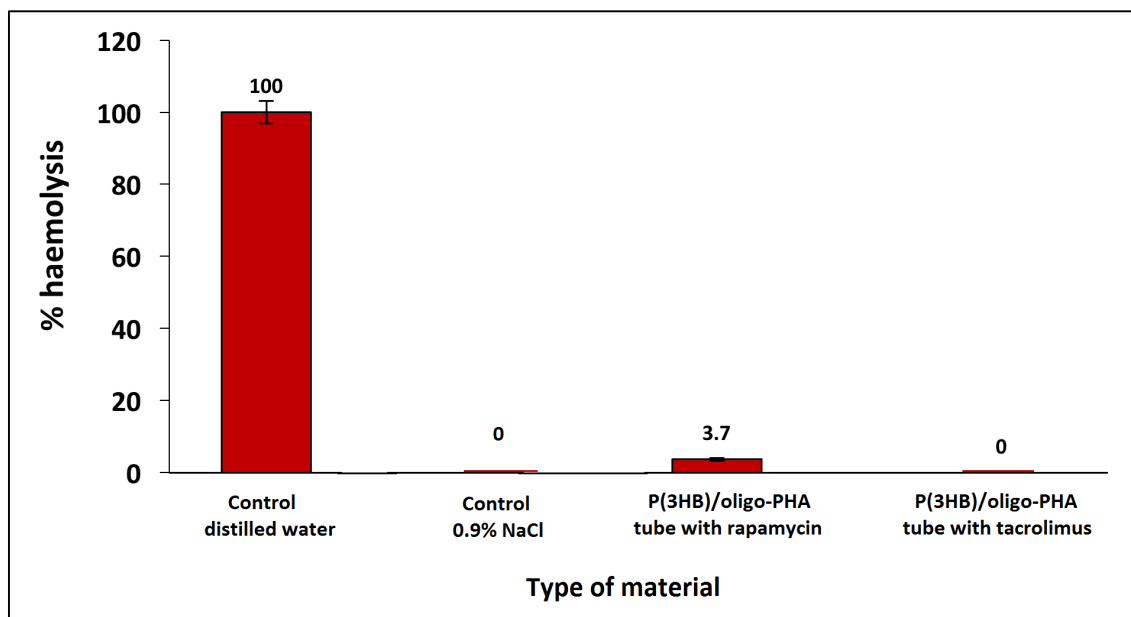


Figure 107: Haemolysis rates of the P(3HB)/oligo-PHA tubes coated with PCI-PEG550 with incorporated rapamycin or tacrolimus after 1h of incubation at 37°C (n=3). * indicates $p < 0.05$ compared to blood control sample containing 0.9% NaCl using ANOVA; no significant difference.

All tubes exhibited non-haemolytic effect on erythrocytes. The percent of haemolysis 3.7%, and 0% was obtained for tube with rapamycin and tacrolimus respectively. According to ISO 10993-4:2002 standard, all tested tubes had low potential to destroy red blood cells.

8.5.2. Whole blood clotting study

Whole blood clotting experiment was performed to investigate the potential thrombogenicity of P(3HB)/oligo-PHA tubes containing different types of drugs incorporated in the polymeric matrix as described previously in the section 2.15.2. The summary of the results obtained after 30 and 90 minutes are demonstrated in Figure 108.

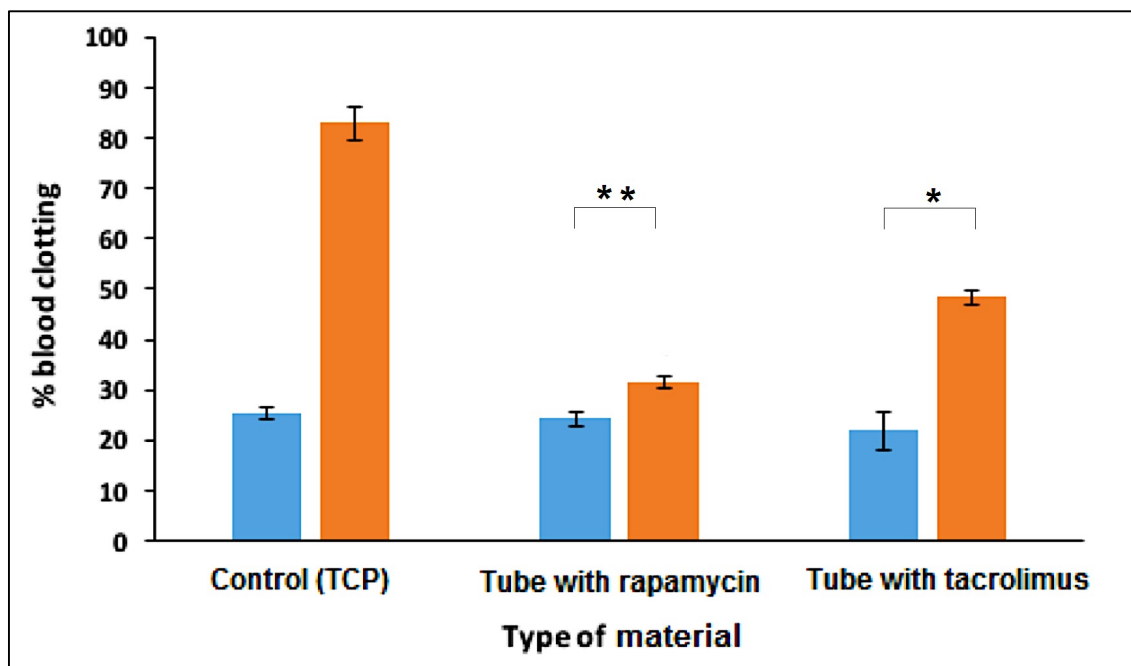


Figure 108: Summary of whole blood clotting results after 30 minutes (■) and 90 minutes (■) of incubation on the P(3HB)/oligo-PHA tubes coated with PCL-PEG550 containing rapamycin or tacrolimus. Tissue culture plastic was used as the control (n=3; error bars=±SD). The data were compared with standard tissue culture plastic using ANOVA. * indicates $p < 0.05$, ** indicates $p < 0.005$.

The results obtained indicate that P(3HB)/oligo-PHA coated tube containing rapamycin or tacrolimus enhanced the activation of the coagulation cascade. After 30 minutes of incubation, P(3HB)/oligo-PHA tube with rapamycin demonstrated $24.2 \pm 1.6\%$ blood clotting. Addition of tacrolimus within the coating resulted in increased % blood clotting after 30 minutes by $21.9 \pm 3.1\%$. The results were not significant in comparison to the control. With the increase of time, the % blood clot increased in all tested materials as well as in positive control. After 90 minutes the blood control demonstrated $82.9 \pm 3.3\%$ blood clotting. P(3HB)/oligo-PHA tube with rapamycin resulted in decrease in the blood clotting rate to $31.5 \pm 1.2\%$. The difference was significant (** $p = 0.0022$). P(3HB)/oligo-PHA coated tube with tacrolimus presented decreased blood clotting rate ($48.4 \pm 1.5\%$) in comparison to the control ($82.9 \pm 3.3\%$). The result was significant (* $p = 0.011$). Addition of drugs resulted in much lower blood clot rate formation than control. To summarise, all tested materials did not demonstrate increased risk of thrombogenicity and can be considered as a biomaterial for medical applications, such as coronary stents.

8.5.3. Monocytes and neutrophil activation

Three different types of tubes: neat P(3HB)/oligo-PHA, coated tube and composite tube were incubated with the whole blood at 37°C overnight and stained with the markers listed in section 2.15.3.1. Summary of the results obtained was demonstrated in Table 37.

Table 37: Summary of median fluorescence intensity (MFI) obtained after incubation of fresh whole blood with P(3HB)/oligo-PHA 90/10 tube coated with PCL-PEG550, P(3HB)/oligo-PHA tube coated with PCL-PEG550 with incorporated rapamycin or tacrolimus and PL38 stained with specific markers in order to evaluate monocyte and neutrophil activity.

Sample	Markers	Monocytes Activity (MFI)	Percentage change (%)	Neutrophils Activity (MFI)	Percentage change (%)
P(3HB)/oligo-PHA 90/10 tube coated with PCL-PEG550	CD86-PE	209.7	82.5	175.3	11.6
	CD45-PerCP	135.9	24.2	76.3	-
	CD11b-PE	498.9	267.1	586.8	316.4
	CD66B-FITC	168.8	-	279.8	71.8
P(3HB)/oligo-PHA 90/10 tube coated with PCL-PEG550 and rapamycin	CD86-PE	188.9	64.4	109.3	-
	CD45-PerCP	66.9	-	98.4	-
	CD11b-PE	642.3	372.6	1104.2	683.6
	CD66B-FITC	131.1	-	168.8	3.7
P(3HB)/oligo-PHA 90/10 tube coated with PCL-PEG550 and tacrolimus	CD86-PE	140.9	22.6	116.7	-
	CD45-PerCP	131.5	20.2	109.4	0
	CD11b-PE	436.7	321.4	546.2	287.6
	CD66B-FITC	249.6	23.2	163.8	0.61

The results obtained after staining blood samples, which were exposed to various types of drugs incorporated within the tubes demonstrated different levels of activity of the monocytes and neutrophils. All tested samples presented higher activity in the activation marker CD11b-PE. The percentage change of MFI for tube containing tacrolimus was 321.4% for monocytes and 287.6% for neutrophils in comparison to control. The tube with rapamycin demonstrated 1.5-2.0-fold higher white cells activation than the neat tube PCL-PEG550 coated tube without any drug. The percentage change of MFI for P(3HB)/oligo-PHA tube containing rapamycin was recorded as 372.6% for monocytes and 683.6% for neutrophils in comparison to control. The results obtained suggested, that addition of rapamycin caused an increased higher activation of neutrophils and monocytes in comparison to tube containing tacrolimus or tube without any drug.

8.6. *In vitro* degradation study

A degradation study was carried out for a period of 3 months at 37°C in phosphate buffered saline solution (PBS) to investigate the degradation behaviour of the P(3HB)/oligo-PHA tubes coated with PCL-PEG550 with incorporated rapamycin or tacrolimus.

8.6.1. Attenuated Total Reflectance Fourier Transform Infrared Spectroscopy (ATR/FT-IR)

FTIR was carried out on the tubes to investigate the changes in the chemical structure during incubation time. Figure 109 illustrates the ATR/FTIR spectra obtained for the tubes after month 1 and 3 of degradation studies.

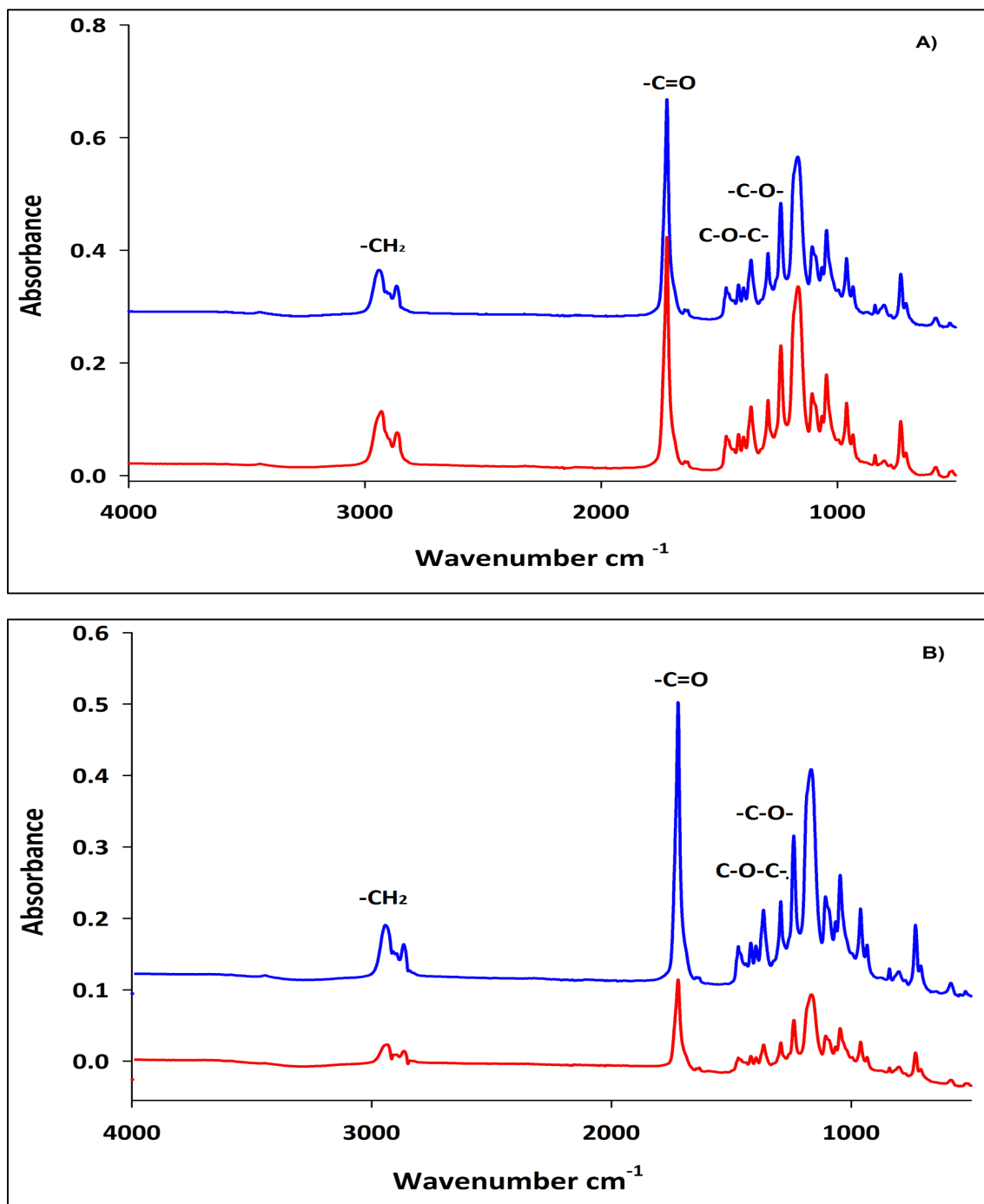


Figure 109: ATR-FTIR spectrum of the P(3HB)/oligo-PHA tubes with rapamycin (A) and tacrolimus (B) after 3 months incubation in PBS indicating characteristic peaks. (■) month 1 of degradation study, (■) month 3 of degradation study.

There were no differences between all spectra obtained after month 1 and 3 for P(3HB)/oligo-PHA tubes with rapamycin or tacrolimus. All the chemical bonds, which were detected are typical of P(3HB)/oligo-PHA blends and PCL-PEG550 coating described previously in Chapter 7.

8.6.2. Thermal properties – Differential Scanning Calorimetry

DSC analysis was carried out in order to study changes in the thermal properties in the material containing drugs, caused by degradation of the tubes. A summary of the results obtained has been listed in Table 38. The first heating cycle thermograms are shown in Figure 110.

Table 38: Summary of the thermal properties of the P(3HB)/oligo-PHA tubes containing rapamycin or tacrolimus after 3 months of degradation study. T_m = melting temperature, T_g = glass transition temperature, T_c = crystallisation temperature, ΔH_f =enthalpy of fusion.

Type of drug	Tube with incorporated Rapamycin			Tube with incorporated Tacrolimus		
	Month 1	Month 2	Month 3	Month 1	Month 2	Month 3
T_g (°C)	0.4	-0.4	-0.1	-3.4	2.3	-1.3
T_m (°C)	64.4	64.9	79.2	62.7	62.5	176.3
	173.1	176.8	176.6	176.3	175.9	
T_c (°C)	58.9	60.5	58.3	52.2	58.4	55.0
ΔH_f (J/g)	10.38	6.85	5.6	3.4	6.12	83.9
	65.5	65.0	66.2	82.43	88.15	

During 3 months of degradation study, the thermal properties of the materials have changed. In the tube with rapamycin, the glass transition temperature slightly decreased from 0.4°C at month 1 to -0.1°C at month 3. There were 2 melting temperatures detected: one related to PCL-PEG550, present in the coating and one related to PHAs. T_m for PCL-PEG550 increased significantly from 64.4°C to 79.2°C after 3 months. The melting temperature for the PHAs also increased from 173.1°C to 176.6°C after month 1 and 3 respectively. The cold-crystallisation temperature increased at month 2 and decreased back to 58.3°C in month 3. The enthalpy of fusion values increased slightly from 65.5J/g to 66.2J/g for PHAs and decreased from 10.38 J/g to 5.6 J/g for PCL-PEG550 after 3 months.

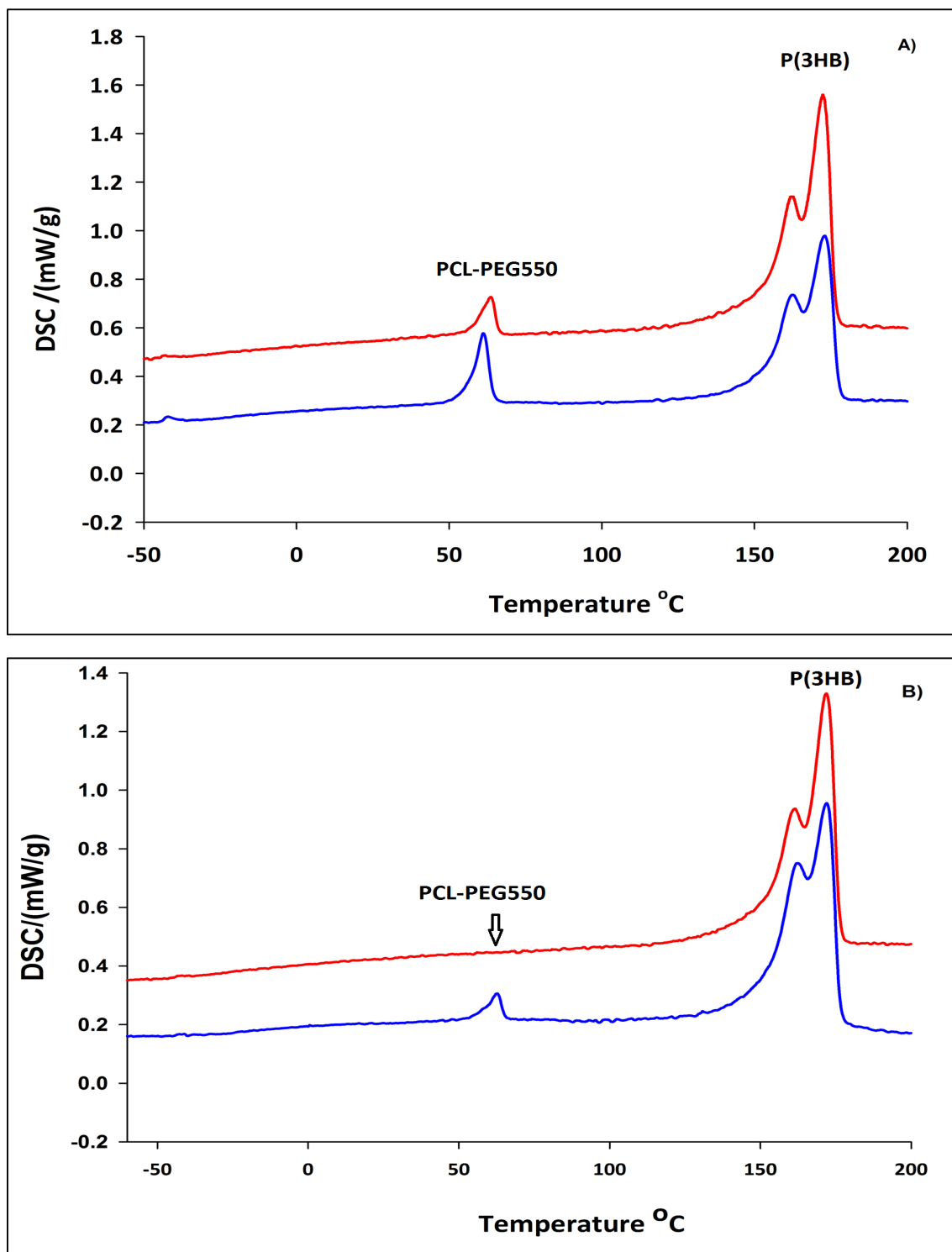


Figure 110: DSC thermograms of P(3HB)/oligo-PHA tubes with incorporated rapamycin (A) and tacrolimus (B) during 3 months of degradation study. (■) month 1 of degradation study, (■) month 3 of degradation study.

In the tube with tacrolimus the glass transition temperature increased from -3.4°C to -1.3°C after 3 months. Cold-crystallisation temperature increased from 52.5°C to 55.5°C

after 3 months. There was significant change in the melting temperature. There was one melting event observed after 3 months of study. This can be explained by degradation of the external layer of the tube. As a result, mostly PHA polymers were left. Degradation study did not affect the melting temperature and was stable around 176.3°C for 3 months in the case of PHAs and 62.5°C for PCL-PEG550 for 2 months. The enthalpy of fusion increased for 2 months from 82.4 J/g to 88.15 after month 2 and decreased back after month 3 to the level 83.9 J/g.

The DSC thermograms in the Figure 110 presents the first heating cycle of tubes with rapamycin (Figure A) and tacrolimus (Figure B) after months 1 and 3 of degradation. In the thermogram obtained from tube with tacrolimus, there was lack of melting event for PCL-PEG550 after month 3, whereas this peak was still present in tube with rapamycin. No other thermal events were observed. Both types of tubes demonstrated different behaviour with respect to their thermal properties during 3 months degradation study.

8.6.3. Mechanical properties of the P(3HB)/oligo-PHA tubes coated with PCL-PEG550 with incorporated drugs

The analysis of the mechanical properties of the P(3HB)/oligo-PHA tubes with rapamycin or tacrolimus incorporated within PCL-PEG 550 polymeric matrices were incubated with PBS at 37°C for 3 months, in order to check the material properties during degradation. The results obtained are summarised in Table 39.

Table 39: Summary of the mechanical properties of the P(3HB)/oligo-PHA tubes with rapamycin or tacrolimus during month 1, 2 and 3 of the degradation study.

Month	Type of drug incorporated	Tensile strength (MPa)	Elongation at break (% strain)	Young's Modulus (GPa)
1	Rapamycin	20.8±1.6	7.8±1.5	0.8±0.1
	Tacrolimus	19.7±1.8	7.4±1.2	0.9±0.06
2	Rapamycin	21.7±0.9	4.4±0.7	1.4±0.15
	Tacrolimus	22.3±0.8	4.1±0.4	1.6±0.04
3	Rapamycin	16.1±2.1	1.7±0.3	1.1±0.05
	Tacrolimus	18.8±0.75	2.6±0.5	1.0±0.12

Mechanical properties of the P(3HB)/oligo-PHA tubes with incorporated rapamycin or tacrolimus after 3 months of incubation in PBS at 37°C had changed. There was a similar trend in the behaviour of both types of the tubes with rapamycin and tacrolimus. In general, the tensile strength and Young's modulus values increased after 2 months and decreased after month 3 of the degradation study. On the other hand, elongation at break values decreased significantly. The results obtained confirmed brittleness of the material, which might be caused by degradation and weight loss of the tubes. Mechanical properties of the tubes incubated with PBS were different than tubes stored at room temperature as described in the section 7.4.3.3. Tubes stored at room temperature for 7 weeks demonstrated higher tensile strength values and elongation at break in comparison to tubes incubated at 37°C in PBS. Young's Modulus after 7 weeks was similar to the incubated tubes after 2 months of degradation study. The hydrolytic environment had a negative effect on the mechanical properties, i.e. decrease in stiffness of the P(3HB)/oligo-PHA tubes coated with PCL-PEG550.

8.6.4. pH measurements of the PBS during degradation studies of neat PHA tubes

The PBS in which the tubes were incubated were studied in order to monitor any changes in the pH during the degradation study. The results obtained were presented in the Figure 111.

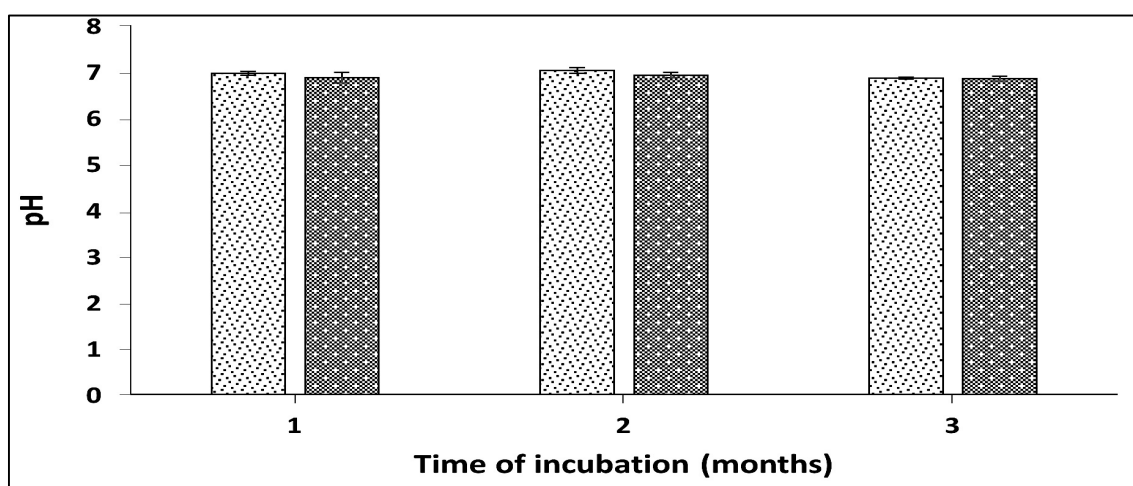


Figure 111: pH changes of PBS after incubation of P(3HB)/oligo-PHA tubes with incorporated rapamycin (□) or tacrolimus (▣) for 3 months (n=3). no significant difference in comparison to month 1.

The pH of PBS was 7.4 in the beginning of the study. After 3 months of incubation at 37°C the final pH was 6.8 ± 0.02 for tubes with rapamycin and 6.8 ± 0.05 for tubes with tacrolimus. These results obtained during this study suggested release of slightly acidic products during degradation process, which resulted in a decrease in pH. However, the pH changes are inconsiderable.

8.6.5. Weight loss (%) of the neat tubes during degradation studies

Percentage of weight loss was measured at month 1, 2 and 3 of degradation study as described previously in the section 2.16.3. The summary of the results has been illustrated in the Figure 112.

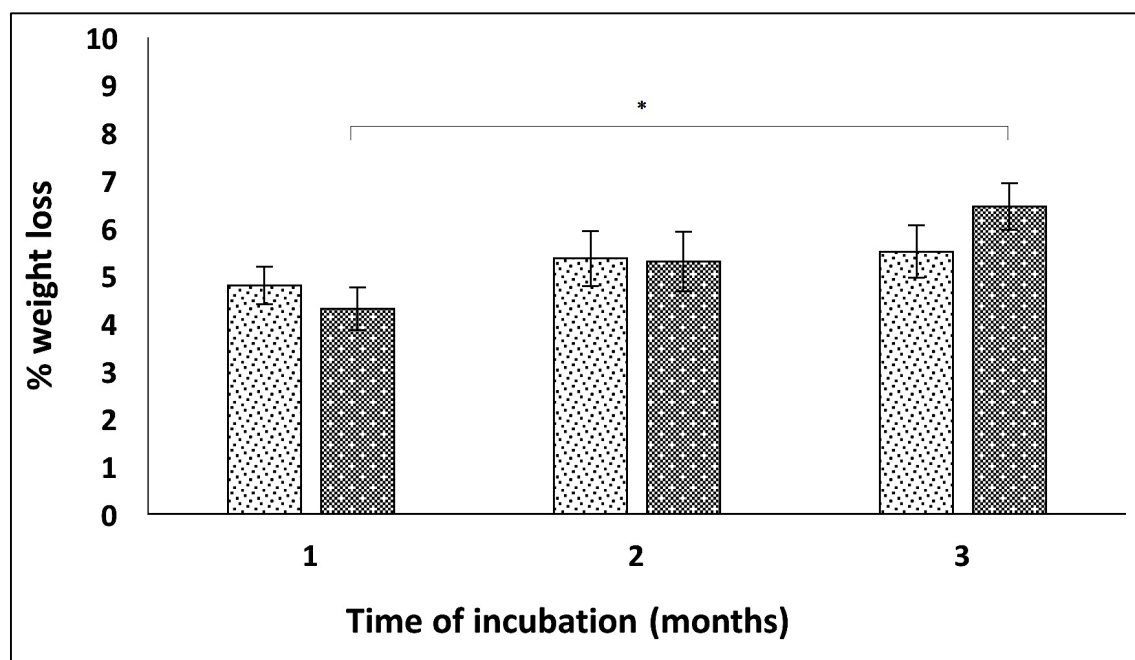


Figure 112: Weight loss (%WL) of the P(3HB)/oligo-PHA tubes with incorporated rapamycin (□) or tacrolimus (▣) for a period of 3 months (n=3). Results were compared to % weight loss after month 1 using ANOVA. * indicates $p < 0.05$.

The results obtained suggest slow increase in weight loss, observed in the tubes during the degradation study. For the tubes containing rapamycin, the initial weight loss at month 1 was slightly above 4%. After 3 months, the % weight loss observed was 5.5%. Similarly, in the tube with tacrolimus weight loss increased from 4.4% after month 1 to 6.4% after month 3.

8.6.6. Water uptake (%) of the neat tubes during degradation studies

Percentage of water uptake (%WU), which is an amount of water absorbed by the material during incubation was measured at month 1, 2 and 3 of degradation study as described previously in the section 2.16.3. the summary of the results has been illustrated in the Figure 113.

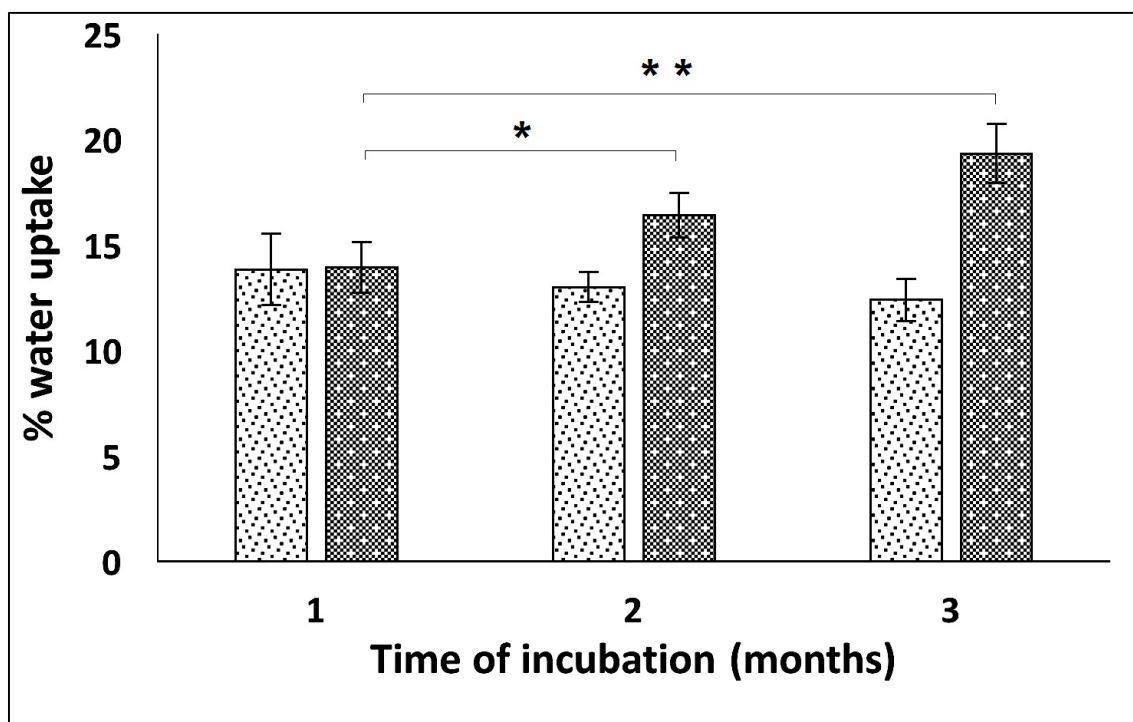


Figure 113: Water absorption (%WU) by the P(3HB)/oligo-PHA tubes with incorporated rapamycin (□) or tacrolimus (▣) for a period of 3 months (n=3). Results were compared to % water uptake after month. * indicates $p=0.04$ and ** indicates $p=0.005$.

The results obtained illustrated the amount of water absorbed by the tubes. In the tubes with rapamycin the water absorption level decreased slightly from 13.8% at month 1 to 12.4% after month 3. For the tube with tacrolimus the water uptake increased steadily from month 1 to 3. The final WU value obtained in this study after month 3 was $19.3 \pm 1.4\%$.

8.6.7. Surface studies of the degraded tubes

After each time point during degradation studies tubes were rinsed with distilled water, dried and imaged using the Scanning Electron Microscope as described in section 2.16.2. SEM analyses of the surface, cross section, wall thickness of the tubes was carried out to analyse any changes on the surface due to degradation. SEM images of the tubes with incorporated drugs, obtained after 3 months of degradation studies are presented in the Figure 114 and 115.

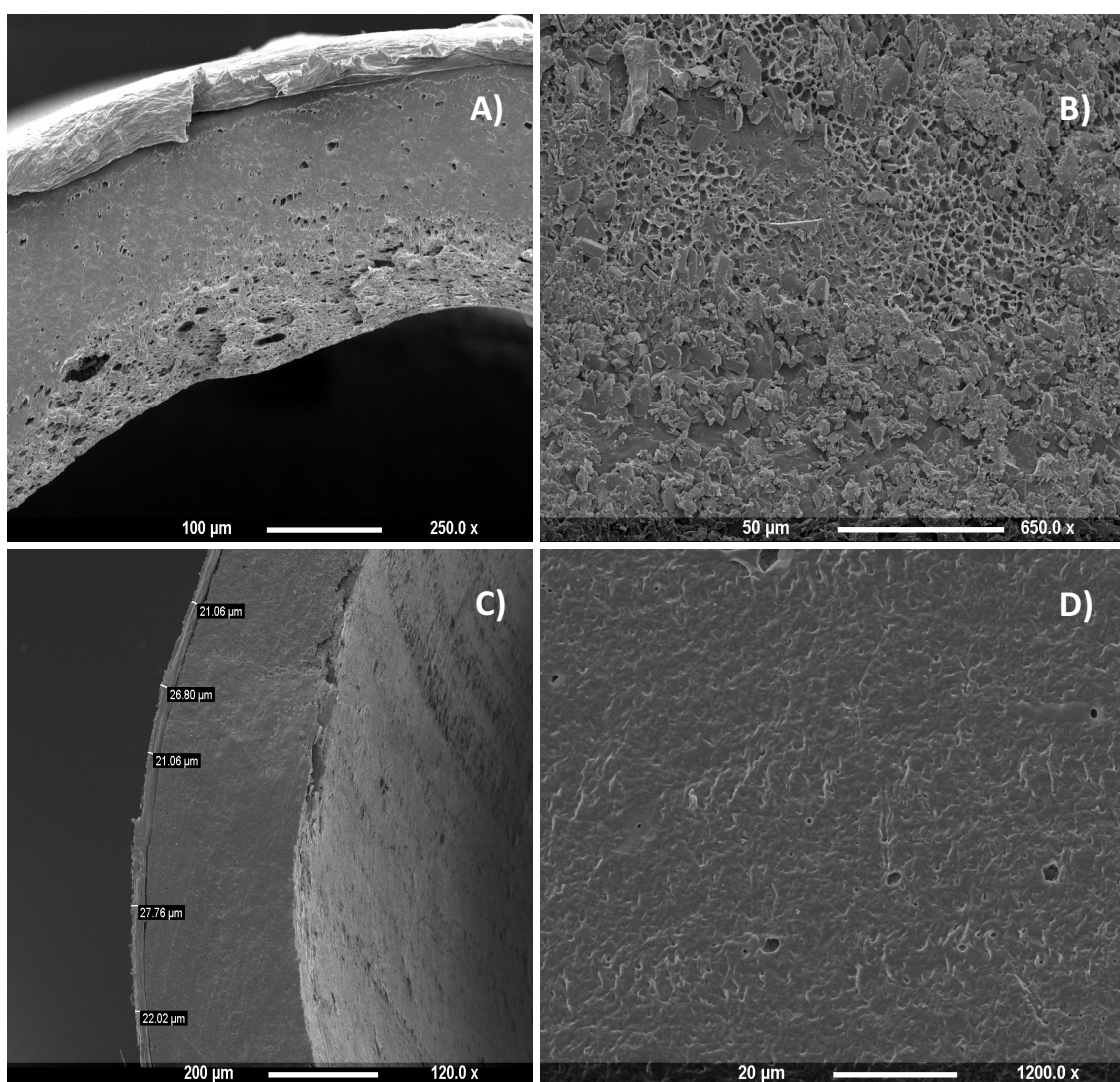


Figure 114: SEM micrographs of the P(3HB)/oligo-PHA tubes with rapamycin after 3 months of degradation study. (A) tube wall structure, (B) tube surface, (C) tube coating thickness, (D) inner surface of the tube.

SEM images of the P(3HB)/oligo-PHA tube with incorporated rapamycin within PCL-PEG550 polymeric coating have confirmed that the degradation process occurred after 3 months. The degradation mechanism seemed to involve the surface erosion from external layer. Therefore, within 3 months only the coating layer was affected by the degradation process. The loss of the coating thickness was 16% (Figure 114C). In the Figure 114B it is clearly visible, how hydrolytic degradation eroded the surface of the tube. The internal layer of the tube (Figure 114D) was however not affected by the hydrolytic environment during the 3 months study. Slightly increased porosity was observed in the wall of the tube (Figure 114A). The monolayer of PCL-PEG550 protected the inner core of the tube before degradation.

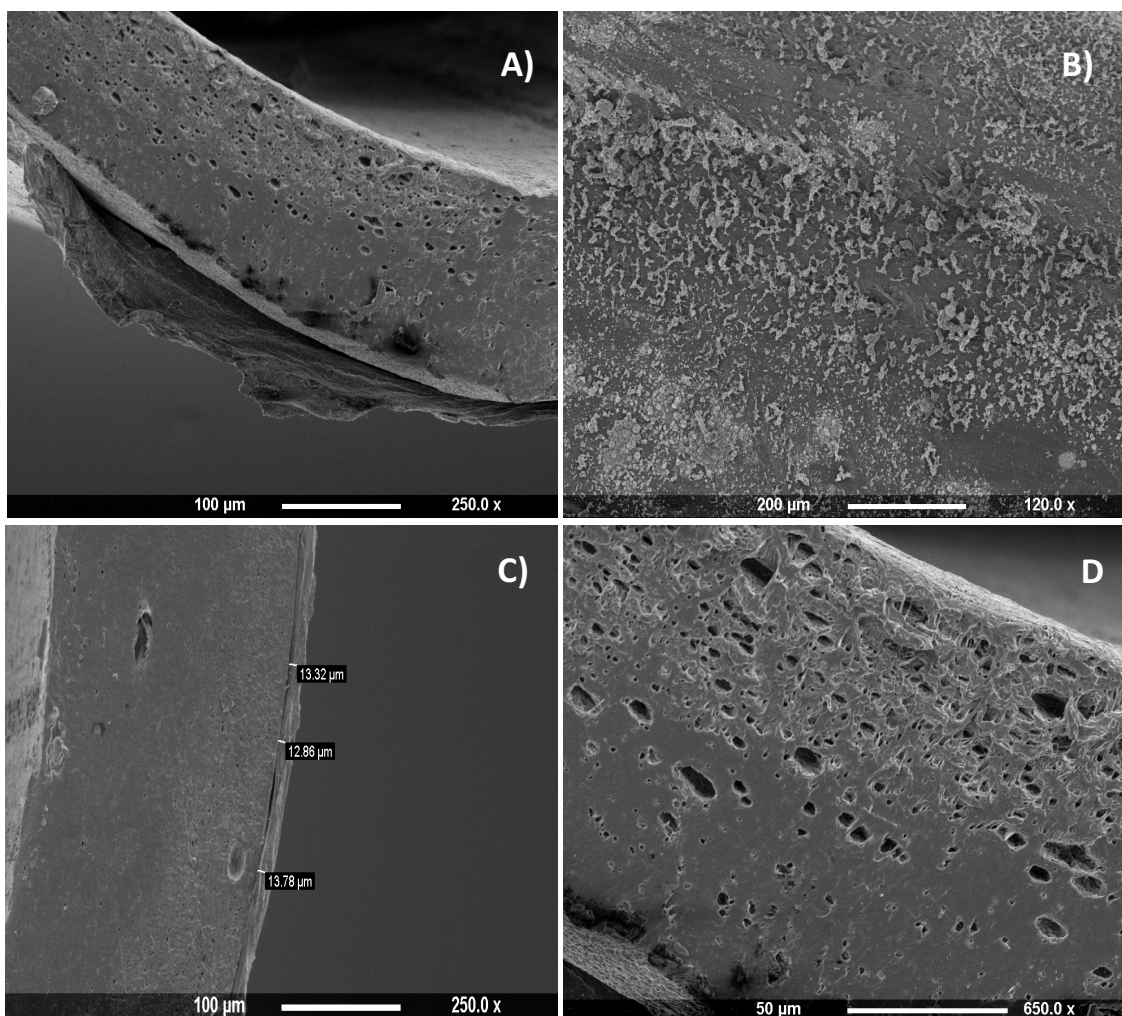


Figure 115: SEM micrographs of the P(3HB)/oligo-PHA tubes with tacrolimus after 3 months of degradation study. (A) tube wall structure, (B) tube surface, (C) thickness of the coating, (D) tube wall structure.

SEM images of the tubes with incorporated tacrolimus confirmed the degradation process has started within 3 months (Figure 115A-D). The degradation had happened by surface erosion from external layer. Separation between coating layer and the P(3HB)/oligo-PHA tube core have been observed. After 3 months time of degradation study mainly coating layer was affected by degradation process. The loss of the coating thickness was 67% (Figure 115C) in comparison to the fresh tube as described previously in Chapter 7. Figure 115B demonstrated outer surface of the tube, which belongs mainly to the PCL-PEG550 coating. Hydrolytic degradation obtained after 3 months of incubation of tubes in PBS at 37°C damaged the coating layer on the surface of the tube. PCL-PEG550 polymeric matrix layer is hardly visible; a lot of polymeric debris on the surface of the tube (Figure 115B). Internal layer of the tube presented increased porosity, caused by hydrolytic environment within 3 months time (Figure 115D). Monolayer of PCL-PEG550 protected core of the tube before degradation. After 3 months the tubes were still stable in the structure and easy to handle, whereas the neat tubes were quite fragile and brittle.

The results obtained in this study suggest that P(3HB)/oligo-PHA tubes with a PCL-PEG550 coating undergo a degradation process by surface erosion. P(3HB)/oligo-PHA tubes with incorporated tacrolimus underwent slightly more intense degradation process in comparison to the P(3HB)/oligo-PHA tubes containing rapamycin. However, in both cases, after 3 months of degradation study, mainly outer layers (PCL-PEG550 coating) of the tubes were affected by hydrolytic environment.

8.7. Discussion

One of the main properties of an ideal stent, require the ability to deliver drugs at the site of injury to allow ordinary healing of the artery wall and to prevent neointimal proliferation, which lead to restenosis (Ako *et al.*, 2007). In this study, P(3HB)/oligo-PHA 90/10 blend tubes were investigated for their ability to deliver immunosuppressive drugs, such as rapamycin or tacrolimus in a controlled manner. The P(3HB)/oligo-PHA 90/10 blend tube coated with polymeric layer of PCL-PEG550 with incorporated drugs were successfully prepared by using the dip moulding and dip coating techniques. The effect of rapamycin or tacrolimus loading on the surface, degradation properties,

biocompatibility and haemocompatibility study of these tubes were performed. *In vitro* drug release studies were carried out. Drug powders were characterised in order to check the thermal properties and the presence of typical chemical bonds. *In vitro* degradation study was performed for 3 months to test the influence of the hydrolytic environment along with higher temperature on the tubes.

The presence of both drugs was confirmed by FTIR analysis. Coated tubes with incorporated drugs showed weak chemical bonds characteristic of rapamycin and tacrolimus in comparison to tubes without loaded drugs (Patel *et al.*, 2013).

SEM was carried out to investigate the effect of drug loading on the surface topography of the blend films using SEM. A uniform surface of the tubes with rapamycin or tacrolimus was observed, similar to the neat tubes coated only with a polymeric layer. Drugs were dissolved completely in a uniform polymeric matrix. Rapamycin have been used previously in coronary stents. The concentration used in this study ($1.2\mu\text{g}/\text{mm}^2$) within the range used in coronary stents, which is $1\text{-}1.5\mu\text{g}/\text{mm}^2$ (Serruys *et al.*, 2002).

The total protein adsorption test was also carried out on the P(3HB)/oligo-PHA tubes coated with PCL-PEG550 containing rapamycin or tacrolimus to assess the effect of the presence of the drugs on proteins adsorption to the surface. As mentioned previously, protein adsorption is generally found to be higher on the hydrophilic surface (Hao and Lawrence, 2006). PCL-PEG550 is more hydrophilic than PHAs. Rapamycin and tacrolimus are hydrophobic drugs. Therefore, the total amount of proteins attached to the material with incorporated drugs should be higher in comparison to neat tubes but lower than coated tubes without drugs (neat PHA tube < PCL-PEG550 coated PHA tube with incorporated drugs < PCL-PEG550 coated PHA tube). This was exactly in agreement with the results obtained in this study. Hence, the higher protein adsorption observed on the coated tube with rapamycin or tacrolimus is most likely due to the increase in the hydrophobicity of the surface gained as a result of the presence of hydrophobic drugs within the matrix.

In vitro release profile of rapamycin confirmed local presence of the drug up to 72 days. On the other hand, only 69.2% of tacrolimus was released within 90 days. Park and co-workers reported release of tacrolimus as well as sirolimus from the polymeric matrix, used to coat bare metallic stent, within 32 days. (Park *et al.*, 2015). Khan *et al.*, 2013 reported controlled release of crystallised rapamycin from stents within 80 days.

Addition of polyethylene glycol (PEG) as a plasticizer further improved the release rate of the drug by acceleration of the degradation of the polymer (Wang *et al.*, 2006). Han and co-workers reported complete release of rapamycin from vascular grafts within 77 days (Han *et al.*, 2013). In conclusion, the drug release kinetics, obtained in this study demonstrated controlled release of rapamycin and tacrolimus throughout the release period. This suggested that the P(3HB)/oligo-PHA 90/10 blend tube with rapamycin or tacrolimus would be suitable for the drug delivery applications.

Another important aspect, that was addressed in these blend tubes with rapamycin or tacrolimus was the *in vitro* degradation study. Polymer hydrolytic degradation can be defined as the scission of chemical bonds in the polymer backbone by molecules of water to form oligomers and finally monomers. After immersing the material in the PBS or other media, the biomaterial absorbs water and swells, and degradation will progress from the external part of the material toward its internal site (Williams and Zhong, 1994). It is well-known fact, that the nature of the materials influences their degradation rate. All biodegradable materials contain hydrolysable bonds within their chemical structures. As first, hydrophilic materials with hydrolysable bonds will degrade followed by hydrophobic materials with hydrolysable bonds. Than hydrophilic and hydrophobic materials with non-hydrolysable bonds respectively (Azevedo and Reis, 2004). However, presence of strong covalent bonds in the backbone (like C-C) and non-hydrolysable groups require longer time for degradation. This is in agreement with the results obtained in this study. *In vitro* degradation studies demonstrated lower percentage of water adsorption and lower rates of weight loss after 3 months of incubation in comparison to neat tubes. Minor changes in the pH suggested absence of the highly acidic products released during polymer degradation. Homopolymer PCL required over 110 weeks to degrade in phosphate buffer (Dai *et al.*, 2009). PCL is well known synthetic polymer, which degrades slowly (up to 4 years) (Woodruff and Hutmacher, 2010; Gunatillake and Adhikari, 2003). However, addition of Poly(ethylene-glycol) (PEG) is a established method for accelerating the degradation rate of homo-polycaprolactone (Bei *et al.*, 1997; Pitt, 1990). Degradation of polymers is highly dependent on the molecular weight. The higher the molecular weight of the polymer, the longer degradation time required, which is in agreement with the results obtained in this study (Pitt *et al.*, 1981). Presence of an additional polymeric layer placed on the surface of the PHA tube as a

coating monolayer demonstrated a protective role for the inner PHA tube structure. In this case, the degradation of the tube might take longer time *in vivo* in comparison to the neat PHA tube without coating.

Presence of PEG550 block to the PCL enhanced hydrolytic degradation of the coating. However, addition of an external layer of PCL-PEG550 polymer into P(3HB)/oligo-PHA neat tube resulted in the initiation of the degradation process on the surface of the tubes. After 3 months, the coating was mainly present as debris on the surface of the tube. In this study, the addition of PCL-PEG550 layer slowed down the degradation rate of the PHA tubes. DSC data of the tube coated with PCL-PEG with incorporated tacrolimus confirmed the absence of the melting peak, characteristic for the PCL-PEG550 from the coating. An increased porosity was observed across the wall of the tube. The mechanical characterisation of the blend tubes coated with PCL-PEG550 with rapamycin or tacrolimus was carried out to investigate the effect of the hydrolytic degradation on their mechanical properties. The Young's modulus values and tensile strength of the degrading samples were lower than the non-degraded samples. Tubes became more brittle and material strength were affected by the degradation.

Another test that was done on these tubes with incorporated drugs was the indirect cytotoxicity study. This experiment was performed to determine the effect of the rapamycin or tacrolimus on the growth of HMEC-1 cells. Considering the potential application of these P(3HB)/oligo-PHA 90/10 blend tubes coated with PCL-PEG550 containing rapamycin or tacrolimus as the platform material for the drug eluting stent application, it is very crucial to investigate compatibility of the tubes with the endothelial cells. Indirect cytotoxicity study confirmed inhibiting effect on the growth of endothelial cells incubated with the extract from the tubes, containing rapamycin. This was confirmed with the results from the literature (Liu *et al.*, 2010). On one side, rapamycin inhibits smooth muscle cells migration, which has a positive effect inhibiting in-stent restenosis. On the other hand, presence of rapamycin leads to undermined endothelialisation, which can cause late stent thrombosis and therefore requires prolonged antiplatelet therapy (Moss *et al.*, 2010). This has weakened the positive effect of rapamycin on the inhibition of the neointimal growth in drug eluting stents (Holmes *et al.*, 2004). Indirect cytotoxicity study confirmed non-toxic effect of an extract released from the tubes with tacrolimus incubated in the media. Moreover, those tubes

demonstrated higher cell viability after day 1 than TCP. The results obtained established the potential of these tubes with tacrolimus in the area of drug eluting biodegradable stents.

The biocompatibility studies resulted in similar or slightly lower cell viability obtained for tube with significantly inhibited cell attachment, proliferation and survival of HMEC-1 cell line. Obtained results were in an agreement with results reported in literature. Gao and co-workers reported significant decrease in the number of endothelial cells after 72 hours incubation in the media with three different concentrations of rapamycin: 0.001, 0.01 and 1 μ g/mL respectively (Gao *et al.*, 2011). The results obtained in this study were in agreement with the literature. It is a well-known phenomenon, that rapamycin inhibits endothelial cell migration and proliferation as well as smooth muscle cells, whereas, tacrolimus does not present such effects. Although the inhibiting effect of tacrolimus on the migration of smooth muscle cells is lower in comparison to rapamycin, the antiproliferative effect of tacrolimus towards endothelial cells is significantly less, which is a positive result. This make tacrolimus a more promising drug for application in drug-eluting stents (Matter *et al.*, 2006). SEM micrographs confirmed these results. Cell attachment and proliferation was much less on the surface of the tubes containing rapamycin. All of the tested tubes did not have any haemolytic effect towards red blood cells. Both types of tubes demonstrated blood clotting rate lower than the control. The presence of immunosuppressive drugs, such as sirolimus and tacrolimus resulted in decelerated blood clot formation. Secondly, both drugs seem to have the same effect on the blood clot formation rate. All tested tubes demonstrated elevated monocytes and neutrophils activity. Surprisingly presence of rapamycin lead to a higher white cells activation, although it is a well-known inhibitor of inflammatory response. Haemocompatibility study was performed after 24hrs, hence only acute mechanisms could be observed. Extended time of this experiment could possibly bring more understanding about mechanisms of reaction of white blood cells with rapamycin incorporated within PHA based tubes and result in different outcome.

In conclusion, P(3HB)/oligo-PHA tubes coated with PCL-PEG550 layer with incorporated rapamycin or tacrolimus were successfully produced and characterised. Controlled local release of both drugs was achieved. However, an incorporation of rapamycin resulted in inhibition of endothelial cells attachment and had toxic effect on the viability of

HMEC-1. Presence of rapamycin had affected the biocompatibility of the tested material significantly. The results obtained confirmed high biocompatibility of HMEC-1 cells to the material with incorporated tacrolimus. Therefore, this drug can be considered for coronary stent application. By demonstrating good cell growth and proliferation, tubes containing tacrolimus are more suitable for medical devices, such as coronary stent application.

Chapter 9

Conclusions and future work

9.1. Conclusions

Polyhydroxyalkanoates are a very attractive group of biomaterials with great potential for biomedical applications (Hazer *et al.*, 2012). They present a broad range of properties and can be processed by using various techniques. Moreover, they are biodegradable and biocompatible (Philip *et al.*, 2007). Varied types of modifications can be applied to PHAs in order to further improve their properties. They can be used to produce blends, composites and grafts. PHAs can be processed into 2D flat films as well as 3D structures, such as fibers, tubes, patches, spheres, films and foams (Williams *et al.*, 1999). There is a high interest in the large-scale production and commercial exploitation of these materials. However, one of the major limitations in the commercialization of PHAs is its high cost of production, which significantly reflects in their market price. Much attention has been devoted to an efficient reduction of these costs, for example by using cheaper carbon sources, solvent-free polymer recovery techniques, genetically modified strains, more productive fermentations strategies (Koller *et al.*, 2017; Anjum *et al.*, 2016; Choi and Lee, 1999).

This research project can be divided into six main parts, which include: scl-PHA and mcl-PHA production and characterisation, development of P(3HB)/oligo-PHA blends, development of radiopaque composites, fabrication of tubes and incorporation of drugs into the polymeric matrix.

The first part of the project focused on scl-PHA production, using various types of bacterial strains and a range of carbon sources. All tested types of bacteria, which included *Bacillus* sp., *Pseudomonas* sp. and *Cupriavidus necator* were able to produce P(3HB). It is a well-known fact, that bacteria from *Bacillus* and *Cupriavidus* genera are able to produce P(3HB) from a variety of carbon sources, following specific metabolic pathways. In this study, P(3HB) was also produced by *P. mendocina*, when mixed carbon sources were used. It is worth highlighting the fact, that the highest polymer yield was obtained from *B. subtilis* OK2, when grown on glucose as the sole carbon source. *B. subtilis* is a Gram-positive bacterium, which does not contain lipopolysaccharides within the cell wall, hence do not trigger enhanced immunogenic response. *B. subtilis* has been classified by FDA as GRAS bacteria, which means: "Generally Recognised as Safe" (Morimoto *et al.*, 2008). This strain has been used in the industry for a large-scale

production of enzymes, proteins and fine chemicals (Zweers *et al.*, 2009). Until today, there is only one report about P(3HB) production from *B. subtilis* OK2. In this study, a batch fermentation mode has been explored. Therefore, further optimisation study is required in order to enhance the polymer productivity and make it competitive in the market. The P(3HB) obtained has been identified and fully characterised. It has similar properties to those, obtained from different bacterial strains. The final properties of the material can be achieved after few weeks, due to organisation of chains at a molecular level.

The second part of this project involved the economical production of mcl-PHAs using renewable and cheap carbon sources such as sugarcane molasses, biodiesel waste and vegetable oils. *Pseudomonas* sp. have been known to produce mainly mcl-PHAs. They utilize both structurally related and unrelated carbon sources and accumulate diverse mcl-PHA monomer units. Homopolymers as well as copolymers with different numbers of monomers within the recurrent monomer unit were produced. *P. mendocina* was able to produce mcl-PHAs from different carbon sources. Utilisation of biodiesel waste as a carbon source, resulted in a PHA yield of 38.9% dcw. The polymer was identified using FTIR and GC-MS. It was found to be a tetramer, which contains: 3HHx, 3HO, 3HD and 3HDD monomer units. From sugarcane molasses, an mcl-PHA copolymer, containing 3HO and 3HD units were obtained and the polymer yield was 14% dcw. When using vegetable oils, various mcl-PHA copolymers were produced. Among all tested oils, waste frying oil resulted in the highest polymer accumulation, which was 38% dcw. The chemical structure of the material was confirmed by FTIR and GC-MS. The results demonstrated that waste frying oil was a promising carbon source for mcl-PHAs production. P(3HHx-3HO-3HD-3HDD) copolymer obtained was very sticky and amorphous in nature. Moreover, a lack of solubility in organic solvents was observed. These results demonstrated that *P. mendocina* was capable of utilising sugarcane molasses, biodiesel waste, various types of vegetable oils, waste frying oil and mixed carbon sources as the feedstock for the production of PHAs. The use of these inexpensive carbon sources could not only effectively reduce the total cost of the production of PHAs but also enhance its competitiveness in various fields (Nor Aslan *et al.*, 2016).

The main objective of this research project was to develop a novel PHA for medical devices, such as coronary stents. To meet this objective, novel blends of P(3HB) with an addition of low molecular weight mcl-PHA copolymer (oligo-PHA) were developed focusing on the potential use of these 2D blend films as a platform material for coronary stents. Physical blending is one of the most economic and comprehensive way of producing novel materials by combining the desired properties of different polymers. This will allow wider range of application of these biopolymers (Ke *et al.*, 2017). Neat P(3HB) and three different types of blends: P(3HB)/5 wt% oligo-PHA, P(3HB)/10 wt% oligo-PHA and P(3HB)/20 wt% oligo-PHA blend films were prepared by solvent casting technique. The blend films were characterised in order to evaluate the effect of an addition of oligomers, acting as plasticising agents on the properties of the polymer. The results obtained emphasized the role of these additives in enhancing the mechanical properties of these blend films. Especially elongation at break was improved in comparison to neat P(3HB). Thermal analysis confirmed miscibility of the obtained system. According to the wettability studies, there was an increase in the water contact angle of the blend films compared to the neat P(3HB) films, due to the addition of the longer chains, indicating an increase in the hydrophobicity of the blend film. Biocompatibility is a crucial requirement from biomaterials considered for biomedical applications. It depends on several factors, such as: chemical structure, hydrophilicity, shape, porosity, microenvironment and degradation products (Wang *et al.*, 2004). Cell proliferation studies were carried out using the HMEC-1 cells over a period of 1, 3 and 7 days, which demonstrated the biocompatibility of the P(3HB)/oligo-PHA blends and neat P(3HB) films. The cell growth and proliferation on the blend films with addition of 10 wt% and 20 wt% oligo-PHA was higher compared to the neat P(3HB) film during 7 days of incubation. P(3HB)/oligo-PHA in ratio 80/20 had the most promising biocompatibility, the highest protein adsorption and surface roughness. However, the material presented the weakest mechanical properties, such as stiffness and strength. Therefore blend, which contains 10% addition of oligo-PHA was selected for further study. In these blend, the mechanical properties were similar to neat P(3HB), but the biocompatibility and surface characteristic were improved significantly. These results indicated that these novel P(3HB)/oligo-PHA blends would be well qualified for tissue engineering applications. Excellent biocompatibility is one of the most important requirements of

any tissue engineering scaffold (O'Brien, 2011). The cell culture data obtained from this study revealed promising results by demonstrating high cell growth and proliferation on the blend films. Tested blends were non-haemolytic in direct contact with fresh whole blood. All tested materials demonstrated low thrombogenic properties. Neat P(3HB) as well as P(3HB)/oligo-PHA blends showed slightly higher activity of monocytes and neutrophils in comparison to the non-activated whole blood. Interestingly, similar trend was observed in PL38, a GMP class material. The results obtained make these blends promising biomaterials for a biomedical application in coronary stent application.

In the next part of the study, P(3HB)/oligo-PHA blend 90/10 was produced selected for development of radiopaque composites. Radiopacity is one of the characteristics, essential for biodegradable stents, which would allow surgeons to monitor the device during deployment and after the procedure. Barium sulphate was selected as a contrast agent in concentration 1 wt%, 3 wt% and 5 wt%. Composites were prepared by solvent casting technique. These materials obtained were characterised with respect to their mechanical, thermal and surface properties. They were also characterised for their bioactivity using HMEC-1 cells. The results highlighted that the addition of barium sulphate within the P(3HB)/oligo-PHA matrix reduced the elastomeric properties of the blends. Materials obtained were much more brittle. There was slight improvement in the tensile strength of the material. Addition of BaSO₄ affected significantly the surface topography of the composite materials. Composites with barium sulphate presented higher surface roughness and protein adsorption in comparison to neat blend. With an increased concentration of barium sulphate the contact angle values decreased, hence material became less hydrophobic. Indirect cytotoxicity results showed that these composite films were not toxic to the HMEC-1 cells. Moreover, addition of 3 wt% and 5 wt% of barium sulphate resulted in significant improvement in cell viability after day 1 and 3 of incubation. The % cell viability on the composite films was higher compared to the neat P(3HB)/oligo-PHA blend film. The results of the cytocompatibility assessment demonstrated increased biocompatibility of these composites with the HMEC-1 cells. Additionally, radiopacity of the materials was achieved and the x-ray adsorption increased with greater amount of BaSO₄. Composites did not demonstrate any haemolytic effect towards red blood cells. The materials had decelerating effect on the blood clot formation. However, presence of barium sulphate resulted in significant

increase in neutrophils and monocytes activity. The results obtained such as improved surface topography and biocompatibility along with radiopacity make these composites an attractive biomaterial for a biomedical application in coronary stent application.

Next part of the project was focused on tubes manufactured by the dip moulding technique using P(3HB)/oligo-PHA blend in the ratio 90:10, obtained in the previous part of study. P(3HB)/oligo-PHA neat tubes, composite tubes with addition of 5 wt% barium sulphate and P(3HB)/oligo-PHA tube coated with PCL-PEG550 were fabricated. Tubes were fully characterised in order to investigate mechanical, thermal properties, conditions of storage, surface topography and biocompatibility. Neat P(3HB)/oligo-PHA 90/10 blend tubes demonstrated promising thermal and mechanical properties. However, the material underwent embrittlement phenomenon within 7 weeks of storage. Incubation of tubes in DMEM media at 37°C influenced the mechanical properties of the tubes in comparison to tubes stored at room temperature without any media. Incubated tubes became more brittle, had much lower values of Young's modulus and slightly lower tensile strength. Mechanical properties of the tubes storage at room temperature were higher than tubes incubated in DMEM media at 37°C. Tubes underwent process called "material aging" within the time and followed similar pathway to this demonstrated by blend films. Overall, material based on P(3HB) became more brittle and stiff. *In vitro* degradation study was carried out for 6 months on the neat tubes. P(3HB)/oligo-PHA 90/10 tubes after 6-month incubation in PBS at 37°C resulted in a weight loss of 30%. P(3HB)/oligo-PHA tubes were characterised with high level of water absorption. The degradation products that leached to the media slightly lowered the pH. After 3-month incubation time the tubes became fragile and brittle. Surface characterisation confirmed the degradation process as well as over 30% loss within the wall thickness. An increased porosity was observed within the tube walls. The coated tubes by covering the blend tube with a monolayer of PCL-PEG550 were prepared to investigate the potential of PHAs as drug delivery vehicles for drug eluting coronary stents. The FTIR and DSC analysis clearly confirmed presence of additional polymer, which demonstrated different properties than PHAs. Presence of an additional polymeric layer had a positive effect on the mechanical properties of the tubes. The strength as well as stiffness of the material had improved. The PCL-PEG550 layer had a protective function on the tube and slowed down the embrittlement process after

storage at room temperature for 7 weeks in comparison to the neat tubes. Addition of the hydrophilic polymer in the external layer resulted in enhanced protein adsorption to the coated surface in comparison to the neat tubes. Barium sulphate was added as a contrast agent in order to obtain radiopacity required for the monitoring of the device inside the body. Addition of barium sulphate to the blend resulted in enhanced brittleness of the tubes. Also, it did affect the microstructure of the tubes. Composite tubes did not have any porosity. A MicroCT scan confirmed the potential radiopaque effect, caused by the presence of BaSO₄. PCL-PEG550 coated tube demonstrated significantly higher protein adsorption, which can be explained by increased hydrophobicity of the material by addition of PCL-PEG550. Biocompatibility study was carried out for 7 days. Composite tubes demonstrated the highest cell attachment and proliferation, which might be the enhanced roughness of the material, due to the addition of BaSO₄ particles resulted in a rougher surface with anchor points for the endothelial cells. Indirect cytotoxicity studies confirmed the non-toxic effect of extracts from all kinds of tested tubes on the HMEC-1 cell line. The tubes did not demonstrate any haemolytic effect on the erythrocytes. PCL-PEG550 coated tube significantly decelerated blood clot formation rate. The coagulation cascade was not activated in the presence of composite tube. Presence of barium sulphate led to higher neutrophils and monocytes activity, as described previously. Further surface modifications of the external layer of the tubes, in order to achieve higher surface roughness, might enhance the cell attachment and proliferation on the neat blend and coated tubes. Additionally, an appropriate stent design, might help to solve the issues raised due to the smooth surface topography.

Finally, an investigation of the P(3HB)/oligo-PHA blend tube with PCL-PEG550 layer containing, as the base material for the development of a drug eluting biodegradable stent was carried out by incorporation of immunosuppressive drugs, such as rapamycin or tacrolimus. Influence of the tubes on surface topography, biocompatibility, haemocompatibility and the degradation rate were investigated. A drug release study was carried out by using UV-VIS Spectrophotometry and High Performance Liquid Chromatography (HPLC) for rapamycin and tacrolimus respectively. Microstructural study demonstrated no influence on the surface topography of the tubes. However, presence of hydrophobic drugs influenced the amount of proteins attached to the

surface, which was lower than P(3HB)/oligo-PHA tube with coating without any drugs. *In vitro* biocompatibility study demonstrated high cell viability on the tubes containing tacrolimus. Rapamycin had an inhibiting effect on cell viability, attachment and proliferation. Presence of drugs lead to the reduction of side effects, such as restenosis, which was the main limitation of bare metallic stent (Alfonso *et al.*, 2014). One of the most important features of the drug eluting biodegradable stent is the local and controlled release of the drugs. Drug release studies showed that there was a controlled release of rapamycin as well as tacrolimus from the coating on the tubes, throughout the release period. After 72 days, over 95% of rapamycin was released. The amount of released tacrolimus after 90 days was around 70%. *In vitro* degradation study, carried out for 3 months confirmed an initiation of hydrolytic degradation process, which progressed from the surface of the tube and result in gradual disappearance of the most external layer, which was PCL-PEG550 coating with incorporated drugs. DSC analysis of tubes with tacrolimus confirmed the disappearance of the melting peak related to the presence of PCL-PEG550. Mechanical properties of the tubes changed within the time of incubation. The tensile strength values decreased slightly, whereas Young's Modulus values increased. Parameter that was the most affected was elongation at break, with tubes becoming much more brittle. The achieved weight loss was 5.5%-6.4% for tubes with rapamycin and tacrolimus respectively. The tube containing tacrolimus had a higher water absorption in comparison to the tubes with rapamycin. Tubes with drugs were identified to be non-haemolytic with very low risk of thrombogenicity. Addition of drugs resulted in higher activation of neutrophils and monocytes, especially in the presence of rapamycin.

In summary, a drug delivery system for the controlled delivery of rapamycin and tacrolimus was successfully developed. P(3HB)/oligo-PHA tubes coated with PCL-PEG550 with and without drugs were prepared using the dip coating technique to investigate their potential as a drug delivery system for the controlled release of rapamycin or tacrolimus. From the drug release pattern, we could conclude that the P(3HB)/oligo-PHA based tubes could be used for the sustained long term drug release. Tacrolimus emerged to be the more promising drug for coronary stents due to its higher biocompatibility.

9.2. Future work

Results obtained in this study demonstrated possibility of production of P(3HB) by using *B. subtilis* OK2 and to use it along with low molecular weight mcl-PHA for medical devices, such as coronary stents. Base on the data, following areas can be explored in order to improve further achieved outcomes.

Optimisation studies of P(3HB) production using *B. subtilis* OK2

P(3HB) was successfully produced and identified during this study. However, the polymer yield needs improvement to lower the total cost of production and become competitive with other plastics in the market. In the first step, the media composition, which will contain the list of all nutrients required for growth and polymer production in optimal concentration needs to be identified. Secondly, various carbon sources as well as different fermentation strategies can be investigated. Additionally, design of experiments can be applied to optimise further the production of P(3HB).

Surface modifications of the material

Various types of surface modifications of these blend tubes can be explored. For example: laser micropatterning (physical method), plasma treatment (biochemical method), chemical modifications of the PHAs. This will create a more attractive surface for endothelial cells attachment and proliferation and improve further material biocompatibility.

Optimisation of coating matrix

Selection of appropriate material for coating is crucial in drug-eluting stents in order to ensure controlled local drug delivery from the device. Also, the degradation profile needs to fulfil those requirements. Therefore, exploration of various types of materials for coating along with drug release studies will be a great interest.

***In vitro* degradation study**

PHAs require several months to degrade. Therefore, intensive degradation study, both: enzymatic and non-enzymatic will be an interesting field of research. This will help to improve further the material properties, if required.

Drug selection

In this study, only two antiproliferative drugs were tested. It will be worth exploring another possible bioactive agent, in order to reduce risk of restenosis, but with minimal reduction of biocompatibility of the construct. Additionally, different types of drug carriers can be explored, such as bioactive glasses, microspheres, fibres loaded with drugs.

Haemocompatibility study

Haemocompatibility studies are required to know the reaction of blood cells after direct contact of developed biomaterial with blood. Special attention needs to be paid to platelet adhesion and white cell activation. Parallel studies of degradation and haemocompatibility would be interesting in order to evaluate the effect of degradation products, such as low molecular weight compounds on whole blood cells.

Stent prototype fabrication and characterisation

In this study, 3D tubular structures were successfully developed. However, due to lack of time it could not be fully fabricated to a stent prototype. Development of a complete stent prototype with a novel stent design and its complete characterisation would be very relevant. Incorporation of antiproliferative drugs or different bioactive agents, such as antibodies within the stent prototype and monitoring their drug release kinetics would be the next step forward. Cell culture and degradation studies of these stent prototypes under dynamic conditions, mimicking the surroundings of blood vessel would be worth exploring.

***In vivo* stent prototype evaluation**

In this study, P(3HB)/oligo-PHA blend tubes were fabricated for their use in the development of biodegradable stents. In the future, *in vivo* evaluation of stent prototypes in small and large animals would be a great addition. *In vivo* study can also be used to evaluate prototype in order to evaluate an appropriate sterilisation techniques, stent deployment, radiopacity, degradation within the body and biological functionality.

References

- Abdelwahaba, M.A., Flynn, A., Chiou, B.S., Imam, S., Orts, W., Chiellinia, E. (2012) Thermal, mechanical and morphological characterization of plasticized PLA–PHB blends. *Polymer Degradation and Stability*. 97, 1822–1828.
- Abe, H., Ishii, N., Sato, S., Tsuge, T. (2012) Thermal properties and crystallization behaviours of medium-chain-length poly(3-hydroxyalkanoate)s. *Polymer* 53, 3026-3034.
- Acharya, G., Park, K. (2006) Mechanisms of controlled drug release from drug-eluting stents. *Advanced Drug Delivery Reviews*. 58, 387-401.
- Aditi, S., D’Souza, S., Narvekar, M., Rao, P., Tembadmani, K. (2015) Microbial production of polyhydroxyalkanoates (PHA) from novel sources: A Review. *International Journal of Research in Biosciences*. 4 (4), 16-28.
- Aggarwal, R.K., Ireland, D.C., Azrin, M.A., Ezekowitz, M.D., de Bono, D.P., Gershlick, A.H. (1996) Antithrombotic potential of polymer-coated stents eluting platelet glycoprotein IIb/IIIa receptor antibody. *Circulation*. 94, 3311–3317.
- Agrawal, C.M., Clark, H.G. (1992) Deformation characteristics of a bioabsorbable intravascular stent. *Investigative Radiology*. 27, 1020-1023.
- Agriculture and Food Development Authority (2000), Waste Oils and Fats as Biodiesel Feedstocks: an assessment of their potential in the EU, ALTENER Program NTB-NETT Phase IV, Task 4, Final Report, March 2000.
- Akaraonye, E., Filip, J., Safarikova, M., Salih, V., Keshavarz, T., Knowles, J.C., Roy, I. (2016a) P(3HB) based magnetic nanocomposites: smart materials for bone tissue engineering. *Journal of Nanomaterials*. 14 pages, doi:10.1155/2016/3897592.
- Akaraonye, E., Filip, J., Safarikova, M., Salih, V., Keshavarz, T., Knowles, J.C., Roy, I. (2016b) Composite scaffolds for cartilage tissue engineering based on natural polymers of bacterial origin, thermoplastic poly(3-hydroxybutyrate) and microfibrillated bacterial cellulose. *Polymer International*. 65(7), 780-791.
- Akaraonye, E., Moreno, C., Knowles, J.C., Keshavarz, T., Roy, I. (2012) Poly(3-hydroxybutyrate) production by *Bacillus cereus* SPV using sugarcane molasses as the main carbon source. *Journal of Biotechnology*. 7(2): 293-303.
- Akaraonye, E., Keshavarz, T., Roy, I. (2010) Production of polyhydroxyalkanoates: the future green materials of choice. *Journal of Chemical Technology and Biotechnology*. 85: 732-743.
- Ako, J., Bonneau, H.N., Honda, Y., Fitzgerald, P.J. (2007) Design criteria for the ideal drug-eluting stent. *American Journal of Cardiology*. (www.AJConline.org). 100 (8B): 3M-9M.
- Alfonso, F., Byrne, R.A., Rivero, F., Kastrati, A. (2014) Current Treatment of In-Stent Restenosis. *Journal of the American College of Cardiology*. 63 (24), 2659-

REFERENCES

- 2673.
- Ali, I., Jamil, N. (2016) Polyhydroxyalkanoates: current applications in the medical field. *Frontiers in Biology*. 11 (1), 19–27. DOI 10.1007/s11515-016-1389-z.
 - Amulya, K., Jukuri, S., Mohan S.V. (2015) Sustainable multistage process for enhanced productivity of bioplastics from waste remediation through aerobic dynamic feeding strategy: Process integration for up-scaling. *Bioresource Technology*. 188, 231–239.
 - Anderson, J.M., Rodriguez, A., Chang, D.T. (2008) Foreign body reaction to biomaterials. *Seminars in Immunology*. 20, 86–100.
 - Anderson, J. (2001) Biological responses to biomaterials. *Annual Review of Material Research*. 31, 81–110.
 - Anderson, J.M. (1993) Chapter 4 Mechanisms of inflammation and infection with implanted devices. In: *Cardiovascular Pathology*. 2 (3), 33-41.
 - Anderson, A.J., Dawes, E.A. (1990) Occurrence, metabolism, metabolic role, and industrial uses of bacterial polyhydroxyalkanoates. *Microbiological Reviews*. 54 (4), 450-472.
 - Anjum, A., Zuber, M., Zia, K.M., Noreen, A., Anjum, M.N., Tabasum, S. (2016) Microbial production of polyhydroxyalkanoates (PHAs) and its copolymers: A review of recent advancements. *International Journal of Biological Macromolecules*. 89, 161-174.
 - Anselme, K., Ploux, L., Ponche, A. (2009) Cell/material interfaces: Influence of surface chemistry and surface topography on cell adhesion. *Journal of Adhesion Science and Technology*. 24, 831-852.
 - Ashby, R.D., Solaiman, D.K.Y., Strahan, G.D., Zhu, C., Tappel, R.C., Nomura, C.T. (2012) Glycerine and levulinic acid: Renewable co-substrates for the fermentative synthesis of short-chain poly(hydroxyalkanoate) biopolymers. *Bioresource Technology*. 118, 272–280.
 - Ashby, D.T., Dangas, G., Mehran, R., Leon, M.B. (2002) Coronary Artery Stenting. *Catheterization and Cardiovascular Interventions*. 56, 83–102.
 - Ashby, R.D., Solaiman, D.K., Foglia, T.A. (2004) Bacterial poly(3-hydroxyalkanoate) polymer production from the biodiesel co-product stream. *Journal of Polymers and Environment*. 12, 105–112. doi:10.1023/B:JOOE.0000038541.54263.d9.
 - Ashby, R.D., Solaiman, D.K., Foglia, T.A. (2002) The synthesis of short- and medium-chain-length poly(hydroxyalkanoate) mixtures from glucose- or alkanolic acid-grown *Pseudomonas oleovorans*. *Journal of Industrial Microbiology and Biotechnology*. 28, 147–153.
 - Azevedo, H.S., Gama, F.M., Reis, R.L. (2004) *In vitro* assessment of the enzymatic degradation of several starches based biomaterials. *Biomacromolecules*. 4, 1703–1712.

REFERENCES

- Balcon, R., Beyar, R., Chierchia, S., De Scheerder, I., Hugenholtz, P.G., Kiemeneij, F., Meier, B., Meyer, J., Monassier, J.P., Wijns, W. (1997) Recommendations on stent manufacture, implantation and utilization. *European Heart Journal*. 18, 1536–1547.
- Bacakova, L., Filova, E., Parizek, M., Ruml, T., Svorcik, V. (2011) Modulation of cell adhesion, proliferation and differentiation on materials designed for body implants. *Biotechnology Advances*. 29(6), 739-67. doi: 10.1016/j.biotechadv.2011.06.004.
- Bagdadi, A., Safari, M., Dubey, P., Basnett, P., Sofokleous, P., Humphrey E., Locke, I.C., Edirisinghe, M., Terracciano, C., Boccaccini, A.R., Knowles, J.C., Harding, S., Roy, I. (2017) Poly(3-hydroxyoctanoate), a promising new material for cardiac tissue engineering. *Journal of Tissue Engineering and Regenerative Medicine*. 12: e495–e512. DOI: 10.1002/term.
- Bala, H., Fu, W., Guo, Y., Zhao, J., Jiang, Y. (2006) *In situ* preparation and surface modification of barium sulfate nanoparticles. *Colloids Surfaces A: Physicochemical and Engineering Aspects*. 274, 71-76. DOI: 10.1016/J.COLSURFA.2005.08.050.
- Baleani, M., Viceconti, M. (2011) The effect of adding 10% of barium sulphate radiopacifier on the mechanical behaviour of acrylic bone cement. *Fatigue and Fracture of Engineering Materials and Structures*. 34(5), 374-382.
- Barham, P.J., Keller, A., Otun, E.L., Holmes, P.A. (1984) Crystallization and morphology of a bacterial thermoplastic: poly-3-hydroxybutyrate. *Journal of Materials Science*. 19(9), 2781-2794.
- Barras, C.D.J., Myers, K.A. (2000) Nitinol—its use in vascular surgery and other applications. *European Journal of Vascular and Endovascular Surgery*. 19, 564–69.
- Basnett, P., Lukasiewicz, B., Marcello, E., Kaur, H., Knowles, J.C., Roy, I. (2017) Production of a novel medium chain length Poly(3-hydroxyalkanoate) using unprocessed biodiesel waste and its evaluation as a tissue engineering scaffold. *Microbial Biotechnology*. 10 (6), 1384-1399.
- Basnett, P., Ching, K.Y., Stolz, M., Knowles, J.C., Boccaccini, A.R., Smith, C., Locke, I.C., Keshavarz, T., Roy, I. (2013) Novel Poly(3-hydroxyoctanoate)/Poly(3-hydroxybutyrate) blends for medical applications. *Reactive and Functional Polymers*. 73, 10. DOI: 10.1016/j.reactfunctpolym.2013.03.019
- Basnett, P., Roy, I. (2010) Microbial production of biodegradable polymers and their role in cardiac stent development [in:] Mendez-Vilas A.: *Current Research, Technology and Education Topics in Applied Microbiology and Microbial Biotechnology*, Formatex, 1405-1415.
- Beauchesne, I., Barnabe, S., Cooper, D.G., Nicell, J.A. (2007) Plasticizers and related toxic degradation products in wastewater sludges. In: IWA Specialist Conf. Biosolids, Moncton, New Brunswick, Canada.

REFERENCES

- Baujard-Lamotte L, Noinville S, Goubard F, Marque P, Pauthe E. (2008) Kinetics of conformational changes of fibronectin adsorbed onto model surfaces. *Colloids Surf B Biointerfaces*. 1, 63 (1), 129-37. doi: 10.1016/j.colsurfb.2007.11.015.
- Bei, J.Z., Li, J.M., Wang, Z.F., Le, J.C., Wang, S.G. (1997) Polycaprolactone-poly(ethylene-glycol) block copolymer. IV: Biodegradation behaviour *in vitro* and *in vivo*. *Polymers for Advanced Technologies*. 8, 693-696. 10.1002/(SICI)1099-1581(199711)8:113.O.CO;2-B.
- Bell, E., Ehrlich, H.P., Buttle, D.J., Nakatsuji, T. (1981) Living tissue formed *in vitro* and accepted as skin equivalent tissue of full thickness. *Science*. 211: 1052.
- Benicewicz, B.C., Hopper, P.K. (1991) Review: Polymers for Absorbable Surgical Sutures—Part II. *Journal of Bioactive and Compatible Polymers*. 6 (1), 64-94. <https://doi.org/10.1177/088391159100600106>.
- Bettinger, C.J. (2009) Synthesis and microfabrication of biomaterials for soft-tissue engineering. *Pure and Applied Chemistry*. 81 (12) 2183–2201. doi:10.1351/PAC-CON-09-07-10.
- Berger, E., Ramsay, B.A., Ramsay, J.A., Chavarie, C., Braunegg, G. (1989) PHB recovery by hypochlorite digestion of non-PHB biomass. *Biotechnology Techniques*. 3, 227–232. DOI: 10.1007/BF01876053.
- Bhattacharyya, A., Pramanik, A., Maji, S.K., Haldar, S., Mukhopadhyay, U.K., Mukherjee, J. (2012) Utilization of vinasse for production of poly-3-(hydroxybutyrate-co-hydroxyvalerate) by *Haloferax mediterranei*. *AMB Express* 2, 1–10.
- Bhattacharyya, D., Xu, H., Deshmukh, R.R., Timmons, R. B., Nguyen, K.T. (2010) Surface chemistry and polymer film thickness effects on endothelial cell adhesion and proliferation. *Journal of Biomedical Materials Research. Part A*. 94(2), 640–648. <http://doi.org/10.1002/jbm.a.32713>.
- BHF CVD statistics compendium 2017 in collaboration with the British Heart Foundation Centre on Population Approaches for Non-Communicable Disease Prevention at the Nuffield Department of Population Health, University of Oxford. Published on March 2017.
- Bhubalan, K., Rathi, D.N., Abe, H., Iwata, T., Sudesh, K. (2010) Improved synthesis of P(3HB-co-3HV-co-3HHx) terpolymers by mutant *Cupriavidus necator* using the PHA synthase gene of *Chromobacterium* sp. USM2 with high affinity towards 3HV. *Polymer Degradation Stability*. 95 (8), 1436-1442.
- Bian, M.H., Hu, W.F., Pang, X., Zuo, Y. (2012) Biocompatibility of polyhydroxyalkanoates synthesized by *Bacillus cereus* BMH. *Advanced Materials Research*. 531, 423-427.
- Bian, Y.Z., Wang, Y., Guli, S., Chen, G.Q., Wu, Q. (2009) Evaluation of poly(3-hydroxybutyrate-co-3-hydroxyhexanoate) conduits for peripheral nerve regeneration. *Biomaterials*. 30, 217–225.

REFERENCES

- Birkenhauer, P., Yang, Z., Gander, B. (2004) Preventing restenosis in early drug-eluting stent era: recent developments and future perspectives. *JPP*. 56, 1339–1356.
- Bissery, M.C., Valeriote, F., Thies, C. (1985) Therapeutic efficacy of CCNU-loaded microspheres prepared from poly(D,L)lactide (PLA) or poly- β -hydroxybutyrate (PHB) against Lewis lung (LL) carcinoma. *Proceedings of the American Association for Cancer Research*. 26, 355–355.
- Bittmann, B., Bouza, R., Barral-Losada, L., Diez, J., Ramirez, C. (2013) Poly(3-hydroxybutyrate-co-3-hydroxyvalerate)/clay nanocomposites for replacement of mineral oil based materials. *Polymer Composites*. 34. 10.1002/pc.22510.
- Bhatia, S.K., Shim, Y.H., Jeon, J.M., Brigham, C.J., Kim, Y.H., Kim, H.J., Seo, H.M., Lee, J.H., Kim, J.H., Yi, D.H., Lee, Y.K., Yang, Y.H. (2015) Starch based polyhydroxybutyrate production in engineered *Escherichia coli*. *Bioprocess and Biosystems Engineering*. 38(8), 1479-84. doi: 10.1007/s00449-015-1390-y.
- Borovetz, H.S., Burke, J.F., Chang, T.M.S. (2004) Application of materials in medicine, biology and artificial organs, in: B.D. Ratner, A.S. Hoffman, F.J. Schoen, J.E. Lemons (Eds.), *Biomaterials Science*, 2nd edition, Elsevier Academic Press, Boston, 455–479.
- Boyandin, A.N., Prudnikova, S.V., Karpov, V.A., Ivonin, V.N., Đỗ Nguyễn, T.H., Hiệp Lê, T.M., Filichev, N.L., Levin, A.L., Filipenko, M.L., Volova, T.G., Gitelson, I.I. (2013) Microbial degradation of polyhydroxyalkanoates in tropical soils. *International Biodeterioration and Biodegradation*. 83, 77-84.
- Braune, S., Lange, M., Richau, K., Lützow, K., Weigel, T., Jung, F., Lendlein, A. (2010) Interaction of thrombocytes with poly(ether imide): The influence of processing. *Clinical Hemorheology and Microcirculation*. 46(2-3), 239-50. doi: 10.3233/CH-2010-1351.
- Brattstrom, C., Wilczek, H.E., Tyden, G., Bottiger, Y., Sawe, J., Groth, C.G. (1998) Hypertriglyceridemia in renal transplant recipients treated with sirolimus. *Transplantation Proceedings*. 30, 3950–3951.
- Braun-Dullaeus, R.C., Mann, M.J., Ziegler, A. (1999) A novel role for the cyclin-dependent kinase inhibitor p27(Kip1) in angiotensin II-stimulated vascular smooth muscle cell hypertrophy. *Journal of Clinical Investigation*. 104, 815–823.
- Brigham, C.J., Sinskey, A.J. (2012) Applications of Polyhydroxyalkanoates in the Medical Industry. *International Journal of Biotechnology for Wellness Industries*. 1, 53-60.
- Bryers, J.D., Giachelli, C.M., Ratner, B.D. (2012) Engineering biomaterials to integrate and heal: the biocompatibility paradigm shifts. *Biotechnology and Bioengineering*. 109, 8, 1898-1911.
- Budde, C.F., Riedel, S.L., Hübner, F., Risch, S., Popović, M.K., Rha, C.K., Sinskey, A.J. (2011) Growth and polyhydroxybutyrate production by *Ralstonia eutropha*

REFERENCES

- in emulsified plant oil medium. *Applied Microbiology and Biotechnology*. 89, 1611–1619/ DOI 10.1007/s00253-011-3102-0.
- Bugnicourt, E., Cinelli, P., Lazzeri, A., Alvarez, V. (2014) Polyhydroxyalkanoate (PHA): Review of synthesis, characteristics, processing and potential applications in packaging. *eXPRESS Polymer Letters*. 8, 11, 791–808. DOI: 10.3144/expresspolymlett.2014.82.
 - Burgos, N., Tolaguera, D., Fiori, S., Jiminez, A. (2014) Synthesis and characterization of lactic acid oligomers: Evaluation of performance as poly(lactic acid) plasticizers. *Journal of Polymers and the Environment*. 22, 227–235.
 - Cadogan, D.F. (1991) Plasticizers: A consideration of their impact on health and the environment. *Journal of Vinyl and Additive Technology*. 13: 104–108. doi:10.1002/vnl.730130209.
 - Camenzind, E., Steg, P.G., Wijns, W. (2007) Stent thrombosis late after implantation of first-generation drug-eluting stents: a cause for concern. *Circulation*. 115 (11), 1440-55.
 - Chanprateep, C. (2010) Current trends in biodegradable polyhydroxyalkanoates. *Journal of Bioscience and Bioengineering*. 110 (6), 621–632.
 - Cara, F.L., Immirzi, B.E., Mazzella, A., Portofino, S., Orsello, G., De Prisco, P.P. (2003) Biodegradation of poly-ε-caprolactone/poly-β-hydroxybutyrate blend. *Polymer Degradation and Stability*. 79, 37–43.
 - Carlo, E.C., Borges, A.P.B., Pompermayer, L.G., Martinez, M.M.M., Eleotério, R.B., Nehme, R.C., Morato, G.O. (2009) Composite for the fabrication of resorbable implants for osteosynthesis: biocompatibility evaluation in rabbits. *Ciencia Rural*, 39 (1), 135-140.
 - Carter, A.J., Brodeur, A., Collingwood, R., Ross, S., Gibson, L., Wang, C.A., Haller, S., Coleman, L., Virmani, R. (2006) Experimental efficacy of an everolimus eluting cobalt chromium stent. *Catheter Cardiovascular Interventions*. 68, 97–103.
 - Cassatella, M.A., Locati, M., Mantovani, A. (2009) *Never underestimate the power of a neutrophil*. *Immunity*. 31, 698–700.
 - Castilho, L.R., Mitchell, D.A., Freire, D.M.G. (2009) Production of polyhydroxyalkanoates (PHAs) from waste materials and by-products by submerged and solid-state fermentation. *Bioresource Technology*. 100 (23), 5996–6009. <http://dx.doi.org/10.1016/j.biortech.2009.03.088>.
 - Cavalheiro, J., De Almeida, A., Grandfils, C., Da Fonseca, M.M.R. (2009) Poly(3-hydroxybutyrate) production by *Cupriavidus necator* using waste glycerol. *Process Biochemistry*. 44, 509–515. doi:10.1016/j.procbio.2009.01.008.
 - Cesario, M.T., Raposo, R.S., Catarina, M., de Almeida, M.D., van Keulen, F., Ferreira, B.S., Manuela, M., da Fonseca, R. (2014) Enhanced bioproduction of poly-3-hydroxybutyrate from wheat straw lignocellulosic hydrolysates. *New Biotechnology*. 31, 104–113. doi: 10.1016/j.nbt.2013.10.004.

REFERENCES

- Chakraborty, P., Gibbons, W., Muthukumarappan, K. (2009) Conversion of volatile fatty acids into polyhydroxyalkanoates by *Ralstonia eutropha*. *Journal of Applied Microbiology*. 106, 1996–2005.
- Chan, B.P., Leong, K.W. (2008) Scaffolding in tissue engineering: general approaches and tissue-specific considerations. *European Spine Journal*. 17 (4), 467–479. <http://doi.org/10.1007/s00586-008-0745-3>.
- Chee, J.Y., Tan, Y., Samian, M.R., Sudesh, K. (2010) Isolation and characterization of a *Burkholderia* sp. USM (JCM15050) capable of producing Polyhydroxyalkanoate (PHA) from triglycerides, fatty acids and glycerol. *Journal of Polymers and the Environment*. 18, 584–592. DOI 10.1007/s10924-010-0204-1.
- Chen, G.Q., Hajnal, I., Wu, H., Li, L., Ye, J. (2015) Engineering biosynthesis mechanisms for diversifying Polyhydroxyalkanoates. *Trends in Biotechnology*. 33 (10), 565-574.
- Chen, C., Hsieh, S.C., Teng, N.C., Kao, C.K., Lee, S.Y., Lin, C.K., Yang, J.C. (2014) Radiopacity and cytotoxicity of Portland cement containing zirconia doped bismuth oxide radiopacifiers. *Journal of Endodontics*. 40(2):251-4. doi: 10.1016/j.joen.2013.07.006.
- Chen, G., Wang, Y. (2013) Medical applications of biopolyesters polyhydroxyalkanoates. *Chinese Journal of Polymer Science*. 31, 719–736.
- Chen, G.Q., Patel, M.K. (2012) Plastics derived from biological sources: Present and future: A technical and environmental review. *Chemical Reviews*. 112, 2082–2099.
- Chen, B.K., Shen, C.H., Chen, S.C., Chen, A.F. (2010) Ductile PLA modified with methacryloyloxyalkyl isocyanate improves mechanical properties. *Polymer*. 51, 21, 4667-4672.
- Chen, G.Q. (2010) Plastics completely synthesized by bacteria: polyhydroxyalkanoates, In: Chen GQ. (eds.) *Plastics from Bacteria*. Microbiology Monographs, 14, 17-37. Springer, Berlin, Heidelberg.
- Chen, G.Q. (2009) A microbial polyhydroxyalkanoates (PHAs) based bio- and materials industry. *Chemical Society Reviews*. 38, 2434-2446.
- Chen, G.Q., Wu, Q. (2005) The application of polyhydroxyalkanoates as tissue engineering materials. *Biomaterials*. 26, 33, 6565-6578.
- Chen, G.C., Junb, X., Wu, Q., Zhang, Z., Ho, K.P. (2001) Synthesis of copolyesters consisting of medium-chain-length β -hydroxyalkanoates by *Pseudomonas stutzeri* 1317. *Reactive and Functional Polymers*, 48, 107–112.
- Chen, G., Page, W. (1997) Production of poly- β -hydroxybutyrate by *Azotobacter vinelandii* in a two-stage fermentation process. *Biotechnology Technology*. 11, 347-350.

REFERENCES

- Cheng, S.T., Chen, Z.F., Chen, G.Q. (2008) The expression of cross-linked elastin by rabbit blood vessel smooth muscle cells cultured in polyhydroxyalkanoate scaffolds. *Biomaterials*. 29, 4187–4194.
- Cheng, S., Wu, Q., Zhao, Y., Zou, B., Chen, G.Q. (2006) Poly(hydroxybutyrate-co-hydroxyhexanoate) microparticles stimulate murine fibroblast L929 cell proliferation. *Polymer Degradation and Stability*. 91, 3191–3196.
- Chiulan, I., Panaitescu, D.M., Frone, A.N., Teodorescu, M., Nicolae, C.A., Casarica, A., Tofan, V., Salageanu, A. (2016) Biocompatible polyhydroxyalkanoates/bacterial cellulose composites: Preparation, characterization, and *in vitro* evaluation. *Journal of Biomedical Materials Research A*, 104A, 10, 2576-2584.
- Cho, H.H., Han, D.W., Matsumura, K., Tsutsumi, S., Hyon, S.H. (2008) The behaviour of vascular smooth muscle cells and platelets onto epigallocatechin gallate-releasing poly(l-lactide-co- ϵ - caprolactone) as stent-coating materials. *Biomaterials*. 29(7), 884-893.
- Choe, E., Min, D.B. (2007) Chemistry of deep-fat frying oil. *Journal of Food Science*. 72, 78-86.
- Choi, D., Hwang, K.C., Lee, K.Y., Kim, Y.H. (2009) Ischemic heart diseases: current treatments and future. *Journal of Controlled Release*. 140, 194–202.
- Choi, J., Lee, S.Y. (1999) Efficient and economical recovery of poly(3-hydroxybutyrate) from recombinant *Escherichia coli* by simple digestion with chemicals. *Biotechnology and Bioengineering*. 62(5), 546-53.
- Choi, J.I., Lee, S.Y. (1997) Process analysis and economic evaluation for poly(3-hydroxybutyrate) production by fermentation. *Bioprocessing Engineering*. 17, 335–342.
- Chorny, M., Fishbein, I., Yellen, B.B., Alferiev, I.S., Bakay, M., Ganta, S., Adamo, R., Amiji, M., Friedman, G., Levy, R.J. (2010) Targeting stents with local delivery of paclitaxel loaded magnetic nanoparticles using uniform fields. *PNAS*. 107, 8346–8351.
- Chung, S., King, M.W. (2011) Design concepts and strategies for tissue engineering scaffolds. *Biotechnology and Applied Biochemistry*. 58(6), 423-38. doi:10.1002/bab.60.
- Ciesielski, S., Mozejko, J., Pisutpaisal, N. (2015) Plant oils as promising substrates for polyhydroxyalkanoates production. *Journal of Cleaner Production*. 106, 408–421. doi: 10.1016/j.jclepro.2014.09.040.
- Ciesielski, S., Mozejko, J., Pisutpaisal, N. (2014) Plant oils as promising substrates for polyhydroxyalkanoates production. *Journal of Cleaner Production*. <http://dx.doi.org/10.1016/j.jclepro.2014.09.040>.
- Collier, D., Calne, R., Thiru, S., Lim, S., Pollard, S.G., Barron, P., DaCosta, M., White, D.S.G. (1990) Rapamycin in experimental renal allografts in dogs and pigs. *Transplantation Proceedings*. 22, 1674-1675.

REFERENCES

- Costa, M.A., Simon, D.I. (2005) Molecular basis of restenosis and drug-eluting stents. *Circulation*. 111, 2257–2273.
- Courtney, J.M., Forbes, C.D. (1994) Thrombosis on foreign surfaces. *British Medical Bulletin*. 50, 4, 966–981, <https://doi.org/10.1093/oxfordjournals.bmb.a072937>.
- Cretois, R., Follain, N., Dargent, E., Soulestin, J., Bourbigot, S., Marais, S., Lebrun, L. (2014) Microstructure and barrier properties of PHBV/organoclays bionanocomposites. *Journal of Membrane Science*. 467, 56–66.
- Cruz, M.V., Sarraguca, M.C., Freitas, F., Lopes, J.A., Reisa, M.A.M. (2015) Online monitoring of P(3HB) produced from used cooking oil with near-infrared spectroscopy. *Journal of Biotechnology*. 194, 1-9.
- Cunha, M., Berthet, M.A., Pereira, R., Covas, J.A., Vicente, A.A., Hilliou, L. (2015) Development of Polyhydroxyalkanoate/beer spent grain fibres composites for film blowing applications. *Polymer Composites*. 1859-1865. DOI 10.1002/pc.
- Dai, Z.W., Zou, X.H., Chen, G.Q. (2009) Poly(3-hydroxybutyrate-co-3-hydroxyhexanoate) as an injectable implant system for prevention of post-surgical tissue adhesion. *Biomaterials*. 30:3075–3083.
- Dai, W., Zhu, J., Shangguan, A., Lang, M. (2009) Synthesis, characterization and degradability of the comb-type poly(4-hydroxyl-ε-caprolactone-co-ε-caprolactone)-co-poly(L-lactide). *European Polymer Journal*. 45:1659–1667.
- D'Amico, D.A., Montes, M.L.I., Manfredi, L.B., Cyras V.P. (2016) Fully bio-based and biodegradable polylactic acid/poly(3-hydroxybutyrate) blends: Use of a common plasticizer as performance improvement strategy. *Polymer Testing*. 49, 22-28.
- Dani, S., Kukreja, N., Parikh, P. (2008) Biodegradable-polymer-based, sirolimus-eluting Supralimus stent: 6-month angiographic and 30-month clinical follow-up results from the series I prospective study. *EuroIntervention*. 4:59–63.
- Danson, M.J., Hough, D.W. (1997) The structural basis of protein halophilicity. *Comparative Biochemistry and Physiology*. 117:307–312.
- Das, K., Bose, S., Bandyopadhyay, A. (2007) Surface modifications and cell-materials interactions with anodized Ti. *Acta Biomaterialia*. 3, 573-585.
- Davis, R., Duane, G., Kenny, S.T., Cerronem F., Guzik, M.W., Babu, R., Casey, E., O'Connor, K.E. (2015) High cell density cultivation of *Pseudomonas putida* KT2440 using glucose without the need for oxygen enriched air supply. *Biotechnology and Bioengineering*. 112, 725–733.
- De Arenaza, M.I., Sadaba, N., Larrañaga, A., Zuza, E., Sarasua, J.R. (2015) High toughness biodegradable radiopaque composites based on polylactide and barium sulphate. *European Polymer Journal*. 73:88–93.
- Deconinck, E., Sohier, J., De Scheerder, I., Van Den Mooter, G. (2008) Pharmaceutical aspects of drug eluting stents. *Journal of Pharmaceutical Sciences*. 97 (12) 5047-5060.

REFERENCES

- Demirbaş, A. (2003) Biodiesel fuels from vegetable oils via catalytic and non-catalytic supercritical alcohol transesterifications and other methods: a survey. *Energy Conversion and Management*. 2093-2109.
- Department of Health and Human Services, Public Health Service, Food and Drug Administration (1987) Guideline on validation of the *Limulus Ameboyte* lysate test as an end-product endotoxin test for human and animal parenteral drugs, biological products, and medical devices.
- De Smet, M., Eggink, G., Witholtm B., Kingma, J., Wynberg, H. (1983) Characterization of intracellular inclusions formed by *Pseudomonas oleovorans* during growth on octane. *Journal of Bacteriology*. 154, 870-878.
- Desvaux, M., Hébraud, M., Talon, R., Henderson, I.R. (2009) Secretion and subcellular localizations of bacterial proteins: a semantic awareness issue. *Trends in Microbiology*. 17(4), 139-45. doi: 10.1016/j.tim.2009.01.004.
- Dhandayuthapani, B., Yoshida, Y., Maekawa, T., Kumar, D.S. (2011) Polymeric scaffolds in tissue engineering application: a review. *International Journal of Polymer Science*. 1-19. doi:10.1155/2011/290602.
- Ding, Y.C., He, J.Y., Yang, Y.Y., Cui, S.J., Xu, K.T. (2011) Mechanical properties, thermal stability, and crystallization kinetics of poly(3-hydroxybutyrate-co-4-hydroxybutyrate)/calcium carbonate composites. *Polymer Composites*. 32, 1134–1142.
- Diós, P., Szigeti, K., Budán, F., Pócsik, M., Veres, D.S., Máthé, D., Pál, S., Dévay, A., Nagy, S. (2016) Influence of barium sulfate X-ray imaging contrast material on properties of floating drug delivery tablets. *European Journal of Pharmaceutical Sciences*. 95, 46-53. doi: 10.1016/j.ejps.2016.09.034.
- Dobranszky, J., Ring, G., Bognár, E., Kovacs, R., Bitay, E. (2014) New method for evaluating the visibility of coronary stents. *Acta Polytechnica Hungarica*. 11. 81-94.
- Doi, Y., Kitamura, S., Abe, H. (1995) Microbial synthesis and characterization of poly(3-hydroxybutyrate-co-3-hydroxyhexanoate). *Macromolecules*. 28, 4822-4828.
- Doi, Y., Mukai, K., Kasuya, K., Yamada, K. (1994) In: Doi, Y., Fukuda, K. (eds.) Biodegradable plastics and polymers. Elsevier, Amsterdam, 39–51.
- Doi, Y., Kanesawa, Y., Kunioka, M., Saito, T. (1990) Biodegradation of microbial copolyesters: poly(3-hydroxybutyrate-co-3-hydroxyvalerate) and poly (3-hydroxybutyrate-co-4-hydroxybutyrate). *Macromolecules*, 23 (1), 26–31. DOI: 10.1021/ma00203a006.
- Doi, Y., Segawa, A., Kunioka, M. (1990) Biosynthesis and Characterization of Poly(3-hydroxybutyrate-co-4-hydroxybutyrate) in *Alcaligenes eutrophus*. *International Journal of Biological Macromolecules*. 12, 106.

REFERENCES

- Doi, Y., Kanesawa, Y., Kawaguchi, Y., Kunioka, M. (1989) Hydrolytic degradation of microbial poly(hydroxyalkanoates). *Macromolecular Rapid Communications*. 10, 227–230. doi:10.1002/marc.1989.030100506.
- Doi, Y., Kunioka, M., Nakamura, Y., Soga, K. (1986) Proton and carbon-13 NMR analysis of poly(β -hydroxybutyrate) isolated from *Bacillus megaterium*. *Macromolecules*. 19, 1274–1276.
- Doyle, C., Tanner, E.T., Bonfield, W. (1991) *In vitro* and *in vivo* evaluation of polyhydroxybutyrate and of polyhydroxybutyrate reinforced with hydroxyapatite. *Biomaterials*. 12, 841-847.
- Drachman, D.E., Edelman, E.R., Seifert, P., Groothuis, A.R., Kalpana, D.A., Kamath, R., Palasis, M., Yang, D., Nott, S.H., Rogers, C. (2000) Neointimal thickening after stent delivery of paclitaxel: change in composition and arrest of growth over six months. *Journal of an American College of Cardiology*. 367, 2325-2332.
- Du, G.C., Yu, J. (2002) Green technology for conversion of food scraps to biodegradable thermoplastic polyhydroxyalkanoates. *Environmental Science and Technology*. 36 (24), 5511–5516.
- Dufresne, A., Vincendon, M. (2000) Poly(3-hydroxybutyrate) and Poly(3-hydroxyoctanoate) blends: morphology and mechanical behaviour. *Macromolecules*. 33.10.1021/ ma991854a.
- Edmund, H., Immergut, F., Herman, M. (1965) Principles of plasticization, In. Plasticization and Plasticizer Processes. *Advances in Chemistry, American Chemical Society, Washington, DC*, 6-10.
- Erbel, R., Di Mario, C., Bartunek, J., Bonnier, J., de Bruyne, B., Eberli, F.R., Erne, P., Haude, M., Heublein, B., Horrigan, M., Ilesley, C., Bose, D., Koolen, J., Luscher, T.F., Weissman, N., Waksman R. (2007) Temporary scaffolding of coronary arteries with bioabsorbable magnesium stents: A prospective, non-randomised multicentre trial. *Lancet*. 369, 1869–1875.
- Eberhart, R.C., Su, S.H., Nguyen, K.T., Zilberman, M., Tang, L., Nelson, K.D., Frenkel, P. (2003) Bioresorbable polymeric stents: current status and future promise. *Journal of Biomaterials Science. Polymer edition*. 14, 4, 299-312.
- Elks, J., Ganellin, C.R. (2014) The dictionary of drugs: chemical data: chemical data, structures and bibliographies. Springer, 366. ISBN 978-1-4757-2085-3.
- El-Taweela, S.H., Hohneb, G.W.H., Mansour, A.A., Stoll, B., Seliger, H. (2004) Glass transition and the rigid amorphous phase in semicrystalline blends of bacterial polyhydroxybutyrate PHB with low molecular mass atactic R, S-PHB-diol. *Polymer*. 45, 983–992.
- Erbel, R., Konorza, T., Haude, M., Dages, N., Baumgart, D. (2002) Future of interventional cardiology in the treatment of coronary artery disease. *Herz* 27, 6:471-480.

REFERENCES

- Erythropel, H.C., Shipley, S., Börmann, A., Nicell, J., Marin, M., Leask, R.L. (2016). Designing green plasticizers: influence of molecule geometry and alkyl chain length on the plasticizing effectiveness of diester plasticizers in PVC blends. *Polymer*. 89. 10.1016/j.polymer.2016.02.031.
- Erythropel, H.C., Maric, M., Nicell, J.A., Leask, R.L., Yargeau, V. (2014) Leaching of the plasticizer di (2-ethylhexyl) phthalate (DEHP) from plastic containers and the question of human exposure. *Applied Microbiology and Biotechnology* 98 (24), 9967-81.
- Escapa, I.F., Morales, V., Martino, V.P., Pollet, E., Avérous, L., García, J.L., Prieto, M.A. (2011) Disruption of β -oxidation pathway in *Pseudomonas putida* KT2442 to produce new functionalized PHAs with thioester groups. *Applied Microbiology and Biotechnology*. 89, 1583–1598. DOI 10.1007/s00253-011-3099-4.
- Follonier, S., Goyder, M.S., Silvestri, A.C., Crelier, S., Kalman, F., Riesen, R., Zinn, M. (2014) Fruit pomace and waste frying oil as sustainable resources for the bioproduction of medium-chain-length polyhydroxyalkanoates. *International Journal of Biological Macromolecules*. 71:42-52. doi: 10.1016/j.ijbiomac.2014.05.061.
- Forrester, J.S., Fishbein, M., Helfant, R. (1991) A paradigm for restenosis based on cell biological clues for the development of new preventive therapies. *Journal of an American College of Cardiology*. 17, 758–69.
- Faccin, D.J.L., Rech, R., Secchi, A.R., Cardozo, N.S.M., Ayub, M.A.Z. (2013) Influence of oxygen transfer rate on the accumulation of poly (3-hydroxybutyrate) by *Bacillus megaterium*. *Process Biochemistry*. 48(3), 420-425.
- Farb, A., Heller, P.F., Shroff, S., Cheng, L., Kolodgie, F.D., Carter, A.J., Scott, D.S., Froehlich, J., Virmani, R. (2001) Pathological analysis of local delivery of paclitaxel via a polymer-coated stent. *Circulation*. 104, 473-479. <https://doi.org/10.1161/hc3001.092037>.
- Fischell, T.A. (2000) Visible Stents: All that glitters ... Is it gold? *Journal of Invasive Cardiology*. 12, 233–235.
- Fischman, D.L., Leon, M.B., Baim, D.S., Schatz, R.A., Savage, M.P., Penn, I., Detre, K., Veltri, L., Ricci, D., Nobuyoshi, M. (1994) A randomized comparison of coronary-stent placement and balloon angioplasty in the treatment of coronary artery disease. Stent Restenosis Study Investigators. *New England Journal of Medicine*. 331 (8), 496-501.
- Francis, L., Meng, D., Locke, I.C., Knowles, J.C., Mordan, N., Salih, V., Boccaccini, A.R., Roy, I. (2016) Novel P(3HB) Composite films containing bioactive glass nanoparticles for wound healing applications. *Polymer International*. 65 (6), 661-674.
- Francis, L., Meng, D., Knowles, J., Keshavarz, T., Boccaccini, A., Roy, I. (2011) Controlled delivery of gentamicin using poly(3-hydroxybutyrate) microspheres. *International Journal of Molecular Sciences*. 12(7), 4294-4314.

REFERENCES

- Francis, L., Meng, D., Knowles, J.C., Roy, I., Boccaccini, A.R. (2010) Multi-functional P(3HB) microsphere/45S5 Bioglass((R))-based composite scaffolds for bone tissue engineering. *Acta Biomaterialia*. 6 (7), 2773-2786.
- Franke, R.P., Jung, F. (2012) Interaction of blood components and blood cells with body foreign surfaces. *Series on Biomechanics*, 27, 1-2, 51- 58.
- Freier, T., Kunze, C., Nischan, C., Kramer, S., Sternberg, K., Sass, M., Hopt, U.T., Schmitz, K.P. (2002) *In vitro* and *in vivo* degradation studies for development of a biodegradable patch based on poly(3-hydroxybutyrate). *Biomaterials*. 23(13), 2649-57.
- Fu, G., Zhanjiang, Y., Chen, Y., Chen, Y., Tian, F., Yang, X. (2016) Direct adsorption of Anti-CD34 antibodies on the nano-porous stent surface to enhance endothelialisation. 2 (3), 273–280.
- Fulkerson, J. D., Bales, T. O., Jahrmarkt, S. L. (2004) Vascular stent with radiopaque markers. US2004/0015229. Syntheon.
- Furukawa, T., Sato, H., Murakami, R., Zhang, J., Noda, I., Ochiai, S., Ozaki, Y. (2007) Comparison of miscibility and structure of poly(3-hydroxybutyrate-co-3 hydroxyhexanoate)/poly(L-lactic acid) blends with those of poly(3-hydroxybutyrate)/poly(L-lactic acid) blends studied by wide angle x-ray diffraction, differential scanning calorimetry, and FTIR microspectroscopy. *Polymer*. 48, 1749–1755.
- Furukawa, T., Sato, H., Murakami, R. (2005) Structure, dispersibility, and crystallinity of poly(hydroxybutyrate)/ poly(L-lactic acid) blends studied by FT-IR microspectroscopy and differential scanning calorimetry. *Macromolecules*. 38, 6445–6454.
- Gallo, R., Padurean, A., Jayaraman, T., Marx, S.O., Roque, M., Adelman, S., Chesebro, J.H., Fallon, J.T., Fuster, V., Marks, A.R., Badimon, J.J. (1999) Inhibition of intimal thickening after balloon angioplasty in porcine coronary arteries by targeting regulators of the cell cycle. *Circulation*. 99, 2164–2170.
- Gamal, R.F., Abdelhady, H.M., Khodair, T.A., El-Tayeb, T.S., Hassan, E.A., Aboutaleb, K.A. (2013) Semi-scale production of PHAs from waste frying oil by *Pseudomonas fluorescens* S48. *Brazillian Journal of Microbiology*. 44 (2), 539-549.
- Ganduri, V.S.R.K., Ghosh, S., Patnaik, P.R. (2005) Mixing control as a device to increase PHB production in batch fermentations with co-cultures of *Lactobacillus delbrueckii* and *Ralstonia eutropha*. *Process Biochemistry*. 40, 257–264.
- Gao, C., Qi, Q., Madzak, C., Lin, C.S. (2015) Exploring medium-chain-length polyhydroxyalkanoates production in the engineered yeast *Yarrowia lipolytica*. *Journal of Industrial Microbiology and Biotechnology*. 42, 1255–1262. DOI 10.1007/s10295-015-1649-y.

REFERENCES

- Gao, X., Chen, J.C., Wu, Q., Chen, G.Q. (2011) Polyhydroxyalkanoates as a source of chemicals, polymers, and biofuels. *Current Opinion in Biotechnology*. 22, 768–774.
- Garcia-Garcia, D., Fenollar, O., Fombuena, V., Lopez-Martinez, J., Balart, R. (2017). Improvement of mechanical ductile properties of poly(3-hydroxybutyrate) by using vegetable oil derivatives. *Macromolecular Materials and Engineering*. 302(2), 12. 3.
- García-Tejada, J., Gutiérrez, H., Albarrán, A., Hernández, F., Velázquez, T., Rodríguez, S., Gómez, I., Tascón, J. (2007) Janus® Tacrolimus-Eluting Carbostent. Immediate and Medium-Term Clinical Results. *Revista Espanola De Cardiologica*. 60 (2), 197-200.
- Gershlick, A., De Scheerder, I., Chevalier, B. (2004) Inhibition of restenosis with a paclitaxel-eluting, polymer-free coronary stent: the European evaluation of pacliTaxel Eluting Stent (ELUTES) trial. *Circulation*. 109 (4), 487-93.
- Gertz, C. (2000). Chemical and physical parameters as quality indicators of used frying fats. *Euro Lipid Science Technology*. 102, 566-572.
- Ghiya, V.P., Dave, V., Gross, R.A., McCarthy, S.P. (1995) Citrate esters as biodegradable plasticizers for poly(hydroxybutyrate-co-valerate). *Polymer Preprints*. 36, 420–1.
- Godbole, S., Gote, S., Latkar, M., Chakrabarti, T. (2003) Preparation and characterization of biodegradable poly-3-hydroxybutyrate-starch blend films. *Bioresourse Technology*. 86, 33–37.
- Gogas, B.D., McDaniel, M., Samady, H., King, III S.B. (2014) Novel drug-eluting stents for coronary revascularization. *Trends in Cardiovascular Medicine*. 24 (7), 305-313.
- Gogas, B.D., Farooq, V., Onuma, Y. (2012) The ABSORB bioresorbable vascular scaffold: an evolution or revolution in interventional cardiology. *Hellenic Journal of Cardiology*. 53, 301–9.
- Gogas, H., Ioannovich, J., Dafni, U. (2006) Prognostic significance of autoimmunity during treatment of melanoma with interferon. *New England Journal of Medicine*. 354, 709–718.
- Gogolewski, S., Jovanovic, M., Perren, S.M., Dillon, J.G., Hughes, M.K. (1993) Tissue response and *in vivo* degradation of selected polyhydroxyacids: polylactides (PLA), poly(3-hydroxybutyrate) (PHB), and poly(3-hydroxybutyrate-co-3-hydroxyvalerate) (PHB/VA). *Journal of Biomedical Material Research*. 27(9), 1135-48.
- Gomez, A., Abonia, R., Cadavid, H., Vargas, H. (2011) Chemical and spectroscopic characterization of a vegetable oil used as dielectric coolant in distribution transformers. *Journal of the Brazilian Chemical Society*. 22 (12), 2292–2303.
- Gomez, J.G.C., Rodrigues, M.F.A., Alli, R.C.P., Torres, B.B., Bueno Netto, C.L., Oliveira, M.S., Silva, L.F. (1996) Evaluation of soil Gram-negative bacteria yielding

REFERENCES

- polyhydroxy-alkanoic acids from carbohydrates and propionic acid. *Applied Microbiology and Biotechnology*. 45, 785-791.
- Gorbet, M.B., Sefton, M.V. (2004) Review: Biomaterial-associated thrombosis: roles of coagulation factors, complement, platelets and leukocytes. The Biomaterials: Silver Jubilee Compendium. The Best Papers Published in *Biomaterials* 1980–2004, 219–241.
 - Gouda, M.K., Swellam, A.E., Omar, S.H. (2001) Production of PHB by a *Bacillus megaterium* strain using sugarcane molasses and corn steep liquor as sole carbon and nitrogen sources. *Microbiological Research*. 156, 201–207.
 - Gould, P.L., Holland, S.J., Tighe, B.J. (1987) Polymers for biodegradable medical devices. IV. Hydroxybutyrate-valerate copolymers as non-disintegrating matrices for controlled-release oral dosage forms. *International Journal of Pharmaceutics*. 38, 1–3, 231-237.
 - Grabow, N., Martin, D. P., Schmitz, K.-P. and Sternberg, K. (2010) Absorbable polymer stent technologies for vascular regeneration. *Journal of Chemical Technology and Biotechnology*. 85, 744–751. doi:10.1002/jctb.2282.
 - Grage, K., Jahns, A.C., Parlange, N., Palanisamy, R., Rasiah, I.A., Atwood, J.A., Rehm, B.H. (2009). Bacterial polyhydroxyalkanoate granules: biogenesis, structure, and potential use as nano-/micro-beads in biotechnological and biomedical applications. *Biomacromolecules*. 10 (4), 660-9. doi: 10.1021/bm801394s.
 - Gregorova, A., Wimmer, R., Hrabalova, M., Koller, M., Ters, T., Mundigler, N. (2009) Effect of surface modification of beech wood flour on mechanical and thermal properties of Poly (3-hydroxybutyrate)/wood flour composites. *Holzforschung*. 63, 565–570.
 - Grube, E., Serruys, P.W. (2002) Safety and performance of a paclitaxel-eluting stent for the treatment of in-stent restenosis: preliminary results of the TAXUS III trial. *Journal of the American College Cardiology*. 39A:58A.
 - Grube, E., Sonoda, S., Ikeno, F., Honda, Y., Kar, S., Chan, C., Gerckens, U., Lansky, A.J., Fitzgerald, P.J. (2004) Six- and twelve-month results from first human experience using everolimus-eluting stents with bioabsorbable polymer. *Circulation*. 109 (18), 2168-71.
 - Grüntzig, A.R., Senning, A., Siegenthaler, W.E. (1979) Non-operative dilatation of coronary-artery stenosis: percutaneous transluminal coronary angioplasty. *New England Journal of Medicine*. 301 (2), 61-8.
 - Gu, Y., Ji, Y., Zhao, Y., Liu, Y., Ding, F., Gu, X., Yang, Y. (2012) The influence of substrate stiffness on the behavior and functions of Schwann cells in culture. *Biomaterials*. 33(28):6672-81. doi: 10.1016/j.biomaterials.2012.06.006.
 - Gunaratne, L.M.W.K., Shanks, R.A. (2005) Multiple melting behaviour of poly(3-hydroxybutyrate-co-hydroxyvalerate) using step-scan DSC. *European Polymer Journal*. 41, 2980-2988.

REFERENCES

- Gurselt, I., Yagmurlu, F., Korkusuz, F., Hasirci, V. (2002) *In vitro* antibiotic release from poly(3-hydroxybutyrate-co-3-hydroxyvalerate) rods. *Journal of Microencapsulation*. 19, 153-64.
- Gumel, A.M., Annuar, M.S.M., Heidelberg, T. (2012) Biosynthesis and characterization of polyhydroxyalkanoates copolymers produced by *Pseudomonas putida* Bet001 isolated from palm oil mill effluent. *PLoS One*. 7: e45214.
- Gunatillake, P.A., Adhikari, R. (2003) Biodegradable synthetic polymers for tissue engineering. *European Cells and Materials*. 5, 1–16.
- Guzik, M.W., Kenny, S.T., Duane, G.F., Casey, E., Woods, T., Babu, R.P. (2014) Conversion of post-consumer polyethylene to the biodegradable polymer polyhydroxyalkanoate. *Applied Microbiology and Biotechnology*. 98, 4223–4232.
- Haas, R., Jin, B., Zepf, F.T. (2008) Production of Poly(3-hydroxybutyrate) from waste potato starch. *Bioscience, Biotechnology and Biochemistry*. 72(1), 253-6.
- Haba, E., Vidal-Mas, J., Bassas, M., Espuny, M.J., Llorens, J., Manresa, A. (2007) Poly 3-(hydroxyalkanoates) produced from oily substrates by *Pseudomonas aeruginosa* 47T2 (NCBIM 40044): Effect of nutrients and incubation temperature on polymer composition. *Biochemical Engineering Journal*. 35, 99–106.
- Hahn, S.K., Chang, Y.K., Kim, B.S., Chang, H.N. (1994) Optimization of microbial poly(3-hydroxybutyrate) recovery using dispersions of sodium hypochlorite solution and chloroform. *Biotechnology and Bioengineering*. 44, 256–261. DOI: 10.1002/bit.260440215.
- Hahn, S.K., Chang, Y.K., Kim, B.S., Lee, K.M., Chang, H.N. (1993) The recovery of poly(3-hydroxybutyrate) by using dispersions of sodium hypochlorite solution and chloroform. *Biotechnology Techniques*. 7 (3), 209-212.
- Hämäläinen, M., Nieminen, R., Uurto, I., Salenius, J.P., Kellomäki, M., Mikkonen, J., Kotsar, A., Isotalo, T., Tammela, L.J., Talja, M., Moilanen, E. (2013) Dexamethasone-eluting vascular stents. *Basic and Clinical Pharmacology and Toxicology*. 112(5), 296-301. doi: 10.1111/bcpt.12056.
- Hamrefors, V. (2017) Common genetic risk factors for coronary artery disease: new opportunities for prevention? *Clinical Physiology and Functional Imaging*. 37, 243–254.
- Han, F., Zhu, C., Guo, Q., Yang, H., Li, B. (2016) Cellular modulation by the elasticity of biomaterials. *Journal of Materials Chemistry B* 4 (1), 9-26.
- Han, J., Farah, S., Domb, A.J., Lelkes, P.I. (2013) Electrospun rapamycin-eluting polyurethane fibres for vascular grafts. *Pharmaceutical Research*. 30, 1735–1748. DOI 10.1007/s11095-013-1016-5.
- Han, J., Hou, J., Liu, H., Cai, S., Feng, B., Zhou, J., Xiang, H. (2010) Wide distribution among halophilic *Archaea* of a novel Polyhydroxyalkanoate synthase subtype with homology to bacterial type III synthases. *Applied and Environmental Microbiology*. 76(23), 7811–7819. doi: 10.1128/AEM.01117-10.

REFERENCES

- Han, S.Y., Kang, Y.S., Jee, Y.H., Han, K.H., Cha, D.R., Kang, S.W. (2006) High glucose and angiotensin II increase β_1 integrin and integrin-linked kinase synthesis in cultured mouse podocytes. *Cell Tissue Research*. 323, 321–32.
- Hanson, S.R., Ratner, B.D. (2004) Evaluation of blood-materials interactions. In: Ratner, B.D., Hoffman, A.S., Schoen, F.J., Lemons, J.E., editors. *Biomaterials Science: An Introduction to Materials in Medicine*. San Diego, 367–378.
- Hänzi, A.C., Gerber, I., Schinhammer, M., Löffler, J.F., Uggowitz, P.J. (2010) On the *in vitro* and *in vivo* degradation performance and biological response of new biodegradable Mg–Y–Zn alloys. *Acta Biomaterialia*. 6 (5), 1824–1833.
- Hao, L., Lawrence, J. (2004) The adsorption of human serum albumin (HSA) on CO₂ laser modified magnesia partially stabilized zirconia (MgO-PSZ). *Colloids and Surfaces B: Biointerfaces*. 34, 87–94.
- Hänzi, A.C., Gerber, I., Schinhammer, M., Loffer, J.F., Uggowitz, P.J. (2010) On the *in vitro* and *in vivo* degradation performance and biological response of new biodegradable Mg–Y–Zn alloys. *Acta Biomaterialia*. 1824–1833.
- Hao, L., Lawrence, J. (2006) Albumin and fibronectin protein adsorption on CO₂-laser-modified biograde stainless steel. *Proceedings of the Institution of Mechanical Engineers H*. 220(1):47–55.
- Hassan, M.A., Shirai, Y., Kusubayashi, N., Karim, M.I.A., Nakanishi, K., Hashimoto, K. (1996) Effect of organic acid profiles during anaerobic treatment of palm oil mill effluent on the production of polyhydroxyalkanoates by *Rhodobacter sphaeroides*. *Journal of Fermentation and Bioengineering*. 82, 151–156.
- Hermann-Krauss, C., Koller, M., Muhr, A., Fasl, H., Stelzer, F., Braunegg, G. (2013) *Archaeal* production of Polyhydroxyalkanoate (PHA) co- and terpolyesters from biodiesel industry derived by-products. *Archaea*, Article ID 129268, 10 pages. <http://dx.doi.org/10.1155/2013/129268>.
- Hiraishi, A., Khan, S.T. (2003) Application of polyhydroxyalkanoates for denitrification in water and wastewater treatment. *Applied Microbiology and Biotechnology*. 61(2), 103–9.
- Hazer, D.B., Kılıçay, E., Hazer, B. (2012) Poly(3-hydroxyalkanoate)s: Diversification and biomedical applications A state of the art review. *Materials Science and Engineering C*. 32, 637–647.
- Hermawan, H., Dubé, D., Mantovani, D. (2010) Developments in metallic biodegradable stents. *Acta Biomaterialia*. 6, 5, 1693–7. doi: 10.1016/j.actbio.2009.10.006.
- Hermawan, H., Alamdari, H., Mantovani, D., Dubé, D. (2008) Iron–manganese: new class of metallic degradable biomaterials prepared by powder metallurgy. *Powder Metallurgy*. 51, 38–45.
- Hirase, T., Node, K. (2012) Endothelial dysfunction as a cellular mechanism for vascular failure. *American Journal of Physiology*. - Heart and Circulatory Physiology. 302 (3), H499–505.

REFERENCES

- Hoffmann, R., Mintz, G.S., Haager, P.K., Bozoglu, T., Grube, E., Gross, M., Beythien, C., Mudra, H., vom Dahl, J., Hanrath, P. (2013) Relation of stent design and stent surface material to subsequent in-stent intimal hyperplasia in coronary arteries determined by intravascular ultrasound. *American Journal of Cardiology*. 89, 1360–1364.
- Hoffman, R., Mintz, G.S. (2000) Coronary in-stent restenosis—predictors, treatment and prevention. *European Heart Journal*. 21, 1739-1749.
- Holmes, D.R., Leon, M.B., Moses, J.W., Popma, J.J., Cutlip, D., Fitzgerald, P.J., Brown, C., Fischell, T., Wong, S.C., Midei, M., Snead, D., Kuntz, R.E. (2004) Analysis of 1-year clinical outcomes in the SIRIUS trial: a randomized trial of a sirolimus-eluting stent versus a standard stent in patients at high risk for coronary restenosis. *Circulation*. 109 (5), 634-40.
- Hong, S.G., Gau, T.K., Huang, S.C. (2011). Enhancement of the crystallization and thermal stability of polyhydroxybutyrate by polymeric additives. *Journal of Thermal Analysis and Calorimetry*. 103, 967–75.
- Horbett, T.A. (2004) The role of adsorbed proteins in tissue response to biomaterials. In: *Biomaterials Science—An Introduction to Materials in Medicine*, 2nd Ed., Elsevier Academic Press: New York, 237–246.
- Horn, O., Nalli, S., Cooper, D., Nicell, J. (2004) Plasticizer metabolites in the environment. *Water Research*. 38, 3693-3698.
- Huang, C.C., Wang, S.H., Tsui, P.H. (2005) Detection of blood coagulation and clot formation using quantitative ultrasonic parameters. *Ultrasound in Medicine and Biology*. 31, 1567–1573.
- Hull, E.H. (1990) Medical grade citrate ester plasticizers. In: *Medical plastics today & tomorrow*. Proceedings of the RETEC Medical Plastics Conference, Anaheim. 1–21.
- Huijberts, G.N.M., Eggink, G., de Waard, P., Huisman, G.W., Witholt, B. (1992) *Pseudomonas putida* KT2442 cultivated on glucose accumulates poly(3-hydroxyalkanoates) consisting of saturated and unsaturated monomers. *Applied and Environmental Microbiology*. 58, 536–544.
- Huisman, G.J., De Leeuw, O., Eggink, G., Witholt, B. (1989) Synthesis of poly-3-hydroxyalkanoates is a common feature of fluorescent pseudomonads. *Applied and Environmental Microbiology*. 55, 1949-1954.
- Hunter, T.B., Taljanovic, M.S. (2003) Glossary of medical devices and procedures: abbreviations, acronyms, and definitions. *RadioGraphics*. DOI: 10.1148/rg.231025136.
- Hwan, S.J., Jeon, C.O., Choi, M.H., Yoon, S.C., Park, W. (2008) Polyhydroxyalkanoate (PHA) production using waste vegetable oil by *Pseudomonas* sp. strain DR2. *Journal of Microbiology and Biotechnology*. 18 (8), 1408–1415.

REFERENCES

- Iakovou, I., Colombo, A. (2005) Contemporary stent treatment of coronary bifurcations. *Journal of the American College of Cardiology*. 46, 1146-1155.
- Ienczak, J.L., Schmidell, W., de Aragao, G.M.F. (2013) High-cell-density culture strategies for polyhydroxyalkanoate production: a review. *Journal of Industrial Microbiology and Biotechnology*. 40, 275–286.
- Iqbal, J., Gunn, J., Serruys, P.W. (2013) Coronary stents: historical development, current status and future directions. *British Medical Bulletin*. 106, 193-211.
- ISO (2002). ISO 10993-4:2002. Biological evaluation of medical devices - Part 4: Selection of tests for interactions with blood.
- Iuliano, D.J., Saavedra, S.S., Truskey, G.A. (1993) Effect of the conformation and orientation of adsorbed fibronectin on endothelial cell spreading and the strength of adhesion. *Journal of Biomedical Materials Research*. 27(8), 1103-13.
- Jacob, J., Mani, R., Bhattacharya, M. (2002) Compatibility and properties of biodegradable polymeric blends. *Journal of Polymer Science: Part A: Polymer Chemistry*. 40 (12), 2003-2014.
- Jamshidi, P., Toggweiler, S., Erne, P. (2008) In-stent restenosis and thrombosis 41 months after drug-eluting stent implantation. *International Journal of Cardiology*. 130, 111-113.
- Jandas, P.J., Mohanty, S., Nayak, S.K. (2014) Morphology and thermal properties of renewable resource-based polymer blend nanocomposites influenced by a reactive compatibiliser. *ACS Sustain. Chemical Engineering*. 2, 377–386.
- Jau, M.H., Yew, S.P., Toh, P.S.Y., Chonga, A.S.C., Chub, W.L., Phang, S.M., Najimudin, N., Sudesh, K. (2005) Biosynthesis and mobilization of poly(3-hydroxybutyrate) P(3HB) by *Spirulina platensis*. *International Journal of Biological Macromolecules*. 36, 144–151. doi: 10.1016/j.ijbiomac.2005.05.002.
- Jeewandara, T.M., Wise, S.G., Ng, M.K.C. (2014) Biocompatibility of coronary stents. *Materials*. 7, 769-786; doi:10.3390/ma7020769.
- Jendrossek, D., Handrick, R. (2002) Microbial degradation of polyhydroxyalkanoates. *Annual Review Microbiology*. 56, 403-32.
- Jian, Y., Zongbao, W., Yang, W., Xiangfa, W., Qun, G. (2010) Crystallization behaviour of incompatible PHBV/PS and PHBV/PMMA crystalline/amorphous blends. *Acta Polymerica Sinica*. 987–994.
- Jiang, X.J., Sun, Z., Ramsay, J.A., Ramsay, B.A. (2013) Fed-batch production of MCL-PHA with elevated 3-hydroxynonanoate content. *AMB Express*. 3, 50. 10.1186/2191-0855-3-50.
- Jin, H., Nikolau, B.J. (2014) Evaluating PHA productivity of bioengineered *Rhodospirillum rubrum*. *PLoS One*. 19, 9(5), e96621. doi: 10.1371/journal.pone.0096621.
- Jirage, A.S., Baravkar, V.S., Kate, V.K., Payghan, S.A. (2013) Poly- β -hydroxybutyrate: Intriguing biopolymer in biomedical applications and pharma

REFERENCES

- formulation trends. *International Journal of Pharmaceutical and Biological Archive*. 4, 1107-18.
- Joner, M., Finn, A.V., Farb, A., Mont, E.K., Kolodgie, F.D., Ladich, E., Kutys, R., Skorija, K., Gold, H.K., Virmani, R. (2006) Pathology of drug-eluting stents in humans: delayed healing and late thrombotic risk. *Journal of the American College of Cardiology*. 48 (1), 193-202.
 - Jung, Y.M., Lee, Y.H. (2000) Utilization of oxidative pressure for enhanced production of poly-beta-hydroxybutyrate and poly(3-hydroxybutyrate-3-hydroxyvalerate) in *Ralstonia eutropha*. *Journal of Bioscience and Bioengineering*. 90, 266–270.
 - Kadouri, D., Jurkevitch, E., Okon, Y. (2005) Ecological and agricultural significance of bacterial polyhydroxyalkanoates. *Critical Reviews in Microbiology*, 31, 55–67. DOI: 10.1080/ 10408410590899228.
 - Kadoya, R., Matsumoto, K., Ooi, T., Taguchi, S. (2015) MtgA deletion-triggered cell enlargement of *Escherichia coli* for enhanced intracellular polyester accumulation. *PLOS ONE*. 10 (6), e0125163. <https://doi.org/10.1371/journal.pone.0125163>.
 - Kahar, P., Tsuge, T., Taguchi, K., Doi, Y. (2004) High yield production of polyhydroxyalkanoates from soybean oil by *Ralstonia eutropha* and its recombinant strain. *Polymer Degradation and Stability*. 83, 79–86. doi: 10.1016/S0141-3910(03)00227-1.
 - Kamath, K. R., Barry, J. J., Miller, K. M. (2006) The Taxus™ drug-eluting stent: A new paradigm in controlled drug delivery. *Advanced Drug Delivery Reviews*. 58, 412- 436.
 - Kandzari, D.E., Leon, M.B., Popma, J.J. (2006) Comparison of zotarolimus-eluting and sirolimus-eluting stents in patients with native coronary artery disease: a randomized controlled trial. *Journal of the American College of Cardiology*. 48 (12), 2440–2447.
 - Kannan, L.V., Rehacek. Z. (1970) Formation of poly-beta-hydroxybutyrate by *Actinomyces*. *Indian Journal of Biochemistry*. 7, 126–129.
 - Kapritchkoff, F.M., Viotti, A.P., Alli, R.C.P., Zuccolo, M., Pradella, J.G.C., Maiorano, A.E., Miranda, E.A., Bonomi, A. (2006) Enzymatic recovery and purification of polyhydroxybutyrate produced by *Ralstonia eutropha*. *Journal of Biotechnology*, 122, 453–462. DOI: 10.1016/j.jbiotec.2005.09.009.
 - Kar, S., Honda, T., McClean, D., (2003) Elution of everolimus and sirolimus from a biodegradable polymer coated stent inhibits neointimal hyperplasia without inflammation or toxicity. *Journal of the American College of Cardiology*. 41, (Suppl A), 6A.
 - Karbasi, F. (2012) Investigation of optimum fermentation condition for PHA production by four species: *Hydrogenophaga pseudoflava*, *Azohydromonas lata*,

REFERENCES

- Cupriavidus necator*, *Azotobacter beijinckii*. *World Applied Sciences Journal*. 20 (12), 1713-1724.
- Kathuria, Y.P. (2006) The potential of biocompatible metallic stents and preventing restenosis. *Materials Science and Engineering*. 417, 1,2, 40-48.
 - Ke, Y., Zhang, X.Y., Ramakrishna, S., He, L.M., Wu, G. (2017) Reactive blends based on polyhydroxyalkanoates: Preparation and biomedical application. *Materials Science and Engineering: C*. 70, 2, 1107-1119.
 - Kenar, H., Kose, G.T., Hasirci, V. (2010) Design of a 3D aligned myocardial tissue construct from biodegradable polyesters. *Journal of Material Science: Materials in Medicine*. 21, 989–997. DOI 10.1007/s10856-009-3917-8.
 - Kereiakes, D., Linnemeier, T.J., Baim, D.S. (2000) Usefulness of stent length in predicting in-stent restenosis (the MULTI-LINK stent trials). *American Journal of Cardiology*. 86, 336–341.
 - Khan, W., Farah, S., Nyska, A., Domb, A.J. (2013) Carrier free rapamycin loaded drug eluting stent: in vitro and in vivo evaluation. *Journal of Controlled Release*. 28, 168(1):70-6. doi: 10.1016/j.jconrel.2013.02.012.
 - Khan, M.O., Leung, S.N., Chan, E., Naguib, H.E., Dawson, F., Adinhrah, V. (2013) Effects of micro-sized and nano-sized carbon fillers on the thermal and electrical properties of polyphenylene sulphide based composites. *Polymer Engineering and Science*. 53 (11), 2398-2406.
 - Khan, W., Farah, S., Domb, A.J. (2012) Drug eluting stents: developments and current status. *Journal of Controlled Release*. 161, 703–712.
 - Khardenavis, A.A., Suresh, Kumar. M., Mudliar, S.N., Chakrabarti, T. (2007) Biotechnological conversion of agro-industrial wastewaters into biodegradable plastic, poly β -hydroxybutyrate. *Bioresource Technology*. 98, 3579–3584. doi: 10.1016/j.biortech.2006.11.024.
 - Khanna, S., Srivastava, A. K. (2005) Recent advances in microbial polyhydroxyalkanoates. *Process Biochemistry*. 40, 607–619.
 - Kim, J.H., Li, Y., Kim, M.S., Kang, S.W., Jeong, J.H., Lee, D.S. (2012) Synthesis and evaluation of biotin-conjugated pH-responsive polymeric micelles as drug carriers. *International Journal of Pharmaceutics*. 427, 2, 435-442.
 - Kim, D.Y., Kim, Y.B., Rhee, Y.H. (2000) Evaluation of various carbon substrates for the biosynthesis of Polyhydroxyalkanoates bearing functional groups by *Pseudomonas putida*. *International Journal of Biological Macromolecules*. 28, 23-29.
 - Kim, B.S., Chang, H.N. (1998) Production of poly(3-hydroxybutyrate) from starch by *Azotobacter chroococcum*. *Biotechnology Letters*. 20, 109-112.
 - Kim, B.S., Lee, S.C., Lee, S.Y., Chang, H.N., Chang, Y.K., Woo, S.I. (1994) Production of poly I (3-hydroxybutyric acid) by fed-batch culture of *Alcaligenes eutrophus* with glucose concentration control. *Biotechnology and Bioengineering*. 43, 892-898.

REFERENCES

- Klugherz, B.D., Jones, P.L., Cui, X.M., Chen, W.L., Meneveau, N.F., DeFelice, S., Connolly, J., Wilensky, R.L., Levy, R.J. (2000) Gene delivery from a DNA controlled-release stent in porcine coronary arteries. *Nature Biotechnology*. 18, 1181–1184.
- Knight, M.A.F., Evans, G.R.D. (2004) Tissue engineering: progress and challenges. *Tissue Engineering Plastic and Reconstructive Surgery*. 114, 2.
- Koller, M., Braunegg, G. (2015) Potential and prospects of continuous Polyhydroxyalkanoate (PHA) production. *Bioengineering*. 2(2), 94-121. doi:10.3390/bioengineering2020094.
- Koller, M., Maršálek, L., de Sousa Dias, M.M., Braunegg, G. (2017) Producing microbial polyhydroxyalkanoate (PHA) biopolyesters in a sustainable manner. *New Biotechnology*. 37, 24-38.
- Koller, M., Salerno, A., Braunegg, G. (2014) Polyhydroxyalkanoates: basics, production and applications of microbial biopolyesters [in:] *Bio-Based Plastics: Materials and Applications*, First Edition. Edited by Stephan Kabasci. John Wiley & Sons, Ltd. Published 2014 by John Wiley & Sons, Ltd.
- Koller, M., Niebelschutz, H., Braunegg, G. (2013) Strategies for recovery and purification of poly [(R)-3-hydroxyalkanoates] (PHA) biopolyesters from surrounding biomass. *Engineering in Life Sciences*, 35, 7, 1023–1028.
- Koller, M., Salerno, A., Dias, M., Reiterer, A., Braunegg, G. (2010) Modern Biotechnological Polymer Synthesis: A Review. *Biotechnological Polymer Synthesis, Food Technology and Biotechnology*. 48 (3), 255–269.
- Koller, M., Salerno, A., Dias, M.D.S., Reiterer, A., Braunegg, G. (2010) Modern biotechnological polymer synthesis: a review. *Food Technology and Biotechnology*. 48, 3, 255–269.
- Koller, M., Bona, R., Braunegg, G., Hermann, C., Horvat, P., Kroutil, M. (2005) Production of polyhydroxyalkanoates from agricultural waste and surplus materials. *Biomacromolecules*. 6, 561-565.
- Komiyama, H., Takano, M., Hata, N., Seino, Y., Shimizu, W., Mizuno, K. (2015) Neoatherosclerosis: Coronary stents seal atherosclerotic lesions but result in making a new problem of atherosclerosis. *World Journal of Cardiology*. 26, 7(11), 776-783.
- König, A., Leibig, M., Rieber, J., Schiele, T.M., Theisen, K., Siebert, U., Gothe, R.M., Klaus, V. (2007) Randomized comparison of dexamethasone-eluting stents with bare metal stent implantation in patients with acute coronary syndrome: Serial angiographic and sonographic analysis. *American Heart Journal*. 153, 979e1–979e8.
- Koning, G.J.M., Kellerhals, M., van Meurs, C., Witholt, B. (1997) A process for the recovery of poly(hydroxyalkanoates) from *Pseudomonads* Part 2: Process development and economic evaluation. *Bioprocess Engineering*. 17, 1, 15–21.

REFERENCES

- Koning, G.J.M., Lemstra, P.J. (1993) Crystallisation phenomena in bacterial poly-(R)-3-hydroxybutyrate: embrittlement and rejuvenation. *Polymer*. 34, 19, 1489-1506.
- Kosseva, M.R., Rusbandi, E. (2018) Trends in the biomanufacture of polyhydroxyalkanoates with focus on downstream processing. *International Journal of Biological Macromolecules. Part A*. 107, 762-778. doi: 10.1016/j.ijbiomac.2017.09.054.
- Koster, R., Vieluf, D., Kiehn, M., Sommerauer, M., Kahler, J., Baldus, S., Meinertz, T., Hamm, CW. (2000). Nickel and molybdenum contact allergies in patients with coronary in-stent restenosis. *Lancet*. 356, 1895–1897.
- Koyama, N., Doi, Y. (1997) Miscibility of binary blends of poly[(R)-3-hydroxybutyric acid] and poly[(S)-lactic acid]. *Polymer*. 38, 1589-1593.
- Knowles, J.C., Hastings, G.W., Ohta, H., Niwa, S., Boeree, N. (1992) Development of a degradable composite for orthopaedic use: in vivo biomechanical and histological evaluation of two bioactive degradable composites based on the polyhydroxybutyrate polymer. *Biomaterials*. 13, 491-496.
- Korovessis, P.G., Deligianni, D.D., Lenke, L.G. (2002) Role of surface roughness of titanium versus hydroxyapatite on human bone marrow cells response. *Journal of Spinal Disorders and Techniques*. 15, 175-83.
- Korsatko, W., Wabnegg, B., Tillian, H.M. (1983) Poly-D-(-)-3-hydroxybutyric acid: a biodegradable carrier for long term medication dosage. II. Comm.: the biodegradation in animal organism and *in vitro* – *in vivo* correlation of the liberation of pharmaceuticals from parenteral matrix retard tablets. *Pharmazeutische Industrie*. 45(10), 1004–1007.
- Köse, G.T., Korkusuz, F., Korkusuz, P., Purali, N., Ozkul, A., Hasirci, V. (2003) Bone generation on PHBV matrices: an *in vitro* study. *Biomaterials*. 24, 4999–5007.
- Kostopoulos, L., Karring, T. (1994) Guided bone regeneration in mandibular defects in rats using a bioresorbable polymer. *Clinical Oral Implants Research*. 5, 66-74.
- Kraak, M.N., Kessler, B., Witholt, B. (1997) *In vitro* activities of granule bound poly-(R)-3-hydroxyalkanoate) polymerase C1 of *Pseudomonas oleovorans*. Development of an activity test for medium-chain-length-Poly(3-hydroxyalkanoate) polymerases. *European Journal of Biochemistry*. 250, 432–439.
- Kumbhakar, S., Singh, P.K., Vidyarthi, A.S. (2012) Screening of root nodule bacteria for the production of polyhydroxyalkanoate (PHA) and the study of parameters influencing the PHA accumulation. *African Journal of Biotechnology*. 11 (31), 7934-7946.
- Kunasundari, B., Arza, C.R., Maurer, F.H.J., Murugaiyah, V., Kaur, G., Sud, K. (2017) Biological recovery and properties of poly(3-hydroxybutyrate) from *Cupriavidus necator* H16. *Separation and Purification Technology*. 172, 1–6.

REFERENCES

- Kunasundari, B., Sudesh, K (2011) Isolation and recovery of microbial polyhydroxyalkanoates. *eXPRESS Polymer Letters*. 5 (7), 620–634. DOI: 10.3144/expresspolymlett.2011.60.
- Kunzler, T.P., Drobek, T., Schuler, M., Spencer, N.D. (2007) Systematic study of osteoblast and fibroblast response to roughness by means of surface-morphology gradient. *Biomaterials*. 28, 2175-82.
- Kurtz, S.M., Villarraga, M.L., Zhao, K., Edidin, A.A. (2005) Static and fatigue mechanical behaviour of bone cement with elevated barium sulfate content for treatment of vertebral compression fractures. *Biomaterials*. 26, 17, 3699-3712.
- Kusaka, S., Iwata, T., Doi, Y. (1999) Properties and biodegradability of ultra-high molecular-weight poly[(r)-hydroxybutyrate] produced by a recombinant *Escherichia coli*. *International Journal of Biological Macromolecules*. 25, 87-94.
- Kushwah, B. S., Kushwah, A.V.S., Singh, V. (2016) Towards understanding polyhydroxyalkanoates and their use. *Journal of Polymer Research*. 23, 153. doi 10.1007/s10965-016-0988-3.
- Kutryk, M. J. B., Serruys, P. W. (2000) Handbook of coronary Stents. 3rd edition. London, Martin Dunitz.
- LaFountaine, J.S., McGinity, J.W., Williams, R.O. (2016) Challenges and strategies in thermal processing of amorphous solid dispersions: a review. *AAPS PharmSciTech*. 17 (1), 43–55. doi: 10.1208/s12249-015-0393-y.
- Lageveen, R.G., Huisman, G.W., Preusting, H., Ketelaar, P., Eggink, G., Witholt, B. (1988) Formation of polyesters by *Pseudomonas oleovorans*: effect of substrate on formation and composition of poly- (r)-3-hydroxyalkanoates and poly-(r)-3-hydroxyalkanoates. *Applied Environmental Microbiology*. 54, 12, 2924-2932.
- Laia, W.C., Liao, W.B., Lina, T.T. (2004) The effect of end groups of PEG on the crystallization behaviours of binary crystalline polymer blends PEG/PLLA. *Polymer*. 45, 3073–3080.
- Langer, R., Vacanti, J. P. (1993) Tissue engineering. *Science*. 260 (5110), 920-6.
- Lao, L.L., Venkatraman, S.S., Peppas, N.A. (2008) Modeling of drug release from biodegradable polymer blends. *European Journal of Pharmaceuticals and Biopharmaceuticals*. 70, 796–803.
- Lane, C.E., Benton, M.G. (2015) Detection of the enzymatically-active polyhydroxyalkanoate synthase subunit gene, phaC, in cyanobacteria via colony PCR. *Molecular and Cellular Probes*. 29, 454–460.
- Lampen, A., Christians, U., Guengerich, F.P., Watkins, P.B., Kolars, J.C., Bader, A., Gonschior, A.K., Dralle, H., Hackbarth, I., Sewing, K.F. (1995) Metabolism of the immunosuppressant tacrolimus in the small intestine: cytochrome P450, drug interactions, and interindividual variability. *Drug Metabolism and Disposition*. 23, 1315–24.
- Lam, S. S., Frantzen, J. J., Khosravi, F. (1998) Radiopaque stent markers. US patent 5725572. *Advanced Cardiovascular System*.

REFERENCES

- Larsson, M., Markbo, O., Jannasch, P. (2016) Melt processability and thermomechanical properties of blends based on polyhydroxyalkanoates and poly(butylene adipate-co-terephthalate). *RSC Advances*. 6, 44354-44363. DOI: 10.1039/C6RA06282B.
- Laschewsky, A. (2014) Structures and synthesis of zwitterionic polymers. *Polymers*. 6, 1544-1601; doi:10.3390/polym6051544.
- Lauzier, C., Marchessault, R.H., Smith, P., Chanzy, H. (1992) Structural study of isolated poly (β -hydroxybutyrate) granules. *Polymer*. 33, 823-827.
- Laycock, B., Halley, P., Pratt, S., Werker, A., Lanta, P. (2013) The chemomechanical properties of microbial polyhydroxyalkanoates. *Progress in Polymer Science*. 38, 536– 583.
- Lazarus, M.D., Cuckler, J.M., Schumacher, H.R., Ducheyne, P., Baker, D.G. (1994) Comparison of the inflammatory response to particulate polymethylmethacrylate debris with and without barium sulfate. *Journal of Orthopaedic Research*. 12, 532–541. doi:10.1002/jor.1100120410.
- Lee, S.Y., Choi, J. (1998) Polyhydroxyalkanoates biodegradable polymer. In: Manual of Industrial Microbiology and Biotechnology. 2nd edition. Demain AL, Davies JE (eds). ASM Press, Washington D.C., 616-627.
- Lee, S.Y. (1996) Plastic bacteria. Progress and prospects for polyhydroxyalkanoate production in bacteria. *Trends in Biotechnology*. 14, 431-438.
- Lee, S.Y. (1995) Bacterial Polyhydroxyalkanoates. *Biotechnology and Bioengineering*. 49, 1-14.
- Lee, E.Y., Jendrossek, D., Schirmer, A., Choi, Y., Steinbuchel, A. (1995) Biosynthesis of copolyester consisting of 3-hydroxybutyric acid and medium-chain-length 3-hydroxyalkanoic acids from 1,3-butanediol or from 3-hydroxybutyrate by *Pseudomonas* sp. A33. *Applied Microbiology and Biotechnology*. 42, 901–909.
- Lemoigne, M. (1926) Products of dehydration and of polymerization of Polyhydroxybutyric acid. *Bulletin of the Chemical Society. Biol.* 8: 770-782.
- Leng, H., Wang, X., Ross, R.D., Niebur, G.L., Roeder, R.K. (2008) Micro-Computed tomography of fatigue microdamage in cortical bone using a barium sulfate contrast agent. *Journal of the Mechanical Behaviour of Biomedical Materials*. 1(1), 68–75. doi: 10.1016/j.jmbbm. 2007.06.002.
- Lewis, G., van Hooy-Corstjens, C.S., Bhattaram, A., Koole, L.H. (2005) Influence of the radiopacifier in an acrylic bone cement on its mechanical, thermal, and physical properties: barium sulfate-containing cement versus iodine-containing cement. *Journal of Biomedical Materials Research B Applied Biomaterials*. 73(1), 77-87.
- Lewis, G. (1997) Properties of acrylic bone cement: state of the art review. *Journal of Biomedical Material Research (Applied Biomaterials)*. 38, 155-182.

REFERENCES

- Li, Z., Yang, J., Loh, X.J. (2016) Polyhydroxyalkanoates: Opening doors for a sustainable future. *NPG Asia Materials*. 8. e265. 10.1038/am.2016.48
- Li, J., Kim, S.G., Blenis, J. (2014) Rapamycin: one drug, many effects. *Cell Metabolism*. 19(3), 373–379. doi: 10.1016/j.cmet.2014.01.001.
- Li, X.T., Zhang, Y., Chen, G.Q. (2008) Nanofibrous polyhydroxyalkanoate matrices as cell growth supporting materials. *Biomaterials*. 29, 3720–3728. doi: 10.1016/j.biomaterials.2008.06.004.
- Li, Y., Wang, C., Wang, G., Qu, Z. (2008) Application of the long-chain linear polyester in plastification of PVC. *Journal of Wuhan University of Technology Materials Science. Edit.* 23: 100. <https://doi.org/10.1007/s11595-006-1100-3>.
- Lillo, J.G., Rodriguez-Valera, F. (1990) Effects of culture conditions on poly(β -hydroxybutyrate acid) production by *Haloferax mediterranei*. *Applied and Environmental Microbiology*. 56(8), 2517–2521.
- Liu, Y., Huang, S., Zhang, Y., Xu, F. (2014) Isolation and characterization of a thermophilic *Bacillus shackletonii* K5 from a biotrickling filter for the production of polyhydroxybutyrate. *Journal of Environmental Sciences*. 26, 1453–1462.
- Liu, H.-T., Li, F., Wang, W.-Y., Li, X.-J., Liu, Y.-M., Wang, R.-A., Wang, H.-C. (2010). Rapamycin inhibits re-endothelialization after percutaneous coronary intervention by impeding the proliferation and migration of endothelial cells and inducing apoptosis of endothelial progenitor cells. *Texas Heart Institute Journal*. 37(2), 194–201.
- Liu, H., Slamovich, E.B., Webster, T.J. (2006) Less harmful acidic degradation of poly(lactic-co-glycolic acid) bone tissue engineering scaffolds through titania nanoparticle addition. *International Journal of Nanomedicine*. 1(4), 541–545.
- Liu, F., Li, W., Ridgway, D., Gu, T., Shen, Z. (1998) Production of poly- β -hydroxybutyrate on molasses by recombinant *Escherichia coli*. *Biotechnology Letters*. 20, 345–348.
- Lizarraga-Valderrama, L., Nigmatullin, R., Taylor, C., Haycock, J.W., Claeysens, F., Knowles, J.C., Roy, I. (2015) Nerve tissue engineering using blends of poly(3-hydroxyalkanoates) for peripheral nerve regeneration. *Engineering in Life Sciences*. 15, 612–621.
- Lo, C.M., Wang, H.B., Dembo, M., Wang, Y.L. (2000) Cell movement is guided by the rigidity of the substrate. *Biophysical Journal*. 79 (1), 144–152.
- Loh, J.W., Yeoh, G., Saunders, M., Lim, L.Y. (2010) Uptake and cytotoxicity of chitosan nanoparticles in human liver cells. *Toxicology and Applied Pharmacology*. 249, 148–157.
- Loo, C.Y., Sudesh, K. (2007) Polyhydroxyalkanoates: Bio-based microbial plastics and their properties. *Malaysian Polymer Journal*. 2 (2), 31-57.
- López-Cuellar, M.R., Alba-Flores, J., Rodríguez, J.N.G., Pérez-Guevaraa, F. (2011) Production of polyhydroxyalkanoates (PHAs) with canola oil as carbon source. *International Journal of Biological Macromolecules*. 48, 74–80.

REFERENCES

- Lowe, H.C., Oesterle, S.N., Khachigian, M.L. (2002) Coronary In-stent restenosis: current status and future strategies. *Journal of the American College of Cardiology*. 39 (2), 183-193.
- Lu, C., Filion, K.B., Eisenberg, M.J. (2016) The safety and efficacy of Absorb bioresorbable vascular scaffold: A systematic review. *Clinical Cardiology*. 39 (1), 48–55.
- Lu, J.N., Tappel, R.C., Nomura, C.T. (2009) Mini-review: biosynthesis of poly(hydroxyalkanoates). *Polymer Reviews*. 49, 226–248. doi: 10.1080/15583720903048243.
- Lu, J., Tappel, R.C., Nomura, C.T. (2006) Mini-Review: biosynthesis of Poly(hydroxyalkanoates). *Polymer Reviews*. 46 (1), 226-248.
- Luckachan, G.E., Pillai, C.K.S. (2012) Biodegradable polymers- a review on recent trends and emerging perspectives. *Journal of Polymers and the Environment*. 19, 637–676.
- Luderer, F., Bler, M., Rohm, H.W., Gocke, C., Kunna, K., Ko, C.K., Kroemer, H.K., Weitschies, W., Schmitz, K.P. (2011) Biodegradable sirolimus-loaded poly(lactide) nanoparticles as drug delivery system for the prevention of in-stent restenosis in coronary stent application. *Journal of Biomaterials Applications*. 25, 851–875.
- Ludman, P.F., Bradley, A., Topham, E., Manuel, S. (2015) National audit of percutaneous coronary interventions. National Institute for Cardiovascular Outcomes Research, Institute of Cardiovascular Science, University College London. Full text available at: www.BCIS.org.uk.
- Luef, K.P., Stelzer, F., Wiesbrock, F. (2015) Poly(hydroxyalkanoate)s in medical application. *Chemical and Biochemical Engineering. Q.*, 29 (2), 287–297.
- Luklinska, Z.B., Bonfield, W. (1997) Morphology and ultrastructure of the interface between hydroxyapatite-polyhydroxybutyrate composite implant and bone. *Journal of Material Science: Materials in Medicine*. 8, 379-383.
- Lyu, S., Untereker, D. (2009) Degradability of polymers for implantable biomedical devices. *International Journal of Molecular Sciences*. 10(9), 4033-4065. doi:10.3390/ijms10094033.
- Ma, Z., Zeng, F., Wang, J., Yang, S., Liu, C. (2017) Enhanced cell affinity of PHBHHx composite scaffold with polylactide-graft-hydroxyapatite as compatibilizer. *Materials Science and Engineering: C*. 80, 472-483.
- Ma, P.M., Hristova-Bogaerds, D.G., Zhang, Y., Lemstra, P.J. (2014) Enhancement in crystallization kinetics of the bacterially synthesized poly(-hydroxybutyrate) by poly(butylene succinate). *Polymer Bulletin*. 71, 907–923.
- Ma, X., Oyamada, S., Gao, F., Wu, T., Robich, M.P., Wu, H., Laham, R. (2011) Paclitaxel/sirolimus combination coated drug-eluting stent: *In vitro* and *in vivo* drug release studies. *Journal of Pharmaceutical and Biomedical Analysis*. 54(4), 807–811. <http://doi.org/10.1016/j.jpba.2010.10.027>.

REFERENCES

- Madison, L.L., Huisman, G.W. (1999) Metabolic engineering of poly(3-hydroxyalkanoates): from DNA to plastic. *Microbiology and Molecular Biology Reviews*. 63, 21–53.
- Malm, T., Bowald, S., Bylock, A., Busch, C., Saldeen, T. (1994) Enlargement of the right ventricular outflow tract and the pulmonary artery with a new biodegradable patch in transannular position. *European Surgical Research*. 298 - 308.
- Malm, T., Bowald, S., Bylock, A., Saldeen, T., Busch, C. (1992). Regeneration of pericardial tissue on absorbable polymer patches implanted into the pericardial sac. An immunohistochemical, ultrasound and biochemical study in sheep. *Scandinavian Journal of Thoracic Cardiovascular Surgery*. 26(1), 15-21.
- Mani, G., Feldman, M.D., Patel, D., Agrawal, C.M. (2007) Coronary stents: a materials perspective. *Biomaterials*. 28, 1689–1710.
- Marang, L., Jiang, Y., van Loosdrecht, M.C.M., Kleerebezem, R. (2014) Impact of non-storing biomass on PHA production: an enrichment culture on acetate and methanol. *International Journal of Biological Macromolecules*. 71, 74-80. doi: 10.1016/j.ijbiomac.2014.04.051.
- Morimoto, T., Kadoya, R., Endo, K., Tohata, M., Sawada, K., Liu, S., Ozawa, T., Kodama, T., Kakeshita, H., Kageyama, Y., Manabe, K., Kanaya, S., Ara, K., Ozaki, K., Ogasawara, N. (2008) Enhanced recombinant protein productivity by genome reduction in *Bacillus subtilis*. *DNA Research*. 15 (2), 73-81. doi: 10.1093/dnares/dsn002.
- Marois, Y., Zhang, Z., Vert, M., Deng, X., Lenz, R., Guidoin, R. (2000) Mechanism and rate of degradation of polyhydroxyoctanoate films in aqueous media: A long-term *in vitro* study. *Journal of Biomedical Materials Research*. 49: 216–224.
- Martin, D.P., Williams, S.F. (2003) Medical applications of poly-4-hydroxybutyrate: a strong flexible absorbable biomaterial. *Journal of Biochemical Engineering*. 16, 97–105.
- Martinez-Sanz, M., Villano, M., Oliveira, C., Albuquerque, M.G.E., Majone, M., Reis, M., Lopez-Rubio, A., Lagaron, J.M. (2014) Characterization of polyhydroxyalkanoates synthesized from microbial mixed cultures and of their nanobiocomposites with bacterial. *New Biotechnology*. 31, 364–376.
- Martinez, G.A., Bertin, L., Scoma, A., Rebecchi, S., Braunegg, G., Fava, F. (2015) Production of polyhydroxyalkanoates from dephenolised and fermented olive mill wastewaters by employing a pure culture of *Cupriavidus necator*. *Biochemical Engineering Journal*. 97, 92-100.
- Martino, L., Cruz, M.V., Scoma, A., Freitas, F., Bertin, L., Scandola, M., Reis, M.A.M. (2014) Recovery of amorphous polyhydroxybutyrate granules from *Cupriavidus necator* cells grown on used cooking oil. *International Journal of Biological Macromolecules*. <http://dx.doi.org/10.1016/j.ijbiomac.2014.04.016>.

REFERENCES

- Marx, S.O., Jayaraman, T., Go, L.O., Marks, A.R. (1995) Rapamycin-Fkbp inhibits cell cycle regulators of proliferation in vascular smooth muscle cells. *Circulation Research*. 76 (3), 412-417.
- Martelli, S.M., Sabirova, J., Fakhoury, F.M., Dyzma, A., Meyer B., Soetaert, W. (2012) Obtention and characterization of poly(3-hydroxybutyric acid-co-hydroxyvaleric acid)/mcl-PHA based blends. *LWT-Food Science Technology*. 47, 386-392.
- Masaeli, E., Morshed, M., Rasekhian, P., Karbasi, S., Karbalaie, K., Karamali, F. (2012) Does the tissue engineering architecture of poly(3-hydroxybutyrate) scaffold affects cell-material interactions? *Journal of Biomedical Materials Research*. A. 100A, 1907–1918.
- Matias, F., de Andrade Rodrigues, M.F. (2011) New PHA products using unrelated carbon sources. *Brazilian Journal of Microbiology*. 42(4), 1354-63. doi: 10.1590/S1517-838220110004000017.
- Matsusaki, H., Abe, H., Doi, Y. (2000) Biosynthesis and properties of poly (3-hydroxybutyrate-co-3-hydroxyalkanoates) by recombinant strains of *Pseudomonas* sp. 61-3. *Biomacromolecules*. 1, 17–22.
- Matter, C.M., Rozenberg, I., Jaschko, A., Greutert, H., Kurz, D.J., Wnendt, S., Kuttler, B., Joch, H., Grünenfelder, J., Zünd, G., Tanner, F.C., Lüscher, T.F. (2006) Effects of tacrolimus or sirolimus on proliferation of vascular smooth muscle and endothelial cells. *Journal of Cardiovascular Pharmacology*. 48 (6), 286-292. doi: 10.1097/01.fjc.0000248233.22570.8b.
- McClean, D.R., Eigler, N.R. (2002) Stent design: implications for restenosis. *Reviews in Cardiovascular Medicine*. 3, S16–S22.
- McFadden, E.P., Stabile, E., Regar, E., Cheneau, E., Ong, A.T., Kinnaird, T., Suddath, W.O., Weissman, N.J., Torguson, R., Kent, K.M., Pichard, A.D., Satler, L.F., Waksman, R., Serruys, P.W. (2004) Late thrombosis in drug-eluting coronary stents after discontinuation of antiplatelet therapy. *Lancet*. 364, (9444), 1519-21.
- Meagher, M.J., Leone, B., Turnbull, T.L., Ross, R.D., Zhang, Z., Roeder, R.K. (2013) Dextran-encapsulated barium sulfate nanoparticles prepared for aqueous dispersion as an X-ray contrast agent. *Journal of Nanoparticle Research*. 15. 2146. 10.1007/s11051-013-2146-8.
- Mekonnen, T., Mussonea, P., Khalilb, H., Bressler, D. (2013) Progress in bio-based plastics and plasticizing modifications. *Journal of Material Chemistry*. A. 1, 13379-13398.
- Mendonca, T.T., Gomez, J.G., Buffoni, E., Sanchez, Rodriguez, R.J., Schripsema, J., Lopes, M.S., Silva, L.F. (2013) Exploring the potential of *Burkholderia sacchari* to produce polyhydroxyalkanoates. *Journal of Applied Microbiology*. 116, 4, 815-29. 10.1111/jam.12406.

REFERENCES

- Mergaert, J., Webb, A., Anderson, C., Wouters, A., Swings, J. (1993) Microbial degradation of poly(3-hydroxybutyrate) and poly(3-hydroxybutyrate-co-3-hydroxyvalerate) in soils. *Applied and Environmental Microbiology*, 59 (10), 3233-3238.
- Mergulhão, F.J., Summers, D.K., Monteiro, G.A. (2005) Recombinant protein secretion in *Escherichia coli*. *Biotechnology Advances*. 23(3), 177-202.
- Meszynska, A., Pollet, E., Odelius, K., Hakkarainen, M., Averous, L. (2015) Effect of Oligo-hydroxyalkanoates on poly(3-hydroxybutyrate-co-4-hydroxybutyrate) - based systems. *Macromolecular Materials and Engineering*. 300 (6), 661-666.
- Meyers, S.R., Grinstaff, M.W. (2012) Biocompatible and bioactive surface modifications for prolonged *in vivo* efficacy. *Chemical Reviews*. 112 (3), 1615–1632. DOI: 10.1021/cr2000916.
- Miller, N.D., Williams, D.F. (1987) On the biodegradation of poly-beta-hydroxybutyrate (PHB) homopolymer and poly-beta-hydroxybutyrate-hydroxyvalerate copolymers. *Biomaterials*. 8(2), 129-37.
- Miller, R.A., Brady, J.M., Cutright, D.E. (1977) Degradation rates of oral resorbable implants (polylactates and polyglycolates): Rate modification with changes in PLA/PGA copolymer ratios. *Journal of Biomedical Material Research*. 11, 711-719.
- Miller, G.L. (1959) Use of dinitrosalicylic acid reagent for determination of reducing sugar. *Analytical Chemistry*. 31, 426.
- Minari, C., Cristofolini, L., Baruffaldi, F., Pierotti, L. (2000) Radiopacity and fatigue characterization of a novel acrylic bone cement with sodium fluoride. *Artificial Organs*. 24(9), 751-757.
- Misra, S.K., Ansari, T.I., Valappil, S.P., Mohne, D., Philip, S.E., Stark, W.J., Roy, I., Knowles, J.C., Salih, V., Boccaccini, A.R. (2010a) Poly(3-hydroxybutyrate) multifunctional composite scaffolds for tissue engineering applications. *Biomaterials*. 31, 2806–2815.
- Misra, S.K., Ohashi, F., Valappil, S.P., Knowles, J.C., Roy, I., Ravi, S., Silva, P., Salih, V., Boccaccini, A.R. (2010b) Characterization of carbon nanotube (MWCNT) containing P(3HB)/bioactive glass composites for tissue engineering applications. *Acta Biomaterialia*. 6 (3), 735-742.
- Misra, S.K., Mohn, D., Brunner, T.J., Stark, W.J., Philip, S.E., Roy, I., Salih, V., Knowles, J.C., Boccaccini, A.R. (2008) Comparison of nanoscale and microscale bioactive glass on the properties of P(3HB)/Bioglass composites. *Biomaterials*. 29, 1750-1761.
- Misra, S.K., Valappil, S.P., Roy, I., Boccaccini, A.R. (2006) Polyhydroxyalkanoate (PHA)/Inorganic phase composites for tissue engineering applications. *Biomacromolecules*. 7, 2249-2258.
- Mokhtari-Hosseini, Z.B., Vasheghani-Farahani, E., Heidarzadeh-Vazifekhoran, A., Shojaosadati, S.A., Karimzadeh, R., Darani, K.K. (2009) Statistical media

REFERENCES

- optimization for growth and PHB production from methanol by a methylotrophic bacterium. *Bioresource Technology*. 100 (8), 2436-2443.
- Möller, A., Iwasaki, K., Kawamura, A. (1999) The disposition of ¹⁴C-labelled tacrolimus after intravenous and oral administration in healthy human subjects. *Drug Metabolism and Disposition*. 27, 633–636.
 - Choi, M.W., Wan, K.T., Park, O.O., Chang, K.Y., Lee, W.J. (2003) Preparation and characterization of poly(hydroxybutyrate-co-hydroxyvalerate)-organoclay nanocomposites. *Journal of Applied Polymer Science*. 90, 525–529.
 - Morales, J.M., Andres, A., Rengel, M., Rodicio, J.L. (2001) Influence of cyclosporine, tacrolimus and rapamycin on renal function and arterial hypertension after renal transplantation. *Nephrology Dialysis Transplantation*. 16 (1), 121-124.
 - Moravej, M., Purnama, A., Fiset, M., Couet, J., Mantovani, D. (2010a) Electroformed pure iron as a new biomaterial for degradable stents: in vitro degradation and preliminary cell viability studies. *Acta Biomaterialia*. 6 (5), 1843-1851.
 - Moravej, M., Prima, F., Fiset, M. (2010b) Electroformed iron as new biomaterial for degradable stents: Development process and structure–properties relationship. *Acta Biomaterialia*. 6, 1726–35.
 - Morice, M.C., Serruys, P.W., Souse, J.E., Fajadet, J., Hayashi, E.B., Perin, M., Colombo, A., Schuler, G., Barragan, P., Guagliumi, G., Molnar, F., Falotico, R. (2002) A randomized comparison of a sirolimus-eluting stent with a standard stent for coronary revascularization. *New England Journal of Medicine*. 346 (23), 1773-1780.
 - Morrisett, J.D., Abdel-Fattah, G., Hoogeveen, R., Mitchell, E., Ballantyne, C.M., Pownall, H.J., Opekun, A.R., Jaffe, J.S., Oppermann, S., Kahan, B.D. (2002) Effects of sirolimus on plasma lipids, lipoprotein levels, and fatty acid metabolism in renal transplant patients. *Journal of Lipid Research*. 43, 1170–1180.
 - Moses, J.W., Leon, M.B., Popma, J.J. (2003) Sirolimus-eluting stents versus standard stents in patients with stenosis in a native coronary artery. *New England Journal of Medicine*. 349, 1315–23.
 - Moskowitz, G.J., Merrick, J.M. (1969) Metabolism of poly-β-hydroxybutyrate. II. Enzymatic synthesis of D-(-)-β-hydroxybutyryl coenzyme A by an enoyl hydratase from *Rhodospirillum rubrum*. *Biochemistry*. 8(7), 2748-55.
 - Mosmann, T. (1983) Rapid colorimetric assay for cellular growth and survival: application to proliferation and cytotoxicity assays. *Journal of Immunological Methods*. 65, 55-63.
 - Moss, S.C., Lightell, D.J., Marx, S.O., Marks, A.R., Woods, C.T. (2010) Rapamycin regulates endothelial cell migration through regulation of the cyclin-dependent kinase inhibitor p27^{Kip1}. *Journal of Biology and Chemistry*. 285(16), 11991–11997.doi:10.1074/jbc.M109.066621.

REFERENCES

- Mothes, G., Schnorpfeil, C., Ackermann, J.U. (2007) Production of PHB from crude glycerol. *Engineering in Life Sciences*. 7(5), 475e9.
- Motlagh, D., Yang, J., Lui, K.Y., Webb, A.R., Ameer, G.A. (2006) Hemocompatibility evaluation of poly(glycerol-sebacate) *in vitro* for vascular tissue engineering. *Biomaterials*. 27 (24), 4315–4324.
- Mozejko-Ciesielska, J., Kiewisz, R. (2016) Bacterial polyhydroxyalkanoates: Still fabulous? *Microbiological Research*. 192, 271-282.
- Mozejko, J., Ciesielski, S. (2014) Pulsed feeding strategy is more favourable to medium-chain-length polyhydroxyalkanoates production from waste rapeseed oil. *Biotechnology Progress*. 30 (5), 1243-1246. DOI 10.1002/btpr.1914.
- Mozejko, J., Ciesielski, S. (2013) Saponified waste palm oil as an attractive renewable resource for mcl-polyhydroxyalkanoate synthesis. *Journal of Bioscience and Bioengineering*. 116(4), 485-92. doi: 10.1016/j.jbiosc.2013.04.014.
- Mozejko, J., Przybytek, G., Ciesielski, S. (2011) Waste rapeseed oil as a substrate for mcl-PHAs production. *European Journal of Lipid Science and Technology*. 113, 1550-1557.
- Mozumder, M.S.I., De Wever, H., Volcke, E.I.P., Garcia-Gonzalez, L. (2014) A robust fed-batch feeding strategy independent of the carbon source for optimal polyhydroxybutyrate production. *Process Biochemistry*. 155, 272–280.
- Muangwong, A., Boontip, T., Pachimsawat, J., Chanprateep, S., Muangwong, N. (2016) Medium chain length polyhydroxyalkanoates consisting primarily of unsaturated 3-hydroxy-5-cis-dodecanoate synthesized by newly isolated bacteria using crude glycerol. *Microbial Cell Factories*. 15, 55. DOI 10.1186/s12934-016-0454-2.
- Muhammadi, S., Afzal, M., Hameed, S. (2015) Bacterial polyhydroxyalkanoates-eco-friendly next generation plastic: Production, biocompatibility, biodegradation, physical properties and applications. *Green Chemistry Letters and Reviews*, 8, 3-4, 56-77. DOI: 10.1080/17518253.2015.1109715.
- Murugan, P., Han, L., Gan, C-Y., Maurer, H.J.F., Sudesh, K. (2016). A new biological recovery approach for PHA using mealworm, *Tenebrio molitor*. *Journal of Biotechnology*. 239, 98–105.
- Naffakh, M., Marco, C., Ellis, G. (2014) Inorganic ws2 nanotubes that improve the crystallization behavior of poly(3-hydroxybutyrate). *CrystEngComm*. 16, 1126–1135.
- Nagarajan, V., Misra, M., Mohanty, A.K. (2013) New engineered biocomposites from poly(3-hydroxybutyrate-co-3-hydroxyvalerate) (PHBV)/poly(butylene adipate-co-terephthalate) (PBAT) blends and switchgrass: Fabrication and performance evaluation. *Industrial Crops and Products*. 42, 461–468.
- Nagy, P. (2014) X-ray examination of integrated stent markers. *IRBM*. 36 (1), 30-34. 10.1016/j.irbm.2014.12.001.

REFERENCES

- Nakano, K., Egashira, K., Masuda, S., Funakoshi, K., Zhao, G., Kimura, S., Matoba, T., Sueishi, K., Endo, Y., Kawashima, Y., Hara, K., Tsujimoto, H., Tominaga, R., Sunagawa, K. (2009) Formulation of nanoparticle-eluting stents by a cationic electrodeposition coating technology. Efficient nano-drug delivery via bioabsorbable polymeric nanoparticle-eluting stents in porcine coronary arteries. *JACC: Cardiovascular Interventions*. 2 (4), 277-283.
- Nakata, Y., Yoshibayashi, M., Yonemura, T. (2000) Tacrolimus and myocardial hypertrophy. *Transplantation*. 69, 1960–1962.
- Nakazawa, G. (2011) Stent thrombosis of drug eluting stent: Pathological perspective. *Journal of Cardiology*. 58, 84–91.
- Naranjo, J.M., Posada, J.A., Higuera, J.C., Cardona, C.A. (2013) Valorization of glycerol through the production of biopolymers: The PHB case using *Bacillus megaterium*. *Bioresource Technology*. 133, 38-44.
- Naveen, S.V., Tan, I.K.P., Goh, Y.S., Raghavendran, H.R.B., Murali, M.R., Kamarul, T. (2015) Unmodified medium chain length polyhydroxyalkanoate (uMCL-PHA) as a thin film for tissue engineering application – characterization and *in vitro* biocompatibility. *Materials Letters*. 141, 55–58.
- Naveen, N., Kumar, R., Balaji, S., Uma, T.S., Natrajan, Sehgal, P.K. (2010) Synthesis of nonwoven nanofibers by electrospinning – a promising biomaterial for tissue engineering and drug delivery. *Advanced Engineering Materials*. 12, B380.
- Nazneen, F., Herzog, G., Arrigan, D.W., Caplice, N., Benvenuto, P., Galvin, P., Thompson, M. (2012) *Journal of Biomedical Materials Research. B*. 100, 1989.
- Nebeker, J.R., Virmani, R., Bennett, C.L., Hoffman, J.M., Samore, M.H., Alvarez, J., Davidson, C.J., McKoy, J.M., Raisch, D.W., Whisenant, B.K., Yarnold, P.R., Belknap, S.M., West, D.P., Gage, J.E., Morse, R.E., Gligoric, G., Davidson, L., Feldman, M.D. (2006). Hypersensitivity cases associated with drug-eluting coronary stents: a review of available cases from the Research on Adverse Drug Events and Reports (RADAR) project. *Journal of the American College of Cardiology*. 47, 175–81.
- Nerkar, M., Ramsay, J.A., Ramsay, B.A., Kontopoulou, M. (2014) Melt compounded blends of short and medium chain-length Poly-3-hydroxyalkanoates. *Journal of Polymers and the Environment*. 22, 236–243.
- Nikodinovic, J., Kenny, S.T., Babu, R.P., Woods, T., Blau, W.J., O'Connor, K.E. (2008) The conversion of BTEX compounds by single and defined mixed cultures to medium-chain-length polyhydroxyalkanoate. *Applied Microbiology and Biotechnology*. 80, 665–673.
- Nicolaou, K.C., Yang, Z., Liu, J.J., Ueno, H., Nantermet, P.G., Guy, R.K., Claiborne, C.F., Renaud, J. *et al.* (1994). "Total synthesis of taxol". *Nature*. 367 (6464): 630–4. doi:10.1038/367630a0.

REFERENCES

- Nigmatullin, R., Thomas, P., Lukasiewicz, B., Puthussery, H., Roy, I. (2015) Polyhydroxyalkanoates, a family of natural polymers, and their applications in drug delivery. *JCTB*. DOI: 10.1002/jctb.4685.
- Nor Aslan, A.K.H., Ali, M.D.M., Morad, N.A., Tamunaidu, P. (2016) Polyhydroxyalkanoates production from waste biomass. *IOP Conf. Series: Earth and Environmental Science*. 36, 012040 doi:10.1088/1755-1315/36/1/012040.
- O'Brien, F.J. (2011) Biomaterials and scaffolds for tissue engineering. *Materials Today*. 14 (3), 88-95. [https://doi.org/10.1016/S1369-7021\(11\)70058-X](https://doi.org/10.1016/S1369-7021(11)70058-X).
- Oberhauser, J., Hossainy, S., Rapoza, R. (2009) Design principles and performance of bioresorbable polymeric coronary scaffolds. *EuroIntervention* 5, 15–22.
- Oberhoff, M., Herdeg, C., Baumbach, A., Karsch, K.R. (2002) Stent-based antirestenotic coatings (Sirolimus/Paclitaxel). *Catheterization and Cardiovascular Interventions*. 55, 404–408.
- OECD/FAO (2017) *OECD-FAO Agricultural Outlook 2017-2026*, OECD Publishing, Paris. http://dx.doi.org/10.1787/agr_outlook-2017-en.
- Oehlmann, J., Schulte-Oehlmann, U., Kloas, W., Jagnytsch, O., Lutz, I., Kusk, K.O., Wollenberger, L., Santos, E.M., Paull, G.C., Van Look, K.J.W., Tyler, C.R. (2009) A critical analysis of the biological impacts of plasticizers on wildlife. *Philosophical Transactions of the Royal Society of London B: Biological Sciences*. 364(1526), 2047–2062. doi: 10.1098/rstb.2008.0242.
- Ojumu, T., Yu, J., Solomon, B. (2004) Production of Polyhydroxyalkanoates, a bacterial biodegradable polymer. *African Journal of Biotechnology* 3 (1), 18-24.
- Okamura, T., Onuma, Y., Garcia-Garcia, H.M. (2010) 3-dimensional optical coherence tomography assessment of jailed side branches by bioresorbable vascular scaffolds: a proposal for classification. *JACC Cardiovascular Interventions*. 3, 836–44.
- Oner, M., Idotlhan, B. (2016) Fabrication of poly(3-hydroxybutyrate-co-3-hydroxyvalerate) biocomposites with reinforcement by hydroxyapatite using extrusion processing. *Materials Science and Engineering C (Materials for Biological Applications)*. 65, 19–26.
- Ong, A.T., Serruys, P.W. (2005) Technology Insight: an overview of research in drug-eluting stents. *Natural Clinical Practice. Cardiovascular Medicine*. 2, 647–658.
- Oren, A. (2008) Microbial life at high salt concentrations: phylogenetic and metabolic diversity. *Saline Systems*. 4, 2. doi: 10.1186/1746-1448-4-2.
- Ormiston, J.A., Serruys, P.W., Regar, E., Dudek, D., Thuesen, L., Webster, M.W., Onuma, Y., Garcia-Garcia, H.M., McGreevy, R., Veldhof, S. (2008) A bioabsorbable everolimus-eluting coronary stent system for patients with single de-novo coronary artery lesions (ABSORB): a prospective open-label trial. *Lancet*. 15, 371 (9616), 899-907. doi: 10.1016/S0140-6736(08)60415-8.

REFERENCES

- Ostuni, E., Chapman, R.G., Holmlin, R.E., Takayama, S., Whitesides, G.M. (2001) A survey of structure–property relationships of surfaces that resist the adsorption of protein. *Langmuir*, 17 (18), 5605–5620. DOI: 10.1021/la010384m.
- Pachence, J.M., Kohn, J. (2000) Bioresorbable polymers for tissue engineering. In *Principles of Tissue Engineering*, ed. Lanza, R.P., Langer, R., Chick, W.L. 267–70.
- Pan, C.J., Tang, J.J., Weng, Y.J., Wang, J., Huang, N. (2009) Preparation and in vitro release profiles of drug-eluting controlled biodegradable polymer coating stents. *Colloids and Surfaces B: Biointerfaces* 73:199–206.
- Panaitescu, D.M., Nicolae, C.A., Frone, A.N., Chiulan, I., Stanescu, P.O., Draghici, C., Iorga, M., Mihailescu, M. (2017). Plasticized poly(3-hydroxybutyrate) with improved melt processing and balanced properties. *Journal of Applied Polymer Science*. 134 (19), 44810-44824.
- Pantazaki, A.A., Papaneophytou, C.P., Pritsa, A.G., Liakopoulou-Kyriakides, M., Kyriakidis, D. (2009) Production of polyhydroxyalkanoates from whey by *Thermus thermophilus* HB8. *Process Biochemistry*. 44, 847–853. doi: 10.1016/j.procbio.2009.04.002.
- Papakonstantinou, V., Papaspyrides, C. (1994) Plasticizer migration from plasticized into unplasticized poly(vinyl chloride). *Journal of Vinyl Technology*. 16. 192 - 196. 10.1002/vnl.730160404.
- Parameswaranpillai, J., Thomas, S., Grohens, Y. (2014) Polymer blends: state of the art, new challenges, and opportunities. Characterization of polymer blends: miscibility, morphology and interfaces. 1-6. 10.1002/9783527645602.ch01.
- Pardo-Ibáñez, P., Lopez-Rubio, A., Martínez-Sanz, M., Cabedo, L., Lagaron, J.M. (2014) Keratin–polyhydroxyalkanoate melt-compounded composites with improved barrier properties of interest in food packaging applications. *Journal of Applied Polymer Science*. 131(4). DOI: 10.1002/app.39947.
- Park, J.H., Joo, C.K., Chung, S.K. (2015) Comparative study of tacrolimus and bevacizumab on corneal neovascularization in rabbits. *Cornea*. 34 (4), 449–455. doi: 10.1097/ICO.0000000000000336.
- Park, D.W., Park, S.W., Park, K.H., Lee, B.K., Kim, Y.H., Lee, C.W., Hong, M.K., Kim, J.J., Park, S.J. (2006) Frequency of and risk factors for stent thrombosis after drug-eluting stent implantation during long-term follow-up. *American Journal of Cardiology*. 98, 352–356.
- Park, J.W., Doi, Y., Iwata, T. (2004) Uniaxial drawing and mechanical properties of Poly[(r)-3-hydroxybutyrate]/poly(l-lactic acid) blends. *Biomacromolecules*. 5 (4), 1557–1566. DOI: 10.1021/bm049905l.
- Parra, D.F., Fusaro, J., Gaboardi, F., Rosa, D.S. (2006) Influence of poly (ethylene glycol) on the thermal, mechanical, morphological, physical-chemical and biodegradation properties of poly(3-hydroxybutyrate). *Polymer Degradation and Stability*. 91, 1954–1959.

REFERENCES

- Paszenda, Z. (2010) Use of coronary stents material and biophysical conditions. *Journal of Achievements in Materials and Manufacturing Engineering*. 43 (1), 125-35.
- Patel, P.V., Patel, H.K., Panchal, S.S., Mehta, T.A. (2013) Self-micro-emulsifying drug delivery system of tacrolimus: Formulation, *in vitro* evaluation and stability studies. *International Journal of Pharmaceutical Investigations*. 3 (2), 95–104. doi: 10.4103/2230-973X.114899
- Patel, P., Patel, H., Panchal, S., Mehta, T. (2012) Formulation strategies for drug delivery of tacrolimus: An overview. *International Journal of Pharmaceutical Investigations* 2 (4), 169–175. doi: 10.4103/2230-973X.106981.
- Patent WO2001019422 A1. Polyhydroxyalkanoate compositions for soft tissue repair, augmentation, and viscosupplementation. 2001.
- Patricio, P., Pereira, F.V., dos Santos, M.C., de Souza, P.P., Roa, J.P.B., Orefice, R.L. (2013) Increasing the elongation at break of Polyhydroxybutyrate biopolymer: Effect of cellulose nanowhiskers on mechanical and thermal properties. *Journal of Applied Polymer Science*. 127, 3613–3621.
- Pawan, G.L., Semple, S.J. (1983) Effect of 3-hydroxybutyrate in obese subjects on very-low-energy diets and during therapeutic starvation. *Lancet*. 1(8314-5), 15-7.
- Pelham, R.J., Jr, Wang, Y.L. (1997) Cell locomotion and focal adhesions are regulated by substrate flexibility. *Proceedings of the National Academy of Sciences of the United States of America*. 94, 13661–13665.
- Peña, C., Castillo, T., García, A., Millán, M., Segura, D. (2014) Biotechnological strategies to improve production of microbial poly-(3-hydroxybutyrate): a review of recent research work. *Microbial Biotechnology*. 7 (4), 278–293. doi: 10.1111/1751-7915.12129.
- Peng, T., Gibula, P., Yao, K., Goosen, M.F.A. (1996). Role of polymers in improving the results of stenting in coronary arteries. *Biomaterials*. 17, 685-694.
- Peuster, M., Hesse, C., Schloo, T., Fink, C., Beerbaum, P., von Schnakenburg, C. (2006) Long-term biocompatibility of a corrodible peripheral iron stent in the porcine descending aorta. *Biomaterials*. 27 (28), 4955-62.
- Peuster, M., Hesse, C., Schloo, T., Fink, C., Beerbaum, P., von Schnakenburg, C. (2006) Long-term biocompatibility of a corrodible peripheral iron stent in the porcine descending aorta. *Biomaterials*. 27, 4955–4962.
- Peuster, M., Wohlsein, P., Brugmann, M., Ehlerding, M., Seidler, K., Fink, C., Brauer, H., Fischer, A., Hausdorf, G. (2001) A novel approach to temporary stenting: degradable cardiovascular stents produced from corrodible metal—results 6-18 months after implantation into New Zealand white rabbits. *Heart*. 86 (5), 563-569. doi: 10.1136/heart.86.5.563.
- Philip S., Keshavarz, T., Roy, I. (2007) Polyhydroxyalkanoates: biodegradable polymers with a range of applications. *Journal of Chemical Technology and*

REFERENCES

- Biotechnology*. 82, 233-247.
- Pitt, C.G. (1990) Poly-caprolactone and its copolymers. In: Chasin M, Langer R, editors. biodegradable polymers as drug delivery systems. New York: Marcel Dekker. 71–120.
 - Pitt, C.G., Chasalow, F.I., Hibionada, Y.M., Klimas, D.M., Schindler, A. (1981) Aliphatic polyesters I.: the degradation of poly(caprolactone) *in vivo*. *Journal of Applied Polymer Science*. 26 (11), 3779–3787.
 - Platzner, N. (1982) The technology of plasticizers. *Journal of Polymer Science: Polymer Letters Edition*. 20(8), 459.
 - Plosker, G.L., Foster, R.H. (2000) Tacrolimus: a further update of its pharmacology and therapeutic use in the management of organ transplantation. *Drugs*. 59 (2), 323-89.
 - Poli, A., Di Donato, P., Abbamondi, G.R., Nicolaus, B. (2011) Synthesis, production, and biotechnological applications of exopolysaccharides and polyhydroxyalkanoates by *Archaea*. *Archaea*. doi: 10.1155/2011/693253.
 - Povolito, S., Toffano, P., Basaglia, M., Casella, S. (2010) Polyhydroxyalkanoates Production by engineered *Cupriavidus necator* from waste material containing lactose. *Bioresource Technology*. 101 (20), 7902-7907.
 - Pouton, C.W., Akhtar, S. (1996) Biosynthetic polyhydroxyalkanoates delivery and their potential in drug delivery. *Advanced Drug Delivery Reviews*. 18, 133-162.
 - Prabhu, S., Hossainy, S. (2006) Modeling of degradation and drug release using biodegradable stent coating. *Journal of Biomedical Materials Research Part A*. 80A (3), 732-741.
 - Preusting, H., van Houten, R., Hoefs, A., van Langenberghe, E.K., Favre-Bulle, O., Witholt, B. (1993) High cell density cultivation of *Pseudomonas oleovorans*: growth and production of poly (3-hydroxyalkanoates) in two-liquid phase batch and fed-batch systems. *Biotechnology and Bioengineering*. 5, 41(5), 550-6.
 - Preusting, H., Nijenhuis, A., Witholt, B. (1990) Physical characteristics of poly(3-hydroxyalkanoates) and poly(3-hydroxyalkenoates) produced by *Pseudomonas oleovorans* grown on aliphatic hydrocarbons. *Macromolecules*. 23, 4220-4224.
 - Puskas, J.E., Munoz-Robledo, L.G., Hoerr, R.A., Foley, J., Schmidt, S.P., Evancho-Chapman, M. (2009) Drug-eluting stent coatings. *Wiley Interdisciplinary Reviews: Nanomedicine and Nanobiotechnology*. 1 (4), 451–462.
 - Qi, Q., Rehm, B.H.A., Steinbuchel, A. (1997) Synthesis of poly(3-hydroxyalkanoates) from *Escherichia coli* expressing the PHA synthase gene PhaC2 from *Pseudomonas aeruginosa*: comparison of PhaC1 and PhaC2. *FEMS Microbiology Letters*. 157, 155-162.
 - Qiu, Z., Ikehara, T., Nishi, T. (2003) Poly(hydroxybutyrate)/ poly(butylene succinate) blends: miscibility and non-isothermal crystallization. *Polymer*. 44, 2503–2508.

REFERENCES

- Qu, X.H., Wu, Q., Liang, J., Qu, X., Wang, S.G., Chen, G.Q. (2005) Enhanced vascular-related cellular affinity on surface modified copolyesters of 3-hydroxybutyrate and 3-hydroxyhexanoate (PHBHHx). *Biomaterials*. 26, 6991–7001. doi: 10.1016/j.biomaterials.2005.05.034.
- Quillaguamán, J., Guzmán, H., Van-Thuoc, D., Hatti-Kaul, R. (2010) Synthesis and production of polyhydroxyalkanoates by halophiles: current potential and future prospects. *Applied Microbiology and Biotechnology*. 85 (6), 1687–1696.
- Quillaguamán, J., Hatti-Kaul, R., Mattiasson, B., Alvarez, M.T., Delgado, O. (2004) *Halomonas boliviensis* sp. nov., an alkalitolerant, moderate halophile bacterium isolated from soil around a Bolivian hypersaline lake. *International Journal of Systematic and Evolutionary Microbiology*. 54, 721–725.
- Ramadugu, P., Alikatte, K.L., Dhudipala, N. (2016) A review on biodegradable and bioabsorbable stents for coronary artery disease. *Journal of Bioequivalence and Bioavailability*. 8, 2. DOI: 10.4172/jbb.1000269.
- Ramcharitar, S., Serruys, P.W. (2008) Fully biodegradable coronary stents: progress to date. *American Journal of Cardiovascular Drugs* 8 (5), 305–314.
- Ramsay, J.A., Berger, E., Voyer, R., Chavarie, C., Ramsay, B.A. (1994) Extraction of poly-3-hydroxybutyrate using chlorinated solvents. *Biotechnology Techniques*. 8, 589–594. DOI: 10.1007/BF00152152.
- Rai, R., Boccaccini, A., Knowles, J., Mordan, N., Salihd, V., Locke, I., Moshrefi-Torbat, M., Keshavarz, T., Roy, I. (2011a) The homopolymer poly(3-hydroxyoctanoate) as a matrix material for soft tissue engineering. *Journal of Applied Polymer Science*. 122 (6), 3606–3617.
- Rai, R., Keshavarz, T., Roether, J., Boccaccini, A., Roy, I. (2011b) Medium chain length polyhydroxyalkanoates, promising new biomedical materials for the future. *Materials Science and Engineering*. 72, 29–47.
- Rai, R., Yunos, D.M., Boccaccini, A.R., Knowles, J.C., Barker, I.A., Howdle, S.M., Tredwell, G.D., Keshavarz, T., Roy, I. (2011c) Poly-3-hydroxyoctanoate P(3HO), a medium chain length polyhydroxyalkanoate homopolymer from *Pseudomonas mendocina*. *Biomacromolecules*. 12 (6), 2126–2136.
- Ranade, V., Hollinger, M. (1996) Drug delivery systems. Boca Raton, CRC Press.
- Randriamahefa, S., Renard, E., Guérin, P., Langlois, V. (2003) Fourier transform infrared spectroscopy for screening and quantifying production of PHAs by *Pseudomonas* grown on sodium octanoate. *Biomacromolecules*. 4, 1092–1097.
- Ratledge, C., Kristiansen, B. (2001) Basic Biotechnology, 2nd edn. Cambridge: Cambridge University Press.
- Ratner, B.D. (2007) Blood compatibility in the 21st century. The catastrophe revisited. *Biomaterials*. 28 (34), 5144–5147. doi: 10.1016/j.biomaterials.2007.07.035.

REFERENCES

- Raval, A.; Parikh, J., Engineer, C. (2010). Mechanism of controlled release kinetics from medical devices. *Brazilian Journal of Chemical Engineering*. 27 (2), 211-225. <http://dx.doi.org/10.1590/S0104-66322010000200001>.
- Ravichandran, R., Sundarrajan, S., Venugopal, J.R., Mukherjee, S., Ramakrishna, S. (2012) Advances in polymeric systems for tissue engineering and biomedical applications. *Macromolecular Bioscience*. 12 (3), 286-311. doi: 10.1002/mabi.201100325.
- Ray, D.K., Mueller, N.D., West, P.C., Foley, J.A. (2013) Yield trends are insufficient to double global crop production by 2050. *PLoS ONE* 8(6), e66428. <https://doi.org/10.1371/journal.pone.0066428>.
- Reddy, S.W., Thirumalam M., Mahmood, S.K. (2009) Production of PHB and P (3HB-co-3HV) biopolymers by *Bacillus megaterium* strain OU303A isolated from municipal sewage sludge. *World Journal of Microbiology and Biotechnology*. 25 (3), 391–397.
- Regar, E., Sianos, G., Serruys, P.W. (2001) Stent development and local drug delivery. *British Medical Bulletin*. 59, 227–48.
- Rahman, A., Linton, E., Hatch, A.D., Sims, R.C., Miller, C.D. (2013) Secretion of polyhydroxybutyrate in *Escherichia coli* using a synthetic biological engineering approach. *Journal of Biological Engineering*. 7, 24. <https://doi.org/10.1186/1754-1611-7-24>.
- Ramadugu, P., Alikatte, K.L., Dhudipala, N. (2016) A review on biodegradable and bioabsorbable stents for coronary artery disease. *Journal of Bioequivalence and Bioavailability*. 8(2), 064-067. DOI:10.4172/jbb.1000269.
- Ramaswamy, V., Vimalathithan, R.M., Ponnusamy, V. (2011) Preparation of barium sulphate nanocrystals in ethanol—water mixed solvents. *Journal of Ceramic Processing Research*. 12 (2), 173–175.
- Ray, S., Kalia, V.C. (2017) Polyhydroxyalkanoate production and degradation patterns in *Bacillus* species. *Indian Journal of Microbiology*. 57, 387. <https://doi.org/10.1007/s12088-017-0676y>.
- Rehm, B.H. (2007) Biogenesis of microbial polyhydroxyalkanoate granules: a platform technology for the production of tailor-made bioparticles. *Current Issues in Molecular Biology*. 9, 41–62.
- Rehm, B.H. (2003) Polyester synthases: natural catalysts for plastics. *Journal of Biochemistry*. 376 (1), 15-33.
- Rehm, B.H.A., Kruger, N., Steinbuchel, A. (1998) A new metabolic link between fatty acid de novo synthesis and polyhydroxyalkanoic acid synthesis. *Journal of Biological Chemistry*. 273, 24044–24051.
- Reinecke, H., Navarro, R., Pérez, M. (2011). Plasticizers. *Encyclopedia of Polymer Science and Technology*.

REFERENCES

- Renard, E., Walls, M., Guérin, P., Langlois, V. (2004) Hydrolytic degradation of blends of polyhydroxyalkanoates and functionalized polyhydroxyalkanoates. *Polymer Degradation and Stability*. 85 (2), 779-787.
- Renstadt, R., Karlsson, S., Albertsson, A.C. (1998) The influence of processing conditions on the properties and the degradation of poly(3-hydroxybutyrate-co-3-hydroxyvalerate). *Macromolecular Symposia*. 127, 241–9.
- Requena, R., Jimenez, A., Vargas, M., Chiralt A. (2016), Effect of plasticizers on thermal and physical properties of compression-moulded poly (3-hydroxybutyrate)-co-(3-hydroxyvalerate) films. *Polymer Testing*. 56, 45-53.
- Reusch, R.N. (2000) Transmembrane ion transport by polyphosphate/poly-(R)-3-hydroxybutyrate complexes. *Biochemistry (Mosc)*. 65 (3), 280-95.
- Ricker, A., Liu-Snyder, P., Webster, T.J. (2008) The influence of nano MgO and BaSO₄ particle size additives on properties of PMMA bone cement. *International Journal of Nanomedicine*. 3(1), 125–132.
- Rijk, T.C., van de Meer, P., Eggink, G., Weusthuis, R. (2005) Methods for Analysis of Poly(3-hydroxyalkanoate) (PHA) Composition. *Biopolymers Online*. 3. 10.1002/3527600035.bpol3b01.
- Ringel, I., Horwitz, S.B. (1991) Studies with RP 56976 (taxotere): a semisynthetic analogue of taxol. *Journal of National Cancer Institute*. 83, 288-291.
- Rossi, S., Azghani, A.O., Omri, A. (2004) Antimicrobial efficacy of a new antibiotic-loaded poly(hydroxybutyric-co-hydroxyvaleric acid) controlled release system. *Journal of Antimicrobial Chemotherapy*. 54, 1013-1018.
- Rowinsky, E.K., Donehower, R.C. (1995) Paclitaxel (taxol). *New England Journal of Medicine*. 332 (15), 1004-14.
- Rowinsky, E.K., Casenave, L.A., Donehower, R.C. (1990) Taxol: a novel investigational antimicrotubular agent. *Journal of National Cancer Institute*. 82, 1247-1249.
- Rydz, J., Sikorska, W., Kyulavska, M., Christova, D. (2015) Polyester-based (bio)degradable polymers as environmentally friendly materials for sustainable development. *International Journal of Molecular Sciences*. 16, 564-596; doi: 10.3390/ijms16010564.
- Ryu, H.W., Hahn, S.K., Chang, Y.K., Chang, H.N. (1997) Production of poly(3-hydroxybutyrate) by high cell density fed-batch culture of *Alcaligenes eutrophus* with phosphate limitation. *Biotechnology and Bioengineering*. 55 (1), 25–32.
- Rzeszutko, L., Depukat, R., Dudek, D. (2013). Biodegradable vascular scaffold ABSORB BVS™ – scientific evidence and methods of implantation. *Postępy Kardiologii Interwencyjnej*. 9(1): 22–30. doi: 10.5114/pwki.2013.34026.
- Sabatini, D.M., Erdjument-Bromage, H., Lui, M., Tempst, P., Snyder, S.H. (1994) RAFTI: a mammalian protein that binds to fkbp12 in a rapamycin-dependent fashion and is homologous to yeast TORs. *Cell*. 78, 35-43.

REFERENCES

- Sabokbar, A., Fujikawa, Y., Murray, D.W., Athanasou, N.A. (1997) Radio-opaque agents in bone cement increase bone resorption. *The Journal of Bone and Joint Surgery British volume*. 79(1), 129-34.
- Sachin, B.S., Ramdas, T.D., Wagh, V.D., Kotade, K.B. (2016) Pharmaceutically used plasticizers: a review. *European Journal of Biomedical and Pharmaceutical Sciences*. 3 (2), 277-285.
- Sádaba, B., Azanza, J.R., García Quetglas, E., Fernández, V. (2004) Treatment with tacrolimus in autoimmune diseases. *Revista de Medicina de la Universidad de Navarra*. 48(3), 24-38.
- Saito, M., Inoue, Y., Yoshie, N. (2001) Cocrystallisation and phase segregation of blends of poly(3-hydroxybutyrate) and Poly(3-hydroxybutyrate-co-3-hydroxyvalerate). *Polymer*. 42, 5573-5580.
- Samorì, C., Abbondanzi, F., Galletti, P., Giorgini, L., Mazzocchetti, L., Torri, C., Tagliavini, E. (2015). Extraction of polyhydroxyalkanoates from mixed microbial cultures: Impact on polymer quality and recovery. *Bioresource Technology*. 189, 195-202.
- Sangiorgi, G., Melzi, G., Agostoni, P., Cola, C., Clementi, F., Romitelli, P., Virmani, R., Colombo, A. (2007) Engineering aspects of stents design and their translation into clinical practice. *Annali dell'Istituto Superiore di Sanita*. 43 (1), 89-100.
- Sathiyarayanan, G., Bhatia, S.K., Song, H.S., Jeon, J.M., Kim, J., Lee, Y.K., Kim, Y.G., Yang, Y.H. (2017) Production and characterization of medium-chain-length polyhydroxyalkanoate copolymer from Arctic psychrotrophic bacterium *Pseudomonas* sp. PAMC 28620. *International Journal of Biological Macromolecules*. 97, 710-720.
- Sbihia, H.M., Nehdia, I.A., Tanb, C.P., Al-Resayesa, S.I. (2015) Characteristics and fatty acid composition of milk fat from Saudi Aradi goat. *Grasas Aceites*. 66 (4), e101. doi: <http://dx.doi.org/10.3989/gya.0233151>.
- Scandola, M., Ceccoruli, G., Pizzoli, M. (1992) Miscibility of bacterial poly(3-hydroxybutyrate) with cellulose esters. *Macromolecules*. 25, 6441-6446.
- Schick, C., Wurm, A., Mohamed, A. (2001) Vitrification and devitrification of the rigid amorphous fraction of semicrystalline polymers revealed from frequency-dependent heat capacity. *Colloid and Polymer Science*. 279 (8), 800-806.
- Schmelzle, T., Hall, M.N. (2000) TOR, a central controller of cell growth. *Cell*. 13, (103), 253-62.
- Schmitz, K.P., Behrend, D., Sternberg, K., Grabow, N., Martin, D.P., Williams, S. F. (2010) Tephra Inc.: Polymeric, degradable drug-eluting stents and coatings, United States patent No.: US8979921.
- Schliecke, G., Schmidt, C. (2003) Hydrolytic degradation of poly(lactide-co-glycolide) films: Effect of oligomers on degradation rate and crystallinity. *International Journal of Pharmacy*. 266, 39-49.

REFERENCES

- Schwartz, R.S., Huber, K.C., Murphy, J.G. (1992) Restenosis and the proportional neointimal response to coronary artery injury: results in a porcine model. *Journal of the American College of Cardiology*. 19, 267–74.
- Scott, H., Ich, O., Yi, Y. (2004) Stent with attached sleeve marker. EP1488763. Endotex Interventional Systems, Inc. 2004.
- Sears, J.K., Darby, J.R. (1982) *The Technology of Plasticizers*, John Wiley, New York.
- Seidman, A.D., Hudis, C.A., Albanell, J., Tong, W., Tepler, I., Currie, V., Moynahan, M.E., Theodoulou, M., Gollub, M., Baselga, J., Norton, L. (1998) Dose-dense therapy with weekly 1-hour paclitaxel infusions in the treatment of metastatic breast cancer. *Journal of Clinical Oncology*. 16 (10), 3353-61.
- Serrano, C.V. Jr, Ramires, J.A., Venturinelli, M., Arie, S., D'Amico, E., Zweier, J.L., Pileggi, F., da Luz, P.L. (1997) Coronary angioplasty results in leukocyte and platelet activation with adhesion molecule expression: evidence of inflammatory responses in coronary angioplasty. *Journal of the American College of Cardiology*. 29 (6), 1276-1283.
- Serruys, P.W., Garcia-Garcia, H.M., Onuma, Y. (2012) From metallic cages to transient bioresorbable scaffolds: change in paradigm of coronary revascularization in the upcoming decade? *European Heart Journal*. 33, 16-U165, ISSN: 0195-668X.
- Serruys, P.W., Ormiston, J.A., Onuma, Y. (2009) A bioabsorbable everolimus-eluting coronary stent system (ABSORB): 2-year outcomes and results from multiple imaging methods. *Lancet*. 373, 897–910.
- Serruys, P.W., Kutryk, M.J.B., Ong, A.T.L. (2006) Coronary-Artery Stents. *New England Journal of Medicine*. 354(5), 483-495.
- Serruys, P.W., Foley, D.P., Suttorp, M.J., Rensing, B.J., Suryapranata, H., Materne, P., van den Bos, A., Benit, E., Anzuini, A., Rutsch, W. (2002) A randomized comparison of the value of additional stenting after optimal balloon angioplasty for long coronary lesions: final results of the additional value of NIR stents for treatment of long coronary lesions (ADVANCE) study. *Journal of the American College of Cardiology*. 39, 393–399.
- Serruys, P.W., de Jaegere, P., Kiemeneij, F., Macaya, C., Rutsch, W., Heyndrickx, G., Emanuelsson, H., Marco, J., Legrand, V., Materne, P. (1994) A comparison of balloon-expandable-stent implantation with balloon angioplasty in patients with coronary artery disease. Benestent Study Group. *New England Journal Medicine*. 331 (8), 489-95.
- Serruys, P.W., Strauss, B.H., Beatt, K.J. (1991) Angiographic follow-up after placement of a self-expanding coronary-artery stent. *The New England Journal of Medicine*. 324, 13–7.

REFERENCES

- Sevastianov, V., Perova, N., Shishatskaya, E., Kalacheva, G., Volova, T. (2003) Production of purified polyhydroxyalkanoates (PHAs) for applications in contact with blood. *Journal of Biomaterial Science. Polymer Edition.* 14(10), 1029-42.
- Shabalovskaya, S.A. (1996) On the nature of the biocompatibility and on medical applications of NiTi shape memory and superelastic alloys. *Biomedical Materials Engineering.* 6 (4), 267-289.
- Shah, K.R. (2014) Optimization and production of Polyhydroxybutarate (PHB) by *Bacillus subtilis* G1S1 from soil. *International Journal of Current Microbiology and Applied Sciences.* 3(5), 377-387.
- Shahid, S., Mosrati, R., Ledauphin, J., Amiel, C., Fontaine, P., Gaillard, J.L., Corroler, D. (2013) Impact of carbon source and variable nitrogen conditions on bacterial biosynthesis of polyhydroxyalkanoates: Evidence of an atypical metabolism in *Bacillus megaterium* DSM 509. *Journal of Bioscience and Bioengineering.* 116 (3), 302-308.
- Shamala, T.R., Chandrashekar, A., Vijayendra, S.V., Sharma, L. (2003) Identification of polyhydroxyalkanoate (PHA) producing *Bacillus* spp. using the polymerase chain reaction (PCR). *Journal of Applied Microbiology.* 94, 369-374.
- Shan, G.F., Gong, X., Chen, W.P., Chen, L., Zhu, M.F. (2011) Effect of multi-walled carbon nanotubes on crystallization behavior of poly(3-hydroxybutyrate-co-3-hydroxyvalerate). *Colloid Polymer Science.* 289,1005–1014.
- Shangguan, Y.Y., Wang, Y.W., Wu, Q., Chen, G.Q. (2006) The mechanical properties and *in vitro* biodegradation and biocompatibility of UV-treated poly(3-hydroxybutyrate-co-3-hydroxyhexanoate). *Biomaterials.* 27, 2349–2357.
- Shapiro, R., Scantlebury, V.P., Jordan, M.L., Vivas, C., Ellis, D., Lombardozzi-Lane S., Gilboa, N., Gritsch, H.A., Irish, W., McCauley, J., Fung, J.J., Hakala, T.R., Simmons, R.L., Starzl, T.E. (1999) Under tacrolimus-based immunosuppression. *Transplantation.* 67(2), 299–303.
- Sharifzadeh, B.M., Tabandeh, F., Yunesi, H., Najafpour, G., Issazadeh, H. (2009) Poly (3-hydroxybutyrate) synthesis by *Cupriavidus necator* DSMZ 545 utilizing various carbon sources, *World Applied Science Journal.* 7(2), 157-161.
- Shen, Y., Li, C., Zhu, X., Xie, A., Qiu, L., Zhu, J. (2007) Study on the preparation and formation mechanism of barium sulphate nanoparticles modified by different organic acids. *Journal of Chemical Sciences.* 119 (4), 319–324.
- Shishatskaya, E.I., Goreva, A.V., Voinova, O.N., Inzhevatkin, E.V., Khlebopros, R.G., Volova, T.G. (2008) Evaluation of antitumor activity of rubomycin deposited in absorbable polymeric microparticles. *Bulletin of Experimental Biology and Medicine.* 145 (3), 358–361.
- Shishatskaya, E.I., Volova, T.G., Puzyr, A.P., Mogilnaya, O.A., Efremov, S.N. (2004) Tissue response to the implantation of biodegradable Polyhydroxyalkanoate sutures, *Journal of Material Science: Materials in Medicine.* 15, 719.

REFERENCES

- Shedden, L., Oldroyd, K., Connolly, P. (2009) Current issues in coronary stent technology. *Proceedings of the Institution of Mechanical Engineers, Part H: Journal of Engineering in Medicine*. 223, 515-524.
- Shilalipi, S., Nirupama, M. (2012) Production and characterization of poly- β -hydroxybutyrate (PHB) polymer from *Aulosira fertilissima*. *Journal of Applied Phycology*. 24 (4), 803–814.
- Siemann, U. (2005) Solvent cast technology – a versatile tool for thin film production. *Progress in Colloid and Polymer Science*. 130, 1–14. DOI 10.1007/b107336.
- Silber, S., Albertsson, P., Aviles, F.F. (2005) Guidelines for percutaneous coronary interventions. The task force for percutaneous coronary interventions of the European Society of Cardiology. *European Heart Journal*. 26, 804–47.
- Silva-Queiroz, S.R., Silva, L.F., Pradella, J.G., Pereira, E.M., Gomez, J.G. (2009) PHA(MCL) biosynthesis systems in *Pseudomonas aeruginosa* and *Pseudomonas putida* strains show differences on monomer specificities. *Journal of Biotechnology*. 143 (2), 111-118. doi: 10.1016/j.jbiotec.2009.06.014.
- Simon-Colin, C., Gouin, C., Lemechko, P., Schmitt, S., Senant, A., Kervarec, N., Guezennec, J. (2012) Biosynthesis and characterization of polyhydroxyalkanoates by *Pseudomonas guezenei* from alkanoates and glucose. *International Journal of Biological Macromolecules*. 51, 1063–1069. doi: 10.1016/j.ijbiomac.2012.08.018.
- Simon-Colin, C., Alain, K., Raguénès, G., Schmitt, S., Kervarec, N., Gouin, C., Crassous, P., Costa, B., Guezennec, J.G. (2009) Biosynthesis of medium chain length poly (3-hydroxyalkanoates) (mcl PHAs) from cosmetic co-products by *Pseudomonas ragenesii* sp. nov., isolated from Tetiaroa, French Polynesia. *Bioresource Technology*. 100, 6033–6039. doi: 10.1016/j.biortech.2009.06.075.
- Simon-Colin, C., Raguénès, G., Costa, B., Guezennec, J. (2008) Biosynthesis of medium chain length poly-3-hydroxyalkanoates by *Pseudomonas guezenei* from various carbon sources. *Reactive and Functional Polymers*. 68, 1534-1541.
- Simon-Colin, C., Alain, K., Colin, S., Cozien, J., Costa, B., Guezennec, J.G., Raguénès, G.H.C. (2008) A novel mcl PHA-producing bacterium, *Pseudomonas guezenei* sp. nov., isolated from a “kopara” mat located in Rangiroa, an atoll of French Polynesia. *Journal of Applied Microbiology*. 104, 581–586. doi: 10.1111/j.1365-2672.2007.03667.x.
- Singer, N.G., McCune, W.J. (1998) Update on immunosuppressive therapy. *Current Opinion in Rheumatology*. 10, 169-73.
- Singh, M., Kumar, P., Ray, S., Kalia, V.C. (2015) Challenges and opportunities for customizing Polyhydroxyalkanoates. *Indian Journal of Microbiology*. 55 (3), 235-249. doi: 10.1007/s12088-015-0528-6.
- Sigwart, U., Prel, J., Mirkoritch, V., Joffre, F., Kappenberger, L. (1987) Intravascular stents to prevent occlusion and restenosis after transluminal

REFERENCES

- angioplasty. *New England Journal of Medicine*. 318, 701-706.
- Singh, M., Patel, S., Kalia, V. (2009) *Bacillus subtilis* as potential producer for polyhydroxyalkanoates. *Microbial Cell Factories*. 8, 38.
 - Skucas, J. (1989) Barium sulfate for examination of the gastrointestinal tract. In: Margulis, A.R., Burhenne, H.J. (eds) *Alimentary Tract Radiology*. CV Mosby, St. Louis.
 - Slepíčka, P., Michaljaničová, I., Rimpelová, S., Švorčík, V. (2017) Surface roughness in action – Cells in opposition. *Materials Science and Engineering: C*. 76, 818-826.
 - Smith, I.O., Ma P.X. (2011) Biomimetic scaffolds in tissue engineering. In: *Tissue Engineering: From Clinic to Lab*. Paulla, N. and Suschek, C.V. (Eds.) Springer-Verlag, Berlin, Heidelberg.
 - Snejdrova, E., Dittrich, M. (2012) Pharmaceutically used plasticizers, in recent advances in plasticizers, Ed. M. Luqman, InTech, 2012.
 - Sodian, R., Hoerstrup, S.P., Sperling, J.S., Daebritz, S.H., Martin, D.P., Schoen, F.J., Vacanti, J.P., Mayer, J.E. Jr (2000a) Tissue engineering of heart valves: *in vitro* experiences. *Annual Thoracic Surgery*. 70(1), 140-4.
 - Sodian, R., Sperling, J.S., Martin, D.P., Egozy, A., Stock, U., Mayer, J.E. Jr, Vacanti, J.P. (2000b) Fabrication of a trileaflet heart valve scaffold from a polyhydroxyalkanoate biopolyester for use in tissue engineering. *Tissue Engineering*. 6(2), 183-8.
 - Solaiman, D.K.Y., Ashby, R.D., Foglia, T.A., Marmer, W.N. (2006) Conversion of agricultural feedstock and coproducts into poly(hydroxyalkanoates). *Applied Microbiology and Biotechnology*. 71 (6), 783–789.
 - Sousa, J.E., Serruys, P.W., Costa, M.A. (2003) New frontiers in cardiology: drug-eluting stents: part I. *Circulation*. 107, 2274–9.
 - Soxhlet, F. (1879) Die gewichtsanalytische Bestimmung des Milchfettes, *Polytechnisches Journal*. (Dingler's), 232, 461.
 - Spencer, C.M., Goa, K.L., Gillis, J.C. (1997) Tacrolimus. An update of its pharmacology and clinical efficacy in the management of organ transplantation. *Drugs*. 54, 925–975.
 - Sridhar, V., Lee, I., Chun, H.H., Park, H. (2013) Graphene reinforced biodegradable poly(3-hydroxybutyrate-co-4-hydroxybutyrate) nanocomposites. *Express Polymer Letters*. 7, 320–328.
 - Stahli, B.E., Camici, G.G., Tanner, F.C. (2009) Drug-eluting stent thrombosis. *Therapeutic Advances in Cardiovascular Disease*. 3 (1), 45–52.
 - Stahli, B.E., Camici, G.G., Steffel, J. (2006) Paclitaxel enhances thrombin-induced endothelial tissue factor expression via c-Jun terminal NH2 kinase activation. *Circulation Research*. 99, 149-155.

REFERENCES

- Staples, C.A., Peterson, D.R., Parkerton, T.F., Adams, W.J. (1997) The environmental fate of phthalate esters: a literature review. *Chemosphere*. 35, 667-749.
- Steinbüchel, A., Hustede, E., Liebergesell, M., Pieper, U., Timm, A., Valentin, H. (1992) Molecular basis for biosynthesis and accumulation of polyhydroxyalkanoic acids in bacteria. *FEMS Microbiological Reviews*. 9 (2-4), 217-30.
- Steinbüchel, A., Wiese, S. (1992) A *Pseudomonas* strain accumulating polyesters of 3-hydroxybutyric acid and medium-chain-length 3-hydroxyalkanoic acids. *Applied Microbiology and Biotechnology*. 37 (6), 691–697.
- Stock, U.A., Nagashima, M., Khalil, P.N. (2000) Tissue engineered valved conduits in the pulmonary circulation. *Journal of Thoracic Cardiovascular Surgery*. 119, 732–740.
- Stock, U.A., Sakamoto, T., Hatsuoka, S., Martin, D.P., Nagashima, M., Moran, A.M., Moses, M.A., Khalil, P.N., Schoen, F.J., Vacanti, J.P., Mayer, J.E. (2000) Patch augmentation of the pulmonary artery with bioabsorbable polymers and autologous cell seeding. *Journal of Thoracic Cardiovascular Surgery*. 120, 1158-68.
- Stoeckel, D., Bosignore, C., Duda, S. (2002) A survey on stent design. *Minimally Invasive Therapy and Allied Technologies*. 11 (4),137–147.
- Sutcliffe, I.C., Alderson, G. (1995) A chemotaxonomic appraisal of the distribution of lipomannans within the genus *Micrococcus*. *FEMS Microbiology Letters*. 133 (3), 233–237.
- Sudesh, K., Abe, H., Doi, Y. (2000) Synthesis, structure and properties of polyhydroxyalkanoates: biological polyesters. *Progress in Polymer Science*. 25, 1503-1555.
- Sui, X., Kujala, P., Janssen, G-J., de Jong, E., Zuhorn, I. S., & van Hest, J. C. M. (2015). Robust formation of biodegradable polymersomes by direct hydration. *Polymer chemistry*, 6(5), 691-696. DOI: 10.1039/C4PY01288G.
- Sukan, A., Roy, I., Keshavarz, T. (2015) Dual production of biopolymers from bacteria. *Carbohydrate Polymers*. 126, 47-51.
- Sun, D., Zheng, Y., Yin, T., Tang, C., Yu, Q., Wang, G. (2014) Coronary drug-eluting stents: From design optimization to newer strategies. *Journal of Biomedical Materials Research. Part A*. 102A, 1625–1640.
- Sun, Z., Ramsay, J.A., Guay, M., Ramsay, B. (2007) Increasing the yield of mcl-PHA from nonanoic acid by co feeding glucose during the PHA accumulation stage in two stage fed batch fermentations of *Pseudomonas putida* KT2440. *Journal of Biotechnology*. 132 (3), 280-282.

REFERENCES

- Suriyamongkol, P.F., Weselake, R., Narine, S., Moloney, M., Shah, S. (2007) Biotechnological approaches for the production of polyhydroxyalkanoates in microorganisms and plants. A review. *Biotechnology Advances*. 25, 148-175.
- Takala, A.J., Jousela, I.T., Takkunen, O.S. (1996) Time course of β 2-integrin CD11b/CD18 (Mac-1, α M β 2) upregulation on neutrophils and monocytes after coronary artery bypass grafting. *Scandinavian Journal of Thoracic Cardiovascular Surgery*. 30, 141-148.
- Takayama, T., Hiro, T., Hirayama, A. (2011) Stent thrombosis and drug-eluting stents, *Journal of Cardiology*. 58 (2),92–98.
- Tamai, H., Igaki, K., Kyo, E., Kosuga, K., Kawashima, A., Matsui, S., Komori, H., Tsuji, T., Motohara, S., Uehata, H. (2000) Initial and 6-month results of biodegradable poly-l-lactic acid coronary stents in humans. *Circulation*. 102, (4),399-404.
- Tamai, H., Igaki, K., Tsuji, T., Kyo, E., Kosuga, K., Kawashima, A., Matsui, S., Komori, H., Motohara, S., Uehata, H., Takeuchi, E. (1999) A biodegradable Poly-l-lactic acid coronary stent in the porcine coronary artery. *Journal of Interventional Cardiology*, 12, 443–450. doi:10.1111/j.1540-8183.1999.tb00673.x
- Tamer, I.M., Moo-Young, M., Chisti, Y. (1997) Optimization of Poly(3-Hydroxybutyric Acid) recovery from *Alcaligenes Latus*: combined mechanical and chemical treatments. *Bioprocess Engineering*. 19, 459-468.
- Tamura, S., Tokunaga, Y., Ibuki, R., Amidon, G.L., Sezaki, H., Yamashita, S. (2003) The site-specific transport and metabolism of tacrolimus in rat small intestine. *JPET*. 306 (1),310–316.
- Tan, G.Y.A., Chen, C.L., Li, L., Ge, L., Wang, L., Razaad, I.M.N., Li, Y., Zhao, L., Mo, Y., Wang, J.Y. (2014) Start a research on biopolymer polyhydroxyalkanoate (pha): a review. *Polymers*. 6(3), 706-754. doi:10.3390/polym6030706.
- Tanadchangsang, N., Yu, J. (2013) Miscibility of natural Polyhydroxyalkanoate blend with controllable material properties. *Journal of Applied Polymer Science*. 2004-2016, doi: 10.1002/APP.38906.
- Tanaka, H., Kuroda, A., Marusawa, H. (1987) Physicochemical properties of FK506, a novel immunosuppressant isolated from *Streptomyces tsukubaensis*. *Transplantation Proceedings*. 14, 11–6.
- Tanaka, H.A., Kuroda, H., Marusawa, H., Hatanaka, T., Kino, T., Goto, T., Hashimoto, M., Taga, T. (1987) Structure of FK-506: A novel immunosuppressant isolated from *Streptomyces*. *Journal of the American Chemical Society*. 109, 5031-5033.
- Taniguchi, I., Kagotani, K., Kimura, Y. (2003) Microbial production of poly(hydroxyalkanoate)s from waste edible oils. *Green Chemistry*. 5, 545–548. doi: 10.1039/B304800B.

REFERENCES

- Thakor, N., Trivedi, U., Pael, K.C. (2006) Microbiological and biotechnological aspects of biodegradable plastics: Poly(hydroxyalkanoates). *Indian Journal of Biotechnology*. 5, 137-147.
- Thellen, C., Coyne, M., Froio, D., Auerbach, M., Wirsén, C., Ratto, J.A. (2008) A processing, characterisation and marine biodegradation study of melt-extruded polyhydroxyalkanoate (PHA) films. *Journal of the Polymers and the Environment*. 16(1), 1-11.
- Tian, W, Hong K, Chen G Q, Wu, Q, Zhang R Huang W. (2000) Production of polyesters consisting of medium chain length 3-hydroxyalkanoic acids by *Pseudomonas mendocina* 0806 from various carbon sources. *Antonie van Leeuwenhoek*. 77, 31-36.
- Timm, A., Steinbuchel, A. (1992) Cloning and molecular analysis of the poly(3-hydroxyalkanoic acid) gene locus of *Pseudomonas aeruginosa* PA01. *European Journal of Biochemistry*. 209, 15-30.
- Trepát, X., Lenormand, G., Fredberg J.J. (2008) Universality in cell mechanics. *Journal of Soft Materials*. 4 (9), 1750-1759.
- Truskey, G.A. (2016) Advancing cardiovascular tissue engineering. *F1000Res*. 5. pii: F1000 Faculty Rev-1045. doi: 10.12688/f1000research.8237.1.
- Tsai, W.B., Grunkemeier, J.M., Horbett, T.A. (1999) Human plasma fibrinogen adsorption and platelet adhesion to polystyrene. *Journal of Biomedical Material Research*. 44(2), 130-139.
- Tsuge, T. (2016) Fundamental factors determining the molecular weight of polyhydroxyalkanoate during biosynthesis. *Polymer Journal*. 48 (11), 1051-1057.
- Tsuji, T., Tamai, H., Igaki, K. (2001) Biodegradable polymer stents. *Current Interventional Cardiology Reports*. 3, 10–17.
- Tsuji, H., Ikada, Y. (2000) Properties and morphology of poly(L-lactide) 4. Effects of structural parameters on long-term hydrolysis of poly(L-lactide) in phosphate-buffered solution. *Polymer Degradation and Stability*. 67(1), 179-189. [https://doi.org/10.1016/S0141-3910\(99\)00111-1](https://doi.org/10.1016/S0141-3910(99)00111-1).
- Valappil, S., Boccaccini, A., Bucke, C., Roy, I. (2007) Polyhydroxyalkanoates in Gram-positive bacteria: insights from the genera *Bacillus* and *Streptomyces*. *Antonie Van Leeuwenhoek*. 91, 1-17.
- Valentin, H.E., Dennis, D. (1996) Metabolic pathway for poly(3-hydroxybutyrate-co-3-hydroxyvalerate) formation in *Nocardia corallina*: inactivation of Mutb by chromosomal integration of a kanamycin resistance gene. *Applied and Environmental Microbiology*. 62(7), 372–379.
- Van Erven, L., Post, M.J., Borst, C. (1991) Arterial wall injury, arterial wall healing and restenosis. *Laser Medical Science*. 6, 271. <https://doi.org/10.1007/BF02030880>.
- Van der Giessen, W.J., Lincoff, A.M., Schwartz, R.S., van Beusekom, H.M.M., Serruys, P.W., Holmes, D.R., Ellis, S.G., Topol, E.J. (1996) Marked inflammatory

REFERENCES

- sequelae to implantation of biodegradable and non-biodegradable polymers in porcine coronary arteries. *Circulation*. 94, 1690-1697; <https://doi.org/10.1161/01.CIR.94.7.1690>.
- Van der Ha, D., Nachtergaele, L., Kerckhof, F.M., Rameiyanti, D., Bossier, P., Verstraete, W., Boon, N. (2012) Conversion of biogas to bioproducts by algae and methane oxidizing bacteria. *Environmental Science and Technology*. 46 (24), 13425–13431. DOI: 10.1021/es303929s.
 - Van der Hoeven, B.L., Pires, N.M., Warda, H.M., Putter, H., Quax, P.H., Schalijs, M.J., Jukema, J.W. (2008) Dexamethasone-eluting stents for the prevention of in-stent restenosis: Evidence for a differential effect in insulin-dependent and non-insulin-dependent diabetic patients. *International Journal of Cardiology*. 124, 166–171.
 - Van der Hoeven, B.L., Pires, N.M.M., Warda, H.M., Oemrawsingh, P.V., van Vlijmen, B.J.M., Quax, P.H.A., Schalijs, M.J., van der Wall, E.E., Jukema, J.W. (2005) Drug eluting stents: results, promises and problems, *International Journal of Cardiology*. 99, 9– 17.
 - Van Thiel, D.H., Wright, H., Carroll, P., Abu-Elmagd, K., Rodriguez-Rilo, H., McMichael, J., Irish, W., Starzl, T.E. (1995) Tacrolimus: A Potential New Treatment for autoimmune chronic active hepatitis: results of an open-label preliminary trial. *American Journal of Gastroenterology*. 90(5), 771–776.
 - Venkataramanan, R., Swaminathan, A., Prasad, T., Jain, A., Zuckerman, S., Warty, V., McMichael, J., Lever, J., Burckart, G., Starzl, T. (1995) Clinical pharmacokinetics of tacrolimus. *Clinical Pharmacokinetics*. 29, 30–404.
 - Venkatraman, S., Boey, F., Lao, L.L. (2008) Implanted cardiovascular polymers: natural, synthetic and bio-inspired. *Progress in Polymer Science*. 33, 853-874.
 - Verhoogt, H., Ramsay, B.A., Favis, B.D. (1994) Polymer blends containing poly(3-hydroxyalkanoates). *Polymer*. 35, 5155-5169.
 - Verlinden, R.A.J., Hill, D.J., Kenward, M.A., Williams, C.D., Piotrowska-Seget, Z., Radecka, I.K. (2011) Production of polyhydroxyalkanoates from waste frying oil by *Cupriavidus necator*. *AMB Express*. 1, 11. doi: 10.1186/2191-0855-1-11.
 - Verlinden, R., Hill, D., Kenward, M., Williams, C., Radecka, I. (2007) Bacterial synthesis of biodegradable polyhydroxyalkanoates. *Journal of Applied Microbiology*. 102, 1437- 1449.
 - Vieira, M.G.A., da Silva, M.A., dos Santos, L.O., Beppu, M.M. (2011) Natural-based plasticizers and biopolymer films: A review. *European Polymer Journal*. 47, 254–263.
 - Volova, T. (2004) Polyhydroxyalkanoates-plastic materials of the 21st century: production, properties, applications. Published by Nova Publishers.
 - Volova, T., Gladyshev, M., Trusova, M., Zhila, N. (2006) Degradation of polyhydroxyalkanoates and the composition of microbial destructors under natural conditions. *Microbiology*. 75(5), 135-143.

REFERENCES

- Wadey, B.L. (2003) An innovative plasticizer for sensitive applications. *Journal of Vinyl Additives*. 9, 172-176.
- Waksman, R., Pakala, R. (2010) Biodegradable and bioabsorbable stents. *Current Pharmaceutical Design*. 16, 4041-4051.
- Waksman, R., Erbel, R., Di Mario, C., Bartunek, J., de Bruyne, B., Eberli, F.R., Erne, P., Haude, M., Horrigan, M., Ilesley, C., Böse, D., Bonnier, H., Koolen, J., Lüscher, T.F., Weissman, N.J. (2009) Early- and long-term intravascular ultrasound and angiographic findings after bioabsorbable magnesium stent implantation in human coronary arteries. *JACC Cardiovascular Interventions*. 2(4), 312-20. doi: 10.1016/j.jcin.2008.09.015.
- Waksman, R. (2006) Biodegradable stents: they do their job and disappear. *Journal of the Invasive Cardiology*. 18(2), 70-4.
- Waksman, R., Bhargava, B., White, L., Chan, R.C., Mehran, R., Lansky, A.J., Mintz, G.S., Satler L.F., Pichard, A.D., Leon, M.B., Kent, K.K. (2000) Intracoronary beta-radiation therapy inhibits recurrence of in-stent restenosis. *Circulation*. 101(16),1895-8.
- Wallemacq. P., Furlan, V., Möller, A. (1998) Pharmacokinetics of tacrolimus (FK506) in paediatric liver transplant patients. *European Journal of Drug Metabolism and Pharmacokinetics*. 23, 367–370.
- Wampfler, B., Ramsauer, T., Rezzonico, S., Hischer, R., Köhling, R., Thöny-Meyer, L., Zinn, M. (2010) Isolation and purification of medium chain length poly(3-hydroxyalkanoates) (mcl-PHA) for medical applications using nonchlorinated solvents. *Biomacromolecules*. 11 (10), 2716–2723. DOI: 10.1021/bm1007663.
- Wang, J., He, Y., Maitz, M.F., Collins, B., Xiong, K., Guo, L., Yun, Y., Wan, G., Huang, N. (2013) A surface-eroding poly(1,3-trimethylene carbonate) coating for fully biodegradable magnesium-based stent applications: toward better biofunction, biodegradation and biocompatibility. *Acta Biomaterialia*. 9 (10), 8678–8689.
- Wang, L., Wang, X.J., Zhu, W.F., Chen, Z.F., Pan, J.Y., Xu, K.T. (2010) Effect of nucleation agents on the crystallization of poly(3-hydroxybutyrate-co-4-hydroxybutyrate) (P3HB4HB). *Journal of Applied Polymer Science*. 116, 1116–1123.
- Wang, Q., Chen, S., Zhang, J., Sun, M., Liu, Z., Yu, Z. (2008) Co-producing lipopeptides and poly- γ -glutamic acid by solid-state fermentation of *Bacillus subtilis* using soybean and sweet potato residues and its biocontrol and fertilizer synergistic effects. *Bioresource Technology*. 99 (8), 3318-3323.
- Wang, Z., Yoshiakitoh, Y., Hosaka, Y., Kobayashi, I., Nakano, Y., Maeda, I., Umeda, F., Yamakawa, J., Kawase, M., Yag, K. (2003) Novel transdermal drug delivery system with polyhydroxyalkanoate and starburst polyamidoamine dendrimer. *Journal of Bioscience and Bioengineering*. 95(5), 541-543.
- Wang, Y., Sun, Z., Shupe, A., Liu, S. (2012) Influence of oxygen mass transfer on the fermentation behavior of *Burkholderia cepacia* for polyhydroxyalkanoates

REFERENCES

- (PHAs) production utilizing wood extract hydrolysate (WEH). *Journal of Bioprocess Engineering*. 4(2), 169–175. doi: 10.1166/jbeeb.2012.1026.
- Wang, J. H., Liu, H.B., Wen, S.G., Shen, Y. (2011) The performance of barium sulfate/nature rubber composites using in sport shoes. *Advanced Materials Research*. 152-153, 1184-1187.
 - Wang, X., Venkatraman, S.S., Boey, F.Y.C., Loo, J.S.C., Tan, L.P. (2006) Controlled release of sirolimus from a multilayered PLGA stent matrix. *Biomaterials*. 27(32), 5588-5595.
 - Wang, Y.X., Robertson, J.L., Spillman Jr, W.B., Clausm R.O. (2004) Effects of the chemical structure and the surface properties of polymeric biomaterials on their biocompatibility. *Pharmaceutical Research*. 21(8), 1362–1373.
 - Wang, F., Lee, S.Y. (1997) Production of poly l(3-hydroxybutyrate) by fed-batch culture of filamentation-suppressed recombinant *Escherichia coli*. *Applied and an Environmental Microbiology*. 63, 4765-4769.
 - Wang, K., Wu, J., Ye, L., Zeng, H. (2003) Mechanical properties and toughening mechanisms of polypropylene/barium sulphate composites. *Composites Part A- Applied Science and Manufacturing*. 34. 1199-1205. 10.1016/j.compositesa.2003.07.004.
 - Wang, F., Lee, S.Y. (1997) Poly(3-hydroxybutyrate) production with high productivity and high polymer content by a fed-batch culture of *Alcaligenes latus* under nitrogen limitation. *Applied and an Environmental Microbiology*. 63, 3703–3706.
 - Wani, M.C., Taylor, H.L., Wall, M.E., Coggon, P., McPhail, A.T. (1971) Plant antitumor agents. VI. The isolation and structure of taxol, a novel antileukemic and antitumor agent from *Taxus brevifolia*. *Journal of the American Chemical Society*. 93, 2325-2327.
 - Weihua, K., He, Y., Asakawa, N., Inoue, Y. (2004) Effect of lignin particles as a nucleating agent on crystallization of poly(3-hydroxybutyrate). *Journal of Applied Polymer Science*. 94, 2466–2474. doi:10.1002/app.21204.
 - Wellen, R.M.R., Rabello, M.S., Fachine, G.J.M., Canedo, E.L. (2013) The melting behaviour of poly(3-hydroxybutyrate) by DSC. Reproducibility study. *Polymer Testing*. 32, 215–220.
 - Welt, F.G., Rogers, C (2002) Inflammation and restenosis in the stent era. *Arteriosclerosis, Thrombosis and Vascular Biology*. 22 (11), 1769–76.
 - Wen, X., Lu, X., Peng, Q., Zhu, F., Zheng, N. (2011). Crystallization behaviors and morphology of biodegradable poly(3-hydroxybutyrate-co-4-hydroxybutyrate). *Journal of Thermal Analysis and Calorimetry*. 109. 1-8. 10.1007/s10973-011-1768-2.

REFERENCES

- Wilkins E, Wilson L, Wickramasinghe K, Bhatnagar P, Leal J, Luengo-Fernandez R, Burns R, Rayner M, Townsend N (2017) European Cardiovascular Disease Statistics 2017. European Heart Network, Brussels.
- Williams, S.F., Martin, D.P. (2005) Applications of polyhydroxyalkanoates (PHA) in medicine and pharmacy. Wiley-VCH Verlag GmbH & Co. KGaA.
- Williams, S.F., Martin, D.P., Horowitz, D.M., Peoples, O.P. (1999) PHA applications: addressing the price performance issue I. Tissue engineering. *International Journal of Biological Macromolecules*. 25, 111–121.
- Williams, D.R., Anderson, A.J., Dawes, E.A., Ewing, D.E. (1994) Production of a copolymer of 3-hydroxybutyric acid and 3-hydroxyvaleric acid from succinic acid by *Rhodococcus ruber*: biosynthetic consideration. *Applied Microbiology and Biotechnology*. 40, 717-723.
- Williams, D.F., Zhong, S.P. (1994) Biodeterioration/ biodegradation of polymeric medical devices *in situ*. *International Biodeterioration & Biodegradation*. 34 (2), 95-130.
- Wilson, W.M., Cruden, N.L.M. (2013) Advances in coronary stent technology: current expectations and new developments. *Research Reports in Clinical Cardiology*. 4, 85–96.
- Windecker, S., Meier, B. (2007) Late coronary stent thrombosis. *Circulation*. 116 (17), 1952-65.
- Widmark, J.M. (2007) Imaging-related medications: a class overview. *Proceedings (Baylor University Medical Centre)*. 20(4), 408–417.
- Wise, L. D. (2000) Handbook of pharmaceutical controlled release technology. Marcel Dekker, Inc. New York, Basel.
- Wong, Y.M., Brigham, C.J., Rha, C.K., Sinskey, A.J., Sudesh, K. (2012) Biosynthesis and characterization of polyhydroxyalkanoate containing high 3-hydroxyhexanoate monomer fraction from crude palm kernel oil by recombinant *Cupriavidus necator*. *Bioresource Technology*. 121, 320–327.
- Woodruff, M., Hutmacher, D. (2010). The return of a forgotten polymer-polycaprolactone in the 21st century. *Progress in Polymer Science*. 35. 10.1016/j.progpolymsci.2010.04.002.
- Wu, T.M., Hsu, S.F., Shih, Y.F., Liao, C.S. (2008). Thermal degradation kinetics of biodegradable poly(3-hydroxybutyrate)/layered double hydroxide nanocomposites. *Journal of Polymer Science. Part B Polymer Physics*. 46, 1207–1213.
- Yamane, T., Chen, X-F., Ueda, S. (1996) Polyhydroxyalkanoate synthesis from alcohols during the growth of *Paracoccus denitrificans*. *FEMS Microbiological Letters*. 135, 207–211.
- Yan, L., Huang, R., Xiao, J., Xia, H., Chao, M., Wiessner, S. (2016) Preparation and properties of a composite made by barium sulfate-containing

REFERENCES

- polytetrafluoroethylene granular powder. *High Performance Polymers*. 28(6), 741–746.
- Yan, C., Wang, Y., Shen, X.Y., Yang, G., Jian, J., Wang, H.S., Chen, G.Q., Wu, Q. (2011) MicroRNA regulation associated chondrogenesis of mouse MSCs grown on polyhydroxyalkanoates. *Biomaterials*. 32 (27), 6435-6444.
 - Yamashita, K., Nakate, T., Okimoto, K., Ohike, A., Tokunaga, Y., Ibuki, R., Higaki, K., Kimura, T. (2003) Establishment of new preparation method for solid dispersion formulation of tacrolimus. *International Journal of Pharmacy*. 28, 267(1-2), 79-91.
 - Yang, J.H., Brigham, C., Willis, L., Rha, C.K., Sinskey, A. (2011) Improved detergent-based recovery of polyhydroxyalkanoates (PHAs). *Biotechnology Letters*. DOI 10.1007/s10529-010-0513-4.
 - Yang, W., Zhang, L., Wang, S., White, A.D., Jiang, S. (2009) Functionalizable and ultra-stable nanoparticles coated with zwitterionic poly(carboxybetaine) in undiluted blood serum. *Biomaterials*. 30 (29), 5617-5621.
 - Yao, Y.C., Zhan, X.Y., Zhang, J. (2008) A specific drug targeting system based on polyhydroxyalkanoate granule binding protein PhaP fused with targeted cell ligands. *Biomaterials*. 29 (36), 4823–4830.
 - Yao, J., Zhang, G., Wu, Q., Chen, G.Q., Zhang, R.Q. (1999) Production of polyhydroxyalkanoates by *Pseudomonas nitroreducens*. *Antonie van Leeuwenhoek*. 75, 345–349.
 - Yavuz, H., Babac, C., Tuzlakoglu, K., Piskin, E. (2002) Preparation and degradation of l-lactide and unknown caprolactone homo and copolymer films. *Polymer Degradation and Stability*. 75, 431–437.
 - Yezza, A., Fournier, D., Halasz, A., Hawari, J. (2006) Production of polyhydroxyalkanoates from methanol by a new methylotrophic bacterium *Methylobacterium* sp. GW2. *Applied Microbiology and Biotechnology*. 73 (1), 211–218.
 - Yoshie, N., Nakasato, K., Fujiwara, M., Kasuya, K., Abe, H., Doi, Y., Inoue, Y. (2000) Effect of low molecular weight additives on enzymatic degradation of poly(3-hydroxybutyrate). *Polymer*. 41,3227–34.
 - Yu, B.Y., Chen, C.R., Sun, Y.M., Young, T.H. (2009) The response of rat cerebellar granule neurons (rCGNs) to various polyhydroxyalkanoate (PHA) films. *Desalination*. 245, 1–3, 639-646.
 - Yu, L., Dean, K., Li, L. (2006) Polymer blends and composites from renewable resources. *Progress in Polymer Science*. 31(6), 576-602.
 - Yusuf, S., Hawken, S., Ounpuu, S., Dans, T., Avezum, A., Lanas, F., McQueen, M., Budaj, A., Pais, P., Varigos, J., Lisheng, L. (2004). Effect of potentially modifiable risk factors associated with myocardial infarction in 52 countries (the INTERHEART study): case-control study. *Lancet*. 2364 (9438), 937-952.

REFERENCES

- Zahora, J., Bezrouk, A., Hanus, J. (2007). Models of stents – comparison and applications. *Physiological Research*. 56 (1), S115-S121.
- Zhang, Y., Sun, W., Wang, H., Geng, A. (2013). Polyhydroxybutyrate production from oil palm empty fruit bunch using *Bacillus megaterium* R11. *Bioresource Technology*. 147, 307.
- Zhang, X., Shanmugam, K.T., Ingram, L.O. (2010) Fermentation of glycerol to succinate by metabolically engineered strains of *Escherichia coli*. *Applied and Environmental Microbiology*. 76, 2397-2401.
- Zhang, X.J., Luo, R.C., Wang, Z., Deng, Y., Chen, G.Q. (2009) Applications of (R)-3-hydroxyalkanoate methyl esters derived from microbial polyhydroxyalkanoates as novel biofuel. *Biomacromolecules*. 10 (4), 707-11. doi:10.1021/bm801424e.
- Zhang, Z., Chen, S.F., Jiang, S.Y. (2006) Dual-functional biomimetic materials: nonfouling poly(carboxybetaine) with active functional groups for protein immobilization. *Biomacromolecules*. 7 (12), 3311–5.
- Zhang, L., Xiong, C., Deng, X. (1996) Miscibility, crystallization and morphology of poly(P-hydroxybutyrate)/poly(d,l-lactide) blends. *Polymer*. 37 (2), 235-241.
- Zhao, W., Chen, G. (2007) Production and characterization of terpolyester poly(3-hydroxybutyrate-co-3-hydroxyvalerate-co-3-hydroxyhexanoate) by recombinant *Aeromonas hydrophila* 4AK4 harbouring genes phaAB. *Process Biochemistry*. 42, 1342–1347.
- Zhou, J., Cidlowski, J.A. (2005) The human glucocorticoid receptor: one gene, multiple proteins and diverse responses. *Steroids*. 70, 407–417.
- Zilberman, M., Eberhart, R.C. (2006) Drug-eluting bioresorbable stents for various applications. *Annual Review of Biomedical Engineering*. 8, 153-180.
- Zinn, M., Witholt, B., Egli, T. (2001) Occurrence, synthesis and medical application of bacterial polyhydroxyalkanoate. *Advanced Drug Delivery Reviews*. 53, 5-21.
- Zweers, J.C., Wiegert, T., van Dijk, J.M. (2009) Stress-responsive systems set specific limits to the overproduction of membrane proteins in *Bacillus subtilis*. *Applied and Environmental Microbiology*. 75 (23), 7356–7364. doi: 10.1128/AEM.01560-09.
- Żwawiak, J., Zaprutko, L. (2014) A brief history of taxol. *Journal of Medical Science*. 1 (83) 47-52.